

1991

The Sedimentology Of The Boss Point Formation (pennsylvanian), Eastern New Brunswick And Northern Nova Scotia (volumes I And Ii)

Gregory Hawtrey Browne

Follow this and additional works at: <https://ir.lib.uwo.ca/digitizedtheses>

Recommended Citation

Browne, Gregory Hawtrey, "The Sedimentology Of The Boss Point Formation (pennsylvanian), Eastern New Brunswick And Northern Nova Scotia (volumes I And Ii)" (1991). *Digitized Theses*. 1943.
<https://ir.lib.uwo.ca/digitizedtheses/1943>

This Dissertation is brought to you for free and open access by the Digitized Special Collections at Scholarship@Western. It has been accepted for inclusion in Digitized Theses by an authorized administrator of Scholarship@Western. For more information, please contact tadam@uwo.ca, wlsadmin@uwo.ca.

**The Sedimentology of the Boss Point Formation
(Pennsylvanian), eastern New Brunswick and
northern Nova Scotia.**

Volume I

by

Gregory Hawtrey Browne

Department of Geology

**Submitted in partial fulfilment
of the requirements for the degree of
Doctor of Philosophy**

**Faculty of Graduate Studies
The University of Western Ontario
London, Ontario
November 1990**

© Gregory H. Browne 1990



National Library
of Canada

Bibliothèque nationale
du Canada

Canadian Theses Service Service des thèses canadiennes

Ottawa, Canada
K1A 0N4

The author has granted an irrevocable non-exclusive licence allowing the National Library of Canada to reproduce, loan, distribute or sell copies of his/her thesis by any means and in any form or format, making this thesis available to interested persons.

The author retains ownership of the copyright in his/her thesis. Neither the thesis nor substantial extracts from it may be printed or otherwise reproduced without his/her permission.

L'auteur a accordé une licence irrévocable et non exclusive permettant à la Bibliothèque nationale du Canada de reproduire, prêter, distribuer ou vendre des copies de sa thèse de quelque manière et sous quelque forme que ce soit pour mettre des exemplaires de cette thèse à la disposition des personnes intéressées.

L'auteur conserve la propriété du droit d'auteur qui protège sa thèse. Ni la thèse ni des extraits substantiels de celle-ci ne doivent être imprimés ou autrement reproduits sans son autorisation.

ISBN 0-315-64249-1

Canada

ABSTRACT

The Westphalian A (Pennsylvanian) Boss Point Formation consists of sandstone and mudrock units which developed within an active pull-apart basin (the Cumberland sub-basin) in Maritime Canada. The bulk of the formation comprises trough cross-bedded sandstones interpreted as braided river deposits. The rivers flowed from largely felsic igneous provenance areas in the west, toward the region of the present-day Bay of Fundy. Paleocurrents indicate a dominant northeast-directed drainage system, which deviated toward the southeast in the vicinity of Cape Maringouin, about a paleogeographic high related to the penecontemporaneous Harvey-Hopewell Fault.

Intercalated with the sand-dominated fluvial rocks, are fine-grained sandstones, ostracod-bearing limestones and coaly shales deposited in a variety of fluvio-lacustrine settings, including distributary channel, crevasse-splay, deltaic and open lacustrine environments. Rootlet horizons, pedogenic features and rills associated with many of the interbedded sandstones indicate that lake depths were probably shallow, and that lake levels fluctuated frequently.

Paleosols occur widely and formed in areas that were starved of sediment for appreciable periods of time. Paleosol geochemistry indicates a high Al content in all pedogenic materials, consistent with extensive *in situ*

weathering. The abundance of calcrete nodules, suggests a semi-arid climate during the time of sedimentation. Calcrete morphologies include ferroan calcite, cryptic plasmic pea material, siltstone aggregates, fragmentary nodules and Mn-rich spherulitic siderites. The paleosols are considered to represent ancient aridisols and vertisols.

At least 8 repetitions of sandstones and mudrocks are recognised through the formation, these defining megacycles as much as 170 m thick. Although faulting may account for the megacycles, it is considered more likely that eustasy was the principal cause for their development. Sandstones were largely deposited during periods of relative eustatic fall, whereas the mudrocks formed during transgressive or high stand periods. Observed stratal relationships are counter to existing published models for fluvial deposition in response to relative sea level change, and modifications are presented based on the Boss Point Formation. The existence of glaciations during the Permo-Carboniferous is well established, suggesting a glacio-eustatic control of the observed stratal geometries, the major glaciation occurring during the Early Pennsylvanian, synchronous with Boss Point Formation sedimentation.

ACKNOWLEDGEMENTS

Guy Plint supervised this thesis, and is thanked for his assistance and stimulating ideas, for his reviews of the manuscript, and for introducing me to some of the varied delights of the Maritimes. Happy memories abound. Wayne Nesbitt (Department of Geology, University of Western Ontario) kindly assisted with the chapter on paleosols. Many others contributed interesting discussions regarding Maritime geology. In particular I wish to thank Chris Dewey (Mississippi State University), Martin Gibling (Dalhousie University), the late Brian Rust (University of Ottawa), Laing Fergusson and David Mossman (Mount Allison University), Gary Yeo (Acadia University), Malcolm McLeod (Department of Natural Resources, New Brunswick), John Calder, Howard Donohoe, Bob Naylor and Bob Ryan (Nova Scotia Department of Mines and Energy). A.D. Smith, Canadian Wildlife Service, Sackville, kindly provided accommodation at Germantown.

Technical assistance was provided by John Forth (thin sections), Charles Wu (XRF) and Dave Kingston (electron microprobe), all of the Department of Geology, University of Western Ontario, and to Ian Craig, Department of Zoology, University of Western Ontario (photography). Sandy Rutherford kindly assisted with computer programming.

The support of Ian Speden, the Director, New Zealand Department of Scientific and Industrial Research Geology and

Geophysics, is greatly appreciated, as is the financial assistance from a DSIR study award. These were difficult times to allow me to take leave and 'abandon' the country for several years. Additional financial support came from a Government of Ontario Scholarship, a University of Western Ontario Graduate Studies Admission Scholarship, and a George Frederic Matthew Research Scholarship from the New Brunswick Museum. These are all greatly appreciated.

The friendship of Maritime people will long be remembered. In particular I would wish to thank Anne-Marie Plint and the Burzynski family of Moncton; to Tony and Brenda for so much that they have done for us. Earl Bourgeois of Joggins provided a lending hand when it was needed most and Mary Evans of Sackville arranged for accommodation at Upper Rockport.

This thesis could not have been accomplished without the endless hospitality of Jack and the late Kay Till of Rockport, who assisted with so many things and made us feel a part of their happy family. Sadly Kay did not live to see this product. You were such an inspiration to all.

My parents are thanked for encouragement and support.

Finally, I wish to thank Viv for patiently accepting such a change to our lifestyle, for forfeiting so much in order that this thesis be completed, and to Chris for putting up with weekends without Dad for so long.

TABLE OF CONTENTS

VOLUME I

	Page
CERTIFICATE OF EXAMINATION.....	ii
ABSTRACT	iii
ACKNOWLEDGEMENTS	v
TABLE OF CONTENTS	vii
LIST OF TABLES	xiii
LIST OF PHOTOGRAPHIC PLATES	xiv
LIST OF FIGURES	xvi
LIST OF APPENDICES	xxiii
CHAPTER 1 - INTRODUCTION	1
1.1 Aim of Study	1
1.2 Presentation of Data	2
1.3 Field Work	7
1.4 Previous Work	8
1.5 Study and Analytical Methods	9
1.6 Economic Geology	11
1.7 Historical Perspective	11
CHAPTER 2 - STRATIGRAPHIC AND DEPOSITIONAL FRAMEWORK	13
2.1 Carboniferous Stratigraphy	14
2.2 Boss Point Formation - Definition	14
2.3 Type Section	25
2.4 Description	26
2.5 Distribution	27
2.6 Thickness	27
2.7 Stratigraphic Relationships	30
2.8 Age	36
2.9 Basin Morphology - The Maritimes Basin	37
2.10 Stratigraphic Patterns within the Cumberland Sub-basin	41
2.10.1 Western Cumberland Sub-basin	51
2.10.2 Eastern Cumberland Sub-basin	52
2.11 Plate Tectonic Considerations	54
2.12 Paleomagnetic Studies	58
CHAPTER 3 - SEDIMENTOLOGY OF COARSE-GRAINED UNITS	60
3.1 Trough Cross-Bedded Gravel	60
3.1.1 Description	60
3.1.2 Interpretation	84
3.2 Planar Cross-Bedded Gravel	87

	3.2.1	Description	87
	3.2.2	Interpretation	89
3.3		Massive Gravel	90
	3.3.1	Description	90
	3.3.2	Interpretation	91
3.4		Breccia	95
	3.4.1	Description	95
	3.4.2	Petrography	95
	3.4.3	Interpretation	96
CHAPTER 4 - SEDIMENTOLOGY OF SANDSTONE UNITS			98
4.1		Trough Cross-Bedded Sandstone	98
	4.1.1	Description	98
	4.1.2	Petrography	108
	4.1.3	Interpretation	114
4.2		Planar Cross-Bedded Sandstone	115
	4.2.1	Description	115
	4.2.2	Interpretation	115
4.3		Current Ripple Cross-Laminated Sandstone	116
	4.3.1	Description	116
	4.3.2	Petrography	120
	4.3.3	Interpretation	120
4.4		Antidunes	121
4.5		Hummocky Cross-Stratification	124
4.6		Horizontally Laminated and Wave Rippled Sandstone	126
	4.6.1	Description	126
	4.6.2	Petrography	127
	4.6.3	Interpretation	130
4.7		Massive Sandstone	130
	4.7.1	Description	130
	4.7.2	Petrography	131
	4.7.3	Interpretation	131
4.8		Pebbly Sandstone	132
	4.8.1	Description	132
	4.8.2	Petrography	134
	4.8.3	Interpretation	138
4.9		Sandstone Dikes	139
4.10		Inclined Heterolithic Stratification (IHS)	139
	4.10.1	Description	139
	4.10.2	Paleochannel Parameters Deduced from IHS	141
	4.10.3	Interpretation	143
CHAPTER 5 - SEDIMENTOLOGY OF FINE-GRAINED UNITS			144
5.1		Massive Mudrock	144
	5.1.1	Description	144
	5.1.2	Petrography and Petrology	150
	5.1.3	Interpretation	151
5.2		Laminated Mudrock	151

5.2.1	Description	151
5.2.2	Petrography and Petrology	204
5.2.3	Interpretation	214
5.3	Siltstone Blocks	217
5.3.1	Description	217
5.3.2	Petrography and Petrology	230
5.3.3	Interpretation	233
5.4	Limestone	237
5.4.1	Description	237
5.4.2	Petrography	238
5.4.3	Paleontology	239
5.4.4	Interpretation	240
5.5	Coal	240
5.5.1	Description	240
5.5.2	Petrography	241
5.5.3	Interpretation	244
 CHAPTER 6 - SEDIMENTOLOGY OF PALEOSOLS		245
6.1	Recognition of Paleosols	247
6.2	Distribution of Soil Profiles	248
6.3	Profile Descriptions	248
6.3.1	Profile Characterisation	248
6.3.2	Sandy Paleosols	256
6.3.3	Silty Paleosols	257
6.4	Petrology and Geochemistry	258
6.4.1	Petrology of Sandy Paleosols	258
6.4.2	Petrology of Silty Paleosols	259
6.4.3	Geochemistry of Sandy and Silty Paleosols	264
6.4.4	Petrography of Calcrete Nodules	290
6.4.5	XRD Analysis of Calcrete Nodules	312
6.4.6	XRF Analysis of Calcrete Nodules	313
6.4.7	What was the Carbonate Source for Calcrete Development?	317
6.5	Soil Taxonomy	318
6.5.1	Aridisols	318
6.5.2	Vertisols	319
6.5.3	Boss Point Formation Paleosol Classification	320
6.6	Paleoclimatic Considerations based on Boss Point Formation Paleosols	323
6.7	Temporal Considerations in Paleosol Development	327
 CHAPTER 7 - VERTICAL FACIES RELATIONSHIPS		332
7.1	Braided River Facies Association	332
7.1.1	Channel-Fill Cycles	334
7.2	Fluvio-lacustrine Facies Association	343
7.2.1	Coarsening-Upward cycles	346
7.2.2	Erosively Based Sandstones	352

7.2.3	Sharp-Based Sandstones	354
7.2.4	Thin-Bedded Sandstones	355
7.2.5	Inclined Heterolithic Stratification Units	356
7.2.6	Hummocky Cross-Stratification Units ...	356
7.3	Recognition of a Large-Scale Stratification Hierarchy - Megacycles	356
CHAPTER 8 - PALEOCURRENT DIRECTIONS		362
8.1	Paleocurrents from Trough Cross- Bedded Sandstones	362
8.1.1	Trough Cross-Bedding	362
8.1.2	Orientation of Logs	370
8.2	Paleocurrents from Planar Cross-Bedded Sandstones	373
8.3	Paleocurrents from Ripple Cross-Laminated Sandstones	374
8.4	Paleocurrents from Parting Lineations in Horizontally Laminated Sandstones	377
 VOLUME II		
CHAPTER 9 - TECTONIC CONSIDERATIONS		383
9.1	Tectonic Deformation in the Boss Point Formation	384
9.1.1	Distribution of Coarse-Grained Clastics Adjacent to Faults	384
9.1.2	Regional Trends in Deformation	385
9.1.3	Stress Indicators from Conjugate Faults	398
9.1.4	The Harvey-Hopewell Fault Zone	403
9.1.5	The Harvey-Hopewell Fault Zone: Alma	412
9.1.6	The Rogers Head Fault: Giffin Pond	421
9.2	Tectonic Relationships in Older Carboniferous Units	424
9.3	Tectonic Models	431
 CHAPTER 10 - CONTROL ON SEDIMENTATION		435
10.1	Dam Mechanisms	436
10.2	Channel Avulsion	437
10.3	Changes in Weather	437
10.4	Changes in Climate and/or Vegetation	438
10.5	Tectonic Effects	438
10.6	Eustatic Effects	442
10.6.1	Sequence Stratigraphy in a Fluvial Setting - Theory	444

10.6.2	A Process-Response Model Based on the Boss Point Formation : Observed Versus Predicted Relationships	450
10.7	What were the Causes of Eustasy?	457
10.7.1	Causes of Glacial Cycles	460
10.7.2	Duration of Boss Point Formation Megacycles	463
CHAPTER 11 - SUMMARY OF CONCLUSIONS		466
APPENDIX I.	LITHOFACIES THICKNESSES AND STATISTICAL PARAMETERS	473
APPENDIX II.	MEASUREMENT OF PALEOCURRENT DIRECTIONS BY THE CARPENTER'S RULE METHOD	493
APPENDIX III.	PETROGRAPHY OF BOSS POINT FORMATION SANDSTONES	494
APPENDIX IV.	OUTCROP DESCRIPTIONS OF BOSS POINT FORMATION PALEOSOL PROFILES	495
APPENDIX V.	MAJOR OXIDE DATA FOR BOSS POINT FORMATION PALEOSOLS DETERMINED BY XRF ANALYSIS	498
APPENDIX VI.	TRACE ELEMENT DATA FOR BOSS POINT FORMATION PALEOSOLS DETERMINED BY XRF ANALYSIS	500
APPENDIX VII.	ELECTRON MICROPROBE DATA FOR RHIZOLITHS	501
APPENDIX VIII.	ELECTRON MICROPROBE DATA FOR SPHERULITIC SIDERITE NODULES	502
APPENDIX IX.	MINERALOGY OF CLAYS WITHIN AND SURROUNDING SPHERULITIC SIDERITE NODULES	504
APPENDIX X.	ELECTRON MICROPROBE DATA FOR CALCITE INFILLING PORE SPACES	506
APPENDIX XI.	MAJOR ELEMENT DATA FOR CALCRETE NODULES DETERMINED BY XRF ANALYSIS	507
APPENDIX XII.	TRACE ELEMENT DATA FOR A REPRESENTATIVE CALCRETE NODULE DETERMINED BY XRF ANALYSIS	508

SUPPLEMENTARY APPENDIX	DETAILED STRATIGRAPHIC COLUMNS USED IN THIS STUDY (Microfiche)	509
REFERENCES		512
VITA		550

LIST OF TABLES

Table	Description	Page
1	Summary of the geology of the Carboniferous sub-basins of the Maritimes Basin	40
2	Ostracod fauna from Boss Point Formation limestone	239

LIST OF PHOTOGRAPHIC PLATES

VOLUME I

Plate	Description	Page
1	Contact between Boss Point Formation and Cumberland Group	24
2	Conglomerate lithofacies from the Boss Point Formation	69
3	Relationship between gravel lithofacies	71
4	Conglomerate and breccia lithofacies from the Boss Point Formation	93
5	Sandstone lithofacies from the Boss Point Formation	101
6	Sandstone lithofacies from the Boss Point Formation	104
7	Sandstone lithofacies from the Boss Point Formation	107
8	Sandstone lithofacies from the Boss Point Formation	119
9	Sandstone lithofacies from the Boss Point Formation	123
10	Sandstone lithofacies from the Boss Point Formation	129
11	Mudrock lithofacies from the Boss Point Formation	147
12	Alternating blue-grey and deep red coloured siltstone beds	149
13	Sandstone structures within mudrock lithofacies	166
14	Sandstone structures within mudrock lithofacies	178
15	Mudrock and limestone lithofacies	225

16	Field relationships of sandy and silty paleosols from the Boss Point Formation	253
17	Field relationships of silty paleosols from the Boss Point Formation	255
18	Petrographic features of sandy paleosols and calcrete nodules from the Boss Point Formation	261
19	Petrographic features of rhizolith and calcrete morphologies from the Boss Point Formation	296
20	Petrographic features of calcretes from the Boss Point Formation	299
21	Petrographic features of calcretes from the Boss Point Formation	303

VOLUME II

22	The shear zone at Owls Head north of Alma, and petrographic features of the Shepody and Maringouin Formations	414
----	---	-----

LIST OF FIGURES

VOLUME I

Figure	Description	Page
1.1	Generalised geological map of eastern Canada	4
1.2	Location of stratigraphic sections used in this study	6
2.1	Devonian-Carboniferous stratigraphic nomenclature for the study area	16
2.2	Devonian-Carboniferous stratigraphic correlation chart for New Brunswick and Nova Scotia	18
2.3	Summary stratigraphic column for the type section of the Boss Point Formation	22
2.4	Tectono-stratigraphic map for Maritime Canada and the northeastern New England States	29
2.5	Basal contacts of the Boss Point Formation	32
2.6	Upper contacts of the Boss Point Formation	35
2.7	Magnetic anomaly map of the study area	43
2.8	Bouguer anomaly map of the study area	45
2.9	Cross-section through the NW-sector of the Cumberland sub-basin	47
2.10	Palinspastic lithospheric plate reconstruction for the Paleozoic	50
2.11	Cartoon depicting the accretion of lithospheric plates during the Paleozoic	57
3.1	Proportions of lithofacies in the Boss Point Formation	62
3.2	Proportions of lithofacies in the Boss Point Formation	65
3.3	Outcrop sketch of cliff face at Hillsborough ...	67

3.4	Triangular diagrams of sphericity-form in trough cross-bedded gravels	74
3.5	Percentage of each sphericity-form class in trough cross-bedded gravels	76
3.6	Discrimination plot of river and beach gravels	79
3.7	Percentage of clast compositions from trough cross-bedded gravels	81
3.8	Paleocurrent directions for Boss Point gravels and sandstones at Hillsborough	86
4.1	Outcrop sketch of cliff face at Alma	110
4.2	Quartz-Feldspar-Lithic triangular plot for Boss Point Formation trough cross-bedded sandstones	113
4.3	Petrography of the pebbly sandstone lithofacies	136
5.1	Representative clay mineralogies determined by XRD	153
5.2	Geological map of Cape Enrage to Bray Beach ...	157
5.3	Composite stratigraphic column for the sequence at Cape Enrage	159
5.4	Geological map of Bays 1 to 6, Cape Enrage ...	161
5.5	Stratigraphic columns for Bays 1 to 6, Cape Enrage	163
5.6	Sketch of the lower siltstone (Unit II) in Bay 3S, Cape Enrage	168
5.7	Sketch of lower siltstone (Unit II) in Bay 3N, Cape Enrage	170
5.8	Plan view maps of bays in the central part of the Cape Enrage section	172
5.9	Paleocurrent directions for the upper siltstone at Cape Enrage	175
5.10	Map of Bay 1N, Cape Enrage	180
5.11	Sketch of upper siltstone (Unit IV) at Bay 2S (Unit IV), Cape Enrage	182

5.12	Sketch of upper siltstone (Unit IV) at Bay 2N, Cape Enrage	184
5.13	Sketch of upper siltstone (Unit IV) at Bay 4S, Cape Enrage	186
5.14	Sketch of upper siltstone (Unit IV) at Bay 4N, Cape Enrage	188
5.15	Sketch of upper siltstone (Unit IV) at Bay 6S, Cape Enrage	190
5.16	Sketch of Bay 6N, Cape Enrage	193
5.17	Orientations of flutes at the base of Unit V, Cape Enrage	195
5.18	Paleocurrent observations for Unit I, Cape Enrage	197
5.19	Paleocurrent observations for Unit III, Cape Enrage	199
5.20	Paleocurrent observations for Unit VI, Cape Enrage	201
5.21	Paleocurrent observations for Unit V, Cape Enrage	203
5.22	Paleocurrent observations for Unit I, Cape Enrage	206
5.23	Paleocurrent observations for Unit III, Cape Enrage	208
5.24	Paleocurrent observations for Unit V, Cape Enrage	210
5.25	Paleocurrent observations for Unit VI, Cape Enrage	212
5.26	Locality map of the Slacks Cove siltstone interval	219
5.27	Geological map of the interval at Slacks Cove East with siltstone blocks	221
5.28	Geological map of the interval at Slacks Cove West with siltstone blocks	223
5.29	Siltstone blocks at Boss Point	227
5.30	Plan view of base of sandstone at Slacks Cove East	232

5.31	Models for the development of the siltstone blocks at Slacks Cove East	236
5.32	Stratigraphic log of coal measures at Slacks Cove West	243
6.1	Geographic and stratigraphic distribution of paleosols in the Boss Point Formation	250
6.2	XRD plots for 2 representative sandy paleosols	263
6.3	XRD plots for 2 representative silty paleosols	266
6.4	Variation in elemental geochemistry through the Cape Enrage sandy and silty paleosols	268
6.5	Variation in elemental geochemistry through the Dorchester sandy paleosol	270
6.6	Variation in elemental geochemistry through the Dorchester and Cape Enrage paleosols, normalised to TiO_2	273
6.7	Variation in elemental geochemistry through the Alma silty paleosol	275
6.8	Variation in elemental geochemistry through the Alma silty paleosol normalised to TiO_2	278
6.9	Variation in Rb, Sr and Ba through the Dorchester and Cape Enrage paleosols	283
6.10	Variation in Cu, Ni and Zn through the Dorchester and Cape Enrage paleosols	283
6.11	Variation in Pb and Ga through the Dorchester and Cape Enrage paleosols	286
6.12	Variation in Nb, Zr and Y through the Dorchester and Cape Enrage paleosols	286
6.13	Variation in Co, V and Cr through the Dorchester and Cape Enrage paleosols	289
6.14	Chemical Index of Alteration determinations for Boss Point Formation paleosols	289
6.15	Major morphologic calcrete types recognised from the Boss Point Formation	292

6.16	Ternary CaCO_3 - MgCO_3 - FeCO_3 and CaCO_3 - MgCO_3 - MnCO_3 diagrams from Boss Point Formation spherulitic siderites	305
6.17	XRD plots of 4 representative calcrete nodules from the Boss Point Formation	310
6.18	Major and minor element geochemistry for 5 representative calcrete nodules from the Boss Point Formation	315
6.19	Model for the development of calcrete	330
7.1	Conceptual model for braidplain deposition in the Boss Point Formation	336
7.2	Idealised fining-upward cycle found in the Boss Point Formation	339
7.3	Fining-upward cycles from 3 representative stratigraphic sections in the Boss Point Formation	341
7.4	Conceptual model for the deposition of the fluvio-lacustrine units in the Boss Point Formation	345
7.5	Facies types developed in the fluvio-lacustrine association	348
7.6	Fluvio-lacustrine successions from 6 representative stratigraphic sections in the Boss Point Formation	350
7.7	Stratigraphic correlation diagram showing megacycle development	359
7.8	Stratigraphic correlation diagram showing megacycle development	361
8.1	Paleocurrents determined from trough cross-bedding in the Boss Point Formation	364
8.2	Paleocurrents determined by previous workers from the Boss Point Formation	367
8.3	A paleogeographic reconstruction of the western margin of the Cumberland sub-basin	369
8.4	Paleocurrents determined from logs in the Boss Point Formation	372
8.5	Orientation of planar cross-beds in the Boss Point Formation	374

8.6	Paleocurrents determined from ripples in the Boss Point Formation	376
8.7	Miscellaneous paleocurrent determinations from the Boss Point Formation	379
8.8	Paleocurrents determined from parting lineations in the Boss Point Formation	381

VOLUME II

9.1	Summary stratigraphic correlations	387
9.2	Summary stratigraphic correlations	389
9.3	Paleocurrent directions for megacycle I	391
9.4	Paleocurrent directions for megacycle II	393
9.5	Paleocurrent directions for megacycle III	395
9.6	Paleocurrent directions for megacycle IV	397
9.7	Tectonic features from the Boss Point Formation	400
9.8	Regional distribution of conjugate fault couples from the Boss Point Formation	402
9.9	Faults from the Boss Point Formation	405
9.10	Fault distribution in the Bay of Fundy region	407
9.11	Sketch of the Harvey-Hopewell Fault, Alma	411
9.12	Tectonic features from the Boss Point Formation	416
9.13	Faults from the Harvey-Hopewell Fault	420
9.14	Tectonic features from the Boss Point Formation	423
9.15	Paleocurrent directions from ripple and climbing ripple lamination in the Maringouin Formation	426
9.16	Paleocurrent directions from trough cross-bedding in the Shepody Formation	428

9.17	Paleocurrent directions from trough cross-bedding in the Claremont Formation	430
10.1	Alluvial sedimentation patterns following initiation of a fault scarp	441
10.2	Response of sedimentation on a depositional profile to a eustatic cycle	447
10.3	Elements of the coastal onlap curve	449
10.4	Cartoon showing the relationship between falling sea level and accommodation	452
10.5	Summary of depositional facies in relation to eustasy	452
10.6	Summary of the deposition of the Boss Point Formation in relation to eustatic change	455
10.7	The stratal relationships of the Boss Point Formation megacycles in relation to eustatic change	459
10.8	Coastal onlap curve for Carboniferous and Permian shelf sediments	462

LIST OF APPENDICES

Appendix	Page
APPENDIX I	Lithofacies thicknesses and statistical parameters473
APPENDIX II	Measurement of paleocurrent directions by the carpenter's rule method493
APPENDIX III	Petrography of Boss Point Formation sandstones494
APPENDIX IV	Outcrop descriptions of Boss Point Formation paleosol profiles495
APPENDIX V	Major oxide data for Boss Point Formation paleosols determined by XRF analysis498
APPENDIX VI	Trace element data for Boss Point Formation paleosols determined by XRF analysis500
APPENDIX VII	Electron microprobe data for rhizoliths ..501
APPENDIX VIII	Electron microprobe data for spherulitic siderite nodules502
APPENDIX IX	Mineralogy of clays within and surrounding spherulitic siderite nodules504
APPENDIX X	Electron microprobe data for calcite infilling pore spaces506
APPENDIX XI	Major element data for calcrete nodules determined by XRF analysis507
APPENDIX XII	Trace element data for a representative calcrete nodule determined by XRF analysis508
SUPPLEMENTARY APPENDIX	Detailed stratigraphic columns used in this study (microfiche)509

The author of this thesis has granted The University of Western Ontario a non-exclusive license to reproduce and distribute copies of this thesis to users of Western Libraries. Copyright remains with the author.

Electronic theses and dissertations available in The University of Western Ontario's institutional repository (Scholarship@Western) are solely for the purpose of private study and research. They may not be copied or reproduced, except as permitted by copyright laws, without written authority of the copyright owner. Any commercial use or publication is strictly prohibited.

The original copyright license attesting to these terms and signed by the author of this thesis may be found in the original print version of the thesis, held by Western Libraries.

The thesis approval page signed by the examining committee may also be found in the original print version of the thesis held in Western Libraries.

Please contact Western Libraries for further information:

E-mail: libadmin@uwo.ca

Telephone: (519) 661-2111 Ext. 84796

Web site: <http://www.lib.uwo.ca/>

CHAPTER 1

INTRODUCTION

The Paleozoic of eastern North America contains a diverse range of lithologies that record 3 orogenies which span Ordovician to Carboniferous time. During this period a number of crustal blocks or terranes were accreted to the North American craton.

Between and during each orogeny, thick sedimentary sequences were deposited. This study examines sediments deposited between the Acadian (Middle Devonian) and Alleghenian (Late Carboniferous) orogenies, rocks which are predominantly continental in origin. The Alleghenian Orogeny (spelling after Lyons 1988), was the last orogeny to affect eastern North America.

1.1 Aim of Study

The purpose of this thesis is to document in detail, the stratigraphy and sedimentology of the Boss Point Formation, an Early Pennsylvanian (Westphalian A) sand-dominated fluvial and lacustrine unit deposited within the Maritimes Basin. The study attempts to elucidate the regional stratigraphy, sedimentary history, facies relationships, and depositional mechanisms which operated

during Boss Point Formation times, and to assess the influence allocyclic factors such as tectonics and relative sea level changes had on sedimentation.

The study area includes eastern New Brunswick in the vicinity of the Bay of Fundy coast, and northern Nova Scotia (Figs. 1.1 & 1.2).

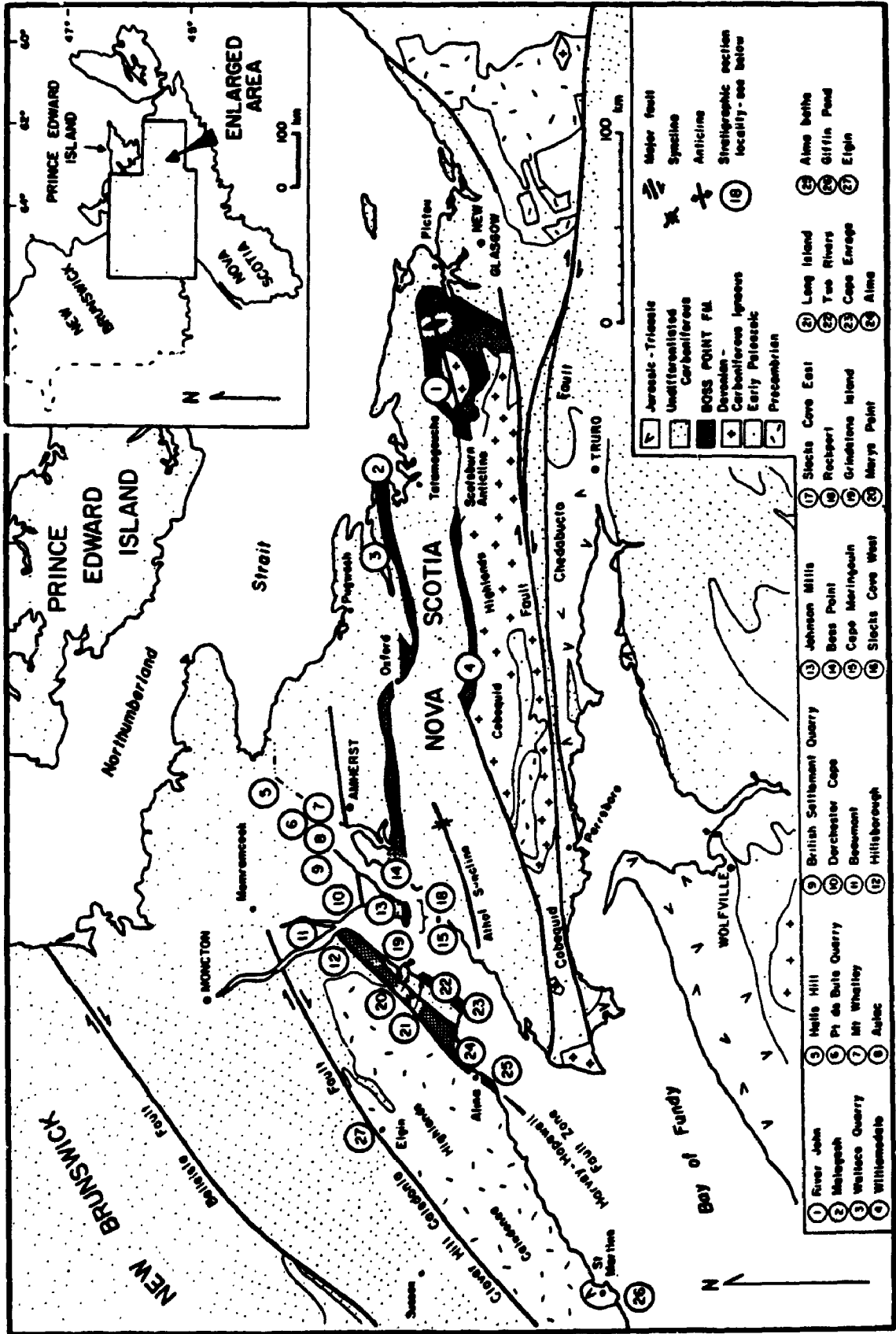
1.2 Presentation of Data

Volume I contains Chapters 1 to 8 of this thesis; Volume II includes Chapters 9 to 11, appendices, and a collection of stratigraphic sections and geological maps. They are referred to in the text as Map 1 etc, and as Stratigraphic Section 18 etc. Full lithological descriptions accompany the stratigraphic columns presented on microfiche (Supplementary Appendix, Volume II), hard copies of which can be obtained on request from Professor Guy Plint, University of Western Ontario.

The lithofacies code used in the text (such as Gt, St, Sr, Fm etc) follows in part the designations of Miall (1978) and Rust (1978) for braided river deposits. A full collation of lithofacies thicknesses and statistical parameters for each of the stratigraphic sections is given in Appendix I.

Fig. 1.1 **Generalised geological map of eastern Canada.**
Inset A indicates the distribution of the
Maritimes Basin.

Fig. 1.2 **Location of stratigraphic sections used in
this study.**



- ▢ Jureale - Triassic
- ▢ Un differentiated Carboniferous
- ▢ BOSS POINT F.M.
- ▢ Devonian Carboniferous Igneous
- ▢ Early Paleozoic
- ▢ Precambrian
- ▬ Major fault
- ▬ Syncline
- ▬ Anticline
- ⊕ Stratigraphic section locality - see below
- ⊙ (18)

- ① Ever John
- ② Malagaish
- ③ Wallace Quarry
- ④ Williamsdale
- ⑤ Halls Hill
- ⑥ Pt de Bois Quarry
- ⑦ Mt Whalley
- ⑧ Aulac
- ⑨ British Settlement Quarry
- ⑩ Dorchester Cape
- ⑪ Bees Point
- ⑫ Cape Maringouin
- ⑬ Johnson Mills
- ⑭ Hillborough
- ⑮ Slechts Cove West
- ⑯ Slechts Cove East
- ⑰ Rectoperi
- ⑱ Grindstone Island
- ⑲ Marys Point
- ⑳ Long Island
- ㉑ Tree Rivers
- ㉒ Cape Enrage
- ㉓ Aims
- ㉔ Aims Belts
- ㉕ Giffin Pond
- ㉖ Elgin

1.3 Field Work

A total of 28 weeks was spent in the field, during the summer months of 1987 to 1989. Most work was undertaken on the excellent shore platform exposures along the Bay of Fundy coast, principally between Hillsborough (near Moncton) in the north and St Martins in the south (Fig. 1.2).

The area is well serviced by sealed and metal roads, access to coastal sections being possible only at periods of low tide. The large tidal range in the Bay of Fundy (up to 15 m in the study area) provided well exposed and extensive shore platform exposures for study, though care has to be exercised to avoid being caught by the tides.

The locations of the stratigraphic sections used in this study are indicated in Fig. 1.2. In total, 27 stratigraphic sections were examined, with thicknesses for each ranging from a few metres to over 800 m (Appendix I). The total thickness of Boss Point Formation rocks logged in this study is 8100 m of which some 6000 m is exposed rock. Numerous other outcrops were also visited, but in general exposure at these sites was too poor to warrant stratigraphic logging.

1.4 Previous Work

In recent years considerable advance has been made in our understanding of Pennsylvanian sedimentary units in eastern Canada (for example, Gibling and Rust 1984, Rust *et al.* 1984, Gibling and Rust 1987, Rust *et al.* 1987, Masson and Rust 1990, Rust and Gibling 1990a, 1990b). With regard to the Boss Point Formation, early work concentrated on stratigraphic description and definition, together with descriptions of the flora (Logan 1845, Bell 1914, 1944, Gussow 1953).

The first sedimentological study of the Boss Point Formation was undertaken by Lawson (1962) who showed that the unit was fluvial in origin, and interpreted it as a delta complex fed by streams and rivers flowing from the west, draining into a large river system which drained to the south.

Subsequently, aspects of Boss Point Formation stratigraphy and sedimentology have been described by van de Poll (1966, 1970, 1972a). van de Poll's studies included extensive discussion of paleocurrents, and in large part formed the basis of our understanding of Boss Point Formation deposition prior to the commencement of this work. McLeod and Ruitenberg (1978), McCabe (1979), McLeod (1980), Fralick (1981), Donohoe and Wallace (1982), Graves (1982), Ryan (1984) added stratigraphic and

sedimentologic contributions regarding the Boss Point Formation. Mitchell (1986) undertook a detailed study of carbonate concretions from Slacks Cove, one of the Boss Point Formation localities used in this study, and Flint (1986, 1989) and van de Poll and Patel (1981, 1989 & 1990) described mudstone blocks with fluted and rilled margins from the formation. These and other previous works will be discussed where relevant throughout the text.

1.5 Study and Analytical Methods

Strata were measured in the field with tape measure, and over covered intervals by either a tape measure and compass, or a pace and compass traverse. Paleocurrent measurements from cross-bedding were made by recording the dip and strike of the trough axis for trough cross-bedding or dip and strike of planar cross-bedding, and restoring these about the horizontal by stereographic projection. In similar fashion, paleocurrent determinations from ripple cross-laminated sandstones were recorded and stereographically restored about the horizontal. Linear paleocurrent measurements (for example orientations of logs, flutes, parting lineations etc.) were restored to the horizontal directly in the field using a carpenter's ruler after the method described in Appendix II.

Black and white aerial photographs were taken by the

author over all stratigraphic section localities on the Bay of Fundy coast. Photographs were acquired from a Cessna 172 fixed-wing aeroplane on 31 August 1987 and 11 August 1989, using a f50 mm SLR camera, and 125 plus-X and ASA 1600 TMZ 5054 black and white film. This imagery proved invaluable for geographic location in the field and for feature recognition.

Petrographic study included carbonate (Evamy 1963) and feldspar staining (Houghton 1980) techniques. Geochemical analyses (whole rock and trace element analyses and clay mineralogy) were made by X-ray fluorescence and X-ray diffraction techniques at the Geology Department, University of Western Ontario. Electron microprobe analyses were made on a JOEL JXA-8600 Superprobe, the data reduced on-line using a Tracor Northern computer, and a ZAF data reduction programme at the Department of Geology, University of Western Ontario.

All stereonet presentations are equal area, lower hemisphere projections. Contoured stereonet data were constructed using a computer programme written in turbo-PASCAL (Longiaru et al. 1989), using a counting area of $100/n^2$ diameter after the method of Starkey (1977). As recommended by Longiaru et al. (1989), for data sets with approximately 50 observations, a contour grid size of 10 (1 cm) was used; for data sets with 100+ observations, a grid size of 20 (0.5 cm) was used.

1.6 Economic Geology

Boss Point Formation sandstones have been a historically important source of grindstones since the middle of the nineteenth century (see section 1.7). Other economic resources include high-grade copper (2-10% Cu) found in sandstone and conglomerate beds at the base of the formation at several localities northeast of Dorchester (New Brunswick), and locally in underground workings (McLeod and Ruitenberg 1978). Mineralisation consists of chalcocite with lesser amounts of chalcopyrite, malachite and azurite (Wright 1950). A first generation of these minerals is typically associated with local replacement of wood material before carbonisation; a second generation of chalcocite and malachite occurs as veinlets and nodules replacing organic material (McLeod and Ruitenberg 1978).

1.7 Historical Perspective

The sandstones of the Boss Point Formation have been one of the most important rock types in New Brunswick and Nova Scotia history. Some of the first rocks quarried by Europeans in Canada came from Aulac, New Brunswick, where they were used to build Fort Beauséjour (Fort Cumberland) during 1755 (Schmeisser 1981). Throughout the nineteenth

and earliest twentieth centuries, sandstone from the Boss Point Formation was the single most important source of grindstone and building blocks in Atlantic Canada and New England. Grindstones up to a standard 1.5 m diameter and 20 cm thick (one ton) were extracted from over 100 quarries in Boss Point Formation sandstone, principally about the Bay of Fundy coast, where the remains of grindstone quarries are still evident. Rock was shipped to Minudie, Nova Scotia, where it was graded, and from there, transported throughout Canada and the United States.

Boss Point Formation sandstone was an important source of building stone, fencing post, stone sinks etc. Features such as Parliament Buildings, Ottawa (quarried from Wallace, Nova Scotia), the Dominion Building, Halifax (quarried from Marys Point, New Brunswick), the Confederation Centre, Charlottetown, Prince Edward Island and the streets of central Boston, Massachusetts, have all used sandstone quarried from the Boss Point Formation.

CHAPTER 2

STRATIGRAPHIC AND DEPOSITIONAL FRAMEWORK

The stratigraphic nomenclature of Carboniferous sedimentary units in eastern Canada is much in need of review. What exists is a complicated assortment of group and formation names, defined on either bio-, chrono-, or lithostratigraphic grounds. Group and formation names are extended over hundreds of kilometres between widely separated depocentres, and are used across major strike-slip faults and interplate boundaries, without regard to specifications of the stratigraphic code (see Boehner *et al.* 1986, Ryan *et al.* 1987).

For example, the Riversdale Group, of which the Boss Point Formation is a part, was defined from Riversdale, Nova Scotia (Bell 1944). This locality is south of the Cobequid-Chedabucto Fault, a major terrane boundary fault system with documented Late Carboniferous strike-slip movement (Eisbacher 1967, 1969), yet the name Riversdale is also used to encompass formations north of this terrane boundary (Port Hood, Claremont and Boss Point Formations).

It is beyond the scope of this work to establish a new stratigraphic format, although revision to the definition of the Boss Point Formation is required.

2.1 Carboniferous Stratigraphy

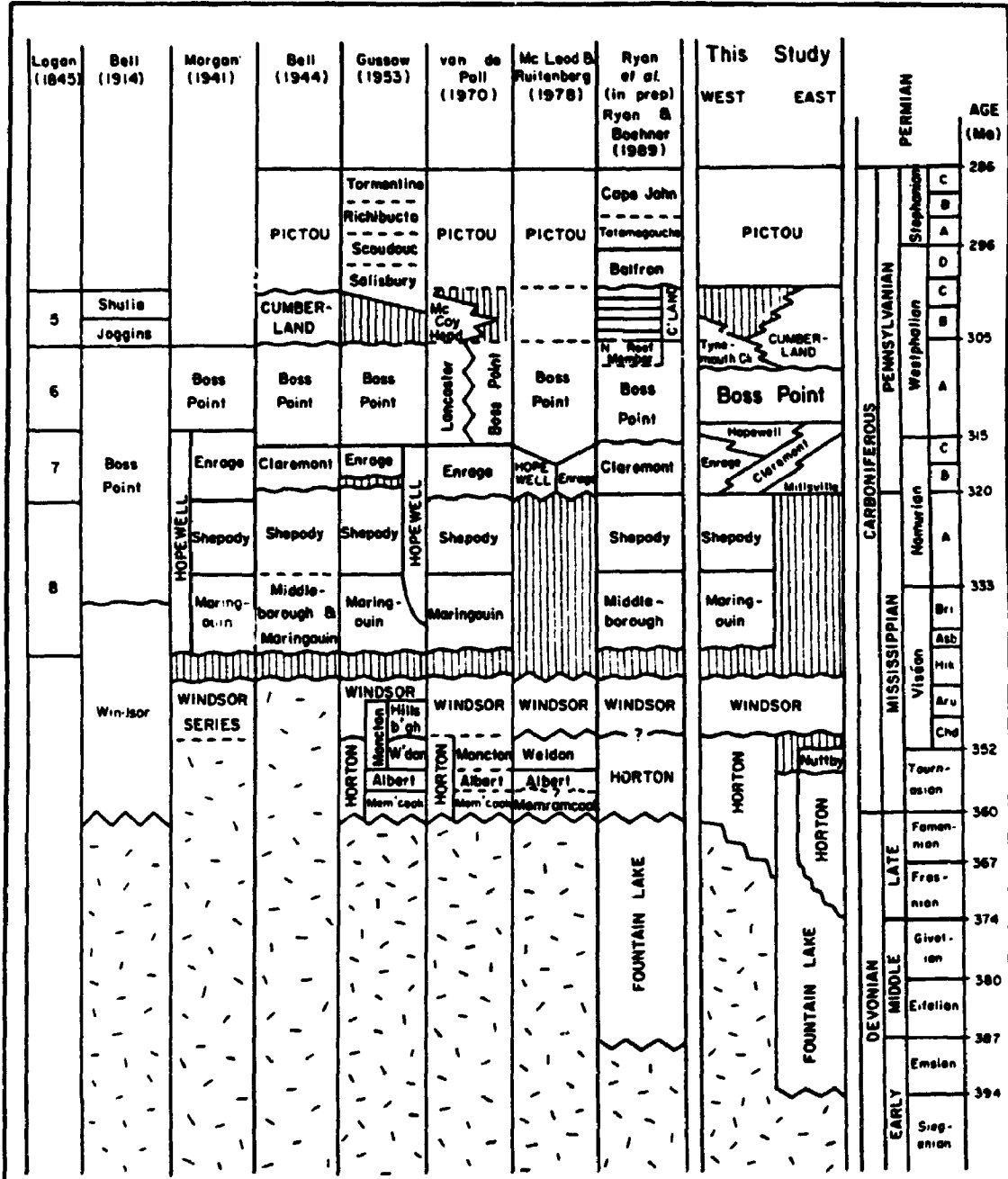
The Carboniferous stratigraphy for the study area is summarised in Figs. 2.1 & 2.2. It is not the intention here to discuss all of these units. Specific aspects of this stratigraphy will be discussed where necessary. A review of the stratigraphic nomenclature can be found in Gussow (1953), van de Poll (1970), Howie and Barss (1975a), and Boehner *et al.* (1986).

2.2 Boss Point Formation - Definition

Logan (1845) was the first to describe the Carboniferous rocks of the study area, and included in his measurement of 4442 m of strata exposed along the Bay of Fundy coast, rocks now assigned to the Boss Point Formation (Fig. 2.1). Logan recognised 7 lithologic groupings (Divisions 1 to 7), but did not formally assign lithostratigraphic names. Dawson (1868), Ells (1885) and Fletcher (1892) all referred to Boss Point Formation strata as the Millstone Grit Formation, because of its similarity to that British formation, though noting that such terminology was "not in all cases lithologically appropriate" (Dawson, 1868, p. 130).

The term 'Boss Point' was first applied by Bell (1914)

Fig. 2.1 Devonian-Carboniferous stratigraphic nomenclature for the study area; previous workers and the nomenclature used in this thesis.



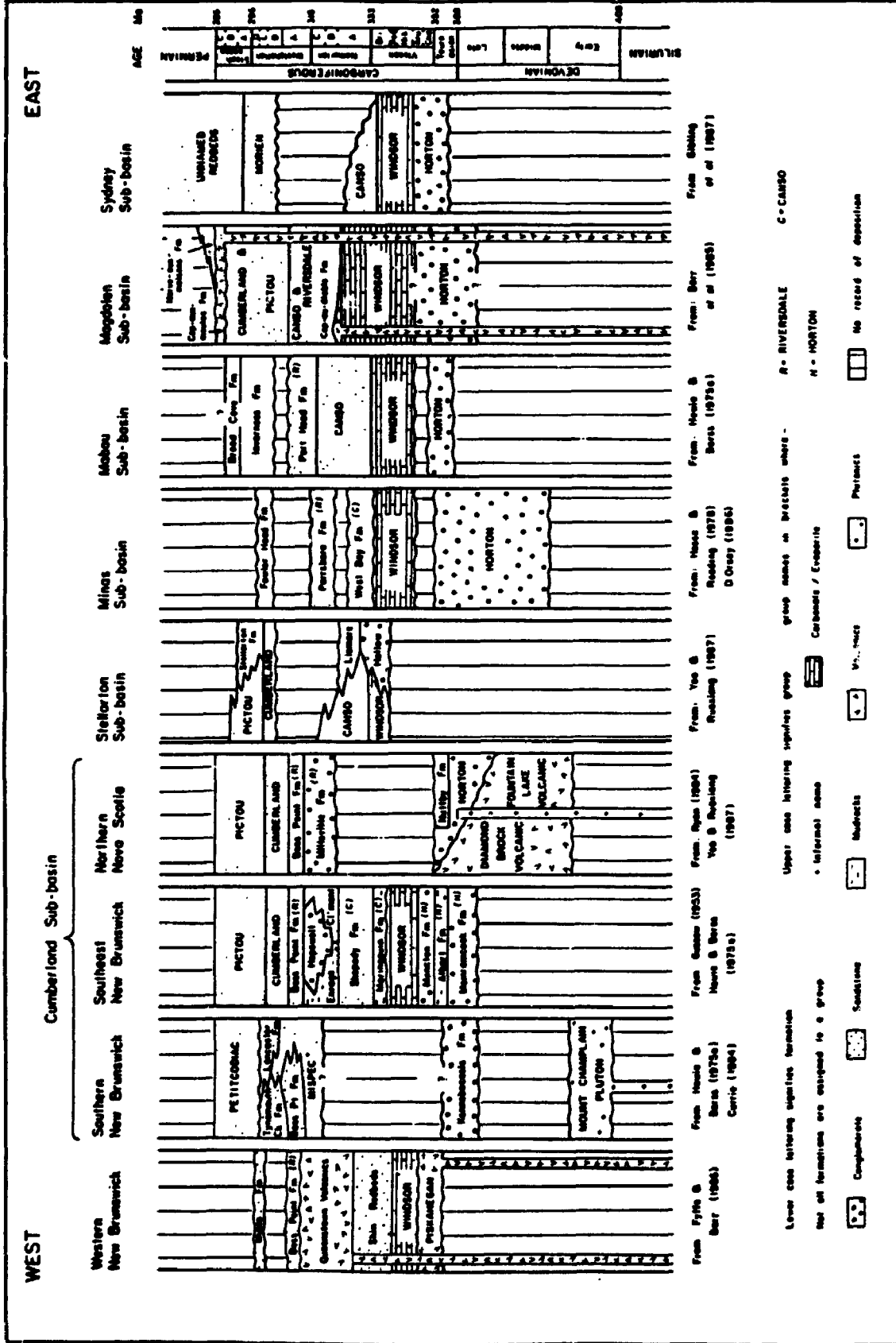
- Precambrian Paleozoic basement
- Angular unconformity
- Disconformity
- Relationship of contact uncertain
- No record of deposition

Lower case lettering signifies formation
 Upper case lettering signifies group
 (unless otherwise stated)

5 formations recognised within
 Cumberland Group being
 Malagash (Top)
 Ragged Reef
 Springhill
 Joggins
 Pelly Brook (Base)

Absolute ages from Harland et al 1962

Fig. 2.2 Devonian-Carboniferous stratigraphic correlation chart for New Brunswick and Nova Scotia.



who defined the formation as "conglomerate, grey sandstone, and shale . . . of Pennsylvanian age, of fresh-water origin, and containing plant remains and thin coal seams" (*op cit.* p. 364), equivalent to Logan's Divisions 7 (198 m thick) and Division 6 (988 m thick).

Norman (1941) revised the Boss Point Formation by excluding the lower unit (Division 7) of Logan (1845), comprising principally quartz pebble conglomerate, red sandstone and shale (Fig. 2.1). Norman placed these units into his Enrage Formation. Further revision was made by Bell (1944), who redefined the base of the Boss Point Formation (Fig. 2.1) to include the uppermost 86 m of Logan's Division 7 (*op cit.* p. 15). The lower part of Logan's Division 7 was placed in the Claremont Formation (Fig. 2.1).

Further revision of the Boss Point Formation is made here. Both the upper and lower contacts are redefined. Bell's (1944) basal contact of the formation occurs between a red sandstone and conglomerate and a concealed interval (probably red shale), 86 m below the top of Logan's Division 7 unit (Fig. 2.1). Lithologies above and below this interval comprise red shale and sandstone in the main, together with conglomerate, the latter becoming more common toward the base. All of Logan's Division 7 is here placed in the Claremont Formation, and its laterally correlative formations, the Enrage and Hopewell Formations to the west,

and the Millsville formation to the east (Figs. 2.1 & 2.2).

The upper contact of the Boss Point Formation was placed at the boundary between Division 5 and Division 6 of Logan's stratigraphy by previous workers. This locality is South Reef, in the central part of Lower Cove at Seaman's Grindstone Quarry (Fig. 2.3). The lithologies through this interval are characterised by red, usually calcareous siltstones, with comparatively minor grey coloured, typically calcareous sandstones (Fig. 2.3). Ryan and Boehner (1989) recognised that the units immediately north of Seaman's Quarry were different from the remainder of the Boss Point Formation, and named them the North Reef member of their Boss Point Formation. However, these rocks are quite distinct from the thick, typically noncalcareous stacked sandstone sequences that dominate Boss Point Formation lithologies below and are more like the overlying Cumberland Group. For these reasons the top of the Boss Point Formation is now placed 174 m stratigraphically below the designation of Bell (1944), approximately 400 m north of Seaman's Quarry, at the base of a prominent 3.4 m thick inclined heterolithic stratification (lateral accretion sandstone) package (Fig. 2.3 & Plate 1).

It should also be noted that several previous authors (without definition) have placed upper and lower boundaries of the Boss Point Formation at different intervals. For example, Graves (1982, fig. 17) placed the base of the Boss

Fig. 2.3 Summary stratigraphic column for the type section of the Boss Point Formation, at Boss Point, Nova Scotia. Seaman's Quarry (South Reef) has previously been taken to be the top of the Formation. This designation is modified; the top is now taken to be approximately 400 m north of the quarry.

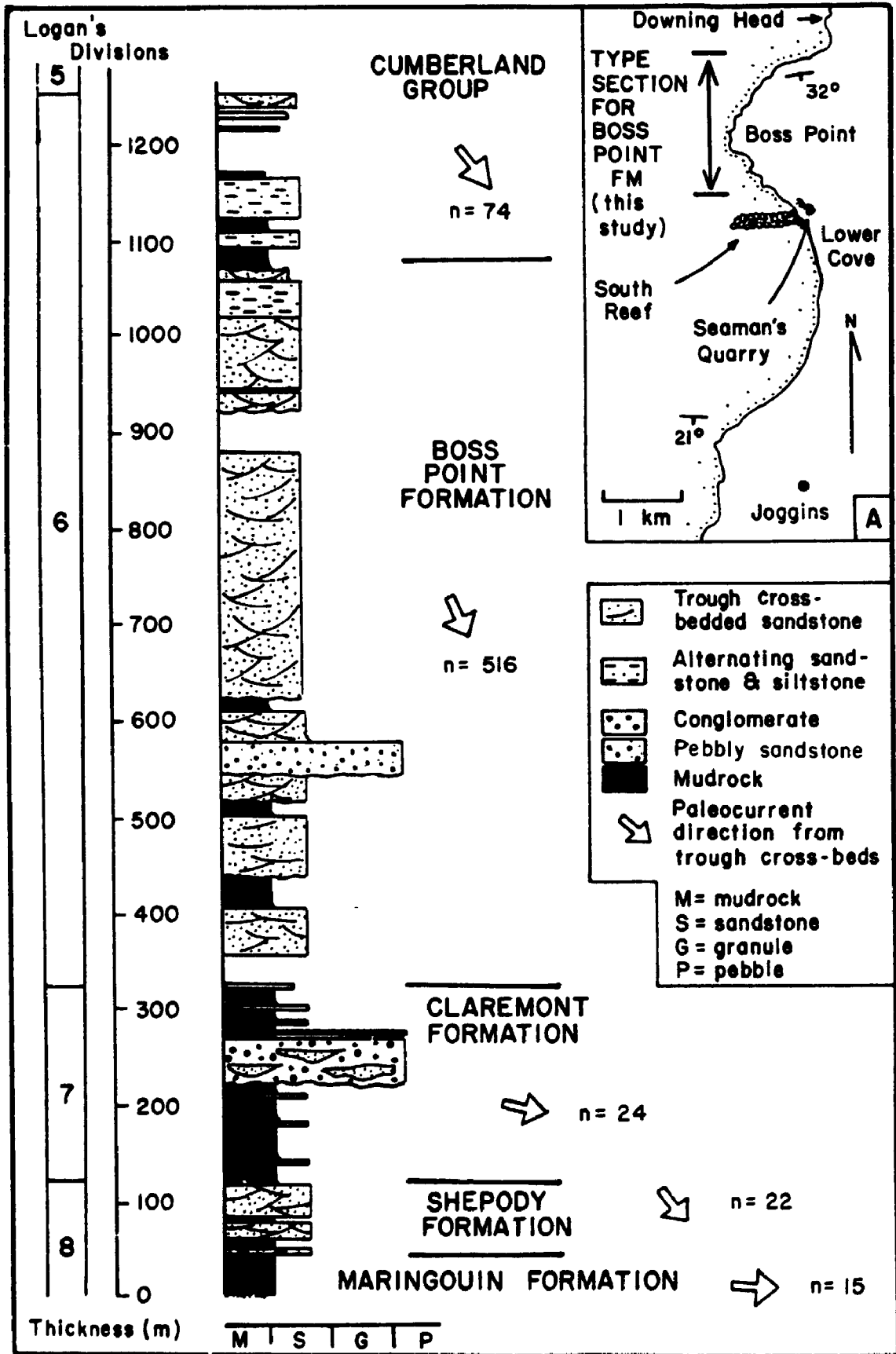
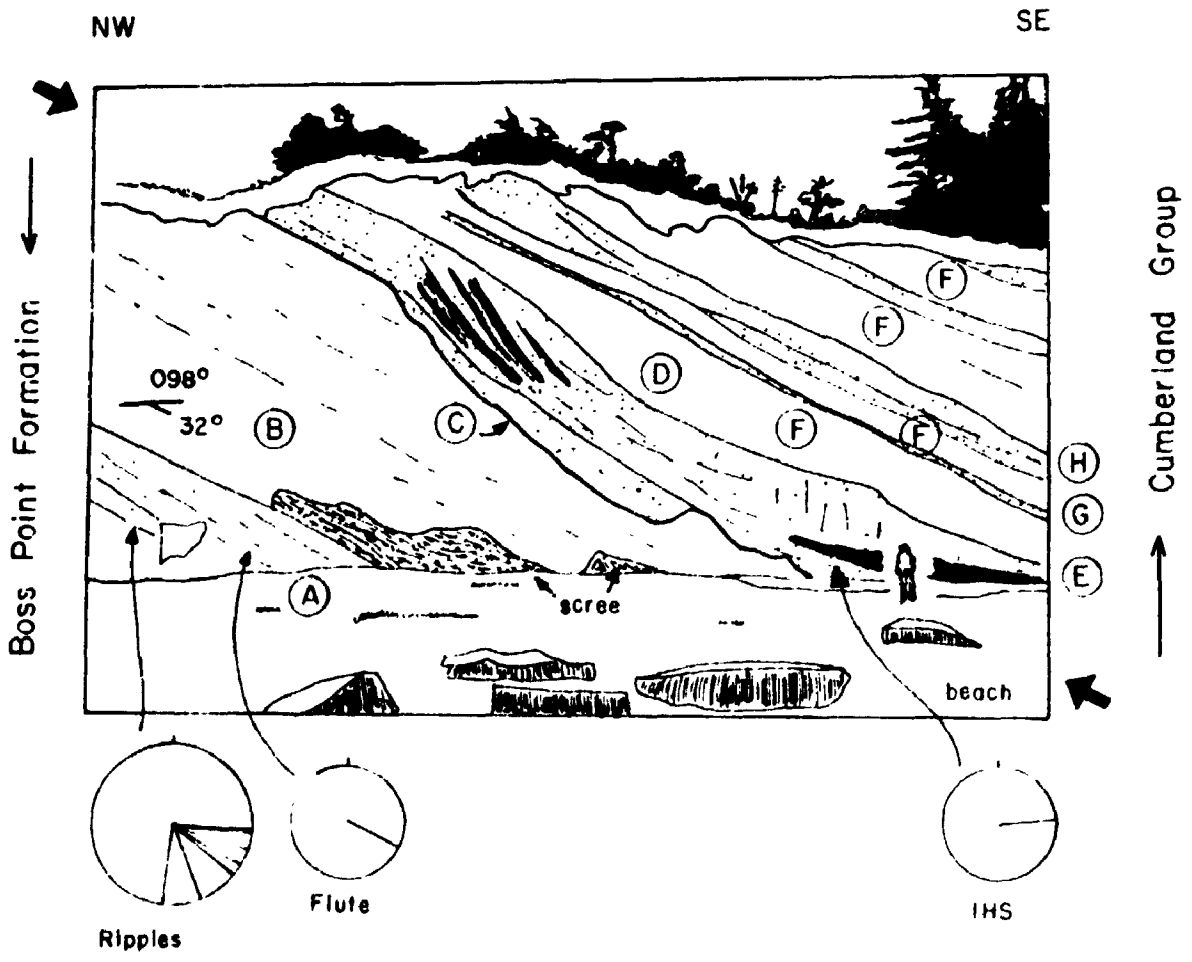


Plate 1

Contact between the Boss Point Formation and the Cumberland Group, approximately 400 m north of Seaman's Quarry, Boss Point, Nova Scotia. A- light grey-green ripple and parallel laminated sandstone; B- green-grey to reddish, noncalcareous and calcareous siltstone; C- green-grey and red, inclined heterolithic stratification (lateral accretion) unit with erosive base; D- reddish grey, fine sandstone and interbedded green-grey and red sandy siltstone inclined heterolithic stratification unit; E- green-grey and red sandy siltstone; F- red, noncalcareous sandy siltstone; G- light green-grey, noncalcareous, fine to very fine trough cross-bedded sandstone; H- decimetre-bedded sandstone as in (G), alternating with decimetre- and centimetre-bedded siltstone as in (F).



Point Formation at Cape Maringouin at the southern end of a small bay (informally known as Ferris Cove), 34 m above the base of the formation as recognised in this study. L. Ferguson and M.R. Gibling (in Donohoe and Grantham 1989) indicate in map form, that the top of the Boss Point Formation occurs at the northern end of Lower Cove, considerably lower stratigraphically than Bell's (1944) definition, and 90 m stratigraphically above the top of the formation as defined in this study.

Several workers have recognised members within the Boss Point Formation. At Dorchester Cape, McLeod and Ruitenberg (1978) divided the formation into 4 units (a to d), and correlated these divisions elsewhere in their study area. These lithostratigraphic subdivisions are not supported by the present study.

2.3 Type Section

No stratigraphic section exposes both the top and basal contacts of the formation. The type locality description given by McCutcheon and Calder (1985, p. 40) is revised in accordance with the new definition given above. The type section is defined from the eastern shore of the Bay of Fundy (Nova Scotia) from the southern end of Boss Cove, south to the northern end of the first small bay north of Lower Cove (Fig. 2.3). At the type locality, the formation

is approximately 750 m thick; the basal contact with the underlying Claremont Formation is not exposed. The upper contact is marked by a local disconformity with the overlying Cumberland Group. Reference sections were suggested as Cape Maringouin (stratigraphic section 15), Big Cape (Hillsborough; stratigraphic section 12), and Dorchester Cape (stratigraphic section 10) by McCutcheon and Calder (1985).

2.4 Description

The Boss Point Formation is dominated by light to medium green-grey, trough cross-bedded sandstone, with less abundant light to medium blue-grey and green-grey parallel, ripple cross-laminated and climbing ripple-laminated sandstone, conglomerate, and pebbly sandstone. These units form stacked sandstone sequences over 100 m thick. They are intercalated with finer-grained medium to dark blue-grey, and reddish siltstone, sandstone, thin coaly shale, coal, paleosols and limestone beds. Carbonaceous matter, ranging from comminuted debris to large logs, and *in situ* tree-stumps, is common at all localities. These lithofacies associations are described in more detail in Chapters 3 to 6.

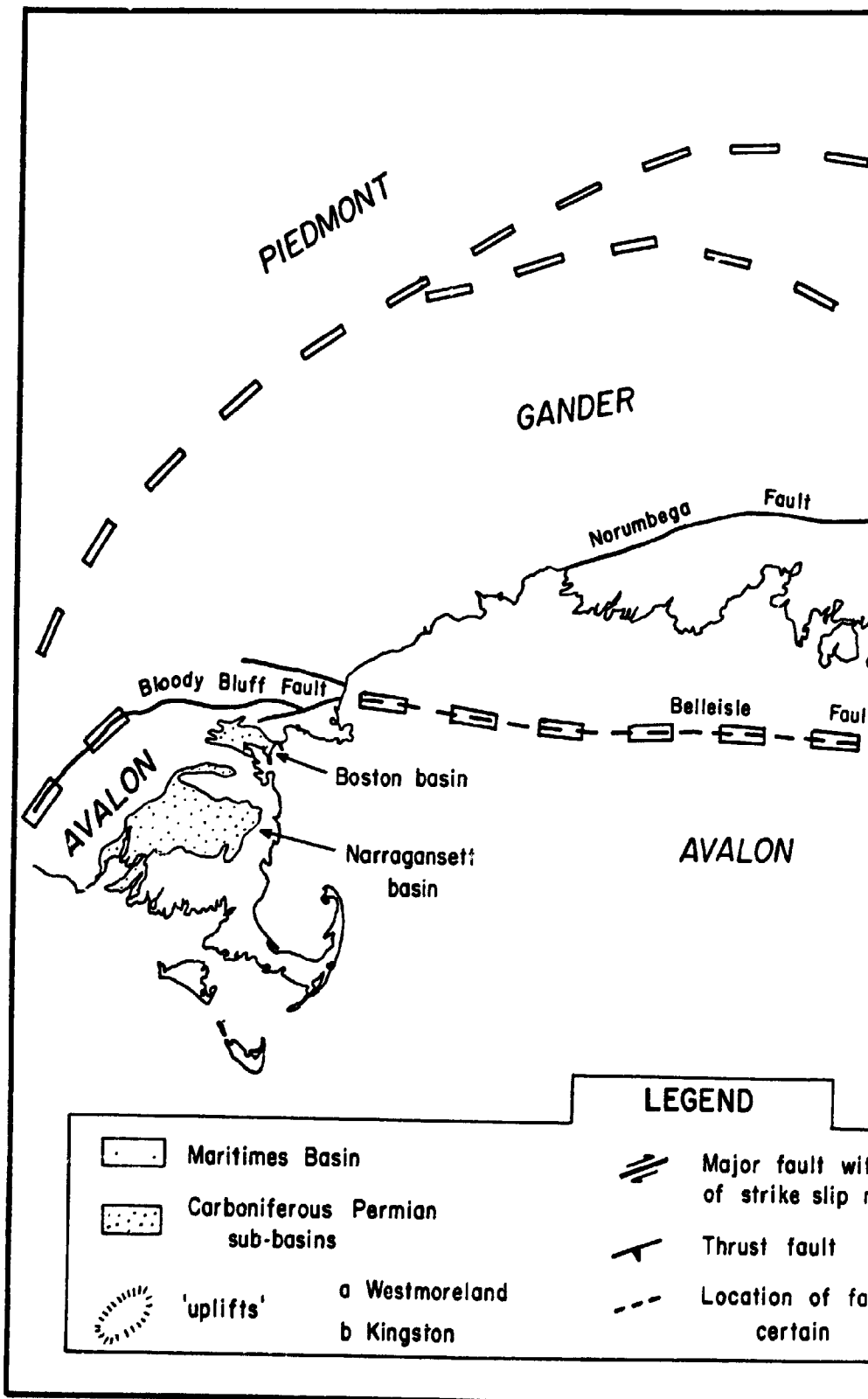
2.5 Distribution

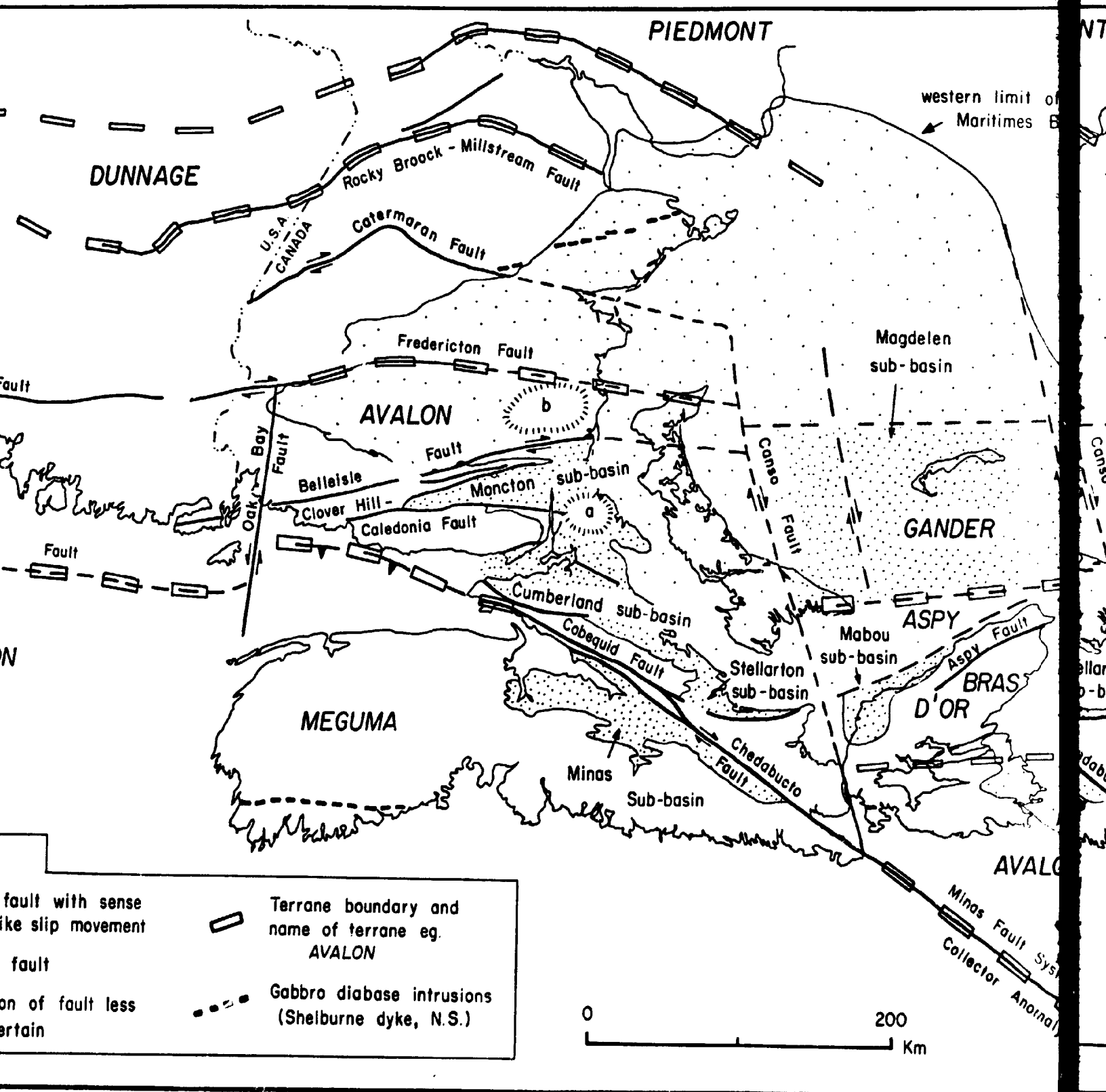
The Boss Point Formation is restricted to the Moncton and Cumberland sub-basins of the Maritimes Basin (Fig. 2.4), and has a present-day distribution from western New Brunswick to central Nova Scotia (Figs. 1.1, 2.4). The best exposures of the formation occur around the Bay of Fundy coast. Less complete sections occur in central Nova Scotia, and along the Northumberland coast. Inferior exposures correlated with the Boss Point Formation occur in central New Brunswick (Ball et al. 1981), and many of these were examined during the course of this study.

2.6 Thickness

The maximum recorded thickness of the Boss Point Formation (in this study) occurs at Johnson Mills (861 m; stratigraphic section 13) in the central part of the study area (Fig. 1.1), though this is slightly less than the true thickness at this locality, for the top of the formation is not exposed. The thickness of the Boss Point Formation exceeds 500 m at Dorchester Cape (810 m; stratigraphic section 10), Boss Point (750 m; stratigraphic section 14), Cape Marigouin (545 m; stratigraphic section 15), Rockport (578 m; stratigraphic section 18) and Marys Point (576 m;

Fig. 2.4 Tectono-stratigraphic map for Maritime Canada and the northeastern New England states, showing terrane boundaries and the distribution of the Maritimes Basin and sub-basins. After Williams (1980), Bradley (1982), Williams and Hatcher (1982), McCutcheon and Robinson (1987), Williams et al. (1988), Barr and Raeside (1989), Loncarevic et al. (1989) and Marillier and Verhoff (1989).





DUNNAGE

PIEDMONT

western limit of
Maritimes B

Rocky Brook - Millstream Fault

Catermaran Fault

U.S.A.
CANADA

Fredericton Fault

AVALON

Magdalen
sub-basin

Belleisle
Fault

Moncton
sub-basin

Canso
Fault

GANDER

Clover Hill -
Caledonia Fault

Cumberland
sub-basin

Mabou
sub-basin

ASPY

Aspy Fault

BRAS
D'OR

MEGUMA

Cobequid
Fault

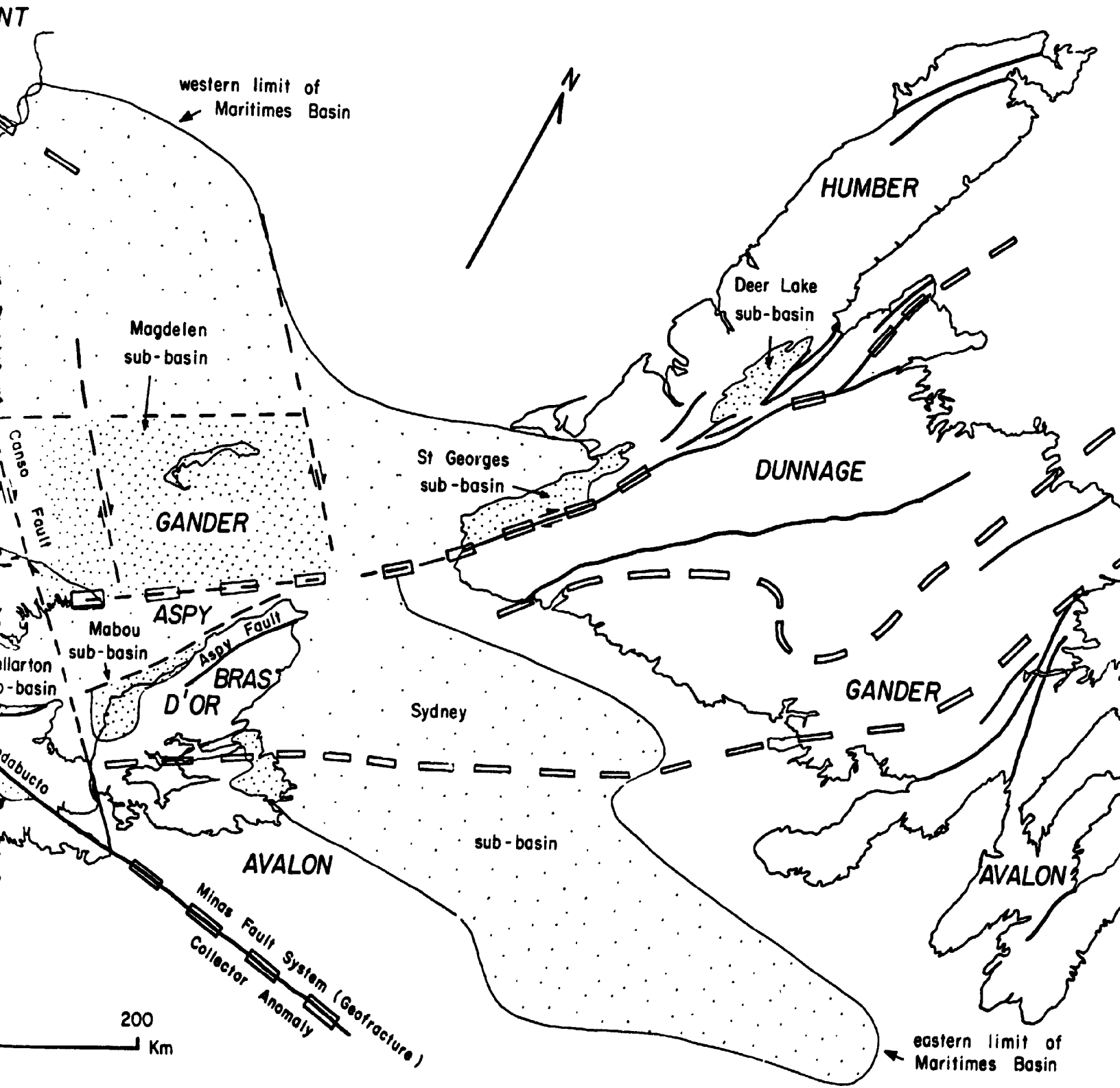
Stellarton
sub-basin

Chedabucto
Fault

Minas
Sub-basin

AVALON

Minas Fault System
Collector Anomaly





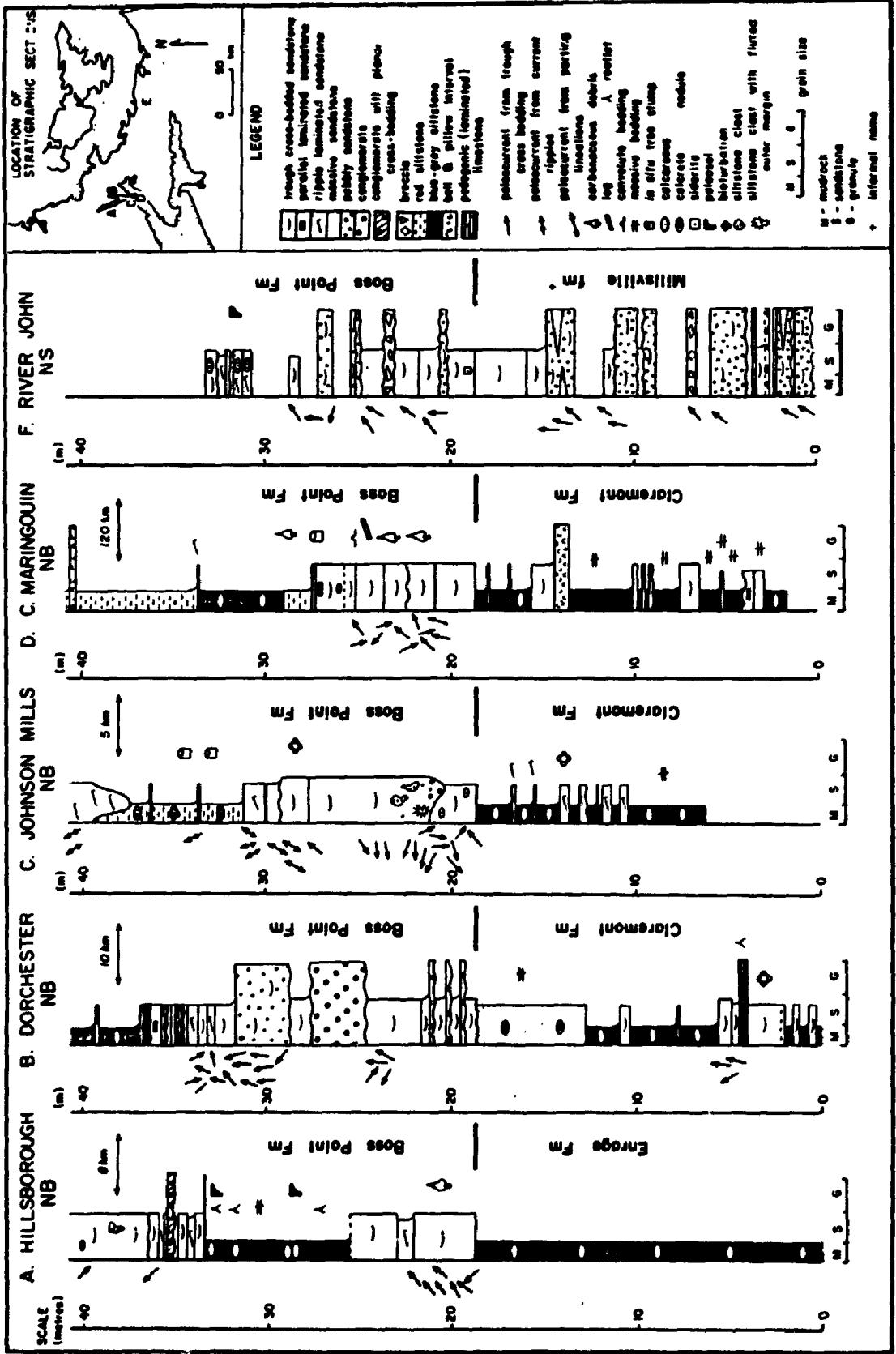
stratigraphic section 20). These thicknesses are considerably less than those reported by previous workers, in the case of the Boss Point locality, because of the revised basal and top definitions. Other workers have recorded a thickness of 1174 m at Boss Point (McCutcheon and Calder 1985). Stratigraphic sections along the west side of the Bay of Fundy expose 200 to 300 m of strata, but the formation thins appreciably in central New Brunswick. In central Nova Scotia, exposures of 100 m occur (though fault bounded), and on the Northumberland coast in northern Nova Scotia, approximately 490 m is exposed (Malagash; stratigraphic section 2).

Drill hole data for the Boss Point Formation in central New Brunswick are summarised by Ball *et al.* (1981, table 9), where up to 350 m are recorded.

2.7 Stratigraphic Relationships

Basal contacts of the Boss Point Formation are shown in Figs. 2.1 & 2.5. At all sections the formation rests conformably on Riversdale and Canso Groups (Enrage, Claremont and Millsville [informal] formations), or unconformably on older Carboniferous and older rocks. At Dorchester the base is marked by slight erosional relief of 20 cm, but beds above and below the contact are conformable (Fig. 2.5). Donohoe and Wallace (1982) indicated a

**Fig. 2.5 Basal contacts of the Boss Point Formation
through the study area.**

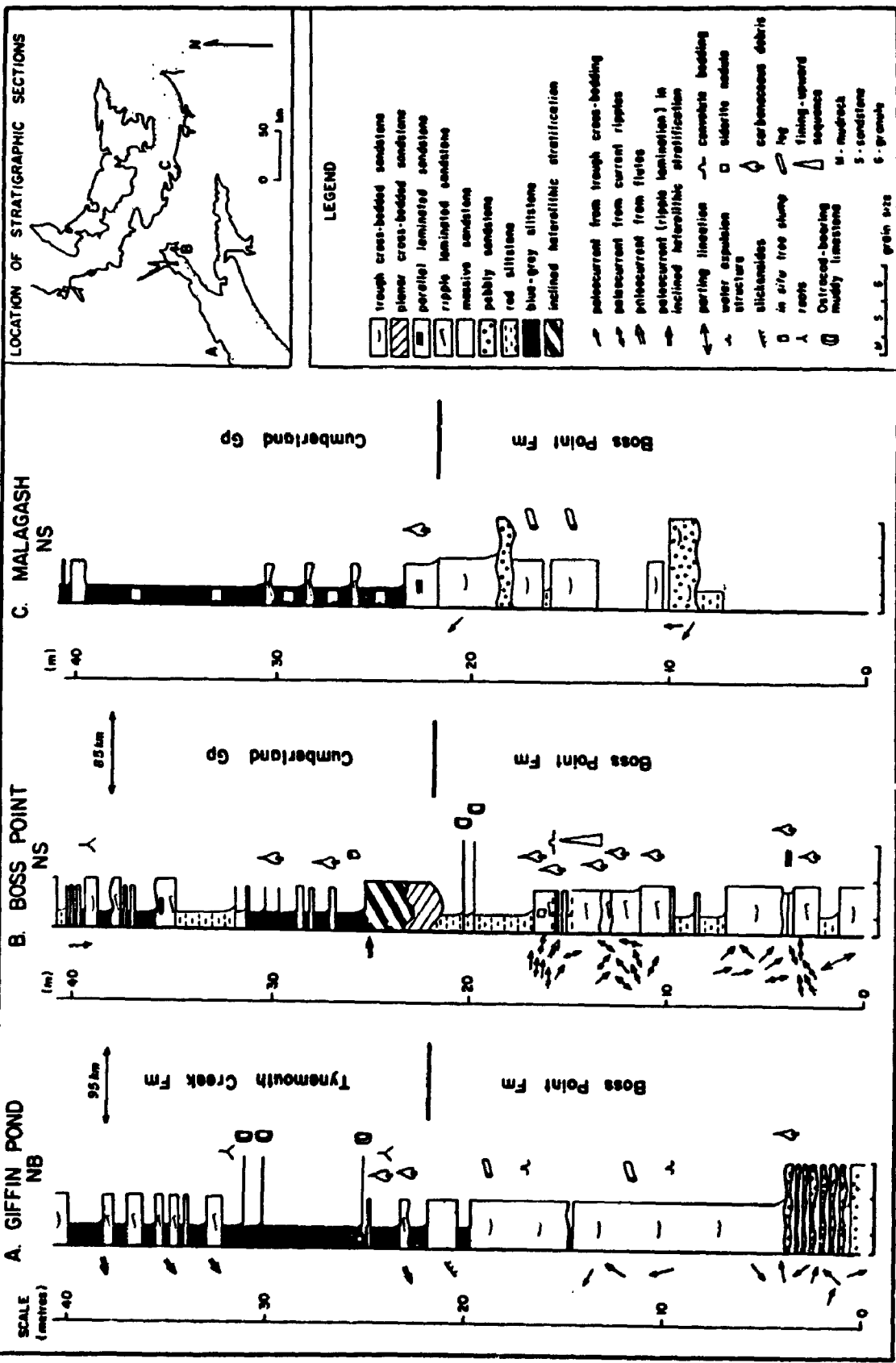


disconformable contact between the Boss Point Formation and the Millville formation at River John, Nova Scotia (stratigraphic section 1). In this study the contact at River John is placed at the stratigraphically lowest green-grey sandstone exposed in the section, a 1.4 m thick sandstone with 5 cm relief at its base (Fig. 2.5). Van de Poll (1970, 1972) noted that the basal part of the Boss Point Formation was everywhere marked by a quartz-pebble conglomerate, and that the formation was disconformable with underlying units. As indicated in Fig. 2.5, these relationships have not been borne out by this study.

The upper contact of the Boss Point Formation is summarised in Fig. 2.6. The Boss Point Formation is conformably overlain by the Tynemouth Creek Formation (Plint and van de Poll 1982, 1984) in the southwest (at Giffin Pond; stratigraphic section 26). The upper contact is marked by a local erosive channel base beneath inclined heterolithic stratification (lateral accretion) units of the Cumberland Group at Boss Point (Plate 1). The same contact is conformable into the Cumberland Group in northern Nova Scotia (at Malagash; Fig. 2.6).

The Boss Point Formation is included within the Riversdale (Bell 1944), Mabou (Fralick (1981), and Petitcodiac Groups (Wright 1922). The Riversdale and Mabou Groups have been used in reference to the Cumberland sub-basin, whereas Boss Point Formation lithologies in the

Fig. 2.6 Upper contacts of the Boss Point Formation
through the study area.



Moncton sub-basin have been included in the Petitcodiac Group. Recently Ryan *et al.* (1990) have suggested that both the Riversdale and the overlying Cumberland Groups are similar both lithologically and in terms of age, and have commented that the "usefulness of the term Riversdale Group becomes obscure."

The Boss Point Formation has been correlated with the Lancaster Formation in southern New Brunswick (van de Poll 1970- Fig. 2.2), with the Port Hood Formation of Cape Breton (Gersib and McCabe 1981- Fig. 2.2), and with the lower part of the Clifton Formation in northern New Brunswick (Graves 1982). Units formerly included in the Grand Anse Formation (Norman 1941) on the Maringouin Peninsula, are now included in the Boss Point Formation.

2.8 Age

The Boss Point Formation has traditionally been assigned a Namurian to Westphalian A age (Barss *et al.* 1963, Kelley 1967). McLeod (1980) believed that the base of the Boss Point Formation was diachronous from the Namurian B to the Westphalian C. At the type section, recent dating indicates that the formation is entirely of Westphalian A age (R.J. Ryan *pers comm.*, 1989). In terms of spore zonation, the basal few tens of metres belong to spore zone 1, the remainder to spore zone 2 (Ryan and

Boehner 1989). Additional samples submitted for dating in this study indicated Viséan to Westphalian ages (R.J. Ryan pers. comm., 1988), with obvious Visean contamination noted in the samples. Westphalian A ages have been reported for the formation in northern Nova Scotia (Ryan 1984, Kalkreuth and Macauley 1987).

2.9 Basin Morphology - The Maritimes Basin

The Boss Point Formation was deposited in the Maritimes Basin (Roliff 1962, Williams 1974), a 1000 by 500 km region in eastern Canada which comprises many smaller sedimentary basins. Up to 15 km of Late Devonian to Permian sediments and minor volcanics occur within the Maritimes Basin (Belt 1968b, Bradley 1982, Donohoe and Wallace 1982, Barr et al. 1985, Fyffe and Barr 1986, McCutcheon and Robinson 1987, Pe-Piper et al. 1989). Some 65,000 km² of the Maritimes Basin is now exposed on land (van de Poll 1970).

Various terms have been used to describe the Maritimes Basin including epieugeosyncline, taphrogeosyncline, horst-graben, wrench, rift, successor, aulacogen, pull-apart, transpression basin, and synclinorium. Most recent workers have adopted the non-genetic term "Maritimes Basin" (after Roliff 1962), and this is adopted here (for discussion see Boehner et al. 1988).

On the western side of the Maritimes Basin, the

Carboniferous sedimentary cover is relatively thin and Mississippian, then Pennsylvanian units onlap deformed Silurian and older rocks toward the northwest (Fig. 1.1). The greatest subsidence occurred in relatively small basins within the larger Maritimes Basin (Fig. 2.4) referred to here as sub-basins. These sub-basins are typically elongate with a length 2 or 3 times their width. They are arranged in an echelon fashion throughout the Maritimes Basin, and are similar to the Narragansett and Boston basins which developed at a similar period further to the south (Skehan *et al.* 1979, McMaster *et al.* 1980, Mosher 1983- Table 1). Some workers have argued that the sedimentary basins of Canada were linked to their southern counterparts in Massachusetts, Connecticut and Rhode Island during the Carboniferous (Gibling 1989, Gibling *et al.* 1989) and that much of the sediment was derived from source areas to the south, principally in the Appalachians of New England (van de Poll 1970, Gibling *et al.* 1989).

Several models have been proposed for the origin of these sub-basins. A rift origin was suggested by Belt (1968a), similar to the passive subsidence model of McCutcheon and Robinson (1987). Fault control models have included formation as wrench basins (Fralick 1981, Fralick and Schenk 1981), whereas most recent work has indicated formation as pull-apart basins (Bradley 1982, D'Orsay 1986, Leger 1986, Yeo and Ruixiang 1987, Fralick 1989), or

Table 1

**Summary of the geology of the Carboniferous sub-basins
of the Maritimes Basin. Modified after Bradley (1982).**

SUB-BASIN	AGE	AREA	BASIN FILL	VOLCANISM/ PLUTONISM	COMMENTS	REFERENCES	
MARITIMES BASIN	MONCTON	Late Devonian- Namurian	3000 km ²	Total: 8.5 km Pictou- clastics Riversdale- clastics Canso- clastics Windsor- carbonates & evaporites Horton- clastics	Visean: 30 m thick ash bed in Windsor Group. Namurian- Westphalian: Queenston Volcanics	Bounding structures Belleisle Fault (west) & Clover Hill-Caledonia Faults (east). Caledonia Massif (east). Faults inferred to be dextral	Gussow 1953 Mabb 1963 Fyffe & Barr 1986
	CUMBERLAND	Tournaisian in west, Emsian in east to Stephanian	3600 km ²	Total: 13 km Pictou- clastics Cumberland- clastics Riversdale- clastics Canso- clastics Windsor- carbonates & evaporites Horton- coarse clastics Fountain Lake- volcanics	Early Devonian: granite & minor gabbro plutons Early Devonian- Tournaisian: rhyolite & basalt(Fountain Lake Group)	Bounding structures Harvey-Hopewell Fault & Caledonia Massif (west), Cobequid Fault & Cobequid Massif (east). Harvey- Hopewell Fault interpreted to be sinistral - all others dextral	Fralick & Schenk 1981 Fralick 1981 Bochner et al. 1986
	STELLARTON	Late Visean- Westphalian	200 km ²	Total: 8 km Pictou- clastics Cumberland- clastics Riversdale- clastics Canso- clastics Windsor- carbonates & evaporites	None known	Bounding structures Hollow Fault (west) Cobequid Fault (east). Interpret- ed to be a pull- apart basin between dextral strike-slip faults	Belt 1968; Yeo & Ruisiang 1987
	MINAS	Middle Devonian- Westphalian	600 km ²	Total: 4 km Riversdale- clastics Canso- clastics Windsor- carbonates & evaporites Horton- clastics & lacustrine	None known	Bounding structures Cobequid-Chedabucto Fault (north)- onlaps basement to south. Interpreted as a dextral pull- bas	Jesse & Leading 1978 D'Orsay 1986
	MAGDELEN	Tournaisian (possibly Devonian)- Permian	25,000 km ²	Total: 13 km Pictou- clastics Cumberland- clastics Riversdale- clastics Canso- clastics Windsor- carbonates & evaporites Horton- not known	Visean: 200 m thick basalt & andesite at top of Windsor Group Permian: basalt (Cap-du-moules, Cap-du-diable & Har-aux-maisons formations)	Bounding structures Fredericton & Belleisle Faults (west) & extension of St Georges Bay Fault (east). Southern boundary marked by Canso Fault. Inferred to be dextral pull- basin	Howie & Barss 1975a Bradley 1982 Barr et al. 1985 Marillier & Verhoef 1989
	MABOU	Tournaisian- Namurian	1500 km ²	Total: 7.5 km Riversdale- clastics Canso- clastics Windsor- carbonates & evaporites Horton- coarse clastics	Late Devonian- Tournaisian: 300 m thick intermediate to siliceous volcanics (Fisset Brook Fm)	Bounding structures Hollow Fault (west) Aspy Fault (east). Tectonic origin uncertain	Howie & Barss 1975a
	SYDNEY	Tournaisian- Permian	36,300 km ²	Total: 4 km Unnamed clastics Horton- clastics Canso- clastics Windsor- carbonates & evaporites Horton- coarse clastics	None known	Bounding structures Southern extension of the Dover-Her- itage Fault (north) & the Mira River- Bateson Fault (south). Interpreted to be a strike-slip faults basin	Howie & Barss 1975a Bird 1987 Gibling & Rust 1987
NEW ENGLAND	MARRAGANSETT	Namurian B- Stephanian B/C	2500 km ²	Total: 4 km Purgatory Fm Dighton Fm Rhode Island Fm Mansurta Fm Pondville Fm -all medium to coarse clastics & volcani- clastics	Westphalian B: 300 m of basalt & rhyolite (Mansurta Cg)	Bounding structures Pontapog Fault (north), onlap to south. Considered to be a pull-apart	Slehan et al. 1979 McMaster et al. 1980 Nesher 1983

strike-slip basins (Gibling et al. 1987, Martel 1987).

Each of these sub-basins is bounded by faulted margins or uplifted blocks which are well delineated by magnetic anomaly and bouguer anomaly maps (Figs. 2.4, 2.7, 2.8 & 2.9). Many of the sub-basins extend offshore, the largest being the Sydney sub-basin, which covers an area of 36,300 km² (Gibling et al. 1987). The largest sub-basin exposed onshore is the Cumberland sub-basin (see below).

Within each sub-basin, a separate and typically distinct sedimentary assemblage accumulated, though each depocentre has many sedimentary features in common. The vast majority of lithologies in the Maritimes Basin are continental in origin, but marine incursions are known during the deposition of the Viséan Windsor Group (Howie 1988), and in the overlying West Bay Formation (D'Orsay 1986). Marine transgression is also recorded by the latest Mississippian Cap-du-Diable Formation in the Magdalen sub-basin (Barr et al. 1985), and in the Westphalian D-Stephanian Sydney Mines Formation, Sydney sub-basin (Bird 1987).

2.10 Stratigraphic Patterns within the Cumberland Sub-basin

The Boss Point Formation was deposited in both the Moncton and Cumberland sub-basins. However exposures of

Fig. 2.7 Magnetic anomaly map of the study area
(after Zietz *et al.* 1980).

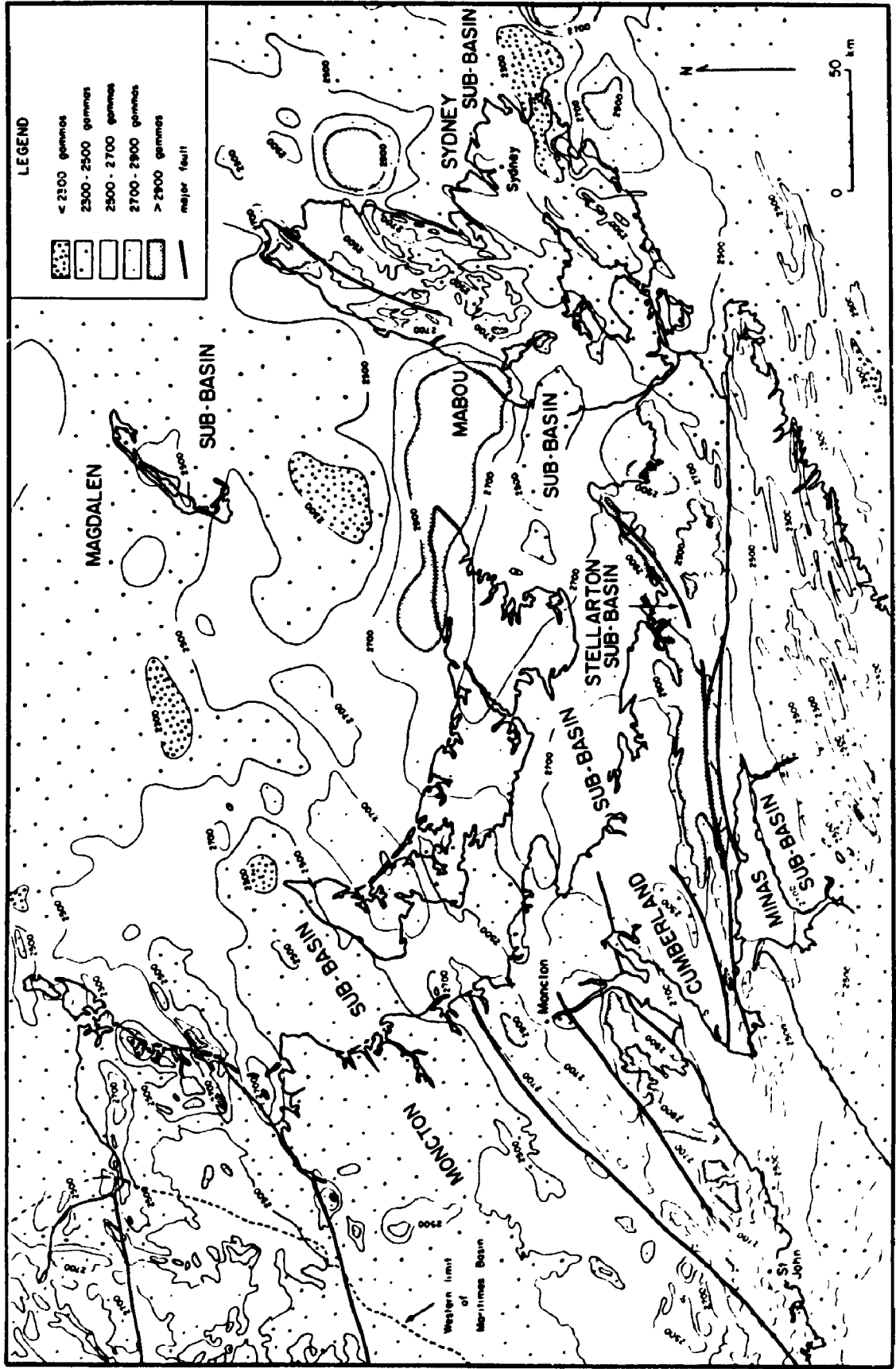


Fig. 2.8 Bouguer anomaly map of the study area
(after Haworth et al. 1980).

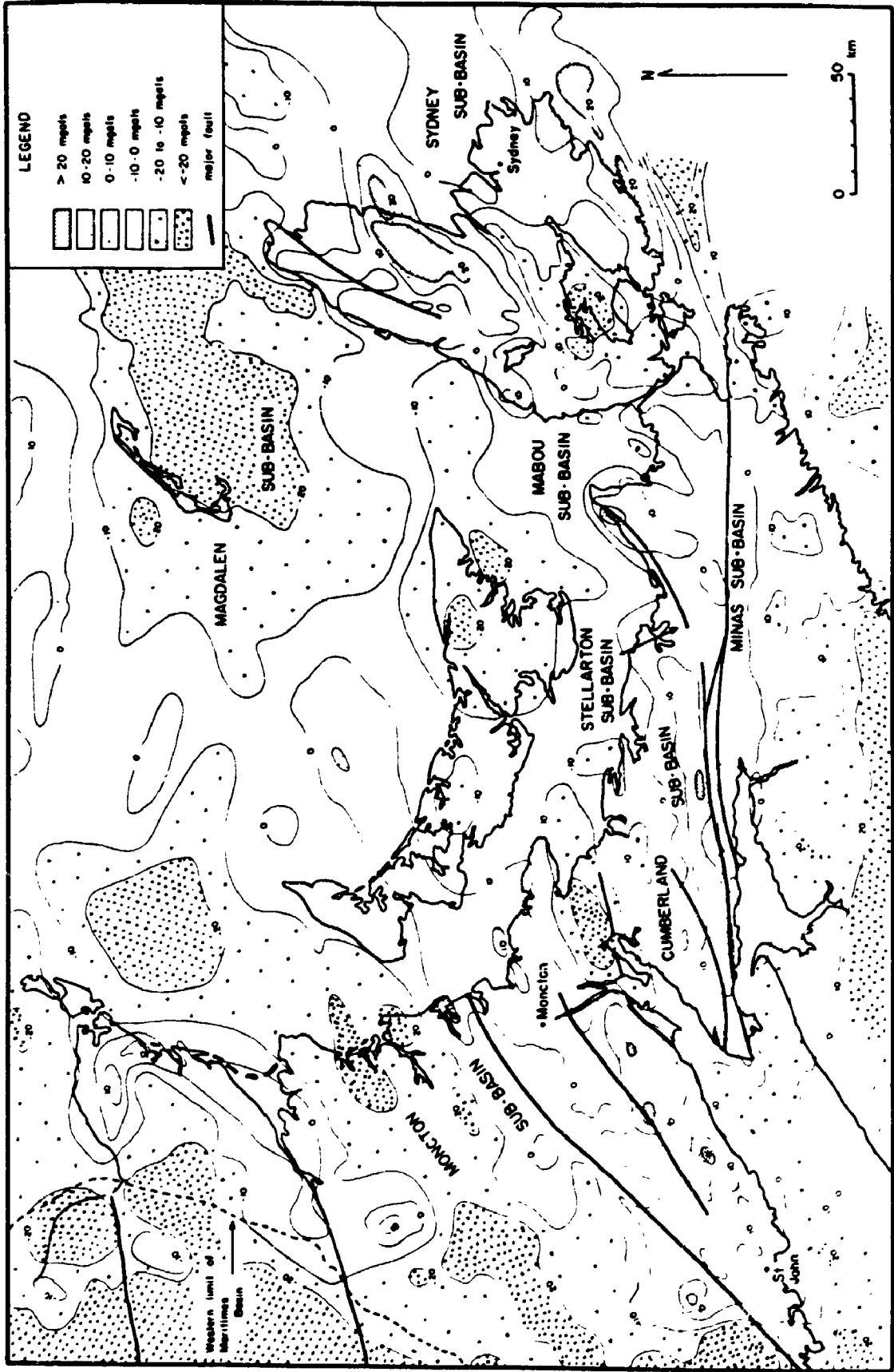
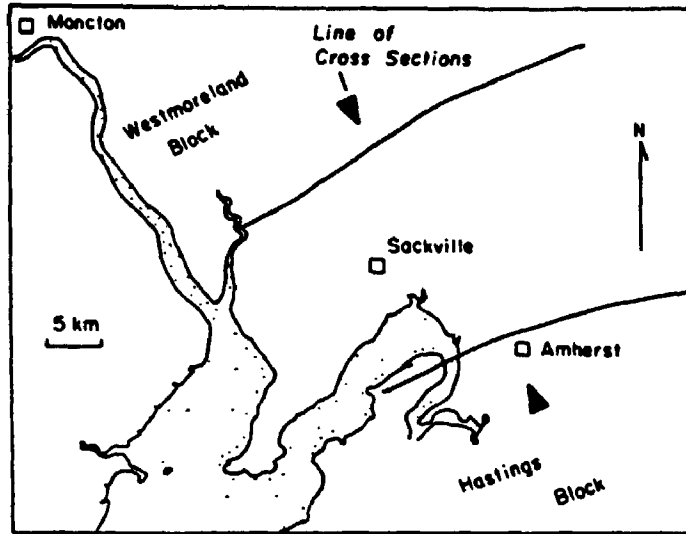
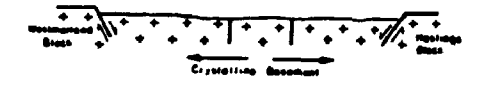


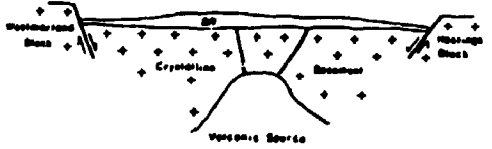
Fig. 2.9 Cross-section through the NW-sector of the Cumberland sub-basin (after Martel 1987). Lithological units are: BR- basal reflectors (lithology unknown), H- Horton Group, W- Windsor Group, MS- Maringouin and Shepody Formations, E- Enrage Formation, BP- Boss Point Formation, P- Petitcodiac Group.



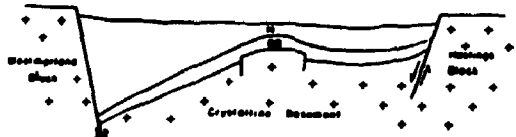
a. Transensional stresses NW SE



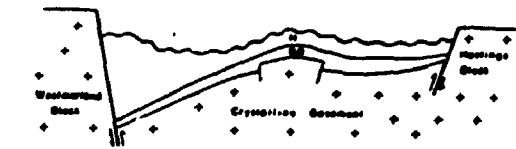
b. Volcanic extrusion - basal reflectors



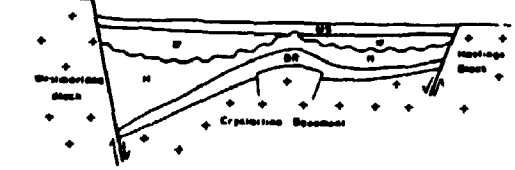
c. Deposition of Horton - transensional



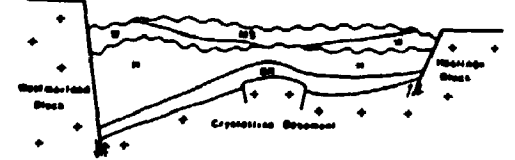
d. Pre-Hillsborough unconformity - transensional



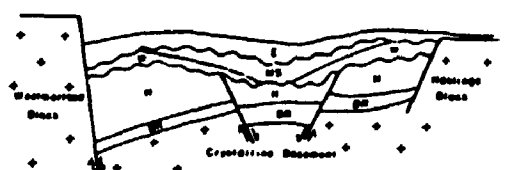
e. Deposition of Windsor and Lower Hopewell - transensional NW SE



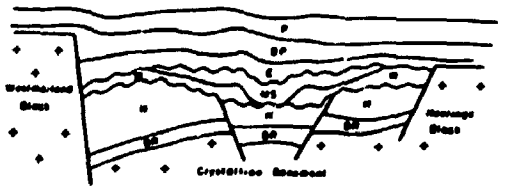
f. Basal Enrage unconformity - transensional



g. Enrage Deposition - transensional?



h. Bass Point and Petitediac deposition - regional subsidence, cooling of lithosphere

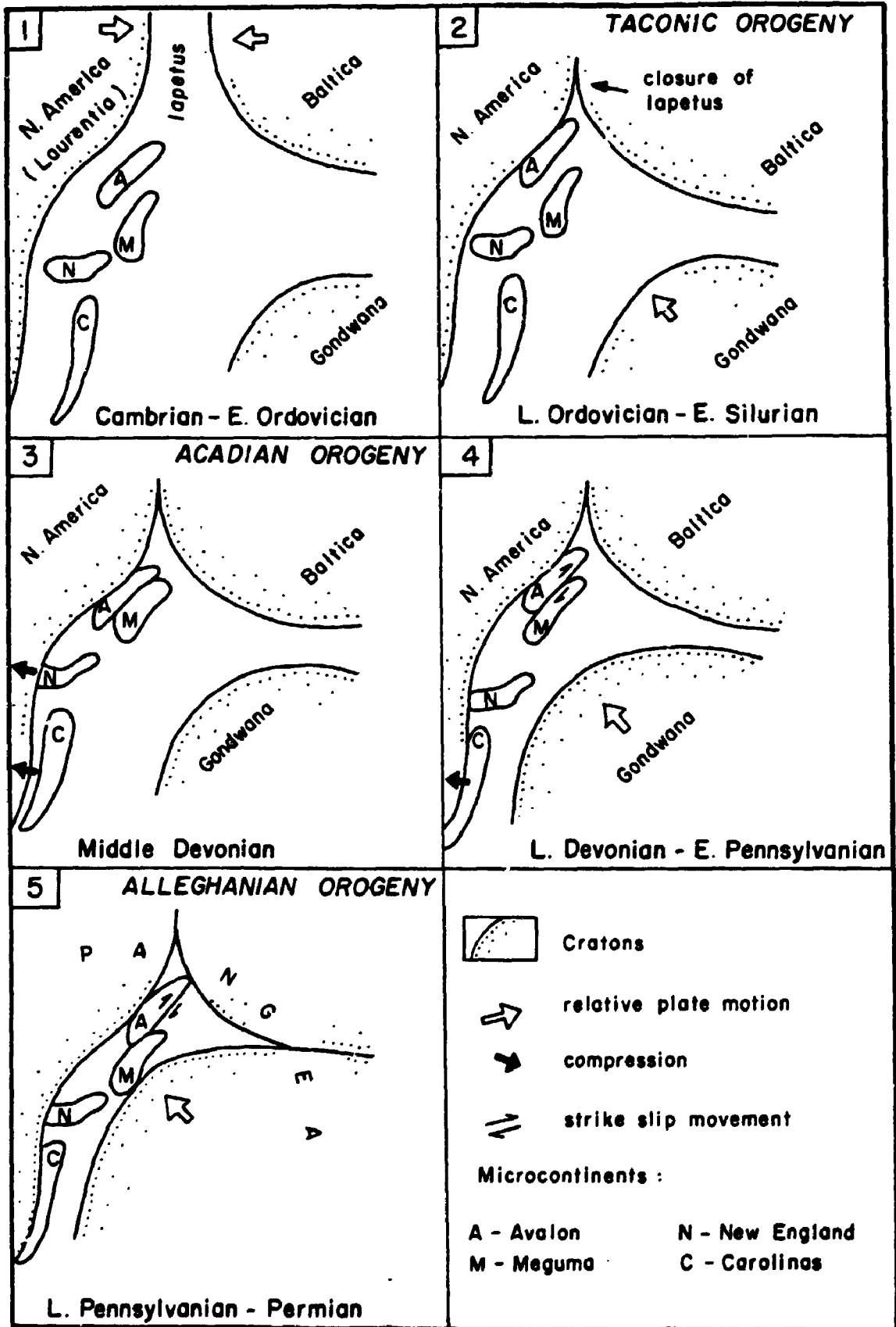


the formation in the Moncton sub-basin are thin, and outcrops are generally poor, and for these reasons, are not dealt with further. Maximum depths to basement in the Cumberland sub-basin are between 8-10 km (Marillier and Verhoef 1989).

The Cumberland sub-basin covers 3600 km² (Table 1) and is bounded in the west by the Caledonia Highlands, a basement complex of metamorphic and plutonic rocks, and by faults associated with the massif: the Harvey-Hopewell and Clover Hill-Caledonia Faults (Figs. 2.4 & 2.10). Recently Martel (1987) has proposed that a smaller depocentre, the Sackville sub-basin developed on the western margin of the Cumberland sub-basin. In the north, the Cumberland sub-basin is bounded by the Westmoreland Uplift, and by west-east trending magnetic and bouguer anomaly highs in the Northumberland Strait region (Figs. 2.4, 2.7 & 2.8). In the south, the sub-basin passes into a structurally complex region where the original controls and morphology of the depocentre have been overprinted by Late Pennsylvanian thrust faulting (Nance 1986). In the east the sub-basin is bounded by the Cobequid Massif, the Cobequid and Chedabucto Faults, and the Hollow Fault (Fig. 2.4).

Essentially two stratigraphic divisions, west and east, can be recognised within the Cumberland sub-basin.

**Fig. 2.10 Palinspastic lithospheric plate
reconstruction for the Paleozoic (modified
after Rast 1988).**



2.10.1 Western Cumberland Sub-basin

In the west, sedimentation began in the Late Devonian and Early Mississippian (Famennian-Tournaisian) following the Acadian Orogeny. Red shale, sandstone and conglomerate (Memramcook Formation), was deposited in proximal areas adjacent to fault margins (Figs. 2.1 & 2.2). These molasse units pass basinward into reddish sandstone and siltstone (Gussow 1953). Either interdigitating or gradationally overlying is the Albert Formation, comprising grey-green to dark grey, thin-bedded and laminated shale and limestone (Kalkreuth and Macauley 1984, Macauley *et al.* 1984, Altebaeumer 1985, Mossman *et al.* 1987, Smith and Gibling 1987). The overlying Moncton Formation is more extensive than the previous formations. It consists of chocolate-brown and red mudstone, and locally near the Cobeguid Highlands in the west, contains a basal conglomerate. These formations comprise the Horton Group and are interpreted as alluvial fan, lacustrine, meandering fluvial or flood plain deposits developed adjacent to active Late Devonian-Mississippian faults.

By the Late Viséan, regional subsidence resulted in a marine transgression (Windsor Group), comprising micrites, black oolitic and stromatolitic limestones and evaporites, together with red shale (Kirkham 1985, Howie 1988).

The unconformably overlying Canso and Riversdale Group rocks are grossly similar to each other. In the western part of the Cumberland sub-basin they comprise two coarsening-upward packages, of deep red siltstone and sandy shale at the base, and green-grey sandstone above. These units include the Maringouin and Shepody Formations as a lower package, and the Enrage and Boss Point Formations as an upper package. The progressively younger formations of the Canso and Riversdale Groups show an increasing degree of onlap onto older lithologies (Fig. 2.10), a feature which is the most widely developed during Boss Point Formation time. The Boss Point Formation therefore was deposited at the concluding stages of basin development, at a time when the depocentre had reached its maximum geographic distribution.

2.10.2 Eastern Cumberland Sub-basin

A different stratigraphic succession is recorded in the eastern part of the Cumberland sub-basin (Fig. 2.2 & Table 1). The oldest rocks are of Early Devonian (Emsian) age, considerably younger than the oldest strata in the western part of the sub-basin. These rocks comprise a thick succession (up to 2 km) of rhyolite and basaltic volcanics of the Fountain Lake Group (Donohoe and Wallace 1982) which have radiometric dates of between 341 and 387 Ma. Recent

work suggests that plutonic rocks, on which the Fountain Lake Group rest, may also be a part of early basin development (Pe-Piper et al. 1989). Unconformably overlying the Fountain Lake Group are Late Devonian and Early Mississippian red-brown and grey, polymict conglomerate and lithic wacke (Falls, Greville River and Nuttby Formations) of the Horton Group (Donohoe and Wallace 1982).

The overlying Windsor Group comprises grey and tan to black and grey limestone, and calcareous siltstone (Boehner et al. 1986).

The Canso Group is absent from this part of the sub-basin, the period between the Early Carboniferous (Viséan to Namurian B) being a period of faulting and uplift along the margin of the Cobequid Massif (Boehner et al. 1986). Riversdale Group rocks rest unconformably upon the Horton Group and comprise up to 700 m of reddish brown breccia, conglomerate and pebbly sandstone, sandstone and minor siltstone (Millville formation [informal name] and Boss Point Formation). The Millville formation is interpreted as alluvial fan conglomerates developed subsequent to the Viséan-Namurian uplift, and adjacent to the fault scarps resulting from that uplift (Boehner et al. 1986).

In northern Nova Scotia, the Boss Point Formation is overlain by up to 600 m of fine-grained, typically calcareous red sandstone and shale lithologies (Table 1),

or by conglomerate of the Cumberland Group (Ryan 1984).

The final record of Carboniferous sedimentation in both western and eastern parts of the Cumberland sub-basin is represented by Pictou Group reddish brown sandstone, mudstone and conglomerate, of Westphalian C to Stephanian age (Gussow 1953, van de Poll 1966, 1970, Ryan 1984). Pictou rocks have been shown to be as young as late Early Permian on Prince Edward Island (van de Poll 1989).

2.11 Plate Tectonic Considerations

Throughout the late Precambrian and Paleozoic a variety of terranes were accreted to the North American craton (Williams 1979, Lefort and van der Voo 1981, Williams and Hatcher 1982). All are structurally uncoupled, their boundaries marked by mélangé, mylonitic zones and ophiolite complexes (Fig. 2.4). Accretion progressed from the craton outward with time, such that the terranes become progressively younger eastward. Accretionary events were marked by major deformation, plutonism and metamorphism, resulting in three major orogenies; the Taconic Orogeny (Late Ordovician and Early Silurian), the Acadian Orogeny (Middle - early Late Devonian), and the Alleghenian Orogeny (Late Pennsylvanian-Middle Permian).

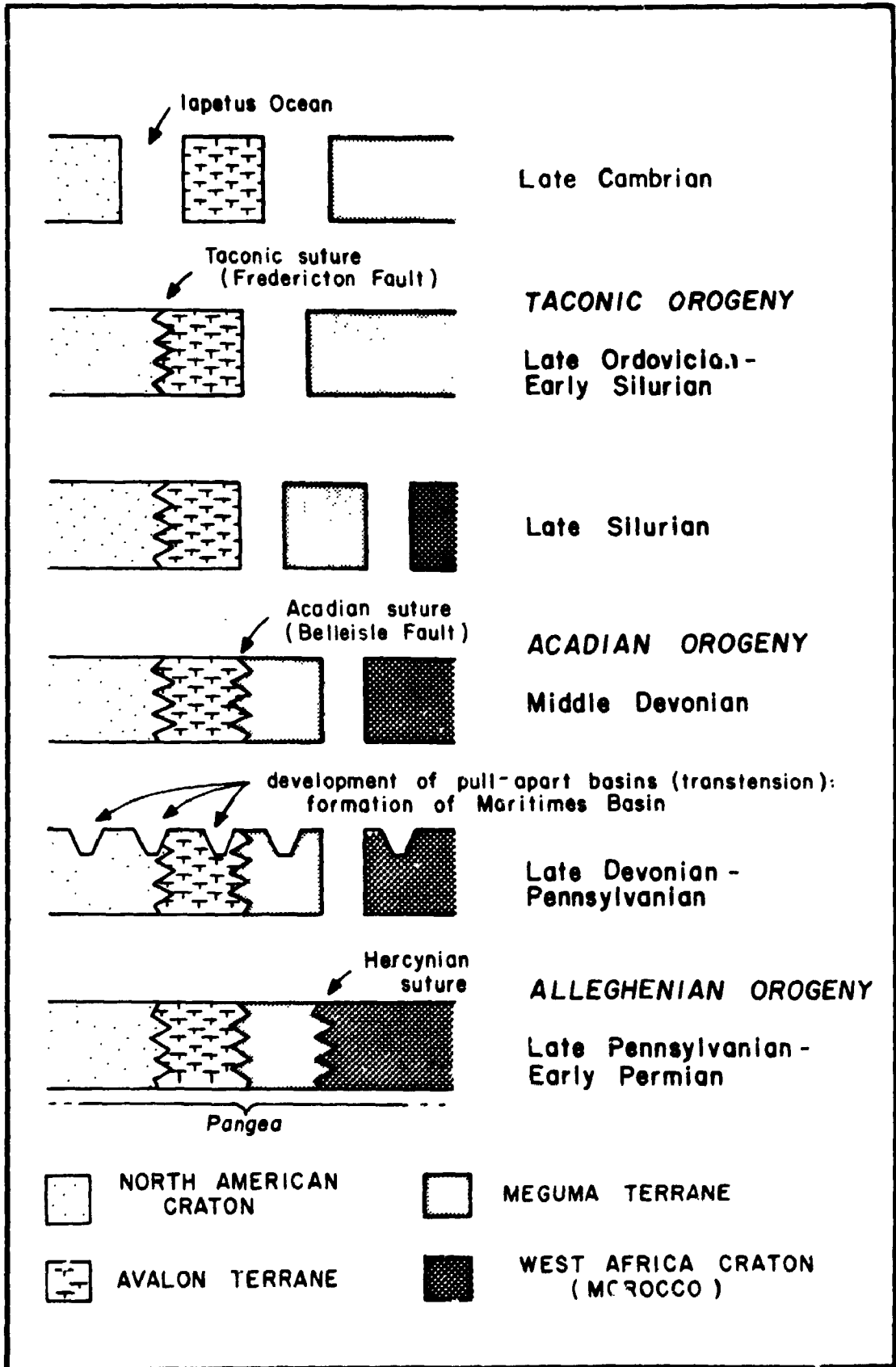
The Maritimes basin developed between the Acadian and Alleghenian orogenies, and are synonymous with the

Caledonian and Variscan (Hercynian) orogenies respectively of Europe (Rast 1988).

During the Taconic Orogeny the western margin of Avalonia, a microplate with west African plate affinities (Avalon terrane), was accreted onto the eastern margin of the North American craton (O'Brien et al. 1983 - Figs. 2.4, 2.10 & 2.11). The Avalon terrane comprises late Precambrian volcanic and sedimentary rocks cut by granites, and overlain unconformably by gently dipping Cambro-Ordovician shallow-water sediments (Schenk 1978, Ruitenberg et al. 1979, Keppie and Dallmeyer 1987, Barr and White 1988).

The Acadian Orogeny represents a later docking of the Meguma microcontinent (Meguma terrane) with the North American craton (Lefort and van der Voo 1981, Schenk 1981, Keppie and Dallmeyer 1987- Figs. 2.4, 2.10 & 2.11). The Meguma terrane has long been recognised as a "displaced," or "exotic," or "suspect" terrane with respect to the remainder of the North American craton. An origin adjacent to western Africa (Morocco) has been suggested by Schenk (1971, 1978, 1981); others (McKerrow and Ziegler 1972, Irving 1979) have suggested an affinity with northeastern South America. Two dominant geologic units are recognised in the Meguma terrane. These are the Cambro-Ordovician siliciclastic sediments of the Meguma Group and the peraluminous granitoids of the southwestern Meguma Zone

Fig. 2.11 Cartoon depicting the accretion of lithospheric plates during the Paleozoic in eastern Canada (modified after Schenk 1981).



which intruded the sediments after they had undergone lower grade greenschist to lower amphibolite facies metamorphism (Schenk 1981, Clarke and Muecke 1985, Keppie and Dallmeyer 1987, Reynolds *et al.* 1987).

During the Alleghenian Orogeny the western margin of the African continent collided with the North American craton, and in so doing united Laurentia (North America), Gondwana (South America, Africa, India, Antarctica and Australia) and Baltica (Europe and Asia) into the super continent Pangea.

Pangea remained a stable block until breakup in the Mesozoic (commencing at 220-230 Ma ago, Reynolds *et al.* 1987), when rifting caused the development of the Atlantic Ocean. In both New Brunswick and Nova Scotia, Triassic gabbro-diabase intrusions (Fig. 2.4), and Triassic-Jurassic basalt flows, and eolian, alluvial fan, playa lake and fluvial sediments (Fundy Group) were emplaced/deposited during this phase of continental rifting (Nadon and Middleton 1985, Hubert and Mertz 1984, Hubert and Forlenza 1988- Fig. 1.1).

2.12 Paleomagnetic Studies

The time of Riversdale Group deposition corresponds to an interval that shows normal, reverse or (most frequently) dual-polarity magnetisations. Above the Boss Point

Formation, the magnetisation is consistently reversed, a period referred to as the Kiaman Magnetic Inter. 1 (Roy and Morris 1983), which persisted for some 85 million years, until the end of the Permian.

Paleomagnetic results for two localities indicate a pole position at 125° E, 33° N and 122° E, 36° N for Riversdale Group strata (Roy 1977). Paleolatitude determinations indicate that the study area was located at about 10° S at the Mississippian-Pennsylvanian boundary, or at approximately Boss Point Formation times (Roy and Morris 1983, Scotese et al. 1983) Through the Pennsylvanian, the paleolatitude moved some 8° north, the study area being very near the paleoequator by the end of the Pennsylvanian (Roy and Morris 1983, Scotese et al. 1983).

CHAPTER 3

SEDIMENTOLOGY OF COARSE-GRAINED UNITS

Conglomerate and breccia units comprise 9.9% of the thickness of the Boss Point Formation (Fig. 3.1a, Appendix I) and occur in areas marginal to the Cumberland sub-basin. Coarse-grained units are absent in central parts of the sub-basin such as at Boss Point, Cape Maringouin, Grindstone Island and Marys Point. Good exposures occur in the north and northwest from Sackville to Hillsborough, in scattered outcrops to the east from Sussex to Elgin, and adjacent to the Cobequid Highlands in the east (Fig. 1.2).

3.1 Trough Cross-Bedded Gravel (Gt)

3.1.1 Description

Trough cross-bedded gravel comprises 1.8% of the thickness of the Boss Point Formation (Fig. 3.1c, Appendix I). Unit thicknesses up to 7.5 m occur, but are generally in the range 0.5 to 2 m (mean thickness 1.3 m) thick (Figs. 3.1d & 3.1e). The lithofacies occurs over most of the study area, but tends to be more abundant in northern localities close to the basin margin or to presumed active

- Fig. 3.1**
- a) Proportions of gravel, sandstone and mudrock as a percentage of the total thickness of the Boss Point Formation.
 - b) Proportions of each lithofacies in the Boss Point Formation in terms of their frequency of occurrence expressed as a percentage. Lithologic code follows that of Miall (1978) and Rust (1978). B= breccia, Z= siltstone blocks, BP= ball and pillow.
 - c) Proportions of each lithofacies in the Boss Point Formation in terms of the percentage of the total thickness. Lithologic code follows that of Miall (1978) and Rust (1978). B= breccia, Z= siltstone blocks, BP= ball and pillow.
 - d) Maximum thickness of each lithofacies in the Boss Point Formation. Lithologic code follows that of Miall (1978) and Rust (1978). B= breccia, Z= siltstone blocks, BP= ball and pillow.
 - e) Mean thickness of each lithofacies in the Boss Point Formation. Lithologic code follows that of Miall (1978) and Rust (1978). B= breccia, Z= siltstone blocks, BP= ball and pillow.

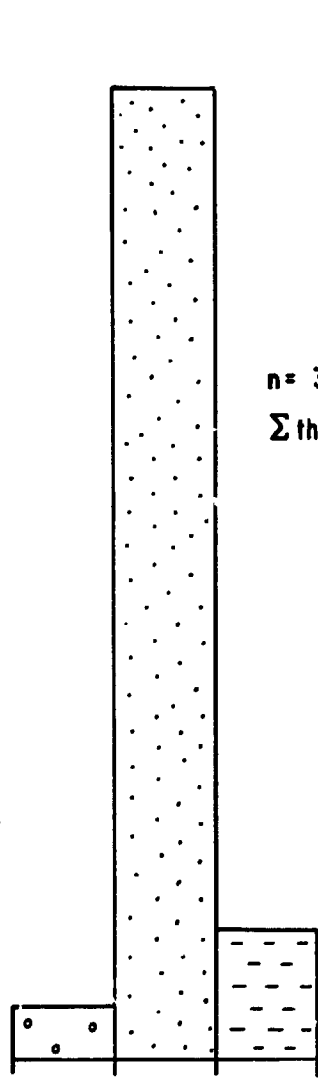
Ⓐ

% OF TOTAL THICKNESS

90
80
70
60
50
40
30
20
10
0

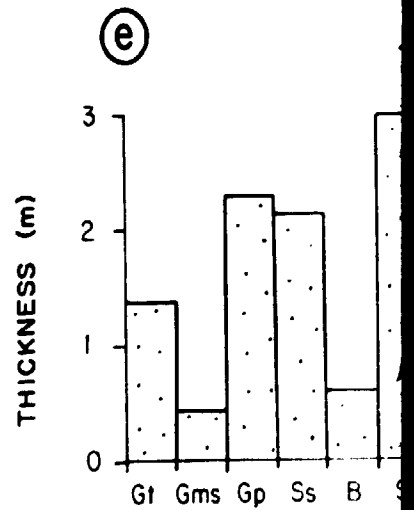
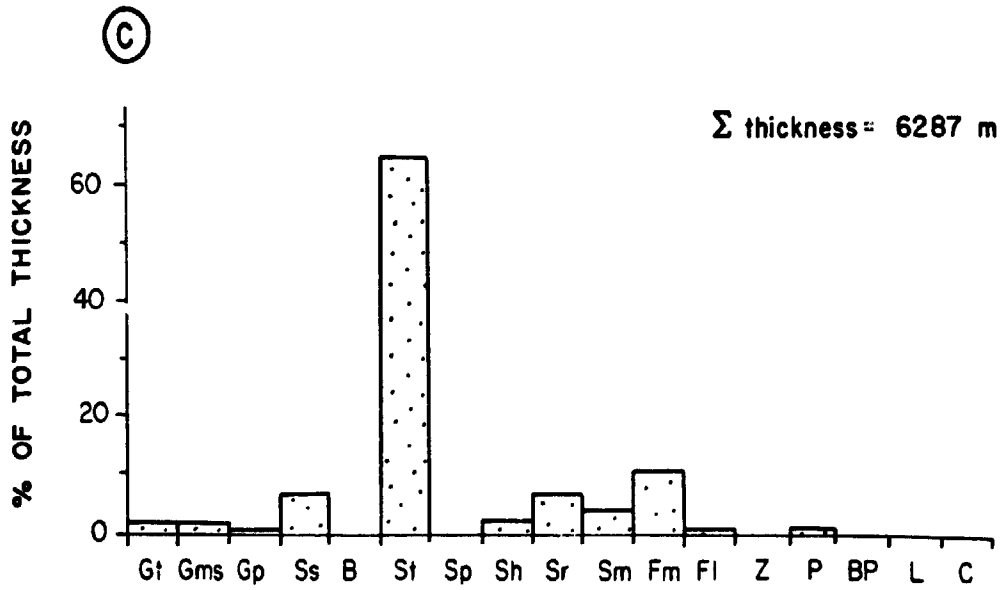
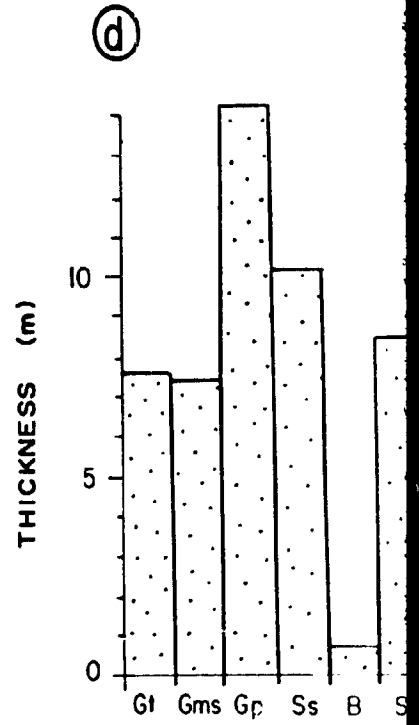
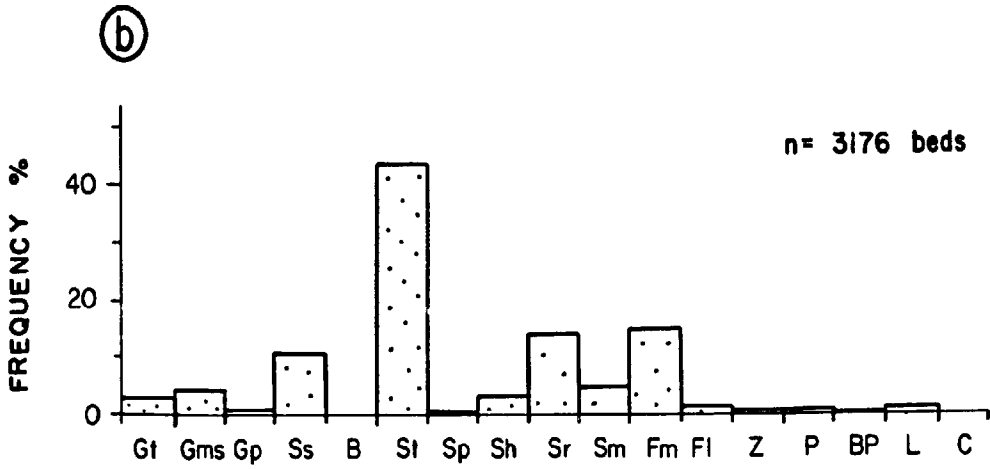
GRAVEL
SANDSTONE
MUDROCK

n = 3176 beds
 Σ thickness = 6287 m

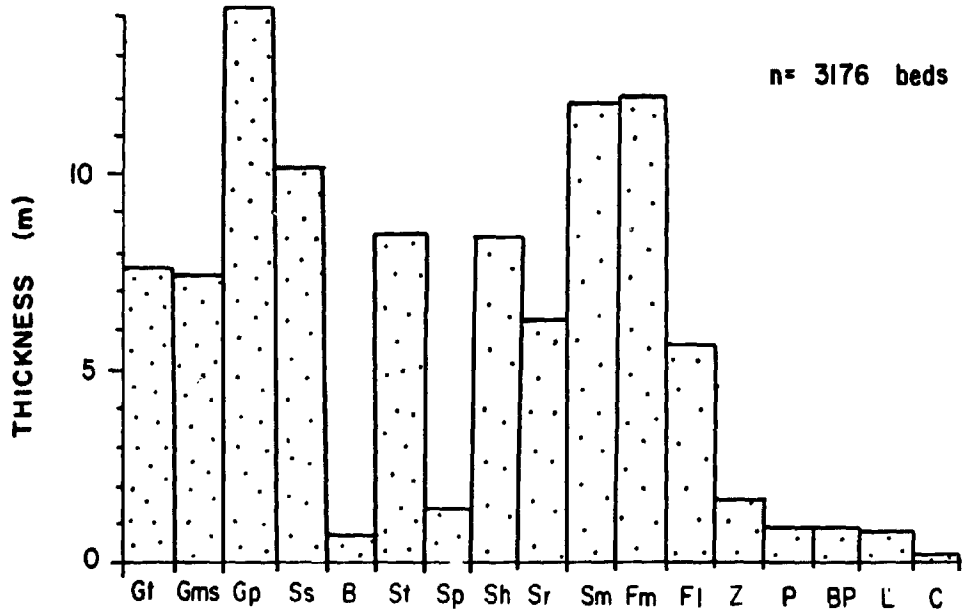


FREQUENCY %

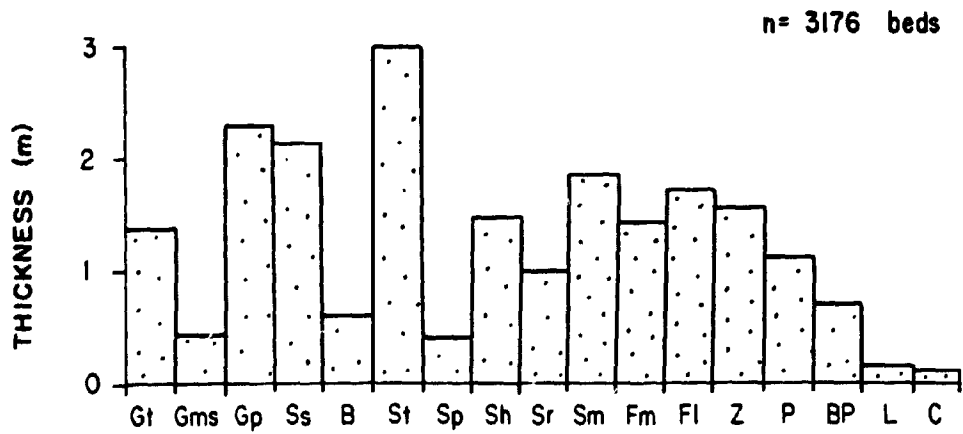
% OF TOTAL THICKNESS



(d)



(e)



Carboniferous faults (Fig. 3.2). Examples include Malagash, Pt de Bute Quarry, Mt Whatley Quarry, Aulac, Dorchester, Beaumont and Hillsborough (Appendix I, stratigraphic sections 2,6,7,8,10,11, and 12).

Well exposed coastal sections at Hillsborough (Fig. 3.3, Plate 2a & Plate 3) exemplify the character of these units and the following discussion is based largely on that locality.

At Hillsborough the <25 m high cliff face is approximately normal to paleocurrent directions. Large scoured surfaces, as much as 4 m thick and up to 100 m wide are exposed. Each scoured surface is overlain by trough cross-bedded cosets, producing a stacked succession 20 to 30 m thick (Fig. 3.3; see Ramos and Sopena 1983). Units are intercalated with trough cross-bedded sandstone (St), planar cross-bedded gravels (Gp) and rarely by horizontally laminated sandstone (Sh) and thinly bedded mudrocks.

Lithofacies Gt consists of poorly sorted granule to pebble conglomerate, with clast size typically between 2-5 cm diameter, although clasts up to 20 cm in diameter are common. In rare cases mudstone clasts as much as 0.7 x 2.0 m diameter occur (Fig. 3.3, Plate 2b & 2c). Clasts are sub-rounded to well rounded and are commonly matrix-supported; clast-support, where it does occur, tends to be more prevalent in areas to the north, such as in the Sackville region. The degree of matrix-support varies

- Fig. 3.2**
- a) Proportions of each lithofacies in the Boss Point Formation in terms of their frequency of occurrence expressed as a percentage. Values are indicated by geographic area in the Bay of Fundy region. N= north, C= central & S= south. Lithologic code follows that of Miall (1978) and Rust (1978). Z= siltstone blocks
BP= ball and pillow.
- b) Proportions of each lithofacies in the Boss Point Formation in terms of the percentage of the total thickness. Lithologic code follows that of Miall (1978) and Rust (1978). Z= siltstone blocks, BP= ball and pillow.

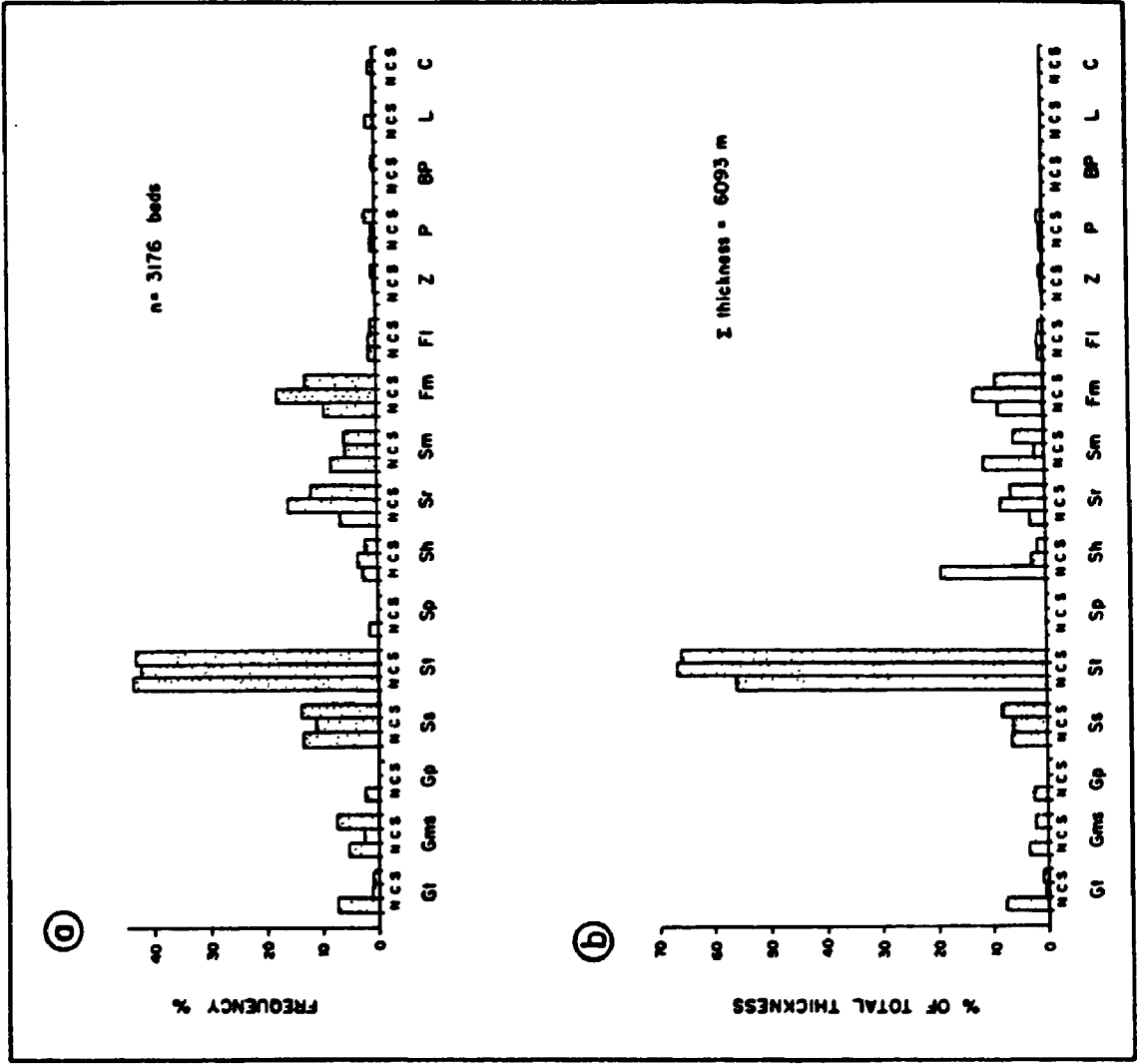
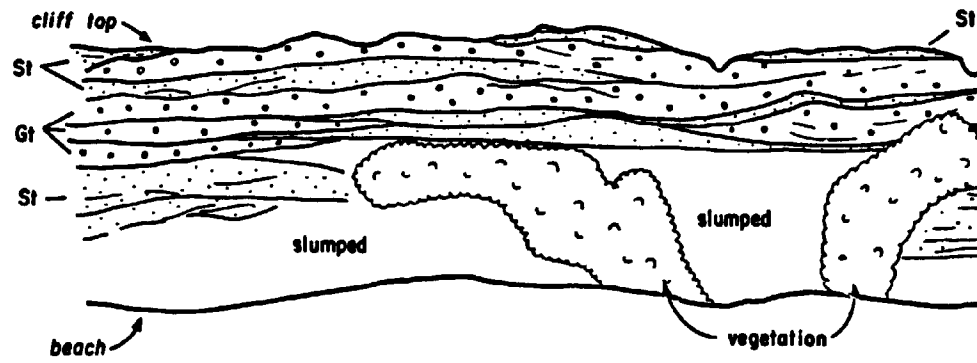
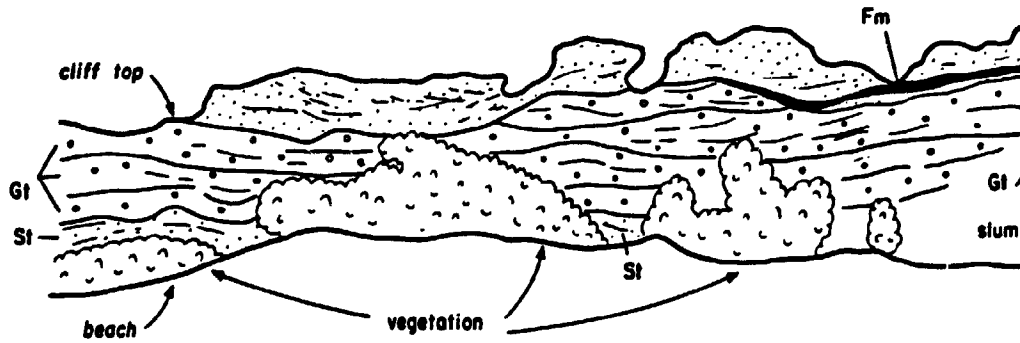


Fig. 3.3 Outcrop sketch of cliff face at Hillsborough showing channelised and stacked geometries of trough cross-bedded gravel (Gt) units and intercalation with planar cross-bedded gravel (Gp), massive gravel (Gms), trough cross-bedded sandstone (St) and massive mudrocks (Fm). Drawn from series of black and white photos.

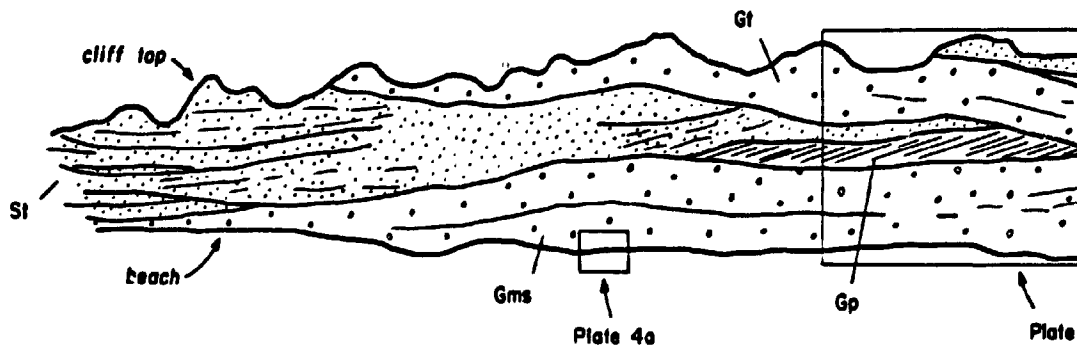
D.

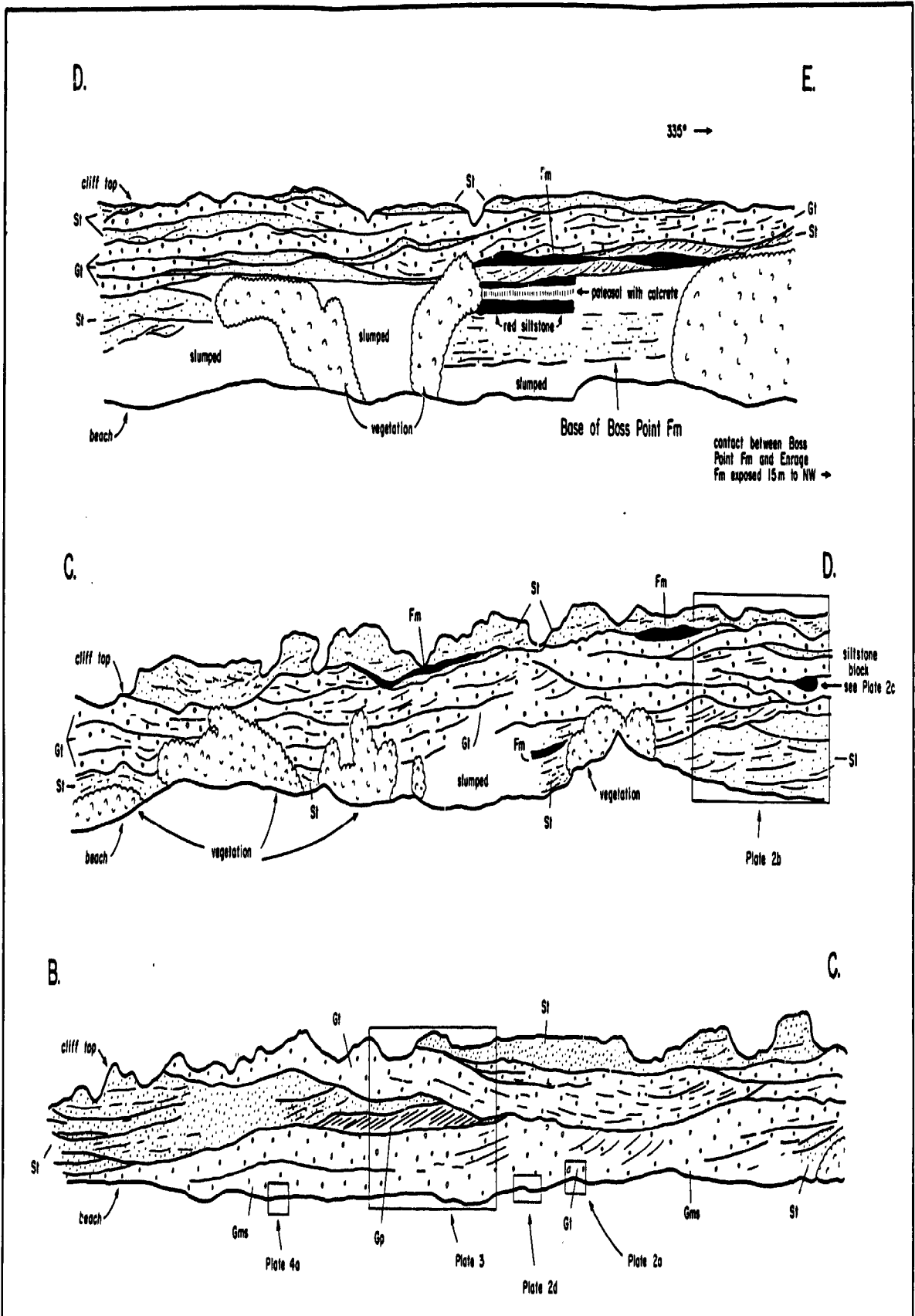


C.



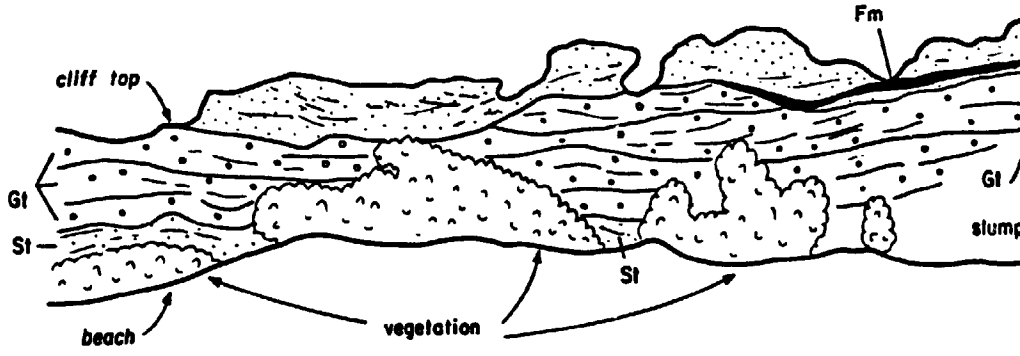
B.



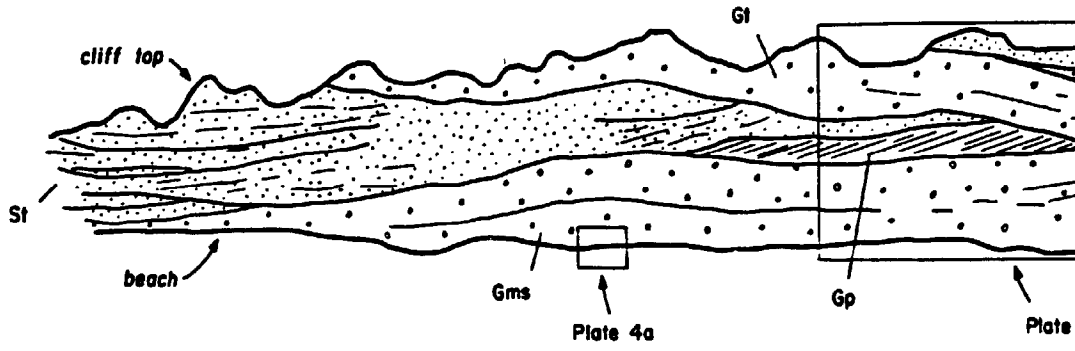




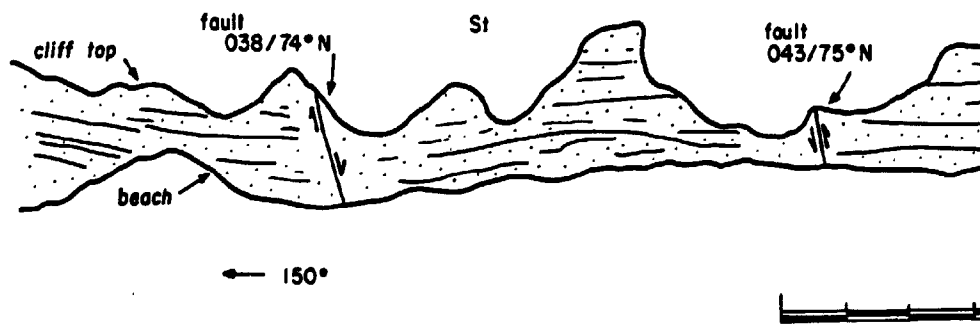
C.

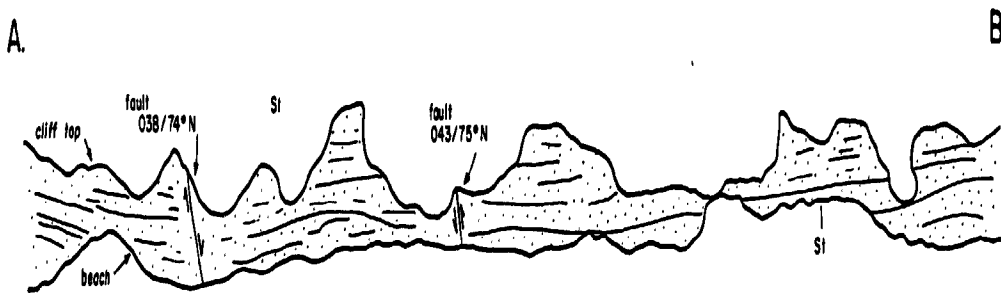
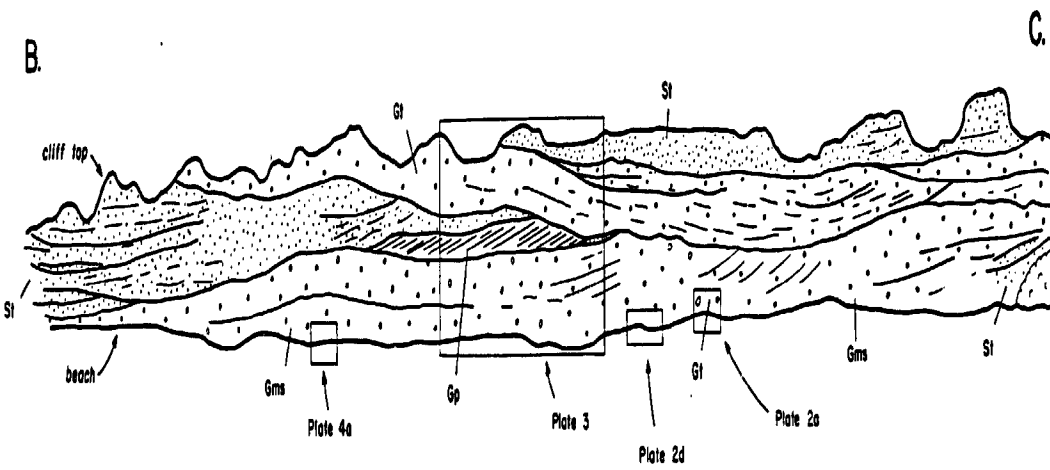
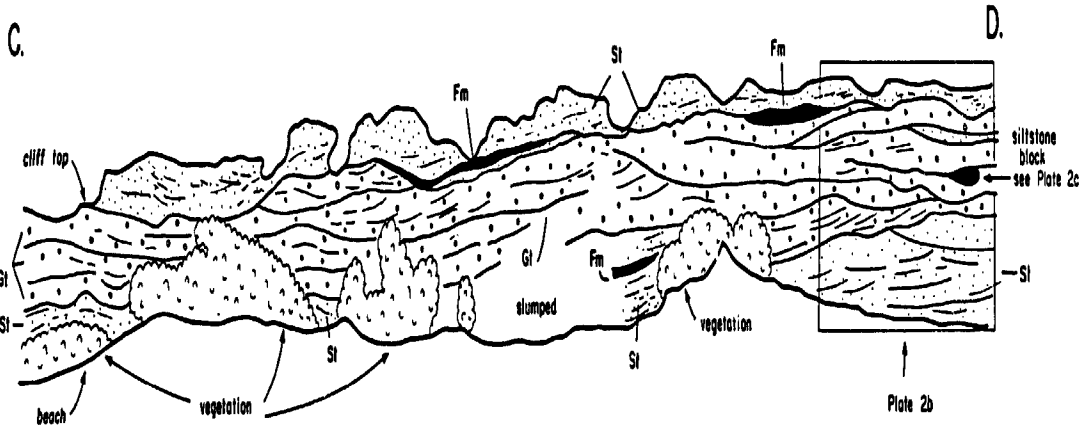
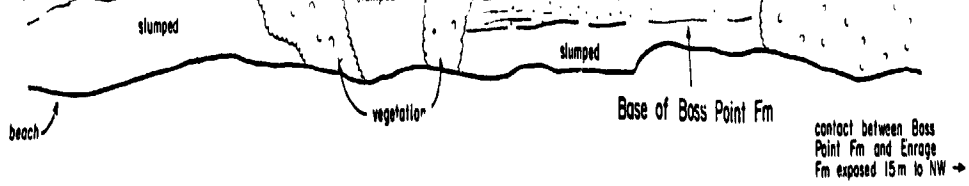


B.



A.





← 150°

25 m No vertical exaggeration

Plate 2

a) Trough cross-bedded gravel (Gt) at Hillsborough. For exact location see Fig. 3.3. Scale is 50 cm long with 10 cm divisions.

b) Outcrop view of Hillsborough section showing trough cross-bedded sandstone units at base of cliff, overlain by stacked channelised trough cross-bedded gravels (Gt), and by trough cross-bedded sandstone near cliff top. For exact location see Fig. 3.3. Outcrop is 35m wide.

c) Detail of 0.7 x 2.0 m diameter siltstone clast interbedded in trough cross-bedded gravel (Gt), Hillsborough section. Siltstone clast can be seen at middle right in Plate 2b.

d) Detail of trough cross-bedded gravel (Gt) in Hillsborough section, showing a cross-section of a silicified log (above scale), and ?Mn-nodules lower centre left and right. For exact location see Fig. 3.3. Scale is 1 m long with 10 cm divisions.

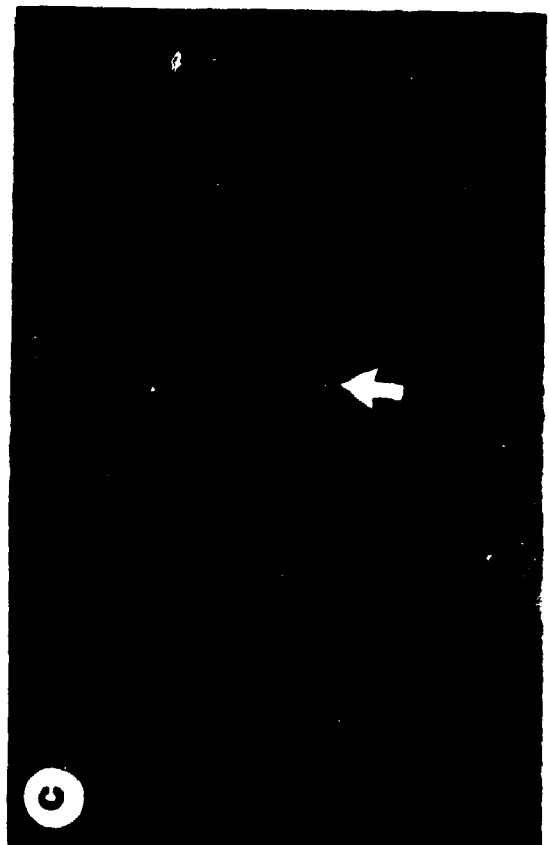
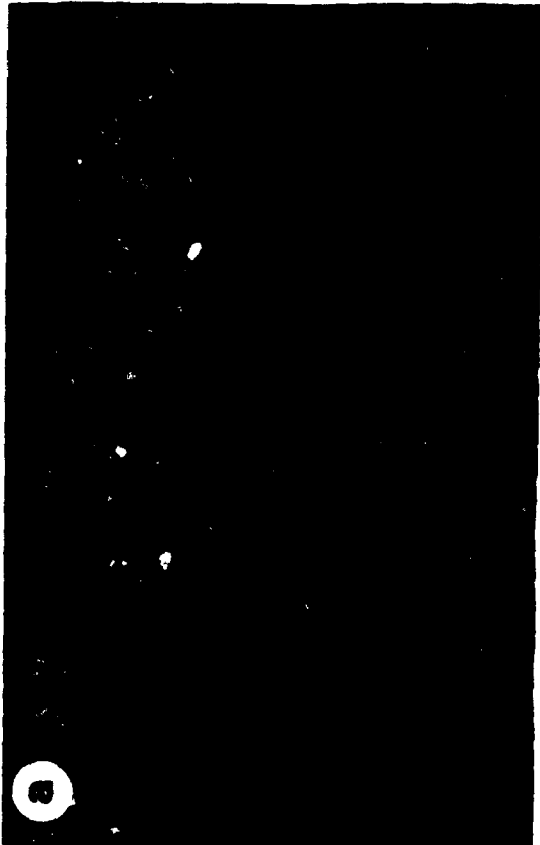
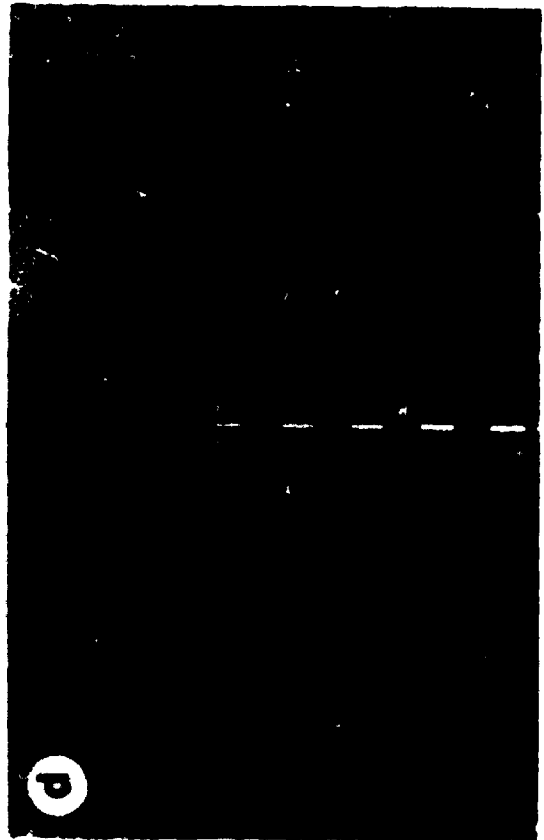
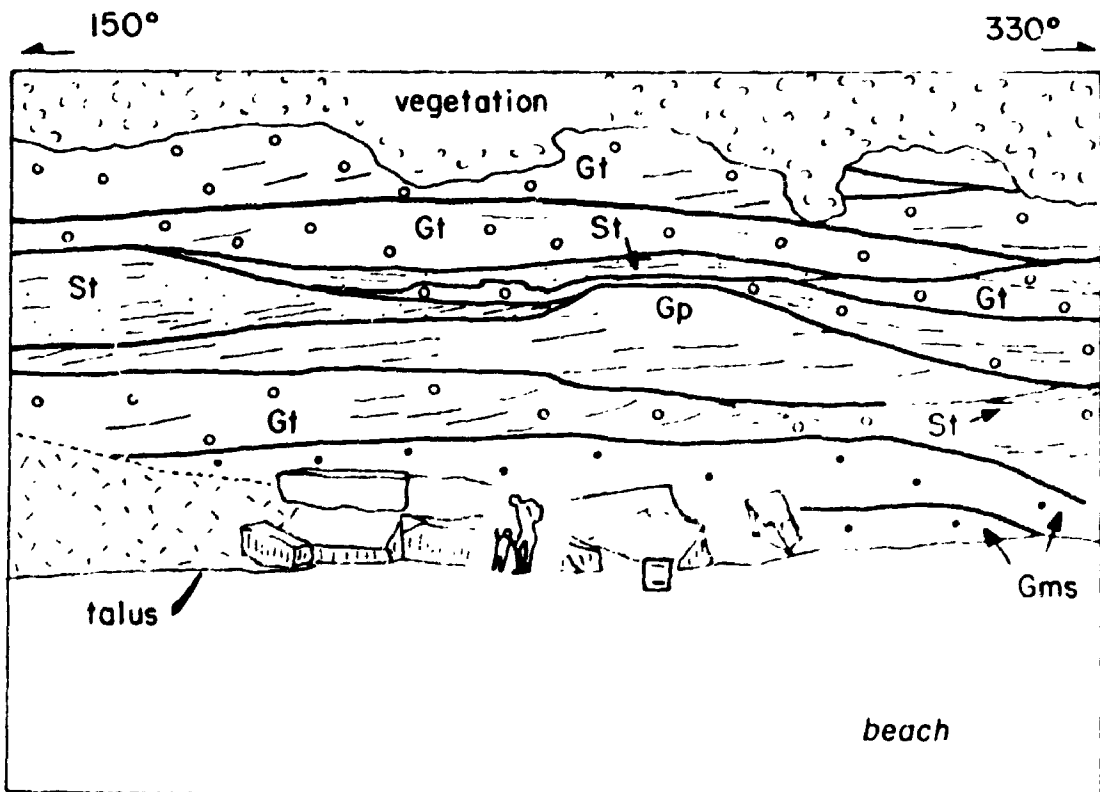
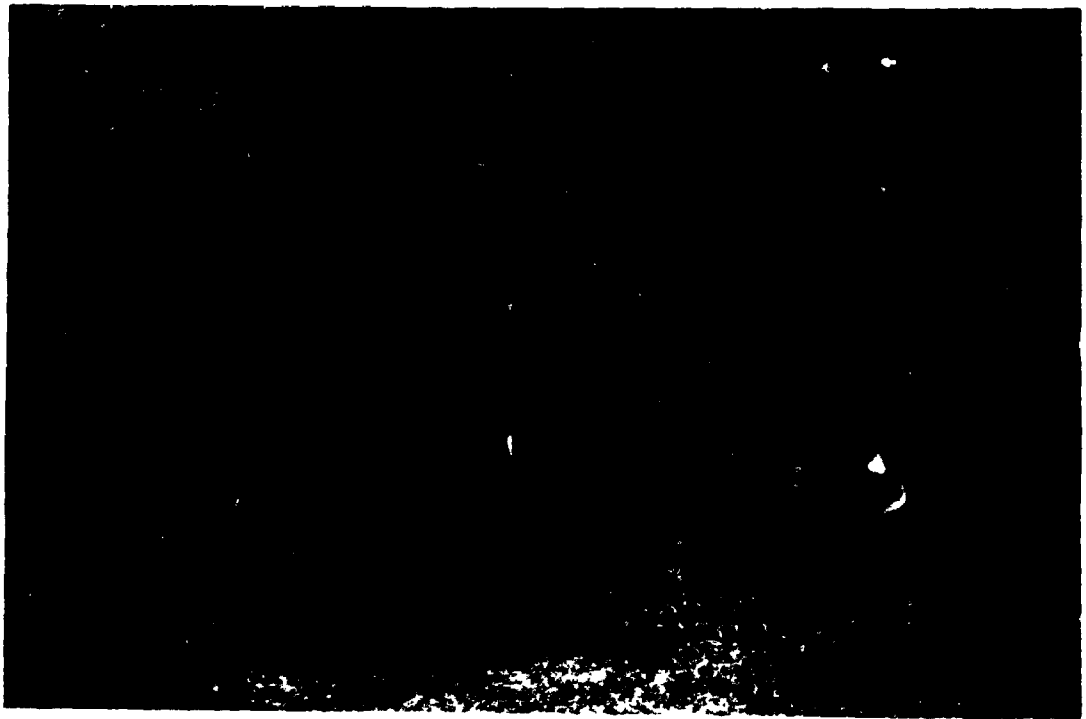


Plate 3

Southern end of Hillsborough section showing relationships between trough cross-bedded gravels and planar cross-bedded gravels. For location see Fig 3.3. Figures in middle foreground for scale.



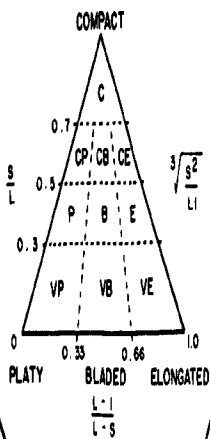
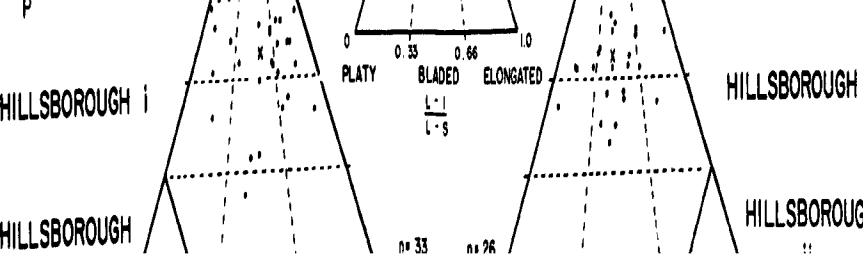
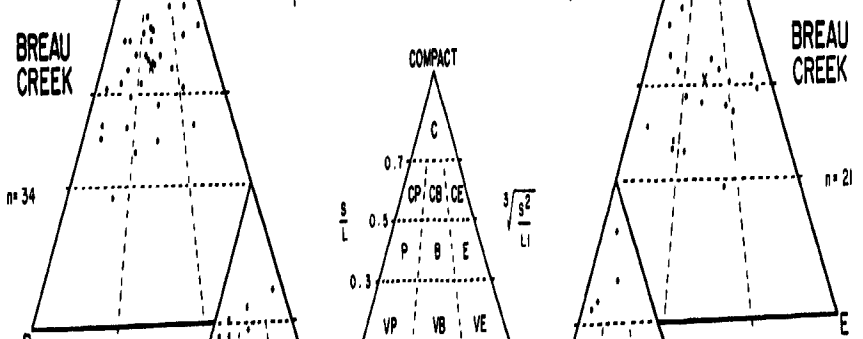
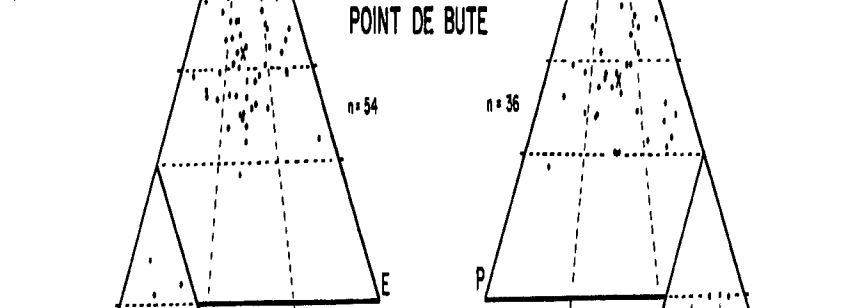
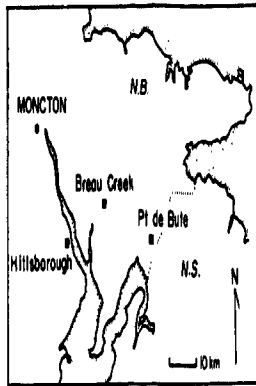
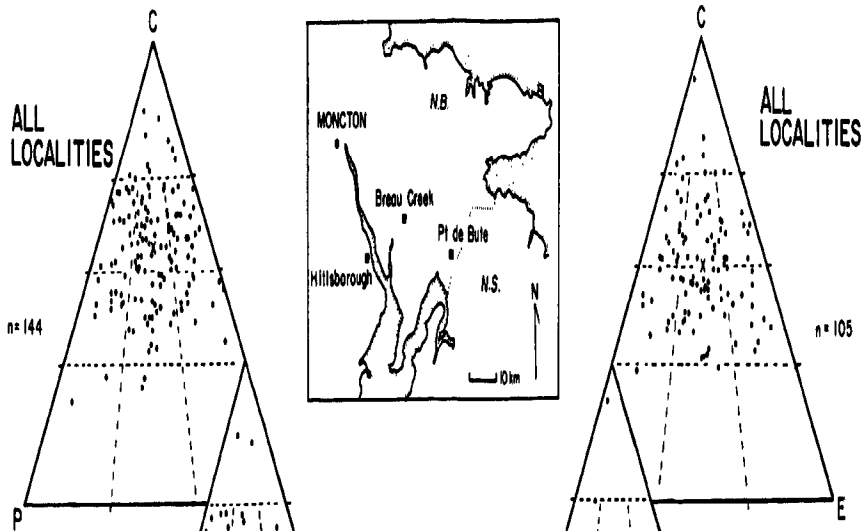
considerably, and locally the lithofacies approaches a pebbly sandstone (Ss) as described in Chapter 4. The matrix is poorly to moderately well-sorted, medium- to coarse-grained sand, similar to sandstone units of the Boss Point Formation as a whole. Black nodules up to 50 cm diameter, comprising sandy conglomerate are common throughout the lithofacies. Their similarity to the nodules that occur in sandstone units described by Mitchell (1986), suggests that they are likely to be Mn-cemented. Calcareous sandstone concretions up to 80 cm in diameter are common, as are large calcified logs with diameters up to 30 cm (Plate 2d).

For the purposes of characterising sphericity-form classes, pebbles were divided into 2 types: quartz and non-quartz (see below). Micrometer measurements of 249 pebbles from 4 sites were used to determine sphericity-form classes (after Sneed and Folk 1958, Folk 1974). Pebbles with one of the three axes less than 1 cm were omitted from the measurements because of difficulties in accurately measuring these smaller diameters. Quartz clasts are typically bladed, whereas other conglomerate lithologies tend to be cubic bladed, with lesser cubic elongate and bladed sphericities (Figs. 3.4 & 3.5). Both quartz and non-quartz clasts have similar sphericity, which tends to be cubic bladed and bladed, though there is a tendency for non-quartz clasts to be more bladed than the more equi-dimensional quartz clasts (Fig. 3.5). This

Fig. 3.4 Triangular diagrams of sphericity-form in trough cross-bedded gravels (Gt) from the Boss Point Formation at 4 localities (see inset map). The method used follows that of Folk (1974). For each diagram, the mean sphericity-form is indicated by a "x".

QUARTZ CLASTS

NON-QUARTZ CLASTS



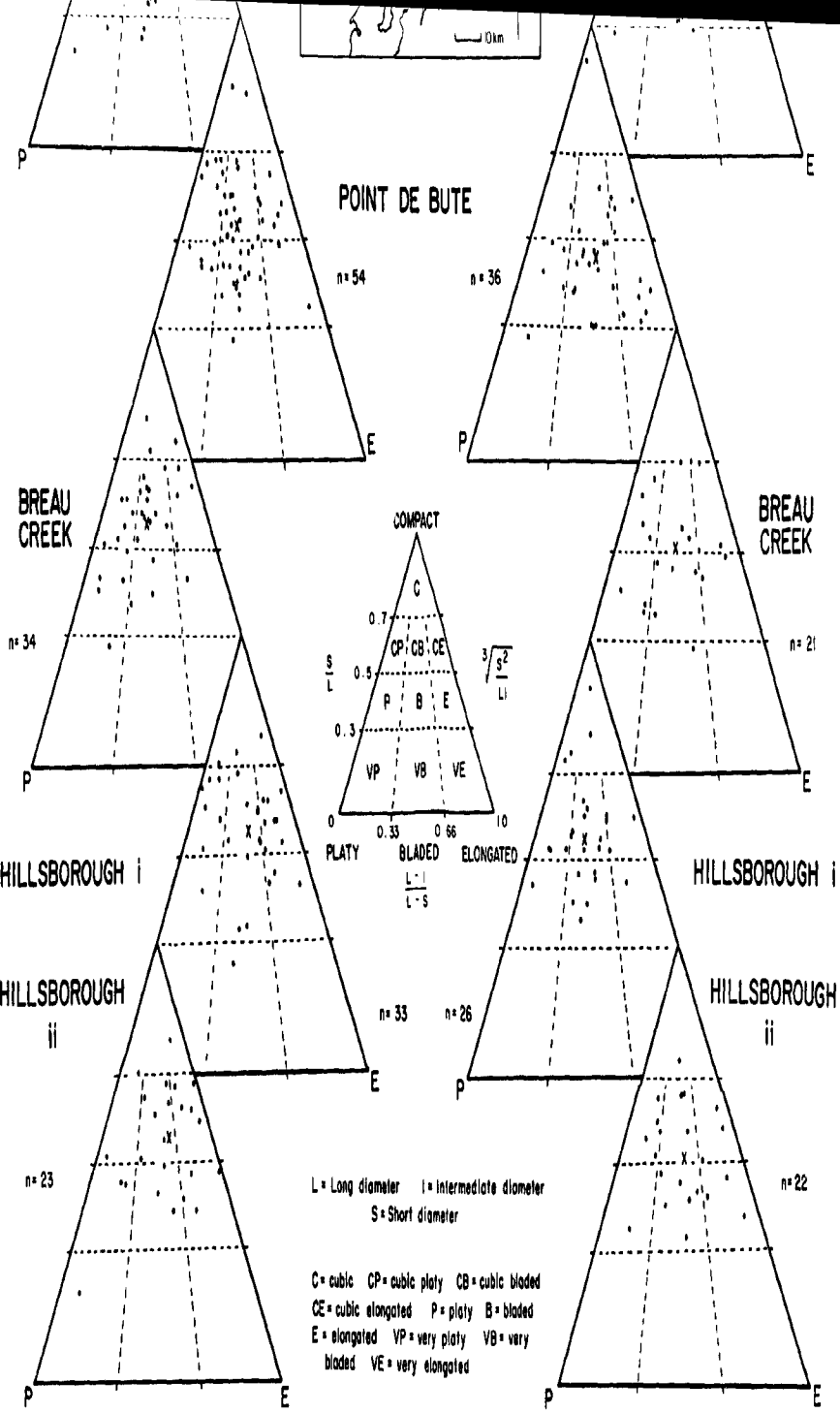
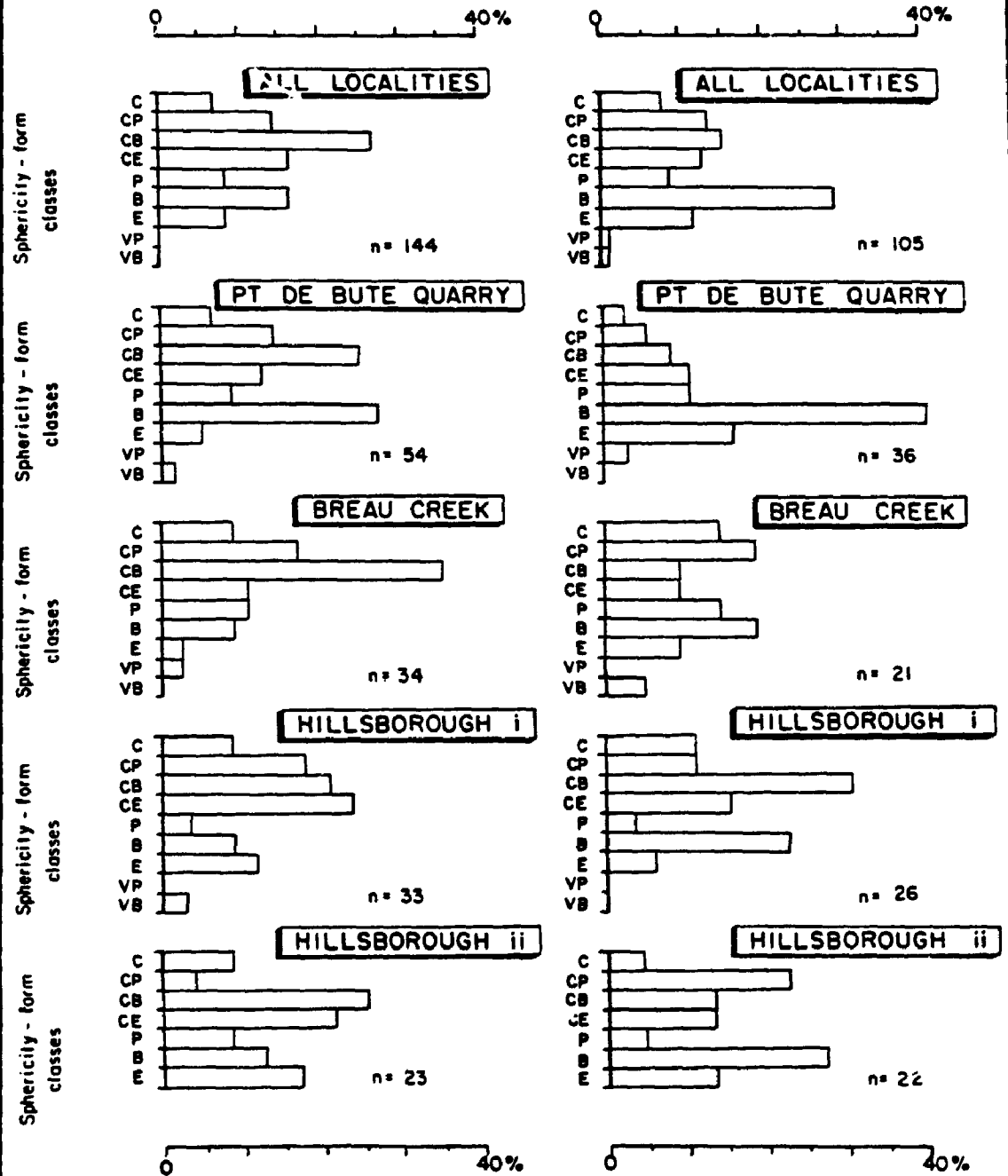


Fig. 3.5 Percentage of each sphericity-form class (based on data from Fig. 3.4) in trough cross-bedded gravels of the Boss Point Formation. For location of samples used, see inset map Fig. 3.4.

QUARTZ CLASTS

NON-QUARTZ CLASTS



is most likely a reflection on inherent inhomogeneities in the non-quartz pebbles such as cleavage and fractures, leading to a more bladed morphology.

Quartz and non-quartz clasts were plotted on an oblate-prolate (OP)/sphericity differentiation diagram, a method that has successfully distinguished fluvial and beach gravels (Dobkins and Folk 1958). Boss Point Formation samples from the 4 localities used in Figures 3.4 and 3.5 plot mostly in the fluvial part of the diagram (Fig. 3.6), although the percentage is only 58%, hardly significant considering that all clasts should fall into the "rivers" field of the diagram. Though often cited as a sedimentary environment discriminating technique (see for example Etheridge and Wescott 1984, Gale 1990), it is concluded that the Dobkins and Folk plot is of limited use in discriminating the depositional environment of Boss Point Formation conglomerates.

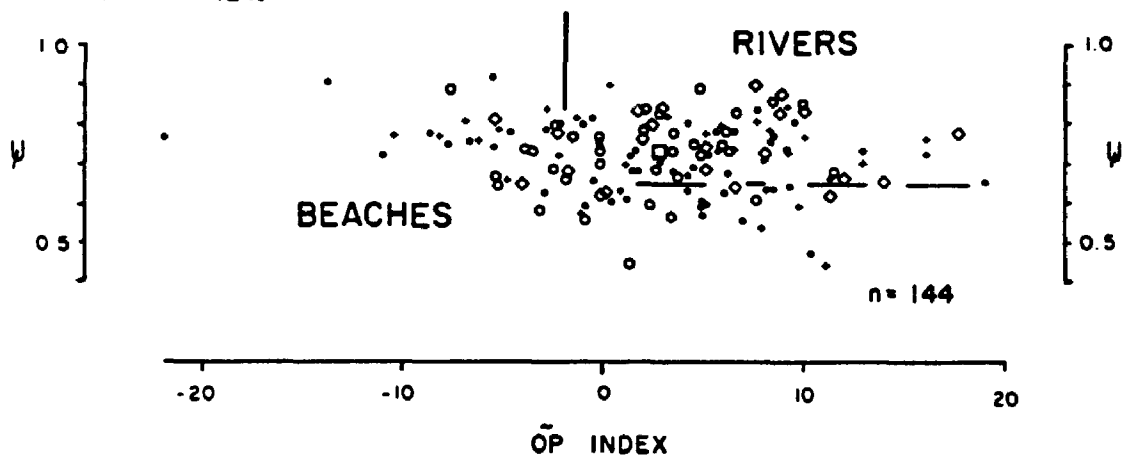
Conglomerate size range and composition were noted in lithologic logs (Volume II) and determined quantitatively at Hillsborough, Point de Bute Quarry and Malagash (Fig. 3.7) by point counting >300 clasts at 5 cm intervals along transects spaced 10 cm apart on outcrops. This analysis indicated that the dominant clast composition is quartz (60-67%), the proportions of other clast types differing at individual sample sites.

At Hillsborough significant amounts of greywacke (8.9%), red chert (5.6%), and rhyolite/dacite in

Fig. 3.6 Discrimination plot of river and beach gravels as devised by Dobkins and Folk (1958). Samples plotted are for trough cross-bedded gravels (Gt) as used in Fig. 3.4.

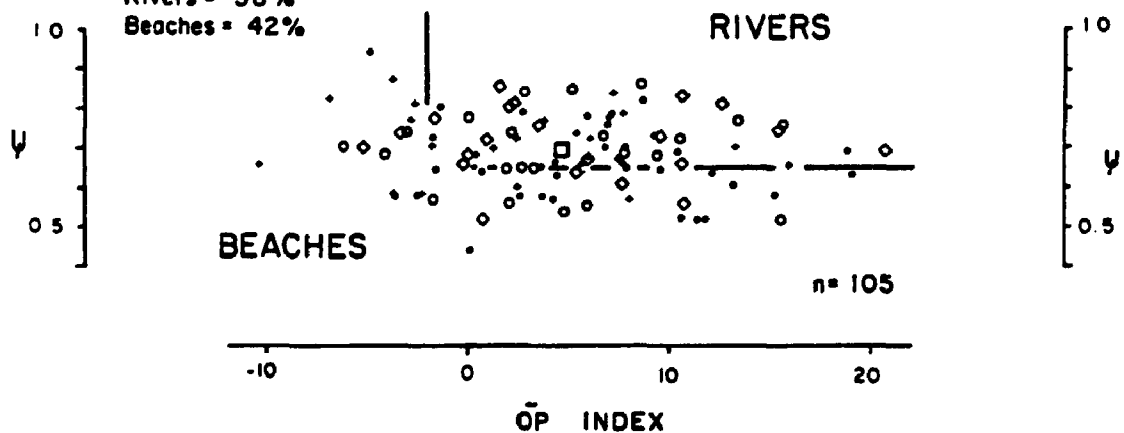
A. QUARTZ CLASTS

Rivers = 58%
Beaches = 42%



B. NON-QUARTZ CLASTS

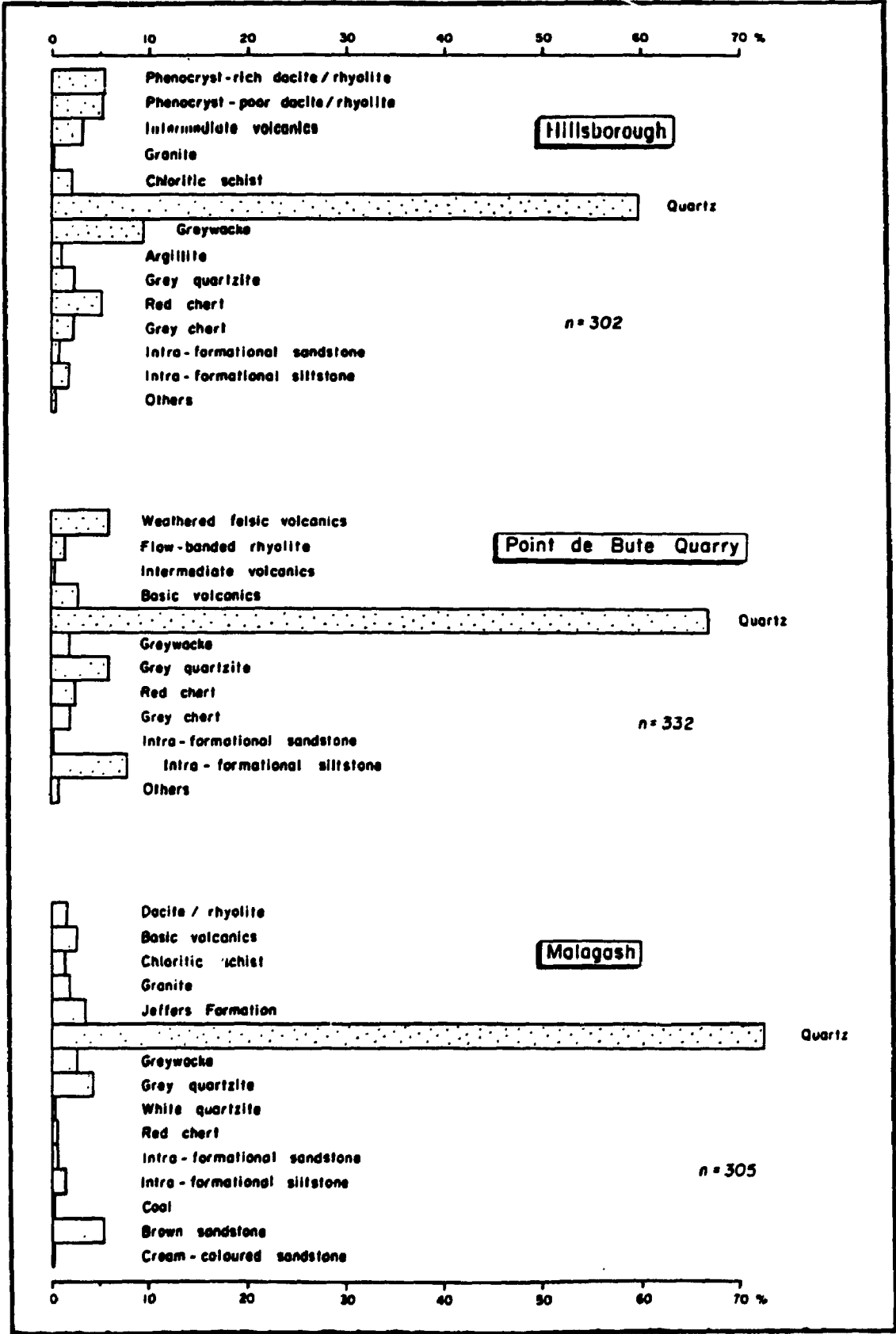
Rivers = 58%
Beaches = 42%



KEY

- Point de Bute quarry
- Breau Creek
- ◊ Hillsborough - locality i
- Hillsborough - locality ii
- ◻ Mean value for group

Fig. 3.7 Percentage of clast compositions from trough cross-bedded gravels (Gt) at 3 Boss Point Formation localities: Malagash, Point de Bute Quarry and Hillsborough. Stratigraphic sections 2, 6, and 12 respectively - see Fig. 1.2 for location.



phenocryst rich (5.6%) and phenocryst poor (5.3%) varieties occur. What is indicated as "grey quartzite" in Fig. 3.7 for Hillsborough and Point de Bute Quarry sites is a grey, very indurated, microcrystalline quartz with vitreous lustre and conchoidal fracture, not unlike silcrete (Langford-Smith 1978). No silcrete is known from the Boss Point Formation. These clasts may have been eroded from Boss Point Formation facies which are presently not exposed, or they may have been derived from older lithologies. At Point de Bute quarry, intraformational siltstone comprises an important proportion of the pebbles (Fig. 3.7), together with felsic volcanics (weathered dacite/rhyolite [6%] and flow-banded rhyolite [1.5%]). At Malagash, major accessory clasts in the conglomerates include brown sandstone (5.6%) presumably an older Devonian-Carboniferous lithology such as the Fountain Lake Group or Millville formation. Distinct green coloured, metavolcanic and metasedimentary clasts recognisable as part of the Jeffers Formation (Donohoe and Wallace 1982) comprise 3.6% of clasts at Malagash. The "grey quartzite" (6%) at this site contains quartz grains, and although they could also be silcrete with brecciated fabric, it is more likely that they are quartzite in the more conventional sense.

A quartz dominated petrology has previously been reported from the formation, van de Poll (1966, 1970) indicating approximately 80% of clasts being sedimentary

and metamorphic quartz, while the remainder are rhyolite and minor andesite (van de Poll 1966, fig. 7), or rhyolite and miscellaneous clasts (van de Poll 1970, fig. 9).

The abundance of felsic volcanic clasts at both Hillsborough and Point de Bute Quarry (approximately 10% of clasts at each site) indicates close proximity of dacite/rhyolite volcanic rocks. Today, these rocks are generally lacking in the source areas for the conglomerates. Acid volcanics are rare in the Caledonia Highlands (Ruitenberg et al. 1979) and are not known from the Westmoreland High. The geology of these areas is now dominated by 'deep-seated' rocks, principally schists and granitoids (Caledonia Highlands) and granite (Westmoreland High). The petrology of the Boss Point Formation conglomerates strongly suggests that during Carboniferous times, felsic volcanic edifices were being eroded; today only the plutonic equivalents of these felsic igneous rocks (such as Calhoun's granite quarry, Memramcook) are exposed. The comparative lack of granite and schist clasts in Boss Point Formation conglomerates supports such a premise.

In most cases, the cross stratification in the conglomerates tends to be poorly displayed, sets ranging between 30 and 120 cm thick. Foresets dip at consistent angles of 15 - 20° (Plate 2a). Paleocurrent directions from the lithofacies are consistent with the paleocurrents determined from trough cross-beds in the interbedded

sandstones (Figs. 3.8a and 3.8b) and from trough cross-bedded sandstones in the entire Hillsborough section (Fig. 3.8h). Although the number of data are limited, trough cross-beds in the conglomerates show a paleoflow directed to the north and east (Fig. 3.8e).

3.1.2 Interpretation

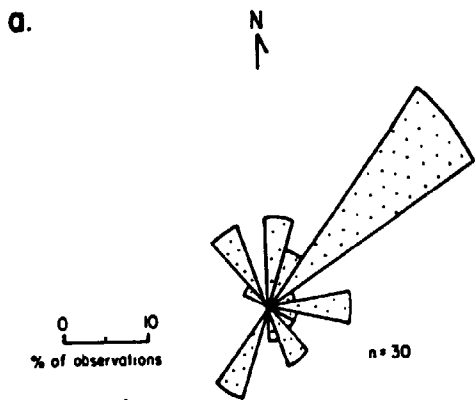
The trough cross-bedded conglomerates are interpreted as coarse bedload braided channel deposits. They are similar to distal gravelly braided fluvial deposits described by Fahnestock and Bradley (1973), Rust (1981), Kraus (1984), Middleton and Trujillo (1984) and Morison and Hein (1987).

The trough cross-bedded nature indicates that the conglomerates moved as coarse bedload within channels, and a high flow velocity or high shear stress braid channel is inferred (cf. Rust and Koster 1984). Such channels were likely to have been at least 100 m wide given the size of channelised geometries shown in the cliff-face exposures at Hillsborough (Fig. 3.3). The abundance of sandy matrix, and the general lack of clast support suggests that flows contained abundant sand as suspended or bedload.

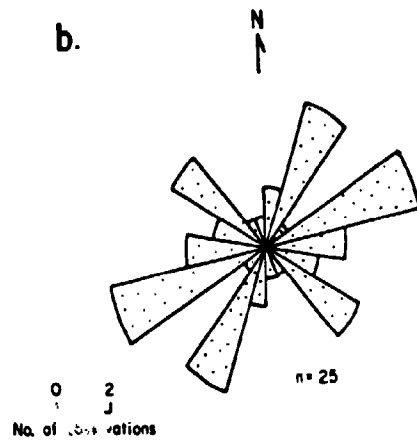
Channelised conglomerates similar to the Boss Point Formation units, described by Ramos and Sopeña (1983) were interpreted as lateral channel deposits adjacent to

Fig. 3.8 Paleocurrent directions for Boss Point Formation
gravels and sandstones at Hillsborough.

Foresets - Trough Cross-Bedded Sandstone (St)
Hillsborough



Logs - Trough Cross-Bedded Sandstone (St)
Hillsborough

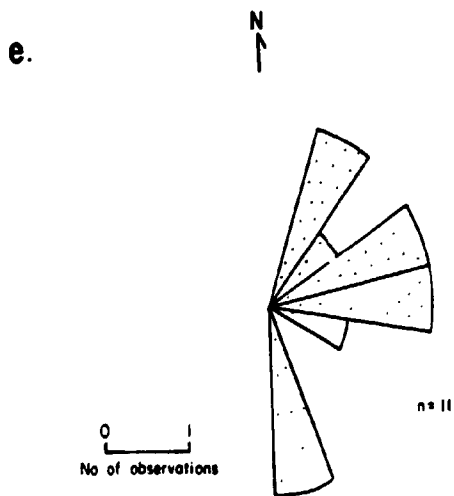


Cross-Beds

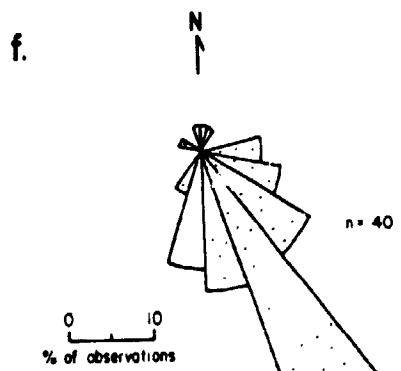
c.

0
No. of observations

Foresets - Trough Cross-Bedded Gravel (Gt)
Hillsborough



Fabric - Planar Cross-Bedded Gravel (Gp)
Hillsborough

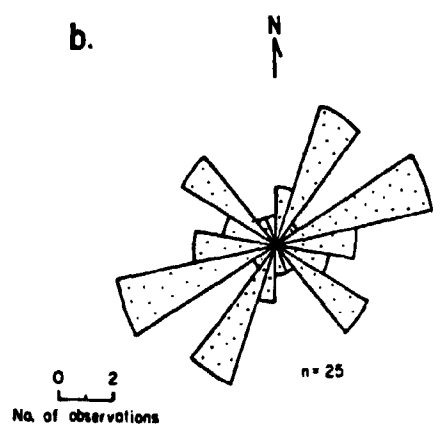


Fab

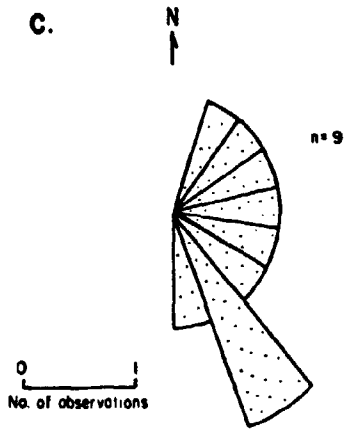
g.

0 10
% of observations

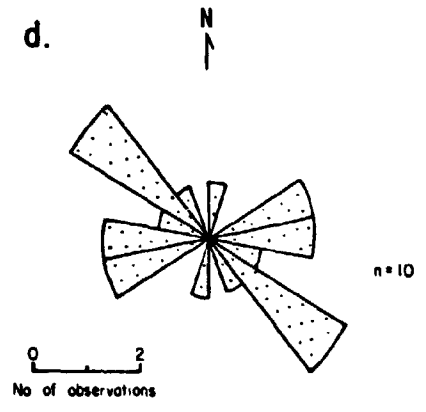
(St) Logs - Trough Cross-Bedded Sandstone (St) Hillsborough



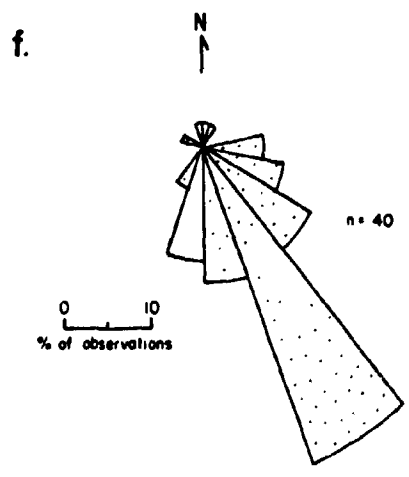
Cross-Beds - Planar Cross-Bedded Gravel (Gp) Hillsborough



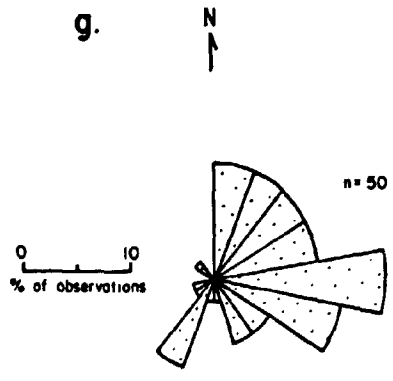
Logs - Planar Cross-Bedded Gravel (Gp) Hillsborough



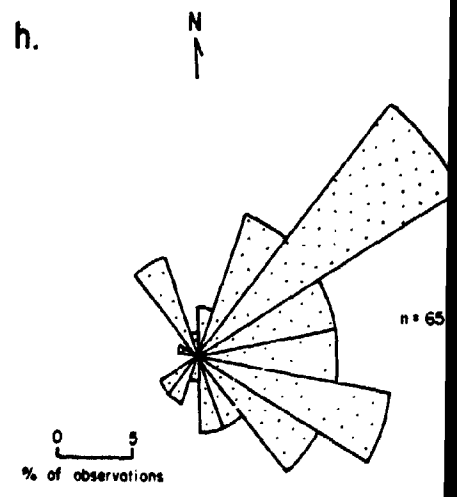
(Gt) Fabric - Planar Cross-Bedded Gravel (Gp) Hillsborough



Fabric - Massive Gravels (Gms) Hillsborough



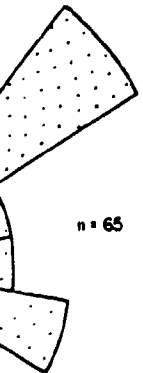
Foresets - Trough Cross-Bedded Sandstone (St) Entire Hillsborough Section



Gravel (Gp)

n = 10

Bedded Sandstone
Section



n = 65

longitudinal bars (cf. Eynon and Walker 1974). The close similarity between the conglomerates described by Ramos and Sopeña to those in the Boss Point Formation suggests a similar origin. This, together with the association of the conglomerates with planar cross-bedded (Gp) and massive conglomerates (Gms) in the Boss Point Formation, units which are interpreted as bar-formed gravels (see below), suggests that the trough cross-bedded, scour-based gravels, developed in channels adjacent to bars.

Although paleocurrent data are limited, trough cross-bedding indicates that flow directions in these Gt dominated channels were generally to the north and east, consistent with paleocurrent measurements in trough cross-bedded sandstone units. The source of the coarse-grained bedload material must have been local, both because of its coarse-grain size, and lack of conglomerate beds in central parts of the sedimentary basin. It is suggested that either local faults were active during sedimentation (see Chapter 9, Martel 1987), or that the Westmoreland High (Fig. 2.4) was growing as an arch during deposition.

3.2 Planar Cross-Bedded Gravel (Gp)

3.2.1 Description

Planar cross-bedded gravels comprise 0.4% of the thickness of the Boss Point Formation (Fig. 3.1c, Appendix

I). The lithofacies is confined to the Hillsborough section (Fig. 3.2, Appendix Id), where a total of 27 m of planar cross-bedded gravels occur (stratigraphic section 12).

The conglomerates form bedded units as much as 15 m thick (Fig. 3.1d) with a mean thickness of 2.2 m (Fig. 3.1e). Foresets dip at angles up to 30°. The lithofacies is composed of granules to pebbles with a variable proportion of poorly-sorted medium-grained sandstone matrix. The clasts are generally well rounded to rounded, and both matrix and clast supported fabrics are present. The lithofacies commonly contains calcified log debris.

The bases of beds are typically sharp with minor erosional relief; the tops are commonly eroded by overlying trough cross-bedded gravels (Gt) and sandstones (St). The lithofacies is interbedded with decimetre to 4 m thick trough cross-bedded gravels (Gt), massive gravels (Gms), trough cross-bedded sandstones (St) and rare laminated sandstones (Sl) and mudrocks (Fm). Black-stained (Mn-rich) and calcareous cemented concretions up to 30 cm diameter are common throughout the conglomerates.

The conglomerates have easterly and southeast dipping foresets and log orientations (Figs. 3.8c & 3.8d); directions which deviate approximately 60° from paleocurrents determined from trough cross-bedding in conglomerates and sandstones (Figs. 3.8a-d). Pebbles are commonly aligned; measurements at Hillsborough for example

show that the long axes (fabric) of clasts dip towards the southeast (Fig. 3.8f). This orientation is at variance with the paleocurrent determinations made from foresets and log orientations (Figs. 3.8c & 3.8d). This anomaly may best be explained if the pebbles are lying in the plane of large foresets, rather than as an imbrication fabric *per se*, much as Hart and Plint (1989, fig.4) have explained from the Cardium Formation, and as recognised from experimental studies by Carling (1990).

3.2.2 Interpretation

The planar cross-bedded gravels of the Boss Point Formation are similar to conglomerates described by Eynon and Walker (1974), Smith (1974), Gustavson (1978), Ramos and Sopeña (1983), Steel and Thompson (1983), Rust (1984) and Billi *et al.* (1987). The lithofacies is interpreted as a bar facies, and a number of barforms may be considered.

Rust (1978) concluded that planar cross-stratified gravels in the Malbaie Formation resulted from falling stage modification of the downstream margin of longitudinal bars. Ramos and Sopeña (1983) have interpreted planar cross-bedded gravels in terms of the migration of transverse bars during periods of low water and sediment discharge. Miall (1978) concluded that planar cross-stratification was produced by linguoid bars,

whereas in the 'Bunter' Pebble Beds, planar cross-stratified gravels overlain by horizontally bedded conglomerate were interpreted to be medial bars (Steel and Thompson 1983). It is concluded that a bar morphology (cf. Smith 1974, Bluck 1979, Church and Gilbert 1979) is consistent with the orientation of foresets oblique (at up to 60°) to the main channel flow direction (cf. Smith 1974, Ferguson and Werritty 1983, Hein 1984).

The predominance of east and southeast dipping foresets in the Boss Point Formation exposures indicates that such bars grew consistently toward the east. To explain this, it is probable that the Hillsborough exposure is only through a cross-section of one channel bend, the beds must dip the other way at the next bend.

3.3 Massive Gravel (Gms and Gm)

3.3.1 Description

Massive gravel units comprise 1.7% of the thickness of the Boss Point Formation (Fig. 3.1c, Appendix I). They tend to occur in the northern parts of the study area, such as at Aulac, Point de Bute Quarry, and in the Sackville area (Fig. 3.2, stratigraphic sections 6 and 8), though significant thicknesses occur at Giffin Pond in the south of the study area (Fig. 3.2, stratigraphic section 26). They form beds up to 7.5 m thick (average thickness

0.4 m, Fig. 3.2) and in all cases are sharp based (usually scoured). At Hillsborough, the base of a massive gravel shows irregularly shaped, erosional lobes that cut into the underlying sandstone to a depth of 20 cm below the base of the main conglomerate unit (Plate 4).

Clasts range in size from 1 to 10 cm, and are well rounded to sub-angular. Most clasts are supported by a coarse-grained poorly sorted sandstone matrix (Plate 4b). Clast supported fabrics occur especially where clasts are large, and for this reason both Gms (predominant) and Gm classes of Miall (1978) and Rust (1978) are recognised. An inclined pebble fabric, although not common, is crudely developed in some beds (Plate 4c).

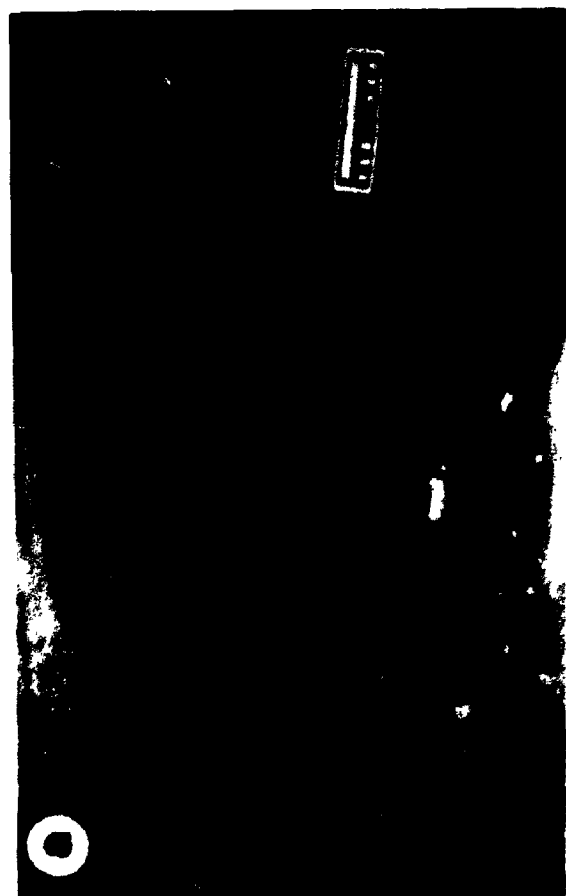
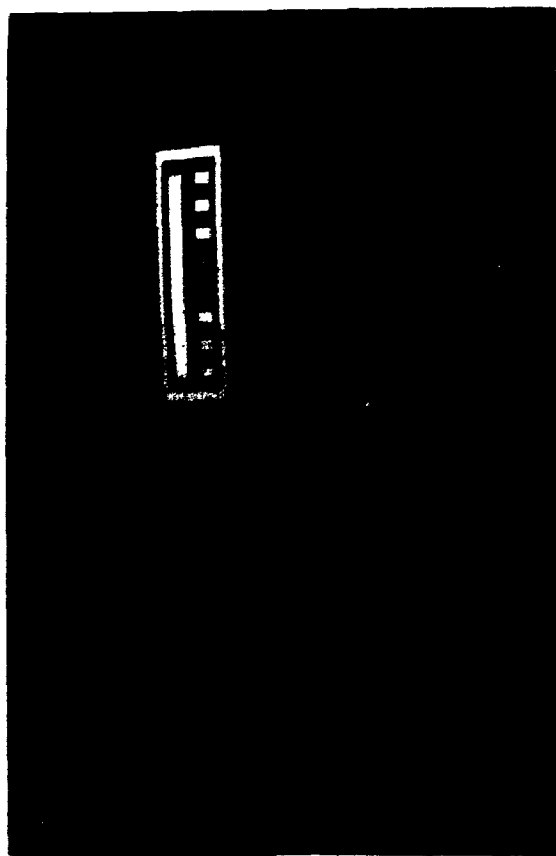
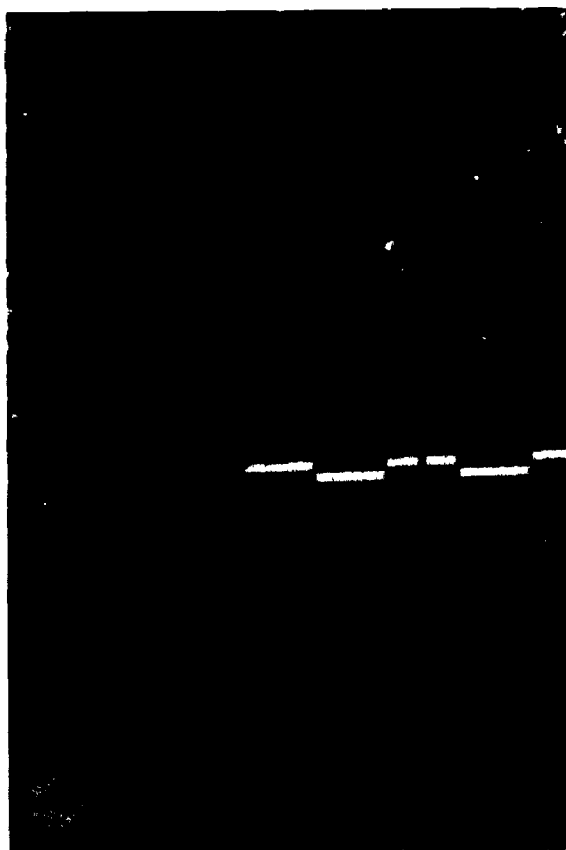
Massive conglomerates are dominated by quartz and their composition appears similar to that of the trough cross-bedded conglomerates described above. However at Giffin Pond, considerable quantities of basalt, derived locally from the Precambrian Coldbrook Volcanics occur. Petrologic data for massive conglomerates at Giffin Pond is similar to that described for gravelly sandstones (Ss - see Chapter 4). No quantitative petrological analyses were performed on the lithofacies.

3.3.2 Interpretation

The Boss Point Formarion massive conglomerates are similar to the matrix supported conglomerates described by

Plate 4

- a) Erosive base of massive gravel (Gms) at Hillsborough (for location see Fig. 3.3) showing irregular shaped erosional lobe extending 20 cm into underlying sandstone.
- b) Typical outcrop of massive gravel (Gms) at Hillsborough showing matrix and clast supported fabric. For location see Fig. 3.3. Scale is 50 cm long with 10 cm divisions.
- c) Massive gravel (Gms and Gm) at Point de Bute Quarry showing a crude inclined pebble fabric (toward bottom right). Scale is 50 cm long with 10 cm divisions.
- d) Breccia unit at River John, Nova Scotia.



Eynon and Walker (1974), Ramos and Sopeña (1983) and Middleton and Trujillo (1984). Massive, matrix supported conglomerates formed in subaerial settings are commonly interpreted as cohesive debris flow deposits (Nemec and Steel 1984), those with clast support fabrics interpreted as non-cohesive debris flows (Miall 1978, Nemec and Steel 1984). The well developed rounding and moderate sorting of Boss Point Formation clasts however, rules out debris flow as a transport mechanism; instead the textural maturity of the Boss Point Formation lithofacies suggests deposition from a subaqueous, in-channel flow (cf. Middleton and Trujillo 1984). In fluvial settings, massive gravels are commonly interpreted as longitudinal bars (Rust 1972, 1975, Boothroyd and Ashley 1975, Ramos and Sopeña 1983) or as lag or sieve deposits (Miall 1978, Rust 1978).

The close association of the massive gravels with the trough (Gt) and planar cross-bedded gravels (Gp) suggests that all three facies relate to bar and adjacent channel development, and in the case of the massive gravels, are interpreted as forming the internal parts of bars (cf. Eynon and Walker 1974). Many studies have shown that massive and crudely stratified conglomerates are deposited at high flow stage in bars, and not by avalanching on the lee sides or lateral flanks of bars (Leopold and Wolman 1957, Smith 1974, Hein and Walker 1977).

The three conglomerate lithofacies, and the

interbedded trough cross-bedded sandstones (Fig. 3.3) conform closely with a Donjek type fluvial succession as described by Miall (1977, 1978) and Rust (1978).

3.4 Breccia (Gms and Gm)

3.4.1 Description

A single breccia bed is recognised from the River John section in Nova Scotia (Plate 4d; stratigraphic section 1). The bed is 60 cm thick and occurs 4.3 m above the base of the formation. Basal and top contacts are sharp and slightly irregular with <5 cm relief. Clasts are up to 5 cm diameter (mean= 1-2 cm) and are compositionally similar to breccia units in the underlying Millsville formation (see Fralick 1981). Both clast and matrix support occurs.

3.4.2 Petrography

The breccia bed was not sampled; full details of clast petrography are given by Fralick (1981). Compositionally the Boss Point Formation breccia is similar to breccia units from the upper part of the Millsville formation. In thin section, these breccias are dominated by rounded greywacke clasts, with less abundant sub-rounded and rounded quartz, schist and basalt rock fragments, cemented

by spar.

3.4.3 Interpretation

The lack of stratification, clast alignment or imbrication, the large proportion of sand matrix and the angularity of clasts suggest deposition from a cohesive debris-flow. A proximal source area is suggested by the angularity of the clasts. Deposition on an alluvial fan, adjacent to active faults (generating fanglomerate) has been suggested for the Millsville formation (Fralick 1981, Boehner et al. 1986), and similar conditions are likely to have prevailed locally during deposition of the lowest parts of Boss Point Formation.

The upward decrease in breccia clast size within the Millsville formation was inferred by Fralick (1981) to reflect

- waning fault activity with time,
- or transition from fan-head to mid-fan and finally outer-fan depositional sites with time. This may have been a consequence of migration of the distributary channel(s) with time, either through avulsion or by strike-slip movement on the adjacent fault(s).

Because of the abundance of trough cross-bedded sandstone at River John, it is likely that at this site the Boss Point Formation represents an outer-fan or proximal braided river setting (Rust and Koster 1984), more distal

in relation to fault blocks than the Millsville formation, and only occasionally influenced by cohesive debris flows which introduced coarse-grained breccia.

CHAPTER 4

SEDIMENTOLOGY OF SANDSTONE UNITS

The great majority of the Boss Point Formation (77.3% of the total thickness) comprises fine-grained sandstone lithologies (Fig. 3.1a, Appendix I). Most are light to medium green-grey and blue-grey in colour, though distinctive red and reddish grey sandstones do occur. Grey coloration is attributed to reducing conditions that existed when the water table was high; the less common red coloration resulted from oxidising conditions formed when water tables were low.

4.1 Trough Cross-Bedded Sandstone (St)

4.1.1 Description

The most abundant lithofacies of the Boss Point Formation is trough cross-bedded sandstone (Fig. 3.1c, Appendix I). In all areas the lithofacies consistently forms between 55 and 70% of the formation (Fig. 3.1b).

Four levels of bedding hierarchy are recognised within the lithofacies, and these are divided into 2 major classes; small-scale and large-scale bedding hierarchies. At the smallest scale are trough cross-bedded sets forming

cosets. Cosets can be traced for distances up to 50 m and are typically 1-2 m thick (Fig. 3.1), with sets in the range 50 to 120 cm thick being common (Fig. 3.1). Large-scale bedding hierarchies consist of channel-fill units marked by large-scale, commonly >1 metre deep scours which cut cosets. Together, the small- and large-scale bedding hierarchies form stacked sandstone successions several 10 s of metres thick, and usually constitute the prominent reef-forming coastal exposures of the formation (Plate 5a). These bedding hierarchies are described below.

Small-Scale Bedding Hierarchy Description

The sandstones that comprise the trough cross-bed sets are a uniform medium green-grey, noncalcareous and less commonly calcareous, well sorted fine- to lower medium-grained sandstone (Plate 5b). Locally the colour varies to blue-grey and reddish grey hues. Grain size varies locally, up to coarse-grained sand. Foresets dip at angles up to 30°, but are more commonly in the range 15 to 20°. Reactivation surfaces are common. Sandstones typically contain carbonaceous debris ranging in size from comminuted fragments to branch-size and log material (Plate 5c); often the logs are calcified, and may be associated with sulphur efflorescence and pyrite. Log debris include the lycopods *Calamites*, *Lepidodendron*, and *Sigillaria*.

Sandstones contain varying amounts of angular to well

Plate 5

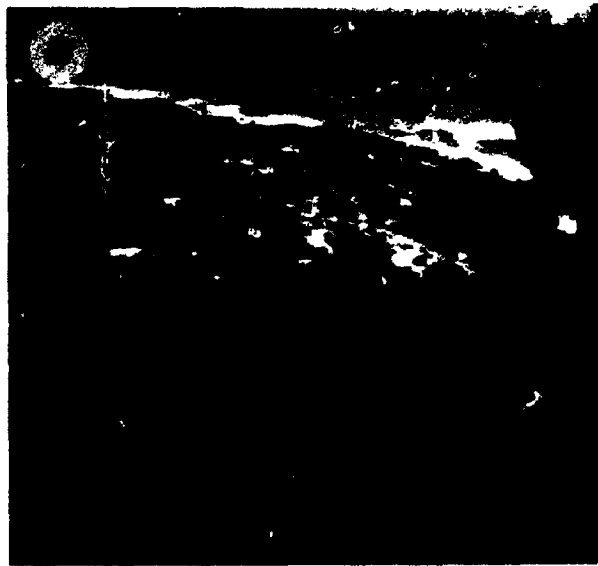
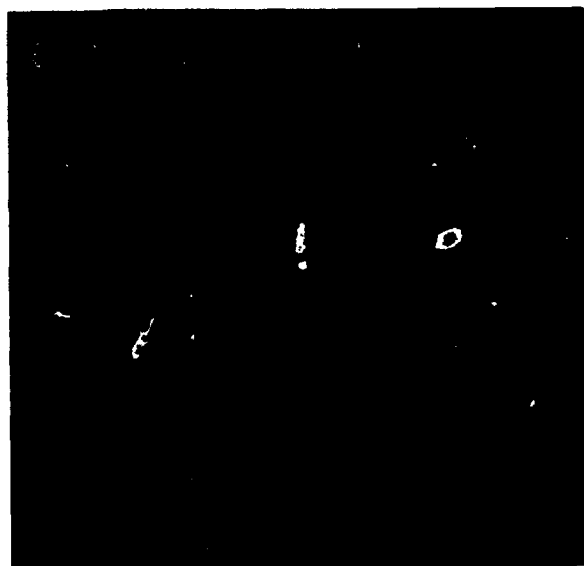
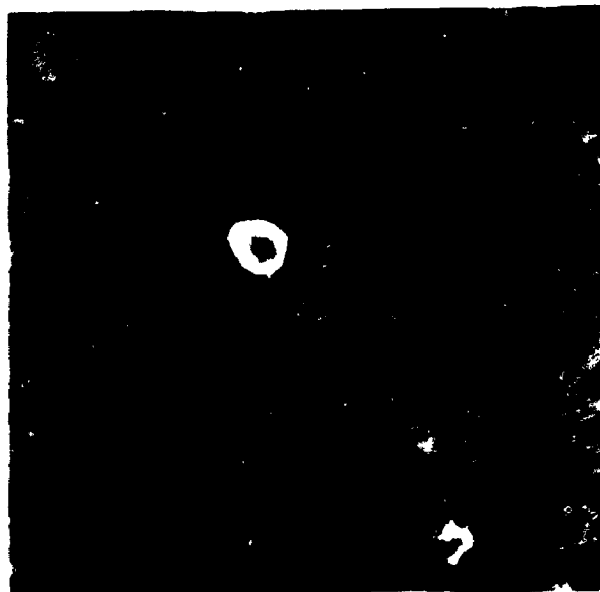
a) Aerial photograph of the shore platform at Boss Point (succession dips approximately 30° S toward upper right), showing the alternating stacked sandstone units interbedded with thinner mudrock units (usually forming small bays). Together these units define megacycles. Note that sandstone units consist of sandstones with little interbedded fine-grained sediment. The sandstones consist of a series of trough cross-bedded units stacked on top of each other, and separated by large scale erosional surfaces. Several such erosion surfaces occur in this image (small arrows). The bases of these sandstone successions are either erosive (large arrow), or planar with respect to the underlying mudrocks. Tops of sandstones are typically sharp and planar with overlying mudrocks. Scale bar is 100 m.

b) Trough cross-bedding preserved on the top of a bedding surface, south shore of Grindstone Island. The paleocurrent was away from the observer in the direction of the scale. Scale is 50 cm with 10 cm divisions.

c) Logs (some with roots) on top of bedding plane exposure at Long Island. Scale bar (bottom left) is 50 cm with 10 cm divisions.

d) Aerial photograph of eroded base of a stacked cross-bedded sandstone succession at Slacks Cove West (arrowed). Rocks dip 50° toward the south (top of photo). Scale bar is 50 m.

e) Photo at the base of stacked sandstone succession at Slack Cove West, showing the extent of erosion (10 m) of underlying siltstone units (arrowed). View is the same locality as shown in Plate 5d). Sandstone shore platform at upper centre is approximately 50 m wide.



rounded light and medium blue-grey siltstone clasts (typically less than 10 cm diameter), some of which display fluted margins and well-developed rill marks (see van de Poll and Patel 1981, Flint 1986, van de Poll and Patel 1990), and less common siderite (<5 cm diameter), quartz, volcanic and granitic clasts (<3 cm diameter). In places granule-size material is so abundant that the lithology is transitional into pebbly sandstones (lithofacies Ss) described below (section 4.8).

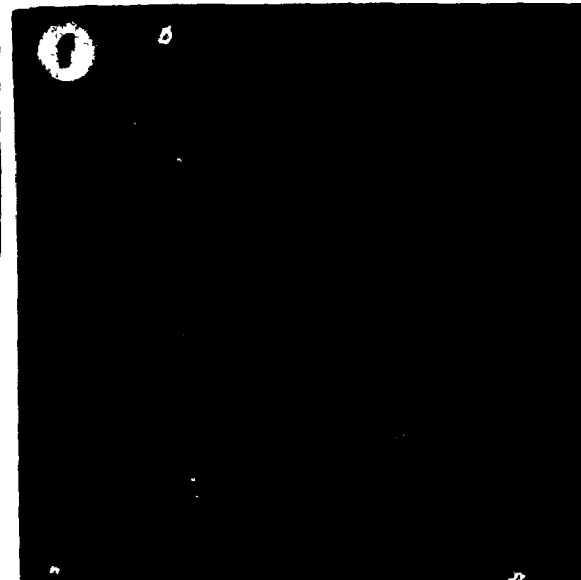
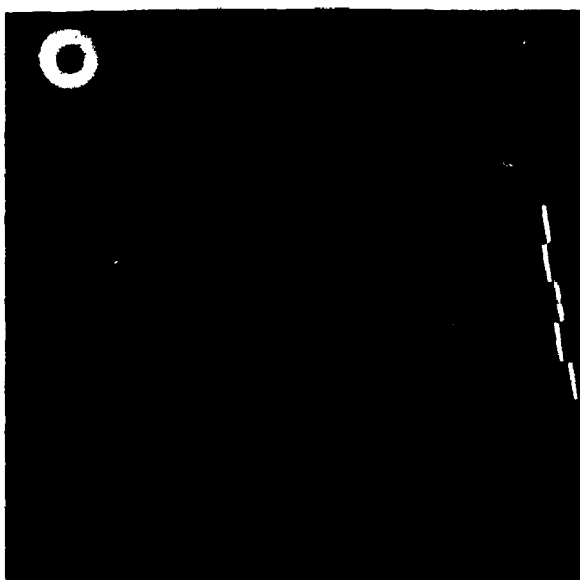
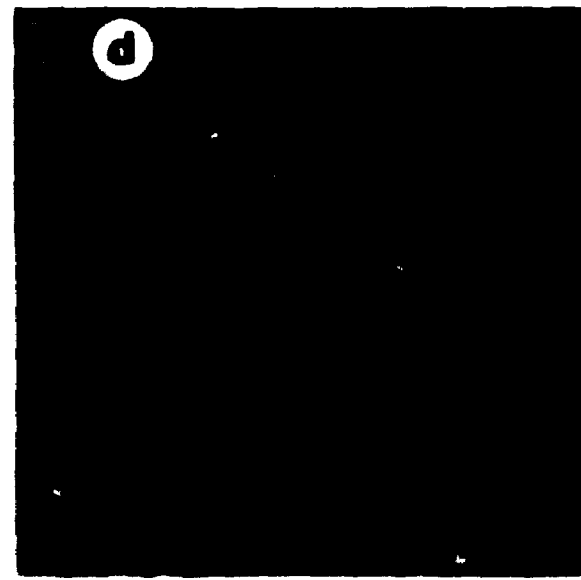
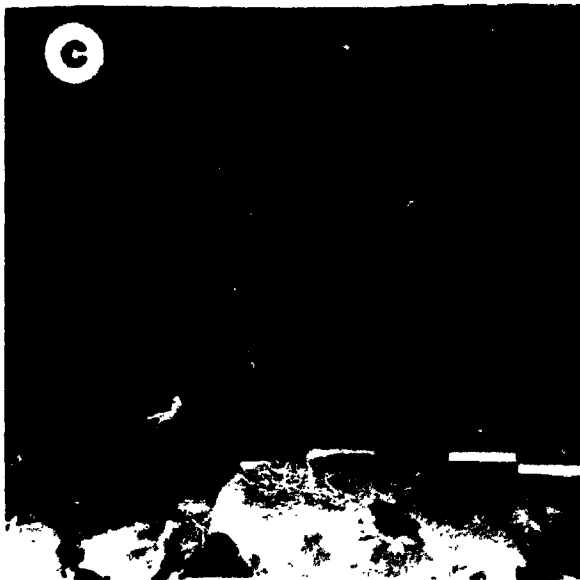
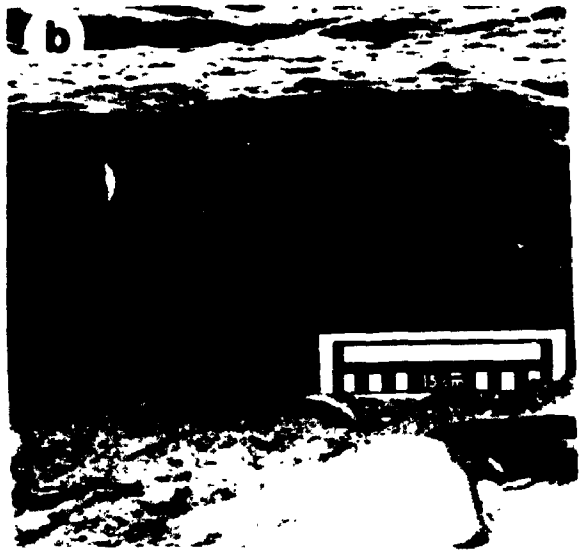
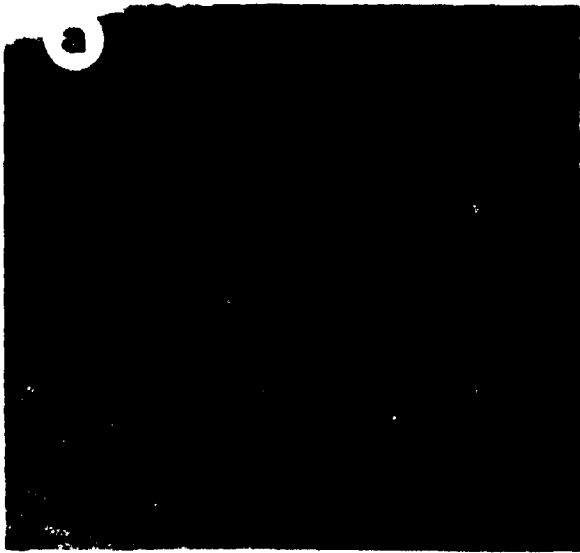
Calcareous sandstone concretions up to 1 m diameter, and <30 cm diameter dark, Mn-rich nodules are common in all sections. The concretionary carbonate occurs both as small intergranular pore-filling and as larger crystals up to 2 mm diameter. Staining with potassium ferricyanide and Alizarin Red S produced no colour change, indicating that the carbonate is dolomite. Both concretions and nodules have previously been described by Mitchell (1986).

The bases of sandstone cosets are in virtually all cases sharp and erosional with underlying units. The scale of erosion varies from a few millimetres to large scale scours, as much as 10 m deep (Plate 5d & 5e). The base of sandstone beds typically preserve flute casts (Plate 6a- see Chapter 5) and in rare cases show obstacle marks (Plate 6b). At Slacks Cove East the base of a trough cross-bedded sandstone shows a transition over a few centimetres from small flutes, changing into rills (Plate 6c).

Load casts may occur where sandstones overlie mudrocks.

Plate 6

- a) Small scale flutes developed at the base of a sandstone bed at Two Rivers. Lens cap is 50 cm diameter.
- b) Obstacle marks at the base of a trough cross-bedded sandstone at Marys Point.
- c) Base of a trough cross-bedded sandstone, Slacks Cove East, showing a transition from flutes (upper right) into rills (at left). Scale is 50 cm with 10 cm divisions.
- d) Load structures preserved on the base of a 90 cm thick sandstone at Cape Enrage. Numerous later-formed micro-faults cut the load casts. Scale at upper left has 10 cm divisions.
- e) Detached load structures consisting of folded sandstone blocks (such as left of scale) enclosed within siltstone, Slacks Cove East. Scale is 50 cm with 10 cm divisions.
- f) Bedding plane surface at Boss Point, showing 70 x 150 cm diameter scour with well preserved wave ripples. Current ripples occur across the flat bedding plane surface adjacent to the scour. Paleocurrent was toward the right. Scale is 50 cm with 10 cm divisions.
-



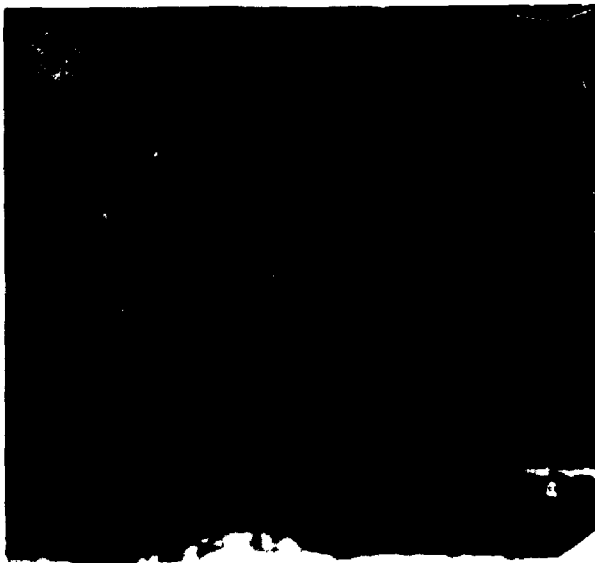
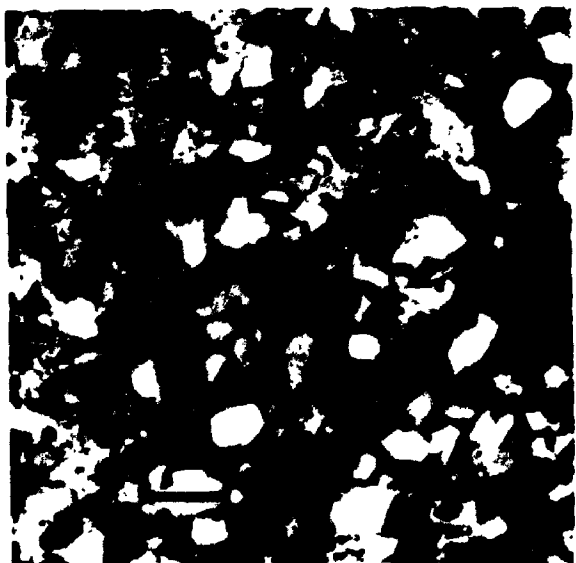
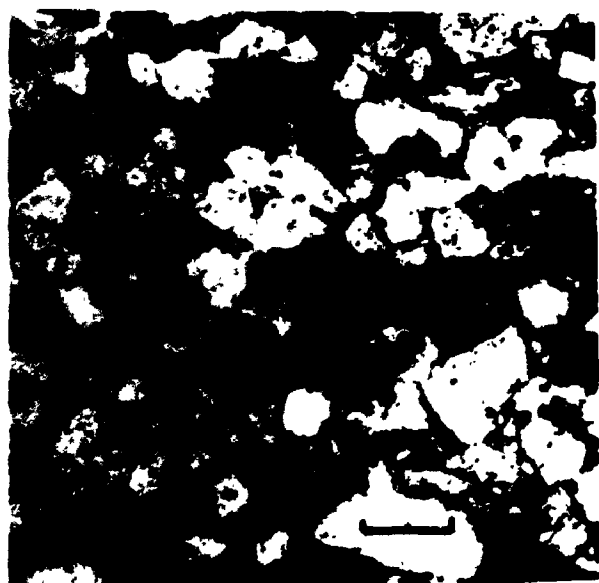
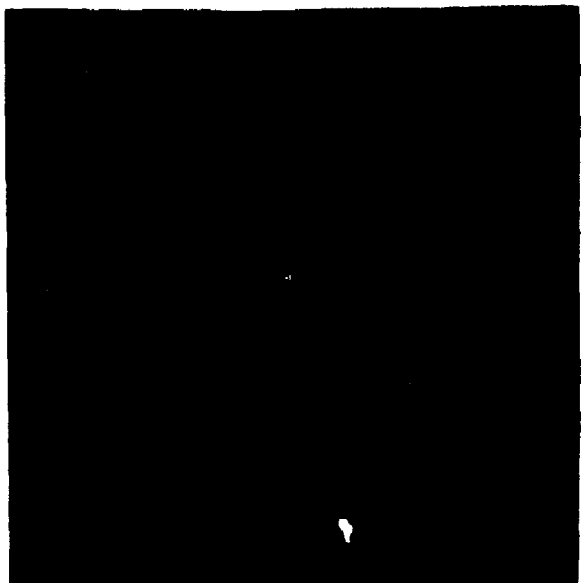
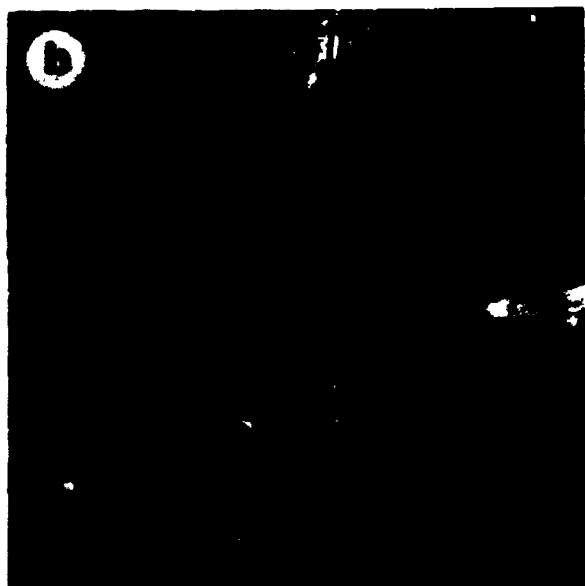
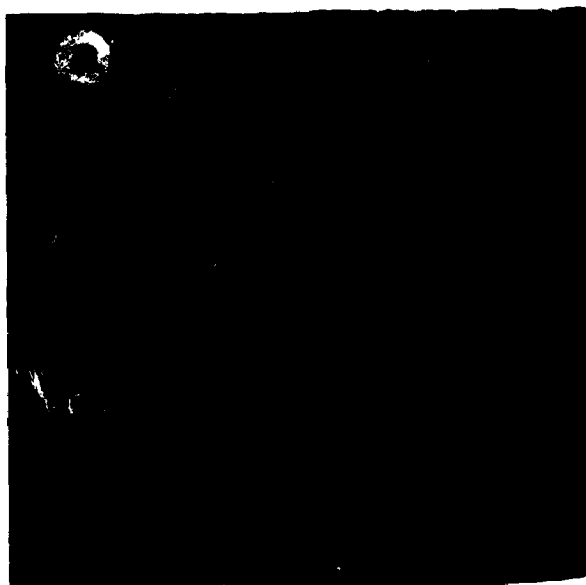
Spectacular examples occur at Cape Enrage at the base of a 90 cm thick trough cross-bedded sandstone, which overlies a 90 cm thick light blue-grey massive siltstone (stratigraphic section 23; 93 m above the base). The loading structures extend 50 cm into the underlying siltstone and are associated with micro-faulting (Plate 6d). At Slacks Cove East (stratigraphic section 17; 284 m above the base) the base of a 50 cm thick sandstone bed shows load structures and some of these extend as much as 80 cm into the underlying siltstone and may be completely detached from the original parent sandstone body above (Plate 6e).

Parting lineations are common in the upper portions of sets and rib and furrow structures are typically preserved on the tops of trough cross-bedded sets. Straight-crested wave ripples are often preserved within circular scour troughs on the tops of bedding plane exposures (Plate 6f). Elsewhere, trough cross-bedded sandstones are gradational into overlying ripple cross-laminated, horizontally laminated or massive sandstone units (see below).

Associated with the trough cross-beds are units with dm-thick sigmoidal foresets that have sharp planar bases, convex tops, and are infilled with foreset laminae with depositional dips as much as 15° (Plate 7a). Units wedge out over lateral distances of up to 15 m, or are erosionally truncated by overlying trough cross-beds. Foreset orientation is consistently oblique to the

Plate 7

- a) Sigmoidal foreset bedding at Grindstone Island. Scale bar is 50 cm with 10 cm divisions.
- b) Large elongate scours preserved on the top of a bedding surface at Slacks Cove West (see Plint 1986). Scale bar (at left) is 50 cm with 10 cm divisions.
- c) Large bedding plane surface showing extensive development of ripples across the entire surface at Slacks Cove West. Cliff face is approximately 15 m high.
- d) Photomicrograph of well sorted trough cross-bedded sandstone, from 184 m above the base of the formation at Rockport. View is in plane-polarised light. The mineralogy is dominated by quartz and orthoclase, together with clays and opaques. Scale bar is 0.5 mm.
- e) Photomicrograph of well sorted calcareous trough cross-bedded sandstone, from 343 m above the base of the formation at Slacks Cove East. View is in cross polarised light. The mineralogy is dominated by common and polycrystalline quartz, with minor plagioclase. Note the fresh appearance of the feldspars. Grains are surrounded by a ferroan poikilotopic calcite. Scale bar is 0.25 mm.
- f) Tabular planar cross-bedded sandstone at Beaumont. Hammer for scale.



paleocurrent trends determined from the trough cross-bedding in stratigraphically adjacent units. These structures are similar to "runoff microdeltas" described by Dalrymple (1984) from the modern in the Bay of Fundy, and to ancient fluvial equivalents (Collinson 1970).

Large-Scale Bedding Hierarchy Description

Scoured surfaces separate groups of cosets, and have previously been described by McCabe (1978a) and Plint (1986). Channel-based scours commonly associated with intraclast pebbles, and immediately overlain by pebble sandstone lithofacies (see below), have a relief of several metres and can be traced across shore platform exposures for several hundred metres (Fig. 4.1). Plint (1986, fig. 9) has previously described linear scour-troughs, the scours being lined with closely-packed mudstone pebbles, in a fine-grained matrix. The elongate scour-troughs are slightly sinuous, are up to 70 cm deep, 1.5 m wide and at least 12 m long (Plate 7b). Generally only the bases of the linear scours display ripples, but at Slacks Cove West, ripples also occur across the planar surfaces between scours (Plate 7c).

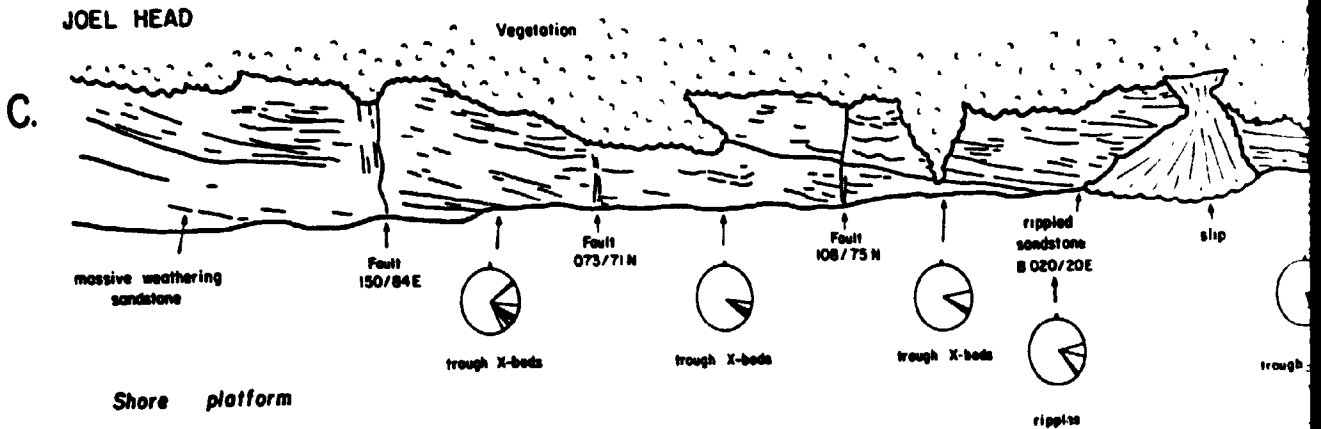
4.1.2 Petrography

Eleven representative samples were petrographically

Fig. 4.1 Outcrop sketch of the cliff face at Alma. "A" is the western-most end of the section (nearest Alma), at the base of the section.

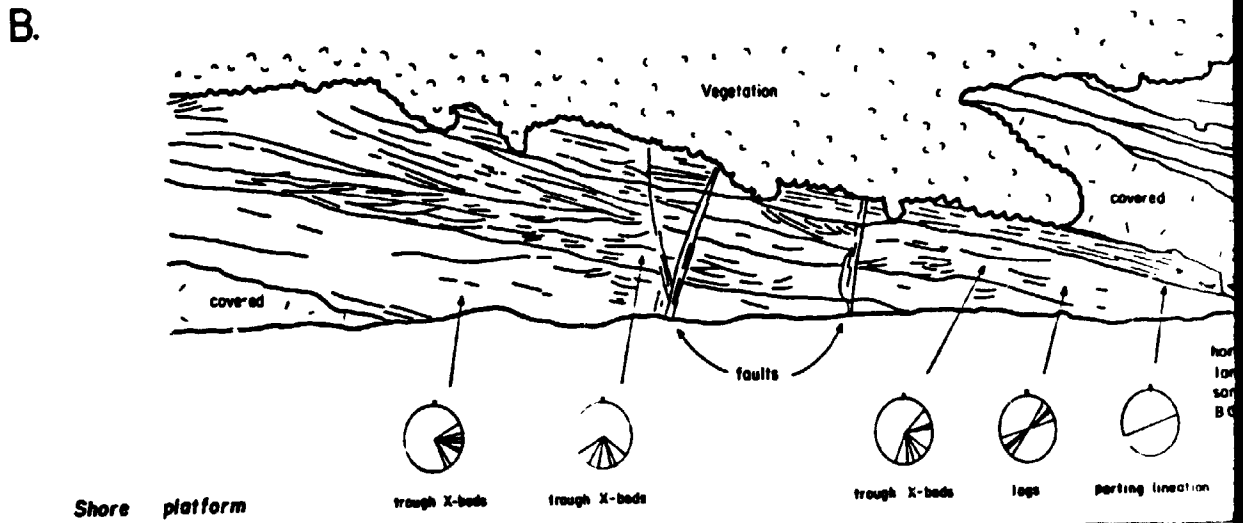
Southwest

060° →



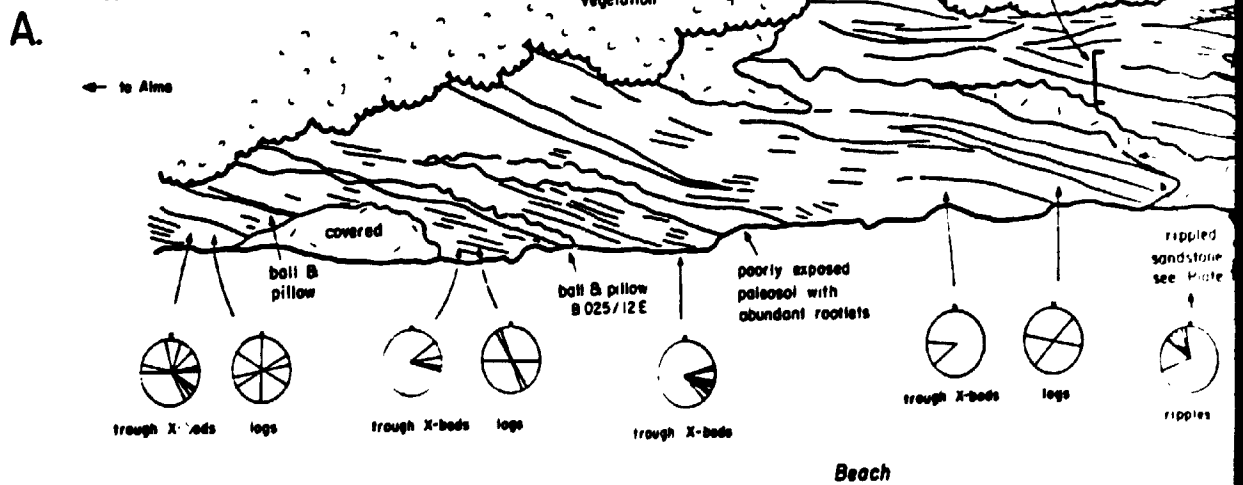
West

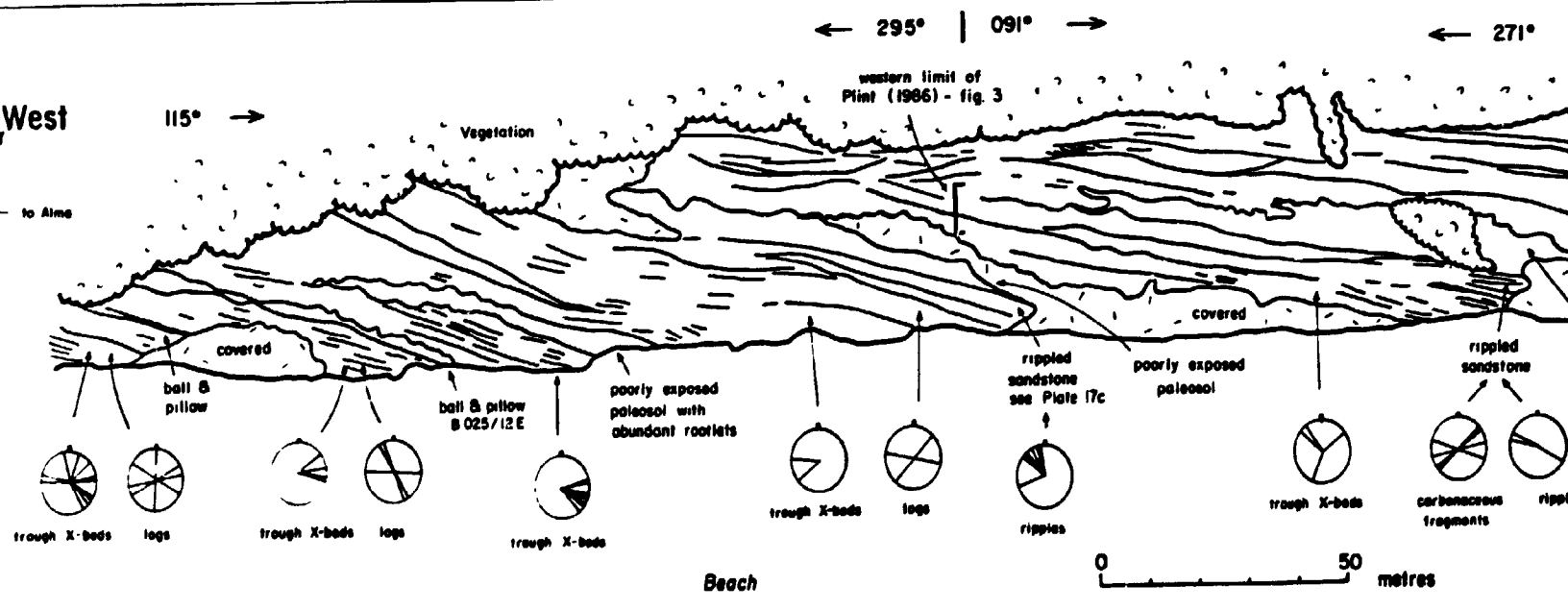
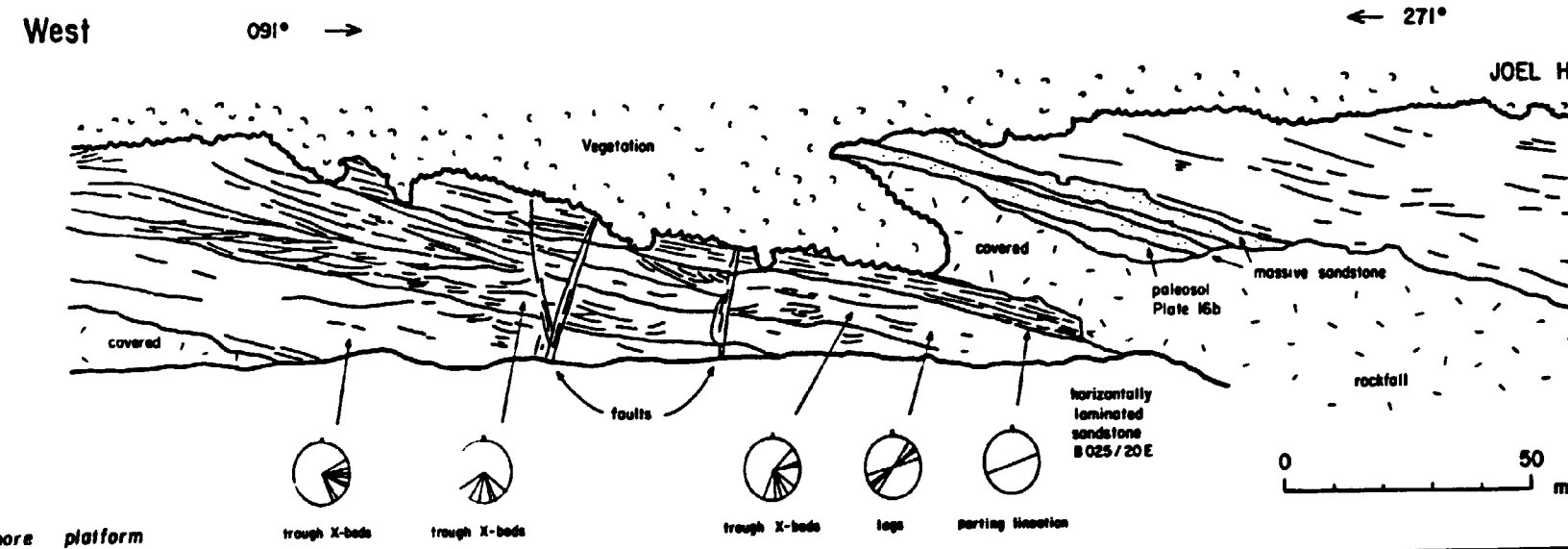
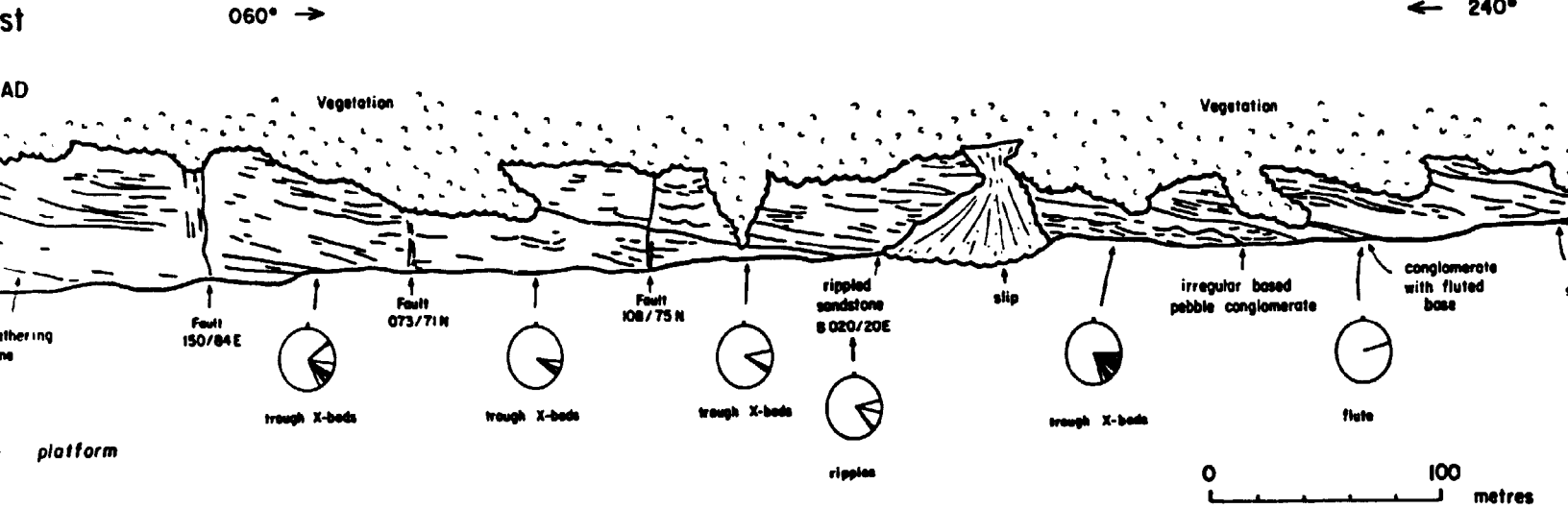
091° →



West

115° →



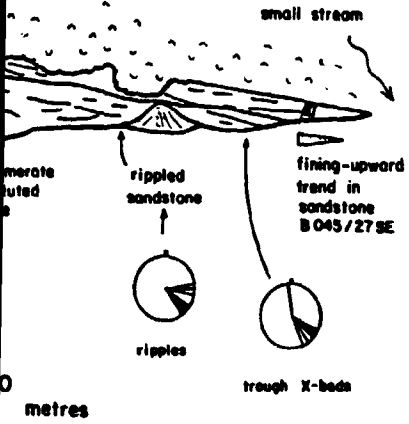


240°

Northeast

D.

small stream



East

JOEL HEAD

C.

massive weathering sandstone

50 metres



271°

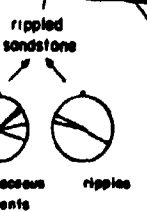
East

B.

eastern limit of Plint (1986) - fig. 3

covered

siltstone blocks for details see Plint (1986)

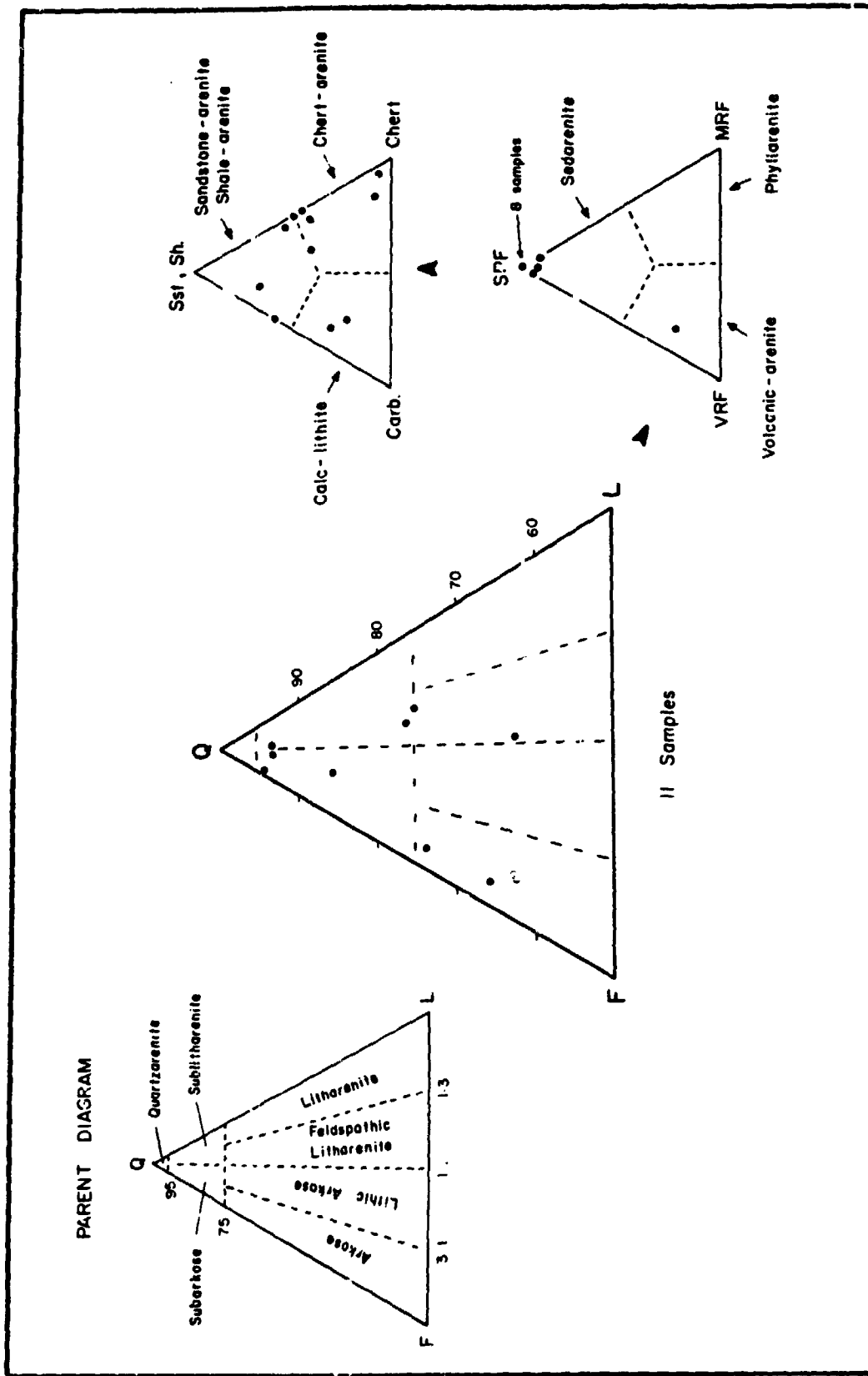


point counted. These samples indicate that Boss Point Formation sandstones contain between 62 and 93% quartz, and may be classified as subarkose, sublitharenite or arkosic sandstones (Fig. 4.2, Appendix III). Areas in the west such as Giffin Pond, contain appreciable quantities of lithic fragments, and are feldspathic litharenites, but elsewhere the composition is dominated by quartz and feldspar (Plate 7d). The feldspar component is almost entirely orthoclase (range 3 to 33%; mean= 16%), indicating felsic source areas. Rock fragments are dominated by sedimentary material (Fig. 4.2); the exception being the sample from Giffin Pond which contains considerable basaltic rock fragments (derived from the Precambrian Coldbrook Group). Sedimentary rock fragments (sedarenites) show considerable spread between the 3 end member compositions, sandstone/shale, carbonate and chert. Samples from areas in the centre of the Cumberland sub-basin, such as Boss Point, contain an abundance of intraformational siderite clasts. Samples rich in chert occur at Hillsborough and Alma; these sites being interpreted as more proximal to uplifted basement lithologies (see below).

Accessory grains not encountered during point counting include biotite, muscovite, plagioclase, microcline, rutile, zircon, chlorite, opaques and matrix.

Where calcareous, the rock has been cemented by spar, the carbonate occurring as both fine-grained pore filling

Fig. 4.2 Quartz-Feldspar-Lithics triangular plot for Boss Point Formation trough cross-bedded sandstones determined from point counting. The nomenclature follows that of Folk (1974). Details appear in Appendix III.



and as poikilotopic spar up to 2 mm diameter. Treatment with potassium ferricyanide and Alizarin Red S indicates that the spar is ferroan calcite (Plate 7e).

4.1.3 Interpretation

Trough cross-bedded sandstones formed as sinuous crested dunes within fluvial channels.

Preservation of dunes and ripple-topped surfaces indicates both temporary bedform modification and more prolonged emergence, probably related to variation in discharge. The presence of parting lineations toward the tops of many sets indicates a change to upper flow regime conditions, and were likely produced when the water level in the channels dropped. High-stage dunes were typically left without substantial modification, and are similar to those described in the Hawkebury Sandstone by Rust and Jones (1987, p. 229). Small, low-stage current ripples were superimposed on the dune field, and are similar to bedforms described by Dam and Andreasen (1990). Similar morphologies have been described from modern rivers and estuaries (Jones 1977, Love et al. 1987) where flow has been abruptly terminated (sometimes artificially such as downstream of damsites).

The sigmoidal foresets with their wedge-shaped morphology suggest that they formed as deltaic lobes that prograded toward the thalweg during falling stage.

Dalrymple (1984) described similar structures ("runoff microdeltas" in his terminology) and showed that they are produced by emergence runoff in periodically exposed areas. In the Boss Point Formation, it is suggested that the sigmoidal foresets developed in a similar fashion when water level in the channels was low.

4.2 Planar Cross-Bedded Sandstone (Sp)

4.2.1 Description

Planar cross-stratified sandstone is a minor component (0.04%) of the formation (Fig. 3.1c, Appendix I). The lithofacies was encountered in the northern Bay of Fundy region at the Beaumont and Hillsborough sections, where the maximum cross-set thickness is 1.3 m (mean= 0.4 m; see stratigraphic sections 11 and 12, Fig. 1.2), and at 206 m above the base of the Rockport section. Foresets have depositional dips between 5 and 20° (mean= 13°) and commonly form wedge-shaped units that thin out over the outcrop width (Plate 7f).

Compositionally the sandstones are equivalent to the trough cross-bedded sandstones described above.

4.2.2 Interpretation

Planar cross-bedded sandstones are interpreted to have

been deposited on the avalanche slip-face of a bar. These bars were either rarely developed or, (more likely), very infrequently preserved in Boss Point Formation rivers. The paleoflow directions determined from the tabular cross-sets indicate that the slip face advanced obliquely in relation to main channel orientations (as determined from trough cross-bedding).

4.3 Current Ripple Cross-Laminated Sandstone (Sr)

4.3.1 Description

Ripple cross-laminated sandstone is an important lithofacies which makes up 6.7% of the formation (Fig. 3.1c, Appendix I). This facies forms units up to 6.2 m thick, and units have a mean thickness of 1.0 m. Various ripple forms occur including linguoid current ripples, climbing ripples, and in-phase ripples.

Current ripple cross-laminated sandstones are consistently finer-grained, more micaceous and more carbonaceous than trough cross-bedded equivalents. Set thickness varies between 2 and 10 cm and is generally between 2 to 5 cm. Locally ripple form sets have an overlying mud drape. In plan view, ripples are weakly to strongly linguoid with ripple indices between 7.3 and 21.8 (mean= 12.7, Standard Deviation= 3.2) for 61 measured ripples.

The lithofacies consists of light to medium blue-grey, noncalcareous, well sorted, very fine- to fine-grained sandstone, seldom with medium-grained sand. They are abundantly carbonaceous, (typically finely comminuted debris throughout), and may display well developed vertical calcareous tubes or stems (Plate 8a). In places rippled sandstone beds contain abundant 'thickets' of *Calamites*, preserved as vertical stems (Plate 8b). *In situ Stigmaria* roots are commonly associated with the facies (Plate 8c & 8d).

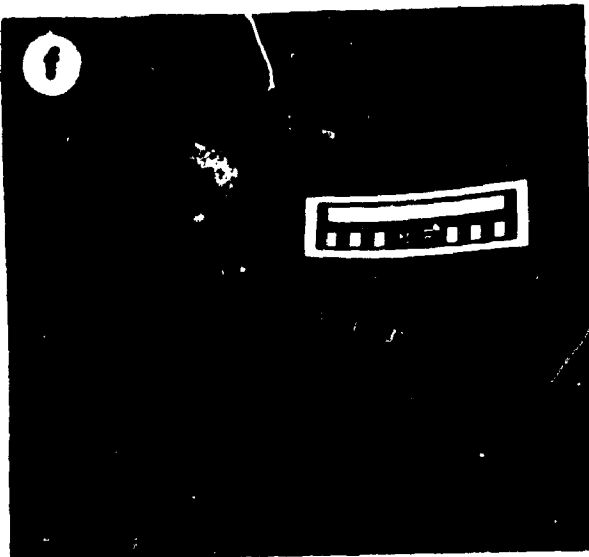
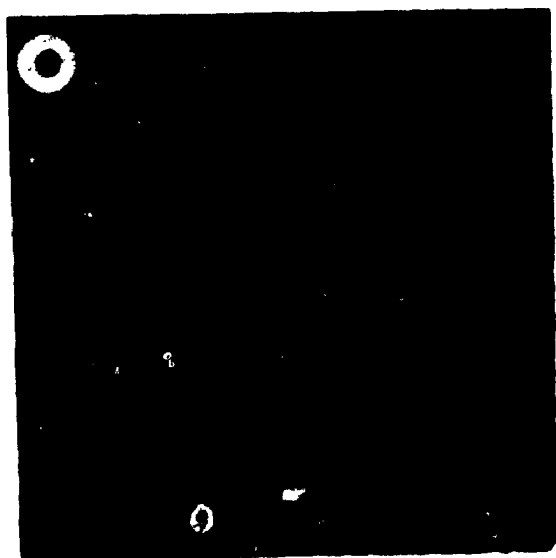
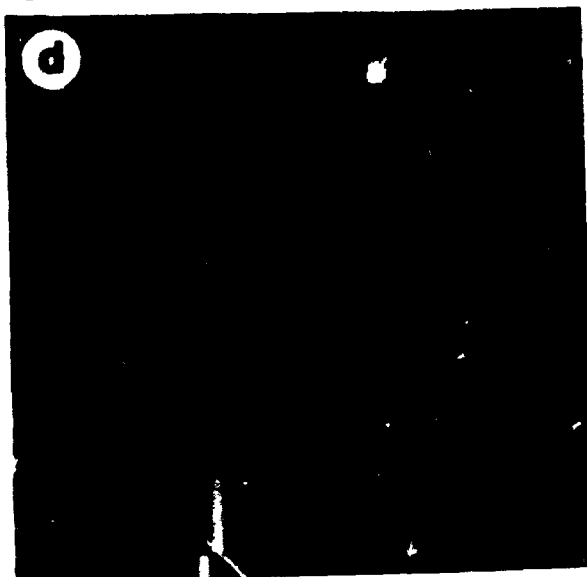
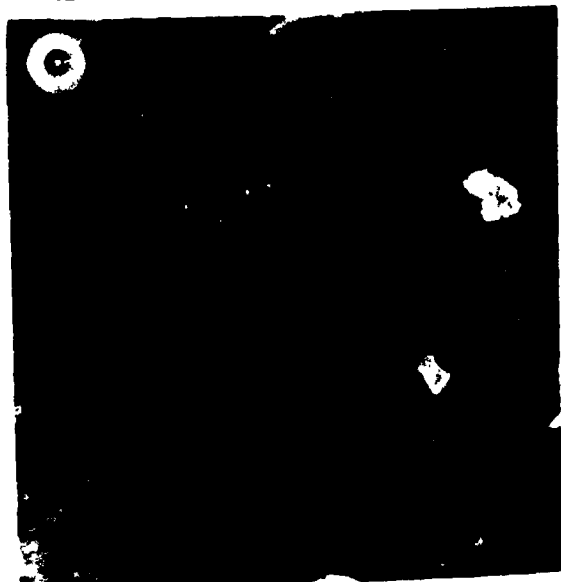
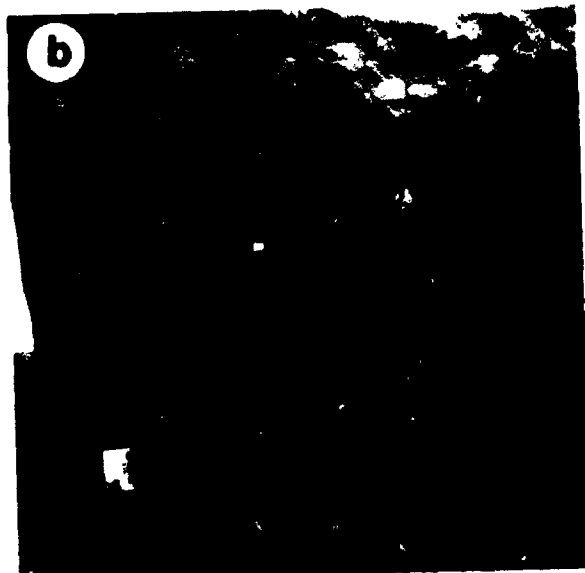
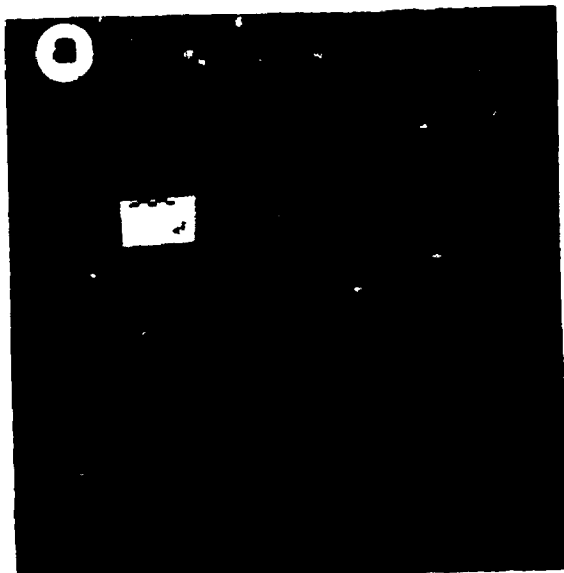
Groove casts with as much as 5 cm erosional relief may be preserved where ripple cross-laminated sandstones directly overlie siltstone (Plate 8e). Load structures associated with the base of ripple cross-laminated sandstone lithologies are not common, but at Dorchester, where rippled sandstones overlie siltstone (stratigraphic section 10; 386 m above the base), loading extends over a vertical interval of 2 m.

Climbing ripples are lithologically equivalent to the ripple cross-laminated units described above, and usually grade upward from such units. Cross-sets are typically 2-3 cm thick and display angles of climb between 1 and 40°.

Rare examples of current ripples, overlain gradationally by climbing ripples and in-phase ripples, capped by plane bed sandstones occur (Plate 8f).

Plate 8

- a) Calcareous vertical tubes (arrowed) interpreted as rhizoconcretions (calcified roots) within ripple laminated sandstone at Johnson Mills. Scale is 5 cm with 1 cm divisions.
- b) Base of sandstone showing *in situ* *Calamites* stems growing through the sandstone. Scale is 5 cm with 1 cm divisions.
- c) *Stigmaria* (labelled St) in growth position within trough cross-bedded sandstone at Johnson Mills. Succession dips steeply to north (left). Scale is 50 cm with 10 cm divisions.
- d) Detail of *Stigmaria* (labelled St) as in Plate 8c, showing main lateral root, with smaller radial rootlets (labelled r) on either side. *Calamites* (labelled Cal) grew *in situ* at the base of the sandstone. Scale bar shows a 10 cm division.
- e) Linear grooves preserved at the base of a ripple laminated sandstone bed at Johnson Mills. Scale is 5 cm.
- f) Climbing ripples (at base) passing up into in-phase ripples and plane bed (top) at Rockport.



4.3.2 Petrography

Current ripple cross-laminated sandstones are subarkose and arkose arenites, dominated by angular to subrounded quartz which forms between 50-90% of the lithology. Grain size typically is between 50 um and 70 um (coarse-grained silt to very fine-grained sand), but may be as much as 0.4 mm (medium-grained sand) in some examples. Carbonaceous debris occurs in all samples (and may locally constitute as much as 40% of the lithology), and typically occurs as finely disseminated material along lamination planes. Accessory minerals include muscovite up to 0.3 mm long (trace to 3%), biotite (trace), chlorite (trace), plagioclase (trace to 10%), opaques (1-10%) and spar (<10%).

4.3.3 Interpretation

Current ripple cross-laminated sandstones are interpreted as low velocity flow regime bedforms. Climbing ripples typically overlie current ripple laminated intervals, and are interpreted to indicate changes in bed aggradation rate, where an increase in the sediment load caused the bed form to aggrade.

4.4 Antidunes

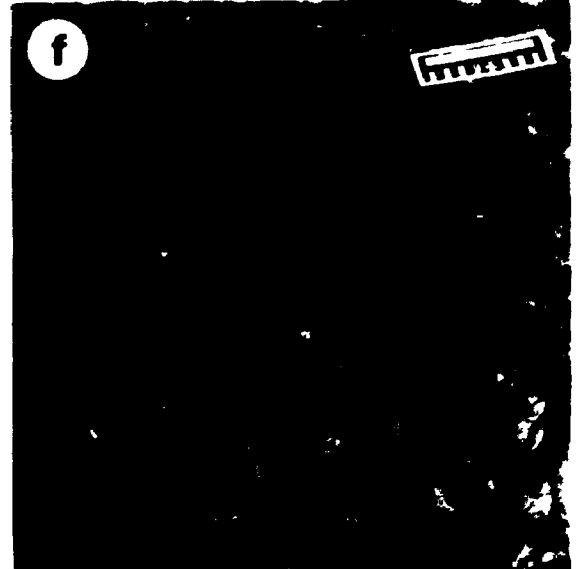
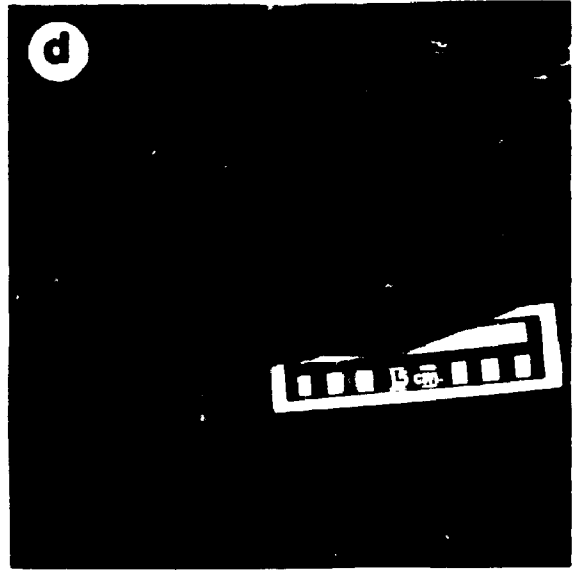
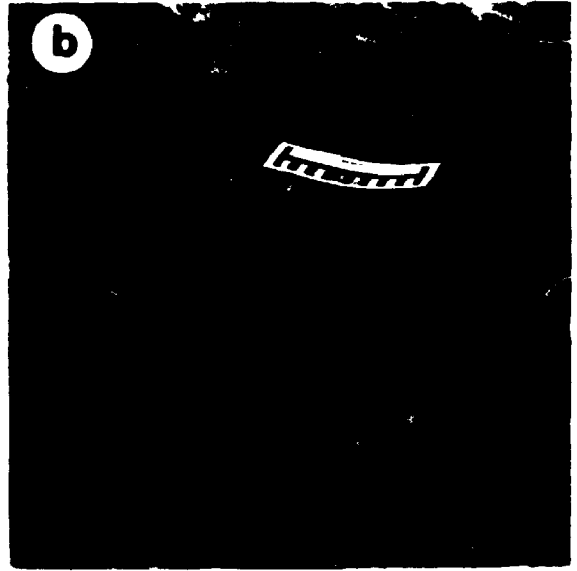
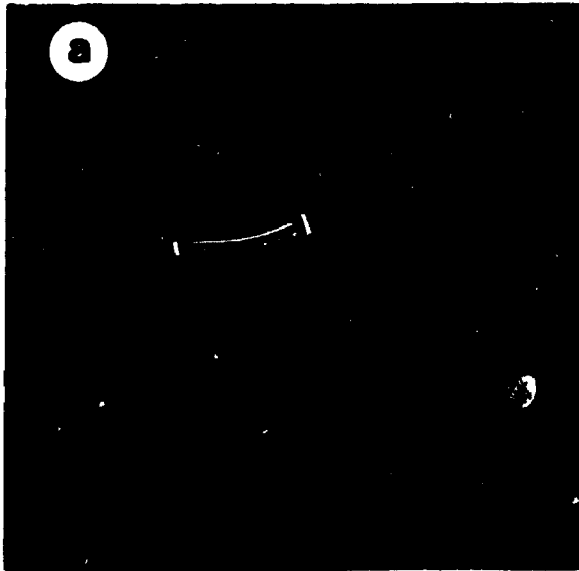
3-dimensional antidunes consist of bedded units which have a 3-D wavy morphology. The only known occurrence occur at 552 m above the base at Rockport (stratigraphic section 18) where the sandstone consists of a light blue-grey, noncalcareous well sorted very fine- to fine-grained sandstone. The undulatory laminae have a height of 5 cm and wave length of 30 to 50 cm, and are sharply overlain by laminated siltstone (Plate 9a). The stratification has a distinct wavy appearance, which on bedding plane surfaces forms domes and swales (Plate 9b), and is distinguished from HCS (described below) on the grounds that there is no truncation of laminae.

The 3-dimensional antidunes occur at the top of a 2.5 m thick fining-upward cycle, resting gradationally above a 1.3 m thick, well sorted, very fine ripple cross-laminated sandstone (below), which in turn gradationally overlies a 60 cm thick very fine to fine ripple laminated sandstone at the base of the fining-upward cycle (stratigraphic section 18).

The antidunes are considered to represent upper flow regime conditions similar to those described by Rust and Gibling (1990b). However, unlike the occurrence described by Rust and Gibling (1990), the Rockport example does not show primary current lineation on the upper surface, although little of the bedding plane is exposed. The

Plate 9

- a) Antidunes in side view at Rockport. Note that the laminae are not truncated. Scale is 15 cm.
- b) Bedding plane exposure of antidunes (same locality as Plate 9a). Note the small domes and swales, suggesting that these structures are antidunes. Scale is 15 cm.
- c) Hummocky cross-stratification preserved at Slacks Cove East. Each HCS couplet consists of massive sandstone (m), overlain by parallel laminated sandstone (p) and hummocky cross-strata (h), with a sharp planar transition into siltstone (above). Scale is 15 cm.
- d) Detail of hummocky cross-strata (same locality as Plate 9c). p= parallel laminated sandstone; h= HCS interval. Laminae in this interval show truncation.
- e) Centimetre-thick horizontally laminated sandstone at Boss Point. Scale is 5 cm with 1 cm divisions.
- f) Bedding plane view of wave ripples with extensive development of runzel marks across the entire surface. Scale is 15 cm.



presence at Rockport of the 3-dimensional antidunes indicates Froude numbers close to 1, and their association above current ripple cross-laminated sandstones suggests a lower/upper flow regime transition between these two units, flow being abruptly terminated at the top of the sandstone, and the surface draped with a 7.5 m thick siltstone.

4.5 Hummocky Cross-Stratification

Hummocky cross-stratification (HCS) was observed at Slacks Cove East at 164 m above the base of the section (stratigraphic section 17). The HCS occurs in association with alternating sandstone/siltstone couplets, sandstone units consisting of medium green-grey, noncalcareous, well sorted fine-grained sandstone, ranging from 20 to 60 cm thick; siltstones being 10-30 cm thick. Each sandstone/siltstone couplet has a sharp base, beginning with massive sandstone, passing upward into parallel laminated sandstone, overlain by hummocky cross-strata, and draped by siltstone (Plate 9c & 9d). The HCS interval developed at the top of the sandstone portion of the couplets consists of sets 5-20 cm thick, with a crest spacing of 30-40 cm. No plan-view outcrops were observed.

HCS differs from the morphologically similar 3-D antidunes described above because individual laminae are truncated in HCS (Rust and Gibling 1990b), and because they are associated with sandstone/siltstone couplets (similar

to those described by Walker *et al.* 1983).

Hummocky cross-strata developed in lakes have been recognised from Pleistocene units of Bonneville Lake, Utah (Duke 1985), and from Lake Huron (Greenwood and Sherman 1986) and paleo-Lake Iroquois, Ontario (Eyles and Clark 1986). Records of HCS in older lacustrine units include the Jurassic of Australia (Fielding 1989), the Permian and Triassic of Australia (Duke 1985), the Permian of South Africa (Hobday 1978, Van Dijk *et al.* 1978), and the Tournasian of Horton Bluff Formation of Nova Scotia (Martel 1990).

The HCS strata in the Boss Point Formation are associated with lacustrine sedimentary units (see Chapter 5) and were produced by flows dominated by strong wave-induced oscillatory motions at or above wave base (for review see Duke 1990). The HCS developed in the Boss Point Formation closely resembles the descriptive divisions recognised by Walker *et al.* (1983). In this scheme the sharp base and massive lower sandstone division (division B) is argued to record sand deposition by storm-related unidirectional flow. Storm-wave reworking produced by upper laminated divisions by oscillatory-flow (divisions P,H,F,X), whereas the mud drape at the top of the sandstone/siltstone couplet (division M) forms by later mud deposition from suspension. Each Boss Point Formation couplet probably represents a distinct storm event or pulse rather than amalgamated hummocky sequences (Dott and

Bourgeois 1982, Leckie and Walker 1982), for successive storms have clearly not eroded into the underlying rippled sandstone and mud drapes.

4.6 Horizontally Laminated and Wave Rippled Sandstone (Sh)

4.6.1 Description

Horizontally laminated sandstone units comprise 2.1% of the Boss Point Formation (Fig. 3.1c, Appendix I), and may form bedded intervals as much as 8.4 m thick (mean thickness = 1.5 m).

Two morphologic varieties are recognised;

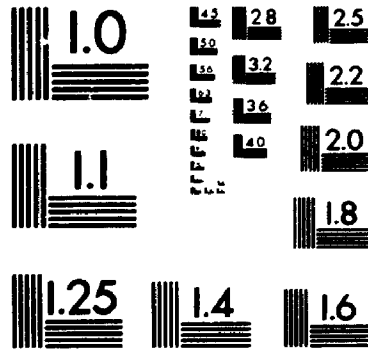
1) The first consists of cm-thick, light to medium blue-grey, noncalcareous and calcareous, well sorted, very fine- to fine-grained parallel laminated sandstone.

Stratification in these units ranges from millimetre to several centimetres in thickness (Plate 9e). Individual laminae are usually parallel but may show minor scouring (up to 15 cm) into underlying laminae. Units extend over lateral distances of a few metres, but seldom greater than 20 m. These units are always associated with fine-grained current ripple cross-laminated and mudrock units.

Comminuted carbonaceous debris is generally absent from sandstone beds, but is ubiquitous on bedding planes which may contain well preserved leaf impressions. The laminations are marked either by concentrations of these

3

Vertical text on the right side of the page, likely a page number or reference code.



MICROCOPY RESOLUTION TEST CHART
NATIONAL BUREAU OF STANDARDS
STANDARD REFERENCE MATERIAL 1010a
(ANSI and ISO TEST CHART No 2)

carbonaceous fragments, or by slight grain size variations. Wave ripples are common on the tops of bedding plane surfaces; ripple crest spacing is consistently between 2-5 cm with ripple heights of 1 to 1.5 cm. Runzel marks are common on both the ripple crests and troughs (Plate 9f). The ripples typically have a concentration of comminuted carbonaceous debris in the troughs between ripple crests (Plate 10a), and have both symmetrical and slightly asymmetric cross sections.

2) The second variety of laminated sandstone consists of dm-bedded, light and medium green-grey, calcareous and noncalcareous, well sorted, fine- to lower medium-grained sandstone, with well defined sharp planar bases (Plate 10b). Primary current lineations are common. Units can be traced for distances of >50 m across shore platform exposures, and are sharp and planar based. They are always associated with trough cross-bedded sandstones. Comminuted carbonaceous debris occurs throughout sandstone beds and along stratification boundaries. These sandstones occur within stacked trough cross-bedded sandstone successions.

4.6.2 Petrography

Horizontally laminated sandstones are well sorted subarkose and arkose arenites. Quartz consists of angular to subrounded equidimensional grains up to 0.3 mm in diameter, but generally in the range 0.1 to 0.2 mm (Plate

Plate 10

a) Bedding plane view of wave ripples at Johnson Mills. Scale is 50 cm with 10 cm divisions.

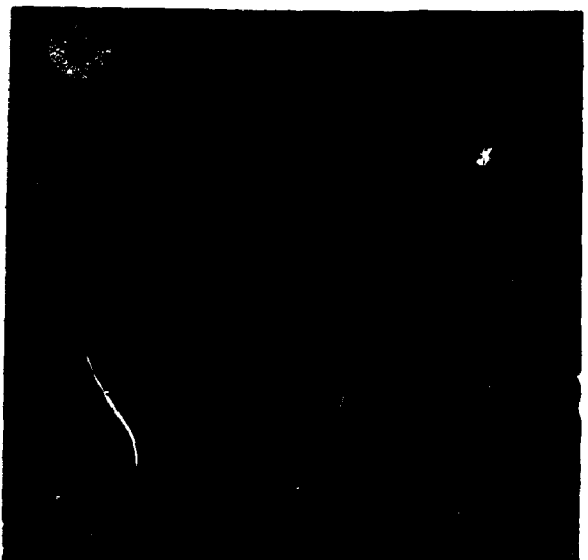
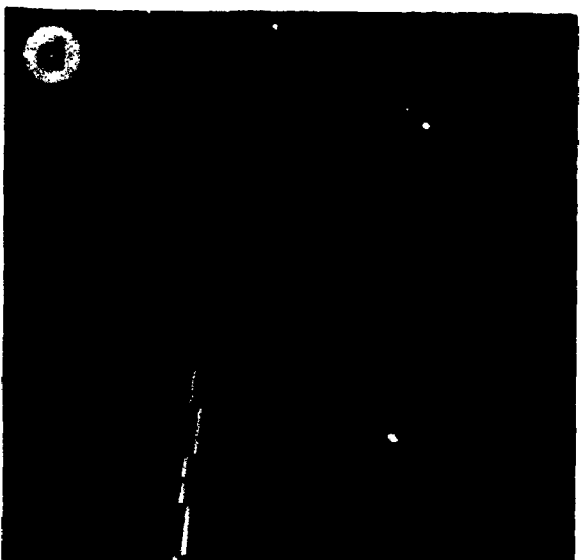
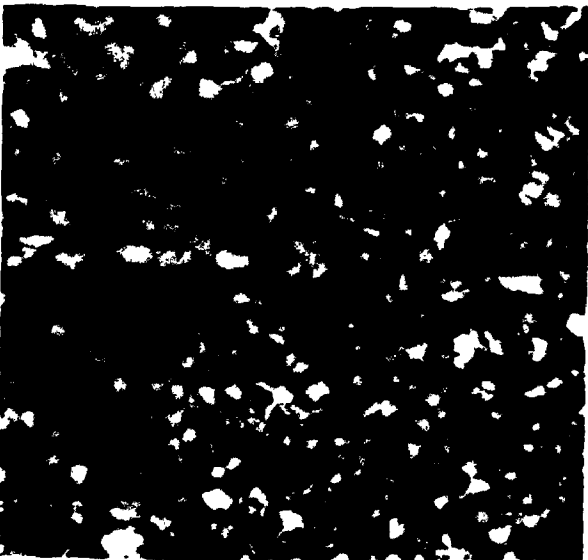
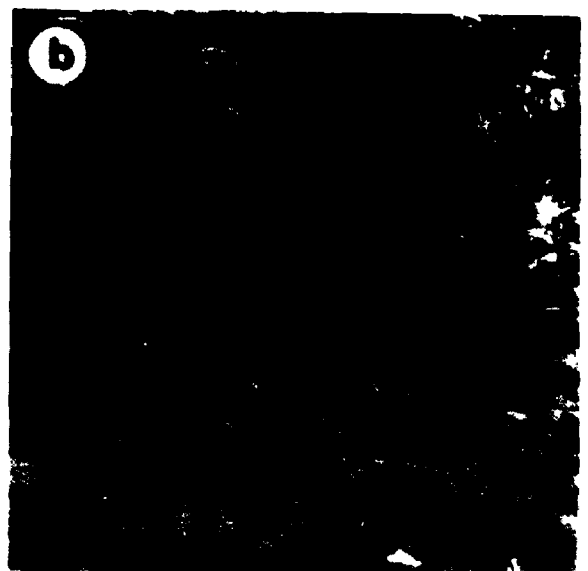
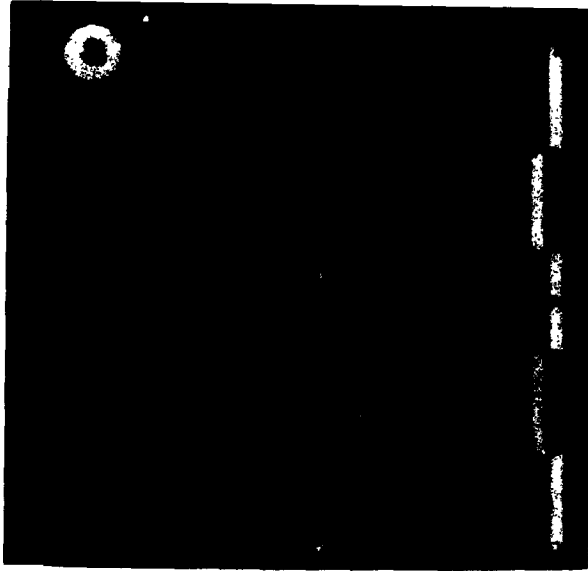
b) Centimetre and decimetre-thick horizontally bedded sandstones at Two Rivers. Scale (centre left) is 50 cm.

c) Photomicrograph of horizontally laminated sandstone from 61 m above the base of the Boss Point Formation at Alma. Note the alignment of quartz grains parallel to stratification in centre. View is in cross-polarised light. Scale bar is 0.5 mm.

d) Pebbly sandstone with well developed dm-metre thick normal-graded intervals. Scale is 50 cm with 10 cm divisions.

e) Centi-metre thick sandstone dikes (arrowed) which intrude into siltstone at Hillsborough. Scale is 50 cm with 10 cm divisions.

f) Inclined heterolithic stratification (IHS) unit (arrowed) consisting of alternating decimetre-thick ripple cross-laminated sandstone and siltstone units, with lacustrine siltstone units above and below. The sandstones below the dead tree are ripple cross-laminated; the sandstone at the extreme left represents the base of a thick stacked sandstone succession (same contact as shown in Plate 5d & Plate 5e). Backpack in foreground (right) for scale.



10c). Quartz forms between 60 and 90% of the rock. Accessory grains include opaques (most likely carbonaceous fragments: 1-15%), elongate muscovite and biotite grains up to 0.8 mm long (trace to <3%), orthoclase, which typically has a weathered "dirty" appearance in thin section (up to 30%), and chlorite (trace). Where present, carbonate infills pore spaces and may constitute as much as 25% of the rock in thin section. Staining indicates that the carbonate is ferroan calcite, similar to the carbonate phase observed in trough cross-bedded sandstones (see above).

4.6.3 Interpretation

The horizontally laminated and wave rippled sandstone lithofacies is interpreted in two ways:

The thinner bedded units associated with the current rippled and mudrock units are interpreted as beach sands. The thicker bedded units associated with trough cross-bedded sandstones are interpreted to be part of crevasse splay units implying upper flat bed conditions.

4.7 Massive Sandstone (Sm)

4.7.1 Description

Massive sandstone units comprise 4% of the formation

(Appendix I), with a maximum thickness of 11.8 m. In many instances, rocks included in this lithofacies are probably trough cross-bedded, especially where the outcrop is too poor to show stratification, which is particularly the case in coastal cliff exposures. Sandstone bases are in most cases sharp, and are both erosive or planar.

The lithology consists of light to medium blue-grey, moderately to well sorted quartz arenite and sublitharenite. Grain-size ranges from fine- to coarse-grained sand, coarse grains being more common than in the trough cross-bedded lithofacies.

4.7.2 Petrography

Massive sandstones are most commonly quartz arenites with less abundant sublitharenites, quartz occurring as subangular to rounded grains up to 1.1 mm in diameter (generally 0.2 mm diameter). Quartz constitutes 70 to 90% of the rock. Accessory grains include lithic fragments (schist, quartzite, greywacke-type sandstone, granite and basalt), orthoclase (up to 30%), muscovite (~1%), feldspar (trace) and opaques.

4.7.3 Interpretation

The massive nature of this lithofacies makes interpretation difficult. Massive sandstones in fluvial

successions such as the Silurian Holmestrand Formation, have been interpreted as upper flow regime bedforms (Dam and Andreasen 1990), deposited very rapidly from highly concentrated currents. Rust and Jones (1987) described massive sandstones from the Hawkebury Sandstone (p. 226-229), and interpreted them as failed or slumped units which liquified as a result of bank collapse. The Boss Point Formation examples however lack the high-angle basal erosion surfaces which occur in the Hawkesbury Sandstone, and it is unlikely that they formed in a similar manner. The Boss Point Formation examples occur in typically weathered outcrops, suggesting that they represent the weathered equivalents of trough cross-bedded sandstones.

4.8 Pebbly Sandstone (Ss)

4.8.1 Description

Pebbly sandstone units occur throughout the study area, comprise 6.0% of the thickness of the Boss Point Formation (Fig. 3.1c, Appendix I) and form bedded units up to 3.0 m thick (mean= 0.6 m). Units have sharp bases which typically have an erosional relief of up to 80 cm, whereas tops are generally sharp.

The lithofacies contains varying proportions of boulder- to granule-sized material, principally quartz, siderite, and light blue-grey siltstone (up to several

metres in diameter), but with significant amounts of red chert, greywacke-type sandstone, intraformational sandstone, basalt and granite. Comminuted and branch-sized carbonaceous debris is ubiquitous throughout.

Typically the lithofacies is trough cross-bedded and resembles the trough cross-bedded lithofacies (St), or less commonly contains dm- to metre-thick normally graded beds (Plate 10d), or crudely stratified, or massive units. The facies is typically found at the base of major stacked trough cross-bedded sandstone units or associated with major scour surfaces.

The lithofacies has previously been described in some detail by van de Poll and Patel (1981), Plint (1986, 1989) and van de Poll (1989), where they have been described as "brecciform" intervals (van de Poll and Patel 1981). These authors have presented differing arguments regarding the origin of flutes, rills, load and groove casts that occur on the outer margins of the siltstone blocks within the pebbly sandstone lithofacies. Plint (1986, 1989) has convincingly shown that these fluted/rilled surfaces are erosional. Some of the blocks are fluted on all sides indicating clast rotation, whereas rill marks indicate emergence and erosion by surging water during surface runoff. In contrast, van de Poll and Patel (1981, 1989 & 1990) proposed that the features on these blocks formed by "rheoplasia", that is by plastic flow-moulding at the interface between two immiscible sediments during

liquefaction. They envisaged the diapiric injection of mudstone bodies through liquified sandstone as a result of reversed density gradients.

Units similar to the pebbly sandstone units described herein, include the intraformational conglomerate units described by Masson and Rust (1990) from the Sydney Mines Formation, Cape Breton Island.

4.8.2 Petrography

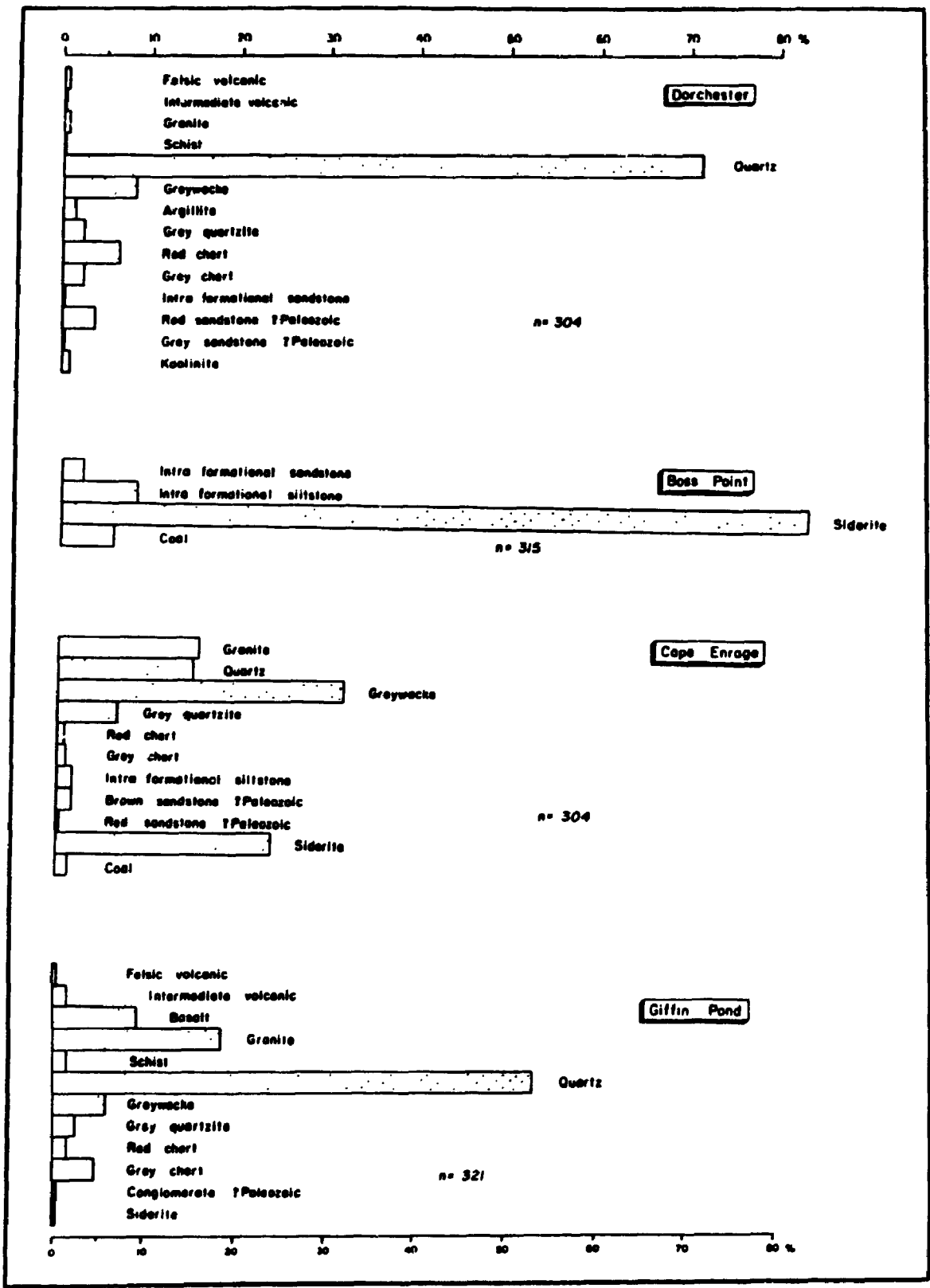
Point counting of outcrop clasts at 4 localities indicates that the dominant composition is quartz, although in the central parts of the basin, siderite may be locally abundant (Fig. 4.3). The abundance of accessory clasts varies considerably with location.

In the north at Dorchester (Fig. 4.3a), 70% of the clasts are quartz. Greywacke and red chert clasts comprise between 5 and 10%, and a significant proportion of Paleozoic red sandstone (~5%) also occurs.

In the middle of the basin (typified by the data presented for Boss Point), extrabasinal clasts are absent. Coarse-grained detritus was restricted to locally provided coal and siderite, and from intraformational sandstone and siltstone.

At Cape Enrage, a 1.5 m thick pebbly sandstone bed near the top of the section (Unit V - Chapter 5) shows an abnormally high proportion of pink granite clasts (Fig.

Fig. 4.3 Petrography of the pebbly sandstone lithofacies determined by point counting outcrop clasts at Dorchester, Boss Point, Cape Enrage and Giffin Pond.



4.3). Point counting indicates that granitic material comprises 15.5% of the granule and pebble clasts at this locality, considerably more than the typical concentrations of <0.5% granite found at other sites in the formation. This, together with an abrupt reversal in paleocurrent direction at this locality, indicates that for a short period clasts were derived from the eastern side of the basin (see Chapter 5).

In the south, at Giffin Pond, basalt, together with schistose and granitic material, is common in the pebbly sandstones (Fig. 4.3), the basalt probably being derived from the nearby Precambrian Coldbrook Volcanics, and granites and schist material being derived from basement lithologies in the adjacent Caledonia Highlands to the west. It is significant that the proportions of these Precambrian/basement lithologies are relatively minor in pebbly sandstones at the base of the Boss Point Formation at Giffin Pond (stratigraphic section 26), but that they increase in abundance toward the top of the section, where they attain the proportions indicated in Fig. 4.3. Point counting from thin section and field estimation from pebbly sandstones at the base of the formation at Giffin Pond (Appendix III), indicates that 5% of the clasts are granite; schist forming about 1% and basalt 12%, as opposed to 17% granite, 2% schist and 9% basalt determined by point counting at the top of the formation.

4.8.3 Interpretation

Pebbly sandstones are interpreted to be a coarse-grained equivalent of the trough cross-bedded sandstones (St), deposited either where flow velocity was higher, perhaps in trunk streams, where coarser grained material was available for transport. The heterogeneous composition of this lithofacies suggests an association with large scale erosion and transport, such as would occur during major floods.

The marked reduction in the range of clast morphologies observed in a W-E direction (Fig. 4.3) suggests a sharp drop-off in the transport ability of Boss Point Formation rivers. Rapid infiltration rates resulting in a reduction of transport capacity are common in ephemeral streams in arid or semi-arid climates (Parkash *et al.* 1983, Reid and Frostick 1986, Love *et al.* 1987, Nanson *et al.* 1988, Dam and Andreassen 1990).

The petrographic observations at Giffin Pond (Fig. 4.3c) indicates penecontemporaneous uplift and erosion, which may have been a precursor to the thrusting of the Boss Point Formation over the Tynemouth Creek Formation as described by Plint and van de Poll (1984), although this tectonism was a little earlier than envisaged by Plint and van de Poll (1984) for this locality.

4.9 Sandstone Dikes

Sandstone dikes were recorded at Hillsborough, Bcss Point and Grindstone Island (stratigraphic columns 12, 14 & 19 - Fig. 1.2), and have been illustrated from Cape Maringouin by van de Poll and Patel (1981, fig. 5). The dikes are <25 cm wide and up to 10 m long and consist of well sorted fine- to coarse-grained (grain size up to 0.65 mm) quartz arenite. Quartz comprises 80-90% of thin sections, other grains consisting of orthoclase, muscovite and opaques. At Hillsborough and Grindstone Island, the 2-5 cm thick dikes cut light and medium blue-grey, noncalcareous very fine-grained sandy siltstone (Plate 10e), but at Boss Point, a dike (20 cm thick) cuts light green-grey and reddish grey, noncalcareous well sorted fine-grained trough cross-bedded sandstone. The dikes do not appear related to any particular stratigraphic interval, or to trends of bedding, faulting or jointing.

4.10 Inclined Heterolithic Stratification (IHS)

4.10.1 Description

Alternating sandstones and siltstones interpreted to be inclined heterolithic stratification units (terminology after Thomas *et al.* 1987) occur at Dorchester, Boss Point, Cape Maringouin and Slacks Cove West (stratigraphic

sections 10, 14, 15 & 16 - Plate 10f). At least 10 such occurrence occur within the formation, and are always intercalated with fine-grained siltstone, and associated thin bedded sandstone, ostracod limestone and coal lithofacies (as described in Chapter 5). The IHS units are analogous to epsilon-cross-stratification (Allen 1963) or to lateral-accretion deposits (Leeder 1973, Elliott 1976, Legun and Rust 1982), the term IHS being adopted here because it lacks the genetic connotations implicit in the other terminology (for full discussion see Thomas *et al.* 1987).

IHS units in the Boss Point Formation consist of interbeds (couplets) of dm-thick well sorted, fine- to medium-grained ripple cross-laminated sandstone and cm- and dm- thick siltstone. IHS couplets are up to 1.5 m thick and can be traced laterally for distances of 50 m. The units have a sharp erosive basal contact, and internally show inclined stratification with depositional dips of between 5 and 15°. The orientation of inclined strata is commonly oblique to the paleocurrent direction determined from trough cross-beds in surrounding sediments. Ripples in sandstone beds indicate paleoflow directions which diverge between 40 to 120° from the main paleoflow direction determined from trough cross-bedded sandstones above and below the IHS unit.

4.10.2 Paleochannel Parameters Deduced from IHS

Width and Depth

Considerable research on modern rivers has established a number of empirical relationships between the hydraulic regime and channel characteristics, and these have been widely applied to model ancient river morphologies. For example the two-thirds relationship of point bar width to bankfull channel width (Moody-Stuart 1966, Leeder 1973, Elliott 1976) can be used to estimate the dimensions of the channels that produced the IHS in the Boss Point Formation. Using the maximum recorded thickness (1.5 m) and width (50 m) of Boss Point Formation IHS units, the maximum channel width is calculated as 75 m (using the two-thirds relationship), giving a width:depth ratio of 50:1.

Sinuosity

Sinuosity (P) may be determined using the equation of Schumm (1963):

$$P = \frac{3.5 w^{-0.27}}{h}$$

where:

w = bankfull width ; h = bankfull depth

Sinuosity is calculated (from the above equation) to have

been 1.22, indicating that the channel pattern was "transitional" using Schumm's (1963) classification.

Discharge

Leeder (1973) defined two methods for determining discharge from IHS units (lateral-accretion units of his terminology). Only his method A can be used here; method B is not applicable in the present study because the channel is of mixed load type (see discussion in Leeder 1973, p. 272). Method A uses two equations to calculate Q (mean annual discharge) and Lm (free meander wave length) where:

$$Q = 10.9w^{1.01}$$

$$Lm = 106Lm^{0.46}$$

Using the values determined above, Q is calculated as 110 m³s⁻¹ and Lm as 850m. However, it should be noted that these equations only apply to rivers with sinuosity >1.7 (the Boss Point Formation example has a calculated P= 1.22 [see above]), so that the above calculations may be in error. Note that in the calculation to determine Q, the equation is non-linear, and feet (not metres) must be used, then converted from ft³s⁻¹ to m³s⁻¹ (conversion factor= 0.028) to determine the final value.

4.10.3 Interpretation

IHS units formed by lateral accretion on point bars of meandering rivers, rivers that flowed into lakes through a system of deltas and crevasse splay units. These paleoenvironments are described further in Chapter 7.

CHAPTER 5

SEDIMENTOLOGY OF FINE-GRAINED UNITS

Fine-grained units include mudrock, limestone and coal, and together comprise approximately 12% of the stratigraphic thickness of the formation (Fig. 3.1). Of these, mudrocks (which include siltstone, claystone and sandy mudstone) are by far the most abundant. Paleosol units which to a large extent are also fine-grained are described separately in Chapter 6.

5.1 Massive Mudrock (Fm)

5.1.1 Description

This lithofacies constitutes 10.8% of the thickness of the formation (Fig. 3.1, Appendix I), though many are likely to be laminated siltstones (F1), the distinction between the two lithofacies not always being easy to determine due to weathered outcrops.

Most occurrences of this lithofacies consist of light and medium blue-grey, occasionally reddish grey, noncalcareous very fine- and fine-grained sandy siltstone, with less common siltstone and claystone units. The lithology forms bedded units up to 10 m thick. Each unit

typically has a sharp base which may be either co-planar with underlying beds, or rest on an erosional surface (Plate 11a). Siderite nodules up to 10 cm diameter are common (Plate 11b) as are calcrete nodules and comminuted carbonaceous debris. Apart from this, the lithofacies lacks fabric, in large part due to the weathered nature of outcrops and to extensive bioturbation (Plate 11c). Perpendicular and bedding parallel burrow structures up to 5 cm long and <1 cm wide were observed in some outcrops.

Although the majority of siltstones are grey in colour, distinctive deep red and greyish red units also occur. At Johnson Mills blue-grey sandstone is overlain by reddish grey and colour mottled, noncalcareous sandy siltstone which is interpreted as a paleosol interval (Plate 12). Sharply overlying this paleosol is a 30 cm thick, deep red, noncalcareous claystone with calcrete nodules. Such a colour change over a thin vertical interval is considered a response to fluctuating water levels, the grey coloration indicative of reducing conditions and relatively high water table levels; the red coloration representing oxidation during conditions of relatively low water table levels.

Little attention has previously been paid to this lithofacies. Lawson (1962) briefly described such units as shale, and interpreted them as swamp, lacustrine and channel fill units with little further elaboration.

Plate 11

a) Vertical airphoto of the shore platform, north side of Grindstone Island, showing erosional top to succession of trough cross-bedded sandstone (arrowed), overlain by siltstone. Units dip approximately 45° toward south (top of photo). Scale bar is 50 m.

b) Siderite nodules within the massive siltstone lithofacies, Slacks Cove East section. Scale is 50 cm long, with 10 cm divisions.

c) Massive siltstone outcrop at Cape Maringouin. Scale is 50 cm with 10 cm divisions.

d) Photomicrograph of pin-stripe lamination formed by the alternation of very fine-grained sandstone (light coloured quartz-rich band) and siltstone. Scale bar is 0.25 mm.

e) Branching burrows within the laminated siltstone lithofacies, Cape Maringouin. The 1 cm thick horizontal bed in the middle of the figure is a very calcareous ostracod-bearing siltstone. Note also siderite nodules left centre. Scale is in 10 cm divisions.

f) Tree stump *in situ* (arrowed) within laminated siltstone, Boss Point. The trunk is approximately 50 cm wide and still has impressions of bark adhering in basal portions. The trunk is cut by a 40 cm thick sandstone bed at the top of photo. Scale is 50 cm long.

g) Laminated siltstone lithofacies at Cape Maringouin with 1 cm thick beds of siderite (lighter zones) throughout. Scale is 50 cm long with 10 cm divisions.

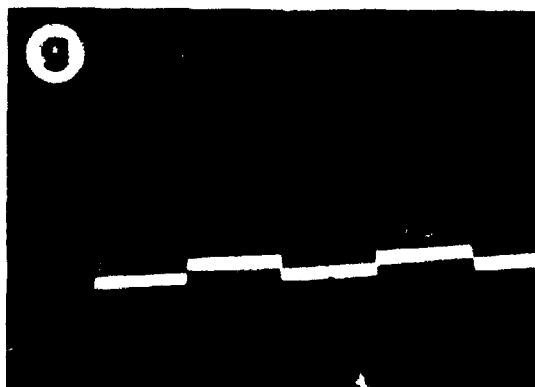
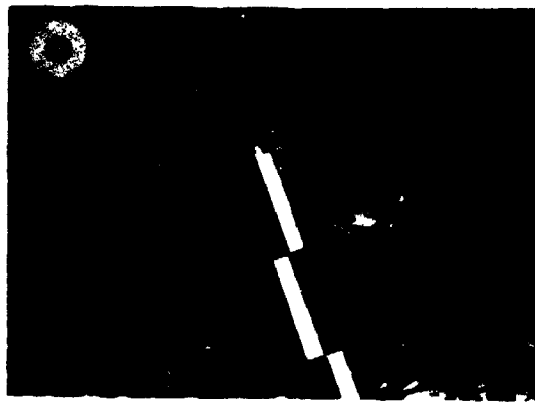
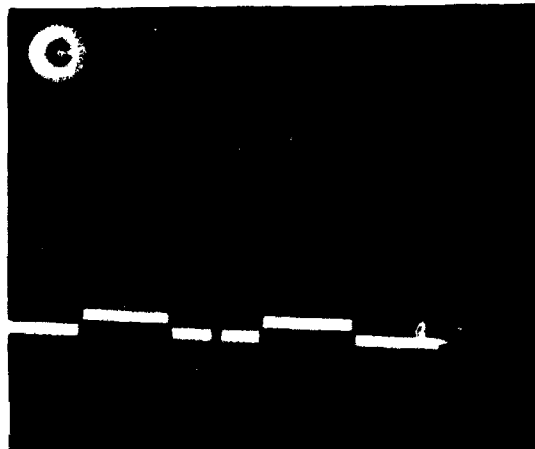
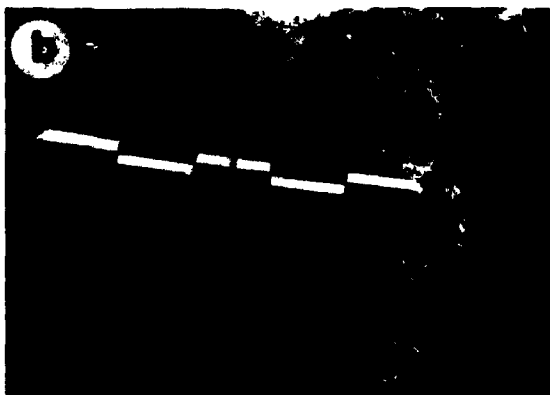
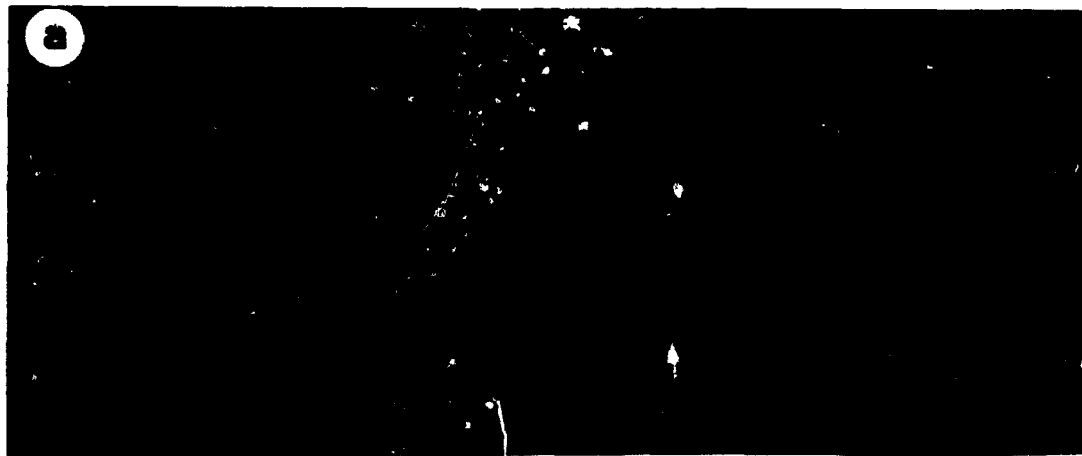
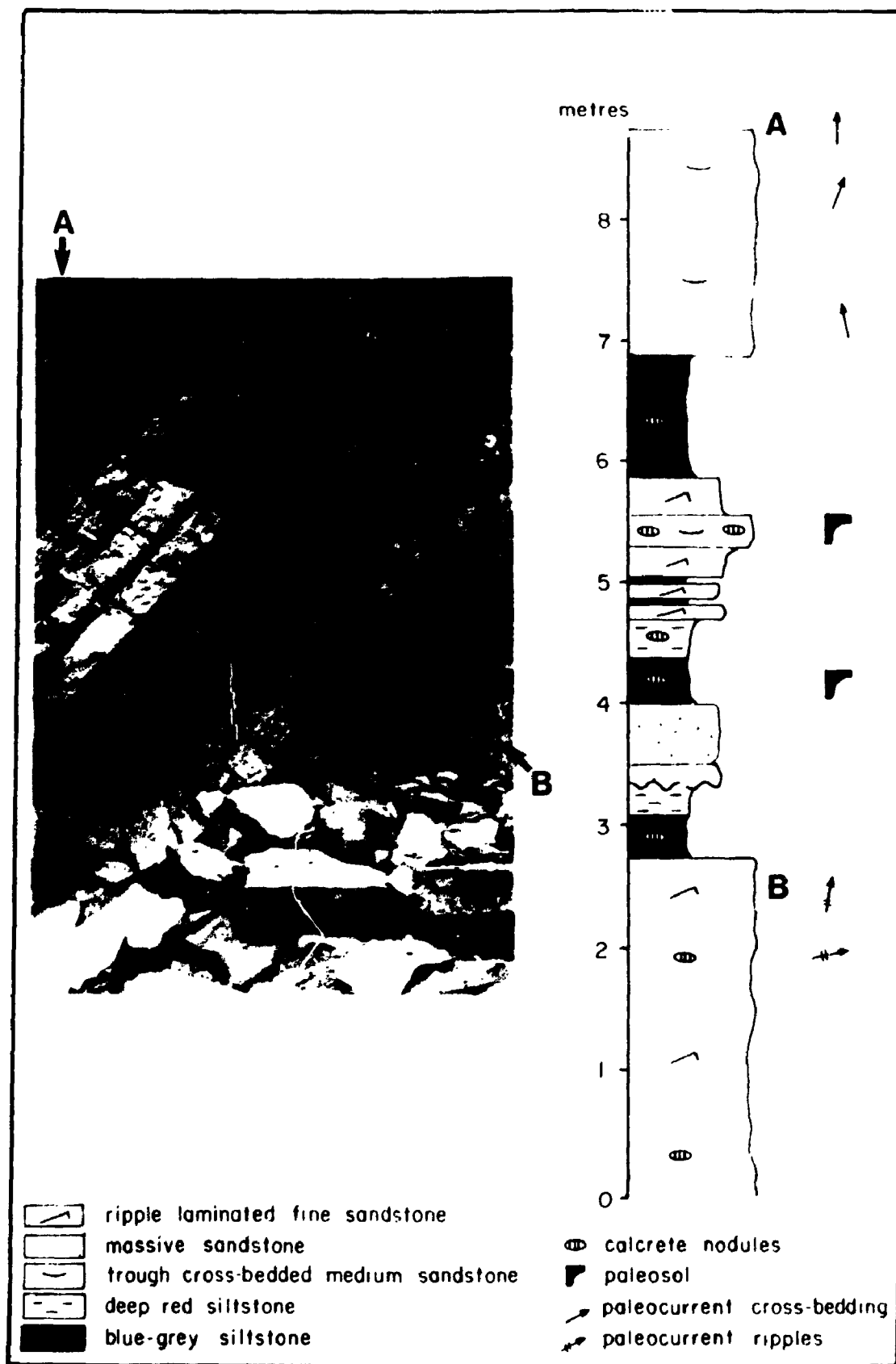


Plate 12

Alternating blue-grey and deep red coloured siltstone beds from Johnson Mills. Such colour changes are attributed to changing water levels. The red coloration formed when water levels were low and oxidising conditions prevailed. The blue-grey coloration is more typical of the formation and indicates relatively high water levels. Stratigraphic column given at right. Scale bar in photo is 50 cm with 10 cm divisions.



5.1.2 Petrography and Petrology

Quartz is the dominant detrital component forming between 10 and 45% of the rock. Grains are very angular to angular and range up to 0.15 mm diameter. Accessory grains in order of abundance include opaques (5-15%), muscovite and less common biotite, typically aligned (presumably parallel to original stratification), and rare green pleochroic chlorite up to 0.15 mm diameter. Angular plagioclase is present in trace amounts and commonly shows brownish weathered margins, though the central parts of grains have a fresh appearance. Vague semi-circular arrangements of quartz grains and elongate mud-filled structures up to 2 mm in size may be bioturbation features, bioturbation being evident in outcrop. However, there is a general lack of bioturbation features in thin section, and this is likely to reflect the high degree of bioturbation, which resulted in extensive reworking of the sediment.

The calcrete nodules that occur within the massive mudrocks have not been systematically studied, but appear analogous to calcrete nodules described from paleosol units (Chapter 6).

Siderite nodules from Boss Point Formation mudrock units have been studied by Mitchell (1986). He concluded that the nodules formed early in diagenesis, initially in response to microbial decay of organic material in

reducing conditions which provided a microenvironment conducive to carbonate precipitation.

XRD analyses indicate a clay mineralogy dominated by kaolinite and illite, with lesser abundances of muscovite and chlorite (Fig. 5.1).

5.1.3 Interpretation

The massive nature of the lithofacies makes it difficult to interpret the mode of formation. From regional considerations (Chapter 7) it is clear that individual siltstone packages can be correlated for >20 km across the basin, suggesting that the massive mudrocks are lacustrine in origin. The alternative explanation, that the mudrocks were related to overbank sedimentation is not consistent with the extensive distribution of the facies across the basin.

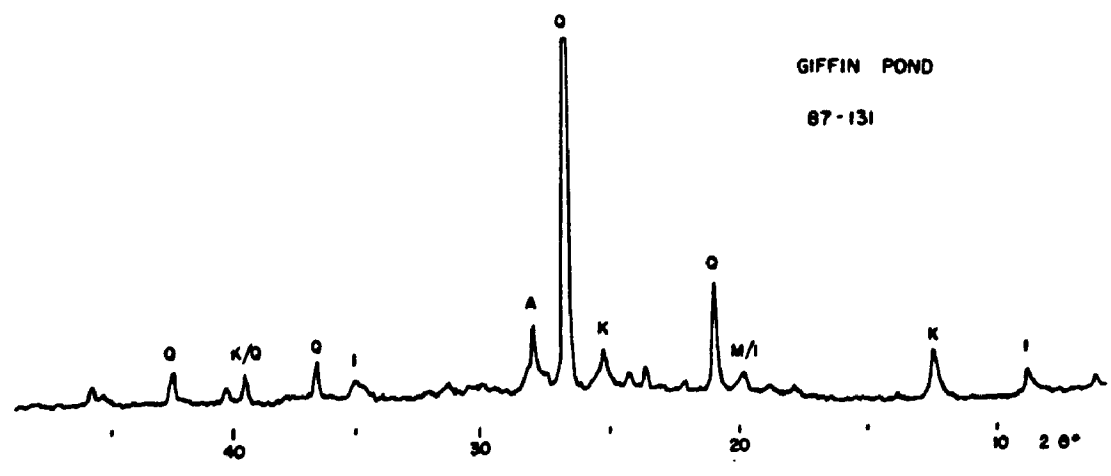
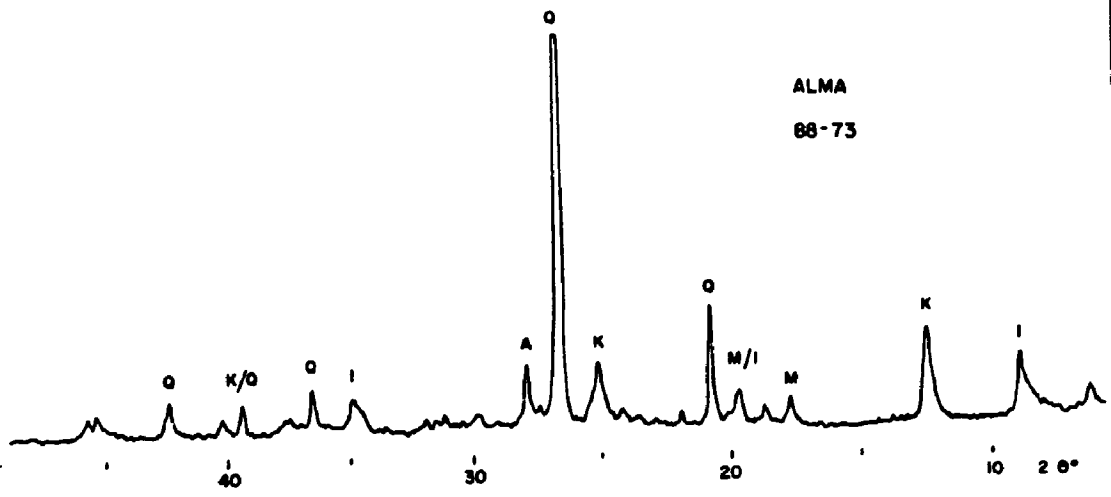
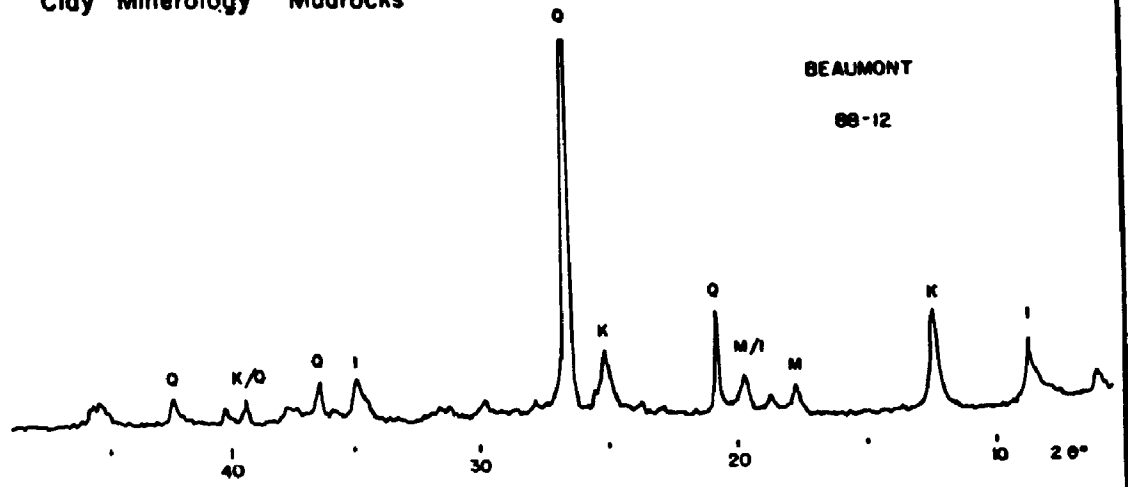
5.2 Laminated Mudrock (F1)

5.2.1 Description

Laminated mudrocks form 0.8% of the lithologic thickness of the formation (Fig. 3.1, Appendix I), though this is probably a gross underestimate, given that it is not always easy to differentiate massive and laminated siltstones due to the weathered nature of outcrops.

Fig. 5.1 Representative clay mineralogies determined by XRD analysis of Boss Point mudrocks. Note that the 12° two-theta peak could be a combined kaolinite/chlorite species.

Clay Mineralogy - Mudrocks



A - Albite I - Illite K - Kaolinite M - Muscovite Q - Quartz

The lithofacies consists of light to medium blue-grey, less commonly reddish grey, noncalcareous finely laminated sandy siltstone, siltstone and clayey siltstone, that form units up to 5.5 m thick (Appendix Ia). A series of such units may form intervals up to 15 m thick.

Pin-stripe lamination up to 5 cm in thickness is common, formed by the interbedding of very fine-grained sand and siltstone laminae (Plate 11d). Bioturbation is common (Mitchell 1986), burrows up to 10 cm long and <1.5 cm wide occur perpendicular to bedding, and are infilled with mudstone or replaced by siderite. Some forms show an upward branching morphology (Plate 11e). Comminuted to small twig-sized carbonaceous debris is commonly associated with the siltstone, and at several localities *in situ* tree stumps were observed (Plate 11f), some with roots at their base. Leaf fragments are occasionally preserved. Siderite nodules up to 10 cm diameter and 1-2 cm thick siderite beds (Plate 11e & 11g) occur at most localities; their occurrence and mode of formation previously was described by Mitchell (1986).

In almost all cases the base of siltstone successions is sharp, and may be conformable with underlying units, or markedly irregular. The latter have a relief of as much as 10.5 m. In such cases the top of the underlying sandstone was clearly eroded, the siltstone infilling an abandoned fluvial channel or series of channels. The top contacts of siltstone successions are sharp, mostly

planar, but commonly erosional.

The Cape Enrage Occurrence (Lithofacies F1)

Laminated mudrocks, interbedded with sandstone and paleosol units, are well exposed for approximately 3 km, immediately north of Cape Enrage (Fig. 5.2). This locality shows many of the characteristics of the lithofacies and therefore serves as a useful case history, which is discussed in detail below. Two siltstone units occur, designated the upper and lower siltstones respectively (Units II & IV - Fig. 5.3 & 5.4). These units can be traced for 3 km north of Cape Enrage. The siltstones are interbedded with trough cross-bedded sandstones (St), designated Units I, III, V and VI on the basis of relative stratigraphic position, petrologic variations and discrete paleocurrent orientations (Fig. 5.4). These lithologies crop out along shore platform exposures, and in small headlands and bays. The embayments are designated Bays 1 to 6, and as north (N) or south (S) for each Bay (Fig. 5.5).

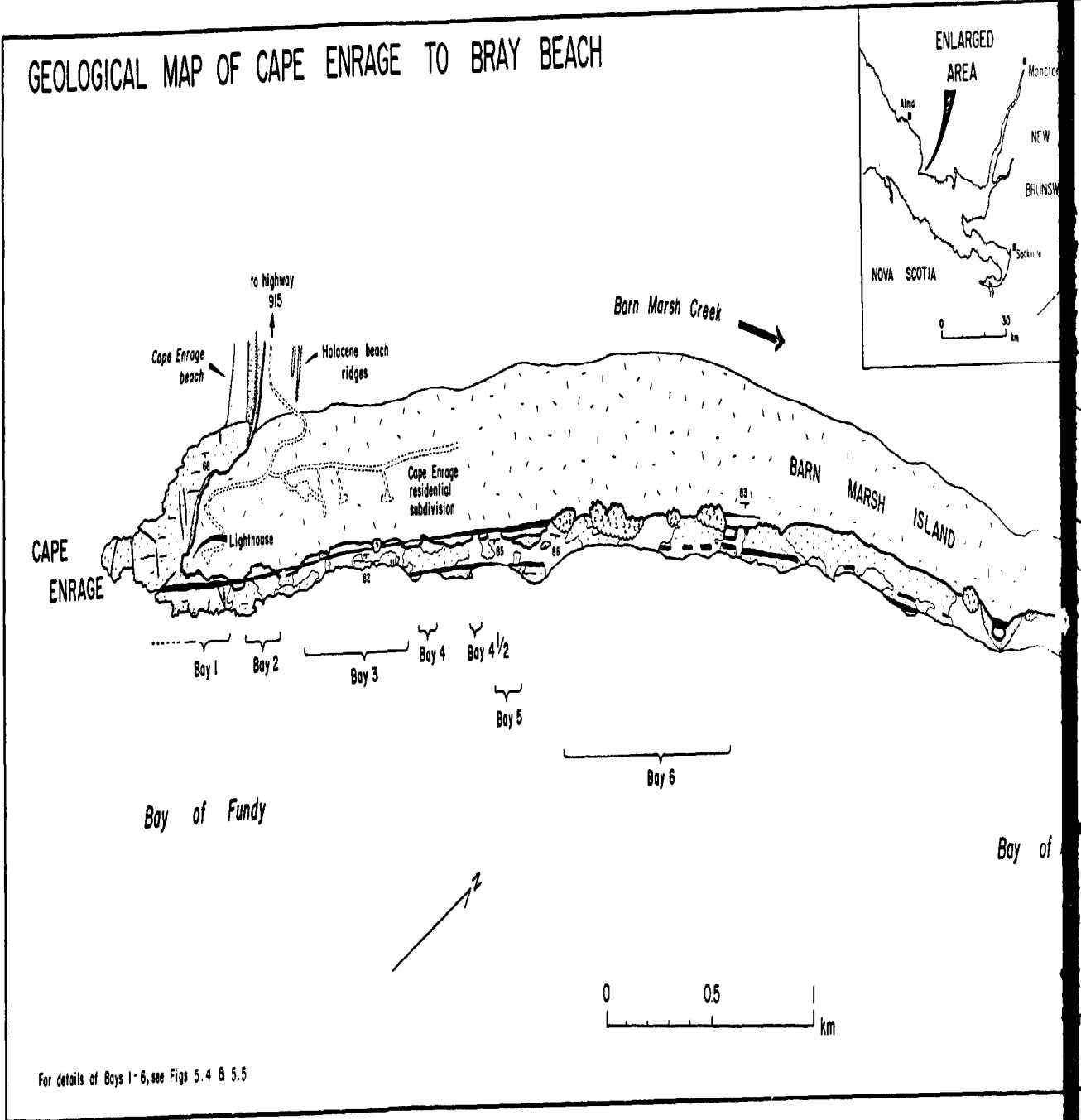
The Lower Siltstone Unit (Unit II)

The lower siltstone unit consists of medium and dark blue-grey laminated claystone, siltstone and fine-grained sandy siltstone up to 3 m thick. At the southern

Fig. 5.2 Geological map of Cape Enrage to Bray Beach, New Brunswick, showing locations of Bays 1 to 6 and lateral extent of some of the siltstone units along the shore platform.

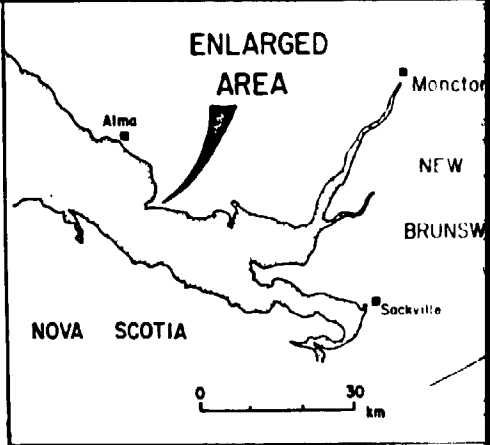
range to Bray Beach, New
ons of Bays 1 to 6 and
the siltstone units

GEOLOGICAL MAP OF CAPE ENRAGE TO BRAY BEACH

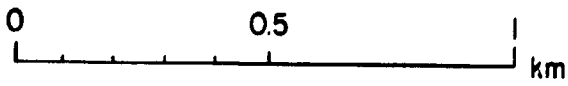
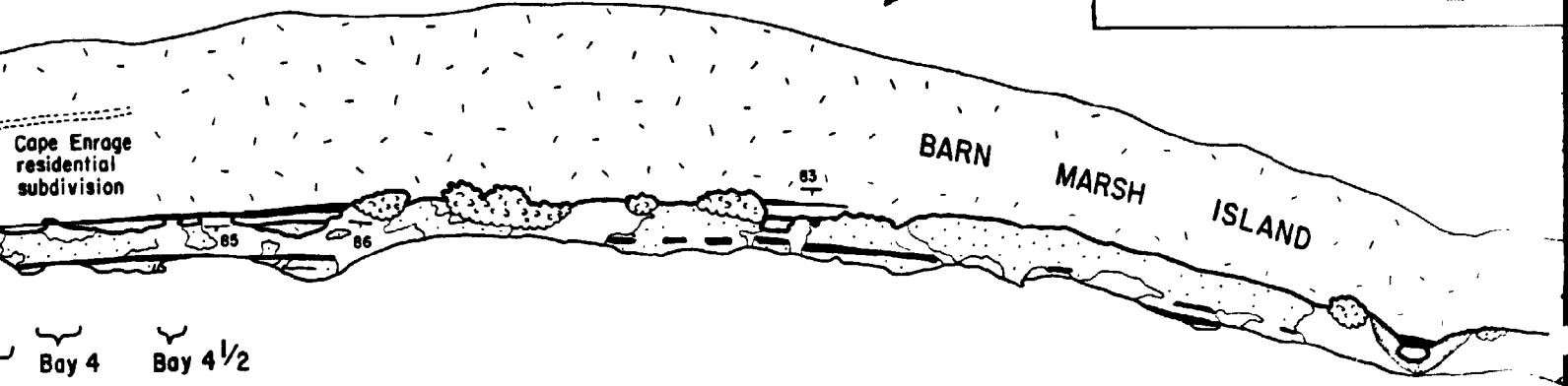


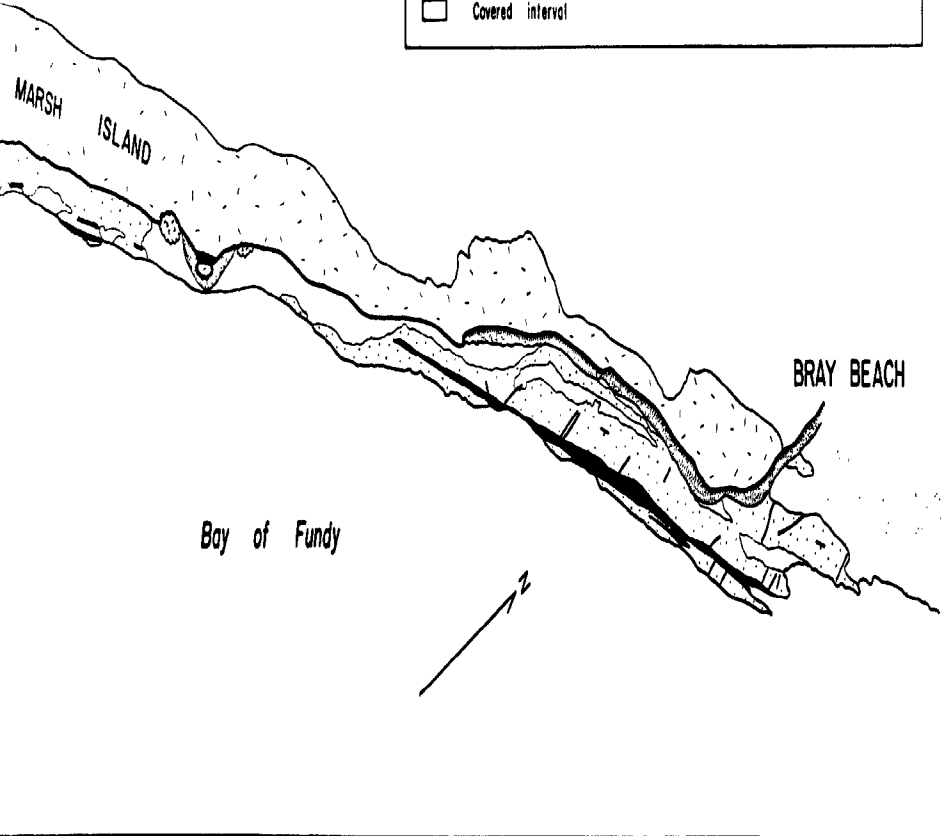
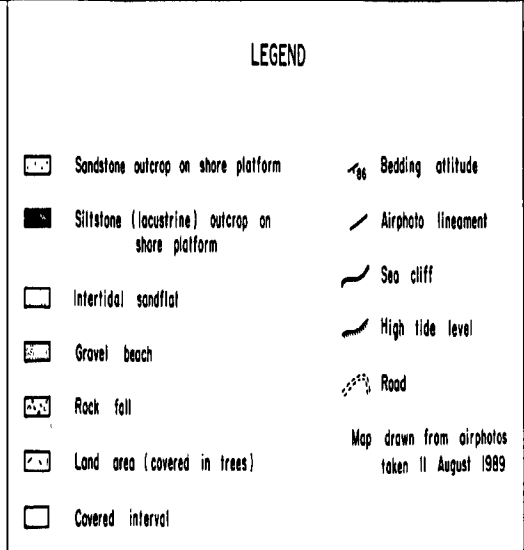
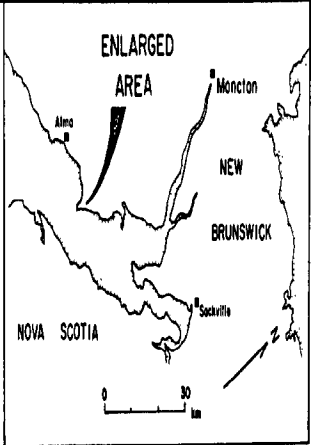
For details of Bays 1-6, see Figs 5.4 & 5.5

TO BRAY BEACH



Barn Marsh Creek →





ding attitude

photo lineament

cliff

h tide level

d

awn from airphotos
en 11 August 1989

BRAY BEACH

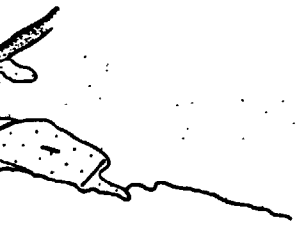


Fig. 5.3 Composite stratigraphic column for the sequence at Cape Enrage. Thicknesses used are the maximum recorded for each stratigraphic unit. The six units are recognised on the basis of lithology and paleocurrent directions.

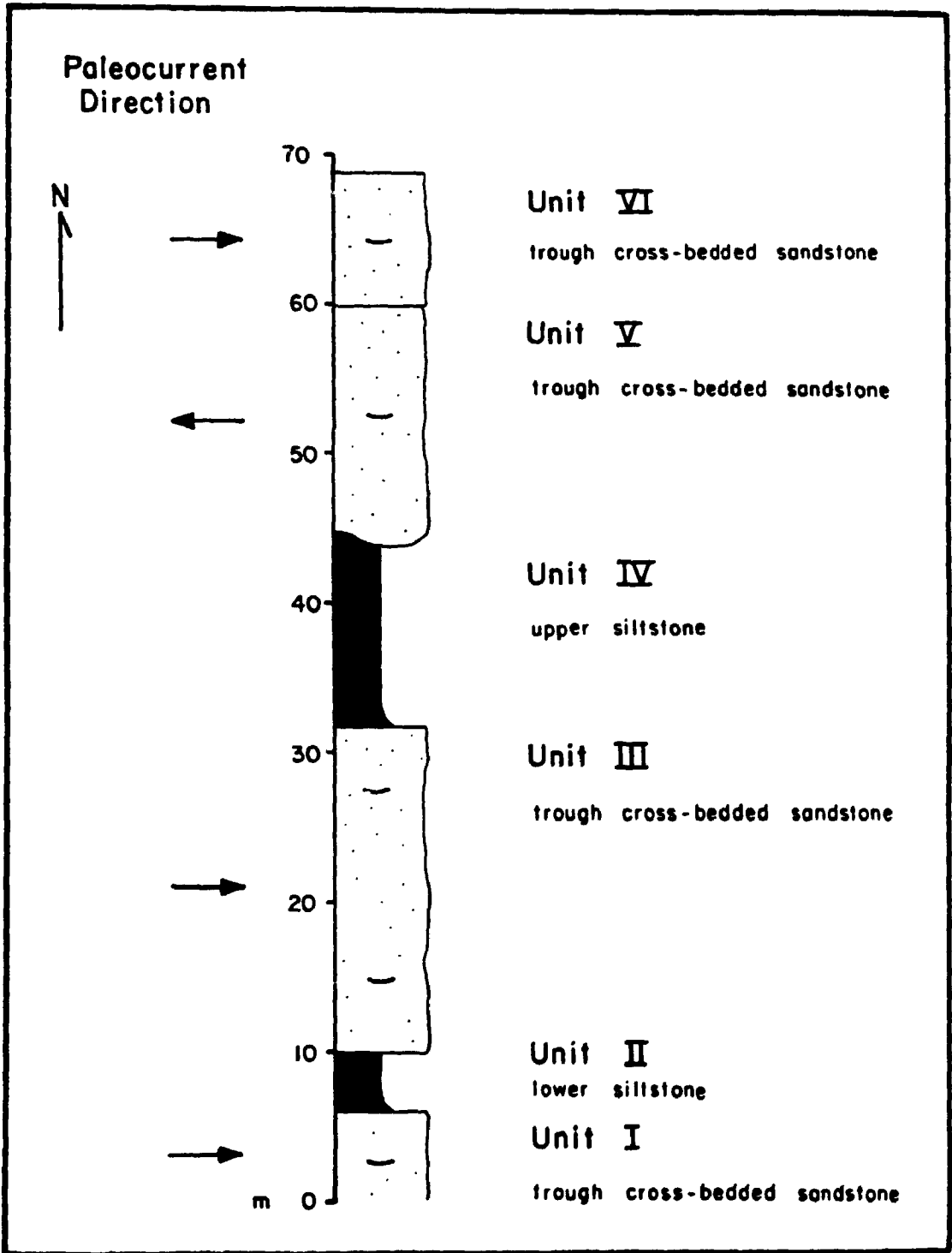
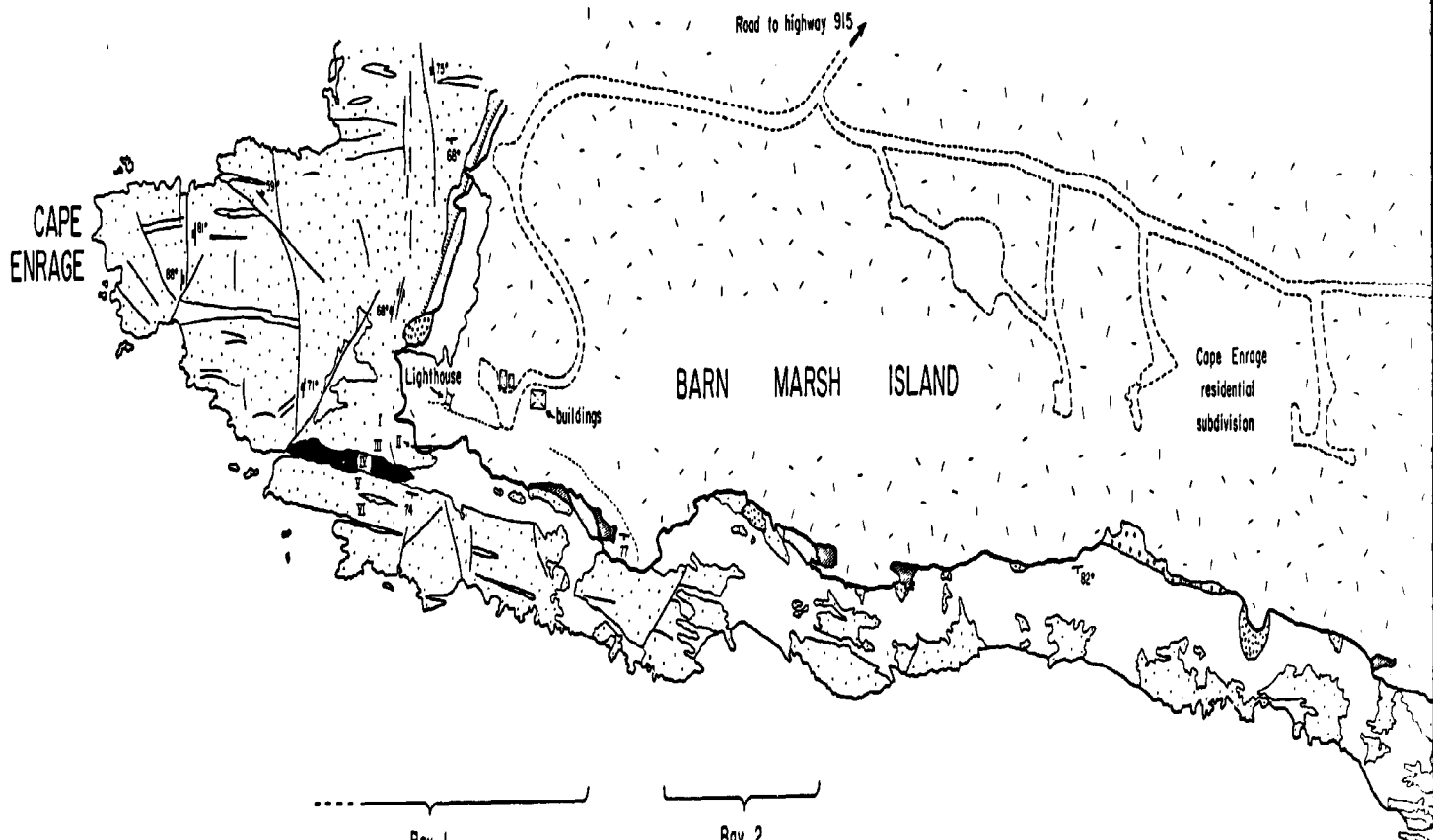
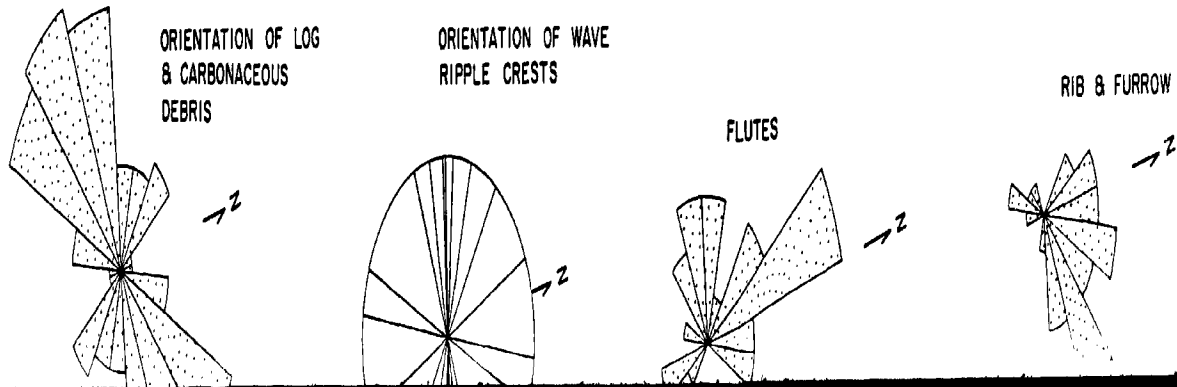
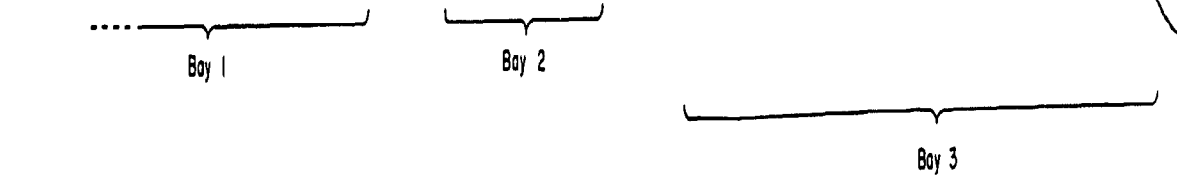


Fig. 5.4 Geological map of Bays 1 to 6, Cape Enrage and
paleocurrent directions for Units I, III, V and VI.

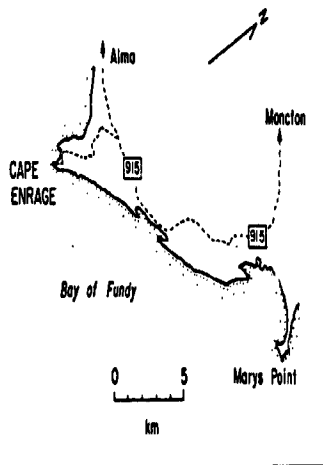
GEOLOGICAL MAP BAYS 1-6, CAPE ENRAGE



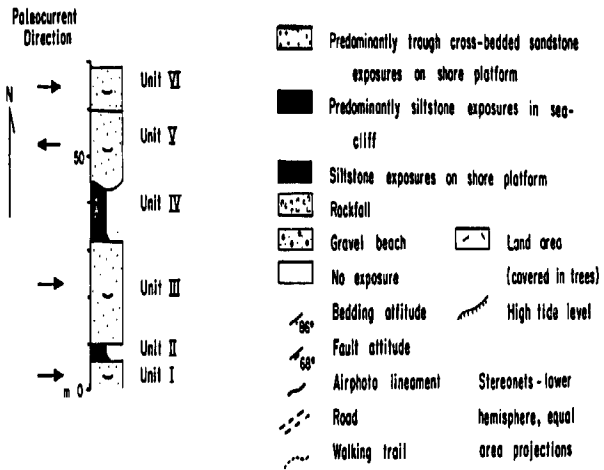
BAY OF FUNDY



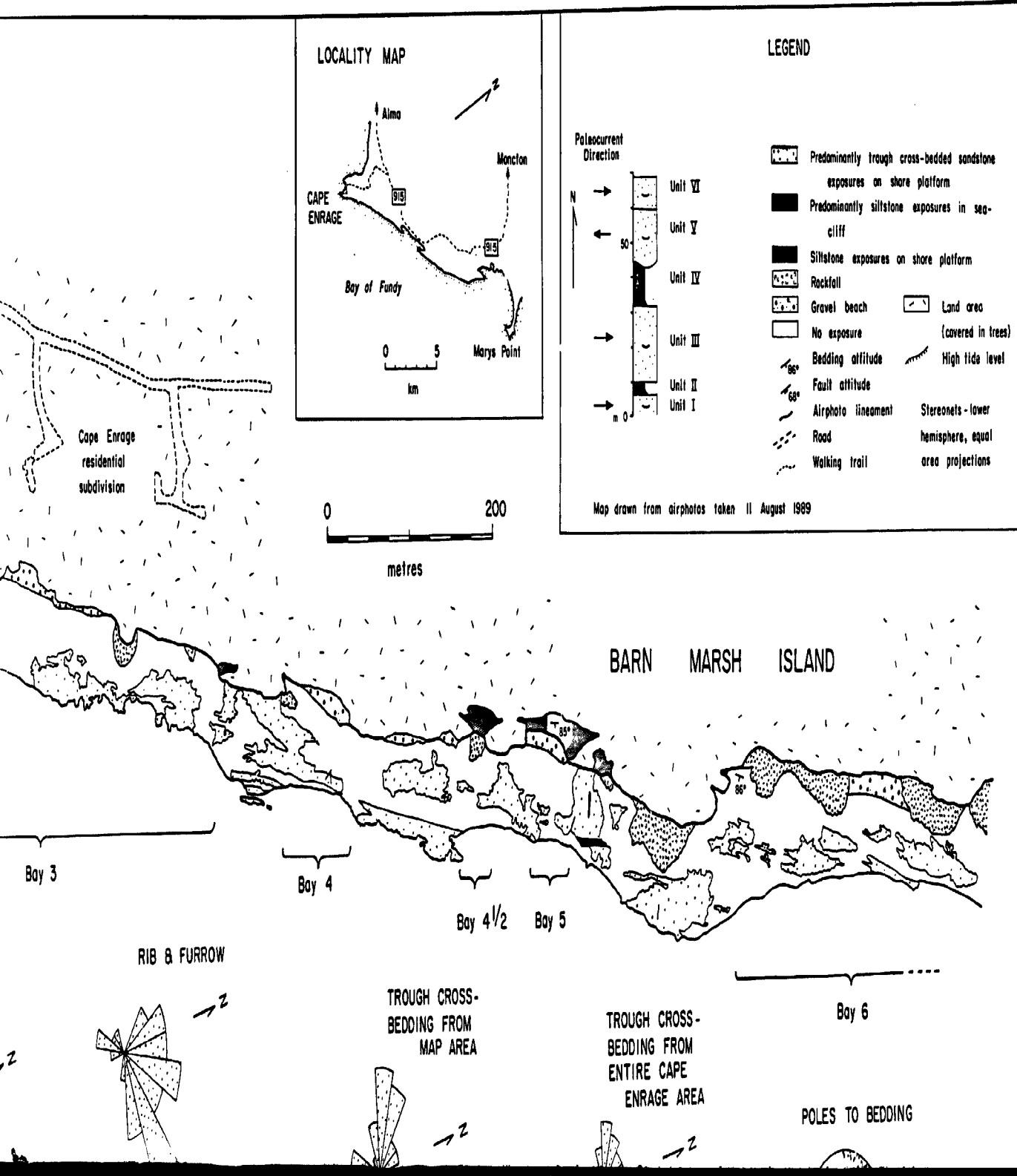
LOCALITY MAP

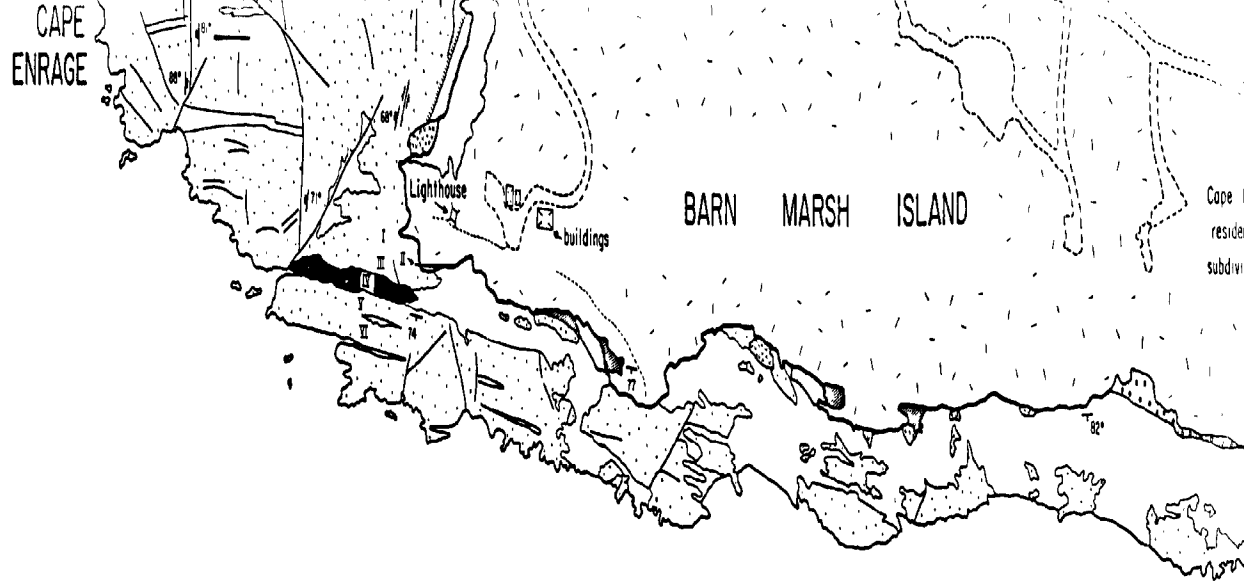


LEGEND

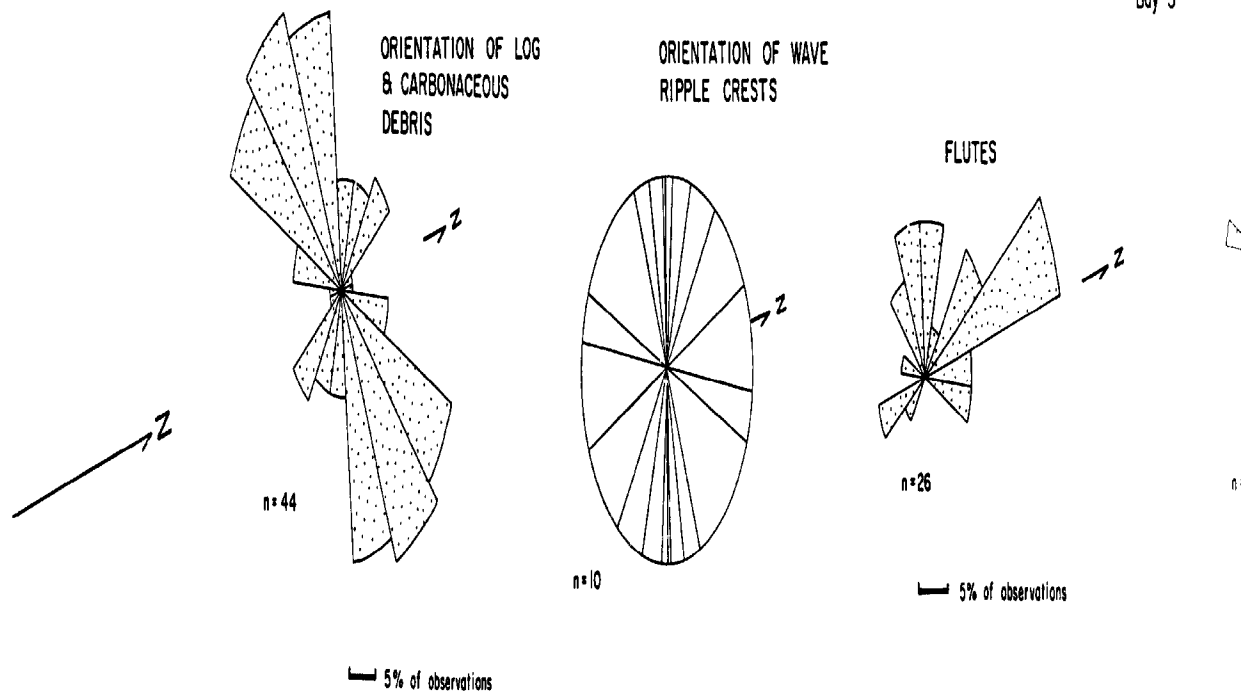
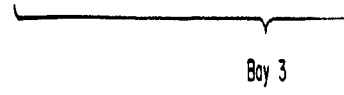
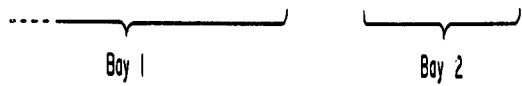


Map drawn from airphotos taken 11 August 1989





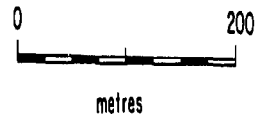
BAY OF FUNDY



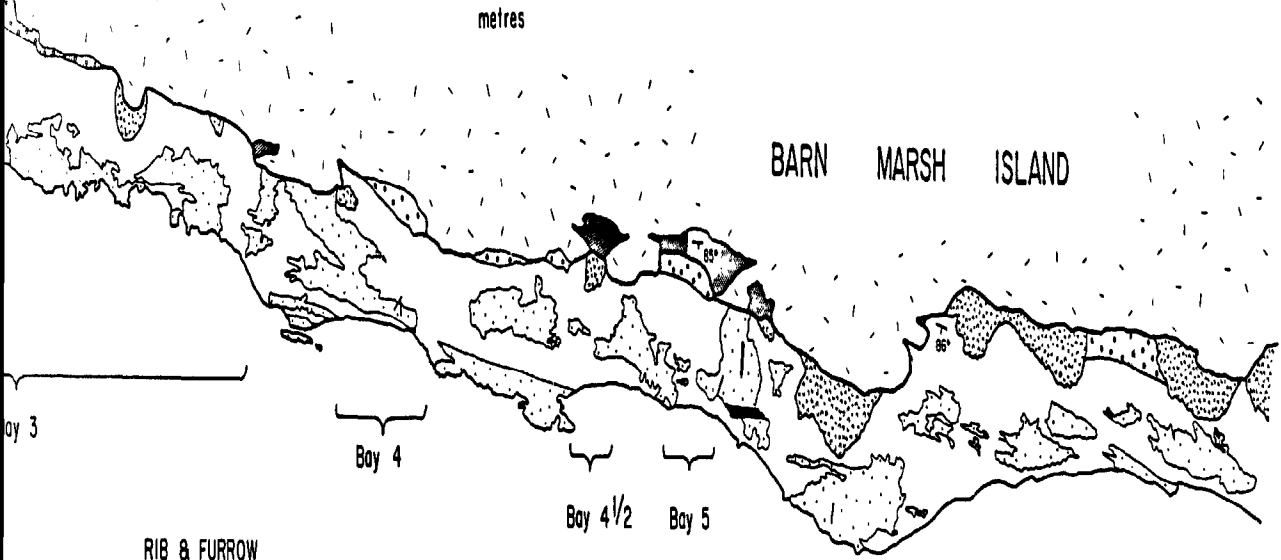
Cape Enrage residential subdivision

Map drawn from airphotos taken 11 August 1989

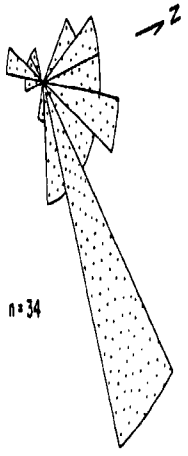
	Airphoto lineament		Stereonets - lower hemisphere, equal area projections
	Road		
	Walking trail		



BARN MARSH ISLAND



RIB & FURROW



5% of observations

TROUGH CROSS-BEDDING FROM MAP AREA



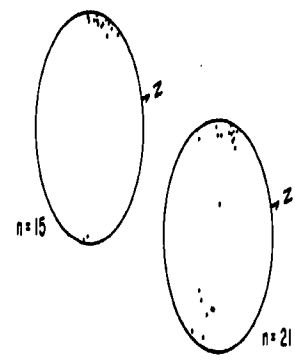
5% of observations

TROUGH CROSS-BEDDING FROM ENTIRE CAPE ENRAGE AREA



5% of observations

POLES TO BEDDING



POLES TO FAULTS

Bay 3

Bay 4

Bay 4 1/2

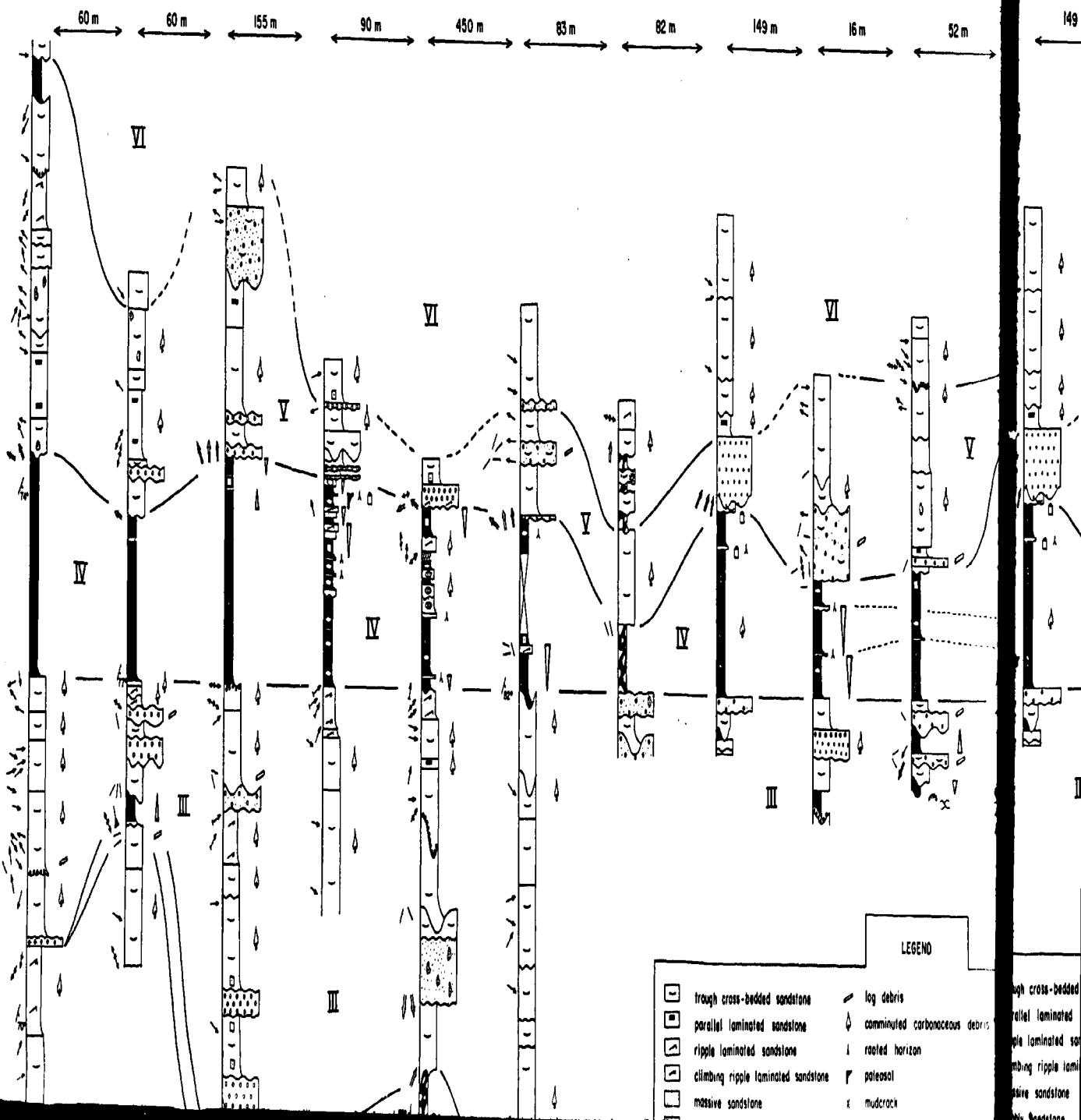
Bay 5

Bay 6

Fig. 5.5 Stratigraphic columns for Bays 1 to 6, Cape Enrage. The base of Unit IV (upper siltstone) has been used as a datum. Correlation between Bays is made on the basis of lithology and paleocurrent directions.

SOUTH

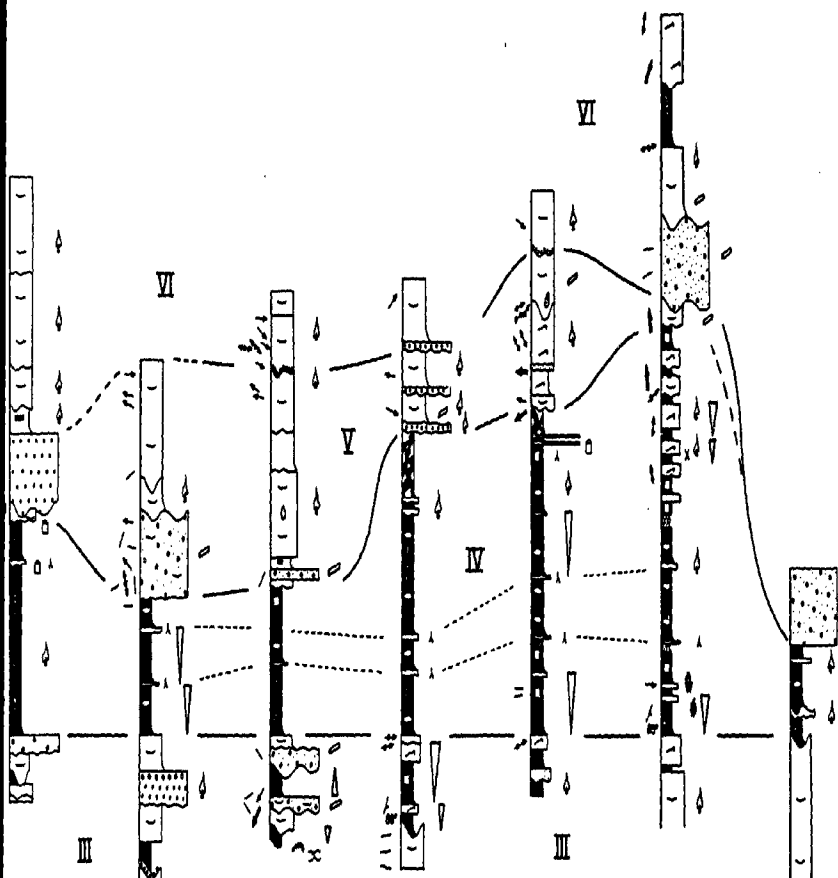
BAY 1S BAY 1N BAY 2S BAY 2N BAY 3S BAY 3N BAY 4S BAY 4N BAY 4 1/2S BAY 4 1/2N BAY 4N



NORTH

BAY 4N BAY 4 1/2S BAY 4 1/2N BAY 5S BAY 5N BAY 6S BAY 6N

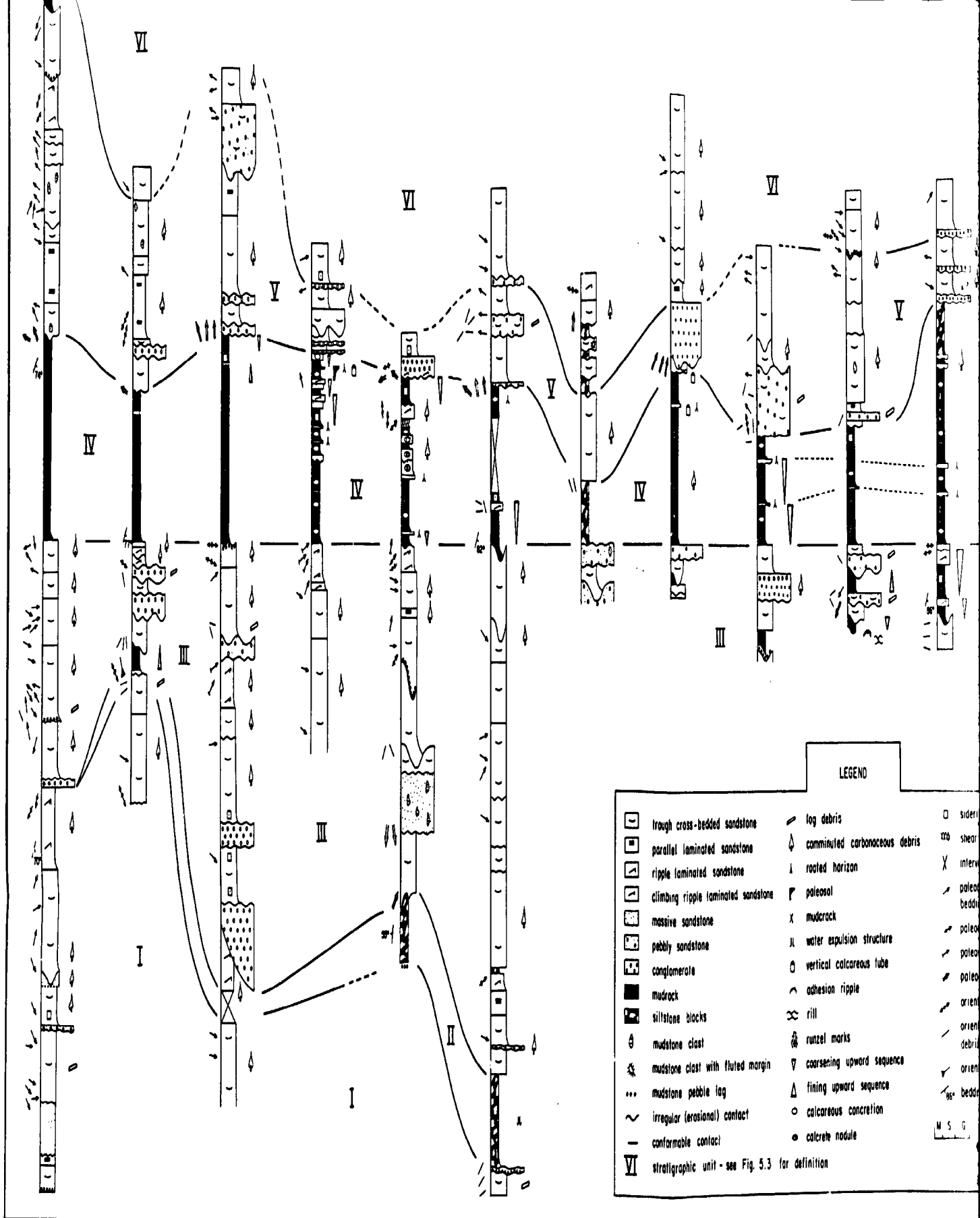
149 m 16 m 52 m 53 m 190 m 875 m



LEGEND

- | | | |
|---------------------------------|--------------------------------|---|
| high cross-bedded sandstone | log debris | siderite nodule |
| parallel laminated sandstone | comminuted carbonaceous debris | shear zone |
| fine laminated sandstone | rooted horizon | interval not exposed |
| high ripple laminated sandstone | paleosol | paleocurrent from trough cross-bedding B rib and furrow |
| fine sandstone | mudcrack | paleocurrent from current ripples |
| shaly sandstone | water expulsion structure | paleocurrent from climbing ripples |

10



LEGEND

- | | | | | | | | | | | | | | | | | | | | | | | | | | | | | | | | | | | | | | | | | |
|-------------------------|------------------------|----------------------|-------------------------------|-------------|------------|------------------|-------------|----------------------|--------------------|---------------------------------------|-------------------------|-----------------------|-------------------------|------------------------|----------------|------------------------------------|--------------------|--------------|--------------|-------------------------------|------------------------------|---------------------|----------|------------------|--------------------------------|----------------------------|---------------------------|---------------------|--------------|-----------|--------------|------------------|--------------|--------------|--------------|---------------------|---------------------|------------------|------------------|-------|
| ▭ (trough cross-bedded) | ▭ (parallel laminated) | ▭ (ripple laminated) | ▭ (climbing ripple laminated) | ▭ (massive) | ▭ (pebbly) | ▭ (conglomerate) | ▭ (mudrock) | ▭ (siltstone blocks) | ⊕ (mudstone clast) | ⊕ (mudstone clast with fluted margin) | ⋯ (mudstone pebble lag) | ~ (irregular contact) | - (conformable contact) | VI (lithographic unit) | ⊕ (log debris) | ⊕ (conminuted carbonaceous debris) | ⊕ (rooted horizon) | P (paleosol) | X (mudcrack) | ⊕ (water expulsion structure) | ⊕ (vertical calcareous tube) | ~ (adhesion ripple) | ∞ (rill) | ⊕ (runzel marks) | ▽ (coarsening upward sequence) | △ (fining upward sequence) | ○ (calcareous concretion) | ● (calcrete nodule) | □ (siderite) | ▭ (shear) | X (interval) | ▭ (paleosol bed) | ▭ (paleosol) | ▭ (paleosol) | ▭ (paleosol) | ▭ (oriented debris) | ▭ (oriented debris) | ▭ (oriented bed) | ▭ (paleosol bed) | M S G |
|-------------------------|------------------------|----------------------|-------------------------------|-------------|------------|------------------|-------------|----------------------|--------------------|---------------------------------------|-------------------------|-----------------------|-------------------------|------------------------|----------------|------------------------------------|--------------------|--------------|--------------|-------------------------------|------------------------------|---------------------|----------|------------------|--------------------------------|----------------------------|---------------------------|---------------------|--------------|-----------|--------------|------------------|--------------|--------------|--------------|---------------------|---------------------|------------------|------------------|-------|

VI lithographic unit - see Fig. 5.3 for definition

end of the section the lower siltstone has been eroded out by an overlying pebbly sandstone (Fig. 5.5). North of this, large siltstone blocks with fluted outer margins exposed at the base of the sea cliff (Plint 1986, fig. 12) are the only remnants of the lower siltstone interval. At Bay 1N, 100 m to the north, the interval coarsens upward from siltstone to fine-grained sandy siltstone (Fig. 5.5), the upper contact of the siltstone displaying well developed rills (Plate 13a). Further to the north at Bay 3S, the siltstone rests on a scoured base, which is lined with a mudstone pebble clast lag (Fig. 5.5), whereas at Bays 3S and 3N, the unit passes into siltstone blocks (Figs. 5.5, 5.6 & 5.7). Further north, the lithology is not exposed.

The Upper Siltstone Unit (Unit IV)

The upper siltstone is separated from the lower siltstone by Unit III, a 5 to 20 m thick trough cross-bedded sandstone with predominantly easterly paleocurrent indicators (Figs. 5.3 & 5.5).

The upper siltstone is 5 to 15 m thick and consists of medium blue-grey and reddish grey laminated claystone, siltstone and sandy siltstone, together with cm- and dm-metre bedded sandstone, rooted sandstone and paleosol units (Figs. 5.5 & 5.8). Sandstone units are typically very fine- to fine-grained, and well sorted, with massive,

Plate 13

a) Branching rills exposed at the top of the lower siltstone (Unit II) at Bay 1N, Cape Enrage. Branched nature indicates that the paleoflow was from the top toward the base of the photo.

b) Mould of small leaf in fine-grained sandstone at base of upper siltstone (Unit IV), Bay 3N, Cape Enrage.

c) Crawling traces preserved in fine-grained sandstone at base of upper siltstone (Unit IV), Bay 3N, Cape Enrage. The traces were probably made by a small myriapod, most likely a diplopoda (millipede).

d) Coarsening-upward cycles at the top of the upper siltstone (Unit IV) at Bay 2N, Cape Enrage. Arrow (at left) points to a bedding parallel shear zone. Scale is 50 cm long with 10 cm divisions.

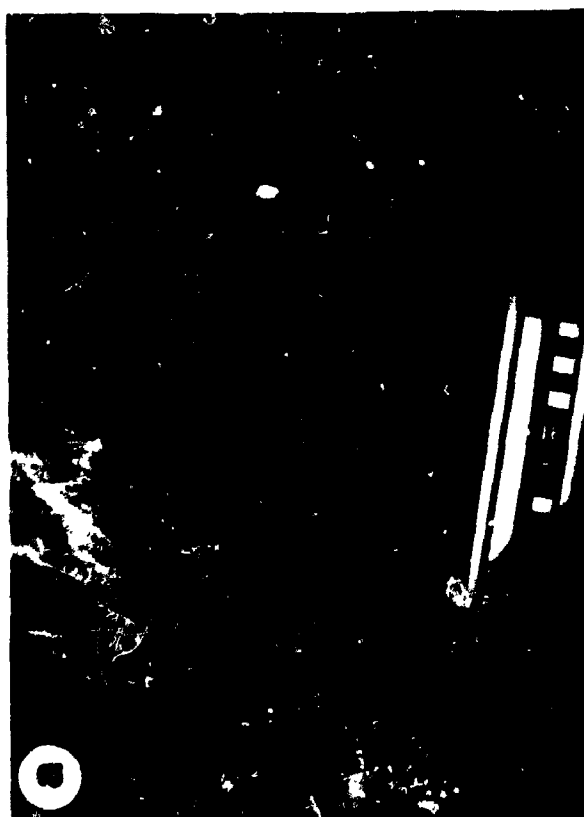


Fig. 5.6 Sketch of the lower siltstone (Unit II) in Bay 3S showing blocky (commonly folded and sheared) nature of the siltstone, intercalated with irregular shaped siltstone pebble conglomerate and sandstone. Note also the irregular contact between Units II and III, and erosional contact between Units I and II. 1 = intraformational pebble lag. 2 = large scour pits at top of sandstone, up to 1.5 m deep and 8 m wide. 3 = large siltstone block; bedding 008/55W. 4 = top of sandstone has numerous small faults. 5 = siltstone block; bedding 039/78E. 6 = tightly folded siltstone block; fold axis 029/16; bedding on west limb 024/85W. 7 = flutes at base of siltstone pebble conglomerate trend 035°. Drawn from field sketch and black and white photograph.

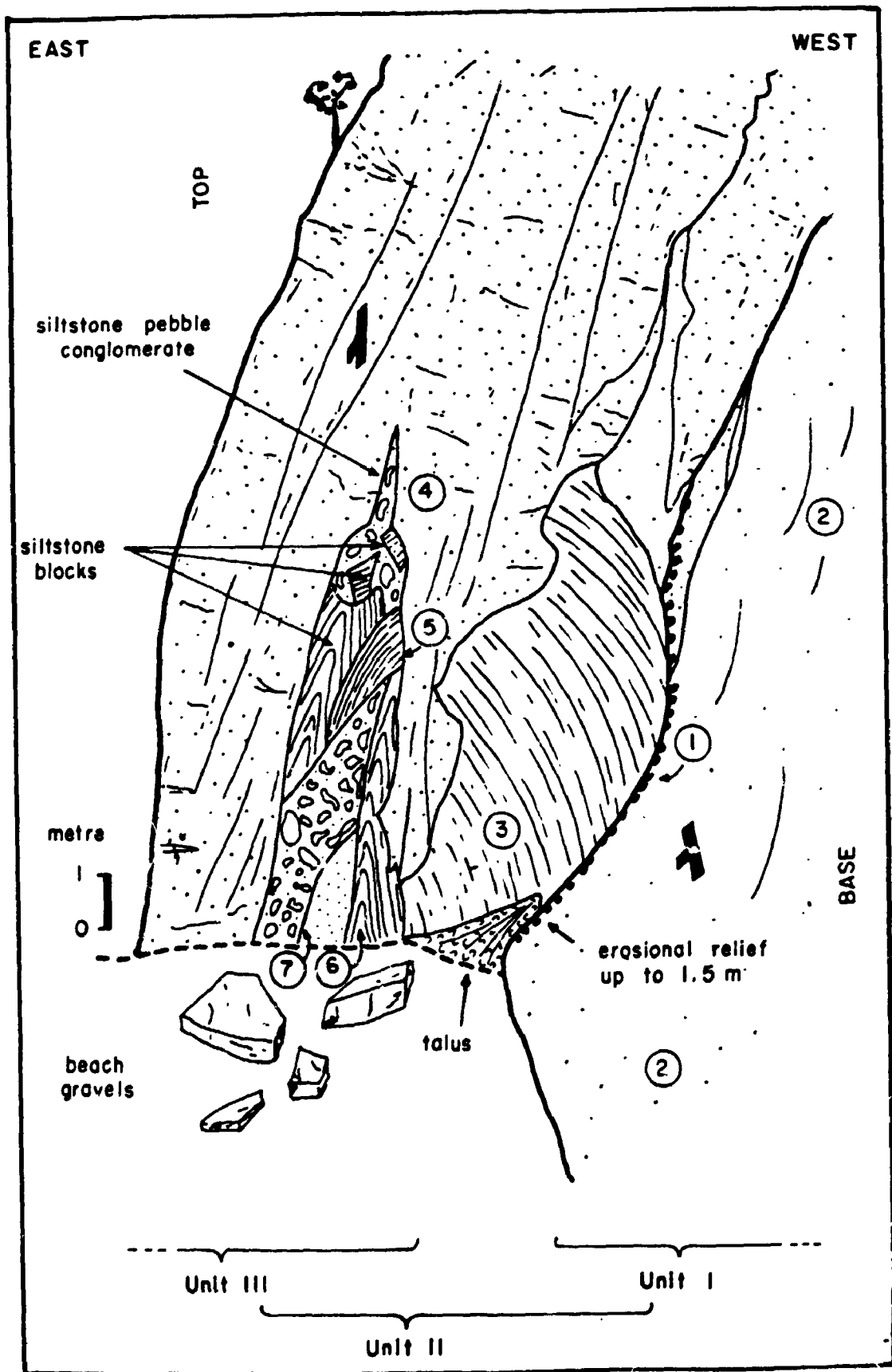


Fig. 5.7 Sketch of the lower siltstone (Unit II) in Bay 3N showing blocky (often folded and faulted) nature of the siltstone. 1 = <1 m diameter sandstone blocks in siltstone. 2 = intraformational pebble lag. 3 = siltstone block, bedding 057/83E. 4 = siltstone block, bedding 173/85E. 5 = siltstone block, bedding 014/85W. 6 = siltstone block, bedding 032/57NW. 7 = siltstone block, bedding 011/71E. 8 = siltstone block, bedding 164/74E. 9 = high angle shear 171/83E. 10 = low angle shear 017/23E. 11 = flutes on base of sandstone trend 003°. Stereonet shows high angle north-south trending bedding poles and north-south trending poles to shears. Lower hemisphere, equal area projection. Drawn from field sketch and black and white photograph.

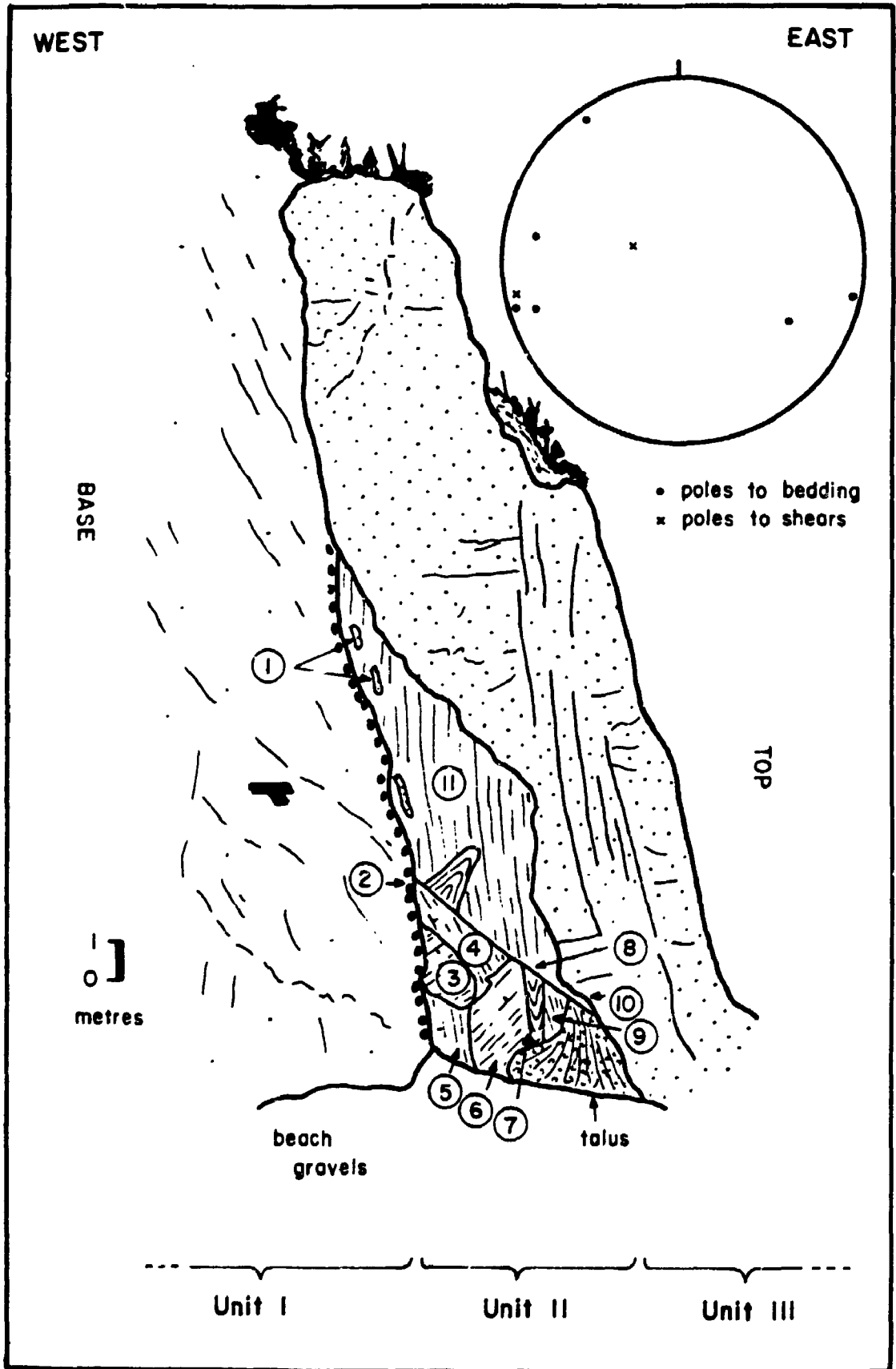
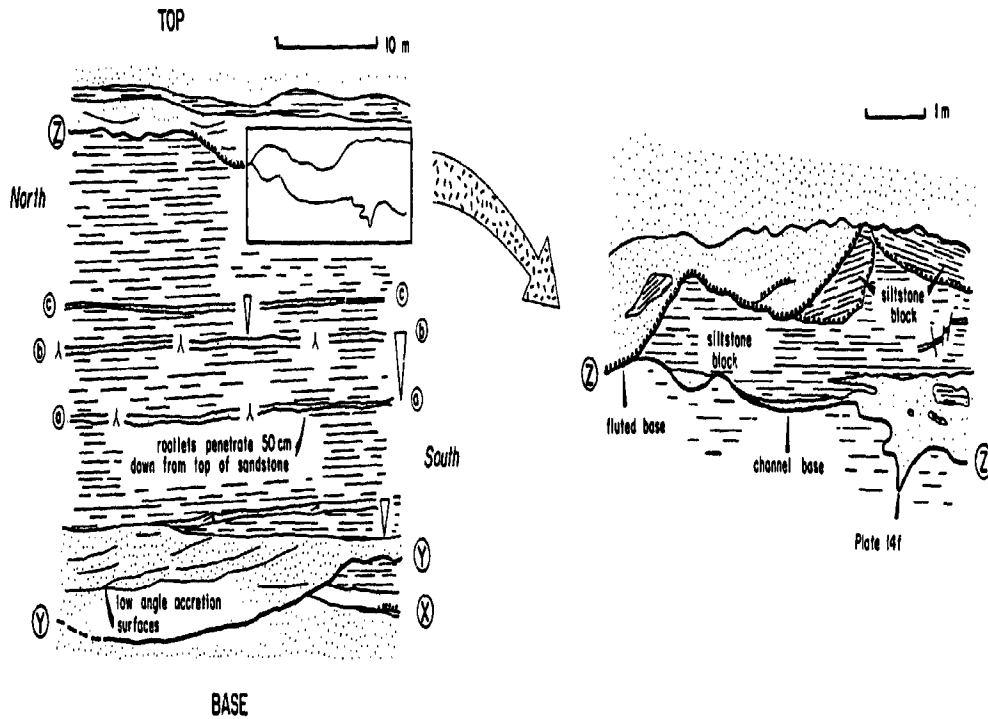
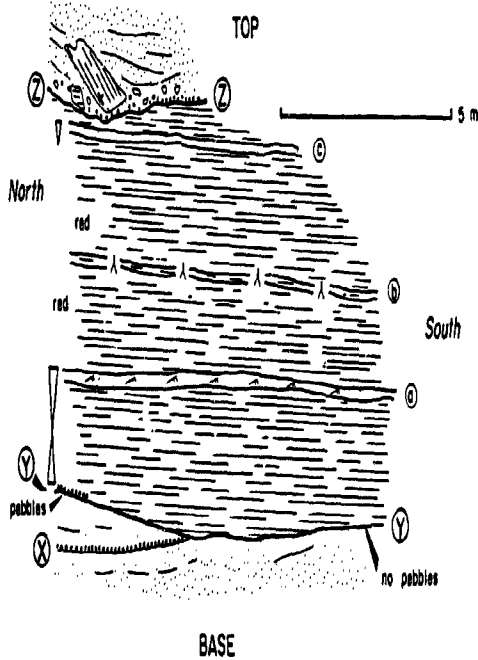


Fig. 5.8 Plan view maps of bays in the central part of the Cape Enrage section. Z = erosive contact at base of Unit V sandstone. Y = erosive contact at base of Unit IV (upper siltstone). X = intra-Unit III erosion surface (Bays 5N and 5S). a, b, and c are thinly bedded sandstone and siltstone units within Unit IV that can be correlated across outcrops and between adjacent bays (see Fig. 5.5). Figure drawn from field sketches by A.G. Plint.

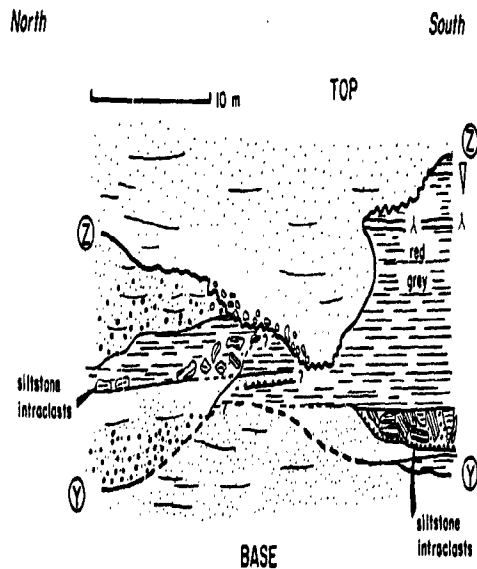
A. Bay 5N

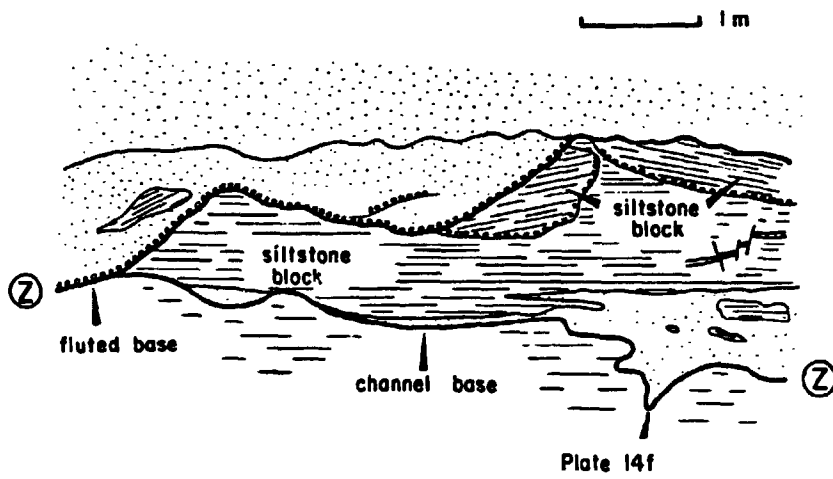


B. Bay 5S



C. Bay 4N

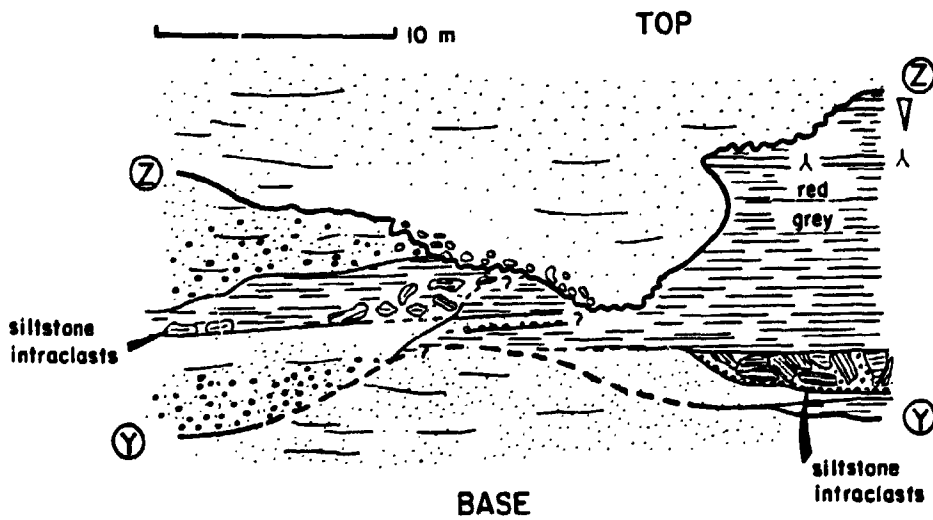




C. Bay 4N

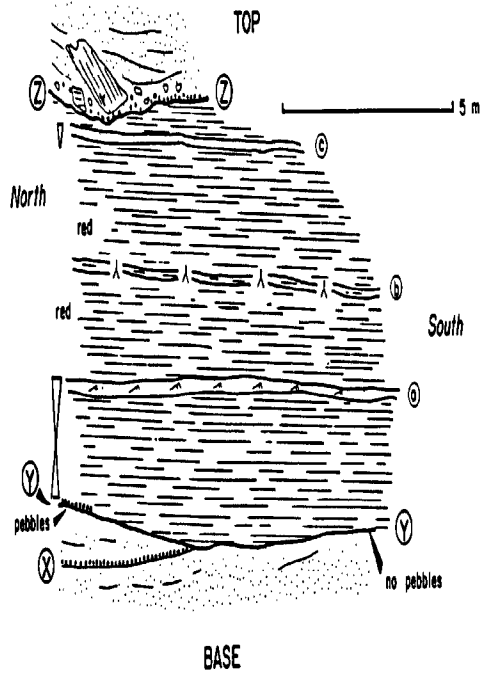
North

South

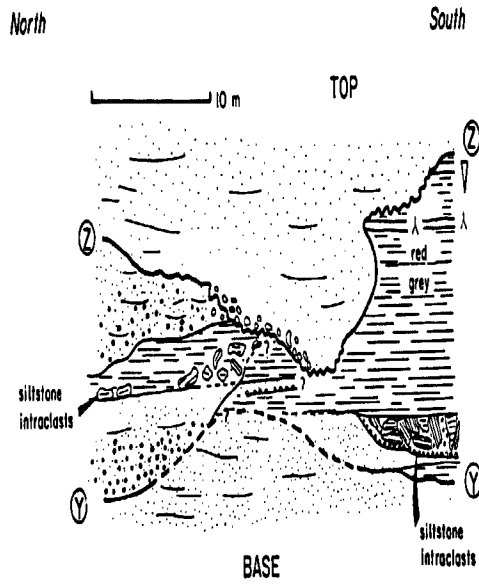


BASE

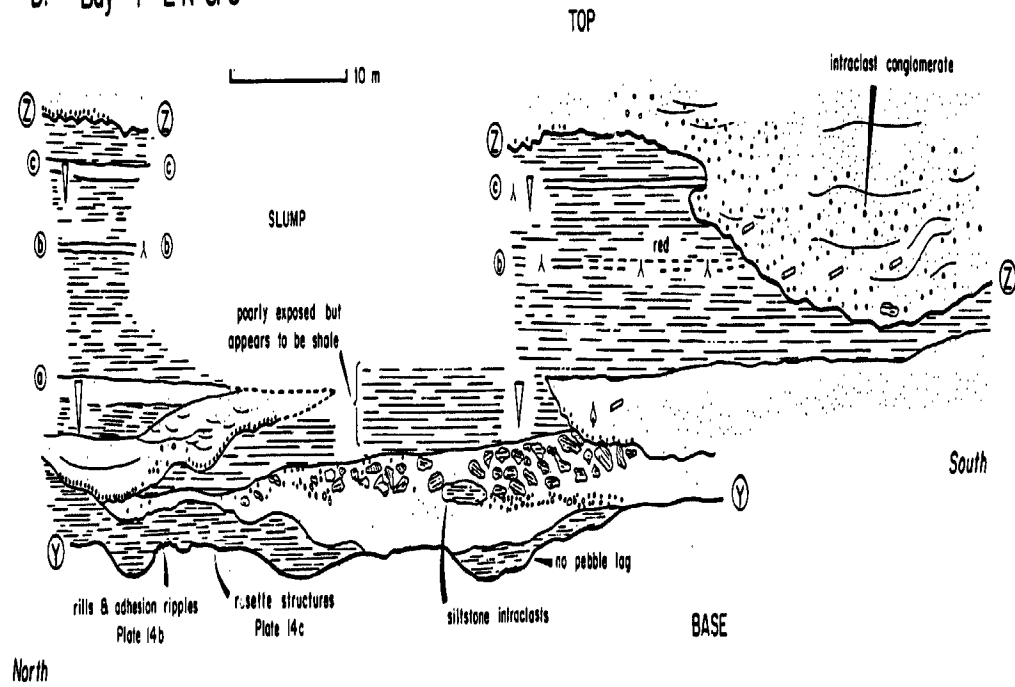
B. Bay 5S



C. Bay 4N



D. Bay 4 1/2 N & S



- Sandstone
- Mudrocks
- Intraclast conglomerate
- Trough X-bedding
- Ripples
- Roots
- Logs
- Carbonaceous debris
- Fining upward
- Coarsening upward

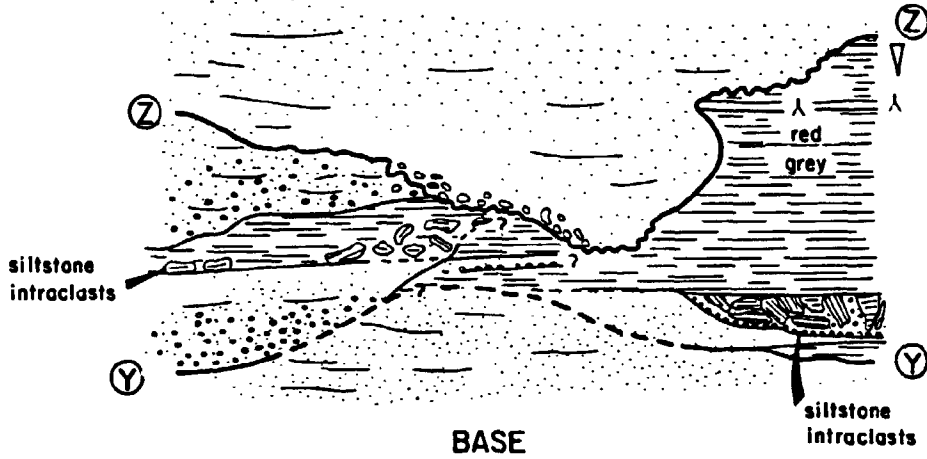
C. Bay 4N

North

South

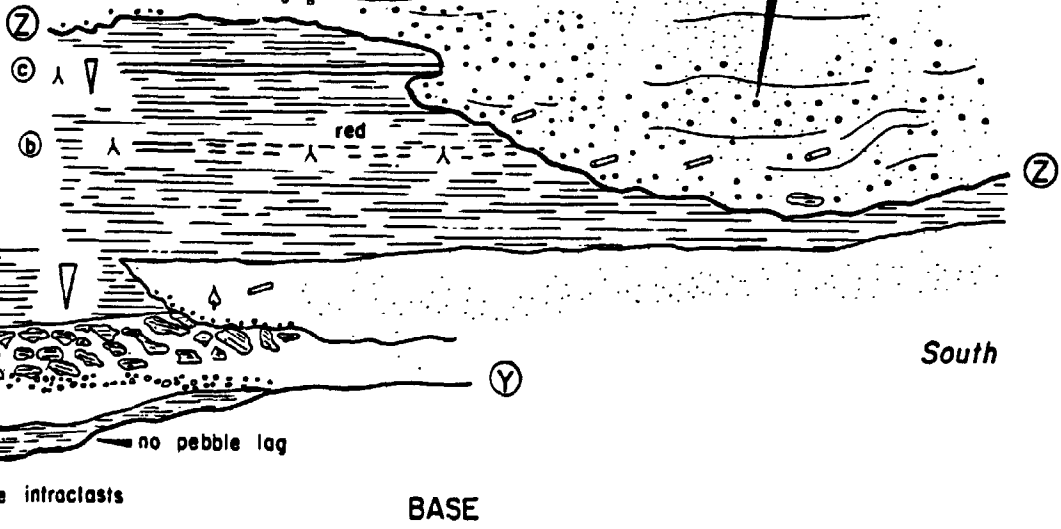
10 m

TOP



TOP

intraclast conglomerate



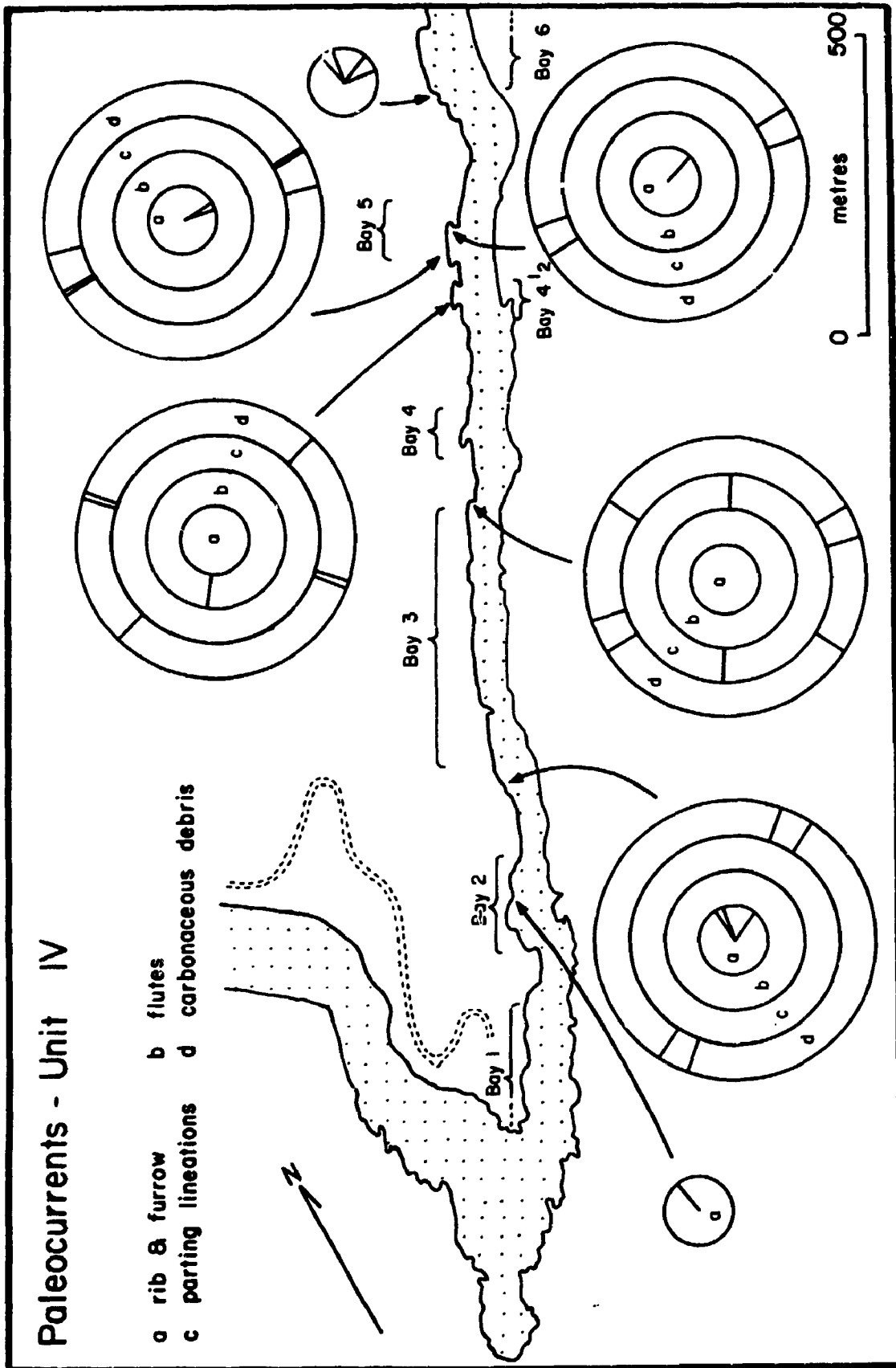
- ripples
- Roots
- Logs
- Carbonaceous debris
- Fining upward
- Coarsening upward

ripple and less common trough cross-bedding. Most sandstones are carbonaceous with occasional coal and well preserved leaf material (Plate 13b). Roots are commonly preserved in the sandstones, some individual rooted horizons traceable laterally for over 300 m (such as between Bays 4½ and 6S -Figs. 5.5 & 5.8). On the top of one sandstone a set of parallel crawling traces 3 cm apart is preserved (Plate 13c), and are interpreted to have been formed by a myriapod (Briggs et al. 1984), probably a diplopoda (millipede). Coarsening-upward cycles 0.5 to 3 m thick are common (Figs. 5.5, 5.8 & Plate 13d). They show a gradation from claystone and siltstone at the base to fine-grained ripple cross-laminated sandstone at the top, and are interpreted as small prograding bodies of sandstone that migrated laterally into the siltstone facies. Bedding parallel shear zones up to 70 cm thick occur in most outcrops (Fig. 5.5), though individual zones could not be correlated with confidence between adjacent sections.

Paleocurrent data include orientation of rib and furrow structures, flutes, parting lineations and carbonaceous fragments. Rib and furrow measurements are likely to be the most reliable paleoflow indicator and indicate flow directions toward the north and east (Fig. 5.9).

The base of the unit is always sharp and is both planar, but more typically erosional (Figs. 5.5 & 5.8)

Fig. 5.9 Paleocurrent directions for the upper siltstone
(Unit IV) at Cape Enrage.



with as much as 2.5 m relief evident. A siltstone pebble lag is associated with the basal contact at Bay 2S and from Bays 4 to 5 (Figs. 5.5 & 5.8). At Bay 4½N (Figs. 5.5 & 5.8) the base is marked by parallel rills spaced 10 cm apart (Plate 14a), which display adhesion ripples or 'warts' (similar to those described by Collinson & Thompson 1982, fig. 6.23) in the interfluves between rill channels (Plate 14b). Enigmatic rosette features are also preserved on the same bedding surface (Fig. 5.8 & Plate 14c), structures that are <10 cm diameter, and consist of radially arranged structures in sandstone, and are most likely feeding traces.

The top contact of the upper siltstone unit is markedly irregular. In the south from Bays 1-2 (Figs. 5.4, 5.5, 5.8, 5.10, 5.11 & 5.12), the base of the overlying sandstone (Unit V) shows abundant flutes (Plate 14d), but little of the upper siltstone has been eroded (Fig. 5.5). To the north from Bays 3S to 5S, Unit V erodes varying amounts of the upper siltstone (Plate 14e); almost all of Unit IV is removed at Bay 4N (Figs. 5.5, 5.8, 5.13 & 5.14). Using the base of Unit IV as a fixed datum, the erosion surface at the base of Unit V climbs upward leaving progressively thicker exposures of Unit IV between Bays 5S and 6S (Figs. 5.5, 5.8 & 5.15). Relationships between Bays 6S and 6N are less certain given the almost 1 km lateral distance between these sections, but it seems that almost all the upper siltstone

Plate 14

- a) Rills in sandstone at base of the upper siltstone (Unit IV) at Bay 4½N, Cape Enrage. Scale is 50 cm long.
- b) Detail of rills shown in Plate 14a. On the interfluves between rills are preserved cm-scale adhesion ripples. Scale 50 cm long, with 10 cm divisions.
- c) Rosette structures preserved on top of sandstone at the base of the upper siltstone (Unit IV) at Bay 4½S, Cape Enrage. These are interpreted as a form of feeding structure. Scale is 50 cm long with 10 cm divisions.
- d) Cork-screw flutes at the base of Unit V at Bay 2S, Cape Enrage. Flutes trend 356, 328 and 358°. Scale 15 cm.
- e) Erosional contact at the base of Unit V, cutting down into underlying siltstone, Bay 3N, Cape Enrage. Scale 15 cm.
- f) Isolated sandstone body (gutter cast) within the upper siltstone (Unit IV), 1 m below the base of Unit V, Bay 5N, Cape Enrage. Relief on base of sandstone is 20 cm and trends 266°. Scale bar is 20 cm.

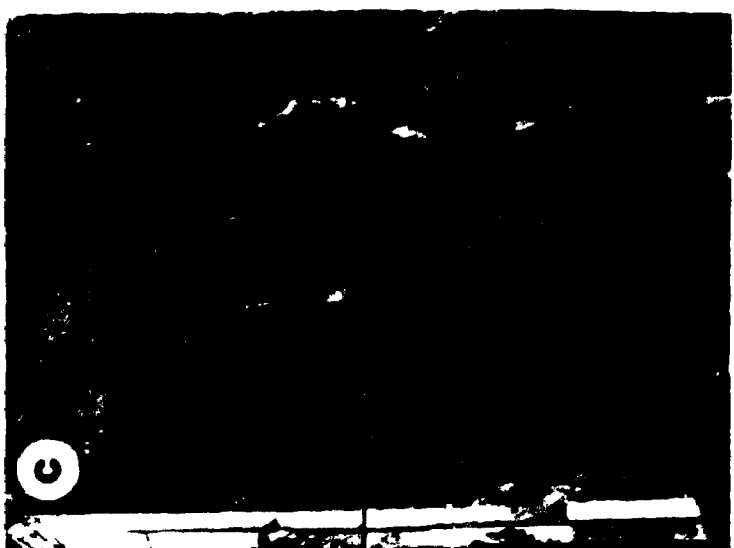
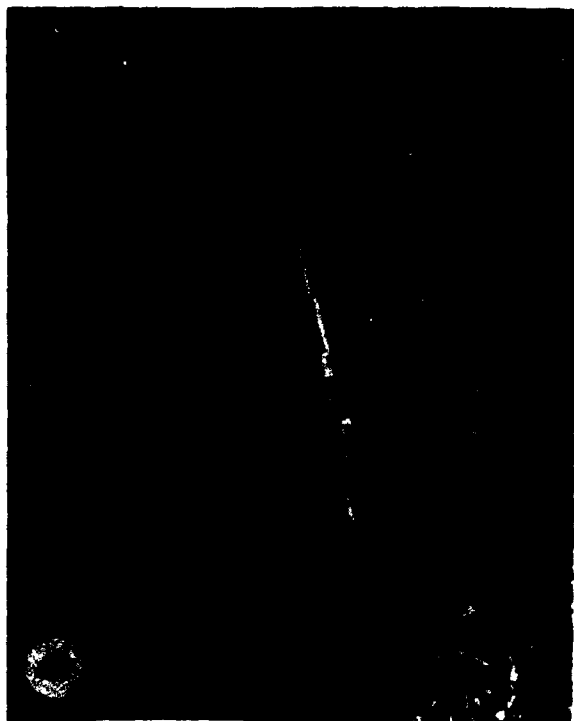


Fig. 5.10 Map of Bay 1N showing the greater thickness of upper siltstone (Unit IV) away from the central part of the Cape Enrage section.

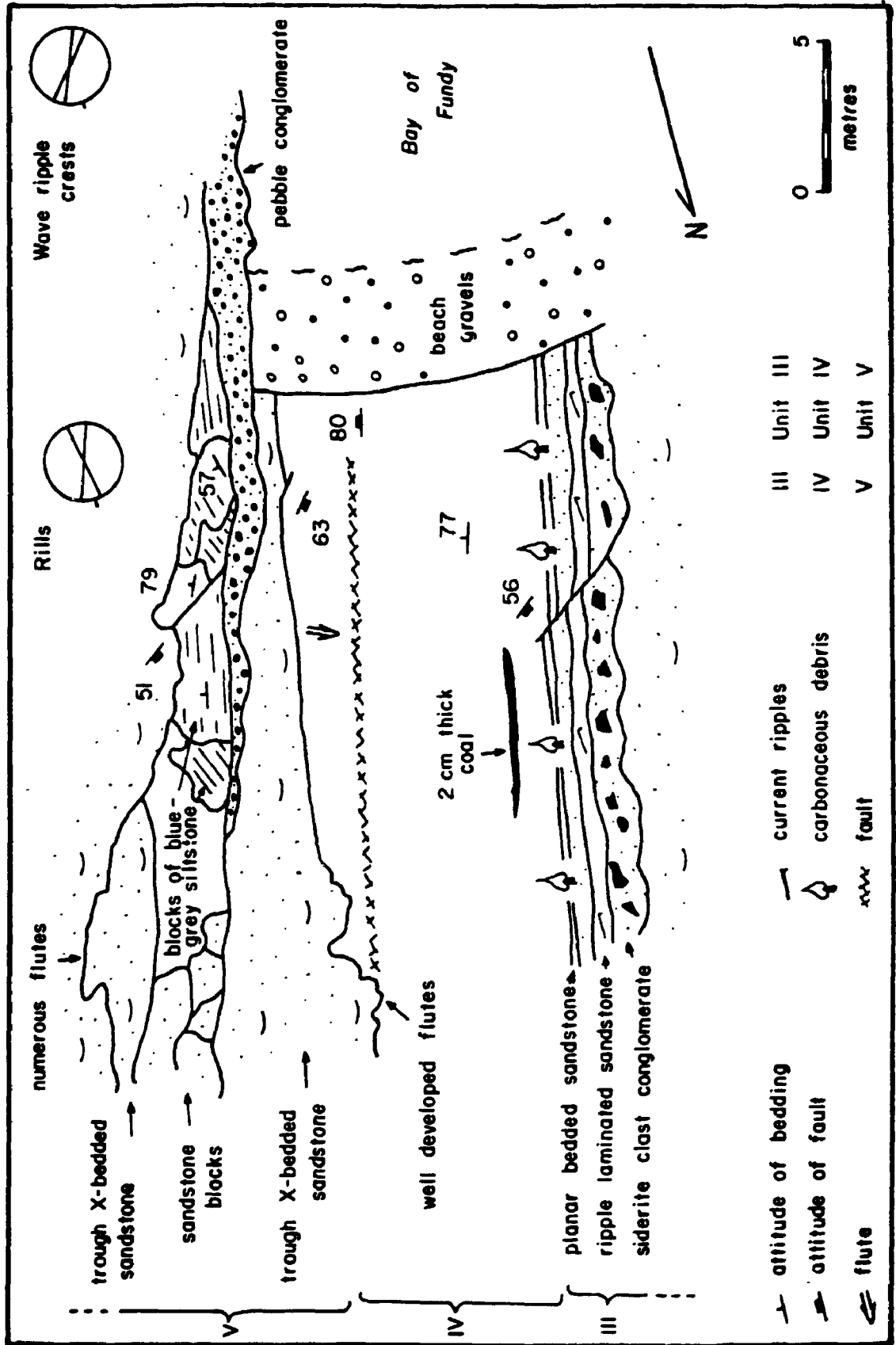


Fig. 5.11 Sketch of upper siltstone (Unit IV) at Bay 2S, Cape Enrage. 1 = Unit III trough cross-bedded sandstone, with ripple lamination at top. 2 = mudstone pebble lag (clasts subrounded to rounded, <15 cm diameter). Unit fines upward over 1 m thick interval. 3 = medium blue-grey fine-grained sandy siltstone. 4 = bedding parallel shear zones trending 031/77°E and 034/72°E. 5 = cork-screw flutes (see Plate 14d). 6 = fining-upward cycle below lower shear zone, and coarsening-upward cycle above. 7 = pebbly sandstone with <3 cm diameter rounded to well rounded granite clasts at base of Unit V. Drawn from field sketch and black and white photograph.

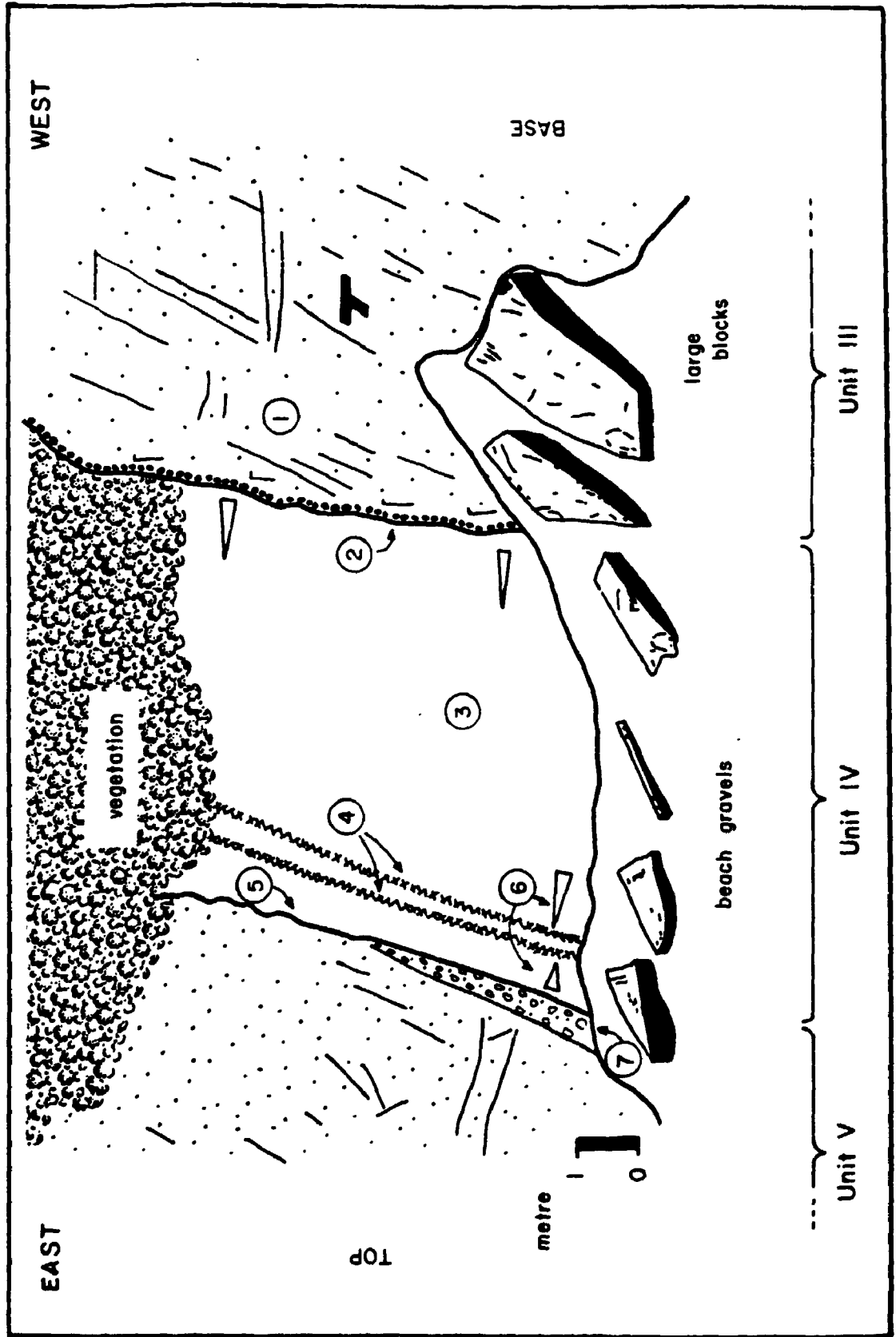


Fig. 5.12 Sketch of upper siltstone (Unit IV) at Bay 2N, Cape Enrage. 1 = trough cross-bedded sandstone passing into ripple (with well preserved straight crested wave ripples trending 169°) and climbing ripple laminated sandstone at top of Unit III. 2 = upward transition from grey siltstone at base, into colour mottled grey and red siltstone into grey siltstone at top. 3 = bedding parallel shear trending $025/83^{\circ}E$. 4 = high angle normal fault. 5 = coarsening-upward cycles (see Plate 13d). 6 = bedding parallel shear trending $016/78^{\circ}E$. 7 = base of Unit V showing extent of erosion into underlying siltstone at the top of the cliff.

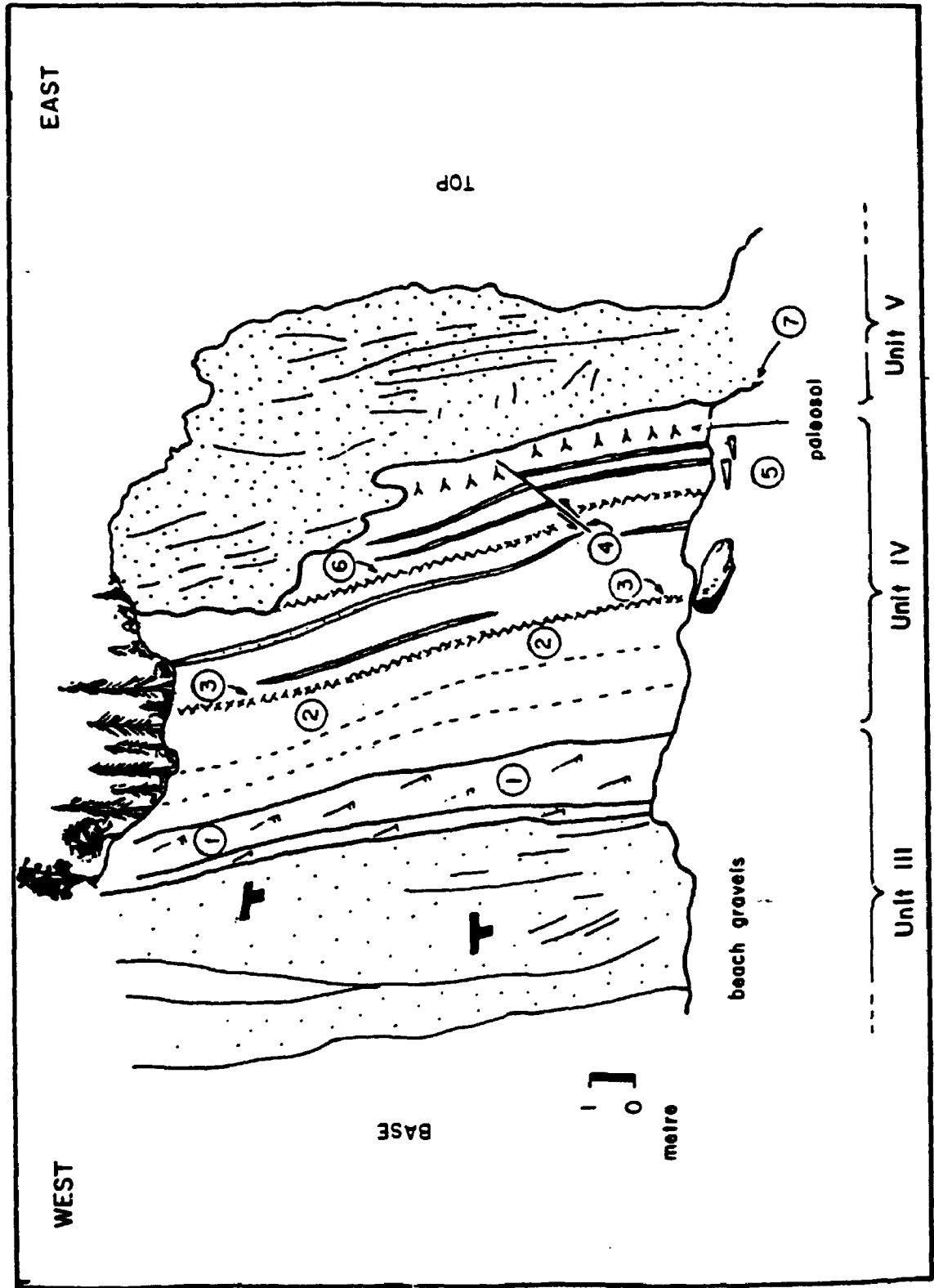


Fig. 5.13 Sketch of upper siltstone (Unit IV) at Bay 4S, Cape Enrage. 1 = trough cross-bedded sandstone (Unit III). 2 = sharp erosional contact with relief up to 2 m, lined with <20 cm diameter blue-grey siltstone pebble lag. 3 = medium blue-grey very fine-grained sandy siltstone overlain by trough cross-bedded sandstone. 4 = laminated siltstone block with bedding trending $048/84^{\circ}\text{E}$. 5 = laminated siltstone block with bedding trending $155/42^{\circ}\text{N}$. 6 = tightly folded siltstone block. 7 = sharp planar base to Unit V, but higher up the cliff face, lower sandstone unit scours into underlying siltstone. 8 = tightly folded siltstone block.

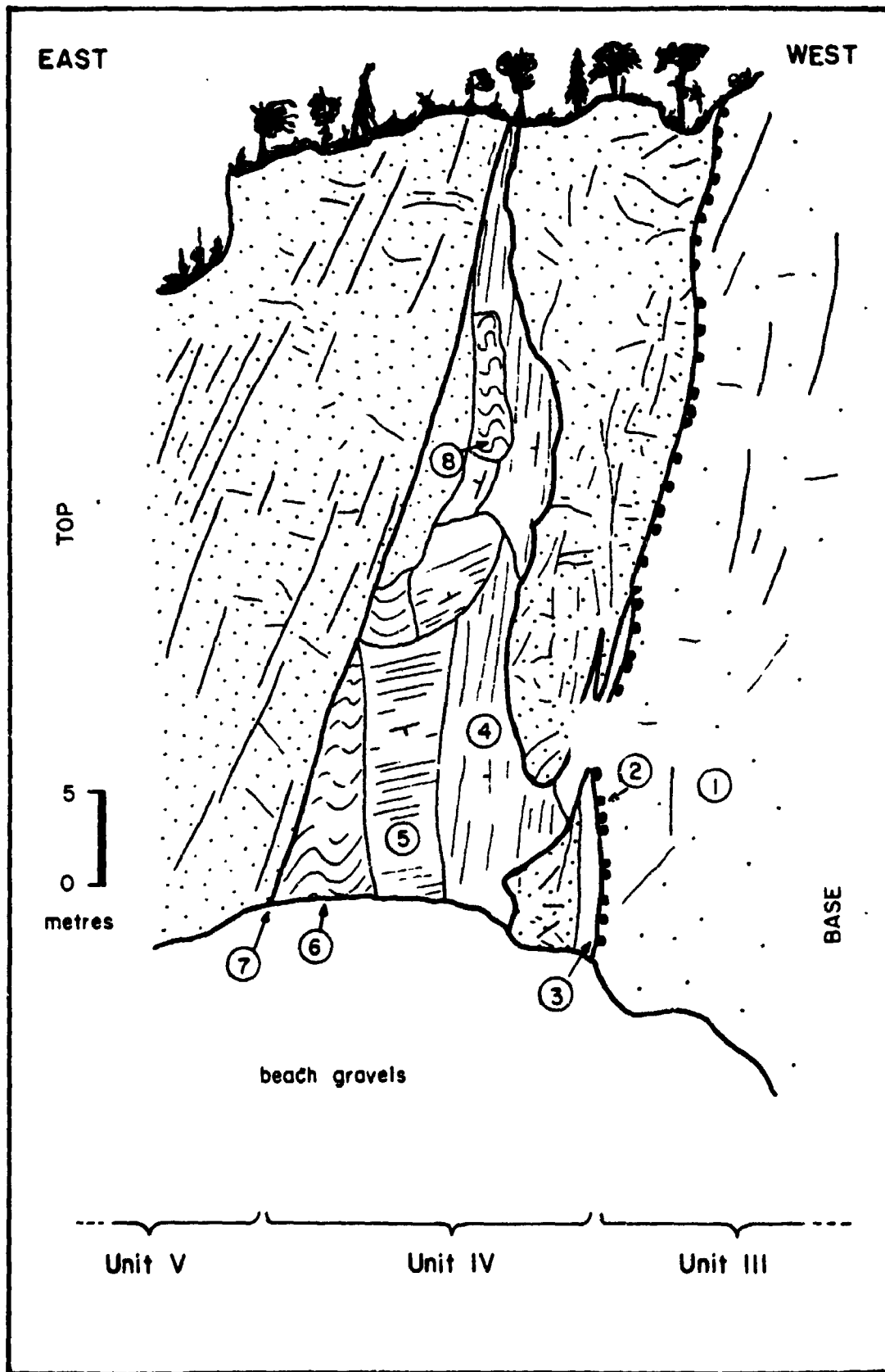


Fig. 5.14 Sketch of upper siltstone (Unit IV) at Bay 4N, Cape Enrage, showing how Unit V erodes underlying Unit IV siltstone. 1 = trough cross-bedded sandstone with occasional <1 cm diameter light blue-grey siltstone clasts scattered throughout. 2 = fine-grained sandy siltstone. 3 = bedding parallel shear zone. 4 = greyish green fine-grained siltstone and clayey siltstone, overlain by 10 cm thick *Stigmaria* bed (5). 6 = high angle normal fault trending 032/85°W with 3.2 m displacement. 7 = sharp erosive basal contact of Unit V (labelled 8) which shows a relief of 6.5 m. Trough cross-bedded sandstone (Unit V) with numerous <20cm diameter angular granite clasts, especially at the base.

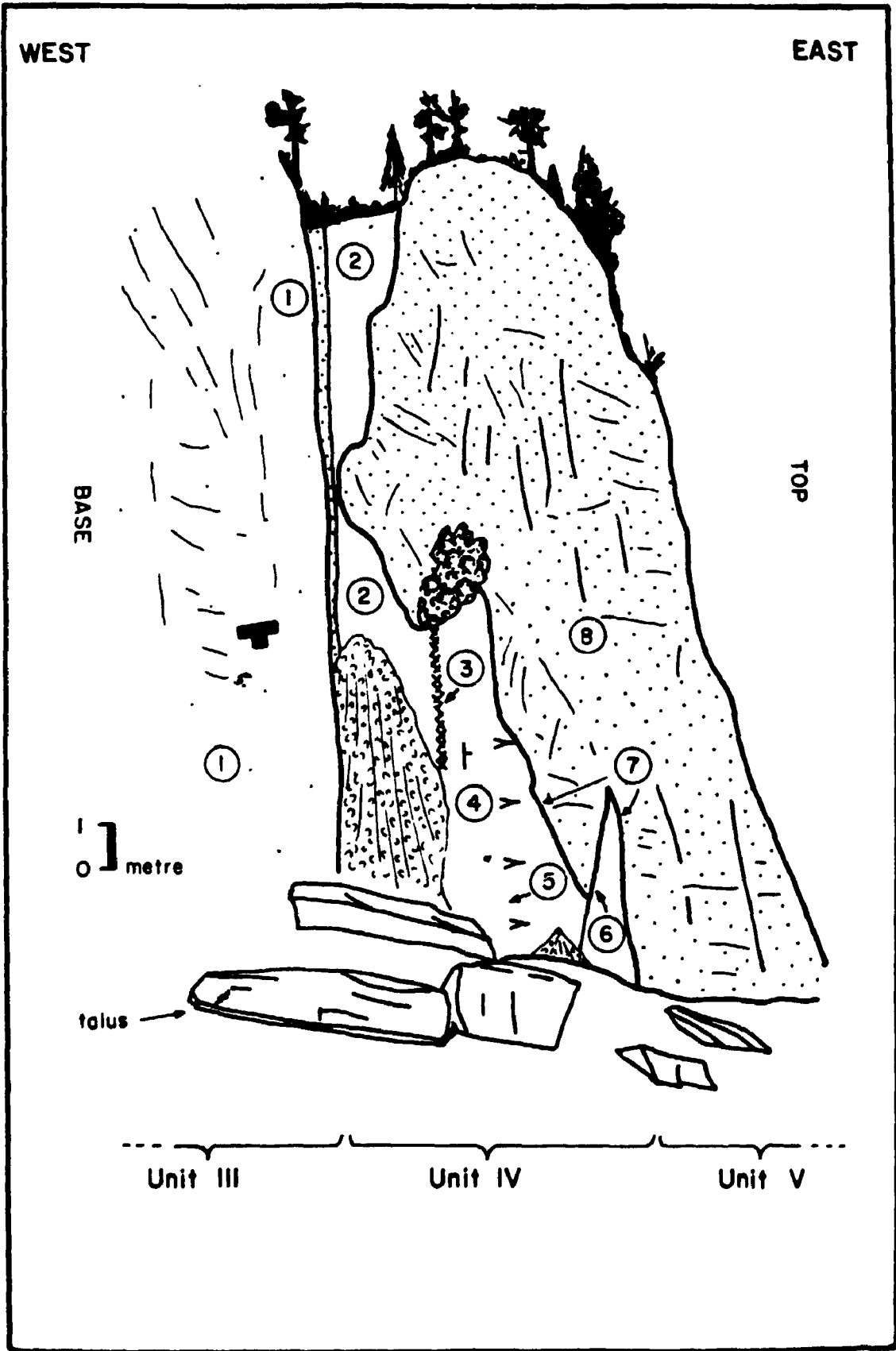
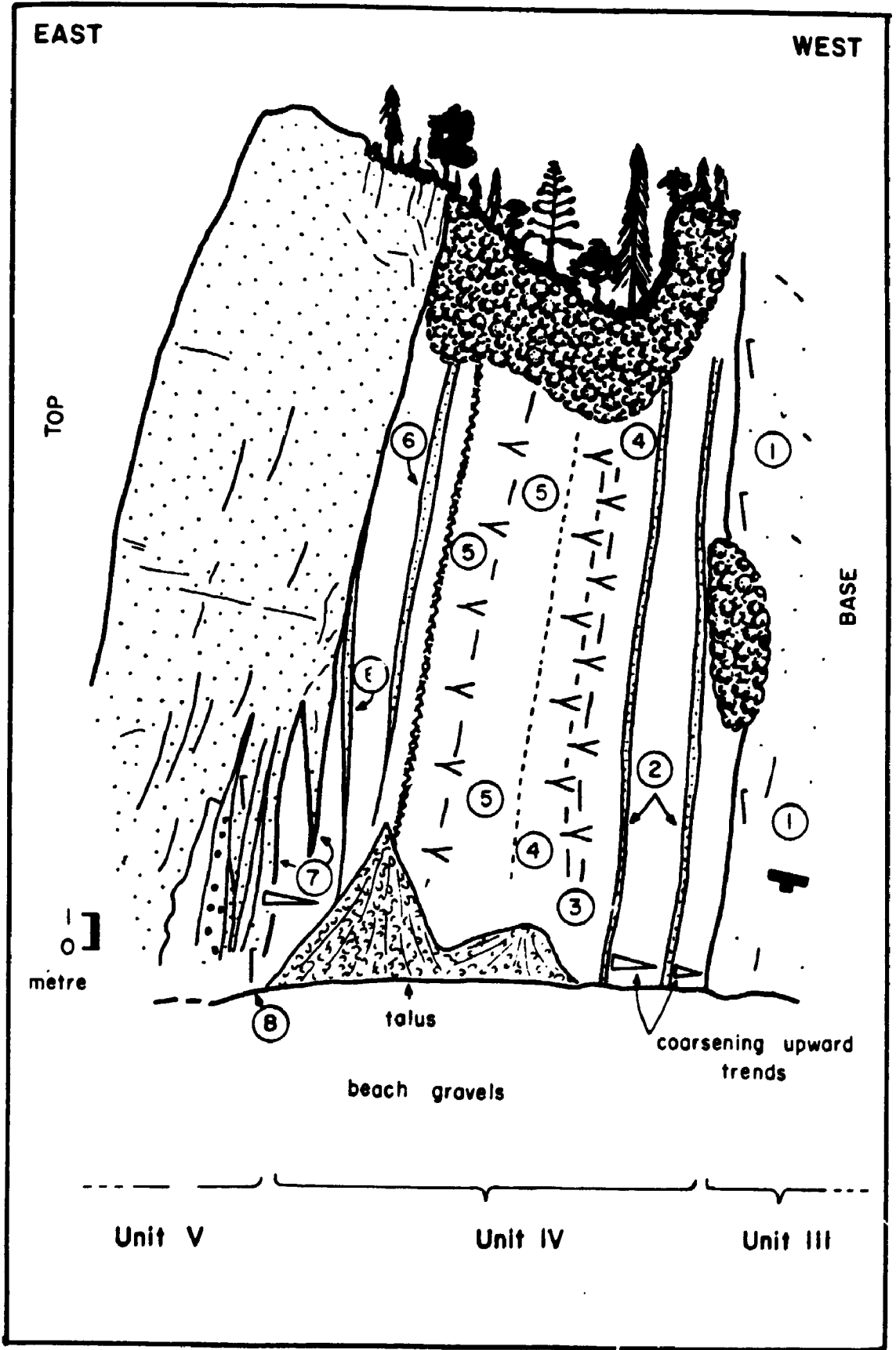


Fig. 5.15 Sketch of upper siltstone at Bay 6S, Cape Enrage. 1 = trough cross-bedded sandstone passing upward into ripple laminated sandstone at top. 2 = coarsening-upward cycles consisting of coarse-grained siltstone at the base and ripple laminated sandstone at top. 3 = 95 cm thick fine-grained siltstone with vertical and sub-vertical rootlets; *Stigmaria* and rhizoconcretions throughout. 4 = colour mottled very sheared siltstone. 5 = colour mottled fine-grained siltstone with 25 cm thick fine-grained sandstone beds at base with calcrete nodules and rootlets throughout. Top marked by bedding parallel shear trending 026/87°E. 6 = medium grey-green coarse-grained siltstone and claystone with interbedded parallel laminated sandstone. 7 = irregular interfingering nature of contact between Units IV and V. Coarsening-upward cycle is capped by 50 cm thick *in situ* *Calamites* sandstone bed (8).



unit is removed at Bay 6N by erosion at the base of Unit V (Figs. 5.5 & 5.16). Up to 13 m of Unit IV was removed by the erosional event at the base of Unit V (Fig. 5.5).

Flutes and cork-screw flutes preserved on the base of Unit V (Plate 14d) indicate north and westerly current directions, changing from a westerly orientation in the south near Cape Enrage lighthouse, to northerly paleoflows at the northern end of the section (Fig. 5.17). At Bay 5N, a sandstone body with a marked erosional base marks the base of Unit V, and is overlain by several large mudstone clasts which were deposited prior to the deposition of the overlying sandstone (Fig. 5.8 & Plate 14f).

Intercalated Sandstone Units (Units I, III, V & VI)

Intercalated with the siltstone units are 5-20 m thick sandstones (Units I, III, V & VI), predominantly trough-cross-bedded, but with less abundant ripple, climbing ripple and parallel laminated sandstone, gravelly sandstone and conglomerate beds (Fig. 5.5). Units I, III and VI all show paleocurrent directions toward the east (Figs. 5.18, 5.19 & 5.20); Unit V, which varies in thickness between 2 and 15 m, consistently shows paleocurrent directions toward the west, 180° from the other sandstone units (Fig. 5.21). Furthermore, Unit V differs compositionally from the remainder of the

Fig. 5.16 Sketch of Bay 6N, Cape Enrage. 1 = well laminated medium dark blue-grey very fine-grained sandy siltstone. 2 = 5.1 m thick light grey-green coarse-grained siltstone, colour mottled sandy siltstone. The correlation between Bay 6S and this locality is not certain, but the siltstone (Unit IV) appears to correlate best with exposure 2 at this locality.

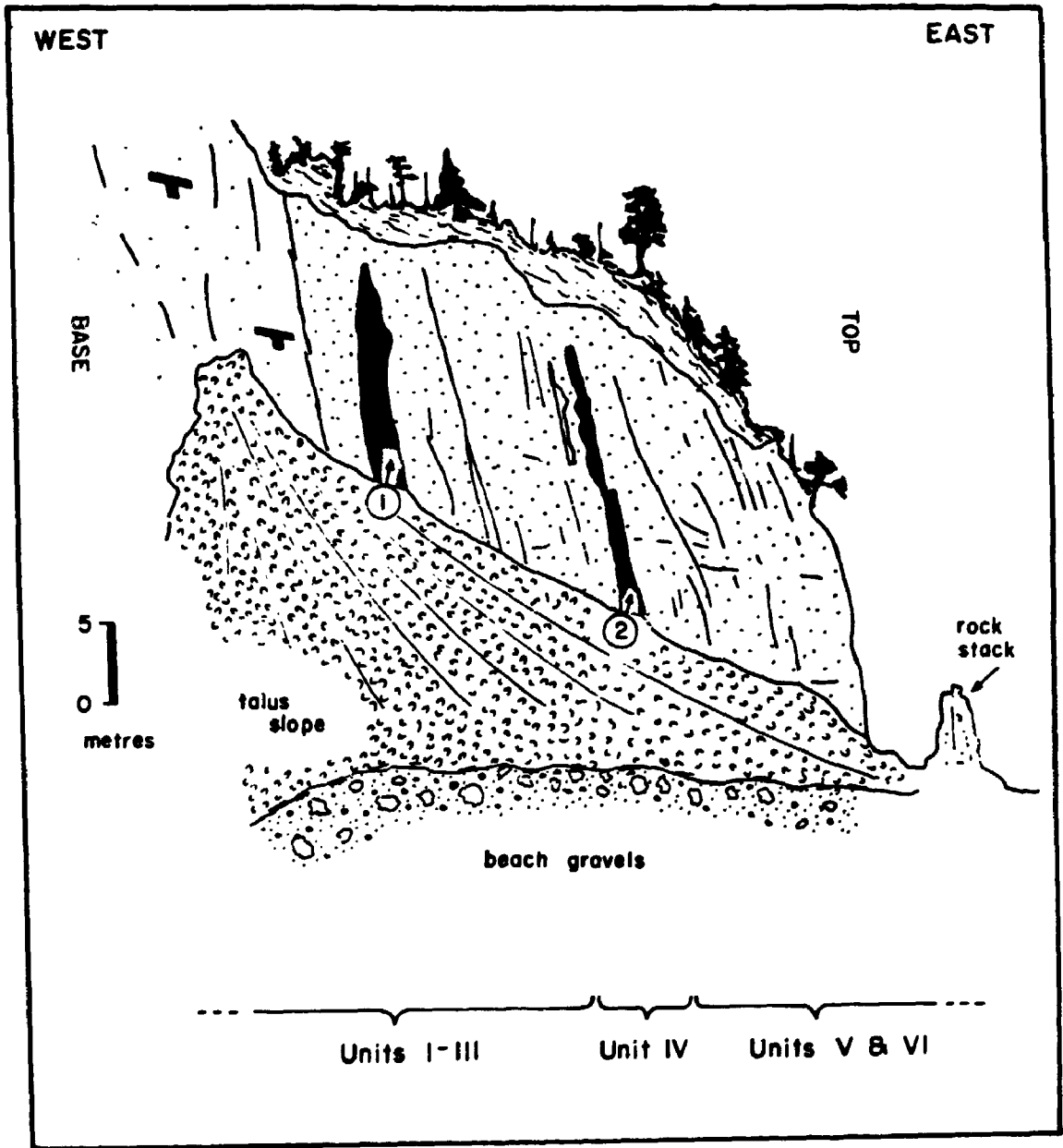


Fig. 5.17 Orientations of flutes at the base of Unit V. Geographic location of flute measurements are shown at base for each Bay. All observations (n= 21) are shown in large diagram.

Orientation of flutes -
base of Unit V

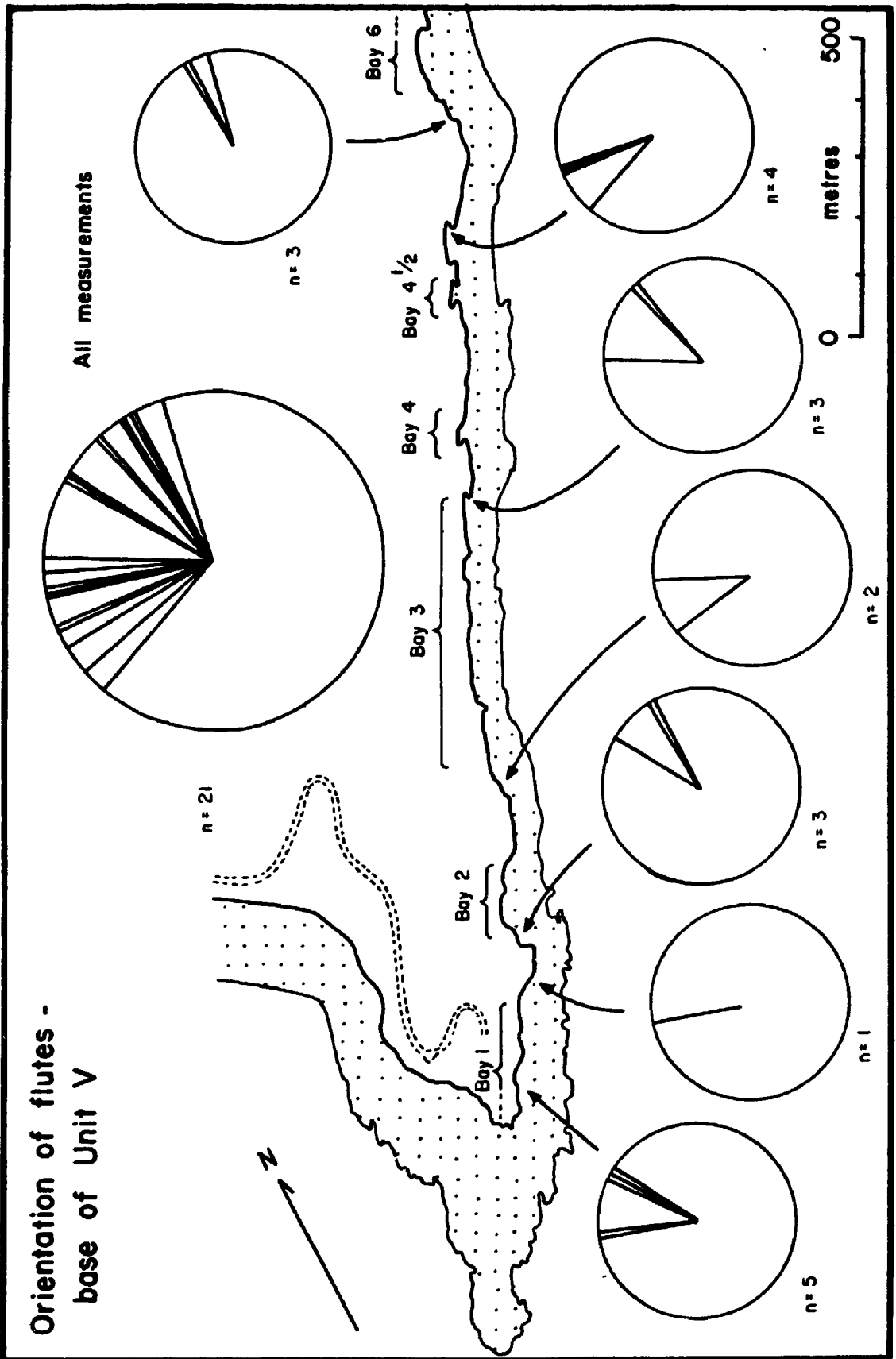


Fig. 5.18 Paleocurrent observations for Unit I. Rose diagrams indicate trough cross-bed orientations from Unit I (n= 18), and from the entire area (n= 147).

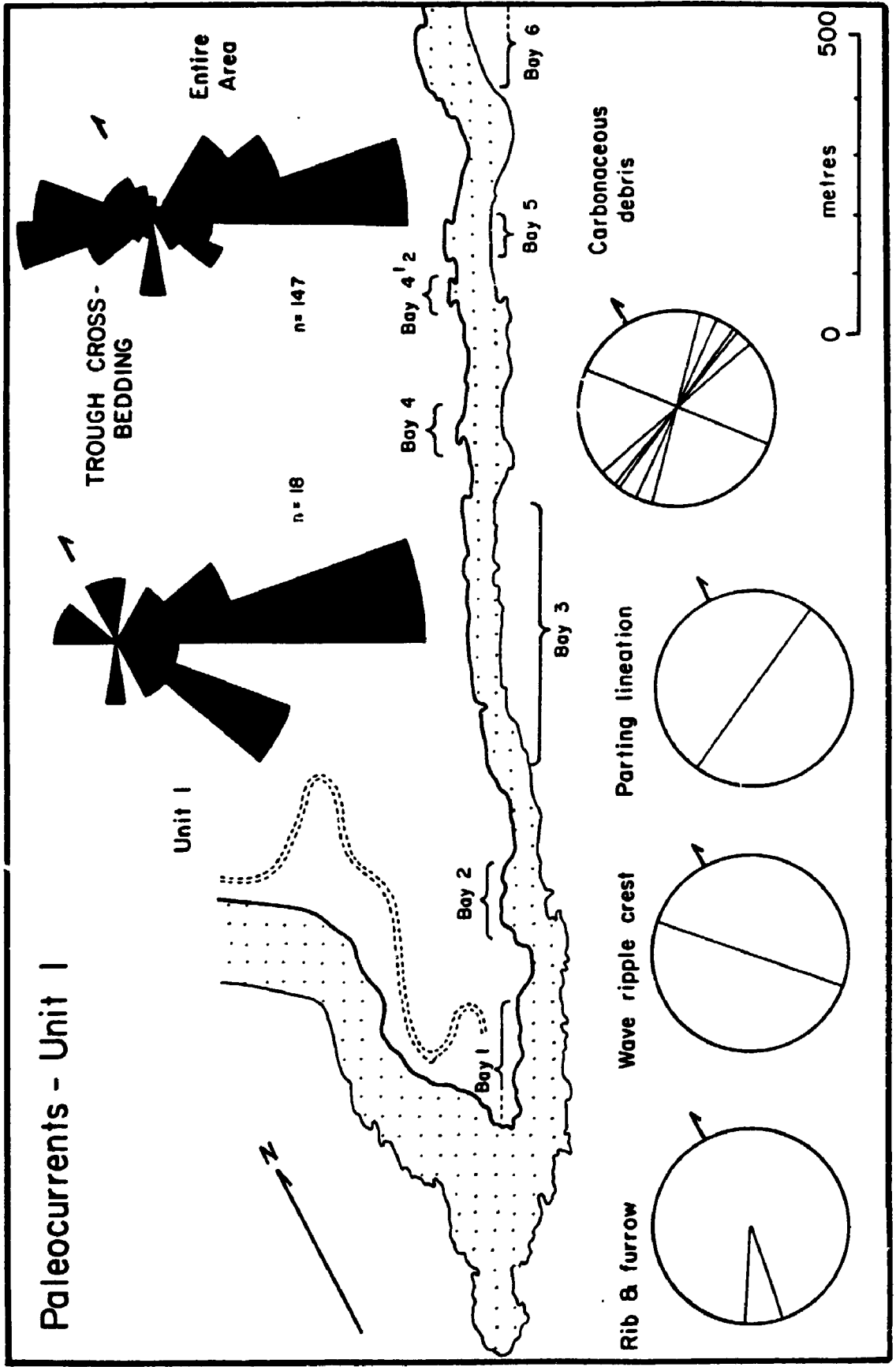
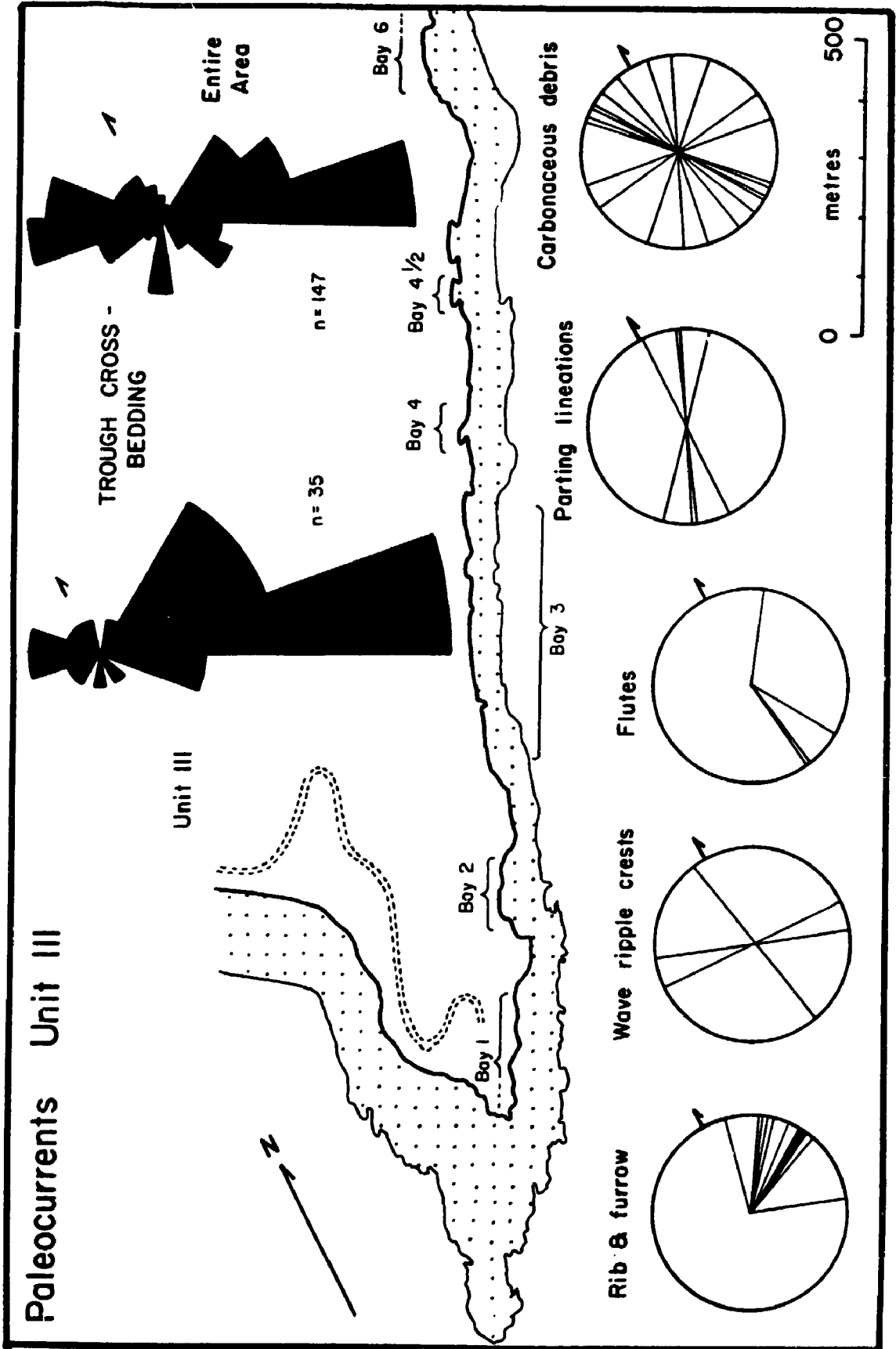


Fig. 5.19 Paleocurrent observations for Unit III. Rose diagrams indicate trough cross-bed orientations from Unit III (n= 35), and from the entire map area (n= 147).



Paleocurrents Unit III

TROUGH CROSS-BEDDING

Unit III

Entire Area

n = 35

n = 147

2

Boy 1

Boy 2

Boy 3

Boy 4

Boy 4 1/2

Boy 6

Rib & furrow

Wave ripple crests

Flutes

Parting lineations

Carbonaceous debris

0 500 metres

Fig. 5.20 Paleocurrent observations for Unit VI. Rose diagrams indicate trough cross-bed orientations from Unit VI (n= 22), and from the entire map area (n= 147).

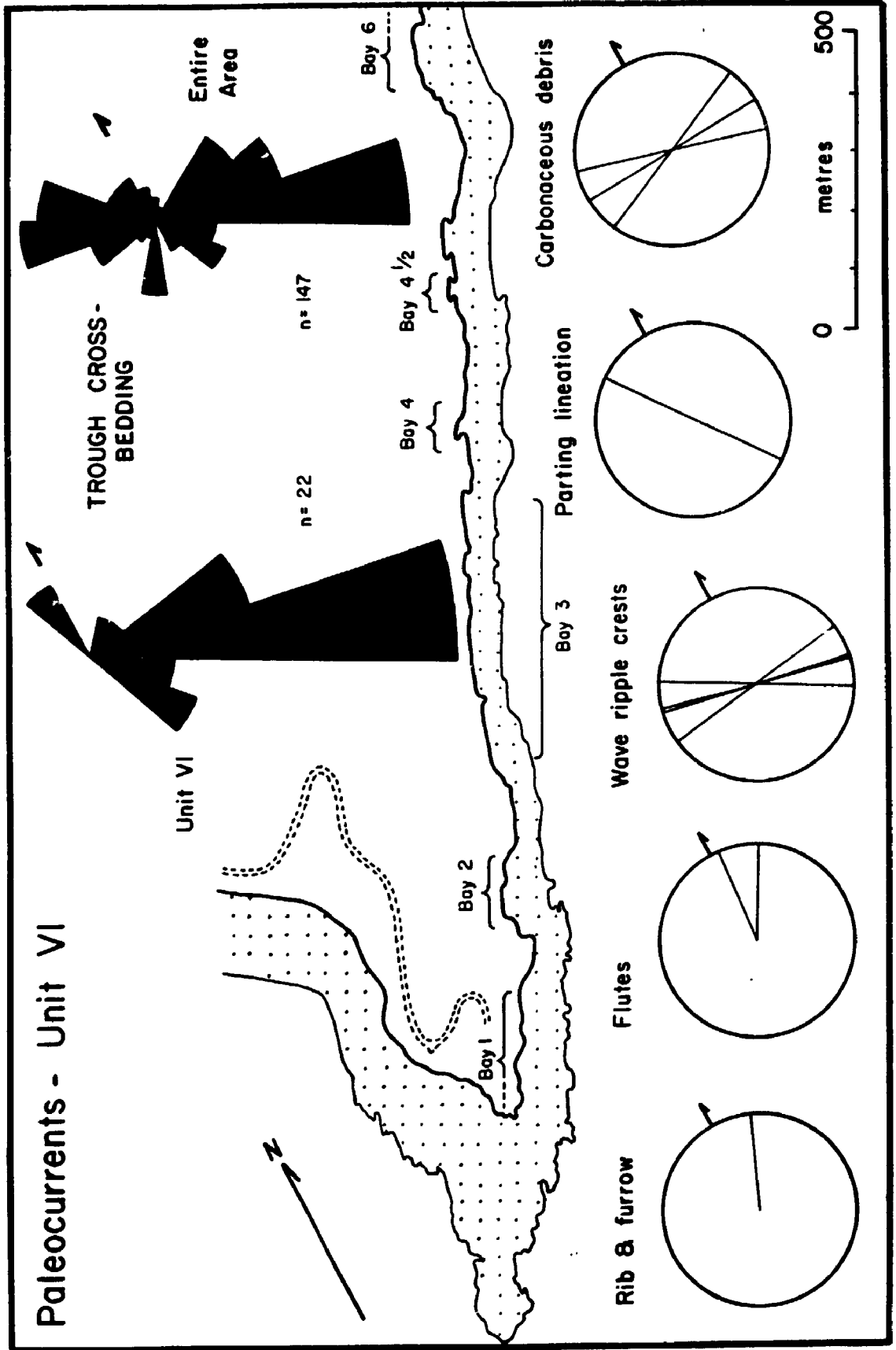
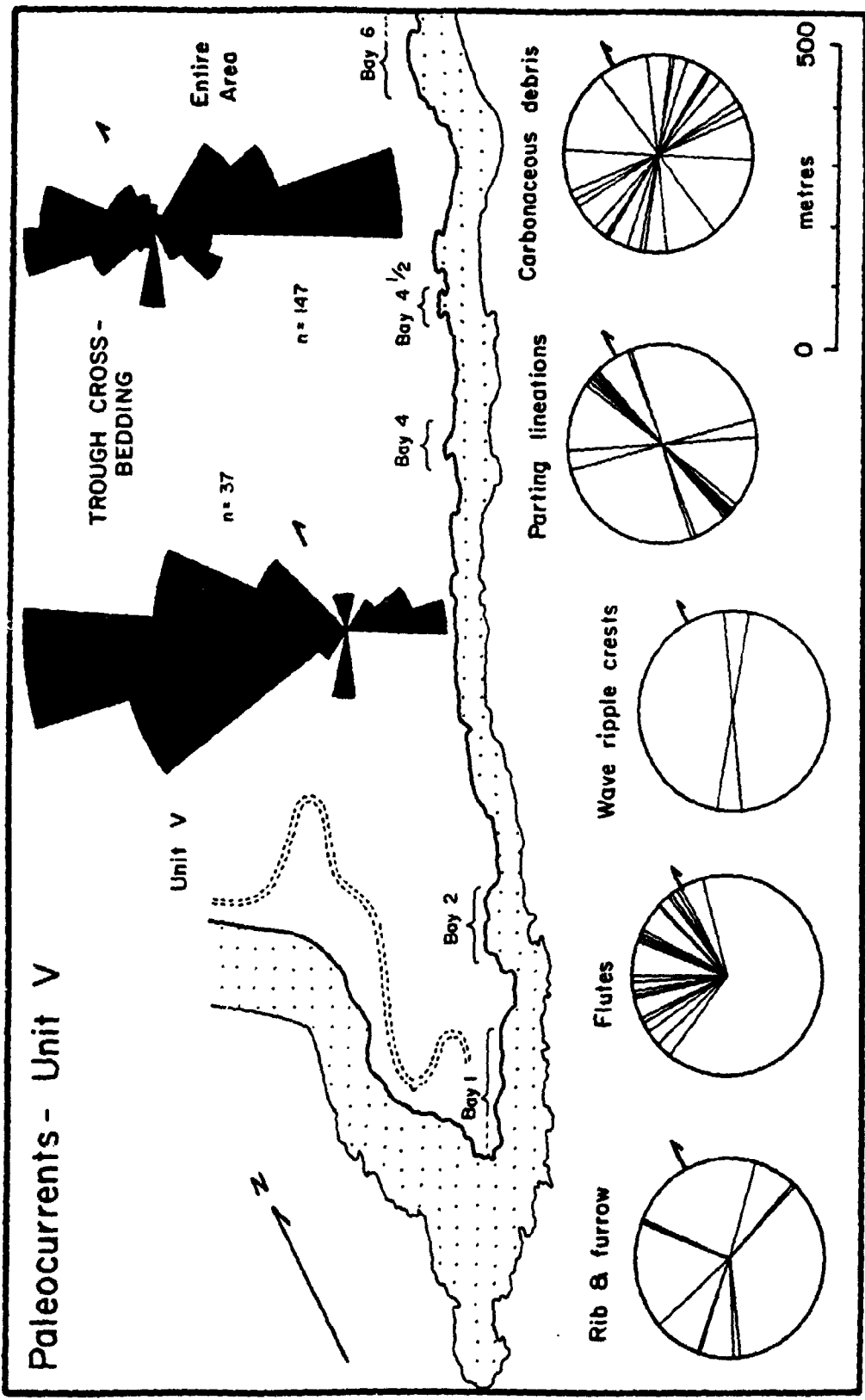


Fig. 5.21 Paleocurrent observations for Unit V. Rose diagrams indicate trough cross-beds from Unit V (n= 37), and from the entire map area (n= 147).



sandstones in containing up to 16% granite clasts; the typical Boss Point Formation pebbly sandstone and conglomerate generally contains less than 0.5% granite detritus (Fig. 4.3).

Other paleocurrent data for Units I, III, V and VI are indicated in Figs. 5.22 - 5.25). Rib and furrow observations are consistent with paleocurrent determinations made from trough cross-bedding. However the number of observations for each sedimentary unit are generally too few to make meaningful assessments of paleocurrent trends between individual bays.

5.2.2 Petrography and Petrology

In thin section, very angular to subangular quartz is the dominant framework grain, constituting 10 to 40% of the lithology in sandy siltstone units. Quartz grains are up to 80 μ m diameter being larger in the more sandy siltstone lithologies. Elongate spindly mica (mostly muscovite, with rare biotite) occurs in all samples, commonly with signs of weathering into "muddy" looking grains. They form <2% of thin section samples and commonly their long axes (up to 0.28 mm long) are aligned sub-parallel and parallel to stratification. Light green chlorite also occurs in sandy siltstones. Opaque grains (presumably carbonaceous or Fe rich), consistently form 15-20% of thin sections.

Fig. 5.22 Paleocurrent observations for Unit I showing the geographic locations of paleocurrent measurements.

Paleocurrents Unit I

- a rib & furrow
- b flutes
- c parting lineations
- d carbonaceous debris
- e wave ripple crests
- f rill

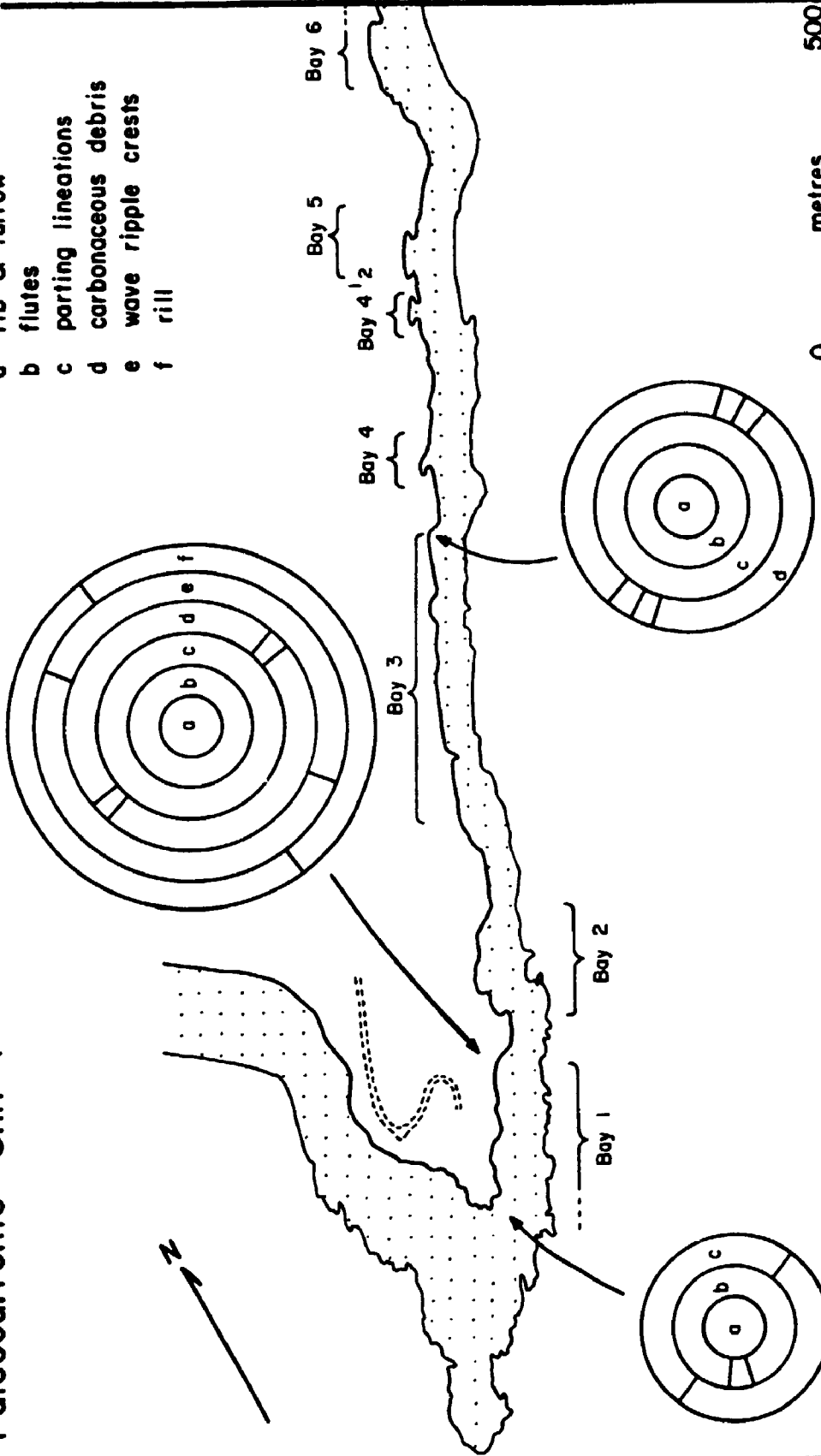


Fig. 5.23 Paleocurrent observations for Unit III showing the geographic locations of paleocurrent measurements.

Paleocurrents Unit III

- a rib & furrow
- b flutes
- c parting lineations
- d carbonaceous debris
- e wave ripple crests

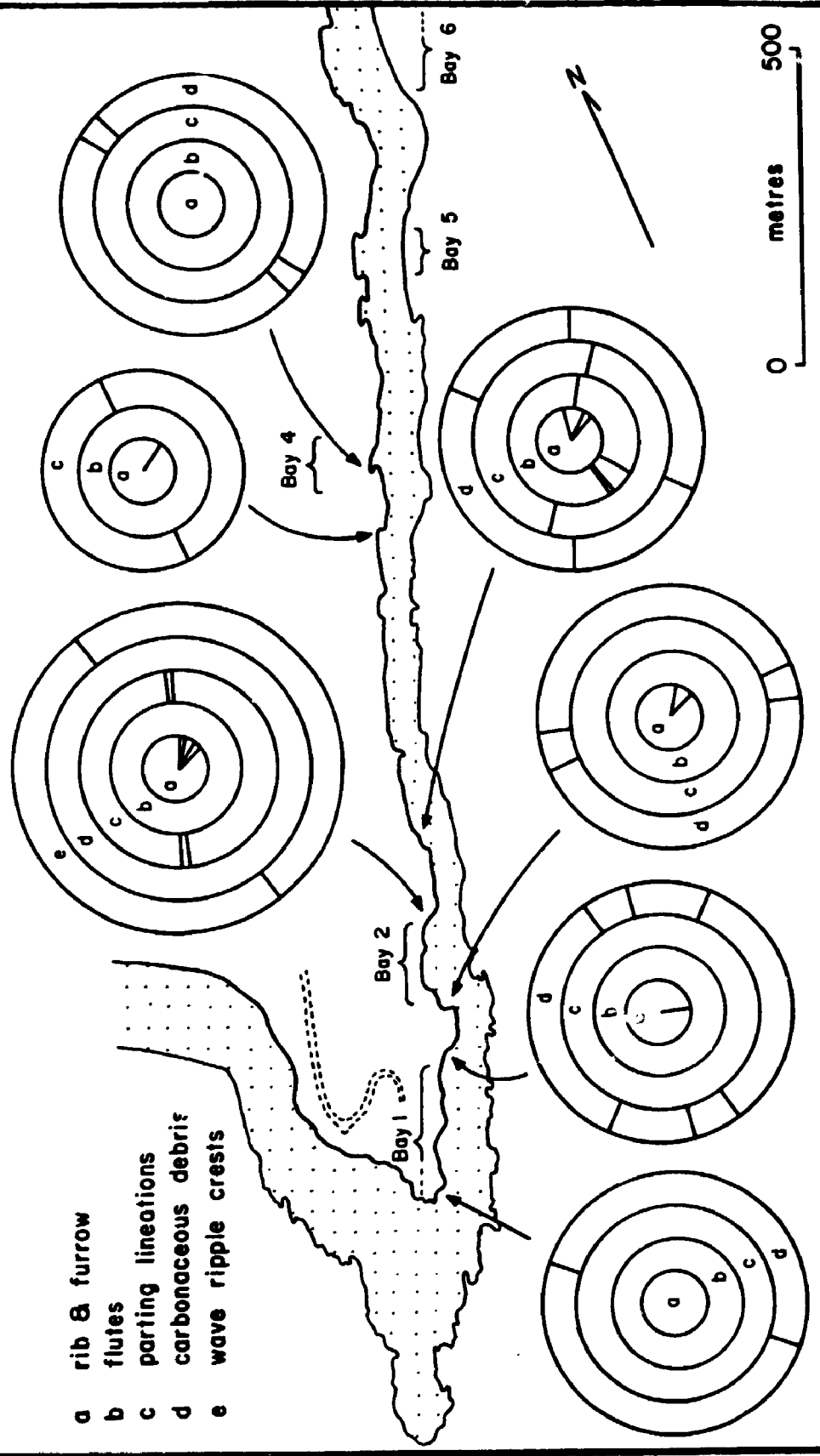


Fig. 5.24 Paleocurrent observations for Unit V showing the geographic locations of paleocurrent measurements.

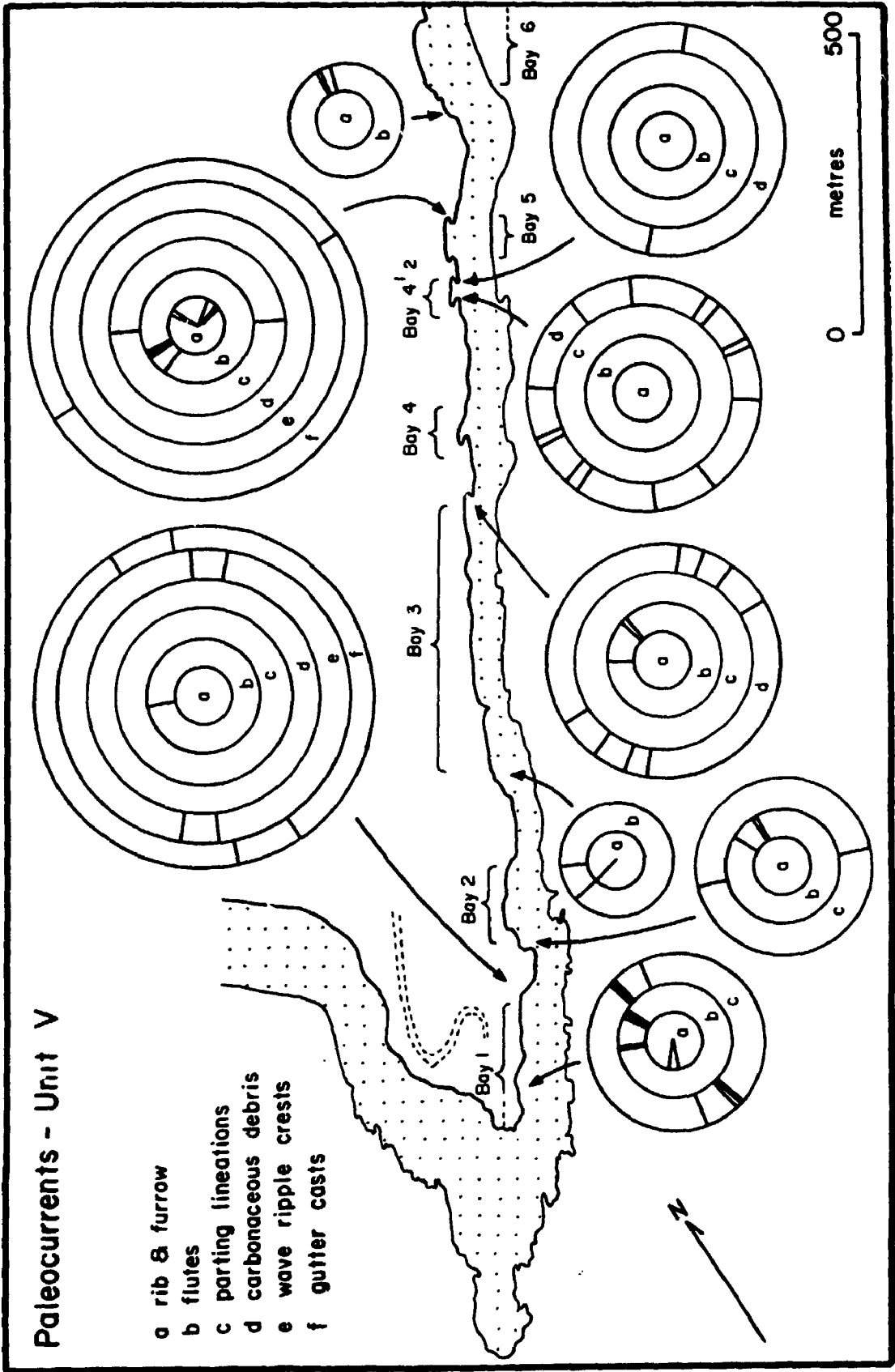
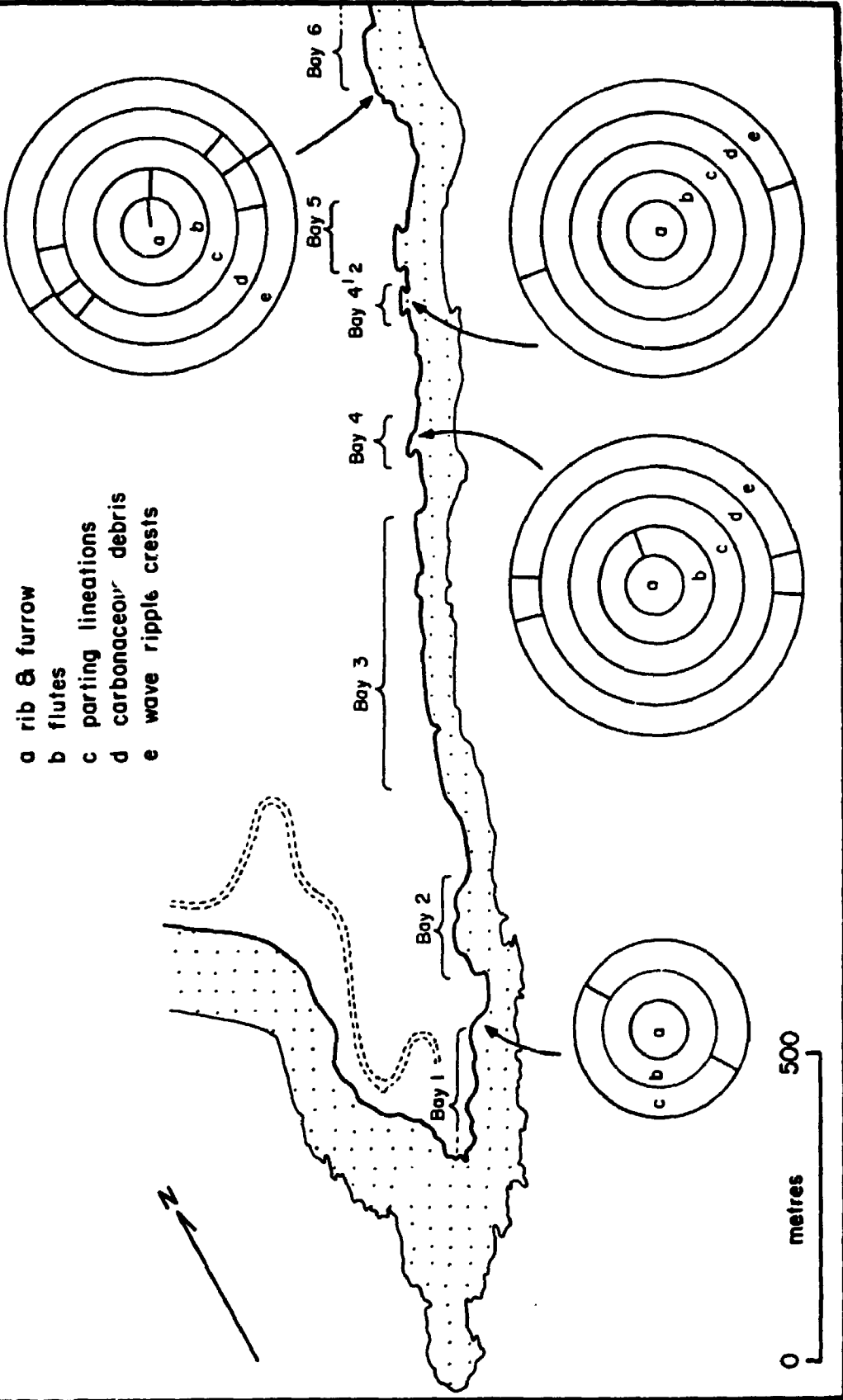


Fig. 5.25 Paleocurrent observations for Unit VI showing the geographic locations of paleocurrent measurements.

Paleocurrents - Unit VI



Laminae are marked by an increase in abundance of very fine, well sorted quartz grains, and is especially marked in pin-stripe laminated siltstones.

XRD analysis shows a very uniform clay composition for the lithofacies. Clay species are dominated by kaolinite and illite, with lesser abundances of muscovite and chlorite (Fig. 5.1).

In thin section siderite nodules consist of massive microcrystalline carbonate. Veinlets 1-2 mm wide, comprising sparry calcite were described by Mitchell (1986), but were not noted in this study. Aspects of siderite petrology and geochemistry have been studied by Mitchell (1986). He showed that the host siltstone sediments are relatively enriched in trace elements with respect to the concretions. Concretions were found to be depleted with respect to the surrounding siltstone in most trace elements (Ba, Rb, Sr, Zr, Nb), but enriched in Y. The increase in Y within siderite nodules was assumed to be related to the carbonates, Y tending to associated with calcium minerals, most notably apatite (Mason 1966, Felsche 1978). Although not mentioned by Mitchell, the Y was presumably being introduced at a late stage of nodule growth, as it has a higher concentration in the outer portion of nodules (cf. Mitchell 1986, p. 33-37).

desiccated to produce calcrete nodules and pedogenic profiles. Similar shallow water lakes with abundant carbonates have been described as palustrine (Tresse and Wilkinson 1982, Platt 1989b) and appear to be very common in arid to semi-arid climatic regions.

Although not directly related to siltstone deposition, the reversal of paleocurrent direction in Unit V sandstones at the Cape Enrage locality, is important in the overall interpretation of these siltstones. This paleocurrent reversal indicates that for a short period, sediment was introduced from a granitic source on the eastern margin of the basin. This is in contrast to the dominant easterly directed paleoflow directions from other Boss Point Formation sandstones (see Chapter 8). This change was probably a response to tilting of the basin floor, related to fault movement; either uplift on the eastern, or subsidence on the western margin of the basin. Reversals in paleocurrent direction have been described from ancient fluvial sediments (eg. Barrett and Kohn 1975, McLean 1977, Eisbacher 1981, Rust 1981, Van Houten 1981, Groll and Steidtmann 1987, Lawrence and Williams 1987), but these changes usually occur over stratigraphic intervals of 100s of metres. Paleocurrent reversals which occur over only a few metres of stratigraphic section as at Cape Enrage are rare. Rust and Jones (1987, p. 226) describe radical changes in paleoflow in the braided Hawkesbury Sandstone between subjacent sheets (switches up

to 135°). Somewhat analogous variations in drainage systems have been documented from modern fluvial settings (Bowler & Harford 1966, Gregory & Schumm 1987).

In situ tree stumps preserved within the siltstone indicate that sedimentation rates for mudrocks were very high. In some instances as much as 1.5 m of siltstone was deposited around the tree as it grew (Plate 11f). Assuming that the lycopod had a life span of 200-500 years, and accounting for rates of compaction in the siltstone (maximum burial depth for the formation = 3 km after Hacquebard & Cameron 1989, equating to a conversion factor of x1.5 after the method of Falvey & Deighton 1982), sedimentation rates for the siltstone would have been between 1.13 m and 0.45 m/100 years.

This rate is exceedingly high, but not atypical for lakes. For example, Picard and High (1981, table 3) show that average sedimentation rates in varved glaciolacustrine settings range between 3.7 mm and 4 m/100 years (Precambrian to Recent successions) with extreme rates up to 100 m/100 years. Sedimentation data based on the depth of burial of tree trunks is rare in the literature. Data presented by Smith (1973) for braided fluvial and overbank environments along reaches in the North Saskatchewan River at Banff National Park, indicated sedimentation rates of 0.34 m/100 years.

to 135°). Somewhat analogous variations in drainage systems have been documented from modern fluvial settings (Bowler & Harford 1966, Gregory & Schumm 1987).

In situ tree stumps preserved within the siltstone indicate that sedimentation rates for mudrocks were very high. In some instances as much as 1.5 m of siltstone was deposited around the tree as it grew (Plate 11f). Assuming that the lycopod had a life span of 200-500 years, and accounting for rates of compaction in the siltstone (maximum burial depth for the formation = 3 km after Hacquebard & Cameron 1989, equating to a conversion factor of x1.5 after the method of Falvey & Deighton 1982), sedimentation rates for the siltstone would have been between 1.13 m and 0.45 m/100 years.

This rate is exceedingly high, but not atypical for lakes. For example, Picard and High (1981, table 3) show that average sedimentation rates in varved glaciolacustrine settings range between 3.7 mm and 4 m/100 years (Precambrian to Recent successions) with extreme rates up to 100 m/100 years. Sedimentation data based on the depth of burial of tree trunks is rare in the literature. Data presented by Smith (1973) for braided fluvial and overbank environments along reaches in the North Saskatchewan River at Banff National Park, indicated sedimentation rates of 0.34 m/100 years.

5.3 Siltstone Blocks (B)

5.3.1 Description

Siltstone blocks forming units up to 4 m in thickness comprise 0.25 % of the Boss Point Formation (Fig. 3.1, Appendix I), and occur throughout the formation. Some Boss Point Formation occurrences have previously been described as "slumped blocks" (Plint 1986). In addition to the outcrops described by Plint (1986; 1989), and van de Poll and Patel (1989, 1990), good exposures occur at Slacks Cove (Figs 5.26, 5.27 & 5.28), at Grindstone Island (Plate 15a) and at Boss Point (Plate 15b).

The lithofacies consists of angular to rounded blocks of medium blue-grey laminated siltstone (F1), intercalated with cm- to dm-metre bedded sandstone. They occur within erosionally based scours which are commonly lined with a siltstone pebble lag (Figs. 5.27 & 5.29, Plate 15c). Blocks of siltstone vary widely in size. The outcrop at Alma consists largely of an unbroken block up to 40 m wide. At the margins, the block shows fragmentation and cracking into blocks, the cracks commonly infilled with sandstone (Plint 1986, fig. 5). This outcrop aside, most occurrences of the lithofacies comprise blocks of siltstone less than 3-4 m wide, with the great majority less than 1 m diameter.

The blocks preserve horizontal lamination (interpreted

Fig. 5.26 Locality map of the Slacks Cove siltstone intervals. Drawn from vertical black and white aerial photography.

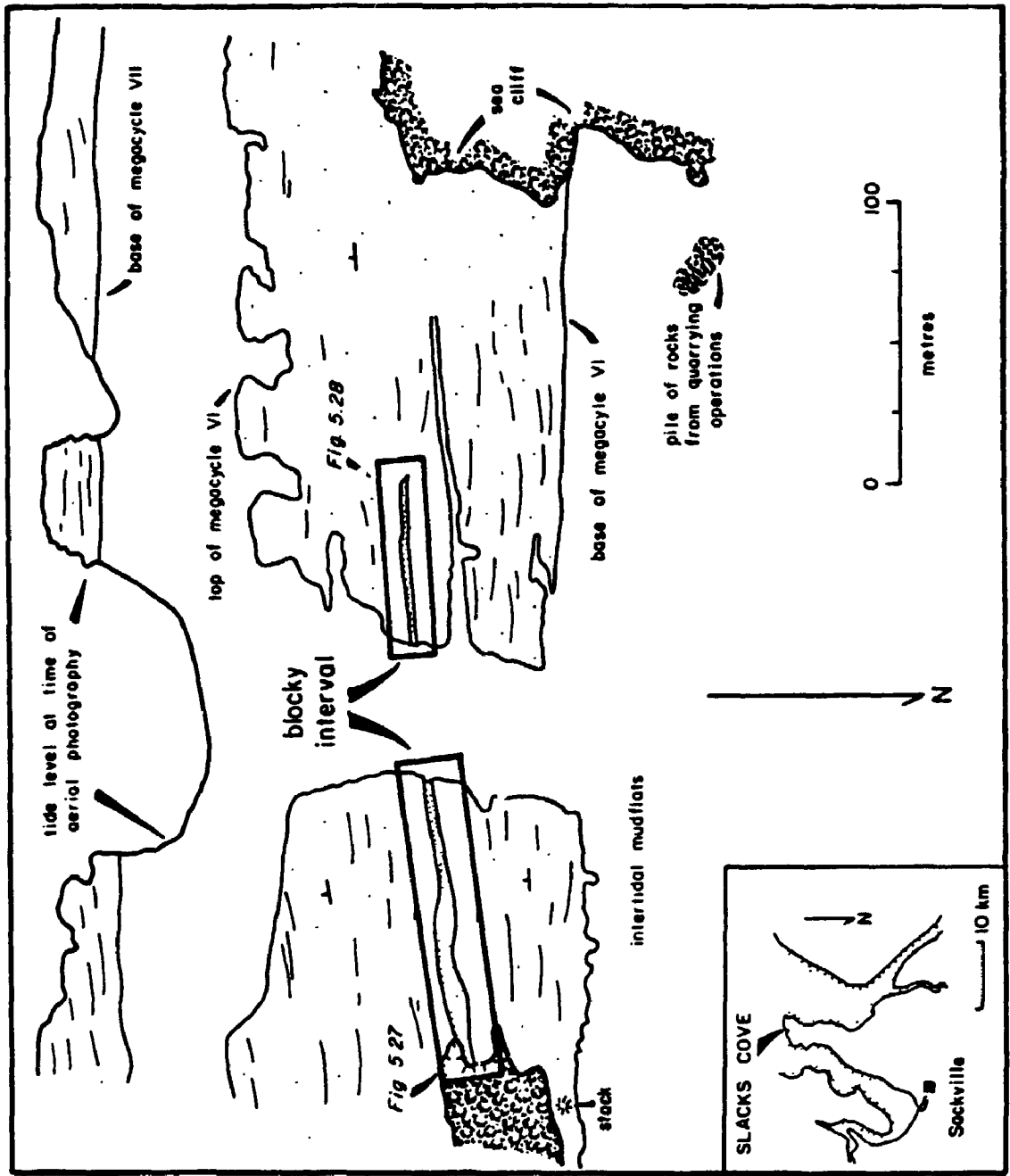
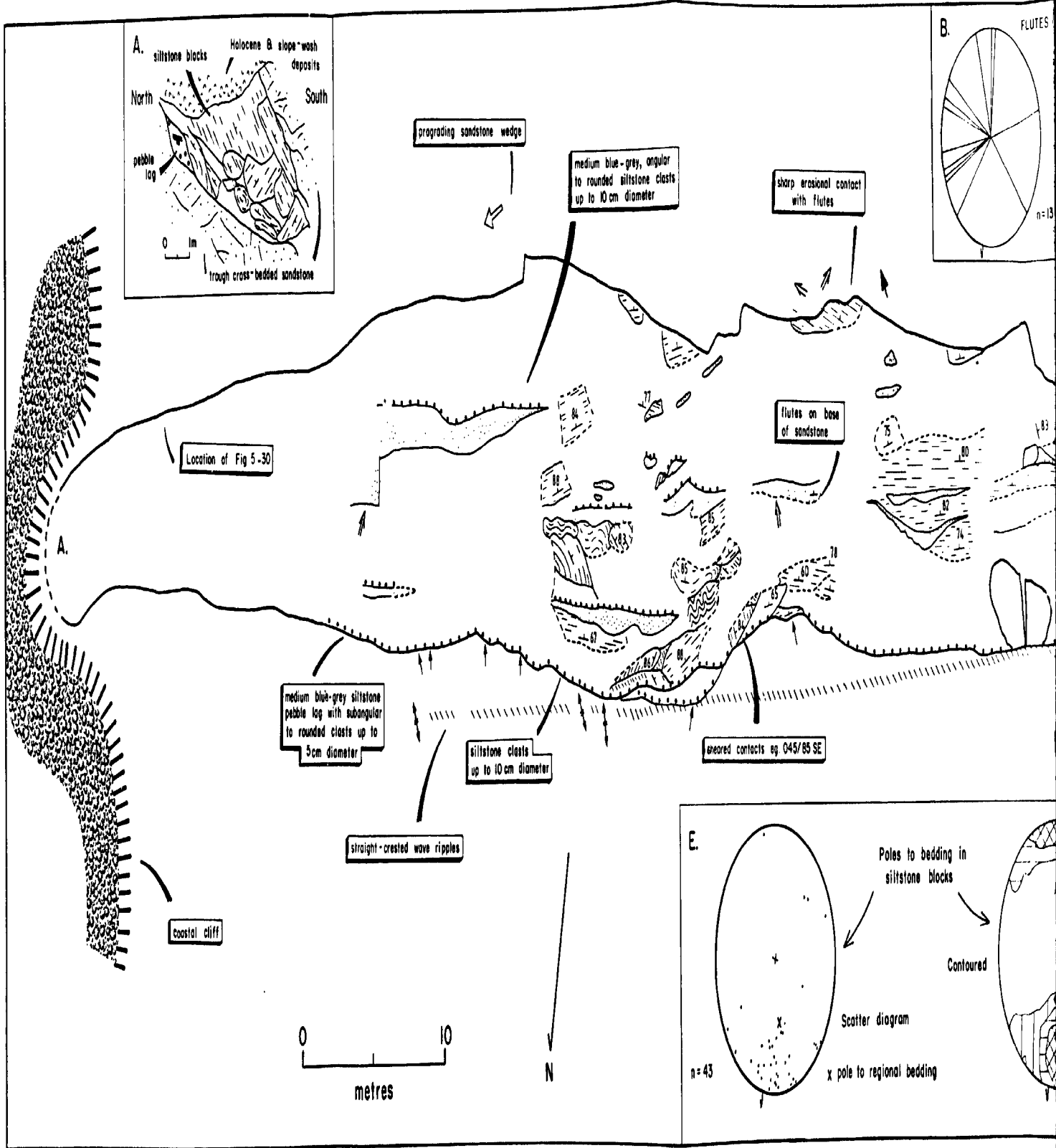


Fig. 5.27 Geological map of the interval at Slacks Cove East with siltstone blocks. Drawn from vertical black and white air photography and field surveys.



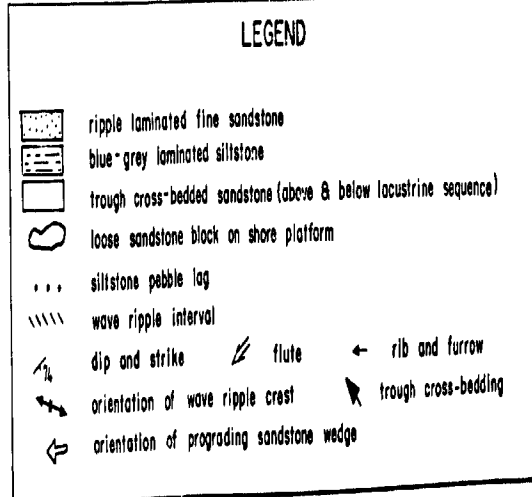
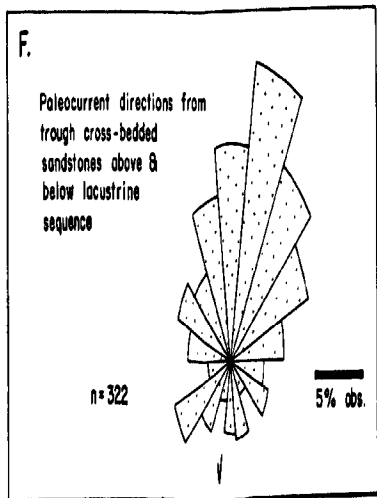
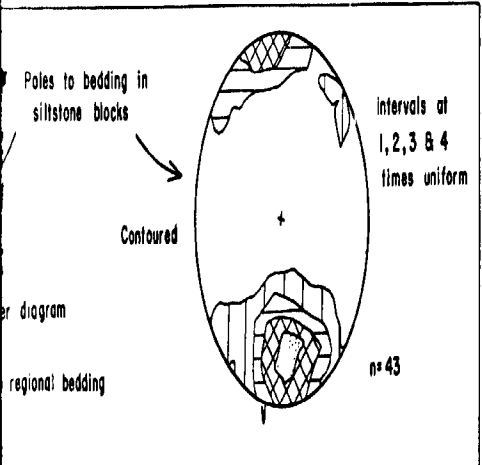
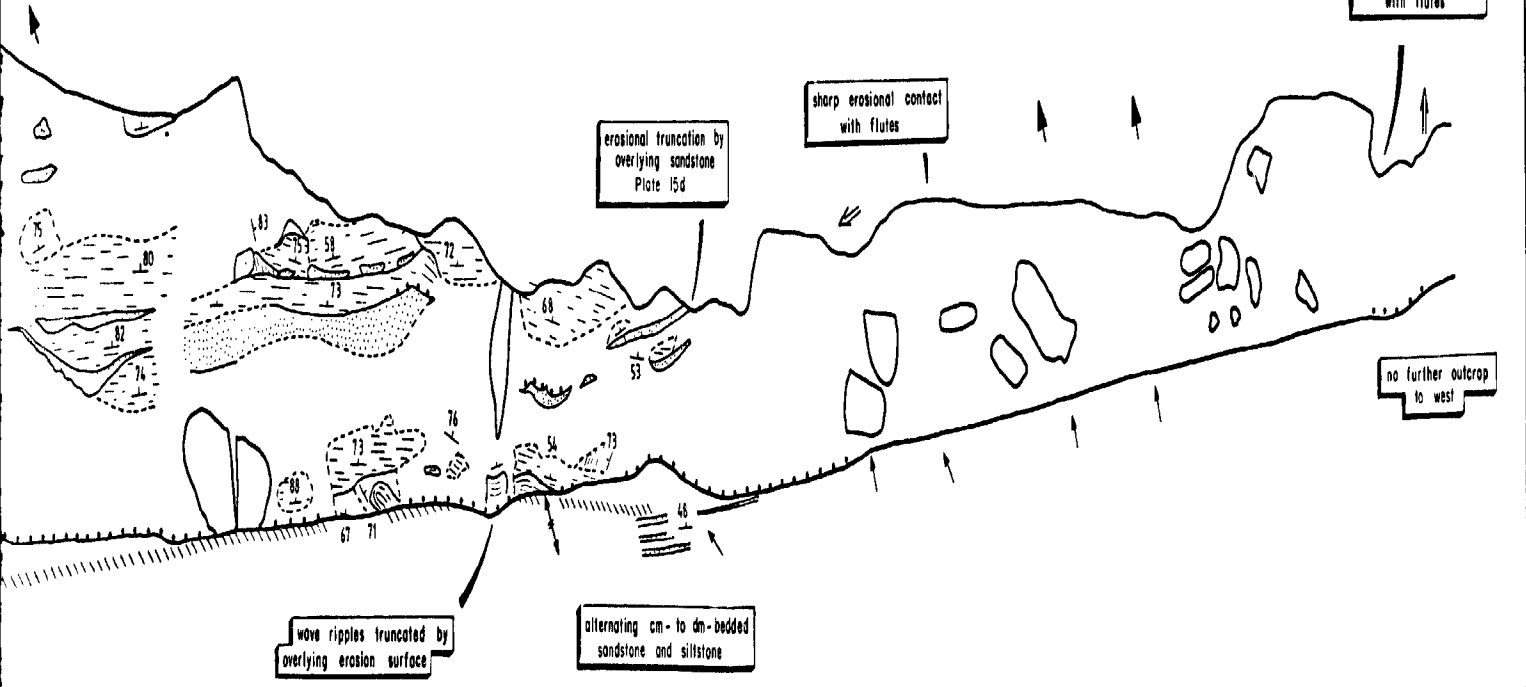
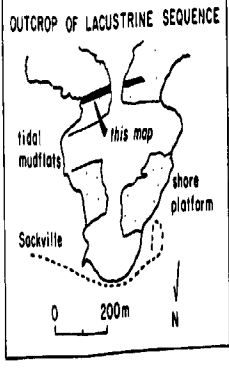
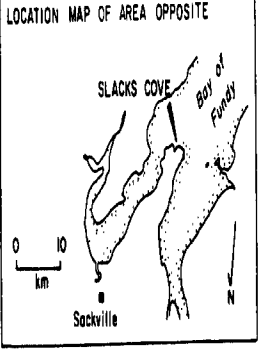
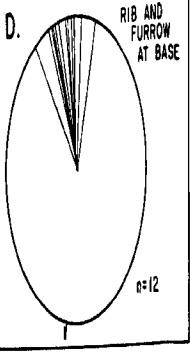
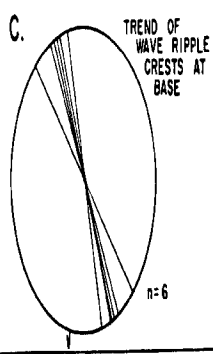
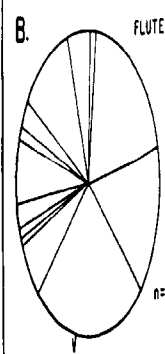
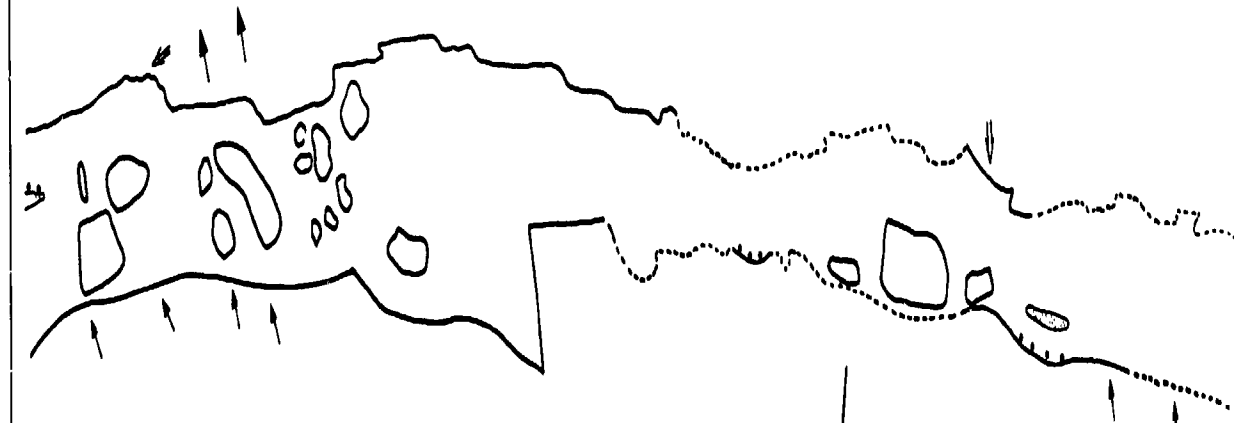
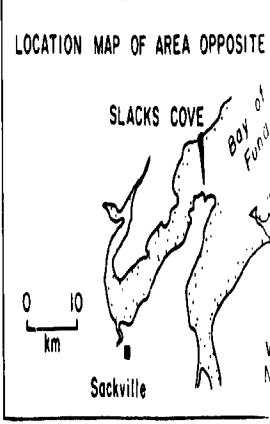
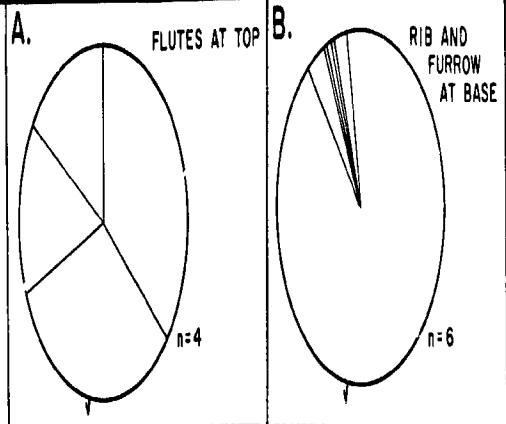









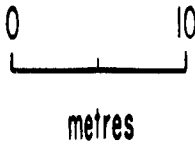
Fig. 5.28 Geological map of the interval at Slacks Cove West
with siltstone blocks. Drawn from vertical black
and white air photography and field surveys.



LEGEND

	ripple laminated fine sandstone
	trough cross-bedded sandstone (above & below lacustrine sequence)
	loose sandstone block on shore platform
	siltstone pebble lag
	flute
	rib and furrow
	trough cross-bedding

N



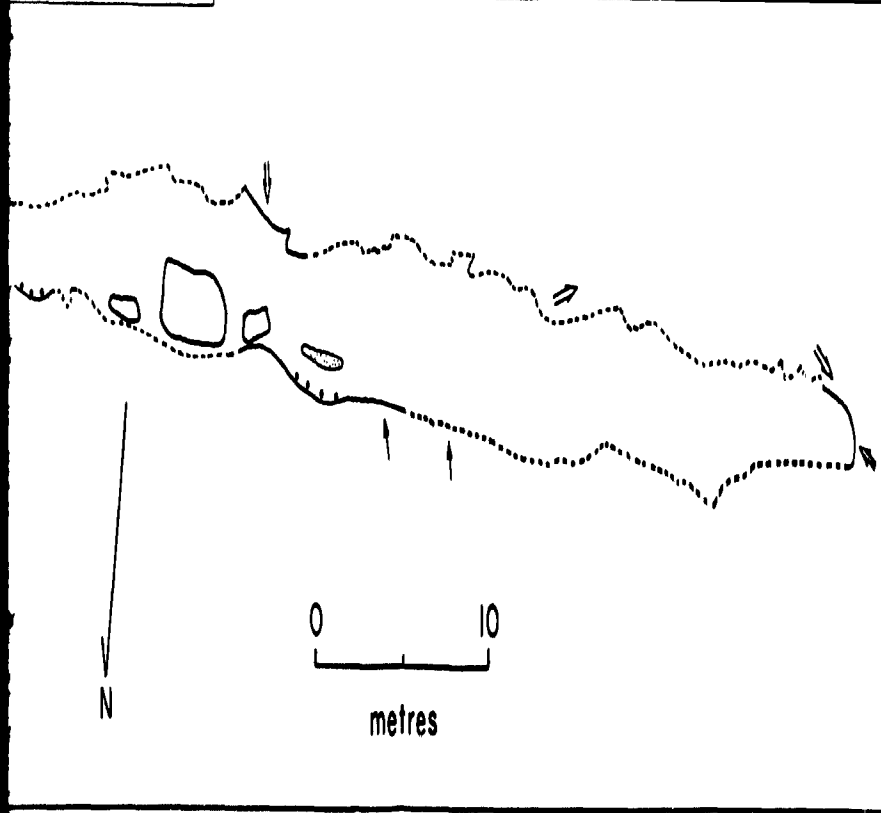
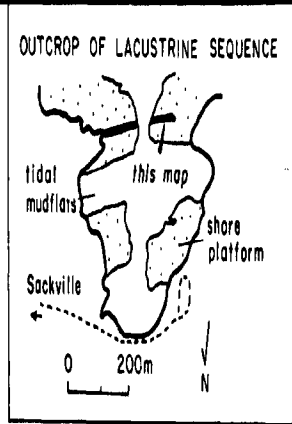
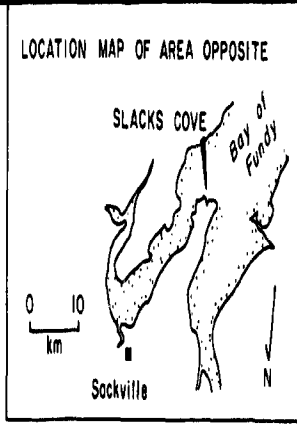
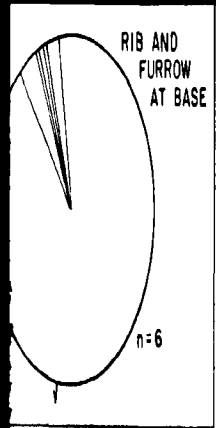


Plate 15

a) Large siltstone "clast" on eastern coast of Grindstone Island. Basal scoured surface (left) has a relief of 2.5 m, and is lined with <2 cm diameter siltstone pebbles. Slickensides on the basal surface trend 142°. The siltstone "block" consists of numerous <2 m diameter siltstone blocks, and at the top displays ball and pillow structures within the siltstone, presumably early formed structures that were incorporated into the block when the block slumped into the channel. Figure centre left for scale.

b) Fine-grained micaceous sandstone block showing soft sediment folding (arrowed) at Boss Point. For location of photograph see Fig. 5.29. Scale has 10 cm divisions.

c) Siltstone pebble clasts at base of blocky siltstone unit, Boss Point. For location of photograph see Fig. 5.27.

d) Siltstone blocks at Slacks Cove East (see Fig. 5.27). Note the bedding in the siltstone unit (marked by erosion resistant ripple laminated sandstone beds [arrowed]) erosively cut by overlying trough cross-bedded sandstone (left). 50 cm scale at centre left.

e) Straight-crested wave ripple lamination exposed in plan view immediately below the blocky siltstone lithofacies at Slacks Cove East section. Scale 50 cm long with 10 cm divisions.

f) Photomicrograph of conjoined ostracod valves from limestone lithofacies from Boss Point. Scale bar is 0.5 mm.

g) Photomicrograph of tightly packed ostracod-bearing limestone from Johnson Mills. This sample also contains abundant gastropods. Staining for carbonate in this sample indicates that the ostracod valves are non-ferroan calcite, whereas pore spaces are filled with ferroan calcite. Scale bar is 0.5 mm.

h) Centimetre thick, erosion resistant coal beds (arrowed) within clayey siltstone, Cape Maringouin section (see Fig. 5.37). Scale is 50 cm long with 10 cm divisions.

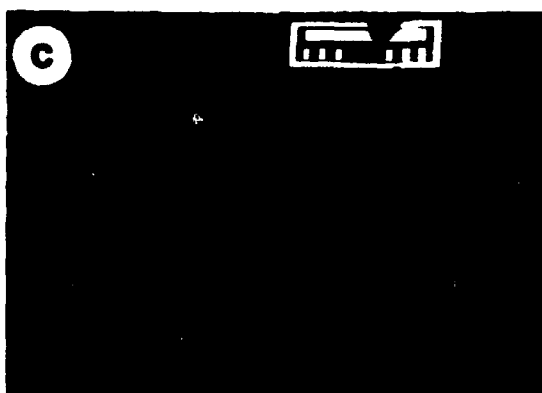
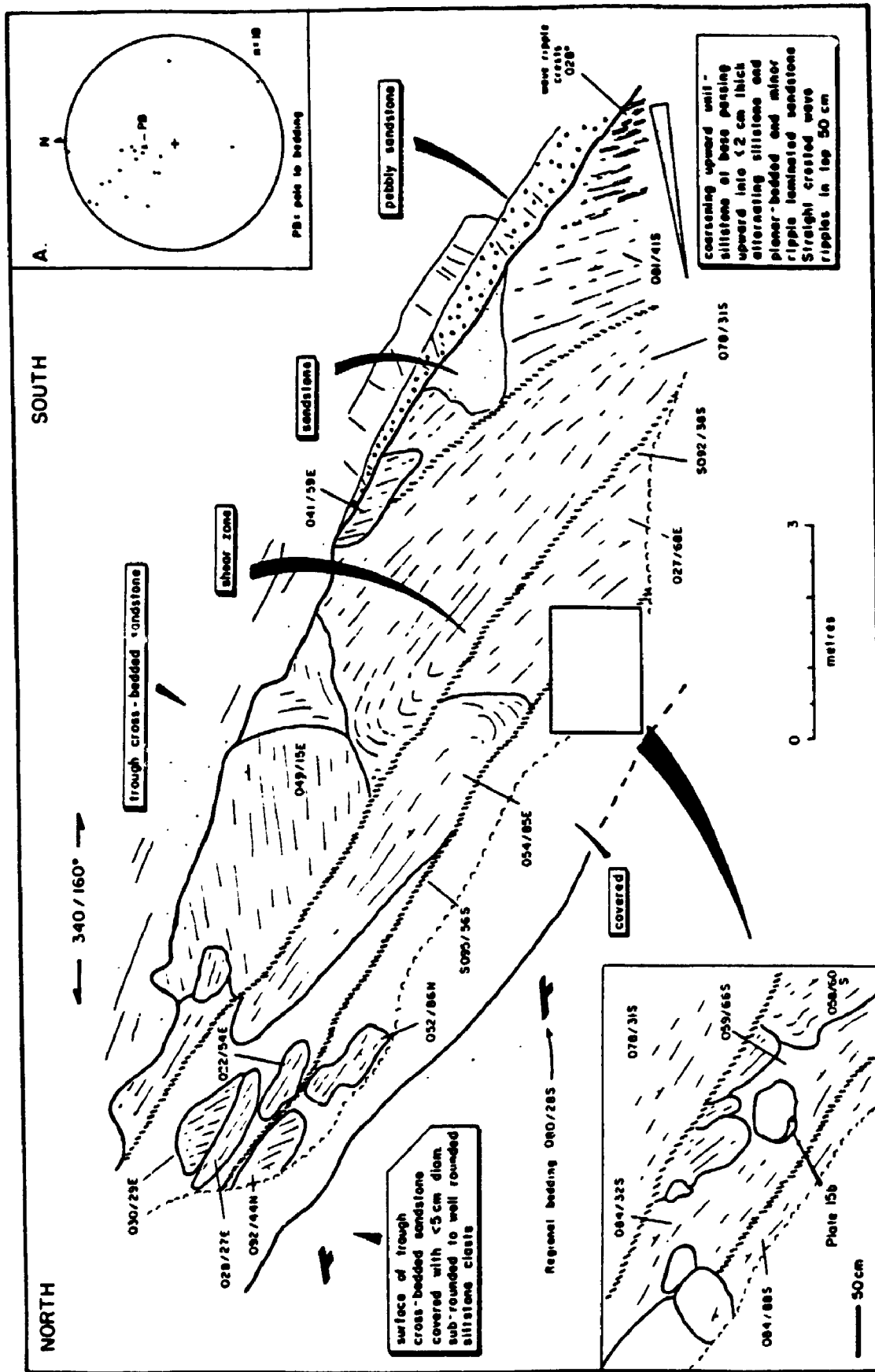


Fig. 5.29 Siltstone blocks at Boss Point. Drawn from black and white photographs and field sketch.



here as primary bedding - cf. Plint 1986, 1989), and not a fabric related to rheoplasia (cf. van de Poll & Patel 1989), and in many cases this stratification has been deformed into open and rare recumbent folds. Siltstone blocks are admixed with smaller (< 50 cm diameter) blue-grey and reddish grey fine- and medium-grained sandstone which commonly show soft sediment folds (Plate 15b), and at Cape Enrage, water expulsion features (Fig. 5.5 at Bay 3N). At first sight, the siltstone blocks appear randomly arranged, but where sufficient numbers of these blocks could be measured, all show a consistent bedding attitude (Figs. 5.27, inset E & 5.29, inset A), invariably 10-15° greater than regional bedding. At Cape Enrage, both the upper and lower siltstone units (F1) can be traced laterally into siltstone blocks over distances between 80 to 450 m (Fig. 5.5), indicating that the siltstone blocks are laterally equivalent to the laminated siltstone lithofacies.

The lithofacies is in all cases overlain and underlain by trough cross-bedded sandstone (St).

The Slacks Cove Occurrence

A well exposed example of siltstone blocks occurs at Slacks Cove where a 4 m thick blocky unit can be traced intermittently over a 150 m wide shore platform exposure (Figs. 5.26, 5.27 & 5.28, Plate 15d). The siltstone

blocks rest on an erosion surface which is typically marked by carbonaceous fragments and a pebble lag consisting of 5-10 cm diameter blue-grey siltstone clasts (Fig. 5.27, Plate 15c). Relief along the contact is as much as 5 m, and in places the surface is smooth and "glassy" suggestive of slickensides or shear plane movement (see Plint 1989).

A climbing ripple laminated unit immediately below the scoured base can be traced across much of the shore platform outcrop (Figs. 5.27 & Plate 15e), and can be seen to be removed in places by an erosion surface (Fig. 5.27). The wave ripple crests are consistently oriented NNW-SSE and NW-SE (Fig. 5.27, inset C). Rib and furrow measurements from the top few centimetres of the sandstone below the blocky interval show a southerly trend, which is consistent with the paleocurrent orientations determined from the entire section (Figs. 5.27, insets D & F, 5.28, inset B). Siltstone blocks are up to 3 m in diameter, and show both undeformed horizontal lamination and folded lamination (Fig. 5.27, inset A). Bedding attitudes measured from the siltstone blocks dip consistently to the south at about 75° , or at about 15° more than the regional bedding (Fig. 5.27, inset E). Not only do blocks of siltstone occur; fine-grained, ripple cross-laminated sandstone blocks and beds are also intercalated, and some of these have siltstone pebble lag clasts on their upper surfaces (Fig. 5.27). Ripple cross-lamination geometry

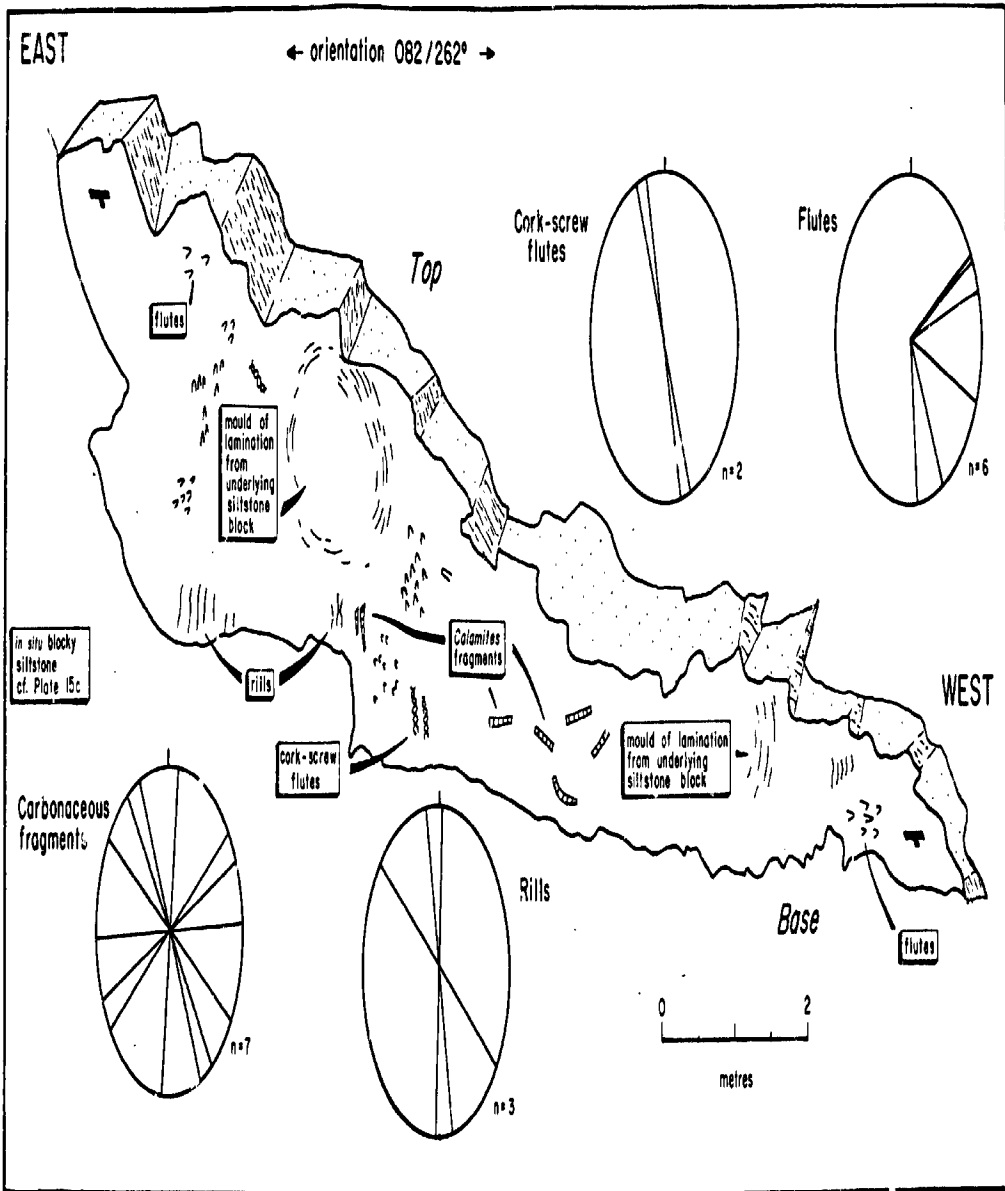
within these sandstone bodies indicate that the sandstones are not overturned, but young in the same direction as the regional bedding, ie. to the south. Occasionally faults separate the blocks (Fig. 5.27), but in most instances blocks appear to rest against each other in a non-sheared manner. Paleocurrent data from within the blocky interval is limited to 2 flute casts preserved at the base of ripple cross-laminated sandstones. These show southerly trends (Fig. 5.27).

The upper contact of the lithofacies is erosional, cutting down as much as 5 m into the underlying blocky interval (Figs. 5.27, Plate 15d). Flutes are common at this contact (Fig. 5.30) and although they show some spread, they generally trend to the south (Fig. 5.27, inset B, Fig. 5.28, inset A), consistent with the regional paleocurrent direction determined from trough cross-beds (Figs. 5.27, inset F, 5.28, inset C) and other sedimentary features (see Chapter 8).

5.3.2 Petrography and Petrology

Petrographically the siltstone units are equivalent to the laminated siltstone lithofacies (F1) described above, comprising laminated very fine-grained sandy siltstone. In thin section the sand grains are dominated by angular quartz (<30%) up to 30 um diameter, with less abundant opaques (10%) and elongate muscovite (<1%) up to 40 um in

Fig. 5.30 Plan view of base of sandstone overlying the siltstone block interval at Slacks Cove East. For location see Fig. 5.27.



length. Flint (1989, fig. 2) observed bioturbation in the deformed siltstone block at Alma, probably formed by roots, but similar structures have not been observed in this study. Sandstone units associated with the lithofacies consist of well sorted, micaceous fine-grained sandstone.

XRD analysis indicates that the siltstone blocks comprise kaolinite and illite clay mineralogy, together with quartz, albite, and muscovite, and is similar to other fine-grained units (Fm & Fl) in the Boss Point Formation (Fig. 5.1).

5.3.3 Interpretation

The lateral equivalence that can be demonstrated between the blocky and laminated siltstone lithofacies at Cape Enrage (Fig. 5.5), is supported by their lithologic and petrologic similarity. It therefore seems likely that they were once part of the same type of unit, the siltstone blocks however being transported and/or dislocated before being emplaced into their present positions.

The consistent orientation of siltstone clasts at both Slacks Cove and Boss Point suggests that a slumping mechanism operated, whereby a backward rotation of dominantly cohesive siltstone material occurred on a curvilinear basal shear plane (rotational slumping under

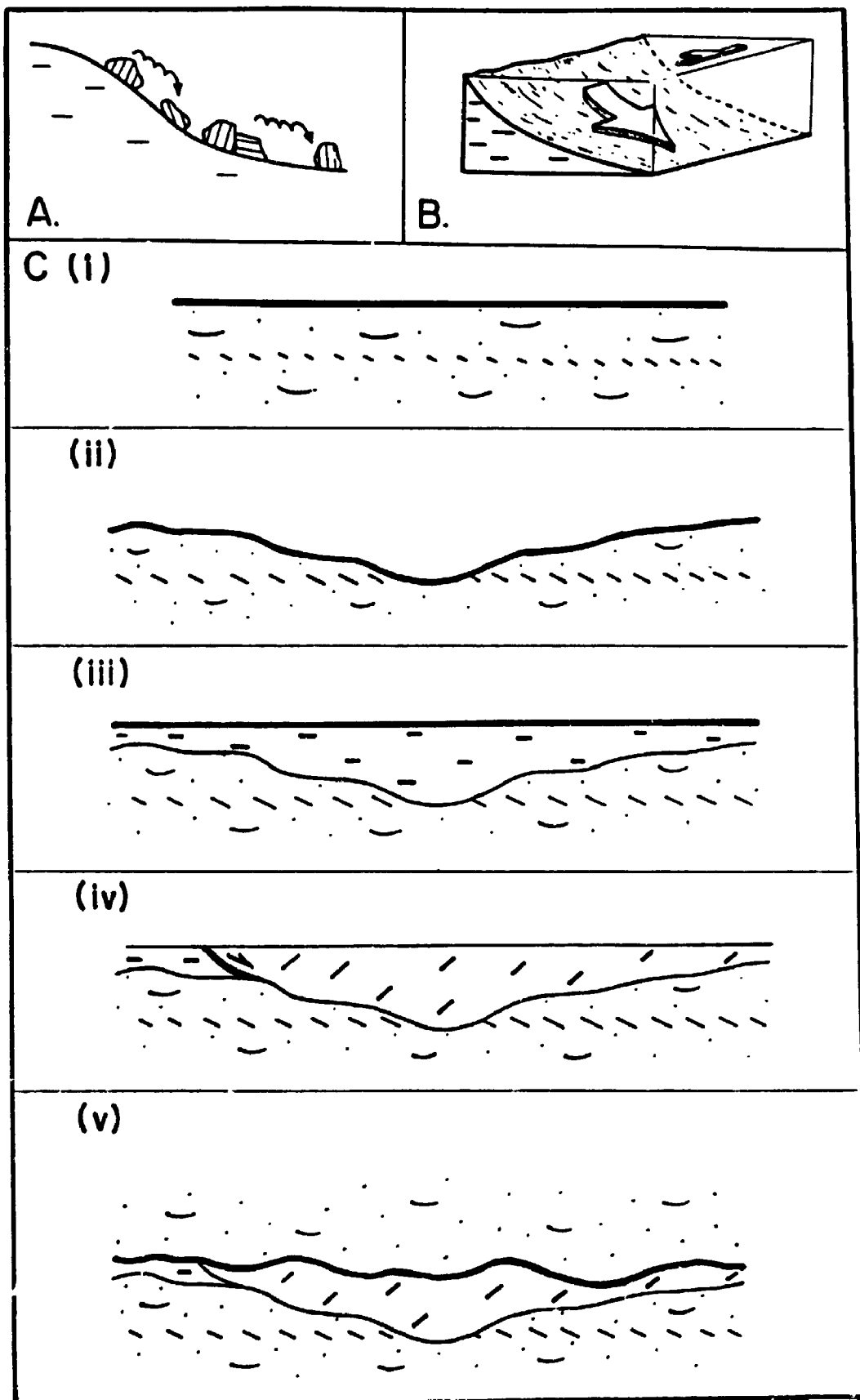
the influence of gravity - Fig. 5.31). The preferred orientation of the clasts within the unit at Slacks Cove and Boss Point rules out the possibility of individual emplacement or toppling of clasts from channel margins (see for example Karcz 1969), or of a debris flow mechanism produced from bank failure (Rust & Jones 1987).

Because of the similarities between the laminated siltstone lithofacies and the siltstone blocks described here, it is assumed that the siltstone blocks forming the blocky sequences were also lacustrine. It is further suggested that the siltstone blocks formed after a scouring event produced a local gradient, slumping being initiated by bank instability, perhaps caused by river undermining of bank materials. The removal of lateral support to the bank may have triggered gravitational slumping toward the thalweg, or alternatively, movement may have been triggered by earthquake mechanisms (see Plint 1985).

Slumping would have involved the backward rotation of a coherent package of sediment along a curved basal shear plane. The orientation of the siltstone blocks is therefore toward the margin of the slide. The 150 m maximum lateral extent recorded for the lithofacies (at Slacks Cove), is the minimum width that this slump attained.

Plint (1986) made a similar proposal, concluding that slumping took place into an abandoned fluvial channel.

Fig. 5.31 Models for the development of the siltstone block unit at Slacks Cove. A) Movement of siltstone blocks downslope would result in a random orientation of blocks at the base of the slope. This model is not supported by the field evidence. B) The favoured model involves a gravitational collapse of the stream bank toward the thalweg, such that the bedding in the slide block is tilted toward the original (failure) slope. C) Evolutionary model for the development of the siltstone units. (i) initial deposition of trough cross-bedded sandstone and wave ripple laminated sandstone. (ii) erosion of units deposited during (i) down to the level of the wave ripple laminated sandstone. (iii) infilling of the scour by lacustrine siltstone. (iv) formation of the blocky siltstone by gravitational collapse of part of the lacustrine interval such that the bedding dips toward the original (failure) slope. (v) erosion of the upper part of the blocky siltstone and deposition of an overlying trough cross-bedded sandstone interval.



Bank collapse causing deformation (folding faulting and local fissuring) of siltstone, was interpreted by Plint to be followed by intense local subaqueous scouring to generate flutes, grooves and linear scours. Slump blocks similar to those described here are common in both modern and ancient fluvial environments (Stanley et al. 1966, Coleman 1969, Williams et al. 1965, Laury 1971, Cant 1978, Guion 1987, Rust & Gibling 1990a). Examples of rotational slumps akin to the Boss Point Formation examples are presented by Stanley et al. 1966, Coleman (1969), and Laury (1971), where collapse occurs into the river toward the thalweg.

5.4 Limestone (L)

5.4.1 Description

In this study, twenty-five limestone beds comprising 0.06% of the thickness of the formation are recorded (Fig. 3.1, Appendix I). The maximum bed thickness is 80 cm (mean thickness = 16 cm). Limestone beds are generally interbedded with fine-grained lithologies, principally massive and laminated siltstone (Fm & Fl) and coal. Limestones occur only in the central part of the Bay of Fundy region, at Marys Point, Cape Maringouin, Slacks Cove, Rockport, Johnson Mills and Boss Point (Fig. 3.2).

The limestone consists of medium to dark grey, richly

carbonaceous wackestone with some packstone, typically with crude to well developed horizontal stratification. Lawson (1962) reported a CaCO_3 content of 80% for the limestone. Bases and tops to beds are planar and sharp. They are typically well cemented and commonly form resistant beds on shore platform exposures.

5.4.2 Petrography

Bioclasts consist almost exclusively of ostracod valves (Plate 15f), with fewer bivalve, gastropod and fish-scale fragments. Ostracods occur as both conjoined and disarticulated valves together with broken shell fragments and are commonly aligned sub-parallel to bedding, giving the rock a well developed stratification. Valves all lack ornament, which is a feature of the genus *Carbonita*. Two forms of ostracod occur; thick-shelled forms with valves between 0.05 - 0.1 mm thick (typically with a porous texture perpendicular to the margin of the valve), and thin-shelled forms with valves <30 μm thick. Both forms range in length between 0.5 and 0.75 mm. They are most commonly infilled with equigranular or drusy textured spar, and in rare cases by micrite. Geopetal structures occur, but are rare. The other bioclasts include bivalve fragments up to 3.5 mm long, gastropod shells and rare fish scales. The apical portions of gastropods are infilled with fine-grained spar which

becomes progressively coarser-grained towards the aperture. Drusy texture is common in the body whorl at the anterior end.

Alizarin Red S and potassium ferricyanide staining indicates that the ostracod valves consist of non-ferroan calcite. The sparry infilling within the ostracod valves is a deep blue (ferroan calcite), with a tendency for the innermost parts of the sparry calcite to be red or non-ferroan (Plate 15g). The molluscan tests did not take the stain and are slightly bluish, suggesting that they have been preferentially dolomitised (ferroan dolomite).

5.4.3 Paleontology

No work has been undertaken on the fauna of the Boss Point Formation limestones since the work of Copeland (1957). Copeland named 4 ostracod species from the genus *Carbonita* at 3 Boss Point Formation localities (Table 2). Considerable scope exists for a modern detailed and systematic paleontologic study on these well preserved faunas.

Table 2 - Faunal List from Boss Point Formation Limestone units after Copeland (1957)

	A	B	C
<i>Carbonita agnes</i> (Jones)		x	
<i>C. atilis</i> (Jones & Kirkby)	x	x	x
<i>C. elongata</i> (Jones & Kirkby)	x	x	
<i>C. fabuina</i> (Jones & Kirkby)	x		x

- A - specimen #1449 (Boss Point type section)
- B - specimen #25633 (Boss Point type section)
- C - specimen #25642 (Cape Maringouin)

5.4.4 Interpretation

The limestones are interpreted as lacustrine on the basis of fauna, fine-grained nature and association with other lithofacies. The complete lack of detrital siliciclastic grains indicates minimal input from adjacent terrigenous sources. Because coals are common immediately beneath limestones, and the two lithologies typically grade vertically into each other (Plate 15h), it is suggested that the limestone represents a deeper water setting with respect to the coal.

5.5 Coal (C)

5.5.1 Description

Fifteen coal beds are recorded from the study area, with a maximum thickness of 70 cm (mean thickness 13 cm; Fig. 3.1, Appendix I). Coal constitutes 0.03% of the formation, and is confined to the central part of the Bay of Fundy region, principally in the Cape Maringouin area. Coal beds occur interbedded with laminated mudrock lithologies (F1), and commonly grade up into ostracod-bearing limestones (Plate 15h). No systematic work was undertaken on coal in this study.

The thickest coal association occurs at Slacks Cove West where black fissile shaley coal with thin vitrain and

clarain bands occur, the coal is intercalated with grey mudrocks (Fig. 5.32). The coal commonly contains pyrite nodules and sulphur efflorescence.

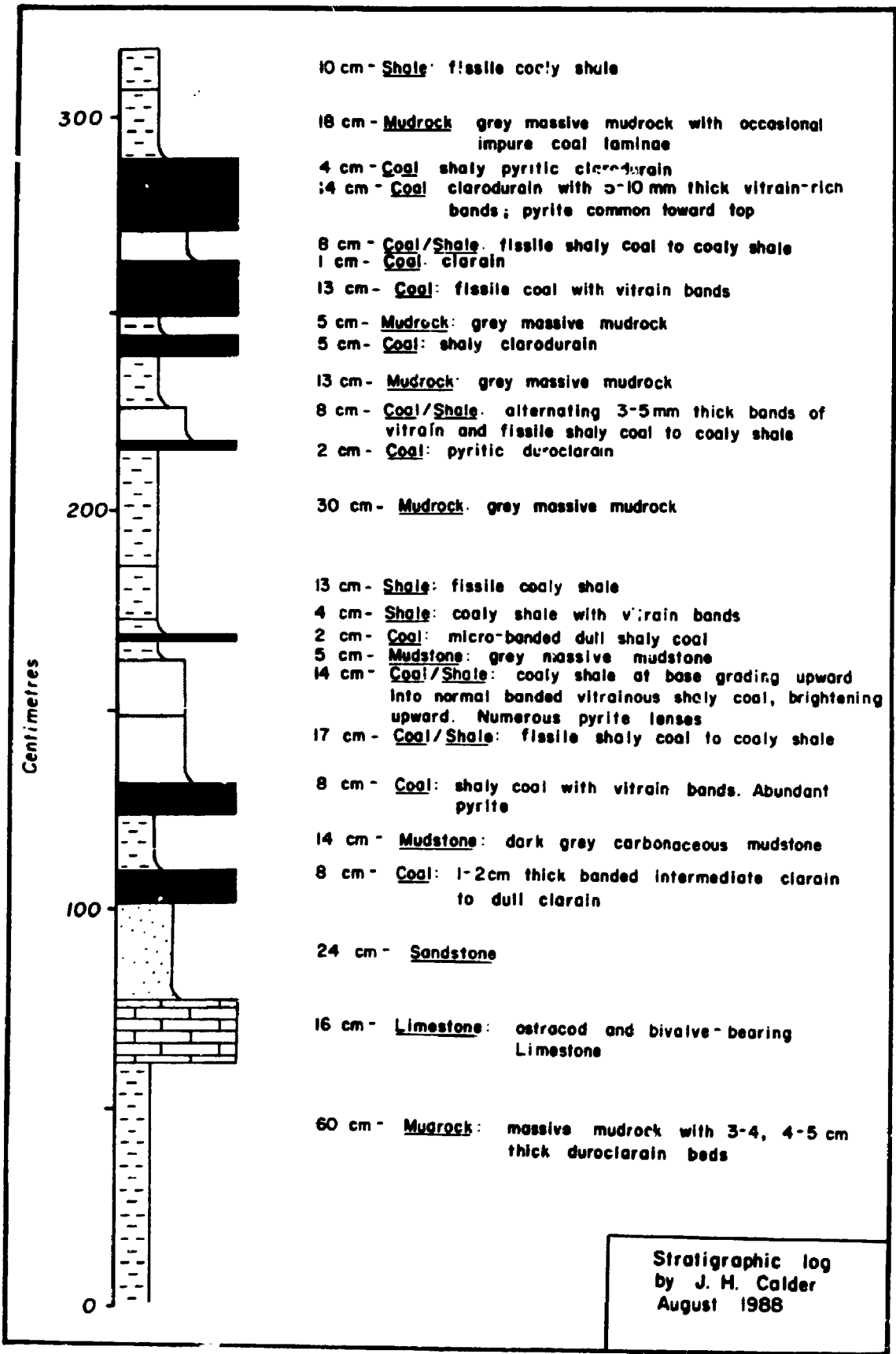
Previous work has indicated that Boss Point Formation coals are high volatile-B (HV-B) bituminous (Hacquebard and Cameron (1989) with vitrinite reflectance ($R_{o \max}$) values between 0.71 and 0.77% (Hacquebard and Avery 1984). These $R_{o \max}$ values indicate that the formation attained a thermal maturity sufficient for hydrocarbon generation (Tissot and Welte 1978), though the small volume of kerogen means that the formation was never a significant source rock for hydrocarbons.

Despite claims by W. Jones and H.A. Ripley of "a 3' 10" wide coal... of excellent quality" at Lower Rockport (Sackville Tribune-Post, November 11, 1907), the only coal ever to be extracted from the formation was by 'hard up' local residents.

5.5.2 Petrography

In thin section the coal consists of durain, with <2 % sub-angular to sub-rounded quartz grains up to 30 μ m diameter, and ostracod valves and fragments. Sparry calcite veins are common. No reflected light microscopy was undertaken in this study.

Fig. 5.32 Stratigraphic log of coal measures at Slacks Cove
West section.



Stratigraphic log
by J. H. Calder
August 1988

5.5.3 Interpretation

The coals are interpreted as autochthonous and *in situ*, formed in the reducing environments of lakes. Coals also form in areas where clastic sedimentation is slight (McCabe 1984), the intercalation of coals with mudrock and limestone lithofacies suggesting a common paleoenvironment.

The most favoured site for coal deposition would have been in swampy or marshy areas marginal to lakes (eg. Tresse & Wilkinson 1982), where terrigenous input was minimal, yet where vegetation could flourish. The commonly observed vertical transition from coal to limestone is interpreted as representing a transition from a shallow lake margin (in which coals developed), to deeper water (with limestone deposition). It is possible that the peat bogs filtered out clastics and preventing them from reaching the deeper water carbonate regions.

SEDIMENTOLOGY OF PALEOSOLS

The recognition of paleosols in alluvial sediments has increased greatly over the past twenty years. Paleosols have been used to interpret a variety of phenomena including rates of sedimentation on flood plains (Allen 1974, Leeder 1975, Wright 1982, 1990b, Kraus and Bown 1986, Leckie et al. 1989), controls on geometries of fluvial channels (Allen and Williams 1979, Retallack 1986, Gibling and Rust 1990), hydrogeologic conditions (G-Farrow and Mossman 1988, Besly and Fielding 1989), paleoclimates (Goudie 1973, Allen 1974, 1986, Steel 1974, Besly and Turner 1983, Searl 1989, Wright 1990a), paleogeomorphology (Retallack 1977, 1983, Allen and Williams 1979, Atkinson 1986, Kraus and Bown 1986, Besly and Fielding 1989), and atmospheric conditions during soil formation (Retallack 1986, G-Farrow and Mossman 1988). Paleosols may also provide important insights into past vegetation patterns (Retallack 1977, 1983, 1985, Francis 1986) and types of burrowing infauna (Retallack 1984). In addition, the significance of the time required to form soils can add to our understanding of rates of flood plain processes (Gile et al. 1966, Goudie 1973, Retallack 1983, Machette 1985, Allen 1986).

Most studies have concentrated on pedologic profile

descriptions and petrography. More recently, pedogenic surfaces or intervals (catena) have been studied across sedimentary basins (Allen 1986, Atkinson 1986), but few studies to date have integrated soil morphology with the sedimentology of the enclosing sediments, or the paleoecology and paleogeography, although important exceptions include Allen (1974), Retallack (1977, 1983, 1986), Bown and Kraus (1987), and Besly and Fielding (1989). The number of studies which attempt geochemical interpretations or isotopic studies of paleosols is growing in number (McPherson 1979, Mount and Cohen 1984, Meyer and Pena dos Reis 1985, Retallack 1986, G-Farrow and Mossman 1988, Naylor et al. 1989, Platt 1989b), and has been aided by significant advances in geochemical studies of weathering processes (cf. Nesbitt and Young 1989).

The aim of this chapter is to describe previously unrecognised paleosol intervals within the Boss Point Formation. Indeed, paleosols have rarely been acknowledged from any part of the Paleozoic of Maritime Canada, and those that have, have received only brief discussion (Legun and Rust 1982, van de Poll 1983, Zaitlin and Rust 1983, Rust and Nanson 1989, Gibling and Rust 1990). To date no published literature exists regarding paleosol geochemistry in the Cumberland sub-basin. The work of Mark Smith (M.Sc. in preparation) currently in progress at the University of Guelph, together with this study, are the first such projects.

6.1 Recognition of Paleosols

Paleosols are characterised by the presence of vivid coloration or colour mottling, intense bioturbation (and/or pedogenic aggregates), mineral accumulations, vertical profile development or root structures (Atkinson 1986, Leckie *et al.* 1989, Rust and Nanson 1989). Of these criteria, the presence of fossil roots preserved in their original growth position is the most diagnostic feature of a paleosol (Retallack 1981, Francis 1986).

To this list can be added calcrete (caliche) nodules (glaebules), which are defined as "terrestrial materials composed dominantly, but not exclusively of CaCO_3 , which occur in states ranging from nodular and powdery to highly indurated, and result mainly from the displacive and/or replacive introduction of vadose carbonate into greater or lesser quantities of soil, rock or sediment within the soil profile" (Watts 1980, p. 663). Calcretes are widely recognised in both modern and ancient sedimentary successions (James 1972, Allen 1974, Steel 1974, Walls *et al.* 1975, Leeder 1976, McPherson 1979, Klappa 1980, Wright 1982).

In this study the presence of any two of the above features was taken to warrant classification as a paleosol; one criterion by itself was deemed insufficient to be confident of pedogenic affinity.

6.2 Distribution of Soil Profiles

Stratigraphically, paleosols occur throughout the Boss Point Formation, and in total, 29 paleosol intervals are recognised (Appendix I). As such, paleosols form a minor percentage of the total formation thickness (0.5%, Fig. 3.1c), and have a maximum thickness of 2.2 m (mean = 1.1 m, Appendix I).

Though the number of paleosols is few in relation to the total thickness of the formation, it is clear that paleosols appear consistently at certain intervals in the Boss Point Formation (for example, at approximately 50 m above the base of the formation in many sections - Fig. 6.1). Paleosols at this stratigraphic position can be traced over an area of at least 900 km², and appear to form one pedogenic horizon or catena.

The paleosols have been recognised in a thin elongate belt extending from Alma in the SE to Dorchester in the NE (Fig. 6.1). Only one paleosol (at River John, stratigraphic section 1) is recognised from outside this zone.

6.3 Profile Descriptions

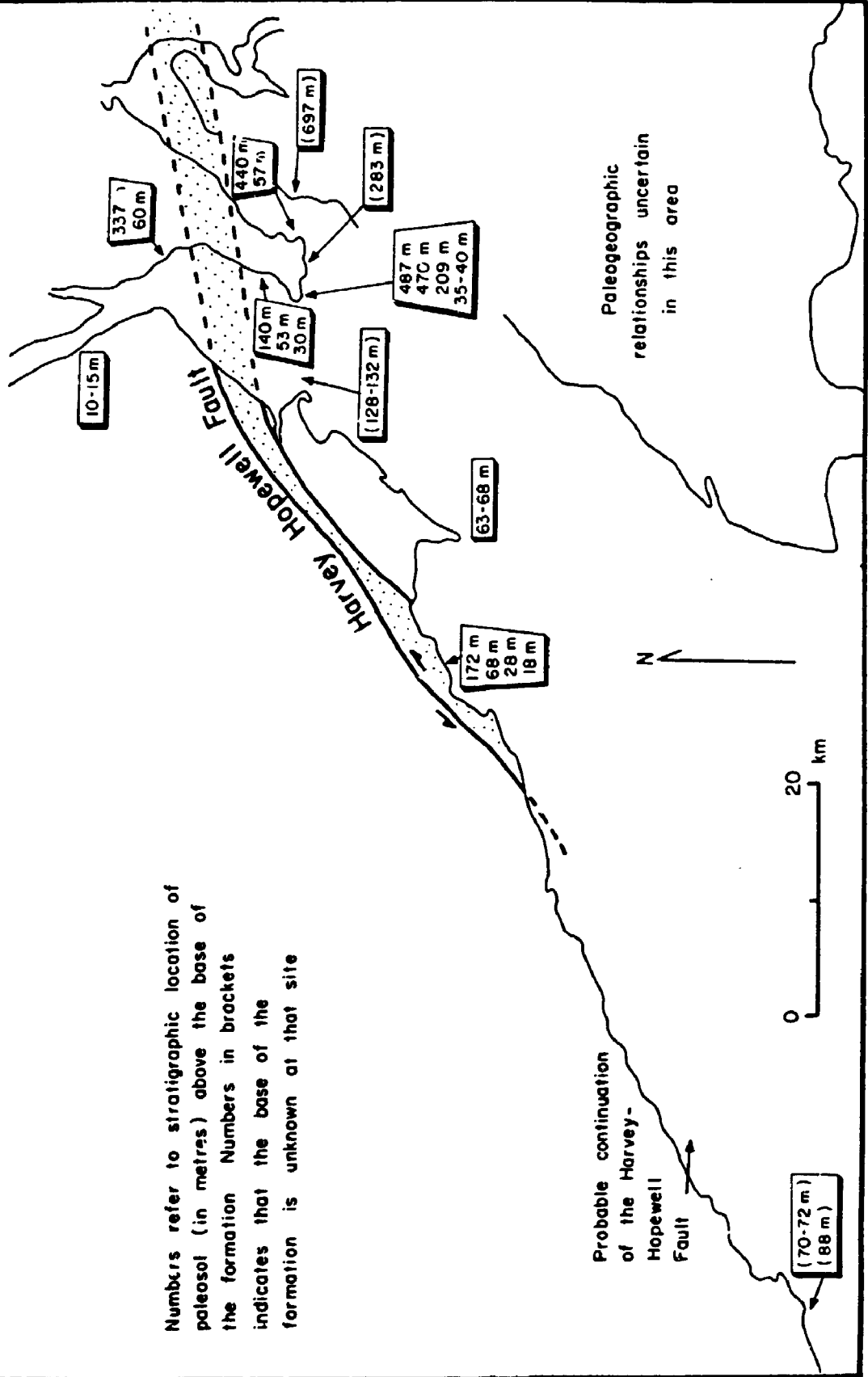
6.3.1 Profile Characterisation

Two pedogenic morphologies, sandy paleosols and silty

Fig. 6.1 Geographic and stratigraphic distribution of paleosols in the Boss Point Formation, Bay of Fundy region.

Paleosols - Geographic & Stratigraphic Distribution

Numbers refer to stratigraphic location of paleosol (in metres) above the base of the formation. Numbers in brackets indicates that the base of the formation is unknown at that site



paleosols are recognised in the Boss Point Formation, both of which developed on a parent material of unconsolidated flood plain alluvium.

Four profiles from a wide geographic area were examined in detail during this study. They were selected on the basis of being typical of sandy and silty paleosols. Descriptive profile logs appear in Appendix IV, and the outcrops are illustrated in Plate 16. The Dorchester sandy paleosol occurs at 337 m above the base of the formation, and is marked by a dense interlocking network of calcrete nodules forming a 20 cm thick resistant band at the top of the profile (Plate 16d & 16e). The two profiles from Cape Enrage are at 67 and 68 m above the base of the formation. The upper silty paleosol contains abundant low-angle conjugate shears (see below) and like other paleosols, displays an upward increase in the density of calcrete nodules toward the top of the profile (Plate 17a), similar to paleosols described by Allen (1974) and McPherson (1979). The Alma profile occurs at 68 m above the base of the formation, and probably represents two stacked paleosols. The central 40 cm of the profile consists of a prominent band of calcrete nodules (Plate 16b & 17b), the top of which is interpreted to mark the contact between the two paleosols.

Samples from these 4 profiles were examined by thin section microscopy, XRD, XRF and electron microprobe analysis. The following discussion is based largely on

Plate 16

- a) Upper portion of the sandy paleosol exposure, Dorchester. 50 cm scale with 10 cm divisions lies just below the top of the paleosol.
- b) Central part of the silty paleosol at Alma. The 40 cm thick erosion resistant calcrete nodule band occurs in the central part of the outcrop. Calcrete nodules protrude from the soft silty paleosol matrix. The calcrete band is overlain by a second silty paleosol (one developed subsequent to the calcrete horizon). Scale is 1 m with 10 cm divisions.
- c) Sandy (A) and silty (B) paleosols at Cape Enrage. Scale in centre foreground is 50 cm with 10 cm divisions. Succession dips (and youngs) 80°E (to right).
- d) Upper planar surface of Dorchester sandy paleosol showing the abundance of calcrete nodules. Scale is 50 cm with 10 cm divisions.
- e) Detail of upper part of Dorchester sandy paleosol shown in section, showing development of calcrete nodules (arrowed) in the sandy matrix. Lens cap is 50 mm diameter.

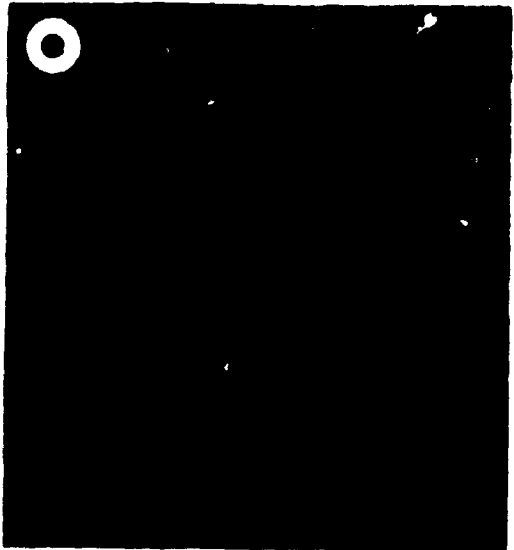
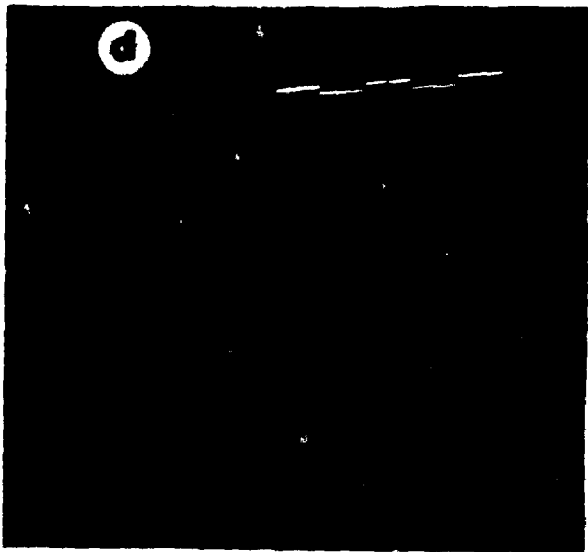
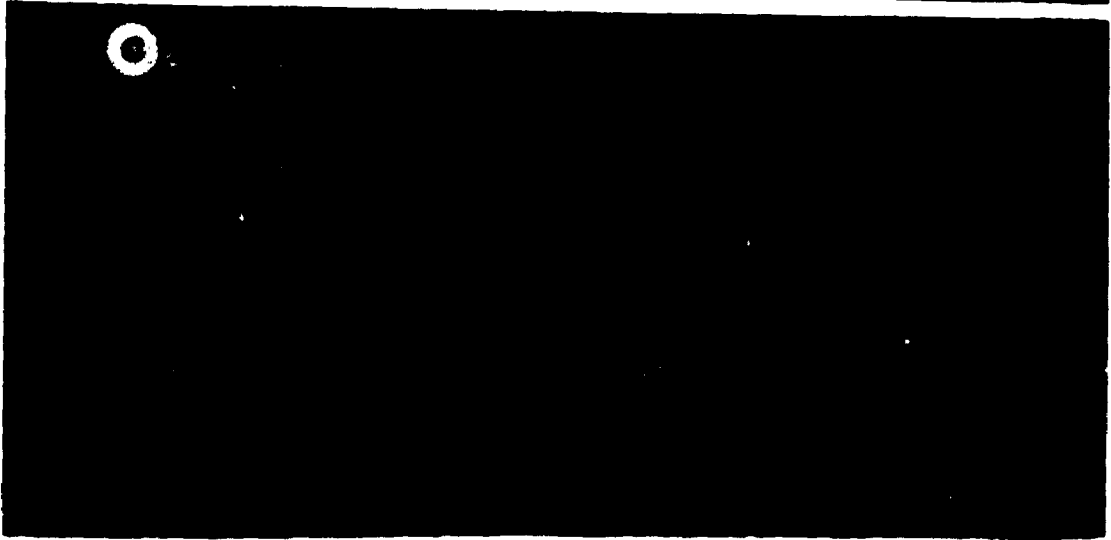
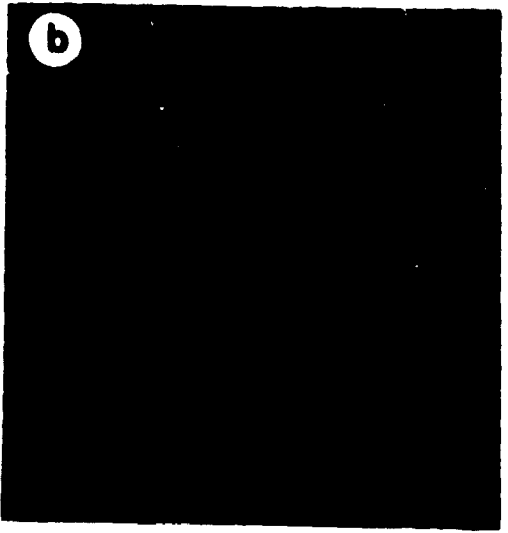


Plate 17

a) Silty paleosol near the base of the Boss Point Formation at Johnson Mills showing the increasing abundance of calcrete nodules upward (to left) through the profile. Some of the large nodules near the top are arrowed. Scale is 50 cm long with 10 cm divisions.

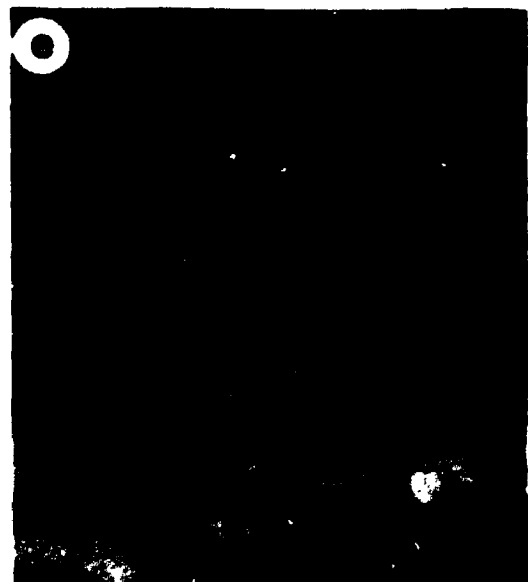
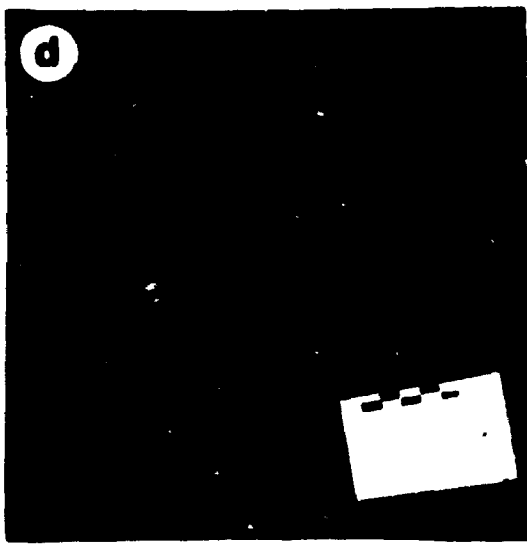
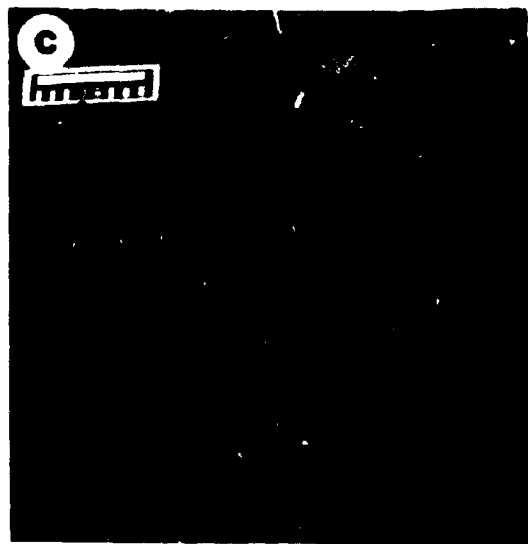
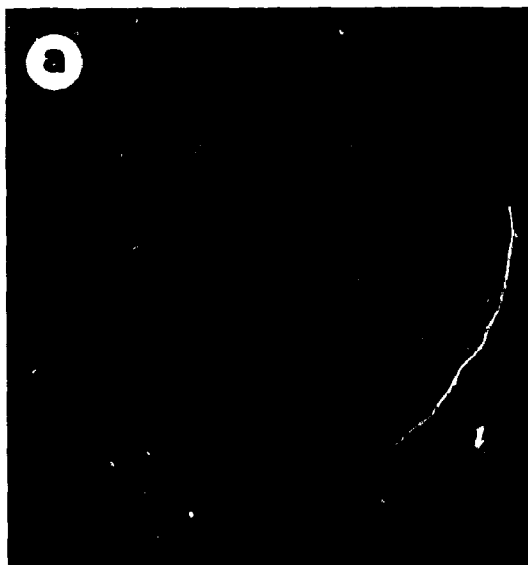
b) Detail of centimetre diameter calcrete nodules (arrowed) in the silty paleosol at Alma. View is from the side of the paleosol profile. Note the vertical cracks giving the paleosol a distinct fabric. Lens cap is 50 mm diameter.

c) Cross-section view (to left below scale) of *Stigmaria* showing the characteristic radiating system of rootlets, branching from the central root (seen in oblique view to right) - Alma section.

d) Rhizoliths (calcareous root structures) developed in a silty paleosol, Dorchester section (arrowed).

e) Low and moderate angle conjugate joints developed in a silty paleosol at Alma. Scale is 1 m with 10 cm divisions.

f) Pseudo-anticlines developed in a silty paleosol at Cape Enrage. Pseudo-anticlines occur in the lower unit (on which the scale bar rests), and is overlain by a 15 cm thick shear-zone (beneath the sandstone at the top of the photograph).



observations made on these 4 representative paleosol profiles, augmented with observations from other Boss Point Formation paleosol localities.

6.3.2 Sandy Paleosols

Sandy paleosols consist of greyish green and brown, colour mottled, calcareous and noncalcareous, well sorted, very fine- to lower medium-grained sandstones. Sandstones include massive, laminated and ripple cross-laminated textures, and may in places be bioturbated. Profile descriptions for two sandy paleosols appear in Appendix IV. Profiles are typified by the presence of nodular calcrete, usually occurring as isolated masses <5 cm diameter. Generally the calcrete glaebules are scattered throughout individual pedogenic layers, but may also be concentrated at the top of soil profiles, where they may form a dense, and almost continuous upper surface (Plate 16d & 16e). Vertical and sub-vertical calcareous tubes as much as 3 cm wide may occur within the sandstone, these being interpreted as rhizoliths (calcified root casts - also known as rhizoconcretions or rhizocretions) and are similar to those described by Klappa (1980 - for detail see section 6.4.4). Comminuted carbonaceous debris also occurs throughout the profile, which in places may also contain well preserved *Stigmaria* (Plate 17c).

At most localities profiles show subtle colour and

textural changes that typically form diffuse horizons a few cm- to dm-thick.

6.3.3 Silty Paleosols

Silty paleosols consist of grey-green and reddish purple (often colour mottled), noncalcareous, slightly sandy siltstone. Greenish coloured units tend to be slightly coarser-grained. Horizon development is not well displayed. Tan to dark reddish brown <15 cm diameter calcrete nodules occur in most profiles, (generally 2-3 cm diameter), and are disorthic (Brewer 1964) in that they possess sharp boundaries and can be easily removed from the enclosing matrix. In many cases the nodular development forms a continuum between poorly defined layers, to dense, erosion-resistant bands comprising a dense packing of calcrete nodules (Plate 16d & 16e, Plate 17b). Vertical and sub-vertical rhizoliths may occur, but tend not to be as common as in the sandy paleosols (Plate 17d). Comminuted carbonaceous debris is present, but is less abundant than in the sandy paleosols. Bioturbation tends not to be obvious in outcrop, but is apparent in thin section, and may be the cause for much of the colour mottling.

Many profiles show low- to moderate-angle conjugate shears which extend for several metres (Plate 17e). Most shears are moderate angle features with respect to the

original depositional dip, and are typically oriented at 90° to each other. Similar structures were described by Wright (1982) and Allen (1986). In recent clay-rich soils, shearing associated with clay expansion leads to the formation of slickensided shear zones at angles of 45° with respect to the surface (Fitzpatrick 1971, Yaalon and Kalmar 1978), an angular relationship that is consistent with ancient examples (Wright 1982) and to some of the observations from the Boss Point Formation.

Arcuate joints which define 3-5 m wide structures are common in the siltstone (Plate 17f), and are analogous to 'pseudo-anticlines' described by Price (1925), Allen (1974), Allen and Williams (1979), Wright (1982) and Allen (1986).

The low- and moderate-angle conjugate shears, and the pseudo-anticlines have been attributed to contraction/expansion phenomena of silty soils, related to an arid or semi-arid paleoclimate and to a montmorillonite mineralogy.

6.4 Petrology and Geochemistry

6.4.1 Petrology of Sandy Paleosols

Sandy paleosols consist of well sorted arkose and subarkose sandstone. Angular to subrounded <2 mm diameter quartz comprises 30-80% (commonly 50-60%) of the rock.

Accessory grains include feldspar (<10%), muscovite (<1%), chlorite (trace) and opaques (<10%), with the remainder of the lithology composed of ferroan calcite spar infilling intergranular spaces (Plate 18a). Circular structures up to 0.1 mm diameter, infilled with equigranular quartz and ferroan calcite are common (Plate 18b) and are interpreted as root structures or very small burrows. Carbonaceous debris is common throughout the sandstone, and is particularly concentrated around the margins of root (rhizolith) structures.

XRD analysis performed on samples from the sandy profiles at Hillsborough and Cape Enrage (Fig. 6.2) indicate that all paleosols have a mineralogy which is similar to that of mudrock units throughout the Boss Point Formation (see Chapter 5). The mineralogy of the sandy paleosols is dominated by quartz, with kaolinite, illite, and albite and muscovite as detrital components (Fig. 6.2).

6.4.2 Petrology of Silty Paleosols

Silty paleosols consist of well sorted very fine- and fine-grained sandy siltstone. Angular to rounded quartz grains, up to 0.15 mm diameter may comprise up to 50% of the rock. Accessory grains include muscovite (1-2%), biotite (1-2%), chlorite (trace to 2%), feldspar (trace) and opaques (1-2%).

XRD analysis performed on samples of silty paleosols

Plate 18

a) Photomicrograph of typical sandy paleosol - from 15 cm below the top of the Dorchester paleosol. Circular structure in centre of section (labelled "a") is a burrow. View is in cross-polarised light. Scale bar= 0.5mm.

b) Burrow structure developed within sandy paleosol - 780 m above the base of the Boss Point Formation, Johnson Mills section. View shows circular cross-section, and a portion of the elongate burrow. View is in plane polarised light. Scale bar= 0.5 mm.

c) Rhizolith consisting of micritic ferroan calcite masses rich in quartz grains, surrounded by a darker, massive, organic rich matrix. Carbonaceous material tends to be common at the outer margin of the rhizolith. Sample is from a silty paleosol, 30 m above the base of the Boss Point Formation at Johnson Mills. View is in plane polarised light. Scale bar= 0.5 mm.

d) Concentrically zoned rhizolith, Cape Enrage sandy paleosol. The majority of the calcrete consists of micritic and ferroan calcite, sometimes with <0.5 mm diameter circular structures (such as "a") which are probably rootlets/root hairs. The inner part of the rhizolith (b) is crudely circular, and contains abundant sparry ferroan calcite veins. View is in plane polarised light. Scale bar= 1 mm.

e) Detail of Plate 18d. View is in plane polarised light. Scale bar= 0.5-mm.

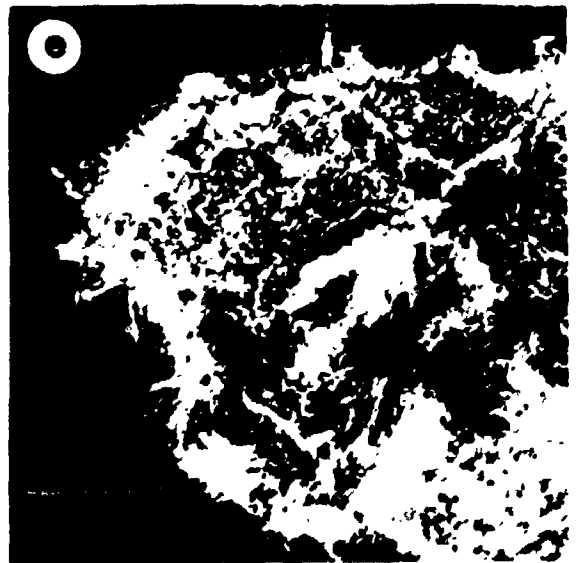
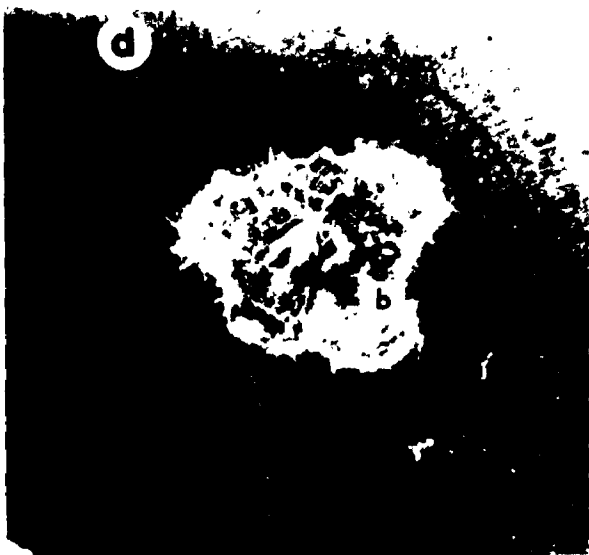
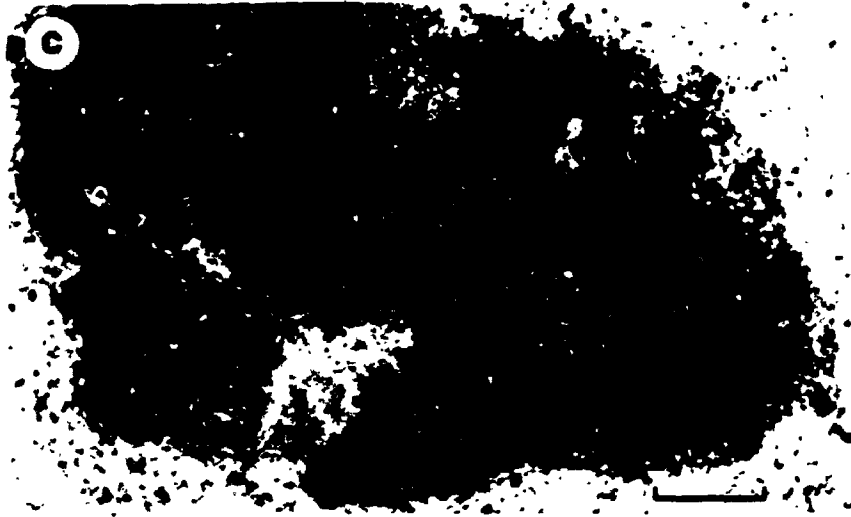
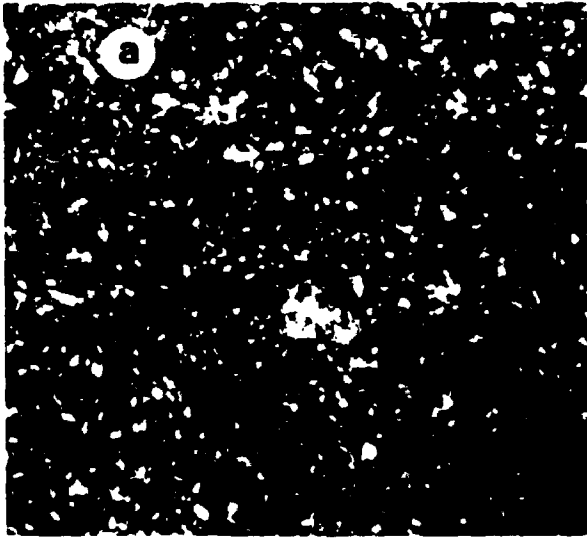
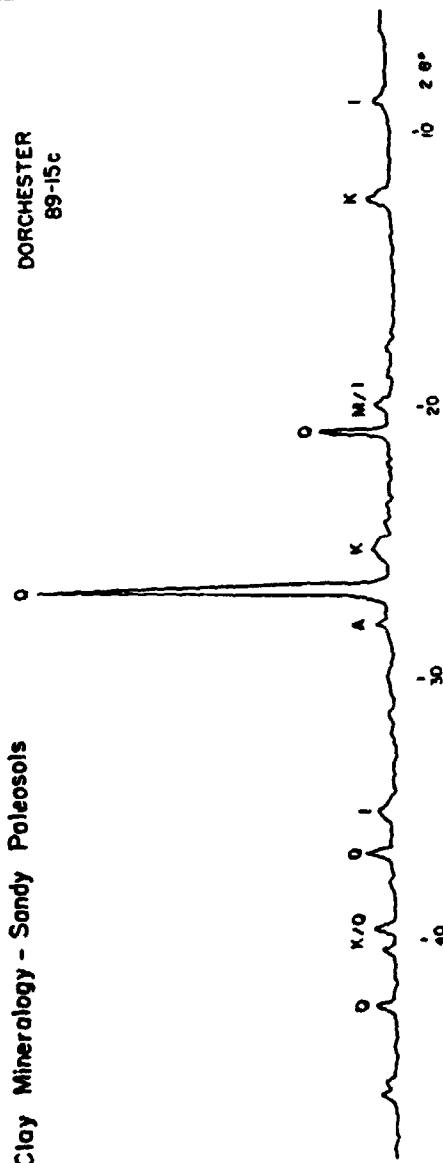


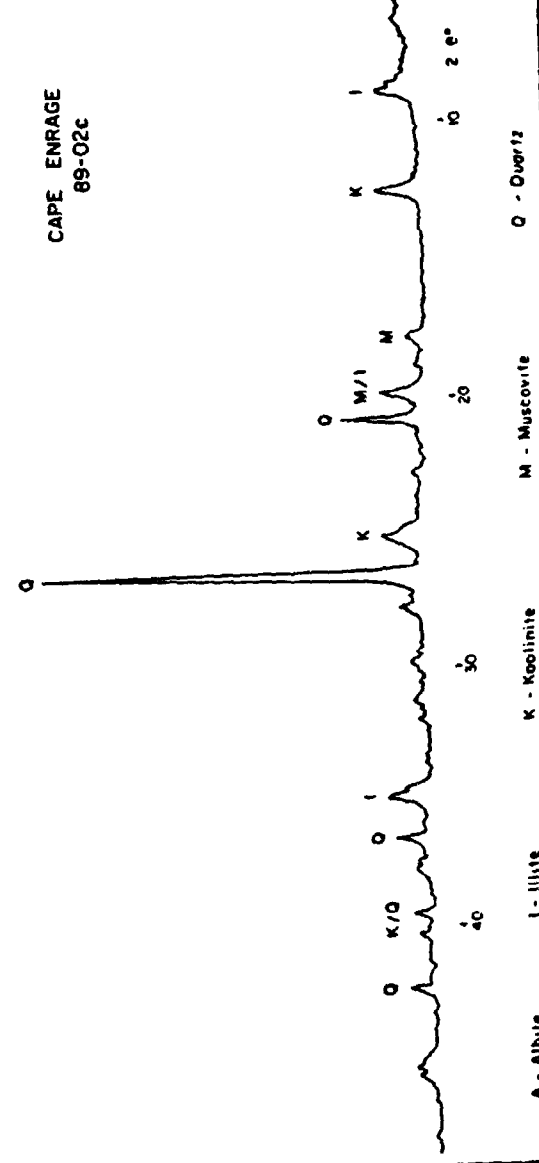
Fig. 6.2 XRD plots for 2 sandy paleosols. These samples are representative of 6 analysed samples from various stratigraphic and geographic locations. Note that the 12° two-theta peak could be a combined kaolinite/chlorite species.

Clay Mineralogy - Sandy Polesols

DORCHESTER
89-15c



CAPE ENRAGE
89-02c



from Cape Enrage and Alma (Fig. 6.3) show little compositional variation throughout the profiles, the mineralogy being similar to that of the mudrocks in the remainder of the Boss Point Formation. The mineralogy of the silty paleosols is dominated by quartz, and also contains kaolinite, illite, albite and muscovite.

6.4.3 Geochemistry of Sandy and Silty Paleosols

Samples from the sandy paleosol profiles at Dorchester and Cape Enrage (Plate 16a & 16c) and the silty paleosol profiles at Cape Enrage and Alma (Plate 16b & 16c) were analysed by XRF methods (after the methods of Norrish and Hutton 1969 for major elements and after Wu 1984 for trace elements). Both matrix material and calcrete nodules were analysed. The results of these analyses are presented in Appendices V and VI.

Silica, Alumina, Iron

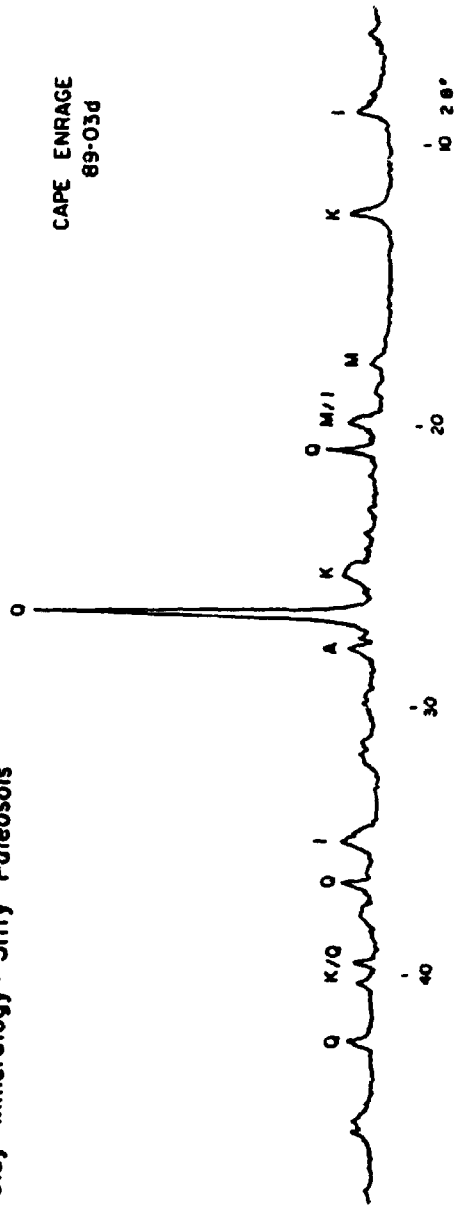
Sandy Paleosols

Silica in the sandy paleosols shows both uniform (Fig. 6.4) and slightly decreasing trends (Fig. 6.5) upward through the profile. Al_2O_3 shows uniform values throughout both paleosols, suggesting that for both these groups, there has been little in the way of Al_2O_3 alteration

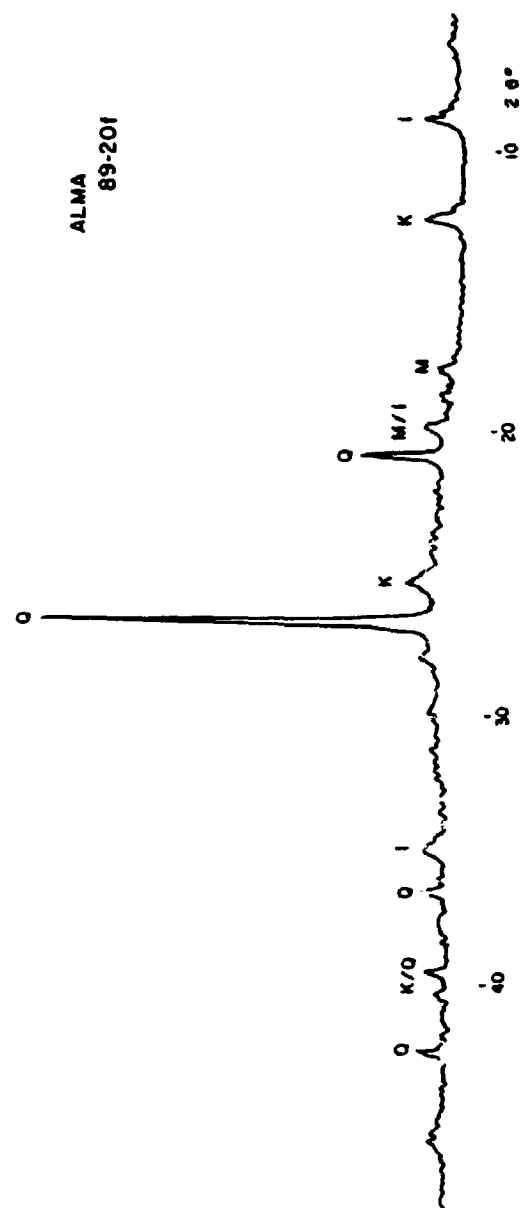
Fig. 6.3 XRD plots for 2 silty paleosols. These samples are representative of 7 analysed samples from various stratigraphic and geographic locations. Note that the 12° two-theta peak could be a combined kaolinite/chlorite species.

Cloy Mineralogy - Silty Paleosols

CAPE ENRAGE
89-03d



ALMA
89-20f



A - Albite
I - Illite
K - K-feldspar
M - Muscovite
Q - Quartz

Fig. 6.4 Variation in elemental geochemistry through the Cape Enrage sandy and silty paleosols determined by XRF.

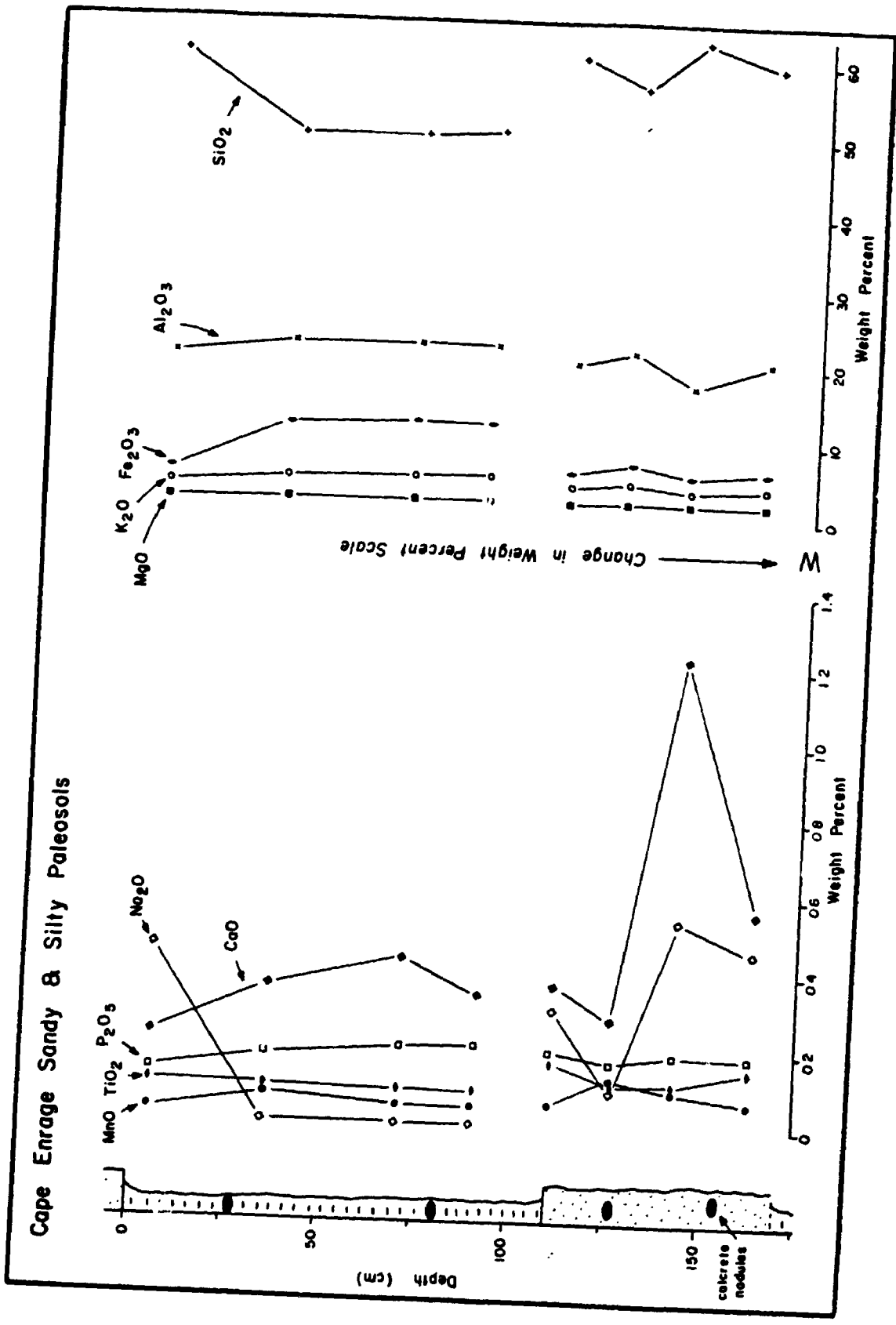
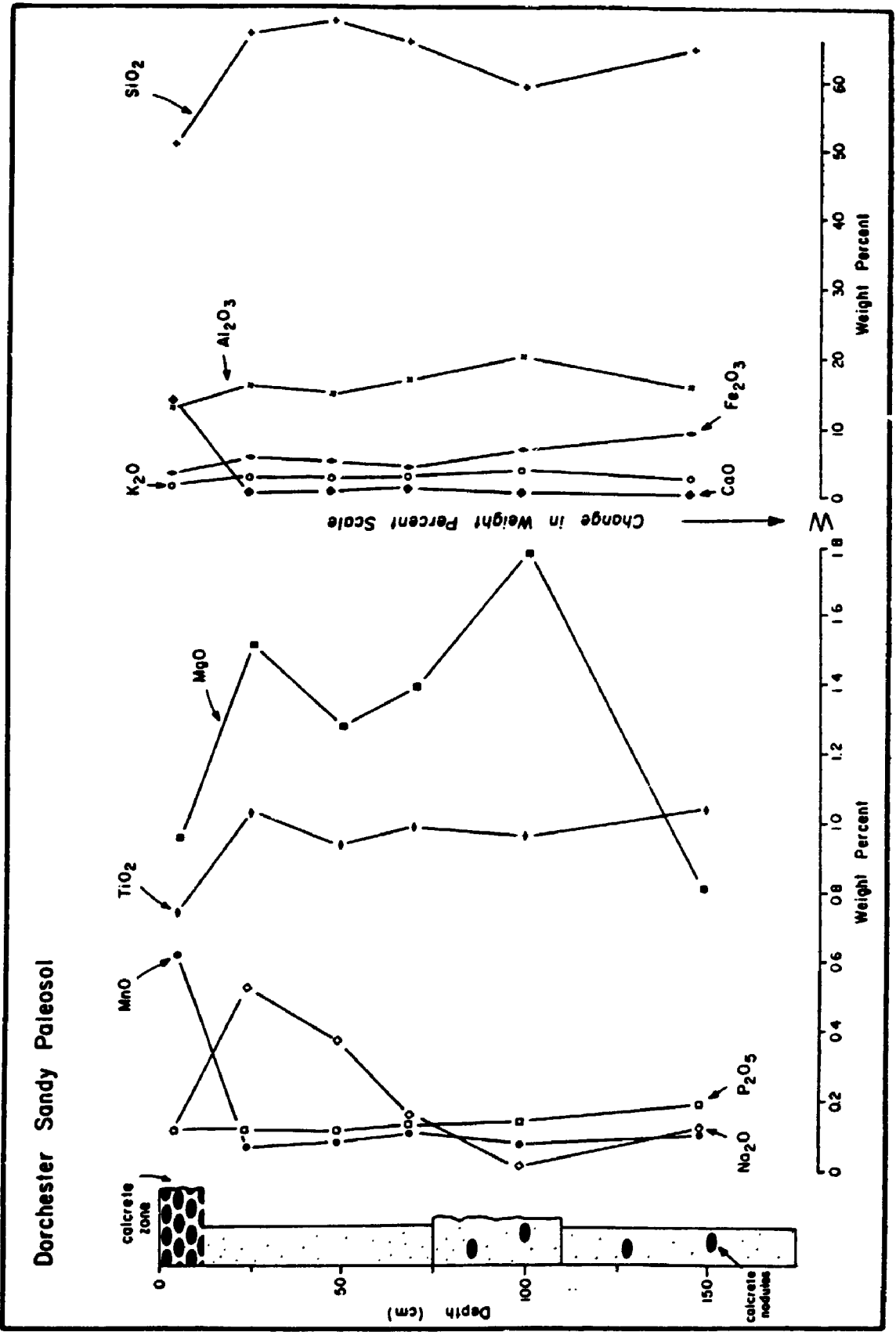


Fig. 6.5 Variation in elemental geochemistry through the
Dorchester sandy paleosol determined by XRF.



through the profile.

TiO₂ values vary little in all profiles and hence it is a useful standard against which to contrast other elemental groups. When the values are normalised with respect to TiO₂ (after Nesbitt 1979), the Dorchester paleosol shows a marked decline in SiO₂ at the top of the profile, in relation to parent materials (Fig. 6.6a). There is also a drop in Al₂O₃ toward the top of the soil profile at this locality (Fig. 6.6a), though less marked. In contrast, the Cape Enrage paleosol profile, after normalisation to TiO₂ shows slightly increasing values for both SiO₂ and Al₂O₃ through the profile (Fig. 6.6b). It should be noted that in the Dorchester profile, the decline in both SiO₂ and Al₂O₃ occurs only in the top 20 cm of the profile, values below that level showing similar levels (Fig. 6.5).

The concentration of Fe₂O₃ in both profiles closely follows that of Al₂O₃, when one increases, so does the other, and vice versa, for both absolute (Figs. 6.4 & 6.5) and normalised data (Fig. 6.6).

Silty Paleosols

Silty paleosols show an increase in SiO₂ up through the profile (Figs. 6.5 & 6.7). Al₂O₃ shows a slight increase to the top of the Alma profile (Fig. 6.7) and constant values in the Cape Enrage profile (Fig. 6.5). Normalising the same data with respect to TiO₂ indicates uniform SiO₂

Fig. 6.6 a) Variation in elemental geochemistry through the Dorchester sandy paleosol, normalised to TiO_2 .

b) Variation in elemental geochemistry through the Cape Enrage sandy and silty paleosols, normalised to TiO_2 .

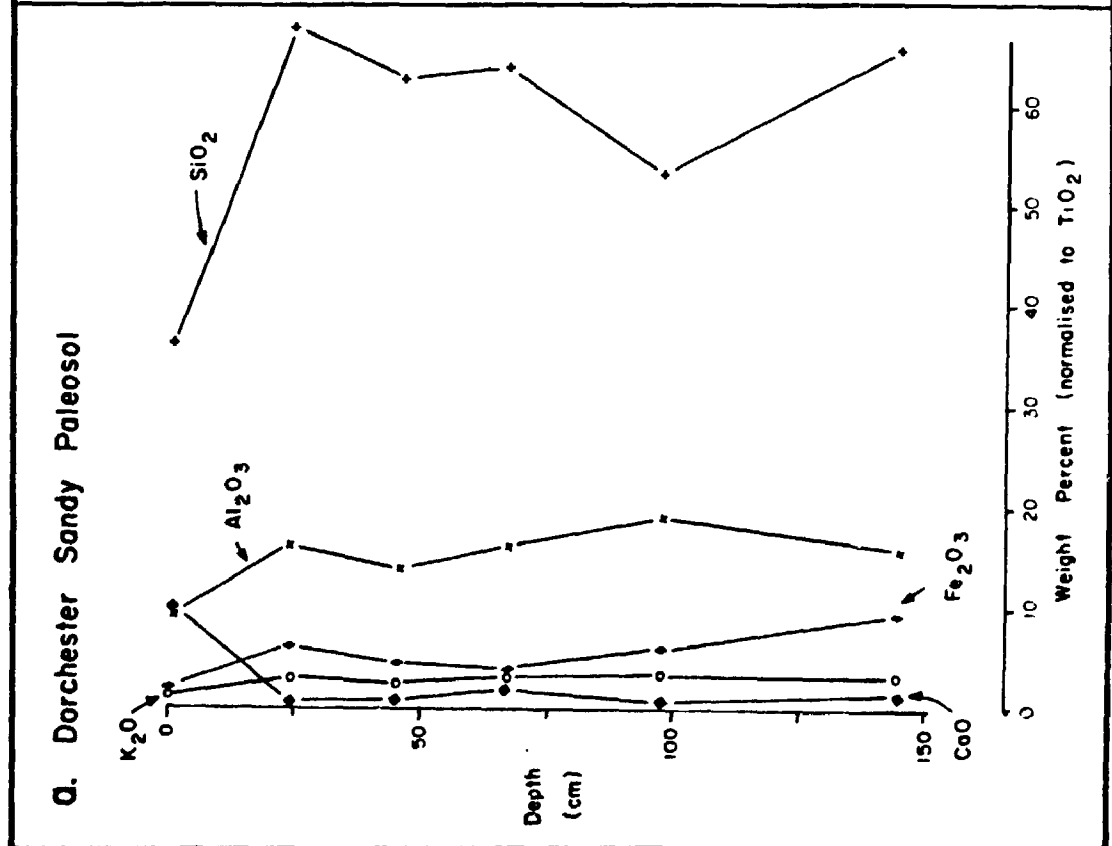
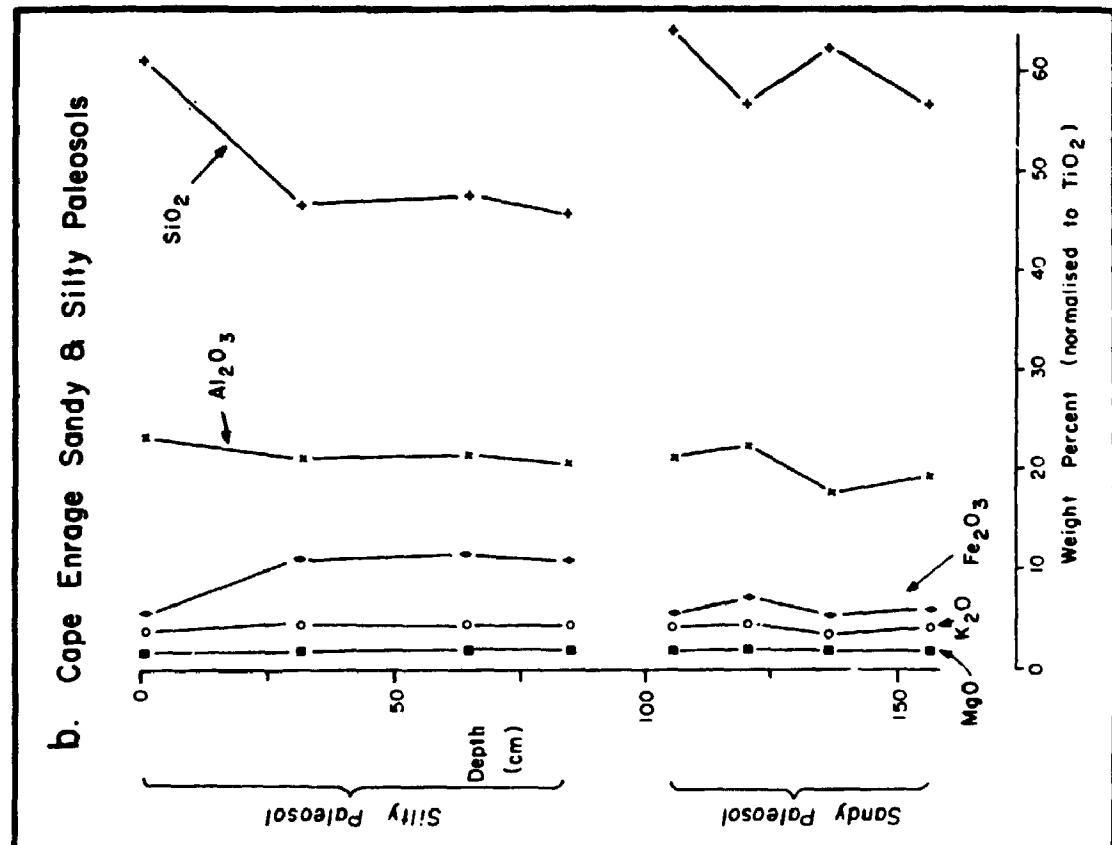
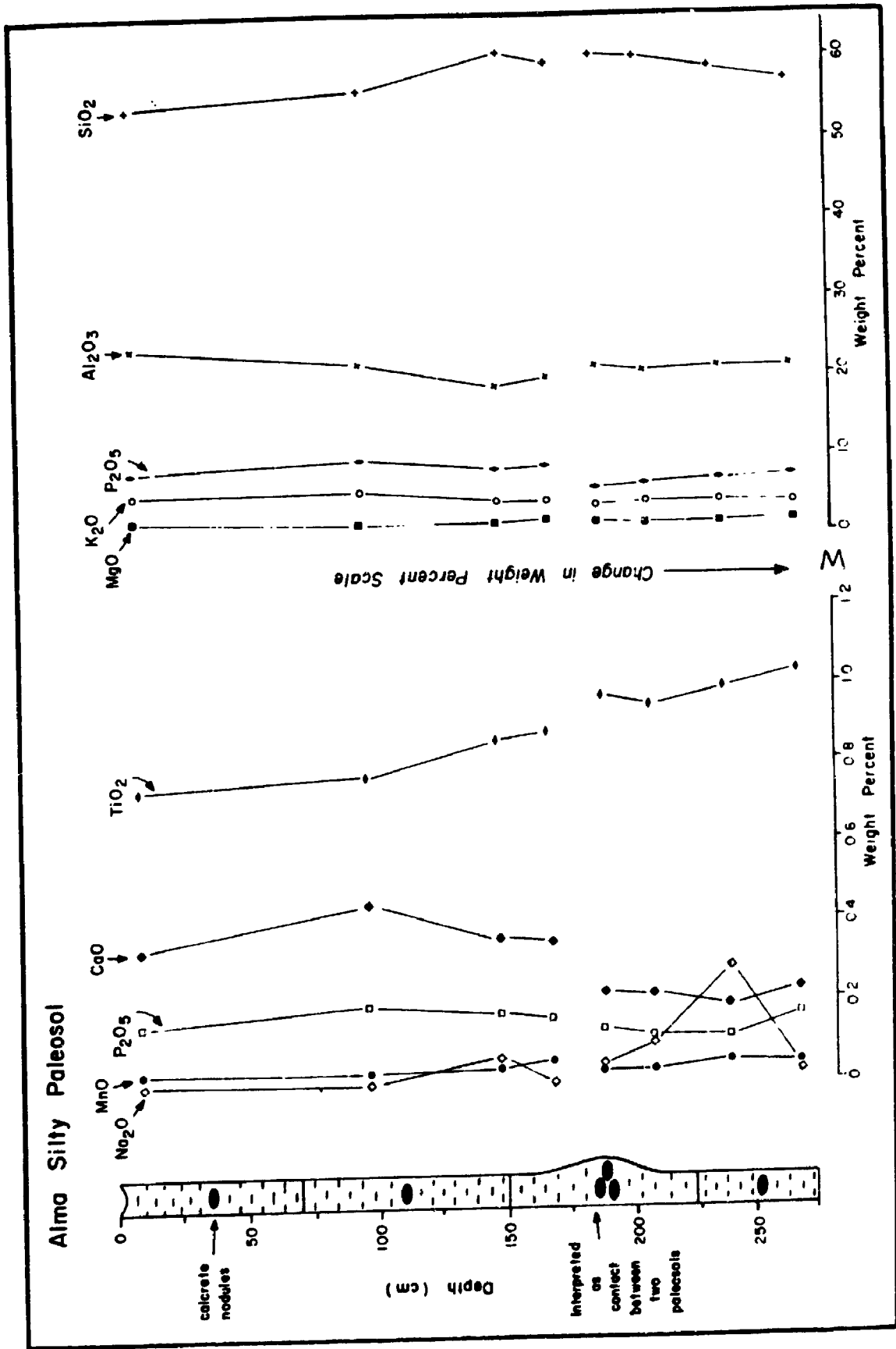


Fig. 6.7 Variation in elemental geochemistry through the Alma silty paleosol determined by XRF.



values through the Alma paleosol profile (Fig. 6.8), and an increase in SiO_2 in the other (Fig. 6.6b). Normalised data for Al_2O_3 show basically uniform levels through the profiles. As with the sandy paleosols, Fe_2O_3 mimics Al_2O_3 (Fig. 6.8), but shows a drop in abundance at the top of the Cape Enrage profile when the data is normalised to TiO_2 (Fig. 6.6b).

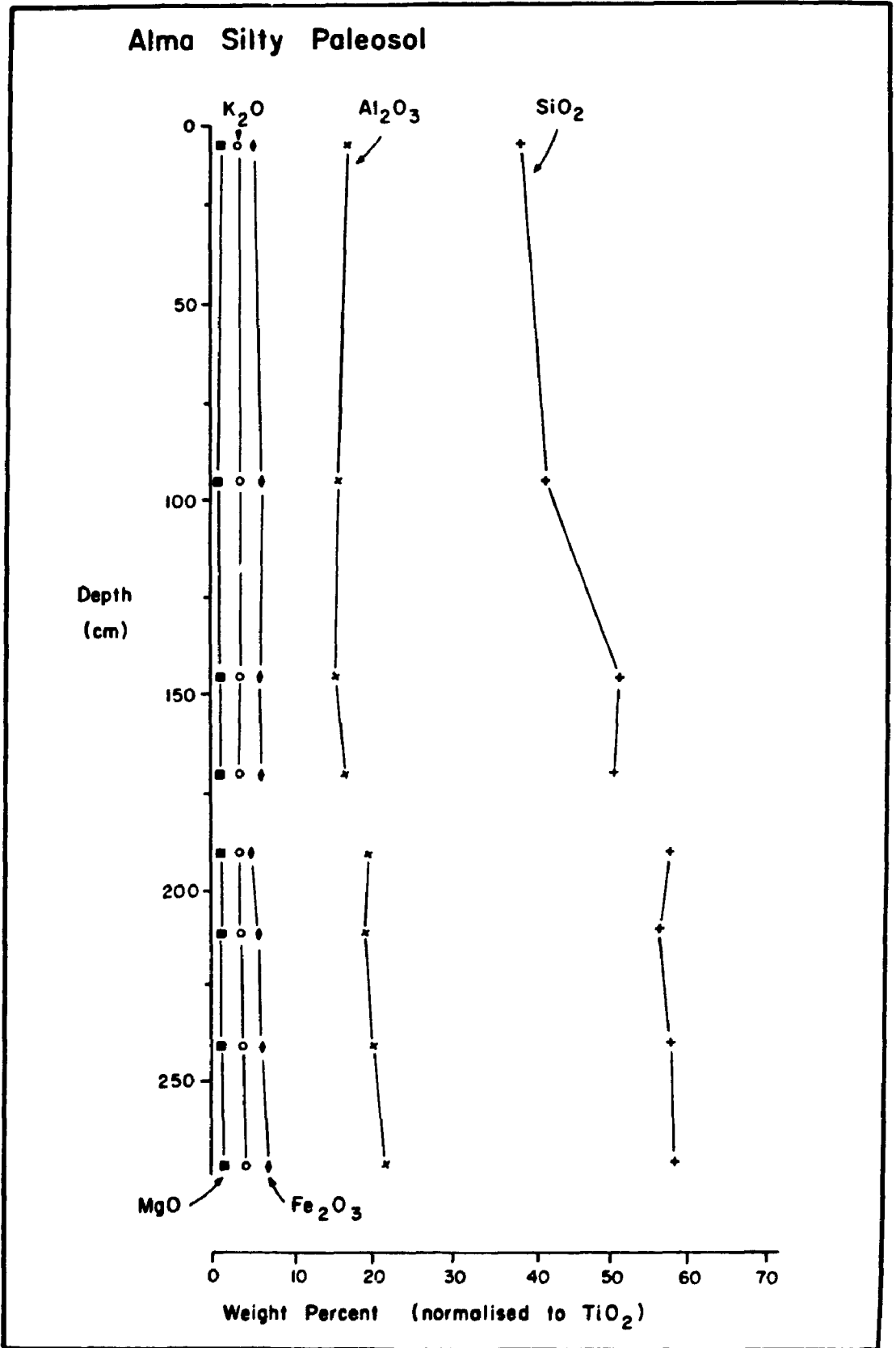
Silicification appears to have played no role in the Boss Point Formation paleosols, and indeed, evidence for silicification is absent from the entire formation. No clear up-profile decrease in silica, and up-profile increase in Al_2O_3 is evident. However, the paleosols are highly weathered because they contain high proportions of Al_2O_3 (typically in the range of 20 weight percent), the weathering most likely occurring *in situ*, although it is possible that weathering could have occurred at any period.

Alkali Elements

In sandy paleosols, K_2O shows only slight variations through the profile (Figs. 6.4 & 6.5) with a range of 3 weight percent. Na_2O shows variations of between 0.1 and 0.5%, values increasing to a maximum, 20 cm below the top of the paleosol at Dorchester (Fig. 6.5) and gradually decreasing upward through the Cape Enrage paleosol (Fig. 6.4).

In silty paleosols, K_2O values are uniform throughout

Fig. 6.8 Variation in elemental geochemistry through the Alma silty paleosol, normalised to TiO_2 .



the profile (Figs. 6.4 & 6.7). Na_2O shows highest values of 0.28 weight percent in the middle portion of the Alma profile (Fig. 6.7), and decreases steadily up profile, whereas in lower part of the Cape Enrage paleosol, values for Na_2O are uniformly 0, but increase to 0.45 weight percent at the top of the profile (Fig. 6.4). The increase in Na_2O at Cape Enrage may be attributed to physical mixing with clastic sediments during burial, as suggested for other paleosols (Kimberley and Grandstaff 1986), or to bioturbation and/or pedoturbation.

During weathering, K_2O is usually lost from the profile (particularly from feldspars). In the Boss Point Formation paleosols K_2O is constant through the profile, despite the fact that the paleosols are highly weathered, suggesting some form of homogenisation (?turbation), or alternatively that the soils were originally high in K.

Alkaline Earths

CaO shows little variation through sandy or silty paleosol profiles (Figs. 6.4, 6.5 & 6.7), calcium instead being concentrated in calcrete nodules (see below). CaO is likely to have been removed from the sandy and silty soil material at both paleosol profiles at Cape Enrage, which both show an up-profile decrease in CaO (Fig. 6.4). This trend is reversed at Dorchester (Fig. 6.5) which shows an increase from 0 to 17 weight percent CaO in the upper 20 cm

of the paleosol profile. In the Dorchester case, the density of calcrete nodules is so great that it is likely that the entire interval was calcified during formation of the calcrete nodules.

MgO values are constant in 3 of the paleosol profiles, but in the middle parts of the Dorchester paleosol, show a marked increase from 0.8 to 1.75 weight percent (Fig. 6.5).

Elements of the First Transition Series

TiO₂ shows a decrease of 30 percent toward the top of the sandy paleosol profile at Dorchester (Fig. 6.5) and slight decreases in the middle portion of the sandy paleosol at Cape Enrage (Fig. 6.4). In both silty paleosols there is a decrease in TiO₂ content toward the top of the profile (Figs. 6.4 & 6.7).

MnO is constant in most profiles, but at Dorchester shows a rapid increase from 0.04 to 0.59 weight percent in the top 20 cm of the paleosol profile (Fig. 6.5). Low MnO content is a good indicator of reducing environments, the high value recorded at the top of the Dorchester profile may indicate the intensity of oxidising conditions experienced at this locality, although Fe, which is probably removed jointly with MnO shows a decrease toward the top of the same profile.

Fe₂O₃ shows a decrease toward the top of the sandy paleosols at Dorchester (Fig. 6.5) and Cape Enrage (Fig.

6.4), an increase in the middle portions of the silty profile at Cape Enrage (Fig. 6.4) and a decrease upward through the profile at Alma (Fig. 6.7). The Fe loss may have resulted from groundwater activity.

Trace Elements

The trace element composition for 9 samples from the Dorchester sandy paleosol, and the Cape Enrage silty paleosol were analysed by XRF, and the results are presented in Appendix VI.

Trace elemental trends for Rb, Sr and Ba show the same basic trends; a marked decline up the paleosol profile in the sandy Dorchester paleosol (Fig. 6.9), and a general decrease upward in the silty Cape Enrage paleosol (Fig. 6.9). However the uppermost sample in both sandy and silty paleosols shows an increase in Ba, Sr and Rb (though Rb in the sandy Dorchester paleosol does not). These trace elements may be concentrated in those parts of the profile with the greatest quantity of clays (as suggested by Nesbitt et al. 1980). The marked increase in the concentration of these trace elements at the top of the paleosol may also relate to surface runoff. Nesbitt et al. (1980) for example concluded that Sr is easily transported in solution from the weathering site. Weathering of Na-feldspar, the original source, may explain the decrease in Sr up-profile (Sawyer 1986).

Fig. 6.9 Variation in Rb, Sr and Ba through the
Dorchester sandy and Cape Enrage silty
paleosols.

Fig. 6.10 Variation in Cu, Ni and Zn through the
Dorchester sandy and Cape Enrage silty
paleosols.

Fig. 6.9

Cape Enrage Silty Paleosol

Dorchester Sandy Paleosol

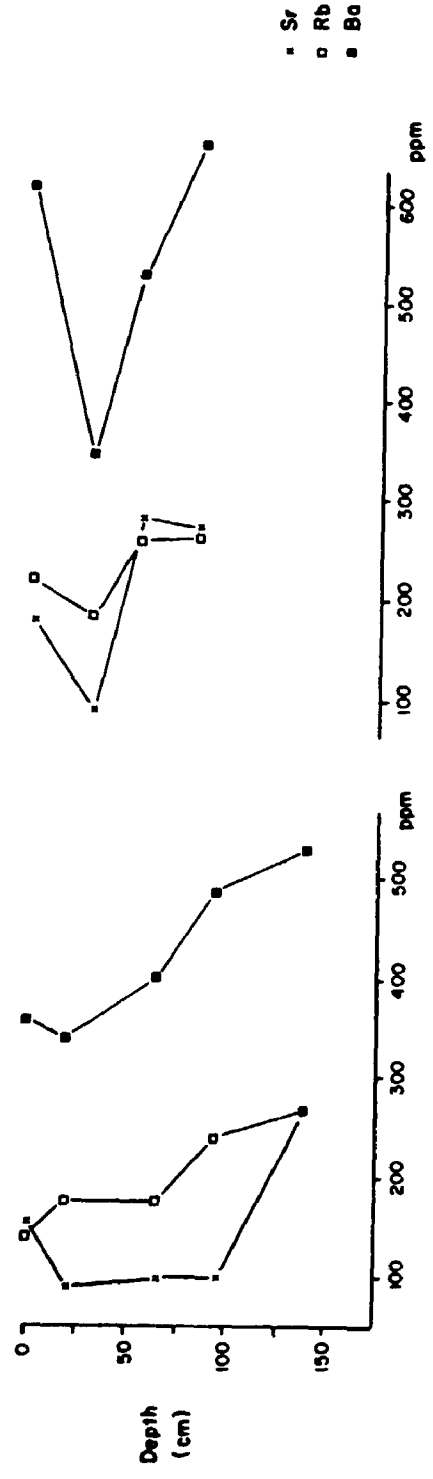
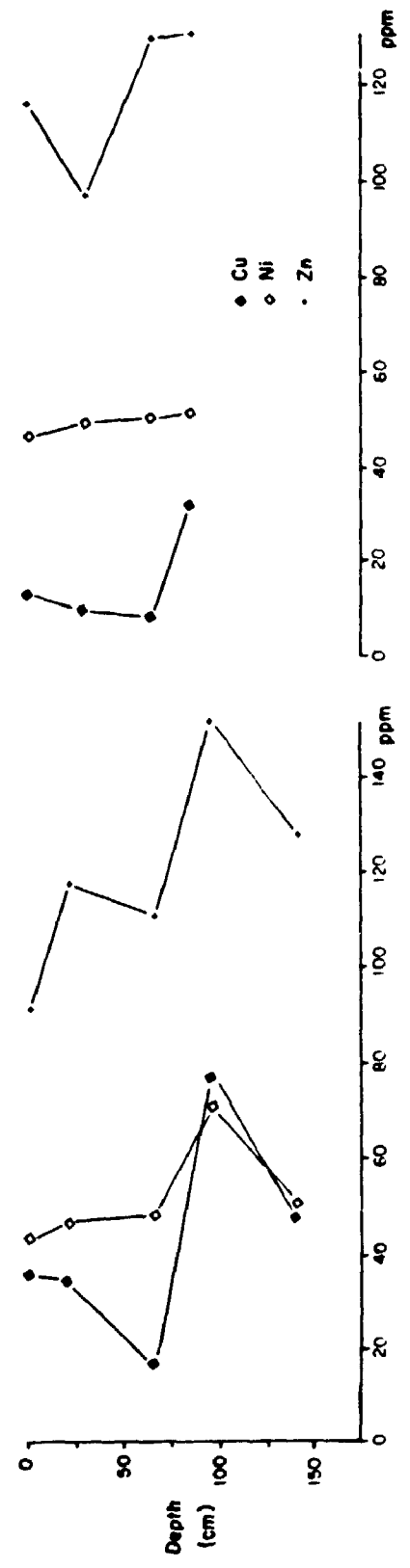


Fig. 6.10

Cape Enrage Silty Paleosol

Dorchester Sandy Paleosol



Trends for Cu, Ni and Zn also show a general upward decrease through the paleosol profiles (Fig. 6.10). Trends in the sandy Dorchester paleosol show high values for each of these 3 elements at a depth of 95 cm below the top of the profile (Fig. 6.10). Relationships in the silty Cape Enrage paleosol are less clear. Although there is a general decrease in Cu, Ni and Zn up-profile, only Ni shows a consistent decline (Fig. 6.10). Cu and Zn both show an increase in elemental concentration in the upper part of the paleosol profile. These decreasing trends are probably related to the degree of oxidation, in view of the adsorption of these elements by ferric hydroxides (Gay and Grandstaff 1980).

Both Pb and Ga in sandy and silty paleosols show a general decrease up-profile; Ga in both samples shows a decrease through the majority of the profile, but the concentration in the upper-most sample is very high (Fig. 6.11).

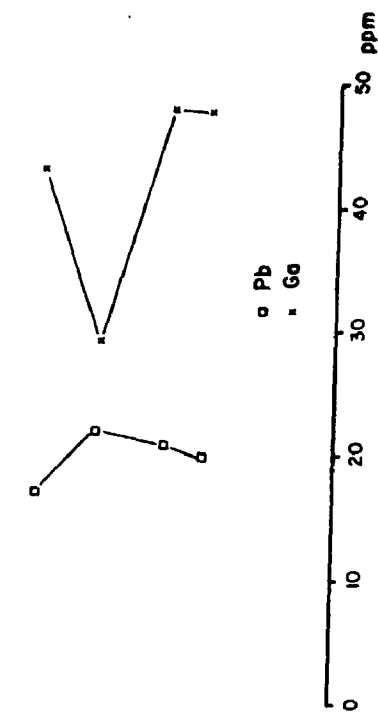
The heavy metals Nb, Zr and Y show less consistent trends (Fig. 6.12). Both Zr and Y show similar trends; a general increase up-profile, with maximum levels at approximately 50 cm below the top of the sandy and silty profiles. Nb shows an upward decrease in the sandy paleosol at Dorchester, and an upward increase in the silty paleosol. These variable trends may relate to uptake of these metals by plants, especially the high concentrations at 50 cm below the top of the profiles (uptake by roots).

Fig. 6.11 Variation in Pb and Ga through the Dorchester sandy and Cape Enrage silty paleosols.

Fig. 6.12 Variation in Nb, Zr and Y through the Dorchester sandy and Cape Enrage silty paleosols.

Fig. 6.11

Cape Enrage Silty Paleosol



Dorchester Sandy Paleosol

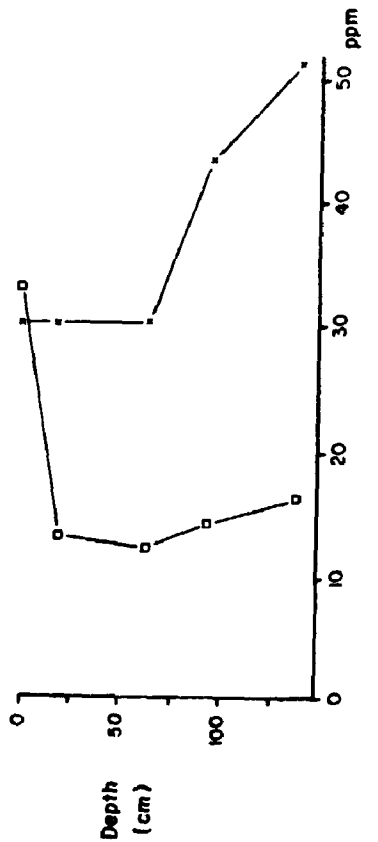
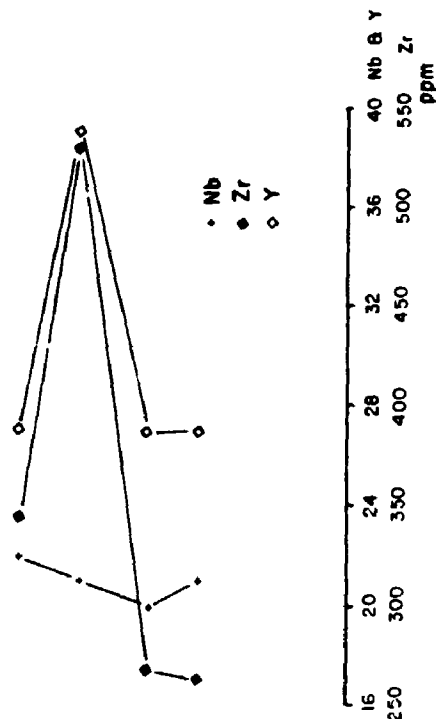
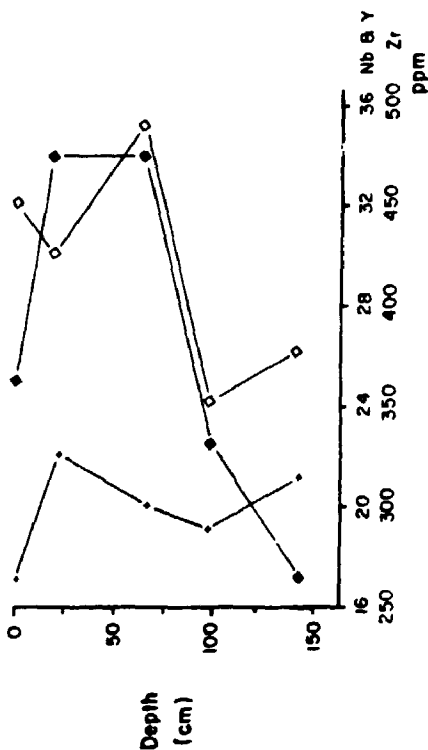


Fig. 6.12

Cape Enrage Silty Paleosol



Dorchester Sandy Paleosol



Co and V show similar trends in both the sandy and silty paleosol (Fig. 6.13), showing an overall decrease up-profile, but with significant high concentrations in the middle portions of the profiles, especially in the case of the sandy Dorchester paleosol. Again this may relate to uptake by roots. Cr trends increase in both profiles (Fig. 6.13), with a general decrease in the upper portions of both paleosols.

Chemical Index of Alteration (CIA)

The CIA is a measure of the degree of weathering using molecular proportions:

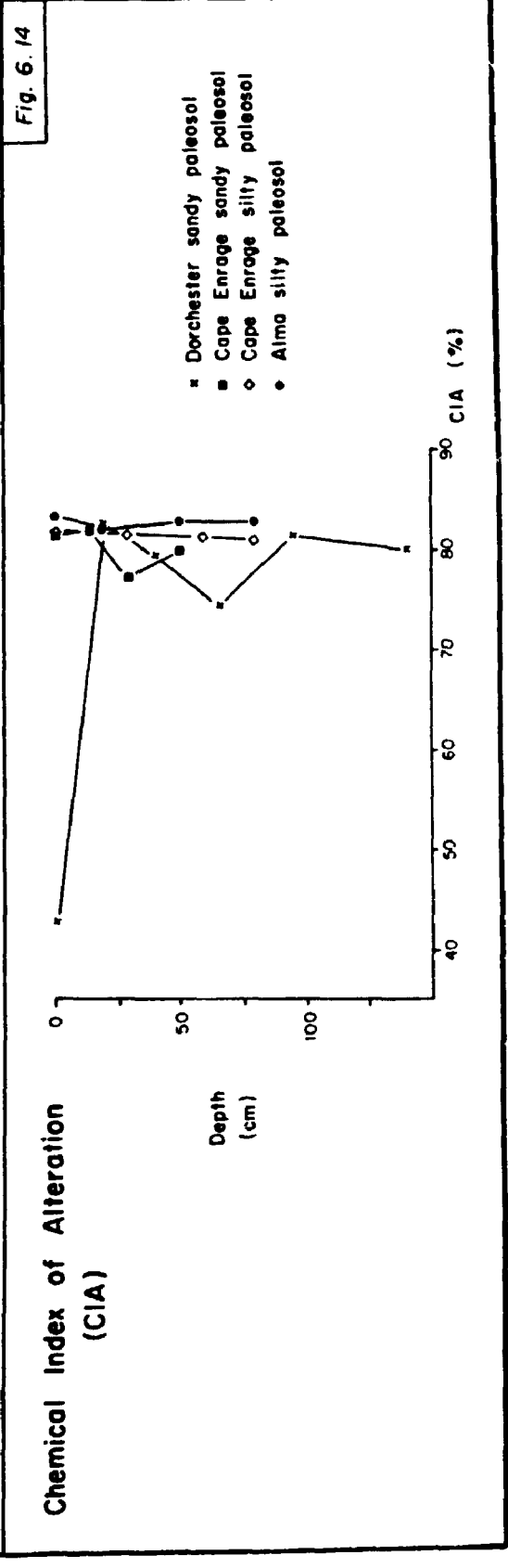
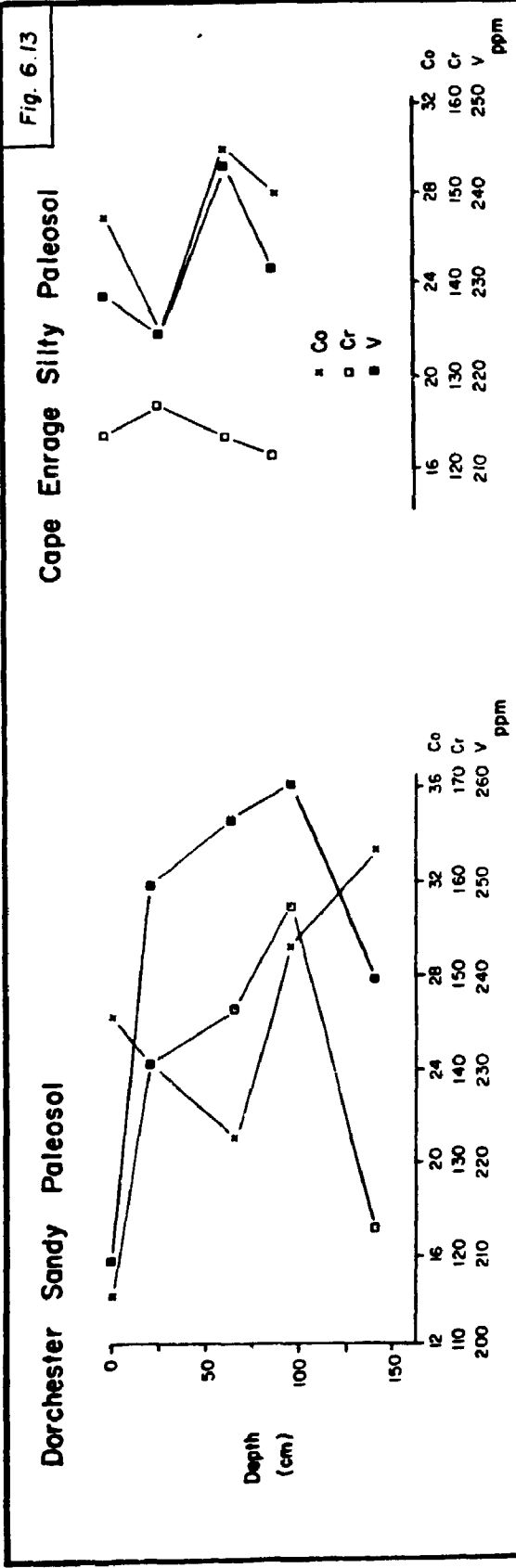
$$\text{CIA} = [\text{Al}_2\text{O}_3 / (\text{Al}_2\text{O}_3 + \text{CaO} + \text{Na}_2\text{O} + \text{K}_2\text{O})] \times 100$$

The resultant value gives the proportion of Al_2O_3 in relation to the labile oxides in the analysed sample. Low values (such as 70%) indicate a lack of weathering, whereas high values (such as 100%) indicate considerable weathering (Nesbitt and Young 1982, 1989). A correction factor has to be made for carbonate, but in the Boss Point Formation examples, all but one sample contains sufficiently low quantities of carbonate, such that the above formula needs no modification.

All the Boss Point Formation paleosols show CIA values that are consistently in the range 74 to 83% (Fig. 6.14;

Fig. 6.13 Variation in Co, V and Cr through the Dorchester sandy and Cape Enrage silty paleosols.

Fig. 6.14 Chemical Index of Alteration (CIA) determinations for Boss Point Formation paleosols.



Appendix V). The one sample from the top of the Dorchester profile (sample 89-15A) which plots outside this range contains abundant calcrete nodules and has a CaO content of 13 weight percent and hence is not meaningful (for the above reasons).

6.4.4 Petrography of Calcrete Nodules

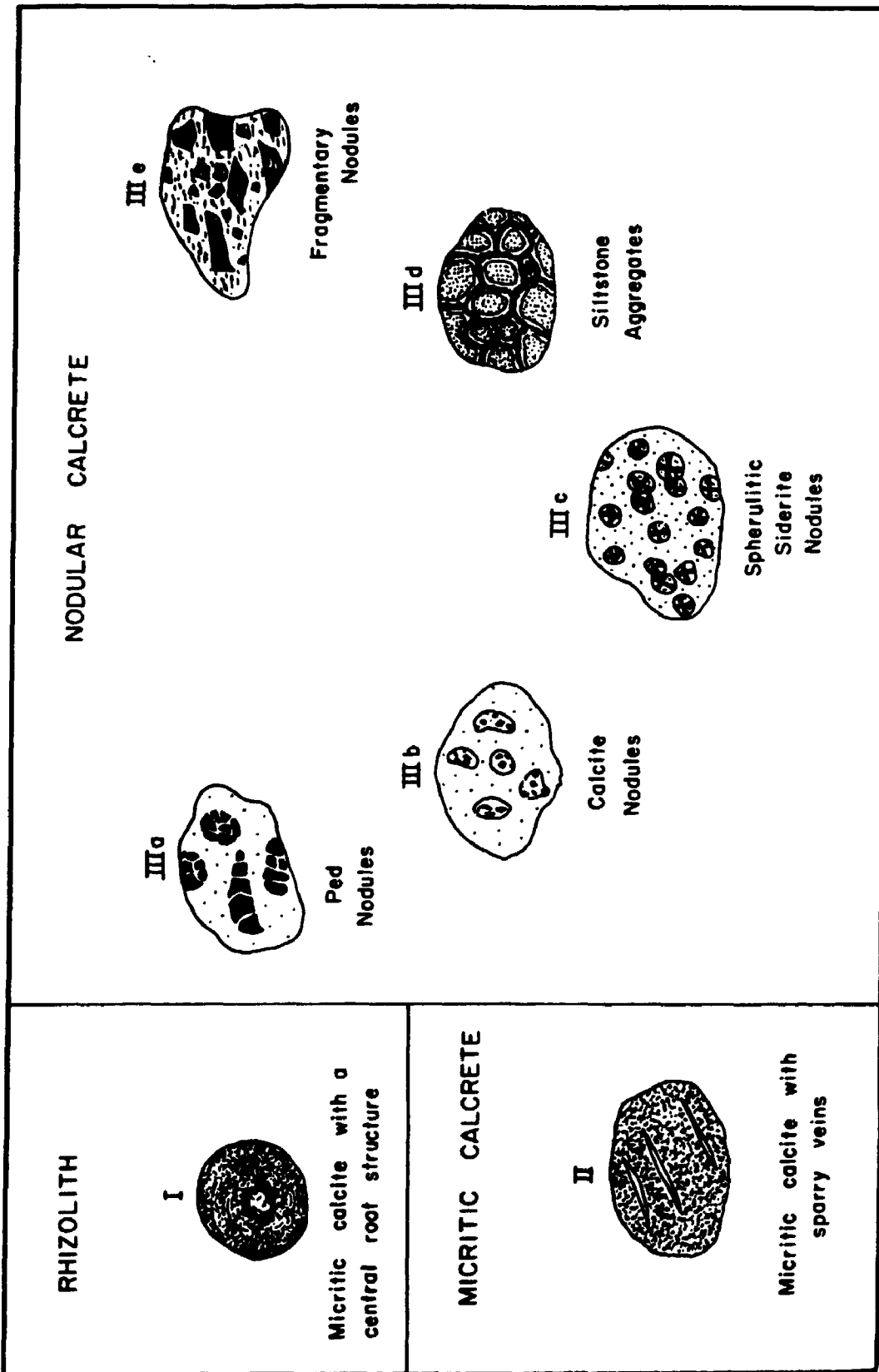
Calcretes occur in both sandy and silty paleosols. Three morphologies are recognised: I) rhizoliths II) micritic and III) nodular and these forms are summarised in Fig. 6.15.

I) *Rhizoliths*

Rhizoliths up to 1.5 cm diameter consist of two basic morphologies - a) comprising irregularly-shaped, poorly defined micritic ferroan calcite masses rich in detrital quartz, and surrounded by a darker, ?organic-rich massive matrix (Plate 18c) and, b) concentrically-zoned rhizoliths (Plate 18d & 18e).

The zoned rhizoliths consist of two main zones, clearly differentiated petrographically. The outer 70% of the structure comprises a crude concentrically banded micritic calcite and ferroan calcite, opaque spherical grains up to 30 um diameter, and rare quartz (Plate 18d & 18e). Small tubules <1 mm diameter, marked by a brown altered margin

Fig. 6.15 Major morphologic calcrete types recognised from the Boss Point Formation. Drawn as if seen petrographically. No scale implied.



are common throughout the micrite, and probably represent small roots or root hairs (cf. Jones and Kwok-Choi Ng 1988, p. 459). Sparry ferroan calcite veins, less than 30 μm wide are common in the micritic outer region. The central region of the rhizolith (<3 mm wide) consists of a cylindrical structure, with abundant <1 mm wide sparry ferroan calcite veins, together with <0.10 μm diameter calcitic micrite and spherical micritic pellets (Plate 18e). The boundary between the outer micritic region and the inner vein-rich zone is clearly differentiated by a medium brown coloured alteration rind.

The rhizolith zonation is interpreted to represent the original root structure; the central region representing the original root material, that would have been an open tube, subsequently infilled with vein material; the outer sheath of micrite forming about this. The concentric nature of the outer sheath is similar to that described from recent rhizoliths (eg. Semeniuk and Meagher 1981). The 2-fold zonation is analogous to zone 2 (micrite) and zone 1 (root) rhizoliths described from the Recent of the British West Indies by Jones and Kwok-Choi Ng (1988, fig. 3). Jones and Kwok-Choi Ng (1988) also describe calcified spherical bodies (which they interpreted as fungal spores or bacteria), and these may be represented in the Boss Point Formation examples by the small spherical pellets observed in both the inner and outer zones of the rhizoliths (Plate 18e).

Analysis by electron microprobe of the region in the upper right of Plate 18e, indicates that these spherical bodies consist of morphologically similar concentrically zoned dolomite, calcite and siderite (Plate 19a & 19b). Representative analyses are presented in Appendix VII. The concentric zonation appears to consist of alternating carbonate and carbonaceous layers, although the latter was plucked during thin section preparation and could therefore not be analysed. Each of the carbonate phases are surrounded by later formed siderite, as much as a few micrometres thick (Plate 19a & 19b). Material surrounding the carbonates consists of clay and dolomite (Plates 19a & 19b).

II) Micritic Calcrete

Micritic calcretes are composed of microcrystalline calcite and <50 um diameter detrital quartz grains, and lack any texture (Plate 19c). Occasional veins or crystallaria as much as 30 um wide cut the nodules, and display at least two (sometimes three) phases of sparry carbonate infill (Plate 19d).

III) Nodular Calcrete

The more common and interesting calcrete nodules consist of nodular material. Five morphologies are

Plate 19

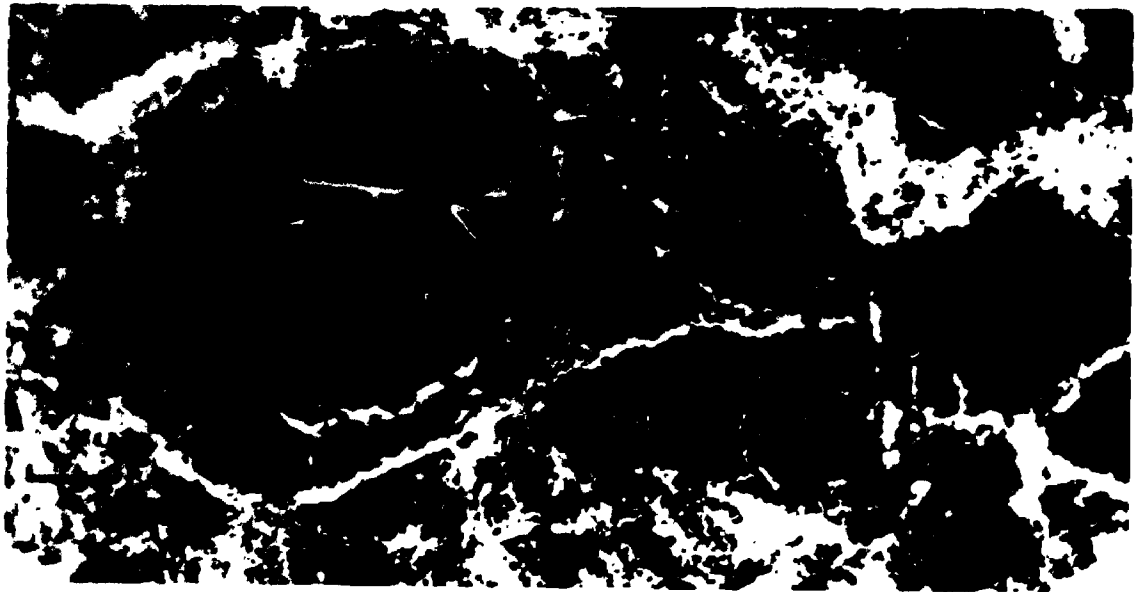
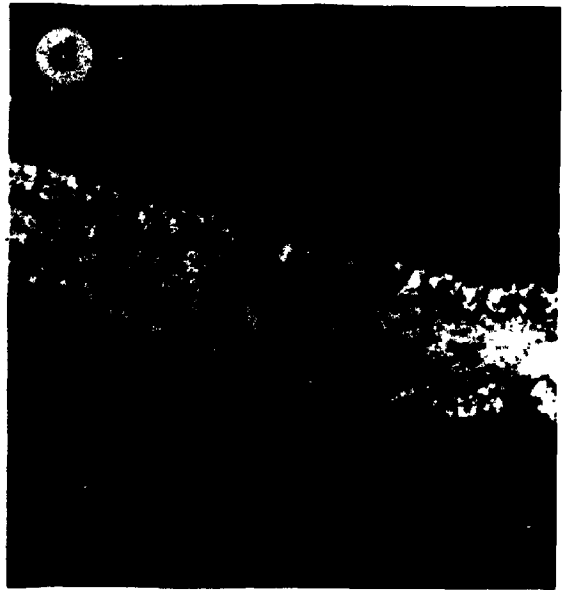
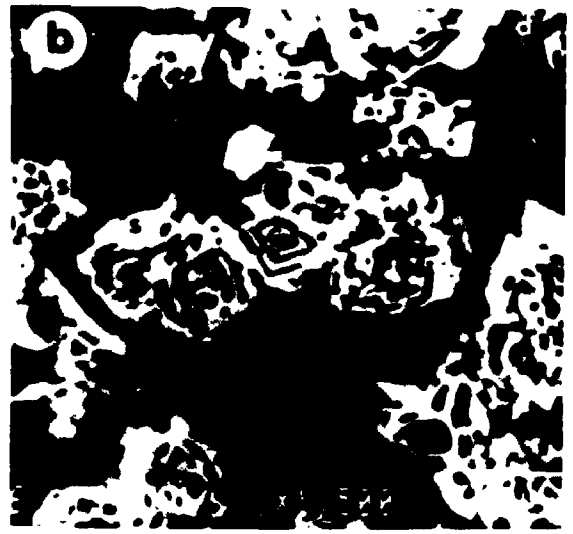
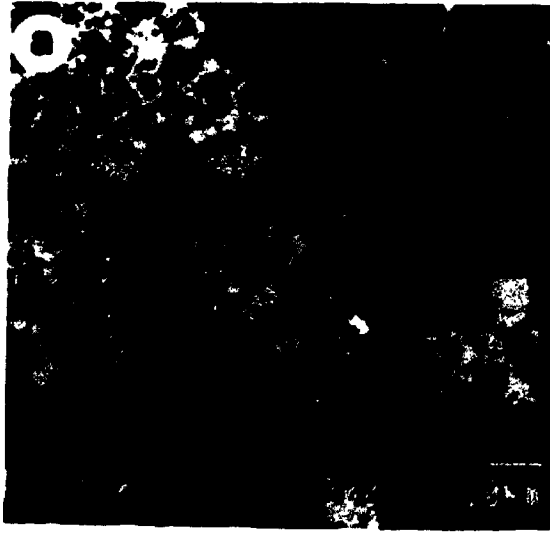
a) Electron microprobe image of carbonate nodules within the central root structure of the rhizolith shown in Plate 18e. Concentrically zoned dolomite nodules surrounded by siderite (s) are enclosed within a matrix of (dark) clay (c) and grey dolomite (dol).

b) Electron microprobe image of carbonate nodules within the central root structure of the rhizolith shown in Plate 18e. Concentrically zoned siderite (s) and calcite (c) surrounded by siderite are enclosed within a matrix of dark clay (cl) and grey dolomite (d).

c) Micritic calcrete nodule (arrowed) composed of microcrystalline calcite, from a sandy paleosol, 760 m above the base of the Boss Point Formation, Johnson Mills. View is in plane polarised light. Scale bar= 1 mm.

d) Sparry vein occurring within micritic calcrete, from the Cape Enrage silty paleosol. Fine, equigranular spar (a) is pink (calcite), the thinner interior zone (b) is blue (ferroan calcite), the central large equigranular area (c) is red (calcite) - determinations made from stained sample (see text). View is in plane polarised light. Scale bar= 0.25 mm.

e) Ped material from Alma silty paleosol. Ped material is black and dark brown and essentially homogeneous (crystic plasmic fabric - see text); small white grains are quartz (qz), with abundant calcite spar veins cutting and enclosing the peds. View is in-plane polarised light. Scale bar= 0.25 mm.



recognised (Fig. 6.15);

- ped nodules
- sparry calcite nodules
- spherulitic siderite nodules
- siltstone aggregates
- fragmentary nodules

These morphologies are not mutually exclusive; several morphologies may appear in the same nodule.

A. Ped Nodules

The term ped is used in the sense of Brewer (1964) and Joeckel (1989) for individual soil aggregates, represented petrographically as dark grey and dark brown, homogenous, fine-grained crystic plasmic fabric (Brewer 1964, Wright 1982). These calcretes show a large petrographic variability. Angular to subrounded quartz (up to 85 μm diameter) is common throughout the nodules, quartz forming as much as 5-30% of the ped material (Plate 19e). Typically the ped nodules are cut by <1 mm wide, irregular and concentrically oriented sparry veins (Plate 19e). Nodules are surrounded by equigranular and drusy textured sparry veins (Plate 20a), and it is consistent for these contain 2-3 phases of carbonate; an outer calcite layer along the walls of the veins, and ferroan calcite in the central parts of the veins (Plate 20b). The outer margin of the veins may be marked by a thin (<15 μm thick), light brown (in plane polarised light) alteration product.

Ped nodules are interpreted as original ped aggregates

Plate 20

a) Drusy textured calcite spar infilling pore space around ped material (seen at left) - Alma silty paleosol. View is in cross-polarised light. Scale bar= 0.5 mm.

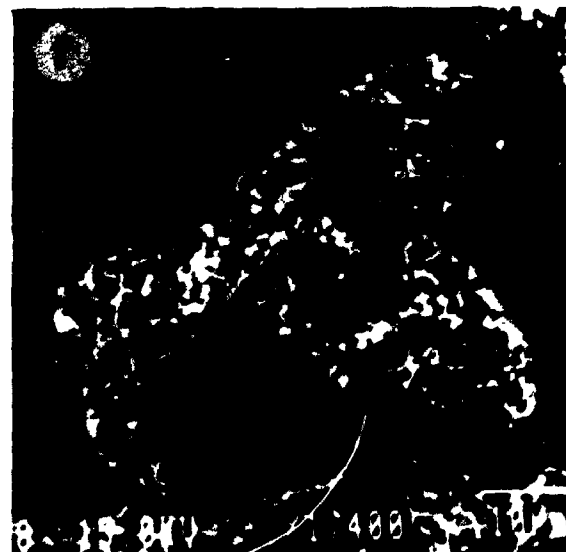
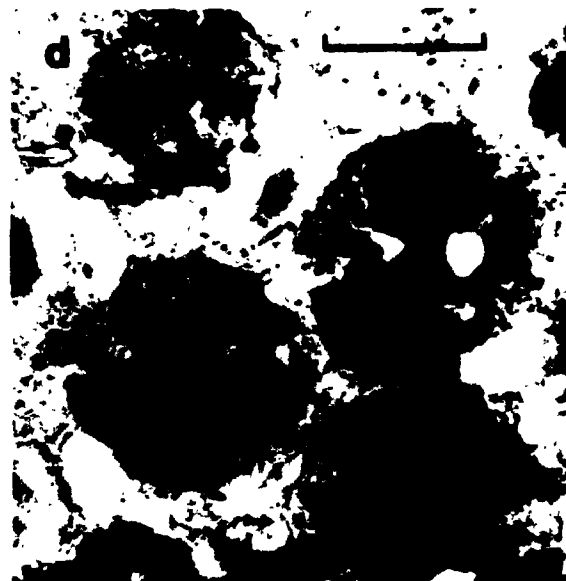
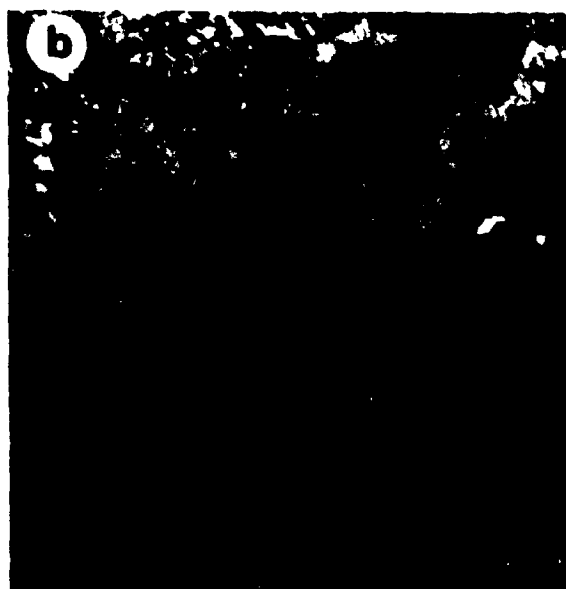
b) Phases of sparry calcite infilling a pore space in the silty paleosol at Alma. Staining indicates that the first carbonate phase (a) was calcite, followed by ferroan calcite (b) and lastly by calcite (c) in the central portions of the pore. View is in plane polarised light. Scale bar= 0.5 mm.

c) Sparry calcite calcrete nodule, Alma silty paleosol. The nodule consists of an interior section of microsparry calcite, quartz and ped material (a), surrounded by equigranular radially oriented microsparry calcite (b). View is in plane polarised light. Scale bar= 0.5 mm.

d) Spherulitic siderite nodules showing typical radial extinction patterns and inclusions of quartz grains. Spherulites occur both as distinct grains or may coalesce (as at bottom left), and are surrounded by a very fine-grained sandy siltstone matrix. Dark coloured ferroan calcite (c) can be clearly differentiated from lighter colored siderite (sid). Sample is from the silty paleosol at Alma. View is in plane polarised light. Scale bar= 0.2 mm.

e) Electron microprobe image of spherulitic siderite nodule from Alma. The majority of the nodule consists of light coloured Mn-rich siderite (sid), with several grey coloured, radial zones of ferroan calcite (c). Black material is quartz (q); white material is polish. The nodule is surrounded by black K-rich clays (?illite) and detrital quartz, and by grey Fe-rich clays (?smectite)

f) Electron microprobe image of spherulitic siderite nodule. View is from upper centre in Plate 20e. Grey coloured zones are Mn-rich siderite (sid); black areas are radial sectors of ferroan calcite (cal).



that have been cut by latter diagenetic sparry crystallaria and are similar to morphologies described by McPherson (1979), Wright (1982) and Atkinson (1986).

B. Sparry Calcite Nodules

A second rare calcrete morphology, consists of orbicular nodules as much as 1 mm diameter composed of microsparry calcite and ped material, containing between 5-20% angular to sub-rounded, medium silt-sized quartz grains (Plate 20c). The spar may be arranged in radial fashion, though this is not typically the case. The outer margin of these sparry calcite nodules is typically an equigranular, radially-oriented microsparry calcite, which forms a rind up to 80 μm thick around the nodules.

Sparry calcite nodules are not easily interpreted. They may represent replacement features of earlier formed hydrous minerals (with radial habit) such as gypsum, subsequently replaced by CaCO_3 , but they are more likely to be a calcareous variant of the ped nodules described above

C. Spherulitic Siderite Nodules

Spherulitic siderite nodules consist of nodules 20 μm to 0.15 mm diameter, always spherical, sometimes coalescing, and composed of radially arranged ferroan calcite and sideritic spar, with accompanying radial

extinction patterns (Plate 20d). Nodules occasionally contain several grains of <20 μm quartz, sometimes at the centres of the spherulites, but more commonly scattered through the nodule (Plate 20d & 20e), and up to three clay species (determined by electron microprobe); Fe-rich clays (probably smectite), and K-rich clays (probably illite) and rare Na-rich clays (probably albite). These clays are commonly surrounded by a very thin (<2 μm thick) Mn-rich sideritic layer (Plate 21a). Margins of the spherical nodules are typically marked by a <20 μm thick dark brown or grey alteration rind. Spherical nodules are supported by a very fine-grained sandy siltstone matrix.

Electron microprobe analyses (Appendix VIII) indicates that the carbonates present in the spherulites are dominated by Mn-rich siderites of uniform composition (MnO between 1.53 and 11.74 weight percent; FeO between 40.17 and 49.85 weight percent for 16 analyses), with less abundant, radially distributed ferroan calcite (Plate 20e & 20f). The high Mn content found in the Boss Point Formation nodules can be attributed to the higher levels of Mn in freshwater as opposed to marine waters, and is typical for siderites formed in fresh or meteoric waters (cf. Mozley 1989).

Data plotted on ternary CaCO_3 - MgCO_3 - FeCO_3 and CaCO_3 - MgCO_3 - MnCO_3 plots (Fig. 6.16) indicate that the siderites are low in Mg relative to Mn, and are therefore comparable with freshwater siderites described by Mozley (1989, fig.

Plate 21

a) Electron microprobe image of small black coloured clay (cl) fragments within spherulitic siderite nodule (from Alma), surrounded by a thin white coloured siderite rind (sid), surrounded by grey coloured calcite (cal).

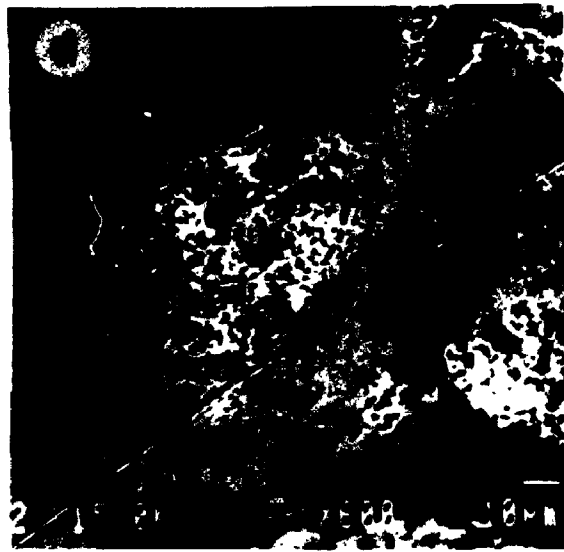
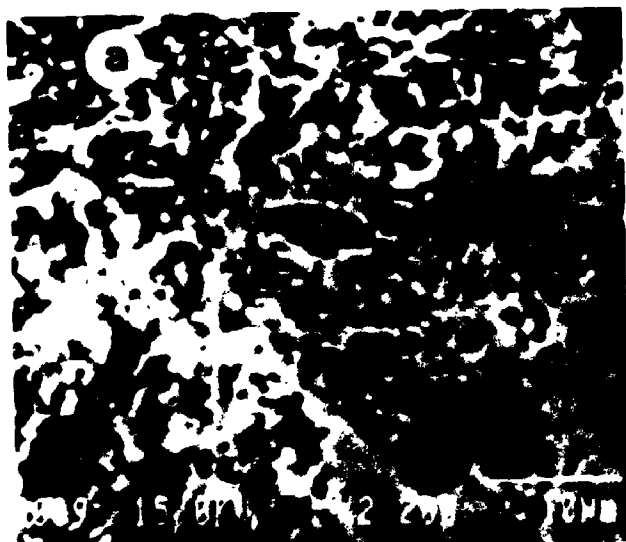
b) Electron microprobe image of spherulitic siderite nodule, in part coalescing with other nodules (as at bottom right and top left). The majority of the nodule consists of light coloured Mn-rich siderite (sid), with less abundant black quartz (qz) and Fe-rich clays (cl). Only minor amounts of radial distributed ferroan calcite (c) occur. The nodule is surrounded by black k-rich clays (?illite) and detrital quartz, and by grey Fe-rich clays (?smectite).

c) Electron microprobe image of zoned spherulitic siderite nodule (left) with abundant clays (upper clay is illite, central grains are ?albite).

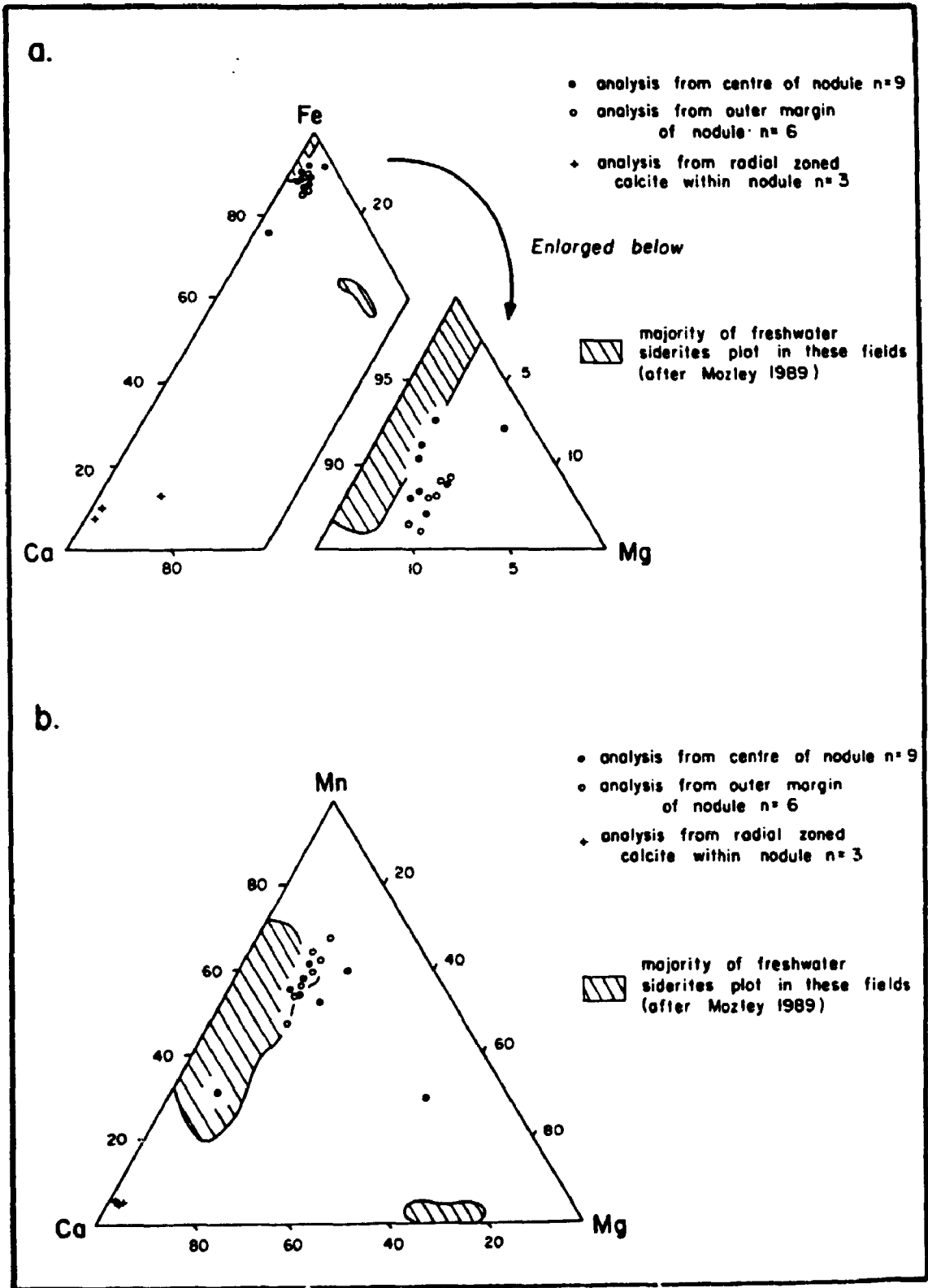
d) Electron microprobe image of zoned spherulitic siderite (detail of Plate 21c), showing grey coloured Mn-rich siderite (sid) in the outer part, and spherical shaped ferroan calcite (cal) in the centre of the nodule. Large black grain (cl) is a Na-rich clay (?albite).

f) Siltstone aggregate nodules from a silty paleosol at 30 m above the base of the Boss Point Formation at Johnson Mills. Grains consist of fine- and medium-grained siltstone and ped material (a), surrounded by a micritic calcite rind (b). View is in crossed polarised light. Scale bar= 0.5 mm.

e) Fragmentary nodules from the silty paleosol at Alma. Dark clasts consist of ped material (ped), with lighter, brown coloured, altered (micaceous) grains (mica). View is in plane polarised light. Scale bar= 0.5 mm.



- Fig. 6.16 a) Ternary CaCO_3 - MgCO_3 - FeCO_3 diagram for Boss Point Formation spherulitic siderite samples analysed by electron microprobe (see Appendix VIII).
- b) Ternary CaCO_3 - MgCO_3 - MnCO_3 diagram for Boss Point Formation spherulitic siderite samples analysed by electron microprobe (see Appendix VIII).



2). With respect to the Ca-Mg-Fe plot (Fig. 6.16a), the Boss Point Formation samples are slightly depleted in Fe and enriched in Mg and Ca with respect to the fields recognised by Mozley (1989). In general, analyses performed at the outer margins of the nodules show a greater degree of Fe-depletion than do samples from central portions of the nodules (Fig. 6.16a). The high Mg siderites recognised by Mozley (1989) were not encountered in this study. Boss Point Formation samples in the Ca-Mg-Mn plot (Fig. 6.16b), are very similar to those recognised by Mozley (1989), but are enriched in Mn relative to the dominant analytical fields of Mozley (1989). Analyses from the outer margins of the nodules are slightly enriched with respect to Mn than are the analyses performed on the central parts of nodules, which show a wide compositional variation (Fig. 6.16b). One sample shows enrichment in Ca, and another shows a high Mg composition, which may be transitional into the high Mg, low Mn analytical field recognised by Mozley (1989). Again, the Boss Point Formation samples do not show the extremely high Mg variants recognised by Mozley (1989).

Composition variation was slight in all siderites (Appendix VIII), though there is a tendency for the outer parts of nodules to be more Mn-rich. This Mn enrichment is attributed to reactions with interstitial meteoric waters at the margins of the nodules during diagenesis, relative to central regions of the nodules. In some spherulites,

ferroan calcite may occur in the centre of the nodules, surrounded by siderite (Plate 21c & 21d), but this is generally uncommon.

The siltstone matrix that surrounds the spherulitic siderites (Plates 20e & 21b), consists of dark coloured Fe- and K-rich ?illite clay (FeO= 6.91 weight percent; K₂O= 5.33 weight percent), and lighter coloured Fe-rich ?smectitic clay (FeO= 32.86 weight percent; see Appendix IX).

Spherulitic siderites have previously been described from pedogenic intervals in western Canada (Fritz et al. 1971, Leckie and Foscolos 1986, Hart 1990) and are equivalent to the sphaeroidite of Fritz et al. (1971), Tucker (1981), Leckie and Foscolos (1986), Gibson (1989) and Gibson et al. (1990). The published literature does not give a clear consensus as to how such spherulites developed, but it is concluded from the Boss Point Formation occurrence that the nodules formed in small standing bodies of water (ponds), under reducing and low sulphate conditions, and were then incorporated into the soil profile, probably as the ponds dried up.

D. Siltstone Aggregates

These nodules consist of <1.5 mm diameter, irregular shaped aggregates that contain medium- (up to 30 um diameter) and fine-grained quartzose siltstone (Plate 21e).

Staining with Alizarin Red S and potassium ferricyanide indicates that ferroan calcite also occurs. The aggregates are coated with a finely crystalline and micritic calcite rind, up to 0.1 mm thick.

These structures are similar to the micrite coated sand grains described by Warren (1983) of South Australia, to the "oolith-like coated particles" of James (1972), or "partially micritized skeletal grains" of Harrison (1977), and "micrite envelopes" of Esteban (1976). Warren (1983) attributed their formation to fluctuations in the volume and salinity of a film of water surrounding the grains. As the water was removed from the pores through evaporation, concurrent changes in the $p\text{CO}_2$ levels caused micrite to precipitate (Warren 1983, fig. 4). A similar origin is likely for the Boss Point Formation calcrete occurrences.

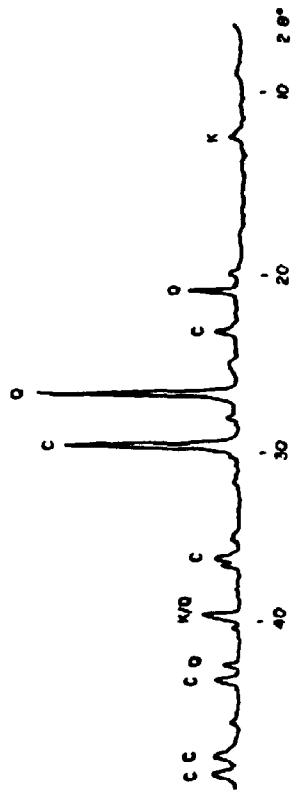
E. Fragmentary Nodules

Fragmentary nodules were observed in one sample, and consist of irregularly-shaped, generally angular fragments of ped material and light brown altered (micaceous) grains (Plate 21f). Ped fragments range up to 5 mm diameter; micaceous fragments are <2 mm diameter. The outer margins of the micaceous fragments are commonly coated by a thin (<30 μm thick) dark brown alteration zone. XRD analysis indicates the presence of hematite (Fig. 6.17), which is probably the mineral forming this alteration rim. Both

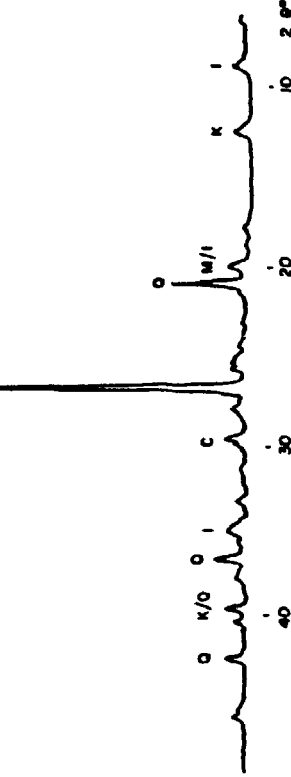
Fig. 6.17 XRD plots for 4 representative calcrete nodules from the Boss Point Formation. Note that the 12° two-theta peak could be a combined kaolinite/chlorite species.

Clay Mineralogy - Calcrite Nodules

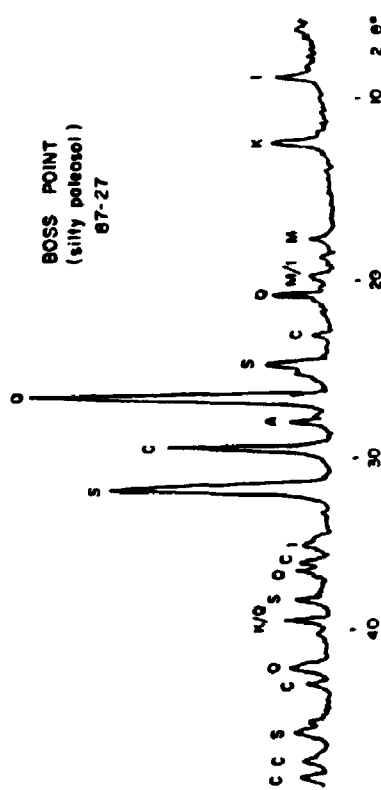
DORCHESTER SANDY PALEOSOL
C89-156



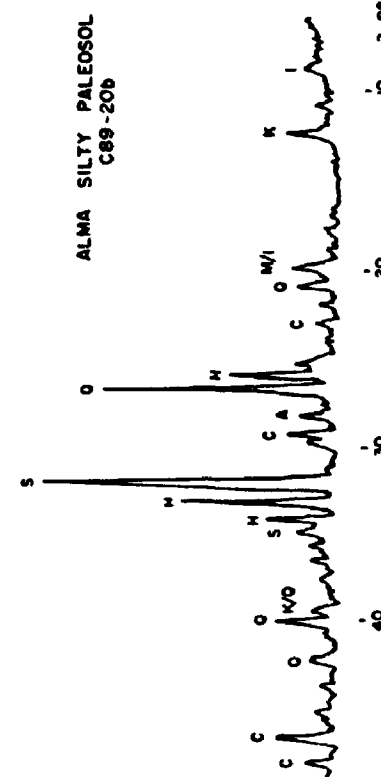
ALMA SILTY PALEOSOL
C88-63



BOSS POINT
(silty paleosol)
87-27



ALMA SILTY PALEOSOL
C89-206



A - Albite C - Calcite H - Hematite I - Illite K - Kaolinite M - Muscovite O - Quartz S - Siderite

mica and ped fragments are cut by ferroan calcite veins (crystallaria). The fragments are supported by a fine-grained quartzose siltstone matrix.

The fragmentary nodules described here are similar to the 'breccias' of Walls *et al.* (1975) and the 'breccioid' calcretes described by Semeniuk and Meagher (1981) from the Recent of Western Australia. In the Australian example it was concluded that they formed as disintegrated or brecciated calcretes. In the Boss Point Formation occurrence, the fragmentary nodules are interpreted as fragmented soil material, both peds and micaceous fragments aggregated into a nodular form. Nodules are not highly cemented and are certainly not as calcareous as the other forms of nodules described above.

Calcrete Matrix

All five types of nodular calcrete material may be surrounded by spar or by sandy siltstone material.

Spar usually occurs as a pore filling; the spar material is drusy textured (crystals as much as 0.4 mm long), and displays several phases of compositional zoning. Staining indicates that outer parts of pore-filling spar consist of calcite, and pass inward to ferroan calcite with calcite (the last formed) in the central parts of pore spaces (Plate 20b). This was confirmed by electron microprobe data from the pore space indicated in Plate 20b

(Appendix X), which indicates that the outer part of the pore is a pure calcite (FeO absent), but becomes increasingly more Mn- and Fe-rich (MnO= 16.53; FeO= 0.62 weight percent) in the central parts of the pore.

Siltstone also surrounds many calcrete nodules and is not dissimilar to the quartzose material that occurs within ped nodules, sparry calcite nodules and spherulitic siderite nodules. This matrix consists of angular to rounded quartz, up to 60 μm diameter, together with less abundant muscovite, chlorite and opaques.

6.4.5 XRD Analysis of Calcrete Nodules

XRD analyses were performed on 4 calcrete samples from the Boss Point Formation (Fig. 6.17). Bulk rock composition is similar to the mineralogy of the surrounding paleosol material and to mudrock units throughout the Boss Point Formation (Figs. 5.1, 6.2 & 6.3). In addition to these mineralogies, calcite is present in all samples, together with hematite and siderite in two of the samples. Based on petrographic observations, the hematite appears to be related to the alteration in the fragmentary calcrete nodules, whereas the siderite appears to be confined to the spherulitic siderite nodules.

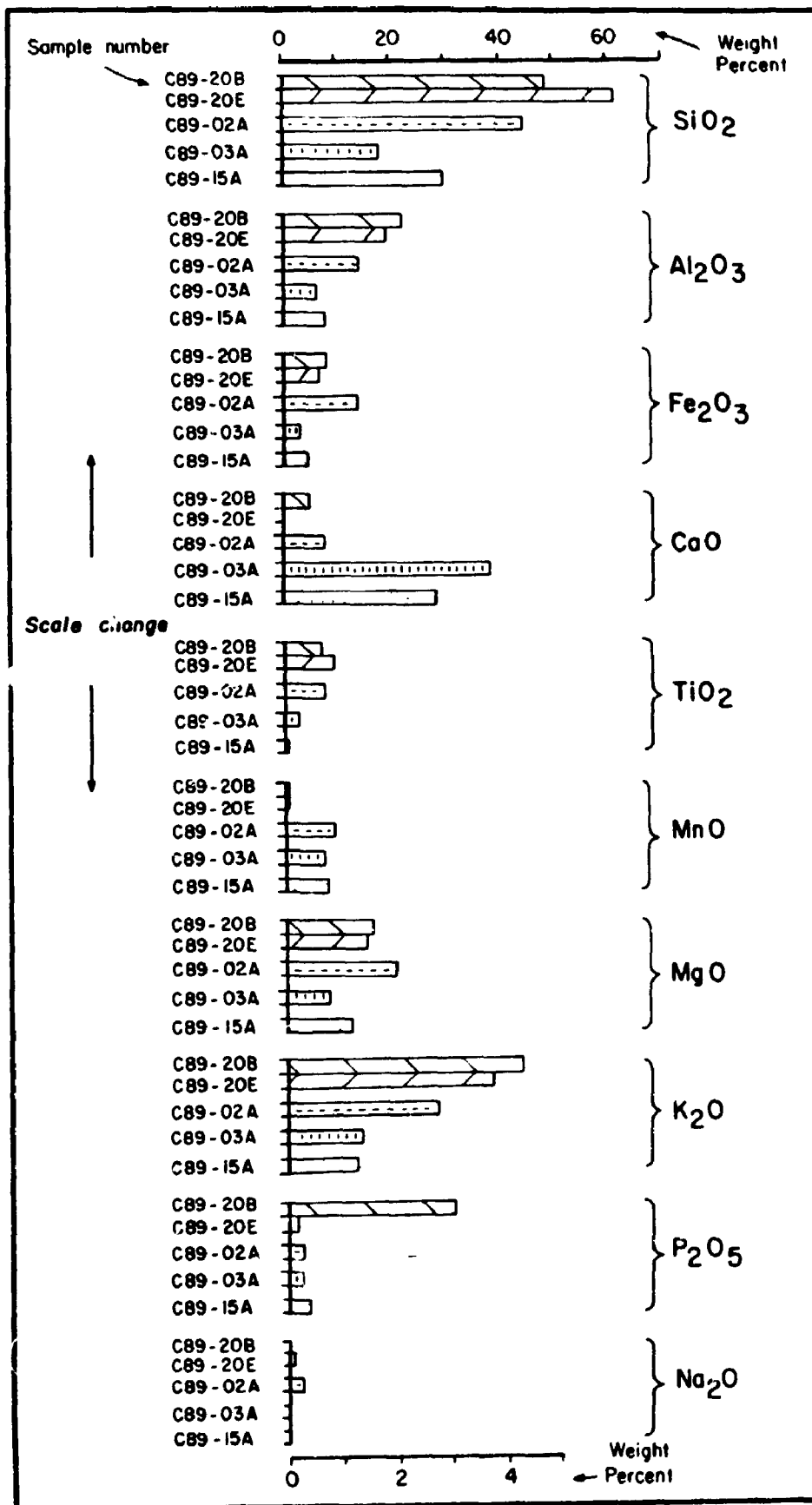
6.4.6 XRF Analysis of Calcrete Nodules

The major element geochemistry of five calcrete nodules was determined by XRF (Appendix XI). Sampled nodules include micritic, ped, sparry calcite, siltstone aggregate and fragmentary nodular calcrete morphologies (see descriptions above).

The high Si content in sample C89-20E (Fig. 6.18) is likely to be a result of the high clastic content of this nodule, silica being observed in thin section both in ped material and in siltstone aggregates (Fig. 6.18).

Calcium varies considerably in the nodules (Fig. 6.18), in the range 1 to 37 weight percent CaO. Silica too shows a wide range from 27 to 61 weight percent; when Si is high, calcium tends to be low (Fig. 6.18). A sample of the fragmentary nodular calcrete (sample C89-20B) has a high Al_2O_3 concentration, and is consistent with the presence of partially weathered mica seen in thin section (Plate 21f). This sample is also high in K_2O , P_2O_5 , and to a lesser extent Fe_2O_3 and MgO (Fig. 6.18). The high K_2O content may relate to the diagenetic alteration of these clays. The abnormally high P content in this sample may reflect the presence of collophane, although the relatively low weight percent CaO (4.50) in the sample suggests that collophane is not present (chemical formula for collophane $\text{Ca}_3\text{P}_2\text{O}_8 \cdot 2\text{H}_2\text{O}$). Collophane was not detected in XRD analysis (Fig. 6.17). An alternative explanation is that the high P

Fig. 6.18 Major and minor element geochemistry for 5 representative calcrete nodules (4 paleosol profiles) - C89-20 (Alma silty paleosol), C89-02 (Cape Enrage sandy paleosol), C89-03 (Cape Enrage silty paleosol) and C89-15 (Dorchester sandy paleosol).



values indicate the presence of phosphatic nodules, such as coprolites, faecal pellets or organic remains (Platt 1989b), perhaps from a burrowing infauna. A source of P from plants is unlikely. In modern soils, phosphate is retained in the upper portions of the soil profile by vascular plants, but if this had been the case in the Boss Point Formation paleosols, there would be an observed increase in P_2O_5 up the paleosol profile. Such a trend was not observed. The high concentrations of Al and Fe may indicate the phosphates of these elements are present.

TiO_2 ranges from 0.05 to 0.9 weight percent, and shows considerably more variation than TiC levels in the remainder of the paleosol profile (see below). The low values of Na_2O is consistent with their removal by weathering or leaching by groundwater (G-Farrow and Mossman 1988). Na has not been retained by clays as effectively as K despite their chemical similarity.

MnO varies from 0.5 weight percent to 9 weight percent for all nodules, values that are consistent with the MnO levels determined from the microprobe analysis of the siderite nodules (see above).

One representative calcrete nodule was examined by XRF for minor and trace element composition (Appendix XII). This sample from the Alma paleosol, is dominated in thin section by ped nodules and crystallaria, and lacks the other varieties of calcrete nodule described above. Minor and trace element data from the calcrete fall within the

range of elemental data obtained from other sandy and silty paleosol material (Appendix VI), indicating that the trace element composition of this calcrete sample is not dissimilar to that of the paleosols in the Boss Point Formation as a whole.

6.4.7 What was the Carbonate Source for Calcrete Development?

The Boss Point Formation sediments are not strongly calcareous and therefore cannot be regarded as a source for the carbonate in calcrete nodules. An origin of the calcium by downward movement of carbonate through the soil profile ("*per descensum* model") was unlikely due to the general decrease in carbonate downward through profiles. Carbonate is known to have been mobilised by upward movement of groundwater saturated with dissolved carbonate, by the widespread occurrence of ferroan calcite throughout paleosols and the Boss Point Formation sandstones as a whole ("*per ascensum* model"). Introduction of eolian carbonate dust into the profile is a possible source of carbonate (see James 1972), but was probably not significant in the Boss Point Formation situation, given the lack of detrital carbonate in the formation as a whole. Although other sources of calcium such as calcium-rich primary minerals, plants which contain calcium in their tissues, and skeletal grains from terrestrial organisms may

have made a contribution (see Klappa 1983), the primary source for the carbonate must be as a biological product of photosynthesis. CO_2 in soils is released by plant roots during respiration, and during decay. The low partial pressure of CO_2 in the soil, promotes precipitation of CaCO_3 . Biogenic carbonate is important in modern calcretes of South Africa (Salomons *et al.* 1978), though tends to be underemphasised in geological situations. Additional minor contributions may have come from Ca^{2+} and HCO_3^- in rainwater (eg. Gardner 1972, Warren 1983), and from flood waters carrying Ca ions from weathered bedrock (eg. Stalder 1975).

6.5 Soil Taxonomy

Although many soil classification schemes exist, one that is widely used by modern workers is the United States Soil Taxonomy (Allen and Fanning 1983). This scheme recognises several Orders and Suborders, of which the two Orders, Aridisols and Vertisols, are the only two which show similarity or relevance to the Boss Point Formation paleosols.

6.5.1 Aridisols

Aridisols are soils of dry climates which show minimal alteration of parent materials. Yet they show at least one distinctive pedogenic horizon which may be either enriched

or depleted of substances by moving water (Allen and Fanning 1983, Nettleton and Peterson 1983). Horizon development may include a/an:

- 1) CAMBIC ZONE- characterised by alteration or removal of mineral matter as indicated by strong chromas, usually grey or red colour mottling
- 2) ARGILLIC ZONE- formation of pedogenic clays
- 3) NATRIC ZONE- an argillic zone but with a blocky, columnar or prismatic structure
- 4) CALCIC ZONE- a zone enriched with secondary carbonates, either calcite or dolomite (petrocalcic), gypsum (petrogypsic), siliceous (silcrete) or containing soluble salts (salic).

Little or no humus accumulates in typical aridisols, and a considerable period of time is required for their formation, largely due to the reduced supply of water for soil forming processes. It is common for aridisols to have some form of surficial or near surface crust, either in the form of a pebble lag or armour (desert pavement), or a duricrust, such as calcrete, silcrete, bauxite or gypcrete. Aridisols are common on alluvial fans, and alluvial surfaces protected from fluvial deposition.

6.5.2 Vertisols

Vertisols are clay-rich (generally montmorillonitic)

soils, which have a very plastic soil consistency when wet, and lack horizon differentiation (Ahmad 1983, Allen and Fanning 1983). The clay content leads to shrinking and swelling with changing water content that result in deep cracks and a self-mixing habit, termed pedoturbation. Present-day vertisols occur under widely differing climatic regimes, although they do tend to occur in tropical and sub-tropical regions (annual rainfall <1500 mm/year), and are very much favoured to develop where this rainfall has a marked seasonality (Ahmad 1983). It is common for vertisols to possess calcium/magnesium nodules, especially when rainfall is low and markedly seasonal.

6.5.3 Boss Point Formation Paleosol Classification

Paleosols of the Boss Point Formation show characteristics of both aridisols and vertisols (United States soil taxonomy).

The sandy paleosols are interpreted as aridisols, based largely on their sandy texture, presence of calcrete nodules, and lack of an E (organic) horizon.

Boss Point Formation sandy paleosols display both cambic and calcic features, but lack pedogenic enrichment in clays (argillication), or blocky texture (natric features). Taxonomically the Boss Point Formation paleosols are most like the Orthid suborder of aridisols, based on the abundance of calcareous material in the

profile.

The silty paleosols are interpreted as vertisols, due to the abundance of clay minerals, presence of low-angle conjugate shears, slickensides, pseudo-anticlines, and calcrete nodules. Several features of the Boss Point Formation paleosols differ, however, from the norm for vertisols.

The Boss Point Formation vertisols are dominated by kaolinite and illite clay groups, whereas modern-day vertisols contain montmorillonite (smectite) as the dominant clay (Ahmad 1983). Several possibilities may account for this. For example, montmorillonite may have been the original clay group even in the Boss Point Formation paleosols, but was diagenetically altered by desilication to kaolinite. Some support for this premise comes from the fact that XRD determinations made on a wide range of mudrocks, of differing ages throughout the Maritimes Basin, all show a very similar kaolinite-illite clay mineralogy (Masson and Rust 1990, A.G. Flint *pers comm.* 1990; see also Besly and Turner 1983). Staub and Cohen (1978) describe kaolinite-rich clays produced from montmorillonite-rich clays through the filtering of acid fluids from overlying peat in the modern. A similar situation may have occurred in the Boss Point Formation, especially in cases where clays are associated with organic layers.

Alternatively, illitisation of smectites, commonly

attributed to increasing temperature during burial diagenesis (Hower *et al.* 1976, Nadeau *et al.* 1985) may have occurred. Two recent studies have shown that illitisation can result from K-fixation by wetting and drying cycles, and not by burial illitisation (Robinson and Wright 1987). Recently Singer (1988) has stressed the importance of pedogenic illitisation operating in Quaternary soils. Another possibility is that kaolinite was the original clay mineralogy, and although it does not have the same water retention capabilities as montmorillonite, it does have the ability to hold considerable water in the crystal lattice. Montmorillonite for example can hold up to 40% of its volume as water, whereas the value for kaolinite is approximately 30% (Sopher and Baird 1982). As such, kaolinite clays can act in much the same way as montmorillonite clays in terms of expansion and contraction upon wetting and drying, and be able to produce low-angle conjugate shears and pseudo-anticlines, although their role in such pedogenic processes has not been acknowledged by previous workers (eg. Allen and Williams 1979, Allen 1986)

Both soil groups are considered to have formed alongside one another, their characteristics being determined primarily by the grain size of the parent material rather than any other factor. Aridisols and vertisols are widely recognised from the Carboniferous in both the central United States and Britain (Allen and Williams 1979, Prather 1985, Allen 1986, Joeckel 1989, Searl 1989, Wright 1990a).

A modern-day analogue is central Australia, where both aridisols and vertisols occur in the same geographic area (Nettleton and Peterson 1983).

6.6 Paleoclimatic Considerations based on Boss Point Formation Paleosols

In the United Kingdom and the United States, considerable importance has been placed on the use of paleosols in reconstructing Carboniferous paleoclimates (Allen 1974, 1986, Steel 1974, Walls *et al.* 1975, Besly and Turner 1983, Searl 1989, Goebel *et al.* 1989, Joeckel 1989, Wright 1990a), but in Canada, no studies of comparable detail based on paleosol petrology and geochemistry have been made for the Carboniferous.

Previous work in Maritime Canada has suggested two contrasting paleoclimates during the Carboniferous. van de Poll (1983) suggested that the paleosols were podzols, formed under tropical conditions, an opinion based largely on the presence of organic matter and coal-forming swamps. D'Orsay and van de Poll (1985) also concluded a tropical climate during the middle Pennsylvanian, on the basis of SEM surface textures of quartz grains. In contrast, Legun (1980), Legun and Rust (1982), Rust and Legun (1983) and Rust and Nanson (1989) have suggested that Carboniferous paleosols in the Maritimes were formed under semi-arid conditions, and base that premise on what they consider

good indicators for a semi-arid paleoclimate (redbeds, mudcracks and other indicators of desiccation). In addition, the high proportion of cellulosic and lignitic tissues in coals has also been used to argue for a dry Carboniferous paleoclimate (Kaplan 1980).

The paleosol descriptions and geochemistry presented in this study overwhelmingly favour a semi-arid paleoclimate during the deposition of the Boss Point Formation. This conclusion is based on the characterisation of these paleosols as aridisols and vertisols, and the presence of calcrete nodules.

Vertisols occur today in areas with a marked seasonality of rainfall. Although the annual rainfall may be as high as 1500 mm/year (Ahmad 1983), there are prolonged periods (as much as 8 months) where evaporation > precipitation. The latter seems to be the key factor determining the occurrence of these soils. These climatic features have also been suggested for ancient vertisols. For example Searl (1989) and Wright (1990a), indicate that for the Early Carboniferous of southern Britain, a monsoonal climate prevailed, with summer rainfall, and a winter dry period as rainfall was deflected by low pressure systems toward Gondwana. In Atlantic Canada, van de Poll (1983) has suggested a marked seasonal (monsoonal) paleoclimate during periods of the Pennsylvanian. Seasonality of precipitation was also likely for the Boss Point Formation paleoclimate.

Modern-day calcrete nodules only form in low or moderate latitude, low rainfall areas (typically <1000 mm/year) where evaporation exceeds precipitation for a considerable period of the year (Reeves 1970, Goudie 1973). Calcretes tend to be best developed in areas where rainfall is <500 mm/year (Goudie 1973, table 6), and in areas that are neither too arid nor too moist (Reeves 1970). Where there is an extreme water deficiency, as in very arid climates, there is insufficient pore water to allow carbonate precipitation; in contrast excessive precipitation causes leaching (Reeves 1970, James 1972). Although calcretes can form in subtropical humid environments (Semeniuk and Searle 1985), these are uncommon, and in all occurrences, evaporation exceeds precipitation.

The final paleoclimatic inferences that can be made from the Boss Point Formation paleosols concern the degree of weathering experienced by the profiles. Petrographically, the 'dirty' appearance of plagioclase feldspars, indicates that some weathering of the soil profile has occurred, the high Al_2O_3 content determined by XRF demonstrating that all the paleosols are highly weathered.

These features are not consistent with the interpretation made by van de Poll (1983) that Carboniferous paleosols in the Maritimes were originally podzols. Podzols have well developed horizon development,

with a strongly leached (eluviated), light grey A2 horizon and a dark brown, B horizon (illuviated) enriched in iron oxide, alumina and organic matter. None of these features are recognised in Boss Point Formation paleosols. Van de Poll's interpretation is based on the presence of ironstone nodules which he argues are common in tropical regions, and the problems of maintaining coal-forming swamps in a semi-arid climate. The presence of coal was interpreted by van de Poll as evidence of abundant rainfall necessary to maintain a tropical rain forest plant community. However, insufficient information is known regarding the physiological requirements of Carboniferous lycopod communities, and it might equally be argued that species such as *Calamites*, with a hollow trunk and stem (much like present-day bamboo), may have been xerophytes, able to store sufficient water within its structure to survive a dry season.

Studies in adjacent areas in the central United States (Prather 1985, Goebel et al. 1989, Joeckel 1989) and Britain (Allen and Williams 1979, Wright 1982, Allen 1986), have all suggested semi-arid or arid paleoclimates at various times during the Carboniferous, whereas Besly and Turner (1983) indicate moist tropical climates for parts of the Upper Carboniferous in Britain.

6.7 Temporal Considerations in Paleosol Development

Paleosols have been used extensively to judge the rates of sedimentation in alluvial basins (Allen 1974, Leeder 1975, Wright 1982, Kraus and Bown 1986, Leckie *et al.* 1989). Because soils require a considerable period of time to develop, it is clear that for a protracted period of time, the particular paleosol locality must have been starved of sediment. Soils may develop when the fluvial channel fails to migrate or avulse across the floodplain (autocyclic mechanisms), or is prevented from doing so by topographic or structurally controlled allocyclic factors (Allen and Williams 1979, Kraus and Bown 1986).

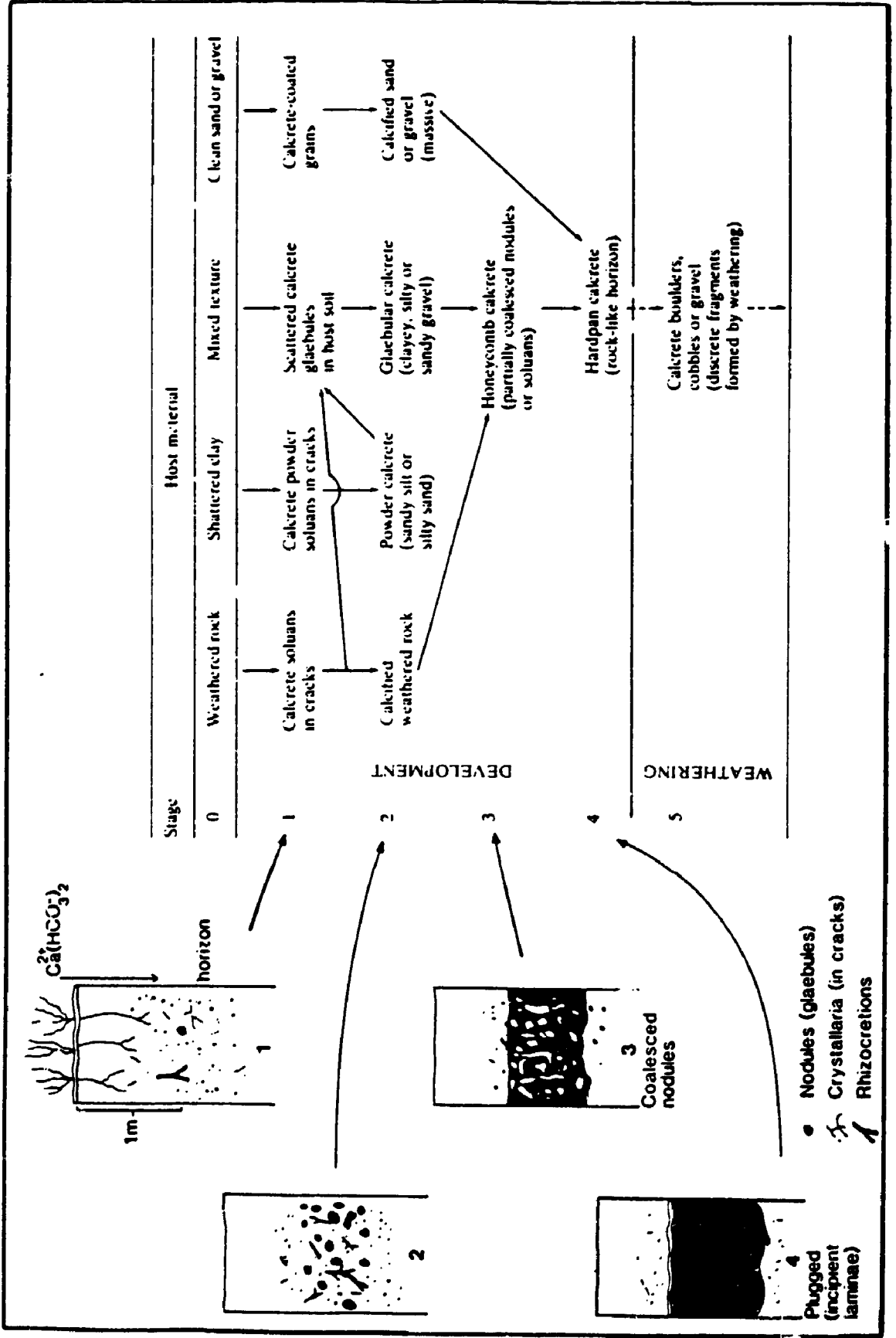
In the Boss Point Formation the paleosols are in large part limited to a thin southwest-northeast strip through the Bay of Fundy region (Fig. 6.1). This zone correlates well with the distribution of the Harvey-Hopewell Fault, which is mapped on the basis of field relationships (Maps 1 & 2) and from its deflection of paleocurrent trends (see Chapter 8). It is suggested that the paleosols developed preferentially atop, or immediately adjacent to this penecontemporaneous high.

Soils of arid climates, and in particular calcrete-bearing soils, have been used to determine sediment accretion rates in ancient alluvial deposits. The proportion of carbonate present in these soils (the 'K' factor of Gile *et al.* 1966), has been used to judge the

relative amount of time required to develop these soils; little carbonate (young soils) versus extensive carbonate (old soils). Numerous evolutionary models (Fig. 6.19) have been devised for carbonate-bearing soils (Price 1933, Goudie 1973, Steel 1974, Leeder 1975, Harrison 1977, Netterberg and Caiger 1983, Machette 1985). All models show a progression with time from a youthful stage (Stage 1) of small incipient carbonate nodules, through to mature and senile profiles that show a dense, continuous calcrete crust (Stages 3 & 4). Clearly the Boss Point Formation paleosols show a range of carbonate nodule development (and by inference several ages), from youthful open fabrics, to mature paleosols with a dense interlocking calcrete nature (Stages 1-3).

Gile *et al.* (1966) assigned approximate time periods required for the development of some of these stages based on ages of geomorphic surfaces that were radiometrically dated (Fig. 6.19). Using these age estimates, the Boss Point Formation paleosols would have required periods of pedogenesis in the range 5×10^3 (for Stage 1 development) to several 100,000 years (for Stages 3-4 development). In addition several empirical mathematical models have been suggested, one of the most commonly cited being that of Goudie (1973) where:

Fig. 6.19 Model for the development of calcrete nodules through a series of stages (1 to 4), with typical pedologic profiles (at left). From Netterberg and Caiger (1983) and Wright (1990b).



$$T = \frac{Ct \ Cd \ CaCO_3\%}{s \ CaCO_3 \ E} \times 10$$

where:

T= time
 Ct= thickness of the calcrete profile
 Cd= dry density of calcrete
 s CaCO₃= calcium carbonate content in ppm of soil water
 E= evaporation in cm/year

Examples where the above methods have been used include Leeder (1975), McPherson (1979), Robbin and Stipp (1979), Machette (1985). However in a recent review paper, Wright (1990b) concluded that it is practically impossible to assume that modern rates of calcrete formation can be applied to ancient examples, and further, that some of the ages originally assigned to modern geomorphic surfaces containing calcrete, have subsequently been shown to be incorrect. Examples are now known of very rapid carbonate accumulation, whereas in other cases, carbonate development is not progressive with time, but can be affected by changing climate and remobilisation of carbonate. Wright (1990b) concludes that assigning specific periods of formation to ancient calcretes is not, at present, justifiable, especially when "extrapolating rates of calcrete formation from Quaternary to mid to early Paleozoic time" (op. cit. p. 275). Probably all that can be concluded for the Boss Point Formation paleosols is that a considerable time would have been required for soil development, and that this was probably in the range of several thousands to tens of thousands of years.

CHAPTER 7

VERTICAL FACIES RELATIONSHIPS

7.1 Braided River Facies Association

Most previous workers have regarded the Boss Point Formation as a meandering fluvial system (Belt 1968a, Plint and van de Poll 1984, Ryan 1984, Plint 1986). Lawson (1962) considered the formation to be a large deltaic complex, with an axial drainage which flowed southwest, down the axis of the present-day Bay of Fundy.

In this study it is concluded that the Boss Point Formation represents a sandy braided fluvial system, which had a source area not too far distant in the Caledonia Highlands to the west. A braided model is favoured because of the relative paucity of mud-filled channels or overbank fines, rare occurrences of IHS (and where these do occur, they are always associated with fine-grained lacustrine units- see below), and the abundance of stacked channel sandstone units relative to lateral accretion and overbank deposits (see the criteria of Jackson 1978 and Bridge 1985). Thick stacked sandstone packages will be produced where the aggradation rate is low relative to avulsion frequency, where there is a large channel-belt/floodplain width, and in areas of preferred tectonic subsidence (Bridge 1985).

In terms of established fluvial facies models, the Boss Point Formation most closely resembles the South Saskatchewan River, and ancient analogue, the Battery Point Formation (Cant and Walker 1976, 1978, Walker and Cant 1984), the Triassic Fremouw Formation of Antarctica (Collinson et al. 1980) and the Westphalian successions of the Isle of Arran, Scotland (Kirk 1989), especially with regard to the predominance of trough cross-bedded sandstone relative to planar cross-bedded units. The virtual lack of planar cross-bedded lithofacies in the Boss Point Formation is at variance with existing models for sandy braided river systems (Platte and South Saskatchewan models). Bars (represented by planar cross-beds) despite their scarcity, must have been a feature of the Boss Point Formation rivers, just as they are in modern braided rivers. It is suggested that bar forms are rare in the formation due to preservation, perhaps related to large discharge fluctuations, or to their formation in the shallowest part of channels. Boss Point Formation units closely resemble other braided sandstone fluvial units, notably the Devonian Battery Point succession, in Quebec (Cant and Walker 1976, Lawrence and Williams 1987), the Fairchild and Buckley Formations, Antarctica (Isbell and Collinson 1988) and the South Bar Formation, Nova Scotia (Rust and Gibling 1990a).

The uniform grain size and dominance of trough cross-bedding over much of the outcrop area suggests that, apart from relatively minor alluvial fans which developed on the

flanks of the basin, most of the Boss Point Formation was deposited on a flat, unconfined braidplain (terminology after Rust and Koster 1984, Rust and Gibling 1990a; Fig. 7.1).

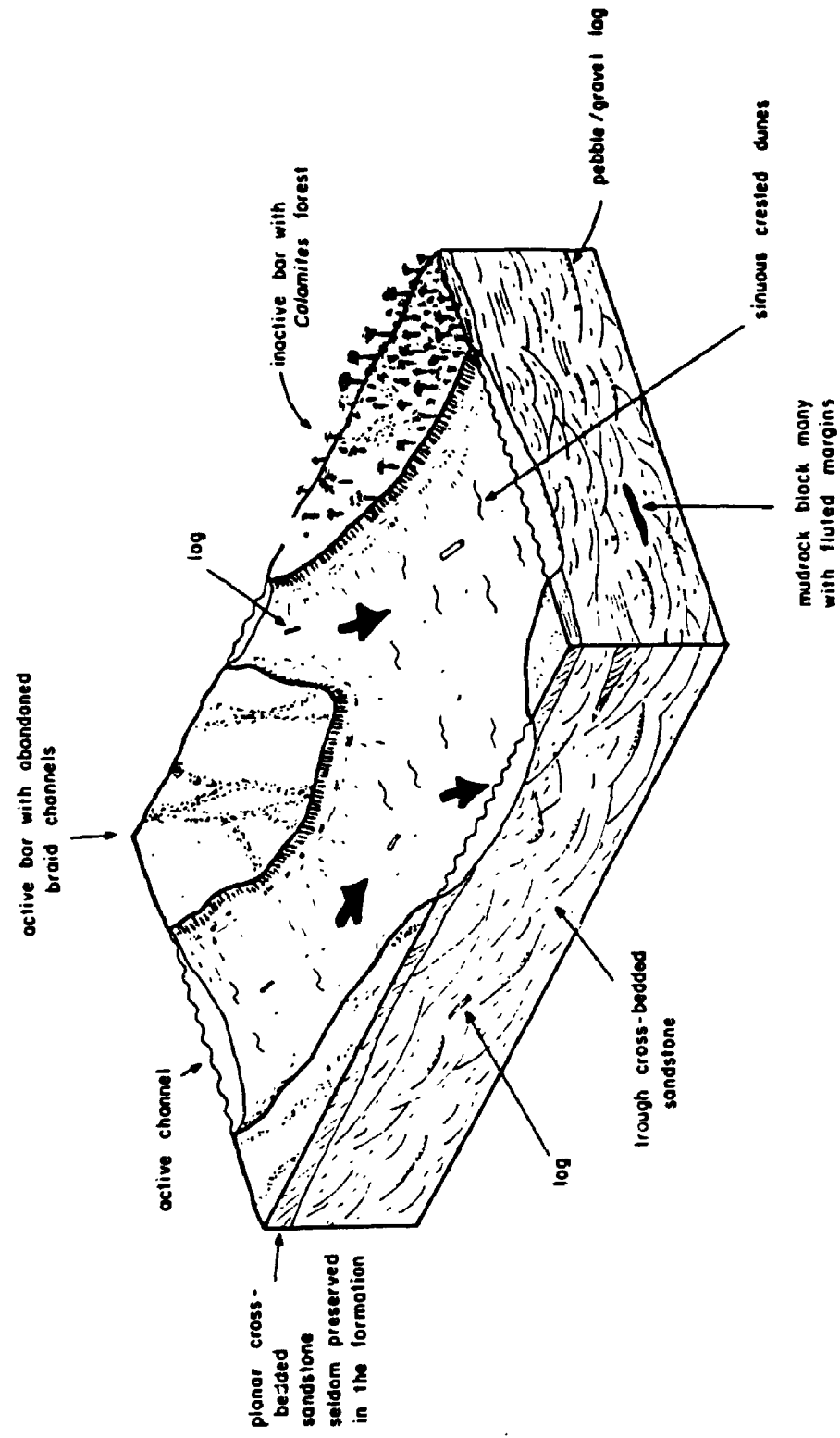
Previous suggestions by van de Poll (1966, 1970) and Gibling *et al.* (1989) that sediment was derived from a great distance to the south, either in New England or further to the south in the Appalachians is not supported by the similarity of pebble clast composition (Chapter 3) and sandstone petrography (section 4.1.2) to rocks presently exposed in the Caledonia Highlands. Gibling *et al.* (1989) suggested that an elongate basin, or series of interconnected basins existed throughout New England and Atlantic Canada, and it was along this corridor that river systems brought sediment from the Appalachians in the south. However recent seismic profiles and derivative maps suggest that such a corridor was unlikely due to the presence of basement highs through the Gulf of Maine region (Hutchinson *et al.* 1987, Hutchinson *et al.* 1988). Rather, it is suggested that separate and geographically distinct sedimentary basins (pull-aparts) were more likely (see Chapter 9).

7.1.1 Channel-Fill Cycles

No statistically derived associations of lithofacies (such as Markov chain analysis, Miall 1973 or facies

Fig. 7.1 Conceptual model for braidplain deposition of sandstone units in the Boss Point Formation.

Model for the Development of Sandy Lithofacies in the Boss Point Formation

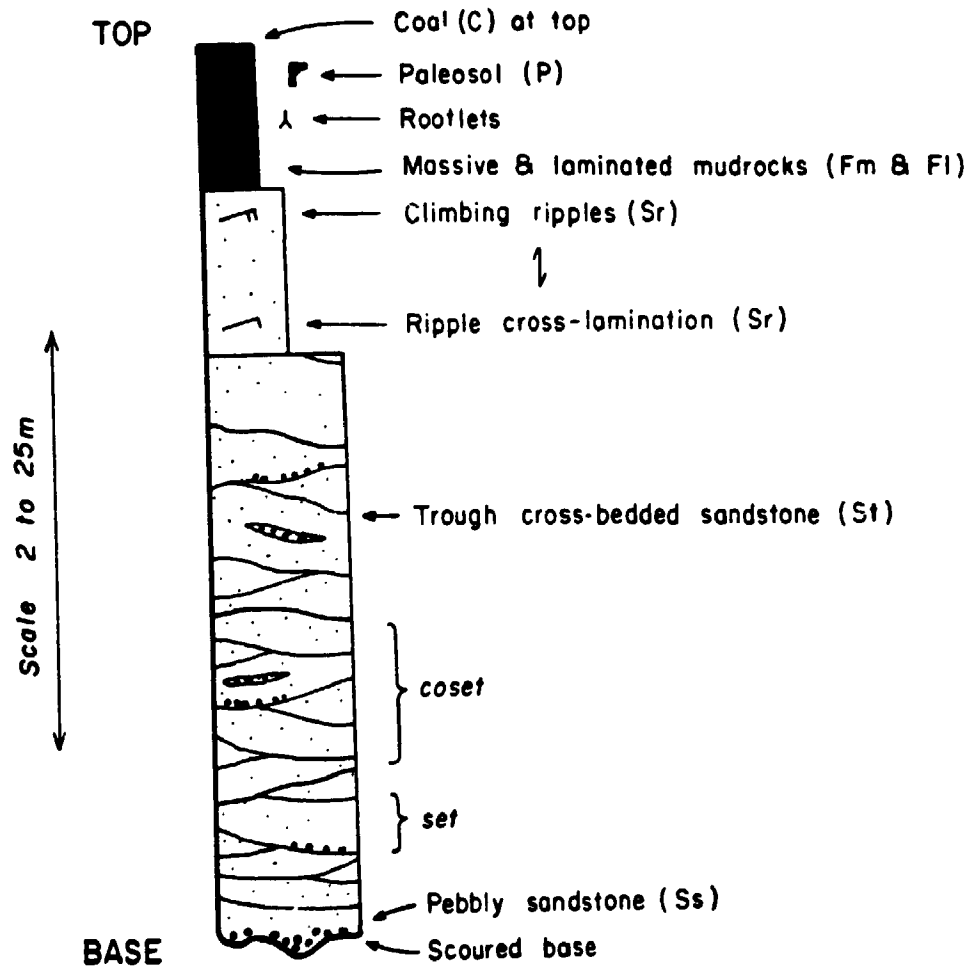


sequence analysis, Cant and Walker 1978) were undertaken in this study. It is clear however from field relationships that certain vertical facies successions are present.

Channel-fill cycles may show fining-upward successions which typically begin with a sharp erosional base, overlain by intraclast pebbles or gravelly sandstone (Ss), or by trough cross-bedded (St) sandstone (Fig. 7.2). The coarse-gravels are usually <2 m thick, and are sharply overlain by a much thicker package of trough cross-bedded sandstone which forms the bulk of the cycle (Fig. 7.3). The tops of St units are gradational upward into ripple cross-laminated sandstones (Sr), with or without climbing ripple laminated sandstones (Sr), horizontally laminated sandstones (Sh) or massive sandstones (Sm). Sandstones may pass upward into mudrocks (Fm and Fl), with minor intercalated sandstone units, whereas the top of the ideal cycle is a paleosol (P). Thus the ideal fining-upward cycle (Fig. 7.2) can be summarised as an erosional base (Ss) → St → Sr → with-or-without climbing ripples, Sh → Fm/Fl → P (top). Massive sandstone (Sm) may occur at any point in this succession (Figs. 7.2 & 7.3). Not all lithofacies are displayed in each cycle; sharp based trough cross-bedded sandstones commonly define the base, mudrocks and paleosols are usually absent from cycles. In the Boss Point Formation the channel-filling cycles are most typically truncated, and this has resulted in the removal of finer-grained lithologies that may have been deposited.

Fig. 7.2 Idealised fining-upward cycle found in the Boss Point Formation.

IDEALISED FINING-UPWARD CYCLE

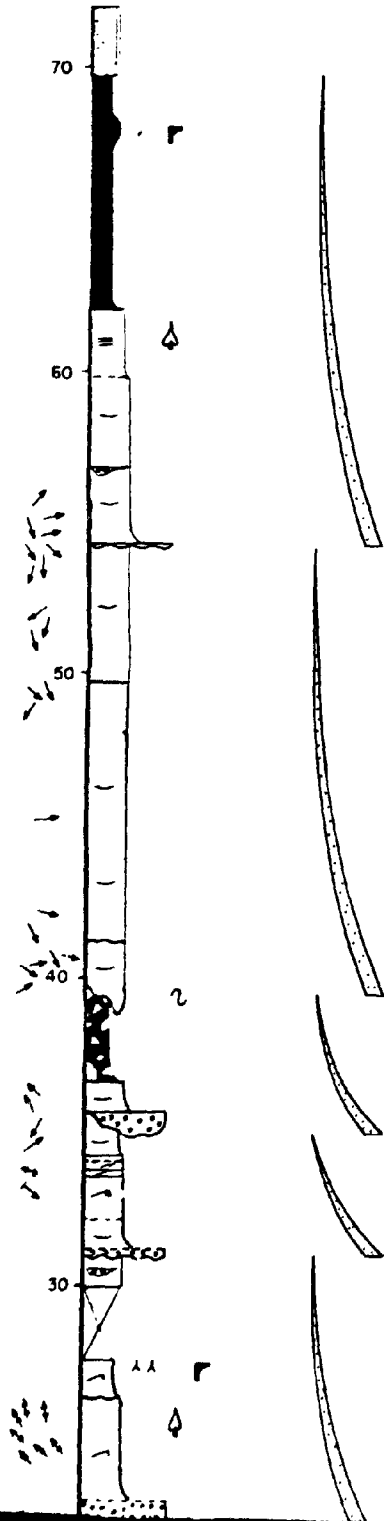


Massive sandstone (Sm), horizontally laminated sandstone (Sh) and pebbly sandstone (Ss) may occur at any position within sandstone successions.

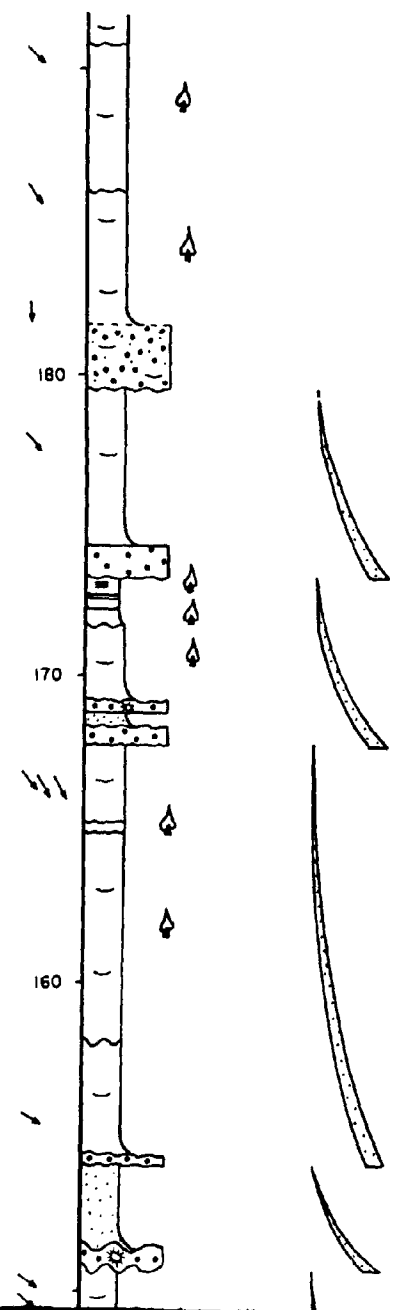
Fig. 7.3 Fining-upward cycles from 3 represent stratigraphic sections in the Boss Formation. Other examples can be found in stratigraphic sections presented in

representative
the Boss Point
can be found in the
printed in Volume II.

ALMA



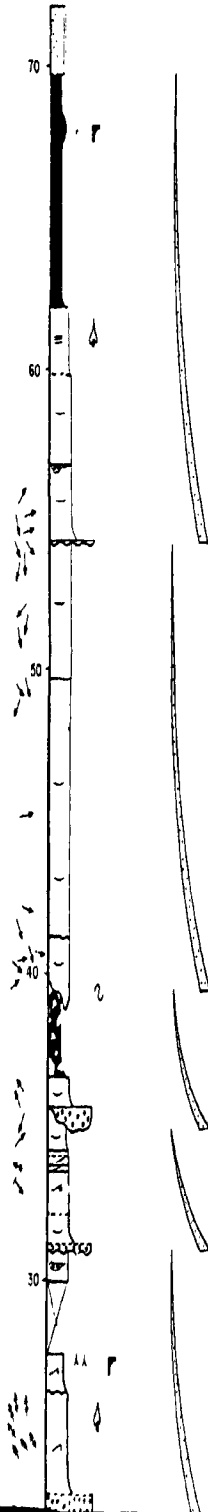
GRINDSTONE ISLAND



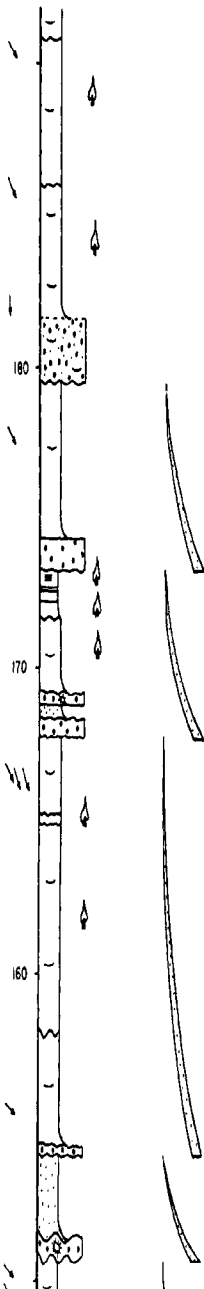
220



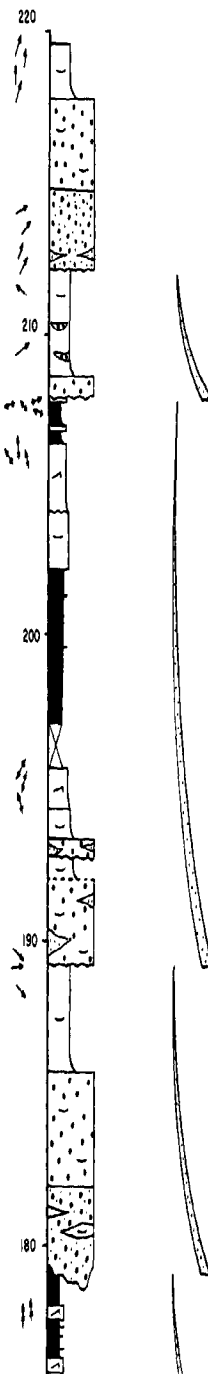
ALMA








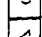





GRINDSTONE ISLAND


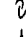


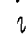






DORCHESTER

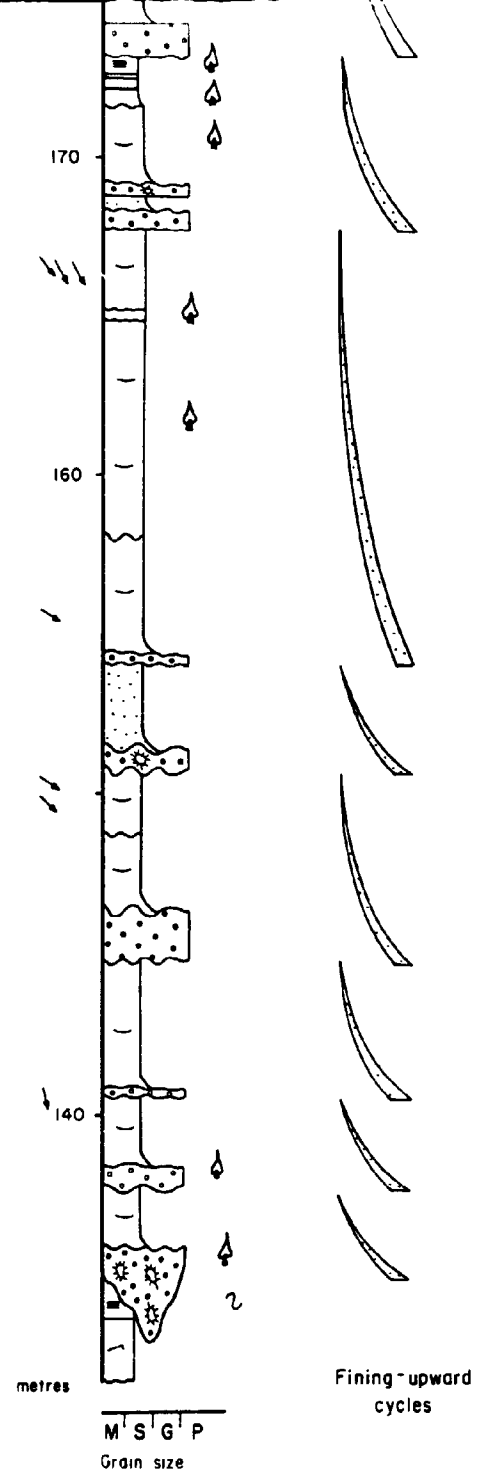
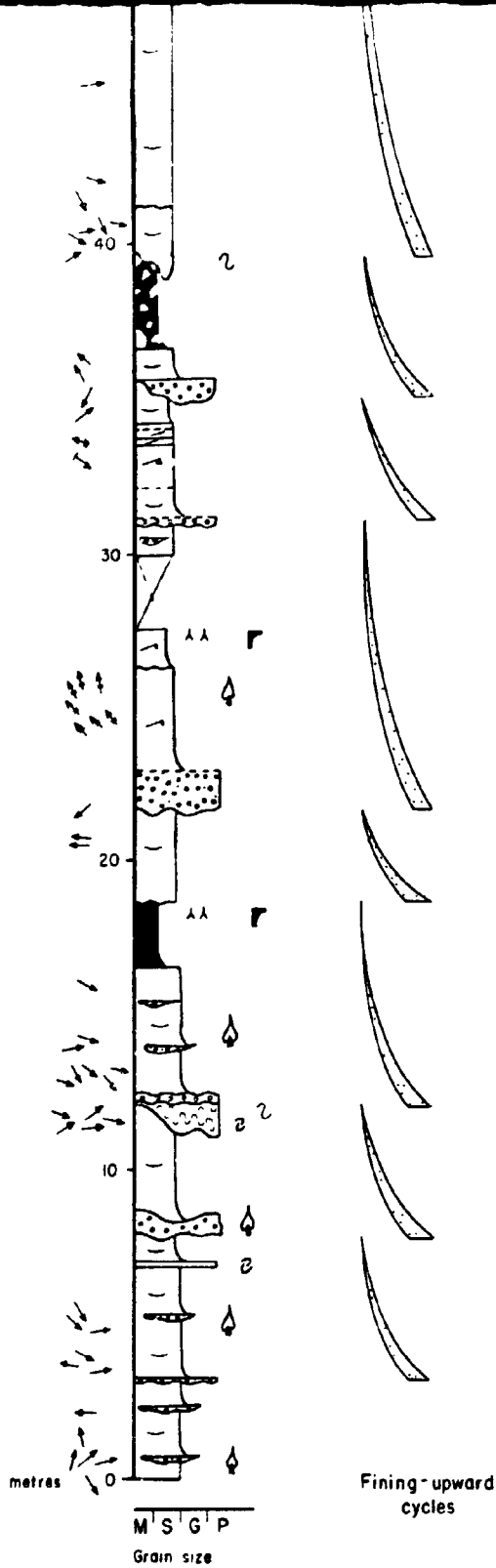


Legend

-  Conglomerate (may have cross-bedding)
-  Pebby sandstone (may have cross-bedding)
-  Ball and pillow
-  Mudrock
-  Siltstone blocks
-  Trough cross-bedded sandstone
-  Ripple laminated sandstone
-  Climbing ripple laminated sandstone
-  Horizontally laminated sandstone
-  Massive sandstone
-  Not exposed

-  Fluted siltstone block
-  Ball and pillow
-  Comminuted carbonaceous debris
-  Rootlet
-  Paleosol
-  Large erosion surface (>1m relief)

- Paleocurrents (north to top of figure)
-  Trough cross-beds
 -  Ripple lamination
 -  Climbing ripple lamination



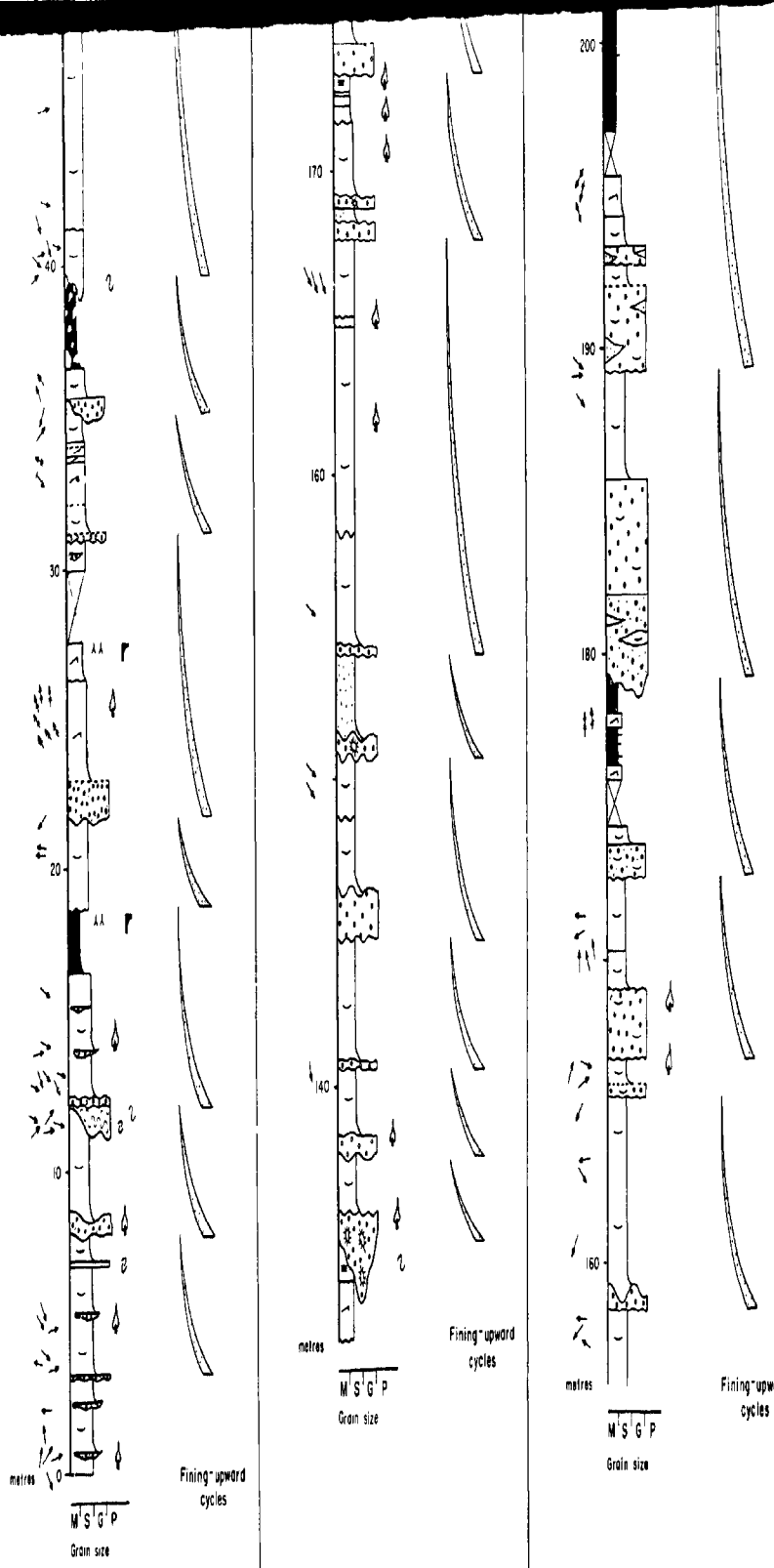
20

190

180

160

metres



Mudrock
 Siltstone blocks
 Trough cross-bedded sandstone
 Ripple laminated sandstone
 Climbing ripple laminated sandstone
 Horizontally laminated sandstone
 Massive sandstone
 Not exposed

Fluted siltstone block
 Boll and pillow
 Comminuted carbonaceous debris
 Rootlet
 Paleosol
 Large erosion surface (>1m relief)

Paleocurrents (north to top of figure)
 Trough cross-beds
 Ripple lamination
 Climbing ripple lamination

Grain size
 M = Mudrock
 S = Sandstone
 G = Granule
 P = Pebble

This results in the thick stacked successions of trough cross-bedded sandstones that characterise the Boss Point Formation.

Channel-filling cycles similar to those described herein have previously been recognised from the Boss Point Formation (McCabe 1978a, Plint 1986) and from a number of other Carboniferous units such as the Shepody and Maringouin Formations (McCabe 1978b), the Port Hood Formation (Gersib and McCabe 1981), the Pictou Group (van de Poll 1970), and the Morien Group of Cape Breton Island (Masson and Rust 1990, Dr M.R. Gibling, Keynote Address to the Canadian Sedimentological Research Group, May 1990).

Both meandering and braided fluvial systems may develop fining-upward cycles (cf. Allen 1965, Leeder 1973).

The Boss Point Formation channel-filling cycles are here interpreted as the product of repeated channel avulsions, and are not unlike the avulsion related cyclicity reported by Bridge (1984). The base of each Boss Point Formation cycle represents the scouring event at the initiation of avulsion, the lack of a fining trend and variation in sedimentary structures throughout much of the cycle, suggests that flow velocity was relatively constant during the deposition of the cycle (when trough cross-beds were deposited). Flow velocity decreased sharply only at the top of the channel and was marked by the transition to ripple cross-laminated sandstones, climbing rippled sandstones and mudrocks. This transition to ripple cross-

laminated sandstone and mudrock units marks either avulsion, passive filling, or the end of the flood episode within the channel. Once the channel had been abandoned, soils may have developed on the abandoned fluvial surface, consistent with the observation of soils at the top of some Boss Point Formation cycles.

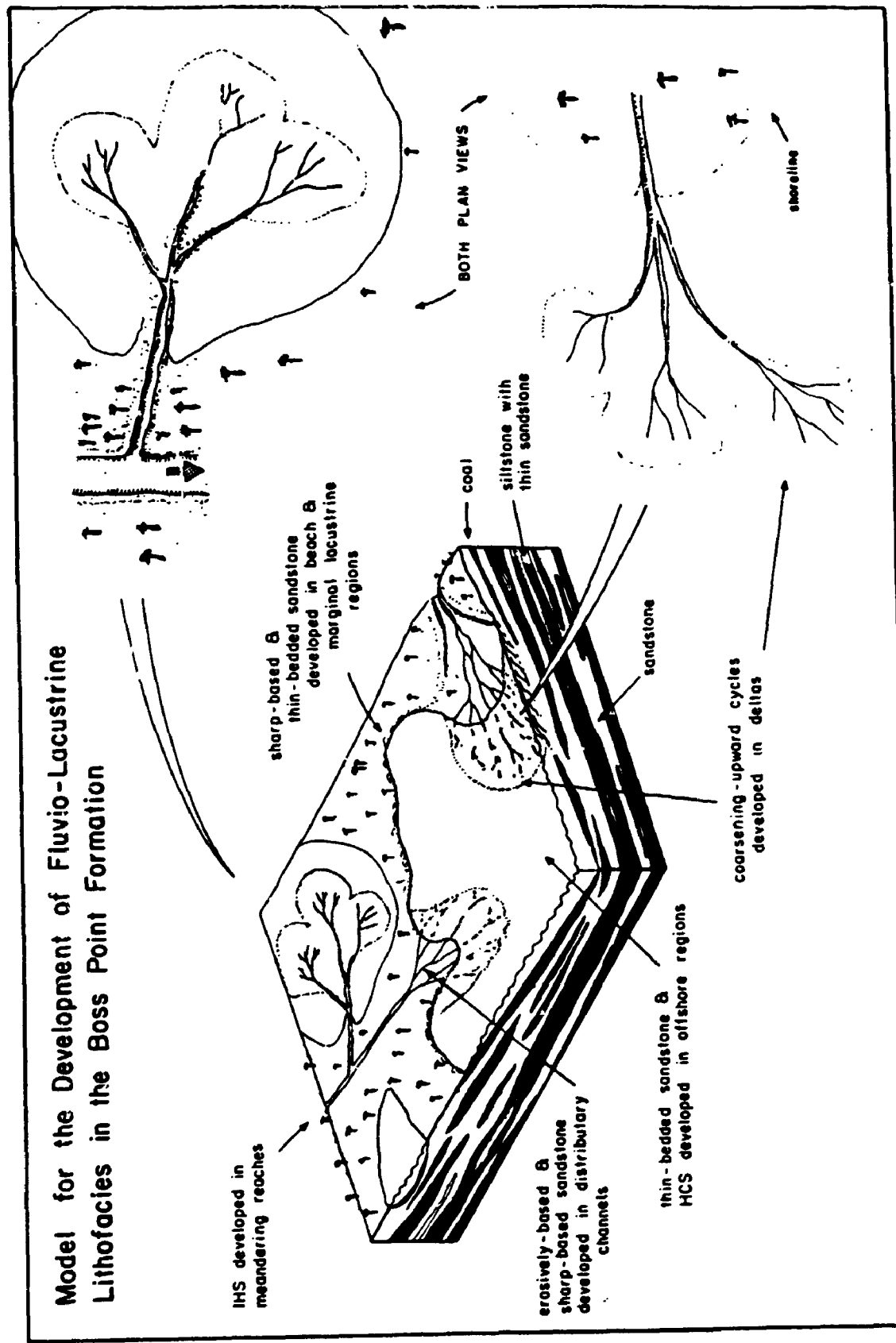
The process of avulsion is typically associated with aggradation (development of an alluvial ridge) and tectonic tilting (Bridge and Leeder 1979), the floodwaters initiating avulsion by the enlargement of crevasse channels (Bridge (1985)).

7.2 FLUVIO-LACUSTRINE FACIES ASSOCIATION

Alternating fine-grained sandstone and mudrock units occur interstratified with the braided fluvial facies association (described above), and form stratigraphic intervals as much as 40 m thick. The fluvio-lacustrine association comprise cm- to dm-bedded, ripple cross-laminated, horizontally bedded, planar cross-bedded and minor trough cross-bedded and massive sandstone units (Sr, Sh, Sp, St and Sm), interstratified with massive or laminated sandy siltstone, siltstone, claystone and paleosols (Fm, Fl and P). Inclined heterolithic stratification (IHS), ball and pillow structures and rooted horizons may also be present (Fig. 7.4). Units of fluvio-lacustrine facies association typically rest abruptly on

Fig. 7.4 Conceptual model for the deposition of the fluviolacustrine units in the Boss Point Formation. Note the similarities in deltaic depositional facies developed from either crevasse splay mechanisms or prograding (subaqueous) deltas.

Model for the Development of Fluvio-Lacustrine Lithofacies in the Boss Point Formation



underlying trough cross-bedded sandstones. The tops of the fluvio-lacustrine association are typically sharp, and erosionally truncated by the overlying units of braided fluvial sandstones. Relief on these erosion surfaces may be 10 m. Tops to the alternating sandstone and mudrock units are typically sharp, and erosionally truncated by the overlying trough cross-bedded sandstone, conglomerate and pebbly sandstone strata.

Many of the attributes of these sandstone-mudrock units have previously been discussed under the respective lithofacies descriptions (Chapters 4 & 5). Vertical facies relationships are described in greater detail here. Six basic variants are recognised (Figs. 7.5 & 7.6); a) coarsening-upward cycles, b) erosively-based sandstones, c) sharp-based sandstones, d) thin-bedded sandstones, e) inclined heterolithic stratification (IHS) units and f) hummocky cross-stratification (HCS) units.

7.2.1 Coarsening-Upward Cycles

Coarsening-upward cycles, have been recognised in this study at Johnson Mills, Slacks Cove West, Grindstone Island, Giffin Pond and within the upper lacustrine unit exposed at Cape Enrage (Figs. 5.5 & 7.6, Plate 13d). Exposures are characterised by dm- to m-thick (up to 15 m) intervals of claystone (base), siltstone and sandy siltstone, which grade upward into very fine-grained

Fig. 7.5 Facies types developed in the fluviolacustrine association. Diagrams not drawn to same scale. Stratigraphic symbols are the same as those used for stratigraphic columns (Volume II).

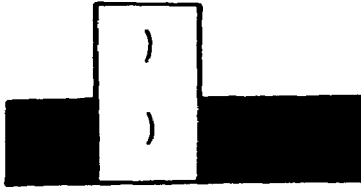
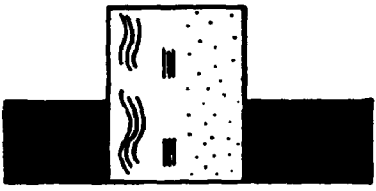
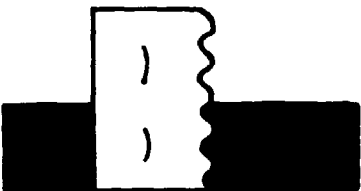

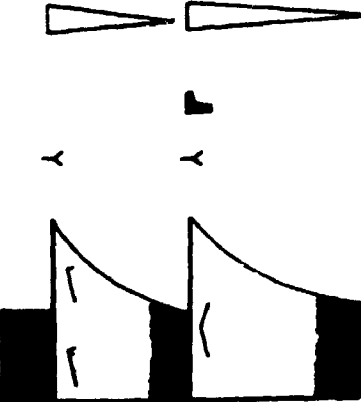
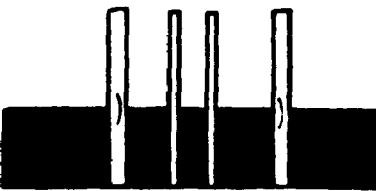
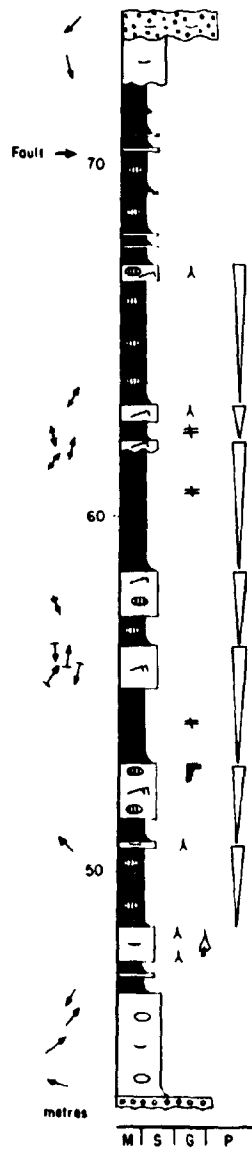
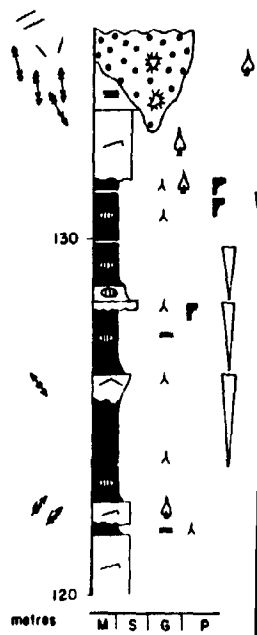
<p>Sharp-based sandstone</p> 	<p>HCS units</p> 
<p>Erosively-based sandstone</p> 	<p>IHS units</p> 
<p>Coarsening-upward cycles</p> 	<p>Thin-bedded sandstone</p> 

Fig. 7.6 Fluvio-lacustrine successions from 6 representative stratigraphic sections in the Boss Point Formation. Other examples can be found in the stratigraphic sections presented in Volume II.

A. Johnson Mills



B. Grindstone Island

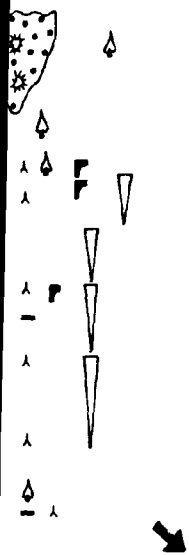


E. Boss Point

TOP OF

F. Boss Point

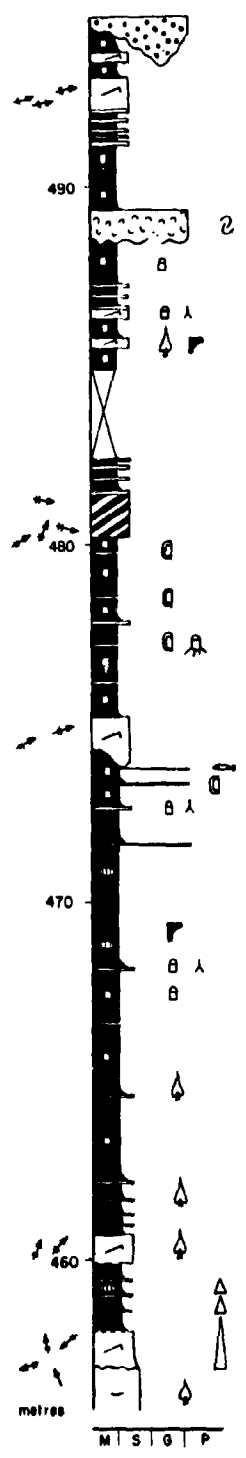
one Island



G | P

Point

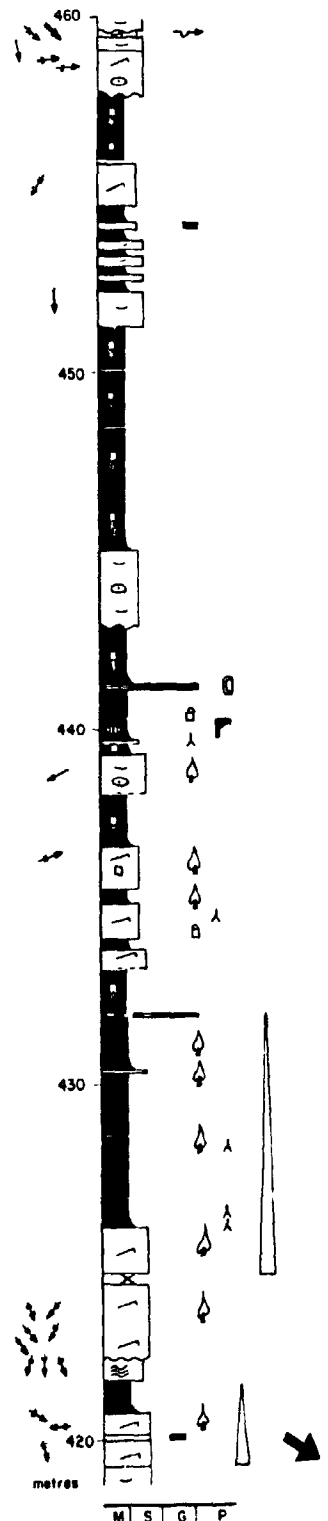
C. Cape Maringouin



metres

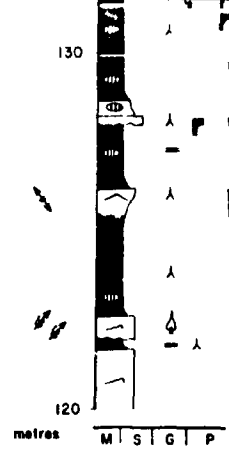
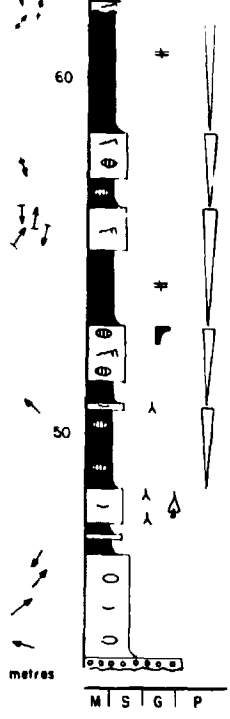
M | S | G | P

D. Rockport

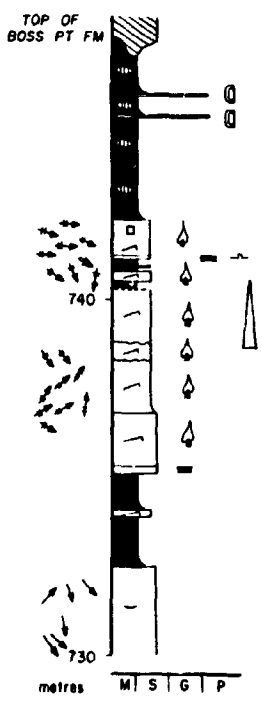


metres

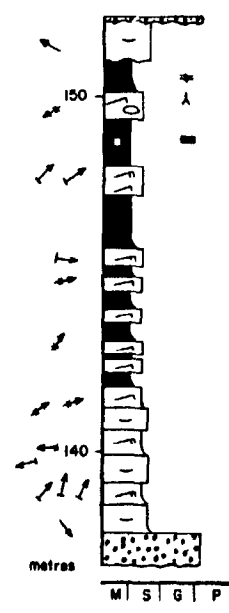
M | S | G | P

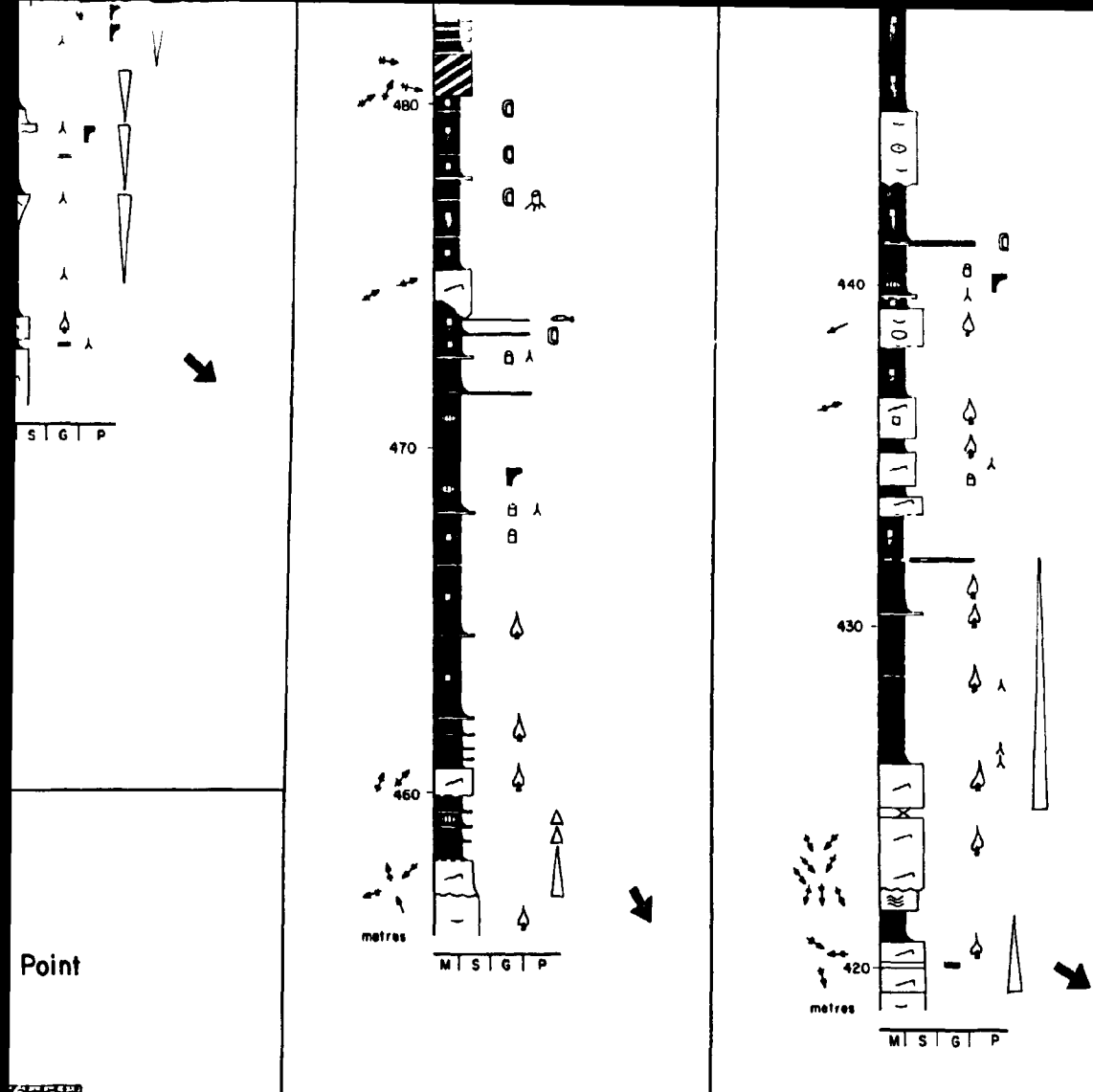


E. Boss Point



F. Boss Point





Point

LEGEND

- | | |
|--|----------------------------------|
| Conglomerate, with fluted siltstone clasts | Pebble sandstone |
| Trough cross-bedded pebbly sandstone | Trough cross-bedded sandstone |
| Planar cross-bedded sandstone | Ripple laminated sandstone |
| Climbing ripple laminated sandstone | Horizontally laminated sandstone |
| Massive sandstone | Wavy bedding - 3D dunes |
| Wave ripple laminated sandstone | Ball and pillow |
| Inclined heterolithic stratification | Mudrock |
| Coal / coaly shale | Not exposed |
-
- | | | |
|--------------------------------|----------------------|---|
| Comminuted carbonaceous debris | Rootlets | Massive bedding |
| Paleosol | Convolute bedding | Concretions |
| Ostracod - limestone | Fish-scale fragments | Flutes |
| Siderite nodules | Calcrete nodules | Vertical or subvertical calcareous tube (rhizolith) |
| In situ tree stump | Fining-upward cycle | |
| Coarsening-upward cycle | | |
- Paleocurrents (north to top of figure):
- | | | |
|----------------------|---|----------------------------|
| Trough cross-bedding | Ripple lamination | Climbing ripple lamination |
| Flutes | Orientation of logs | Rib and furrow |
| Parting lineations | Dominant paleocurrent trend from entire section - see Fig 8 1 | |
- All sections drawn to same scale. Numerical values which appear with each column refer to stratigraphic position (in metres) above the base of each section.
- Grain size:
 M = mudrock S = sandstone G = granule P = pebble

current and wave rippled sandstones, together with horizontally bedded and trough cross-bedded sandstones. Tops of sandstones typically contain rootlets (such as *Stigmaria*- Fig. 7.6) or paleosols, and at Cape Enrage, one example shows runzel marks (Plate 14a & 14b). Pedogenic calcrete nodules are common in both sandstone and finer-grained siltstone units. Ripple cross-lamination and climbing ripple lamination show a wide variation in paleocurrent trends, from parallel to divergent with respect to paleocurrents from trough cross-bedding (Fig. 7.6).

Coarsening-upward cycles similar to those recognised in the Boss Point Formation have been described by Elliott (1974, 1976), Schäfer and Sneh (1983), Fielding (1984), Guion (1987) and Tye and Coleman (1989) who attribute them to fluvio-deltaic deposition.

The Boss Point Formation examples are similar to the distal lacustrine delta model of Guion (1987), although in the Nottinghamshire case described by Guion (1987) the mudrocks at the base of the cycles consist of interbedded siltstone and sandstone. The general lack of sandstone suggests that such deltas were very small, and the preferred depositional model is the lacustrine delta front setting described by Coleman and Gagliano (1965), Elliott (1974, 1976), Fielding (1984) and Tye and Coleman (1989). The delta front is an area of shoaling and rapid deposition associated with a relatively small prograding distributary

channel (Coleman and Gagliano 1965, fig. 3), and is dominated by small-scale ripple cross-lamination (Tye and Coleman 1989). The horizontally laminated sandstones likely represent beaches which developed in shallow areas on these deltas, although some of them (see below), certainly represent beach facies developed around the margins of the lakes, not necessarily associated with deltas.

Shoaling may also be enhanced by the colonisation of the deltas by vegetation and ultimately this may lead to rooted horizons, paleosols or the development of coals at the top of the coarsening-upward cycles (Elliott 1986, Fielding 1984, Guion 1987, Tye and Coleman 1989). Although coal was never developed on the tops of the Boss Point Formation cycles (as was the situation in the Carboniferous Yoredale successions described by Elliott 1976), the presence of paleosols atop some of the cycles in the Boss Point Formation indicate that some of the distributary mouth bars became subaerial and experienced prolonged periods of sediment starvation and pedogenesis.

7.2.2 Erosively-Based Sandstones

These units consist of erosively-based, dm- to m-thick, fine- to medium-grained, ripple cross-laminated, and trough cross-bedded sandstones. Paleocurrents display a wide spread. Typically the erosively-based sandstones show calcrete nodules and other signs of paleosol development,

such as rooted horizons, and therefore subaerial exposure.

The lithofacies is similar to the distributary mouth bar facies of Tye and Coleman (1989) in terms of both the thickness of individual channel sand deposits, and abundance of ripple cross-laminated and trough cross-beds. In the Boss Point Formation the erosively-based sandstones do not form extensive thicknesses (unlike the Mississippi situation), suggesting that if they were deposited as part of a distributary mouth bar, that such distributary channels were either small or short lived, or provided little sediment.

The erosively-based sandstones are similar to the channelised, erosively-based sandstones described by Fielding (1984), who regarded them as crevasse splay channels. The proximal crevasse splay channels described by Fielding from the Westphalian Durham Coalfield are characterised by erosively-based trough cross-bedded and ripple cross-laminated sandstones. These units however are up to 7 m thick, much thicker than units found in the Boss Point Formation. The Durham units also show unimodal paleoflow directions, unlike the wide paleocurrent spread found in the Boss Point Formation.

These features may suggest more distal crevasse splay settings, equivalent to the medial or distal crevasse splay facies of Fielding (1984), but these are characterised by interbedded sandstone and siltstone lithologies, erosive contacts at the base of sandstones, and abundant trough-

cross-bedding. The Boss Point Formation examples, however, lack the interbedded sandstone and siltstone units and the coarsening-upward trends recorded from this facies by Fielding. Both the medial and distal crevasse splay facies were deposited by high energy traction currents and by density induced underflow mechanisms (Fielding 1984), underflow being common in crevasse-initiated lake delta systems (Gilbert and Shaw 1981, Weirich 1986), though nothing of a classic turbidite Bouma subdivision was observed in the Boss Point Formation.

7.2.3 Sharp-Based Sandstones

Sharp-based trough and ripple cross-laminated sandstones are morphologically similar to the erosively-based channel sandstone deposits described above, except that the base (and top) of beds are sharp. Many of them were clearly associated with subaerial conditions for they contain calcrete nodules, rootlets and paleosols.

Similar facies have been described from delta front environments in the modern (Tye and Coleman 1989), and from distal crevasse splay/minor delta facies by Fielding (1984), but not in association with (subaerial) rootlets and pedogenic features. The sandstones are regarded as either sharp-based equivalents of the erosively-based sandstone lithofacies developed in distributary channels on deltas (Fig. 7.4), or were formed in marginal lacustrine

regions such as beaches, shore face or interdistributary bays, that experienced frequent lake level fluctuations. Water level fluctuations are common in most lakes (Picard and High 1981), especially those in semi-arid or arid climates, a semi-arid climate being suggested during the time of Boss Point Formation sedimentation (see Chapter 6).

7.2.4 Thin-Bedded Sandstones

Centimetre-thick, sharp-based ripple cross-laminated and horizontally laminated sandstones are common throughout the fluvio-lacustrine intervals. The sandstones are associated with rootlet and rhizolith horizons, abundant comminuted carbonaceous debris, ostracod-bearing limestones and paleosols.

These units are similar to the minor delta/overbank claystone facies described by Fielding (1984), the distal lacustrine delta facies described by Guion (1987) and to the prodelta (horizontally laminated) and delta front (ripple cross-laminated) sediments described by Tye and Coleman (1989). Delta front sediments usually display abundant soft sediment or scour-and-fill structures, features which are absent in the Boss Point Formation units.

It is suggested that the thin-bedded sandstones in the Boss Point Formation were deposited in beach, shore face or interdistributary bay settings, which were subject to

pedogenic development during periods of emergence, similar to the sharp-based sandstone lithofacies described above.

7.2.5 Inclined Heterolithic Stratification Units

Inclined heterolithic stratification units have previously been described in Chapter 4, where it was suggested that they formed when meandering fluvial channels entered lacustrine settings. As such they probably represent the feeder channels to the deltas or mouth bars described above.

7.2.6 Hummocky Cross-Stratification Units

Hummocky cross-stratification developed in offshore lacustrine areas and has previously been described in Chapter 4.

7.3 Recognition of a Large-Scale Stratification Hierarchy- Megacycles

Erosionally-based fining-upward cycles in the order of a few to 25 m in thickness have already been described in section 7.1. In the Boss Point Formation, these fining-upward cycles occur stacked on top of each other, and as such, form sandstone packages 10's of metres to 130 m in thickness. Alternating with these stacked trough cross-

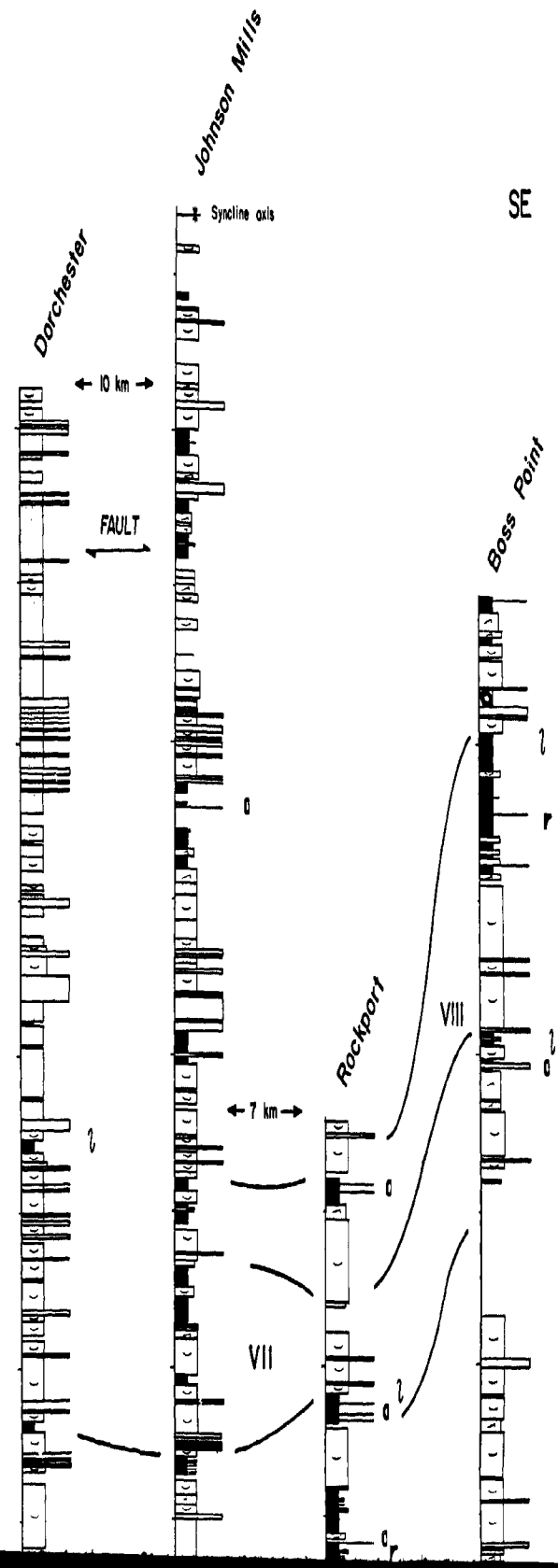
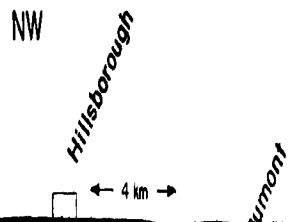
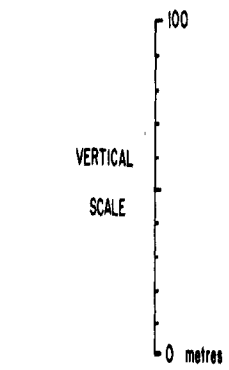
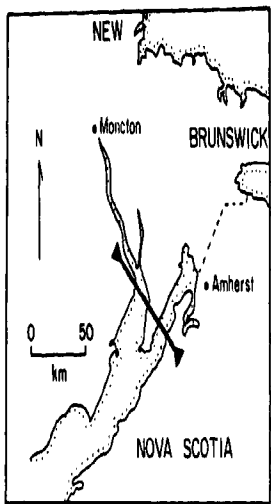
bedded sandstone units are typically thinner bedded, up to 60 m thick, siltstone and fluvio-lacustrine mixed siltstone and sandstone units.

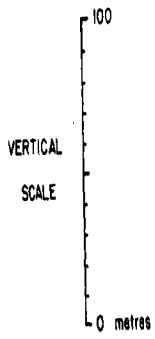
Together these sandstone and siltstone units form the largest stratification hierarchy recognised from the formation, and are called megacycles. Each megacycle consists of a sharp (typically erosive) sandstone base, overlain by stacked sandstone units (Plate 5a, 5d & 5e), which are overlain sharply by the siltstones of each megacycle. Megacycles can be traced between adjacent stratigraphic sections (Figs. 7.7 & 7.8), and can be recognised over lateral distances of up to 20 km across the Bay of Fundy region.

At least 8 such megacycles (referred to as megacycles I to VIII) are recognised from the formation, and there is a possibility that other megacycles occur at the top of the formation, though these are poorly defined due to lack of sufficient stratigraphic control. The significance of these megacycles is considered further in Chapter 10.

7

Fig. 7.7 Stratigraphic correlation diagram from Hillsborough to Boss Point (NW to SE), showing the development of megacycles (labelled I to VIII) in the Boss Point Formation. Inset locality map shows relative position of NW-SE transect.





NW

Hillsborough

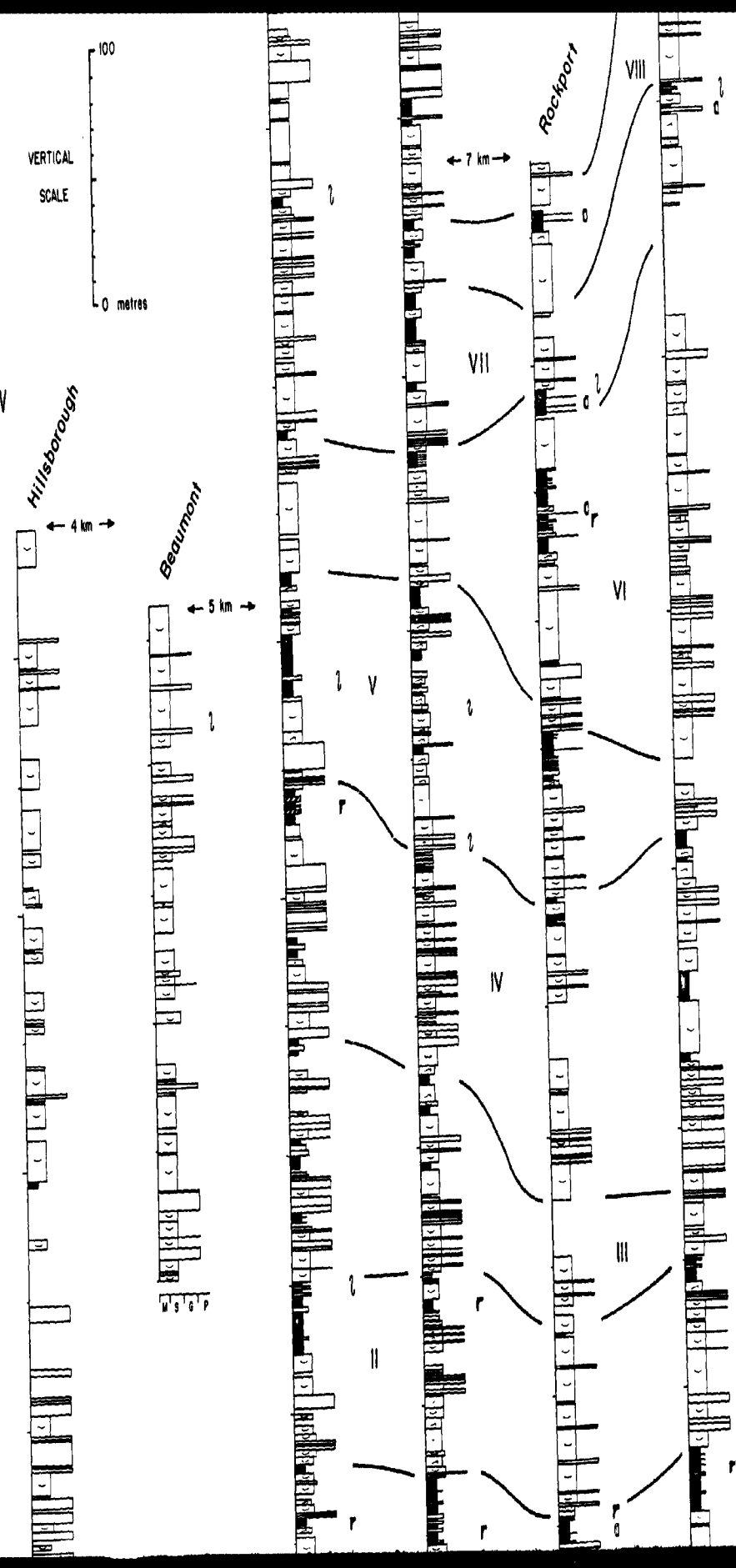
4 km

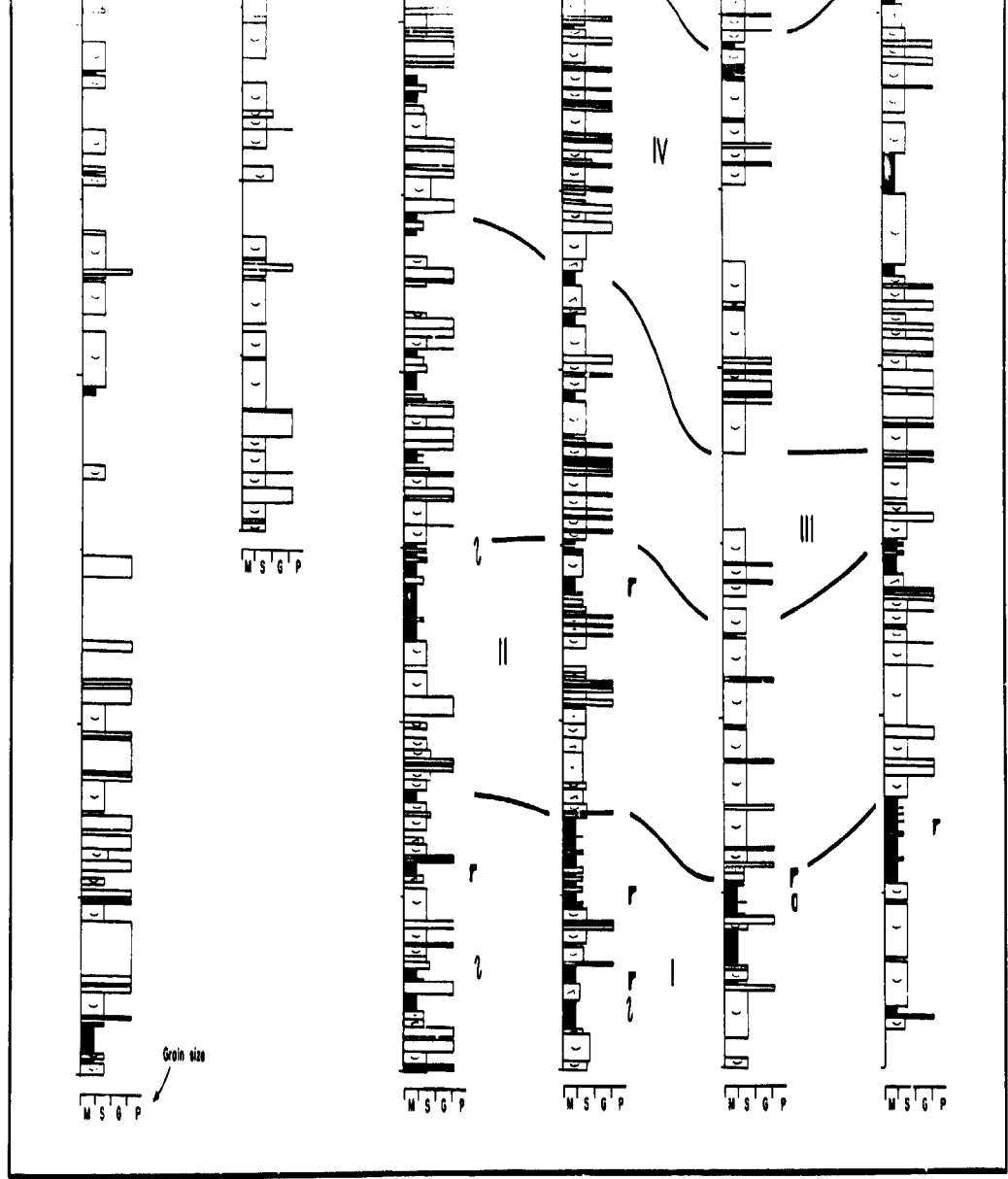
Beaumont

5 km

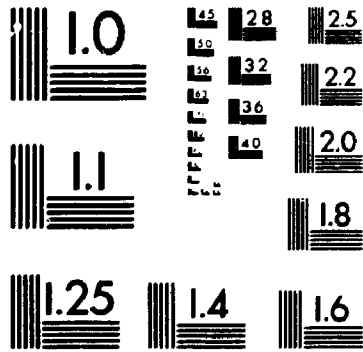
Rockport

7 km



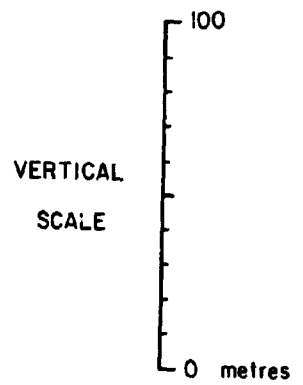
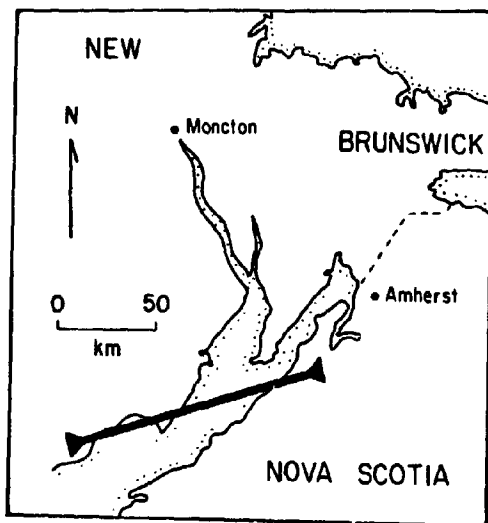


7



MICROCOPY RESOLUTION TEST CHART
NATIONAL BUREAU OF STANDARDS
STANDARD REFERENCE MATERIAL 1010a
(ANSI and ISO TEST CHART No. 2)

Fig. 7.8 Stratigraphic correlation diagram from Boss Point to Alma (NE to SW), showing the development of megacycles (labelled I to VIII) in the Boss Point Formation. Inset locality map shows relative position of NE-SW transect.



← 4 km

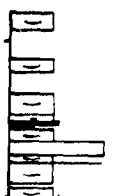
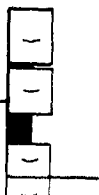
SW

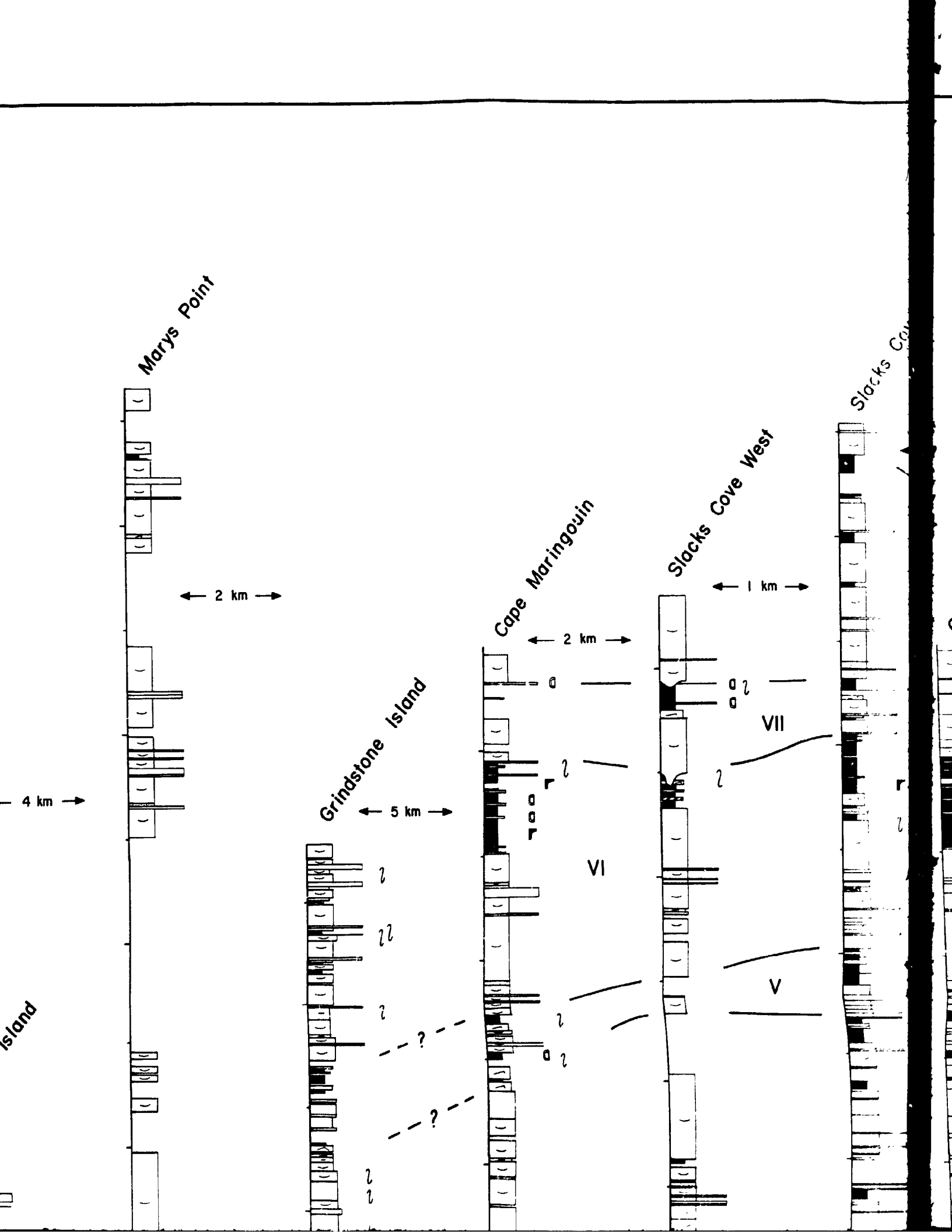
Cape Enrage

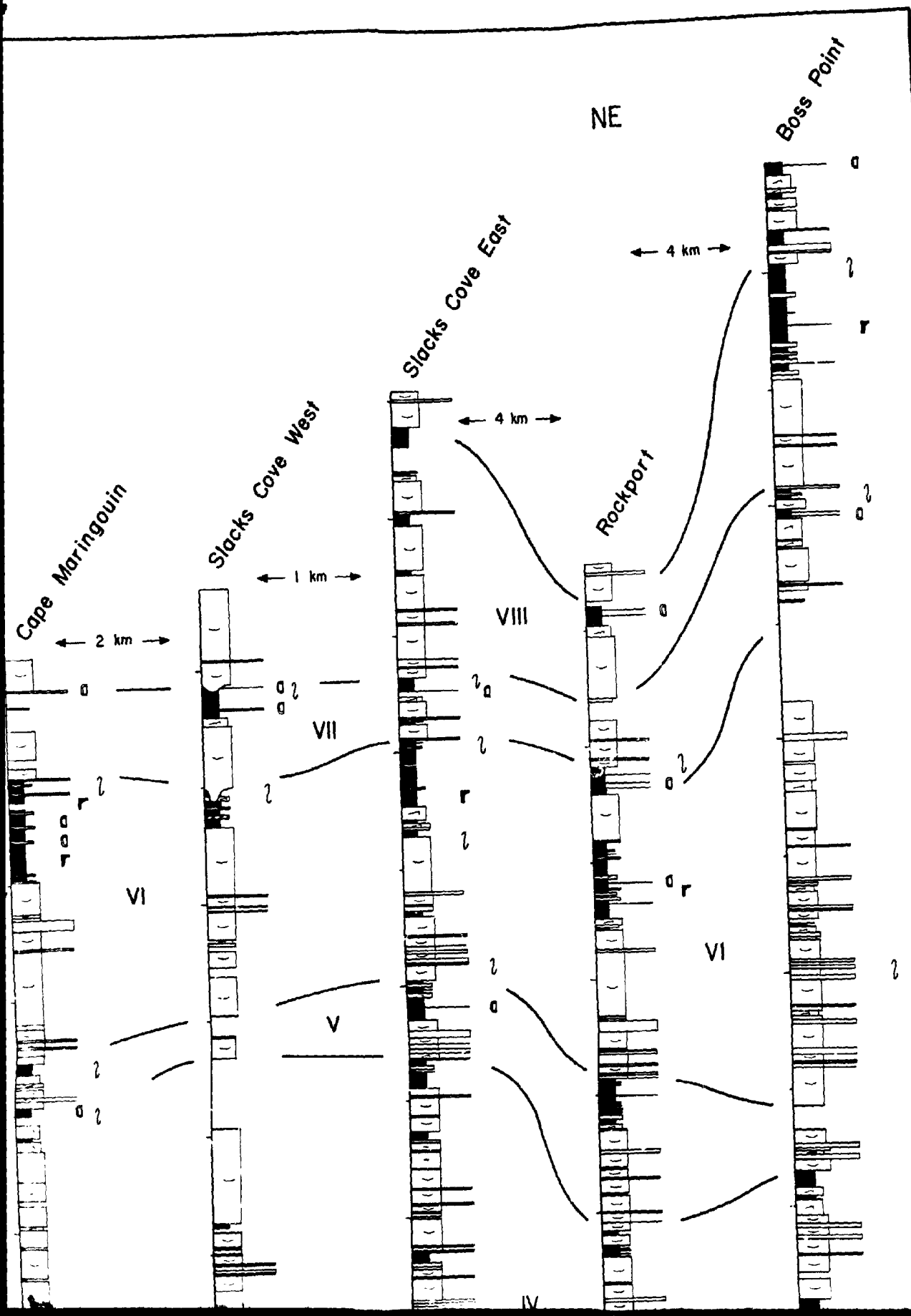
Long Island

← 16 km →

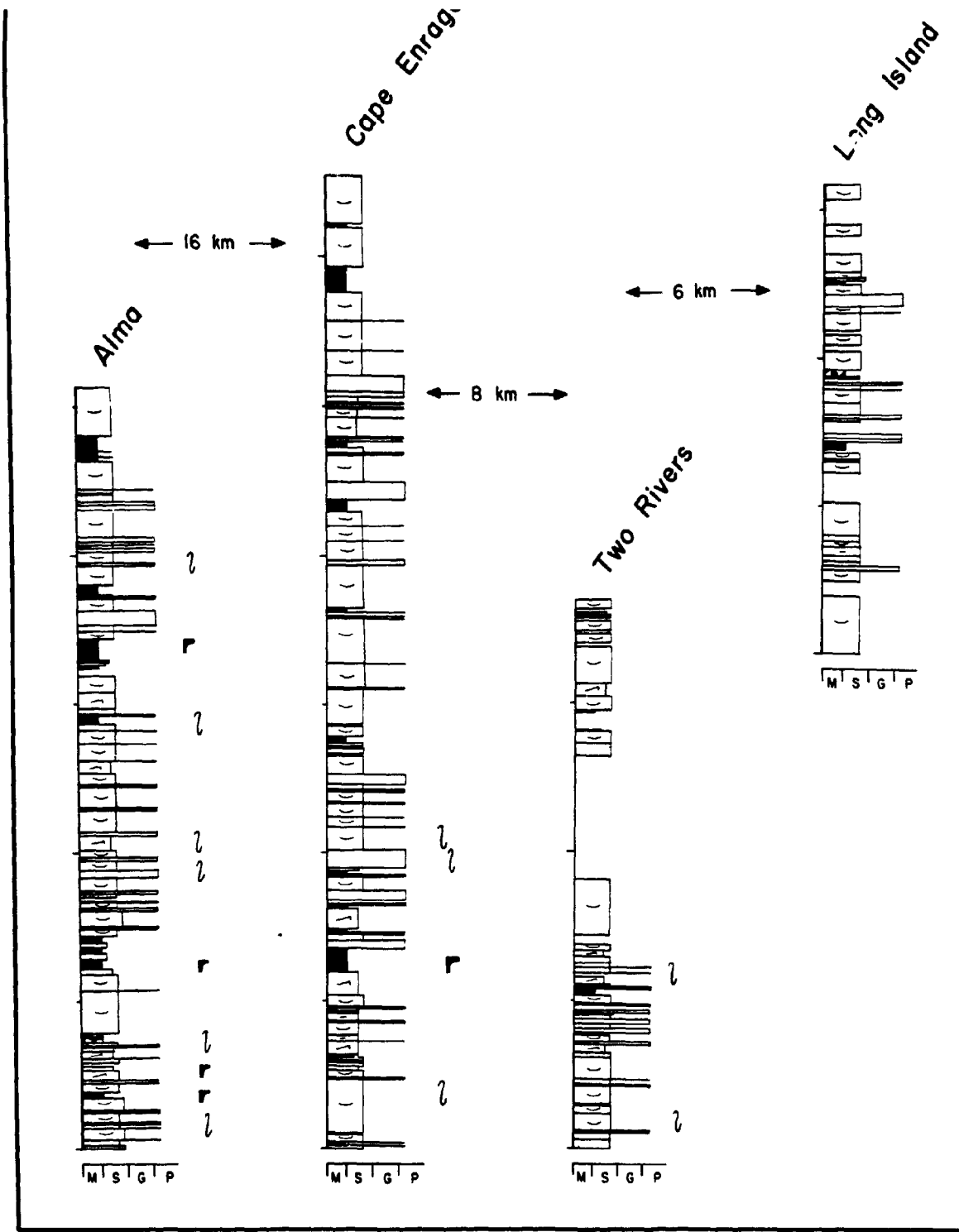
← 6 km →



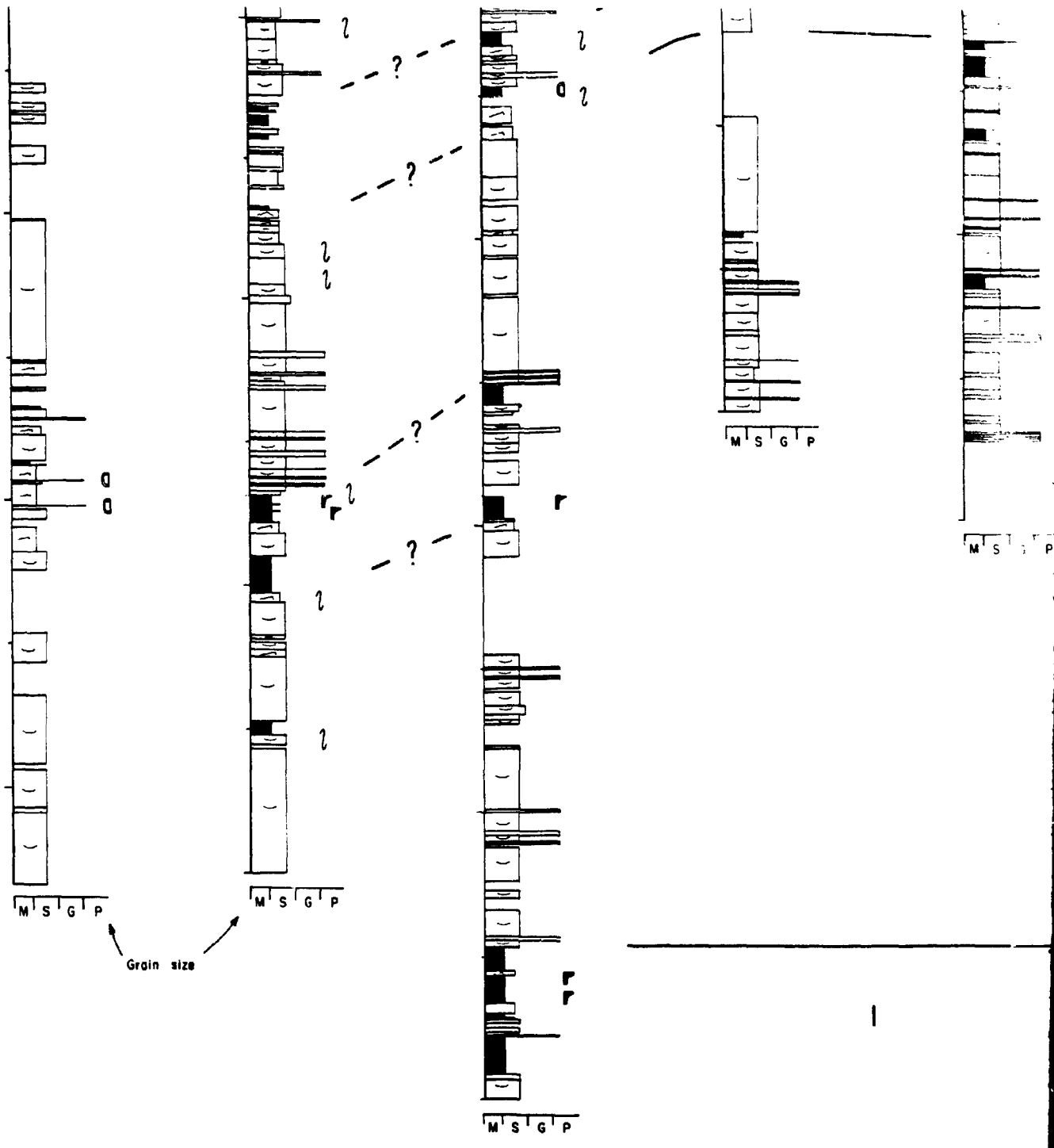








Quartz



Grain size

M S G P

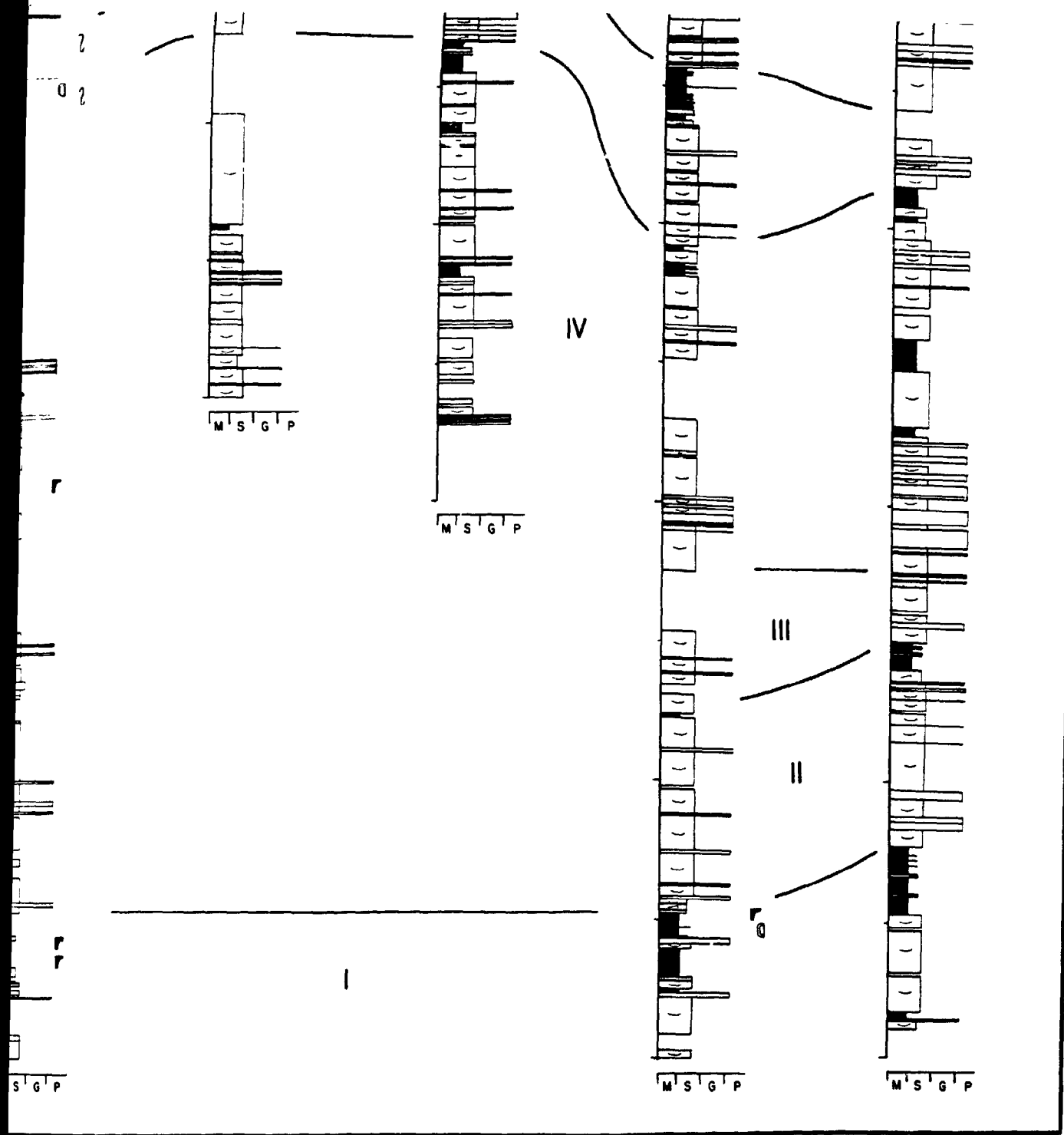
M S G P

M S G P

M S G P

M S G P

M S



2

0 2

M S G P

M S G P

IV

M S G P

M S G P

S G P

r

r

I

II

III



CHAPTER 8

PALEOCURRENT DIRECTIONS

Paleocurrents measurements were obtained from a variety of lithofacies within the formation. These are described in detail below.

8.1 Paleocurrents from Trough Cross-Bedded Sandstones

8.1.1 Trough Cross-Bedding

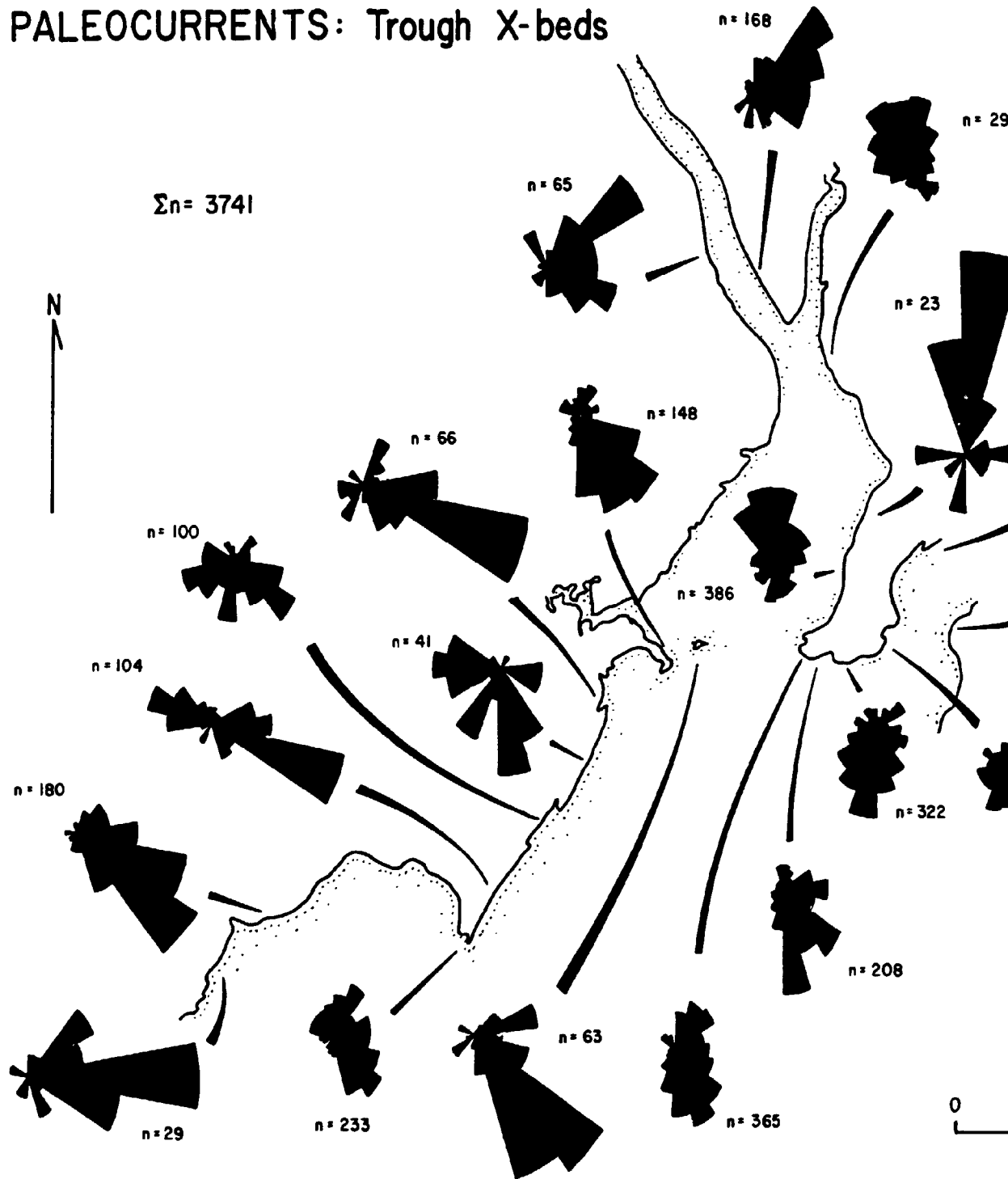
Shore platform exposures have facilitated measurement of over 4100 paleocurrent azimuths from trough cross-bedding. The trough cross-sets represent 3-dimensional dune structures which migrated within channels, and are therefore regarded as the most reliable paleocurrent indicator in the formation. They indicate paleoflow directions to the east in the southern and central parts of the Bay of Fundy region, and toward the northeast in northern Nova Scotia (Fig. 8.1). However many local variations are evident, and these indicate important features of the Carboniferous paleogeography (see also Chapter 9).

No paleocurrent measurements were obtained from the Moncton sub-basin largely because of poor exposure. However in that region, van de Poll (1966, fig. 5; 1970,

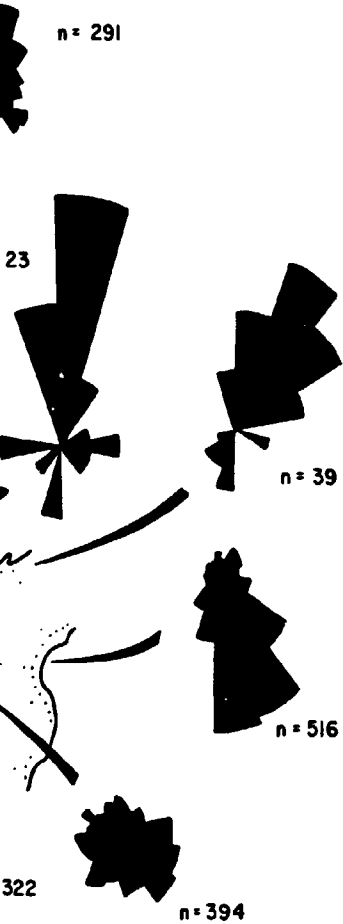
Fig. 8.1 Paleocurrents determined from trough cross-bedding in the Boss Point Formation. Map (i) is a detailed representation of the Bay of Fundy region.

PALEOCURRENTS: Trough X-beds

$\Sigma n = 3741$



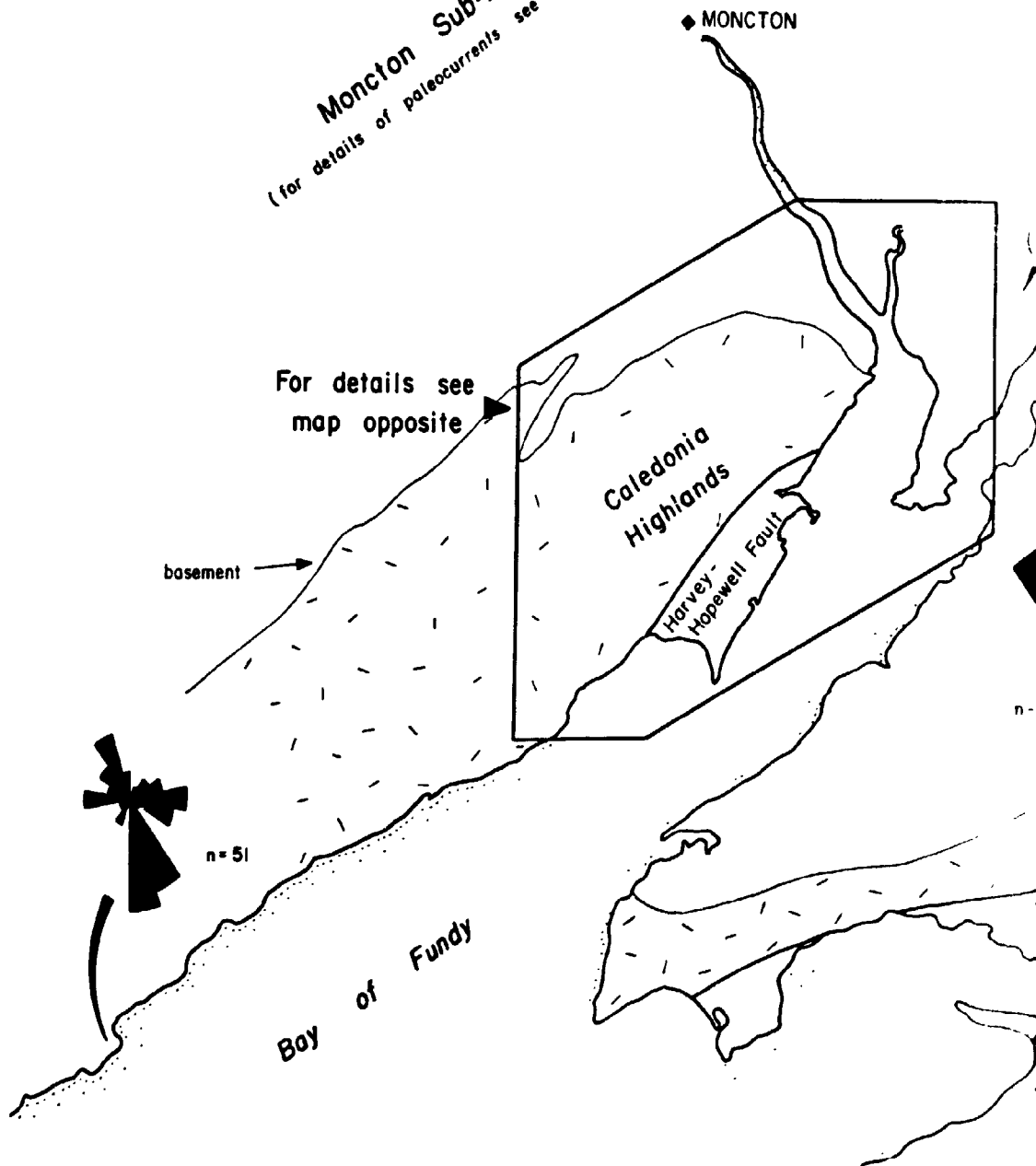
(i)



0 10 km

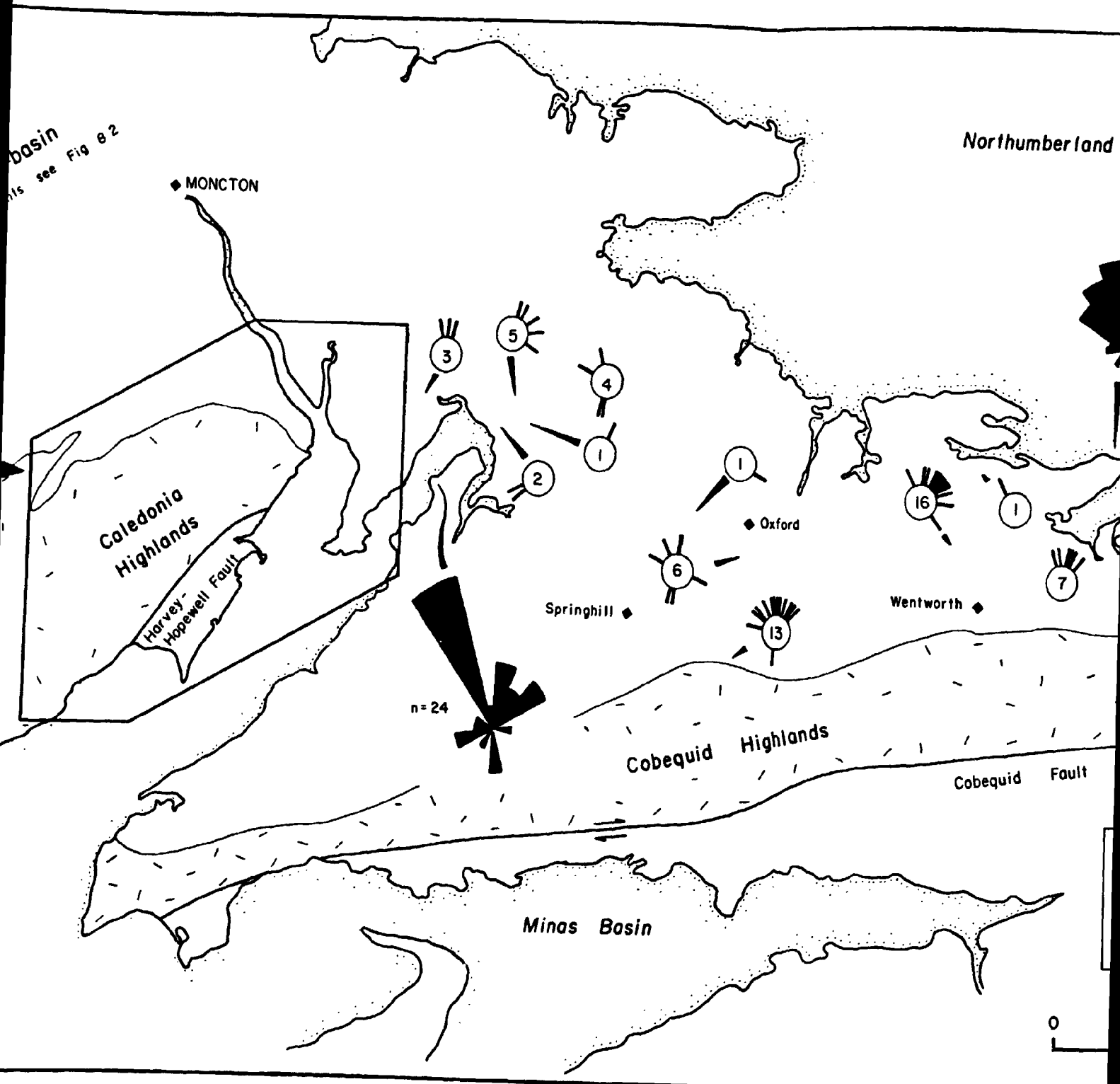
$\Sigma n = 366$

Moncton Sub-basin
(for details of paleocurrents see Fig. 8.2)



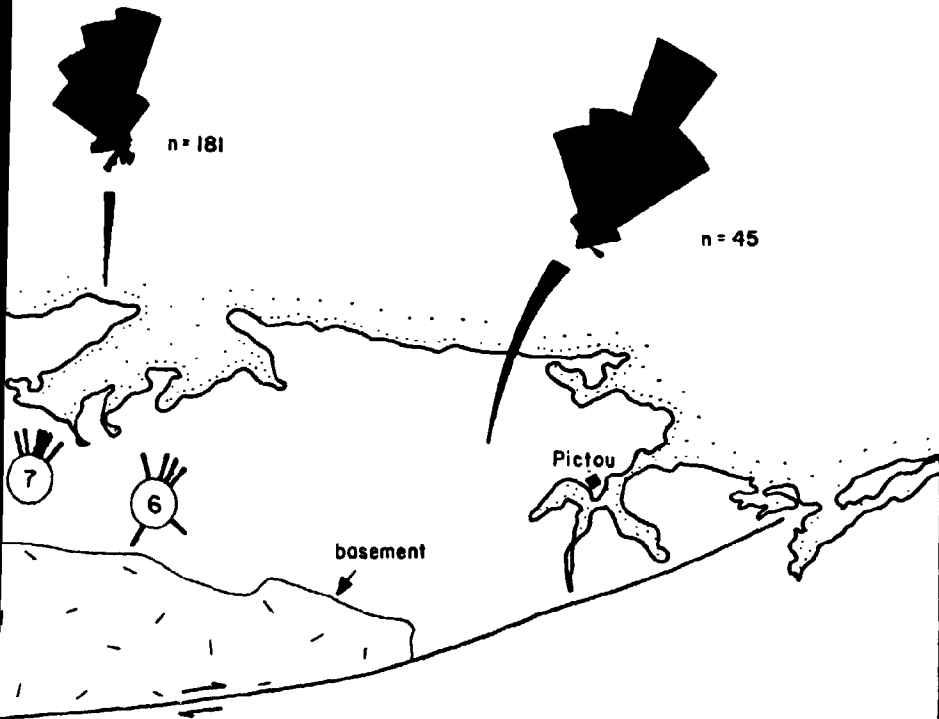
basin
see Fig 8 2

Northumberland



(ii)

erland Strait



Fault

② Paleocurrents & number of observations at each site

0 10 % of observations (rose diagrams)

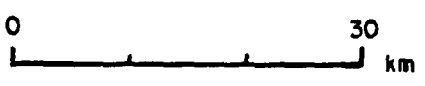


fig. 18) indicated uniform north and northeasterly paleocurrents (Fig. 8.2).

With regard to the western side of the Cumberland sub-basin, paleocurrents show consistent easterly trends in the south and central parts of the Bay of Fundy region, with a swing to a more southerly azimuth in the vicinity of Cape Maringouin and Boss Point (Fig. 8.1). North and northwest of these localities, trough cross-bedding indicates predominantly northeasterly paleocurrent trends, approximately opposite to trends observed further to the south. A demarcation therefore exists between predominantly southerly paleocurrents south of (and including) the Cape Maringouin area, whereas north of this, northerly paleocurrent trends are evident (Figs. 8.1 & 8.3).

These patterns are similar to those reported previously for the Boss Point Formation in the Bay of Fundy region (Lawson 1962, Fig. 8.2), though they were interpreted differently. Similarities can also be seen with the paleocurrents recorded from a large group of Carboniferous rocks (Gibling *et al.* 1989). The trends recorded in the present study however are approximately at right angles to those reported by van de Poll for the Boss Point Formation (van de Poll 1966, 1970 - reproduced as Fig. 8.2B & 8.2C). van de Poll's studies indicated consistent northeasterly paleocurrents for the entire western Cumberland sub-basin and the Moncton sub-basin. The trends reported in this

Fig. 8.2 Paleocurrents determined by previous workers from the Boss Point Formation. Maps are all based on measurements of trough cross-bedding. Maps B and C are from van de Poll and show mean azimuth directions.

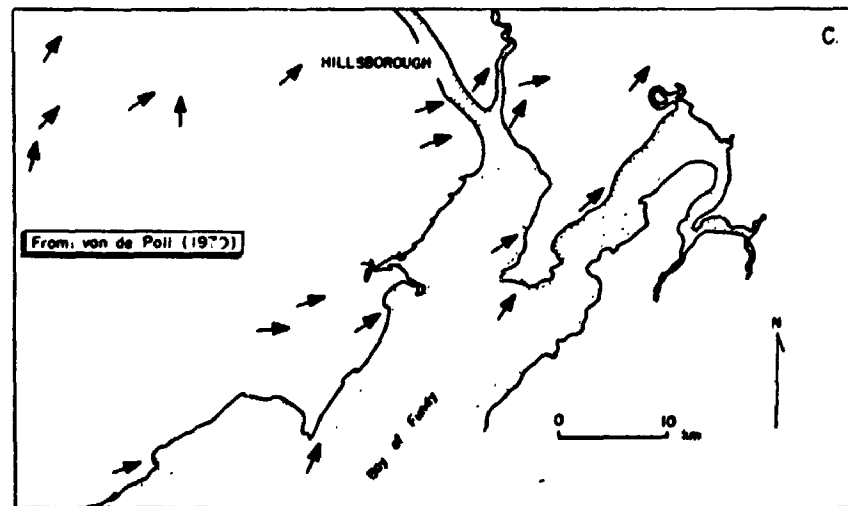
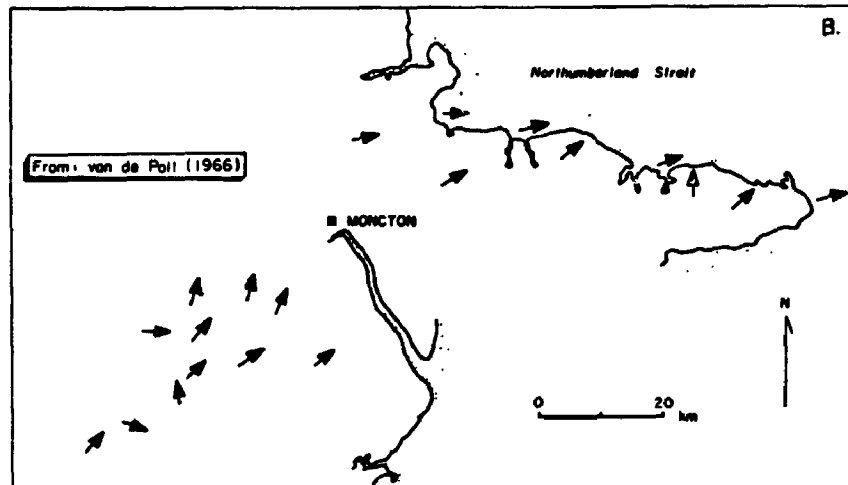
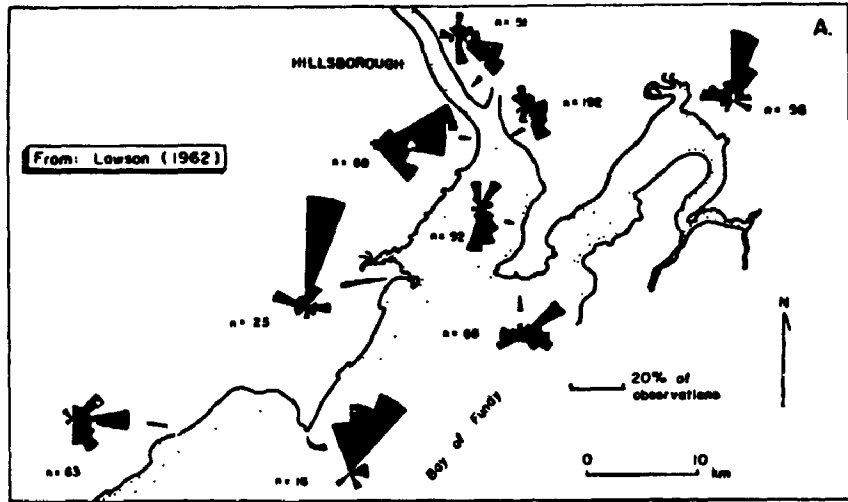
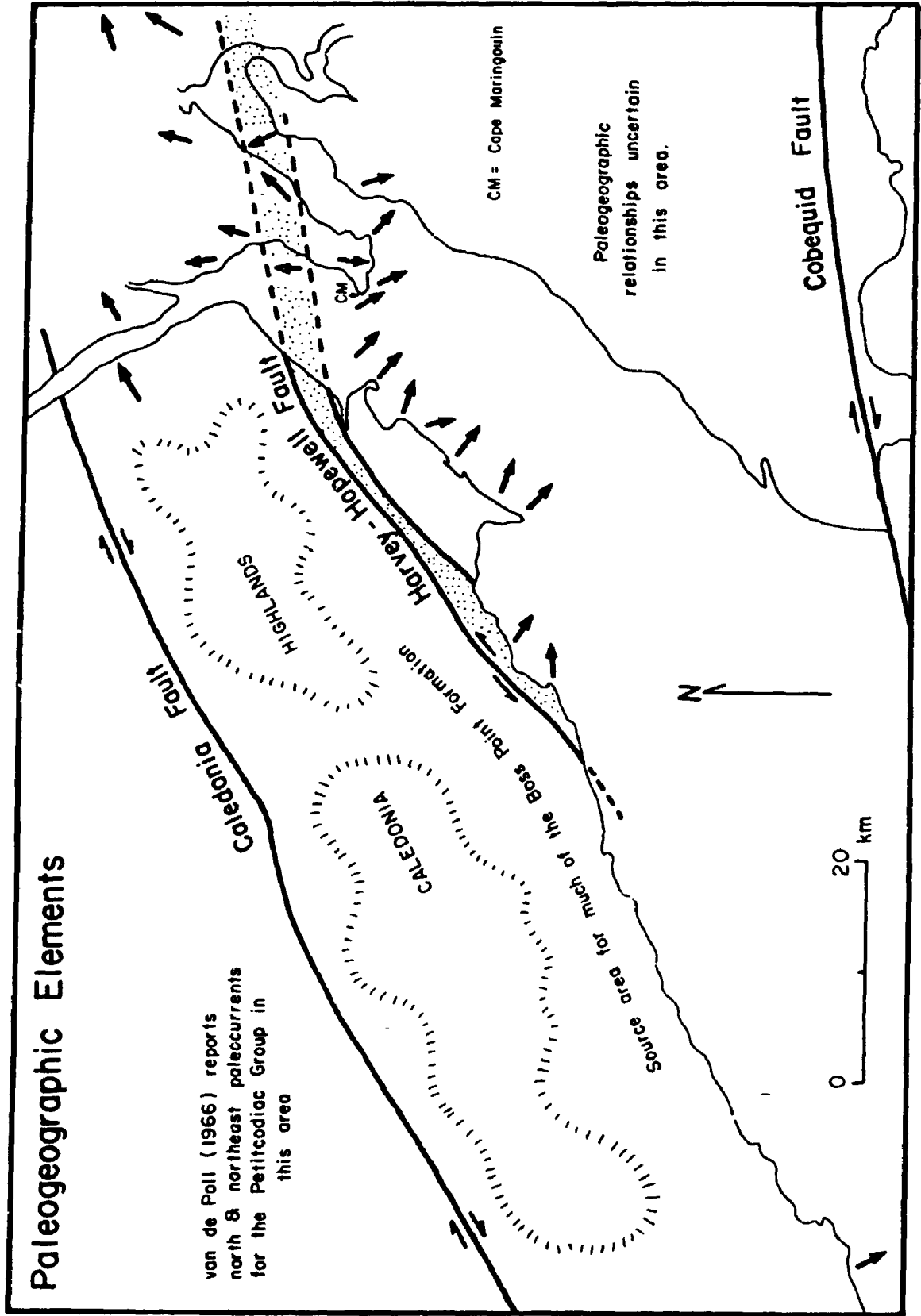


Fig. 8.3 A paleogeographic reconstruction of the western margin of the Cumberland sub-basin, with dominant paleocurrent directions (from trough cross-bedding) indicated. Note the existence of the paleogeographic high through the central parts of the map area, and its close association with the Harvey-Hopewell Fault.



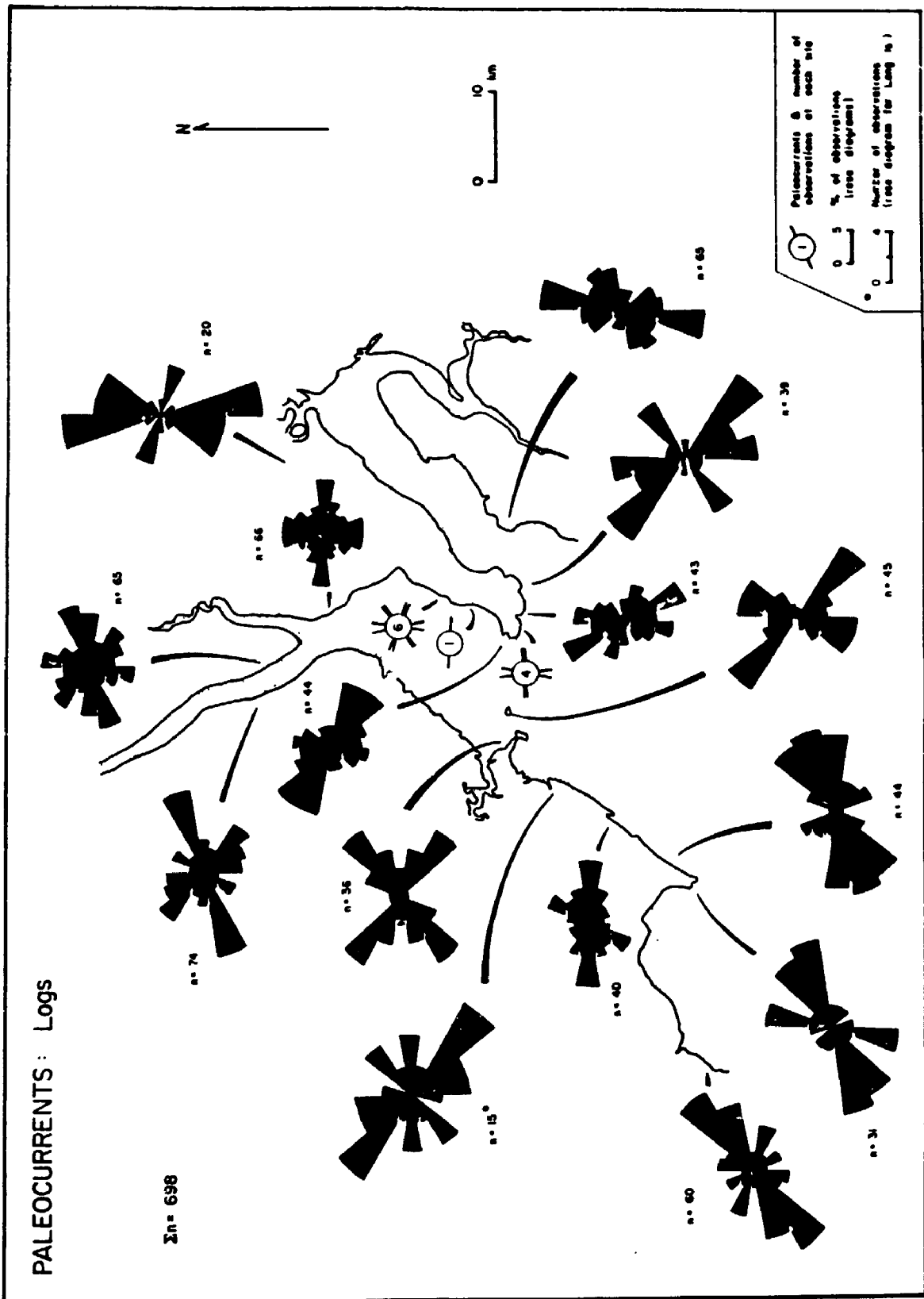
study are also at variance to the northwest source area determinations suggested by McLeod and Ruitenberg (1978) for the Boss Point Formation.

In northern Nova Scotia, paleocurrents determined from trough cross-bedding trend north and northeast, essentially away from the Cobequid Highlands, and are similar to trends reported from Late Carboniferous rocks by other workers (Fralick 1981, Yeo 1985, Gibling *et al.* 1989). Similar northerly sediment dispersal patterns have been documented for Late Carboniferous rocks in Cape Breton Island (Gersib 1979, Rust and Gibling 1990a). South of the Cobequid Fault, D'Orsay (1986) and Fralick (1989) have reported southerly paleoflow directions in the Westphalian West Bay and Parrsboro Formations.

8.1.2 Orientation of Logs

Considerable data is available from logs. In Fig. 8.4 the orientation of only large logs (diameters >10 cm) are recorded. They show northeast-southwest trends in the vicinity of Cape Enrage, but further to the north, show either unimodal east-west and southeast-northwest trends, or bimodal southeast-northwest and northeast-southwest trends. These data are in general agreement with paleocurrents determined from trough cross-beds (Fig. 8.1), but differ especially with regard to the Cape Enrage area where the log orientation appears normal to paleoflow

Fig. 8.4 Paleocurrents determined from logs in the Boss Point Formation.



directions determined from trough cross-bedding. To explain these anomalies, Boss Point Formation rivers at such sites may have travelled only short distances east of the Harvey-Hopewell Fault, and from a topographically elevated area to the west, corresponding to the present-day Caledonia Highlands. These rivers for reasons such as confinement of channels, small size, low discharge, or low flow velocities may not have been capable of sorting log debris in flow parallel orientations as efficiently as more distal river systems (most of the study area) further to the northeast and east. It is also possible that log jams were common, or that the logs had more side branches in the more proximal areas, and therefore did not orient themselves to flow parallel positions particularly well.

Lawson (1962) presented data for 604 "plant fragment orientations" (Lawson 1962, map 4), and these show good agreement with data presented in this study (Fig. 8.4).

8.2 Paleocurrents from Planar Cross-Bedded Sandstones

Although the number of observations are few, paleocurrents determined from planar cross-sets are oblique to paleocurrent trends determined from trough cross-bedding in adjacent sections. At Beaumont, planar cross-bedding indicates trends to the north (vector mean= 20°), whereas at Hillsborough they indicate paleocurrents dominantly to the southeast (vector mean= 90° ; Fig. 8.5).

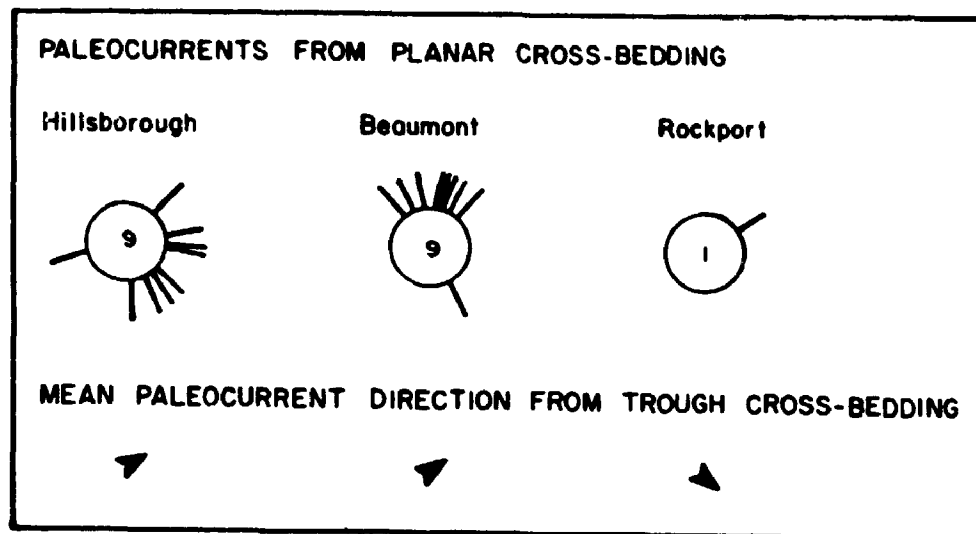


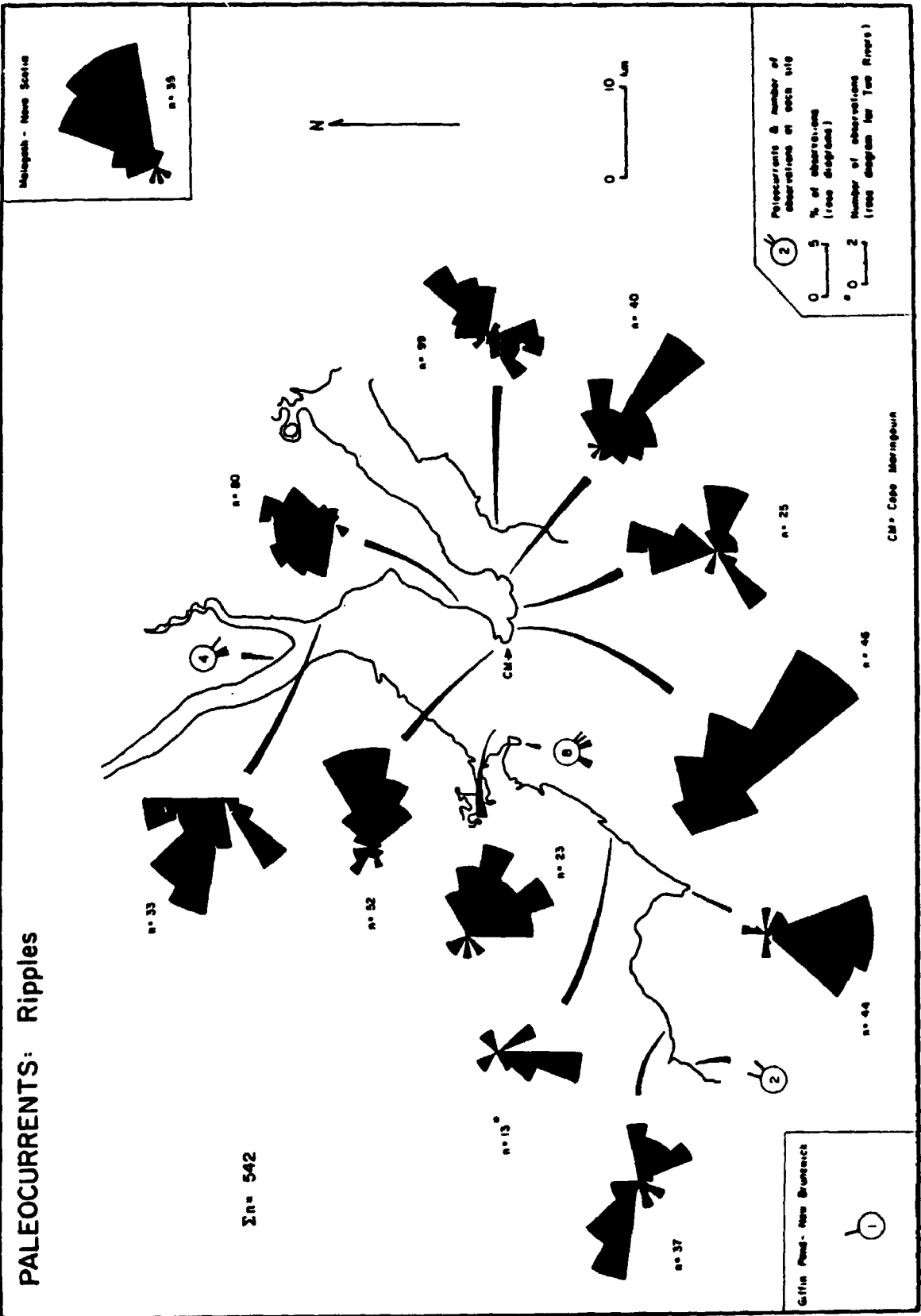
Fig. 8.5 Orientation of planar cross-beds in the Boss Point Formation.

These trends are 30° west and 40° east respectively, relative to paleocurrents determined from trough cross-beds at the same position in the stratigraphic section.

8.3 Paleocurrents from Ripple Cross-Laminated Sandstones

Paleocurrent measurements from ripple cross-laminated sandstones indicate dominant southeasterly trends south of Cape Maringouin, and northerly paleoflows north of the Cape (Fig. 8.6). These patterns are in agreement with paleocurrents determined from trough cross-bedded sandstones (Fig. 8.1), though several variations occur, notably at Cape Enrage and Two Rivers. There, ripples show southerly trends, approximately at right angles to trough cross-bed trends. At Alma, ripples show a significant paleocurrent trend to the NW, 180° from paleoflows

Fig. 8.6 Paleocurrents determined from ripples in the Boss Point Formation.



determined from trough cross-bedding at this locality (Fig. 8.6). Cases such as Cape Enrage and Two Rivers can best be explained if the ripples are considered to have formed from flows oblique to the main channel axes, such as small prograding deltas or crevasse-splay deposits. In the Alma situation where ripples indicate flow in an upstream sense, ripples may have formed on the foresets of dunes by counter or reverse flow, in the zone of separated flow at the bottom of the avalanching foresets.

Wave ripple crests are consistently normal to paleocurrent directions determined from trough cross-bedding (Fig. 8.7).

Rib and furrow measurements appear to closely resemble paleocurrent determinations made from trough cross-bedded sandstones (Fig. 8.7).

8.4 Paleocurrents from Parting Lineations in Horizontally Bedded Sandstones

Parting lineations consist of primary current lineations and parting-step lineations (definitions after McBride and Yeakel 1963). Parting lineation trends show a wide spread and many localities display two modes, one of which conforms to the paleocurrents determined from trough cross-bedding (Fig. 8.8). At other localities (Alma, Cape Enrage and Two Rivers) parting lineation trends are at right angles to paleocurrents determined from trough cross-

Fig. 8.7 Miscellaneous paleocurrent determinations from the Boss Point Formation, based on flutes, rib and furrow structures and the orientation of wave ripple crests.

PALEOCURRENTS: Miscellaneous Determinations

Flutes n = 57
 Rib & furrow n = 85
 Wave ripple crests n = 45

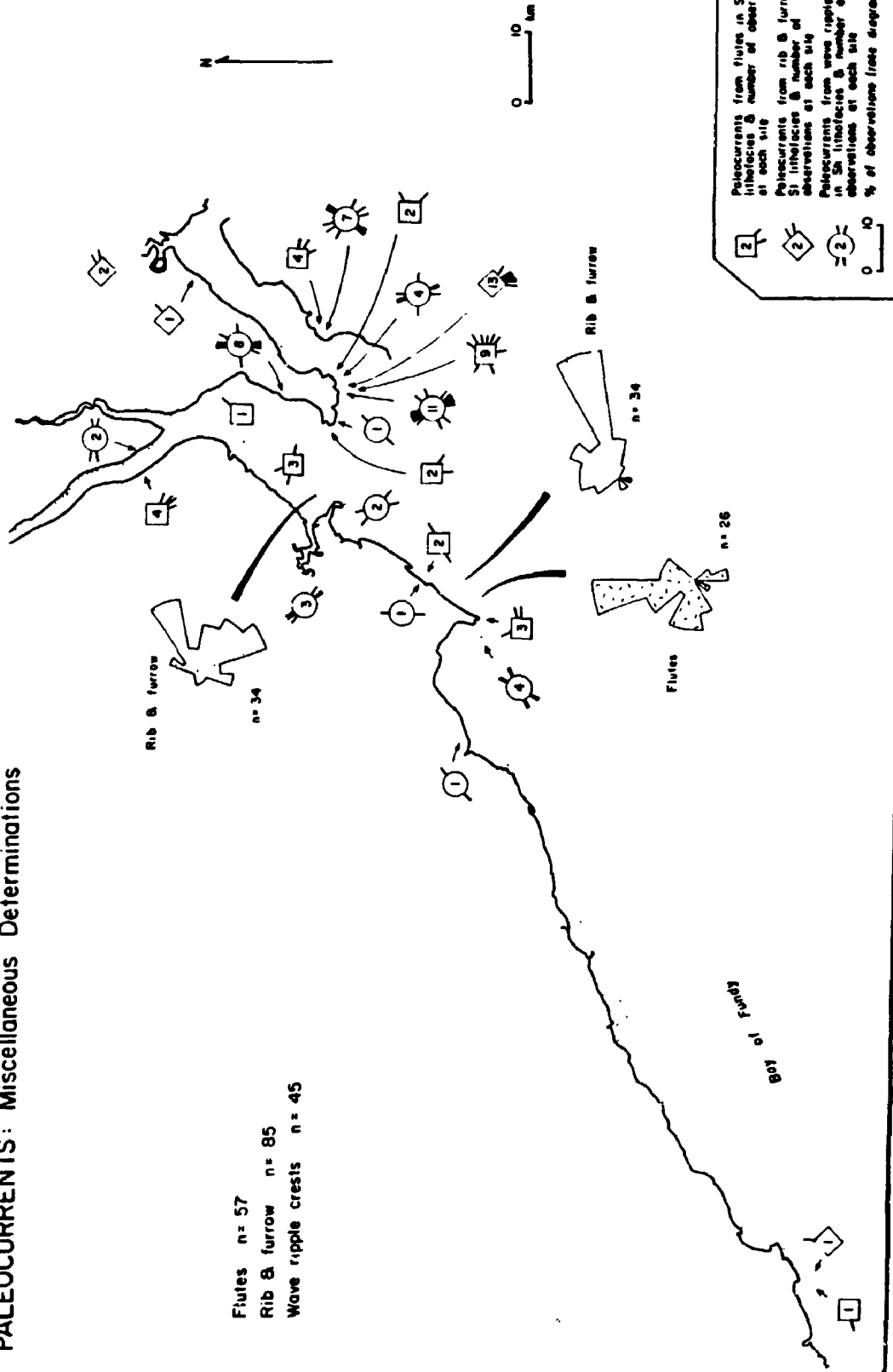
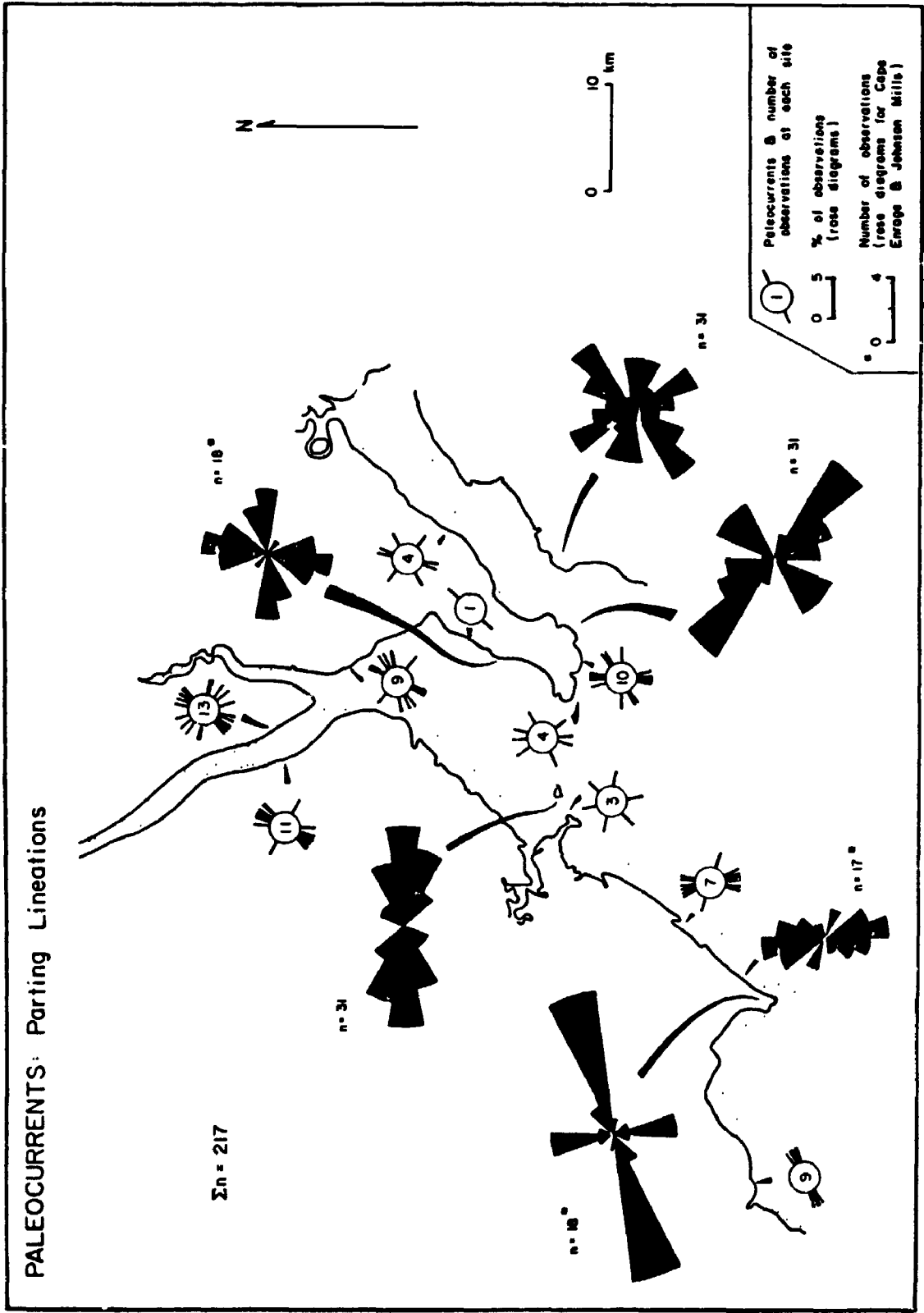


Fig. 8.8 Paleocurrents determined from parting lineations in the Boss Point Formation.



bedding. Because the lineations formed from currents passing over the surfaces of active dunes (trough cross-beds) they should be expected to show considerable variations in trend.

The Sedimentology of the Boss Point Formation
(Pennsylvanian), eastern New Brunswick and
northern Nova Scotia.

Volume II

by

Gregory Hawtrey Browne

Department of Geology

Submitted in partial fulfilment
of the requirements for the degree of
Doctor of Philosophy

Faculty of Graduate Studies
The University of Western Ontario
London, Ontario
November 1990

© Gregory H. Browne 1990

TABLE OF CONTENTS

VOLUME II

	Page
TABLE OF CONTENTS	xxv
LIST OF PHOTOGRAPHIC PLATE	xxvii
LIST OF FIGURES	xxviii
LIST OF APPENDICES	xxx
CHAPTER 9 - TECTONIC CONSIDERATIONS	383
9.1 Tectonic Deformation in the Boss Point Formation	384
9.1.1 Distribution of Coarse-Grained Clastics Adjacent to Faults	384
9.1.2 Regional Trends in Deformation	385
9.1.3 Stress Indicators from Conjugate Faults	398
9.1.4 The Harvey-Hopewell Fault Zone	403
9.1.5 The Harvey-Hopewell Fault Zone: Alma	412
9.1.6 The Rogers Head Fault: Giffin Pond	421
9.2 Tectonic Relationships in Older Carboniferous Units	424
9.3 Tectonic Models	431
CHAPTER 10 - CONTROLS ON SEDIMENTATION	435
10.1 Dam Mechanisms	436
10.2 Channel Avulsion	437
10.3 Changes in Weather	437
10.4 Changes in Climate and/or Vegetation	438
10.5 Tectonic Effects	438
10.6 Eustatic Effects	442
10.6.1 Sequence Stratigraphy in a Fluvial Setting - Theory	444
10.6.2 A Process-Response Model Based on the Boss Point Formation : Observed Versus Predicted Relationships	450
10.7 What were the Causes of Eustasy?	457
10.7.1 Causes of Glacial Cycles	460
10.7.2 Duration of Boss Point Formation Megacycles	463
CHAPTER 11 - SUMMARY OF CONCLUSIONS	466

APPENDIX I.	LITHOFACIES THICKNESSES AND STATISTICAL PARAMETERS	473
APPENDIX II.	MEASUREMENT OF PALEOCURRENT DIRECTIONS BY THE CARPENTER'S RULE METHOD	493
APPENDIX III.	PETROGRAPHY OF BOSS POINT FORMATION SANDSTONES	494
APPENDIX IV.	OUTCROP DESCRIPTIONS OF BOSS POINT FORMATION PALEOSOL PROFILES	495
APPENDIX V.	MAJOR OXIDE DATA FOR BOSS POINT FORMATION PALEOSOLS DETERMINED BY XRF ANALYSIS	498
APPENDIX VI.	TRACE ELEMENT DATA FOR BOSS POINT FORMATION PALEOSOLS DETERMINED BY XRF ANALYSIS	500
APPENDIX VII.	ELECTRON MICROPROBE DATA FOR RHIZOLITHS	501
APPENDIX VIII.	ELECTRON MICROPROBE DATA FOR SPHERULITIC SIDERITE NODULES	502
APPENDIX IX.	MINERALOGY OF CLAYS WITHIN AND SURROUNDING SPHERULITIC SIDERITE NODULES	504
APPENDIX X.	ELECTRON MICROPROBE DATA FOR CALCITE INFILLING PORE SPACES	506
APPENDIX XI.	MAJOR ELEMENT DATA FOR CALCRETE NODULES DETERMINED BY XRF ANALYSIS	507
APPENDIX XII.	TRACE ELEMENT DATA FOR A REPRESENTATIVE CALCRETE NODULE DETERMINED BY XRF ANALYSIS	508
SUPPLEMENTARY APPENDIX	DETAILED STRATIGRAPHIC COLUMNS USED IN THIS STUDY (Microfiche)	509
REFERENCES	512
VITA	550

LIST OF PHOTOGRAPHIC PLATE

VOLUME II

Plate	Description	Page
22	The shear zone at Owls Head north of Alma, and petrographic features of the Shepody and Maringouin Formations	414

LIST OF FIGURES

VOLUME II

Figure	Description	Page
9.1	Summary stratigraphic correlations	387
9.2	Summary stratigraphic correlations	389
9.3	Paleocurrent directions for megacycle I	391
9.4	Paleocurrent directions for megacycle II	393
9.5	Paleocurrent directions for megacycle III	395
9.6	Paleocurrent directions for megacycle IV	397
9.7	Tectonic features from the Boss Point Formation	400
9.8	Regional distribution of conjugate fault couples from the Boss Point Formation	402
9.9	Faults from the Boss Point Formation	405
9.10	Fault distribution in the Bay of Fundy region	407
9.11	Sketch of the Harvey-Hopewell Fault, Alma	411
9.12	Tectonic features from the Boss Point Formation	416
9.13	Faults from the Harvey-Hopewell Fault	420
9.14	Tectonic features from the Boss Point Formation	423
9.15	Paleocurrent directions from ripple and climbing ripple lamination in the Maringouin Formation	426
9.16	Paleocurrent directions from trough cross-bedding in the Shepody Formation	428
9.17	Paleocurrent directions from trough cross-bedding in the Claremont Formation	430
10.1	Alluvial sedimentation patterns following initiation of a fault scarp	441

10.2	Response of sedimentation on a depositional profile to a eustatic cycle	447
10.3	Elements of the coastal onlap curve	449
10.4	Cartoon showing the relationship between falling sea level and accommodation	452
10.5	Summary of depositional facies in relation to eustasy	452
10.6	Summary of the deposition of the Boss Point Formation in relation to eustatic change	455
10.7	The stratal relationships of the Boss Point Formation megacycles in relation to eustatic change	459
10.8	Coastal onlap curve for Carboniferous and Permian shelf sediments	462

LIST OF APPENDICES

Appendix	Page
APPENDIX I Lithofacies thicknesses and statistical parameters	473
APPENDIX II Measurement of paleocurrent directions by the carpenter's rule method	493
APPENDIX III Petrography of Boss Point Formation sandstones	494
APPENDIX IV Outcrop descriptions of Boss Point Formation paleosol profiles	495
APPENDIX V Major oxide data for Boss Point Formation paleosols determined by XRF analysis	498
APPENDIX VI Trace element data for Boss Point Formation paleosols determined by XRF analysis	500
APPENDIX VII Electron microprobe data for rhizoliths ..	501
APPENDIX VIII Electron microprobe data for spherulitic siderite nodules	502
APPENDIX IX Mineralogy of clays within and surrounding spherulitic siderite nodules	504
APPENDIX X Electron microprobe data for calcite infilling pore spaces	506
APPENDIX XI Major element data for calcrete nodules determined by XRF analysis	507
APPENDIX XII Trace element data for a representative calcrete nodule determined by XRF analysis	508
SUPPLEMENTARY APPENDIX Detailed stratigraphic columns used in this study (microfiche)	509

TECTONIC CONSIDERATIONS

The Cumberland sub-basin is bounded to the south by the Cobequid Fault and to the northwest, by the Harvey-Hopewell Fault. The Cobequid Fault (and related Chedabucto Fault) is one of the best known strike-slip fault systems in the Maritimes. They have been shown to have had a complicated structural history, with both Pre-Carboniferous sinistral as well as dextral movement during the Carboniferous (Eisbacher 1967, 1969, Fralick and Schenk 1981, Bradley 1982, Donohoe and Wallace 1982, 1988, Yeo and Ruixing 1986). The Cobequid Fault is outside the geographic area of this study.

The northwestern margin of the Cumberland sub-basin is bounded by the Harvey-Hopewell Fault, the Westmoreland High, and the Caledonia Highlands (Figs. 2.4, 2.7 & 2.8). The Harvey-Hopewell Fault is thought to have had post-Mississippian sinistral movement, although little in detail is known (see Webb 1963, Nance 1987).

Although it was not the aim of this study to document tectonic features in a comprehensive manner, the Harvey-Hopewell Fault exposure near Alma involves the Boss Point Formation, and is described in some detail below.

9.1 Tectonic Deformation in the Boss Point Formation

9.1.1 Distribution of Coarse-Grained Clastics Adjacent to Faults

It has already been demonstrated that penecontemporaneous faults were active during Boss Point Formation time, and that these strongly influenced the nature of paleocurrent directions and sedimentary facies (Chapters 3, 4, 5, 6 and 8). In Chapter 8 it was shown that paleocurrents in the Boss Point Formation trend away from a NE-SW trending fault block which divides the western margin of the Cumberland sub-basin into two depositional domains (Figs. 8.1 & 8.3).

At Dorchester and Johnson Mills (stratigraphic sections 10 & 13), coarse-grained units (conglomerate and pebbly sandstone) increase in abundance at approximately 150 m above the base of the Boss Point Formation, and persist to a position about 350 m above the base (Figs. 7.7 & 7.8). These coarse-grained lithologies become less abundant in stratigraphic sections north and south of Dorchester and Johnson Mills sections. A fault is mapped between these two sections (Maps 1 & 2), and it is suggested that faulting was active during Boss Point Formation sedimentation, with a pulse of activity corresponding to a stratigraphic position between 150 and 350 m above the base of the formation.

In terms of the megacycles recognised in Chapter 7, the coarse-grained lithologies appear at the base of megacycle III and persist through to megacycle IV. If the fault block was active during the lower part of Boss Point Formation time, it may be possible to see a trend in paleocurrents before, and after fault movement. Using the megacycle hierarchy of Chapter 7 (summarised as Figs. 9.1 & 9.2), 4 maps are presented of paleocurrents for stratigraphic sections adjacent to the fault block (Figs. 9.3 to 9.6). These maps show that the paleocurrents were directed away from the fault block throughout the deposition of megacycles I to IV, suggesting that the fault block was a topographic feature throughout deposition, although the evidence from the abundance of coarse-grained clastics suggests that the fault was only active during deposition of megacycles III and IV.

9.1.2 Regional Trends in Deformation

Much of the Boss Point Formation shows no evidence of faulting, either in terms of major offsets or minor structures. Areas in the southwest however, adjacent to the Harvey-Hopewell Fault (the "Fundy coastal zone" of Nance 1987), and in the east, adjacent to the Cobequid Fault (eg. River John), show considerable evidence for penecontemporaneous faulting. For the present purpose, two structural domains are recognised; a largely unfaulted

Fig. 9.1 Summary stratigraphic sections, showing major megacycles (I to VIII) in the Boss Point Formation. For details see Figs. 7.7 and 7.8.

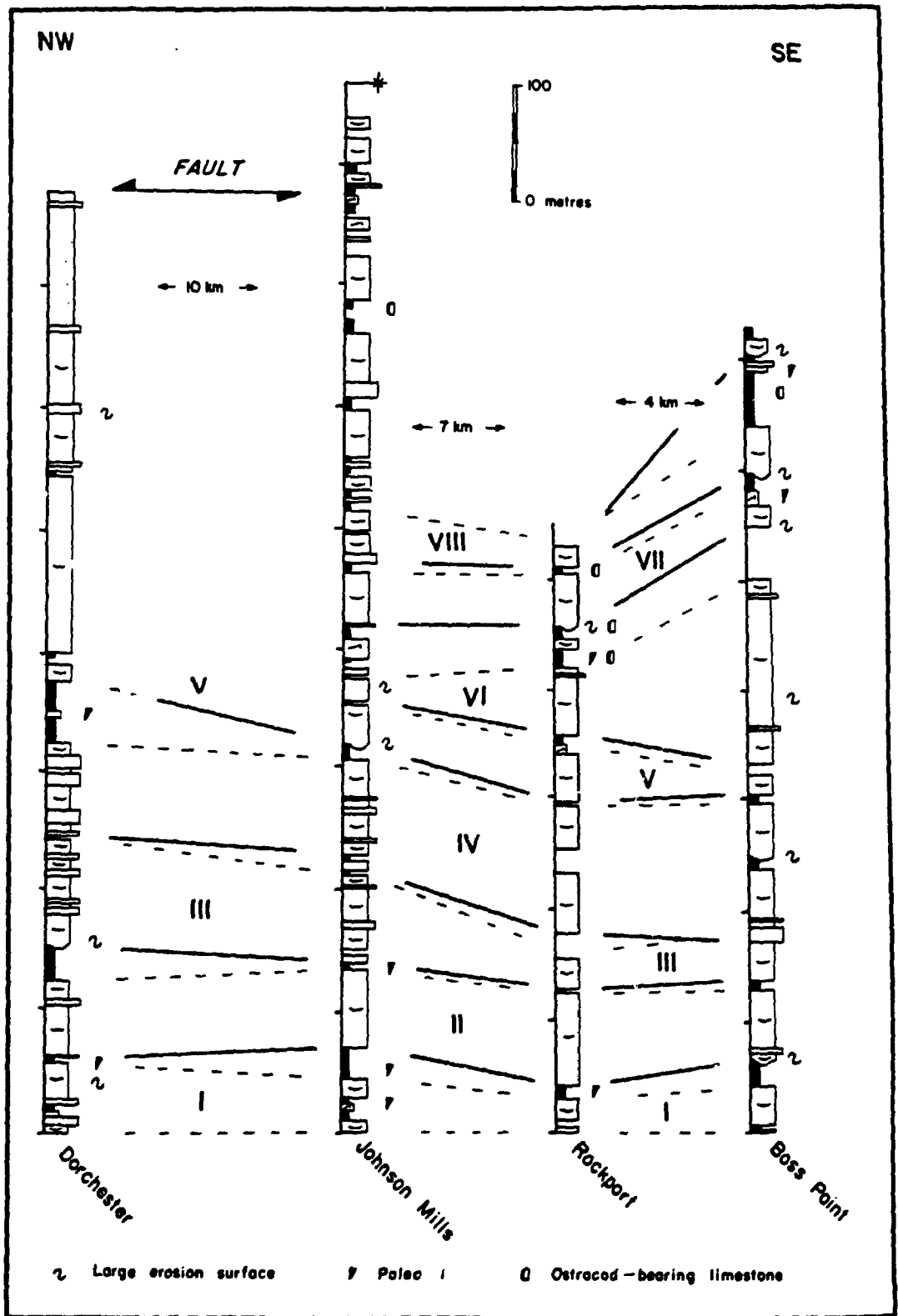


Fig. 9.2 Summary stratigraphic sections, showing major megacycles (I to VIII) in the Boss Point Formation. For details see Figs. 7.7 and 7.8.

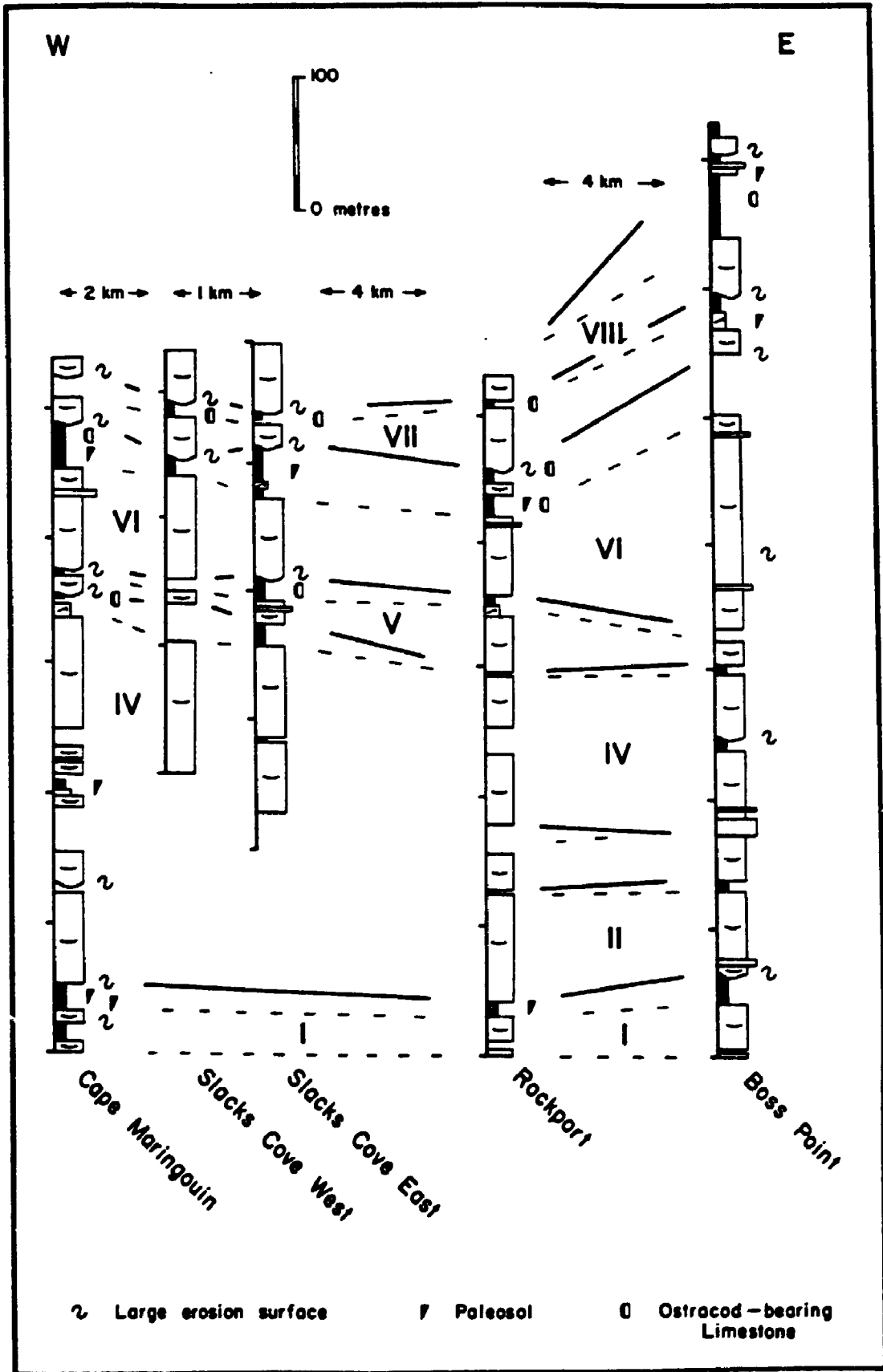


Fig. 9.3 Paleocurrent directions for megacycle I, based on trough cross-beds (number of observations at each locality given with each rose diagram), in relation to the contemporaneous high.

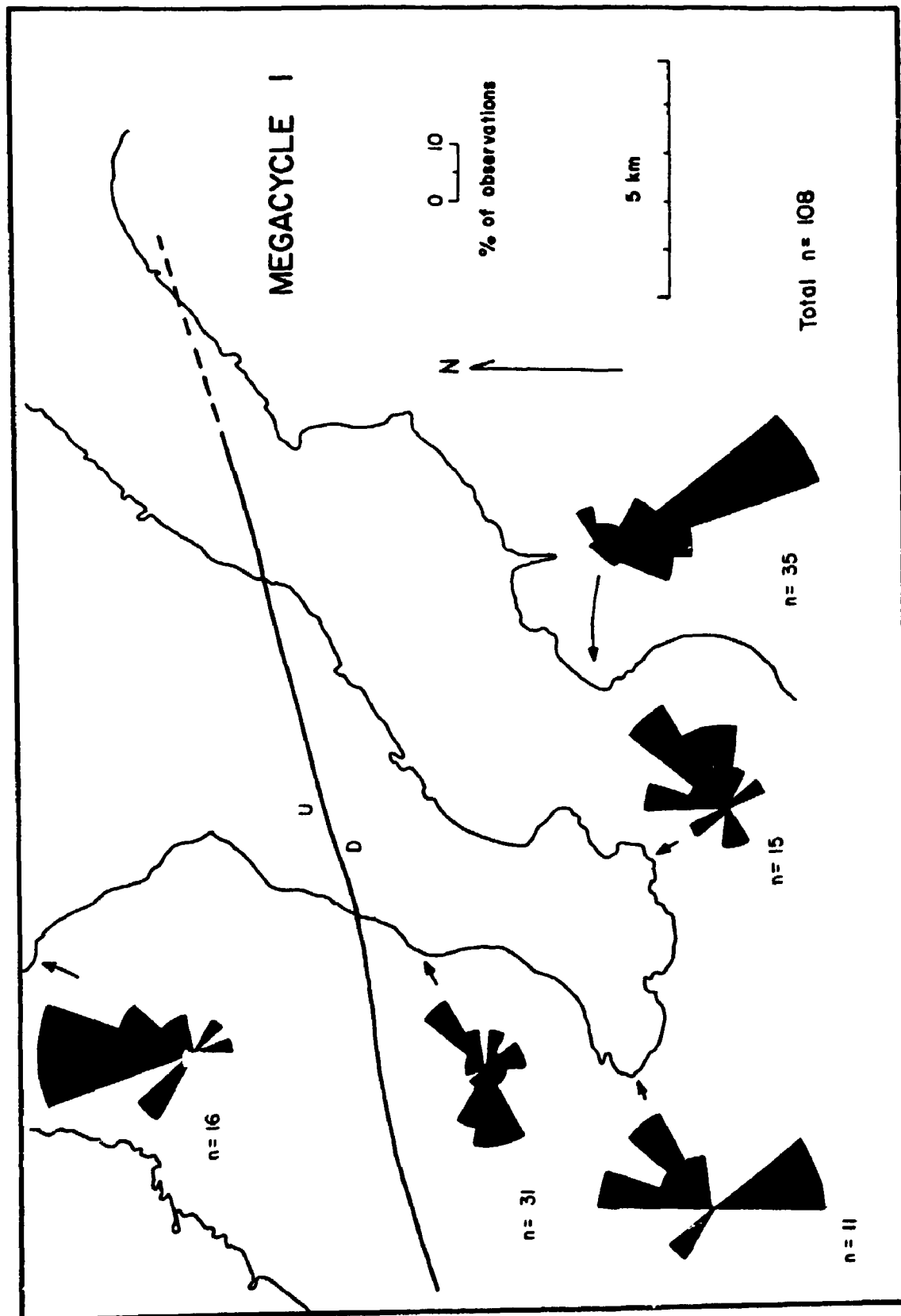


Fig. 9.4 Palaeocurrent directions for megacycle II, based on trough cross-beds (number of observations at each locality given with each rose diagram), in relation to the contemporaneous high.

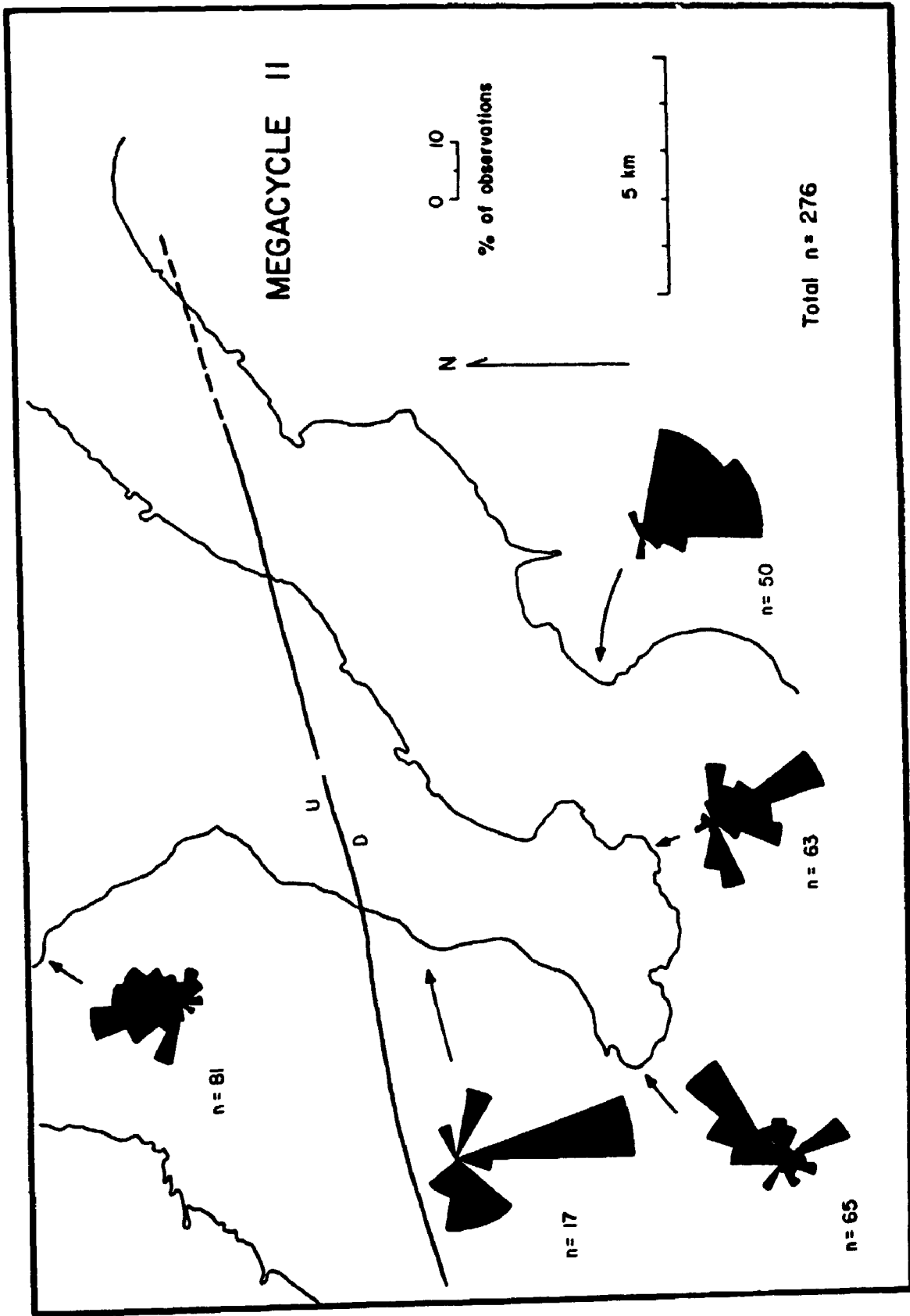


Fig. 9.5 Paleocurrent directions for megacycle III, based on trough cross-beds (number of observations at each locality given with each rose diagram), in relation to the contemporaneous high.

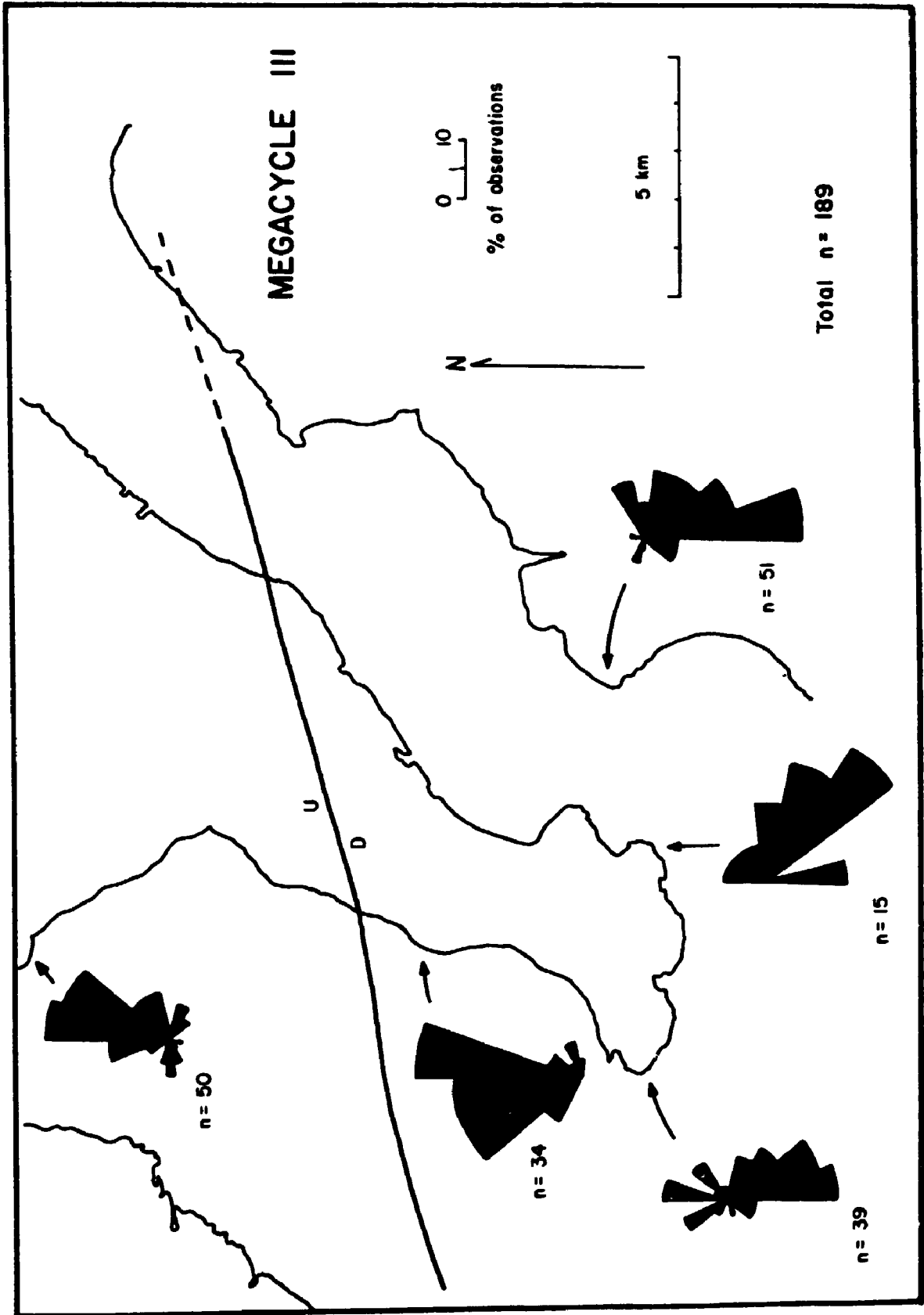
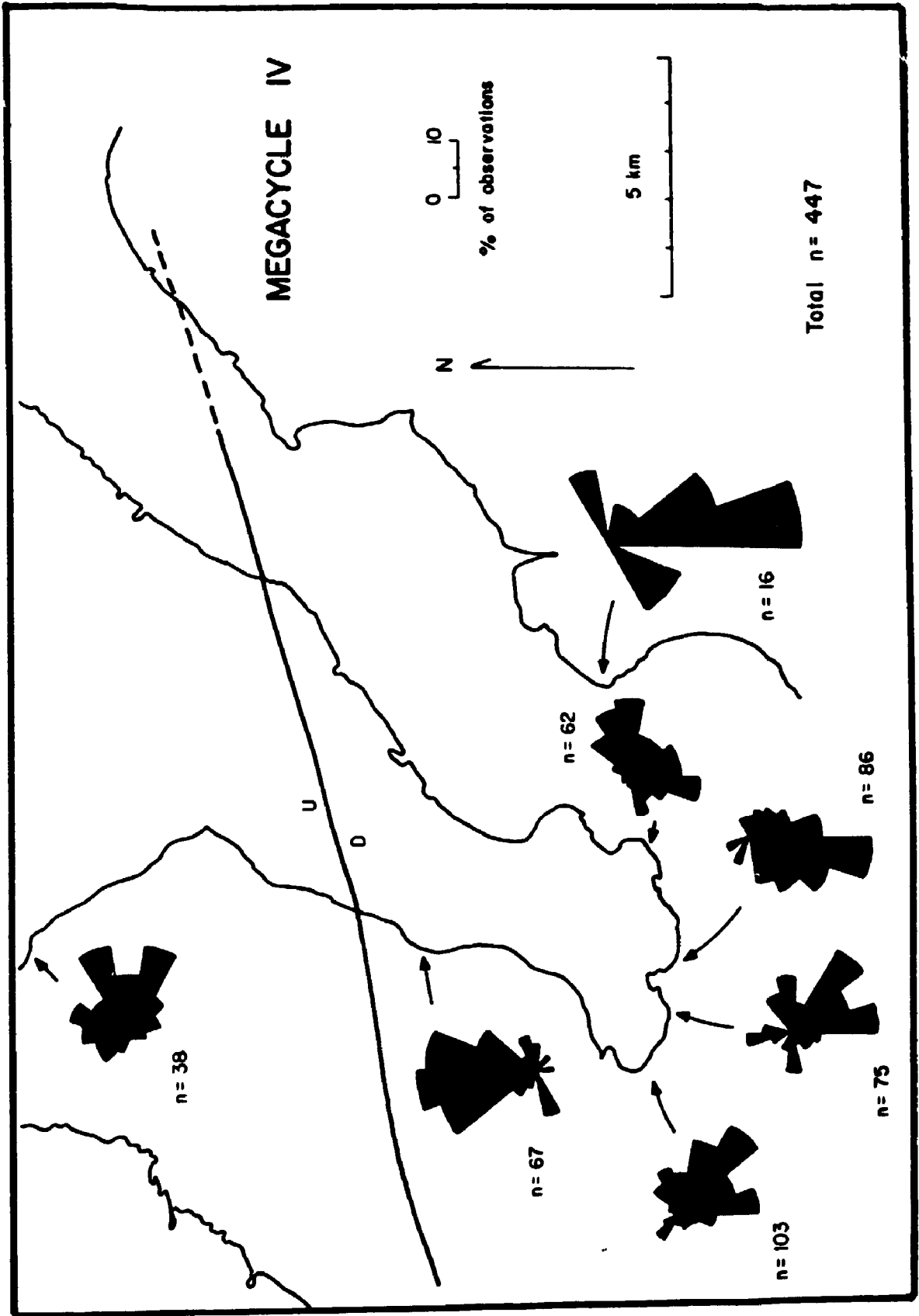


Fig. 9.6 Paleocurrent directions for megacycle IV, based on trough cross-beds (number of observations at each locality given with each rose diagram), in relation to the contemporaneous high.



sedimentary sequence in the north (north of Cape Enrage), and a more deformed zone to the south.

The northern region is dominated by moderate to high bedding attitudes, that define gently W-E plunging fold axes (Fig. 9.7a). Faulting tends to be minor in relation to that in the south, with fault planes trending ENE-WSW at moderate angles (Fig. 9.7b), with a wide scatter in the trend of striations (Fig. 9.7c).

Brittle deformation is much more pervasive in the southwest adjacent to the Harvey-Hopewell Fault, with a strong NE-SW fault alignment at Alma (Fig. 9.7d) and N-S and NE-SW trending faults at Giffin Pond (Fig. 9.7e). Striations too are more common in the south, but show the same wide spread as in the northern domain (Fig. 9.7f). Both these areas are described in more detail below.

9.1.3 Stress Indications from Conjugate Faults

Conjugate fault couples indicate stress orientations predominantly directed N-S and NE-SW, consistent with the strike-slip on regional faults (transpression), whereas a lesser number of conjugate couples show NW-SE compression (Fig. 9.8). Although the available data is limited, NE-SW directed compression seems to occur in the north and south of the Bay of Fundy region, whereas at Alma and Cape Enrage, NW-SE directed compression appears to predominate. The significance of this is unclear.

- Fig. 9.7
- a) Pi plot for the Maringouin Anticline, Maringouin Peninsula (fold axis 092/05).
 - b) Poles to faults from the northern part of the Bay of Fundy region (north of Cape Enrage).
 - c) Striations from the northern part of the Bay of Fundy region (north of Cape Enrage).
 - d) Poles to faults from the Harvey-Hopewell Fault zone between Owls Head and Dennis Beach.
 - e) Poles to faults immediately beneath the Rogers Head Fault, north of Giffin Pond.
 - f) Striations from the Harvey-Hopewell Fault zone between Owls Head and Dennis Beach.

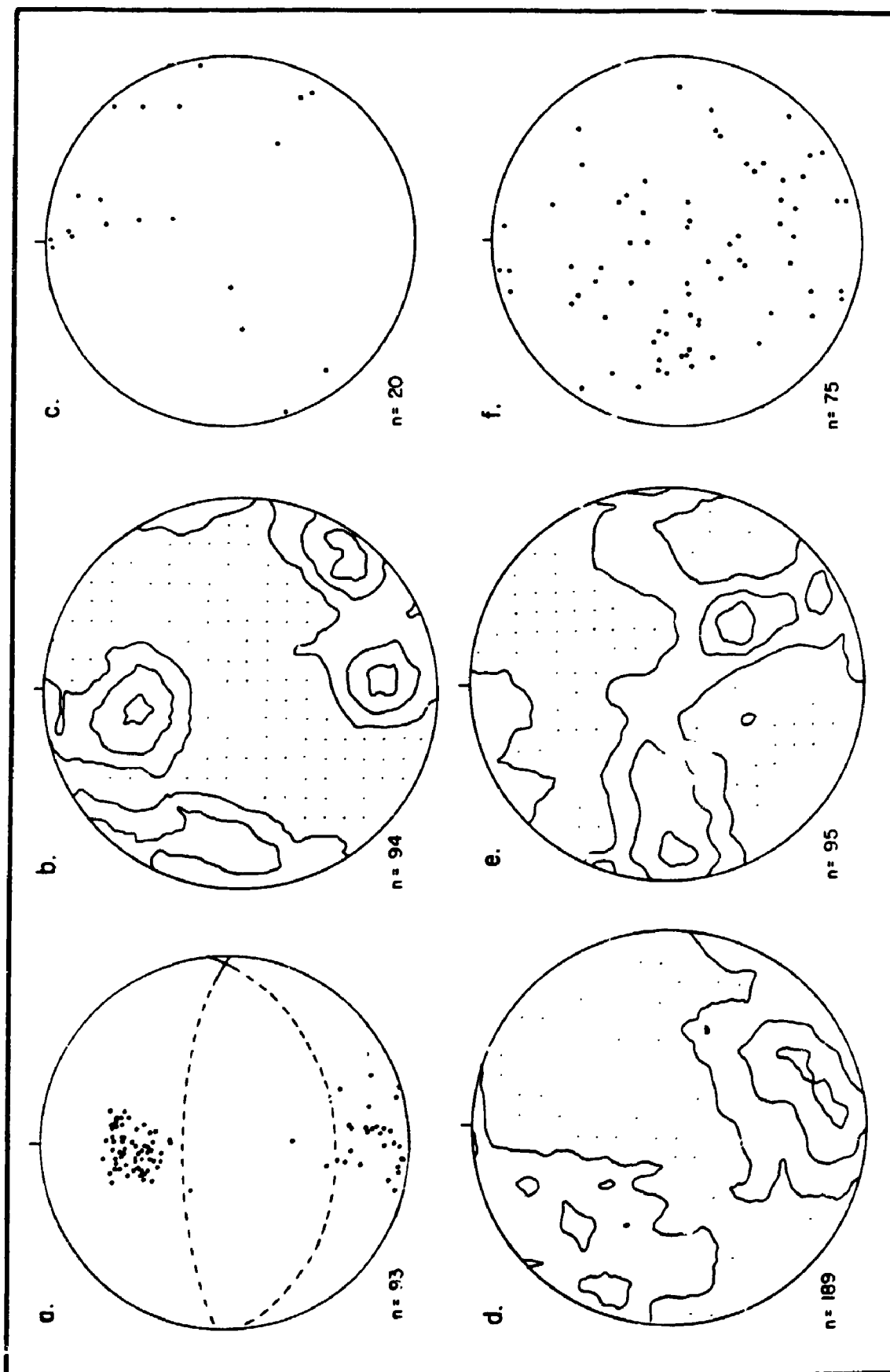
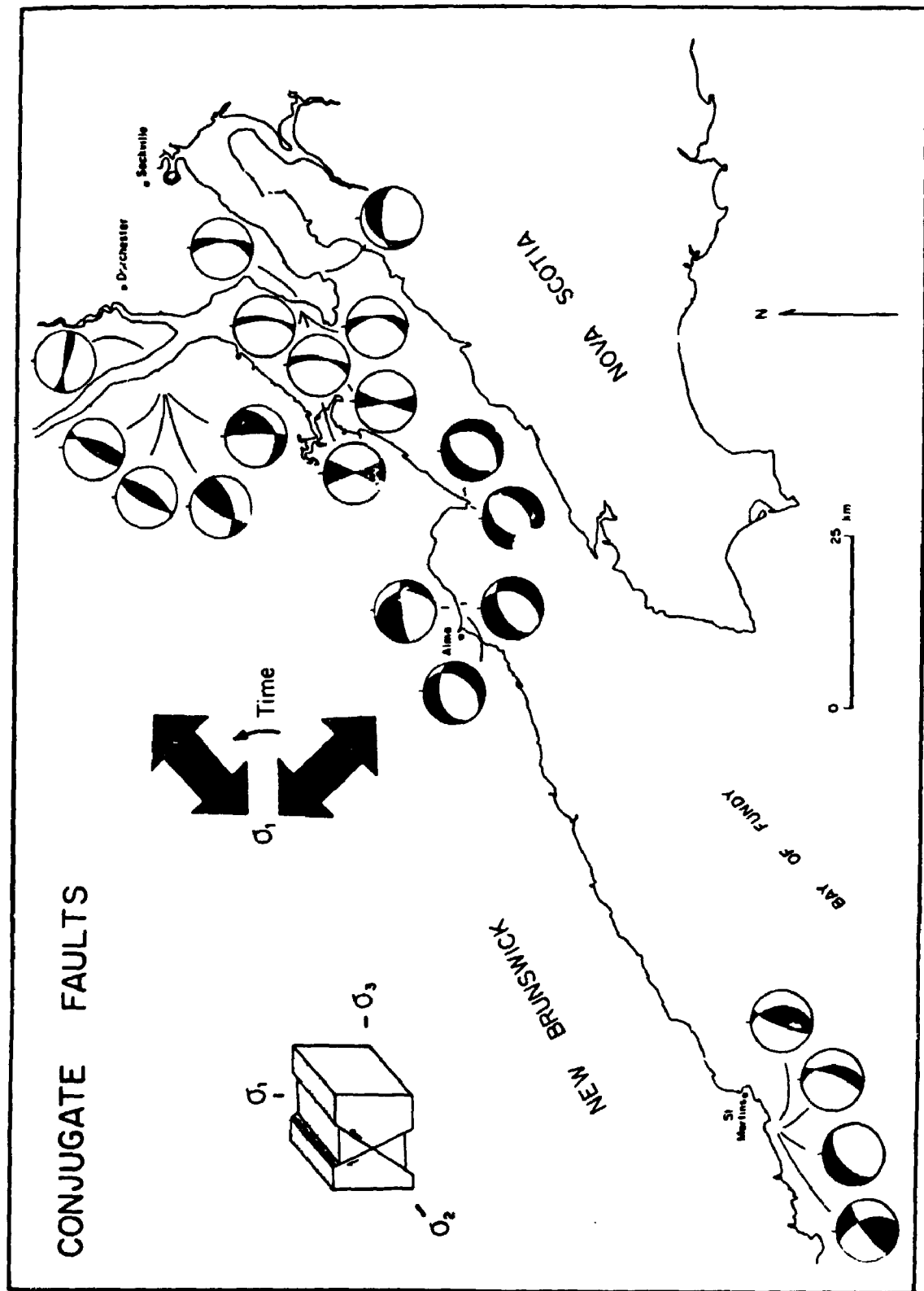


Fig. 9.8 Regional distribution of conjugate fault couples from the Boss point Formation. Black sectors in each stereonet indicate compression directions. Sneck and Nance (1988) have suggested that with time the dominant compression direction changed from NW-SE to NE-SW.



Recently Sneek and Nance (1988) have suggested from a detailed study of the Musquash Harbour region (southern New Brunswick), that an early NW-SE directed compression changed in approximately middle Pennsylvanian time to a NE-SW directed regime. It may be that the 2 different stress orientations recorded by the conjugate faults in this study relate to this temporal variation in stress.

It is however very difficult to separate structures generated during Boss Point Formation time with those related to subsequent events. Conjugate faults from the Boss Point Formation show a predominant NW-SE movement direction (Fig. 9.9a & 9.9b) indicative of NW-SE extension, and this is assumed to relate to Triassic and Jurassic extension and the opening of the Atlantic Ocean (Olsen and Schlische 1990). Faults from the Triassic Fundy Group at Dennis Beach, north of Alma (Fig. 9.9c), are consistently W-E structures, and conjugate faults from this same sequence show high angle NE and SE directed compression (Fig. 9.9d).

9.1.4 The Harvey-Hopewell Fault Zone

One of the key faults of the Cumberland sub-basin is the NE-SW trending Harvey-Hopewell Fault in the southwest sector of the Bay of Fundy region (Fig. 9.10). The fault is in essence a fault zone, defined by a number of subparallel traces. The western-most fault separates

- Fig. 9.9
- a) Conjugate faults from the entire Bay of Fundy region. Poles to compression, intermediate and extension axes indicated.
 - b) Conjugate faults from the entire Bay of Fundy region. Partial great circles connecting axes represent a movement plane at right angles to intermediate axes (or intersection line) of conjugate set. A dominant NW-SE movement direction is indicative of NW-SE extension, assumed to be Jurassic in age. The less prominent NE-SW movement directions indicate NE-SW extension, and are assumed to be of Carboniferous age.
 - c) Poles to faults from the Triassic Fundy Group, Dennis Beach.
 - d) Conjugate fault couples from the Triassic Fundy Group at Dennis Beach.

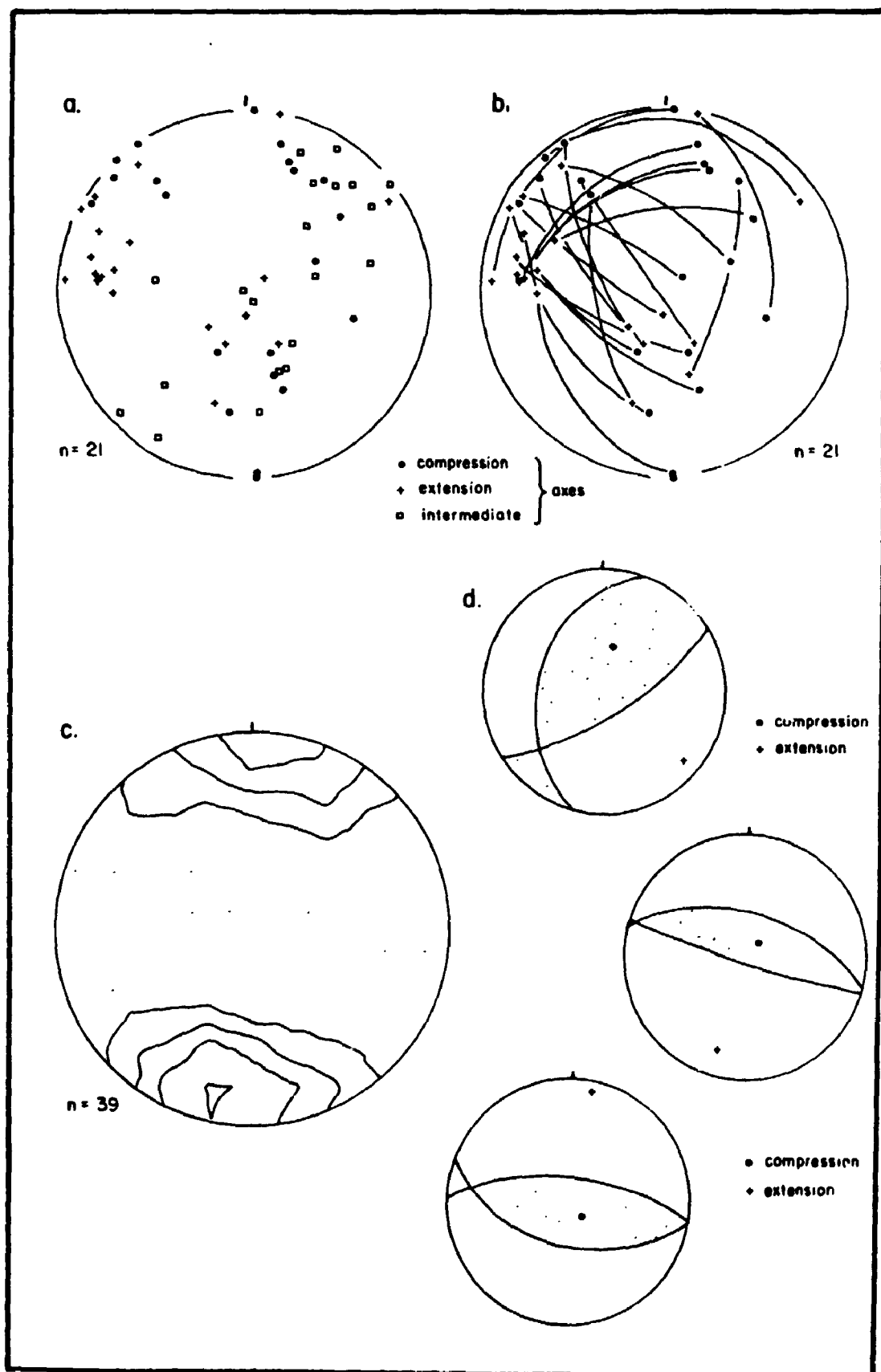
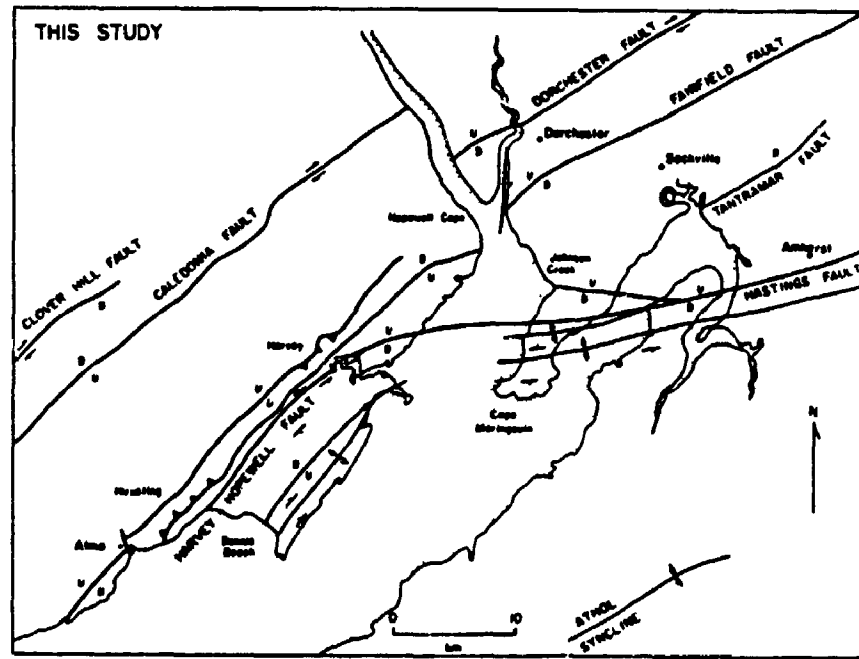
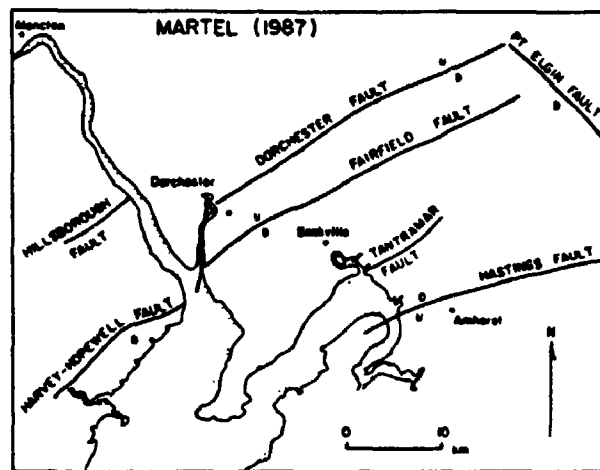
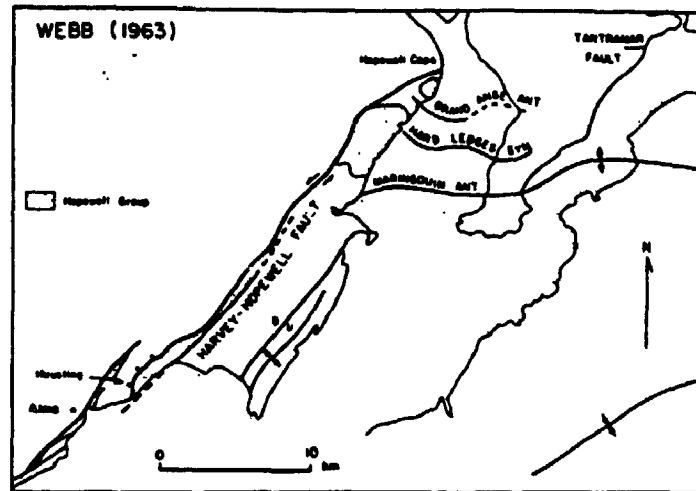


Fig. 9.10 Fault distribution in the Bay of Fundy region from Webb (1963) and Martel (1987), and reinterpreted in this study. Location of cross section (Fig. 9.13a) across the Harvey-Hopewell Fault zone is indicated in lower map.



Precambrian basement lithologies to the west from Boss Point Formation sandstones in the east (Map 2), and as such must be the master or major fault trace, though it has never been recognised as such by previous studies (cf. Webb 1963). Two faults occur further to the east (Map 2); the more westerly of these offsets Boss Point Formation lithologies against the Hopewell Group (Fig. 9.10), and locally involves thrusting of Hopewell rocks over the Boss Point Formation (see below). The eastern fault offsets Hopewell Group from the Maringouin Formation (Map 2, Fig. 9.10). Traditionally, the Harvey-Hopewell Fault has been taken as the eastern most fault of the three shown in Fig. 9.10, at the western end of Dennis Beach (Webb 1963). The fault is mapped from this locality (with probable continuation further to the southwest; see Webb 1963), to Hopewell Cape in the north (Fig. 9.10). The exact nature of the Harvey-Hopewell Fault north of Hopewell Cape is uncertain. Authors have suggested that the fault may change strike, that it remains hidden beneath younger strata, or that it may die out abruptly (Webb 1963, p. 1909-1910).

The problems of correlating faults in the vicinity of Hopewell Cape were well recognised by Webb (1963), who suggested that the fault may link up with northeasterly trending structures in northern Nova Scotia, such as the Tantramar Fault (*op cit.* p. 1910, Fig. 9.10).

In this study the Harvey-Hopewell Fault is mapped in a

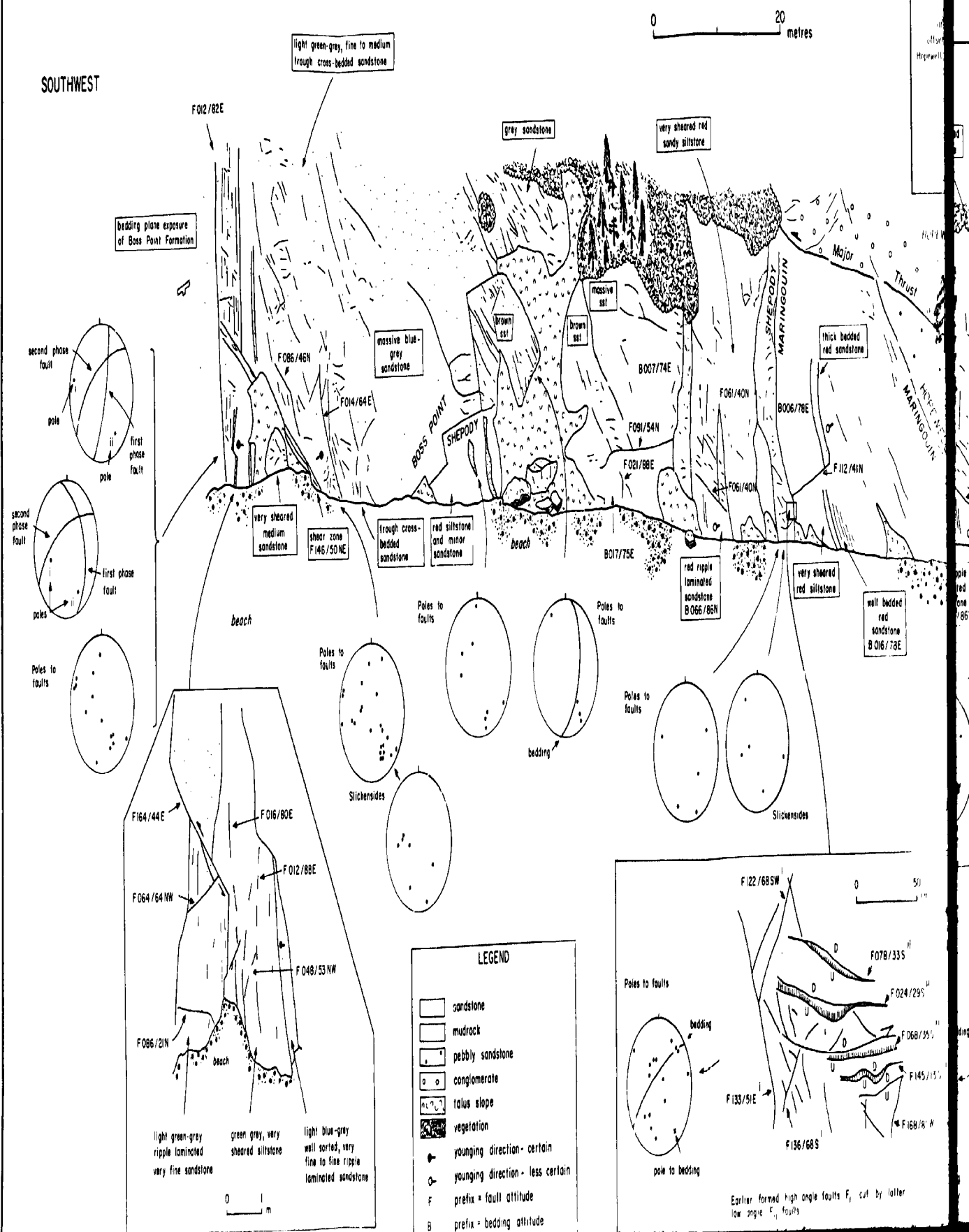
similar manner to that of van de Poll (1972b) and Howie (1988). The western master fault extends from Point Wolfe, near Alma, north to Harvey, where local thrusting occurs, and probably signifies that the fault plane flattens out into some form of low-angle shear. The fault which crops out at Owls Head (Figs. 9.10 & 9.11), extends from Owls Head to Hopewell Cape, and probably continues eastward, to join up with the Tantramar or Fairfield Faults (Fig. 9.10). The eastern-most fault exposed at Dennis Beach (ie. the Harvey-Hopewell Fault of previous workers) is interpreted in this study to change trend at Harvey, and to cross the Maringouin Peninsula south of Johnson Creek, to link with the Hastings Fault (see Martel 1987) of northern Nova Scotia (Fig. 9.10). Supporting evidence for this interpretation comes from a previously unmapped 90 m wide shear zone exposed on the shore platform just north of the Johnson Mills section.

At Johnson Creek on the Maringouin Peninsula (Fig. 9.10) a splinter fault occurs to the north of the Hastings Fault, and is downthrown to the south, where Viséan Windsor Group anhydrite and gypsum (to the north), are in contact with Boss Point Formation sandstones on the downthrown block, south of the fault (Maps 1 & 2).

The Harvey-Hopewell Fault is an important structure, for it, along with the Dorchester Fault (Map 1), is the only fault in the Maritimes thought to have undergone sinistral movement during the Carboniferous (Webb 1963,

Fig. 9.11 Sketch of the Harvey-Hopewell Fault, Owls Head,
northeast of Alma.

SKETCH OF HARVEY-HOPEWELL FAULT ZONE, OWLS HEAD



SOUTHWEST

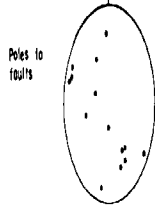
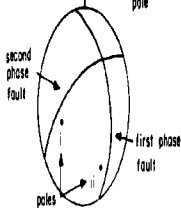
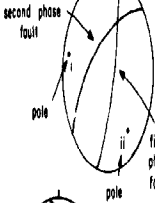
0 20 metres

light green-gray, fine to medium trough cross-bedded sandstone

gray sandstone

very sheared red sandy siltstone

bedding plane exposure of Boss Point Formation



massive blue-gray sandstone

F014/64E

brown sst

brown sst

massive sst

B007/74E

F091/54N

F021/88E

F061/40N

thick bedded red sandstone

B006/78E

F112/41N

very sheared medium sandstone

shear zone F146/50NE

trough cross-bedded sandstone

red siltstone and minor sandstone

beach

B017/75E

red ripple laminated sandstone B066/86N

very sheared red siltstone

well bedded red sandstone B016/78E

beach

Poles to faults

Poles to faults

Poles to faults

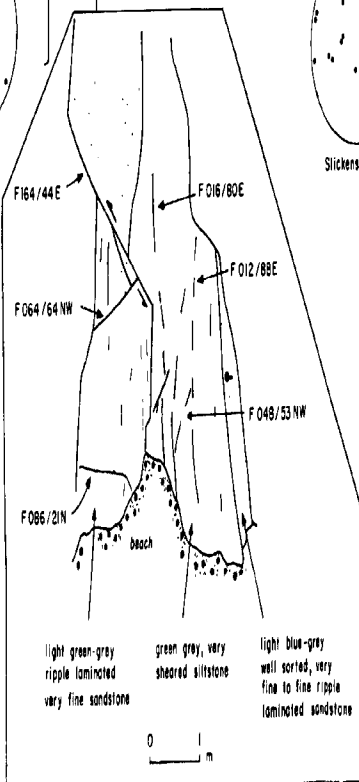
Poles to faults

Poles to faults

Slickensides

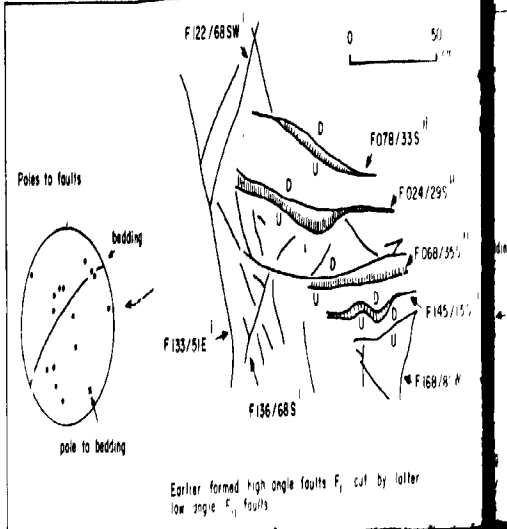
bedding

Slickensides

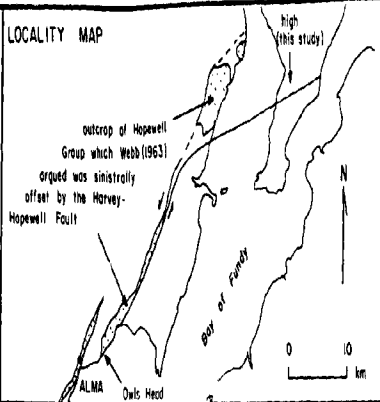


LEGEND

- sandstone
- mudrock
- pebbly sandstone
- conglomerate
- talus slope
- vegetation
- younging direction - certain
- younging direction - less certain
- F prefix = fault attitude
- B prefix = bedding attitude

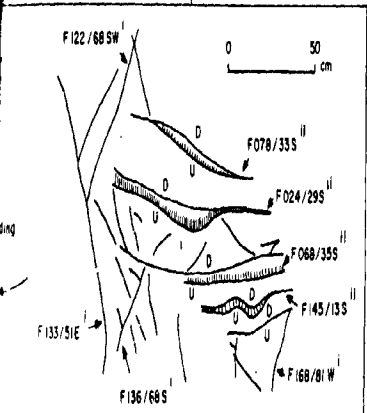
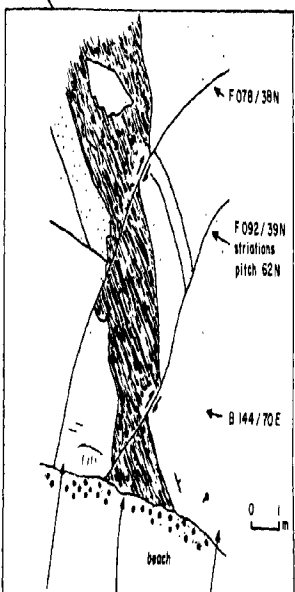
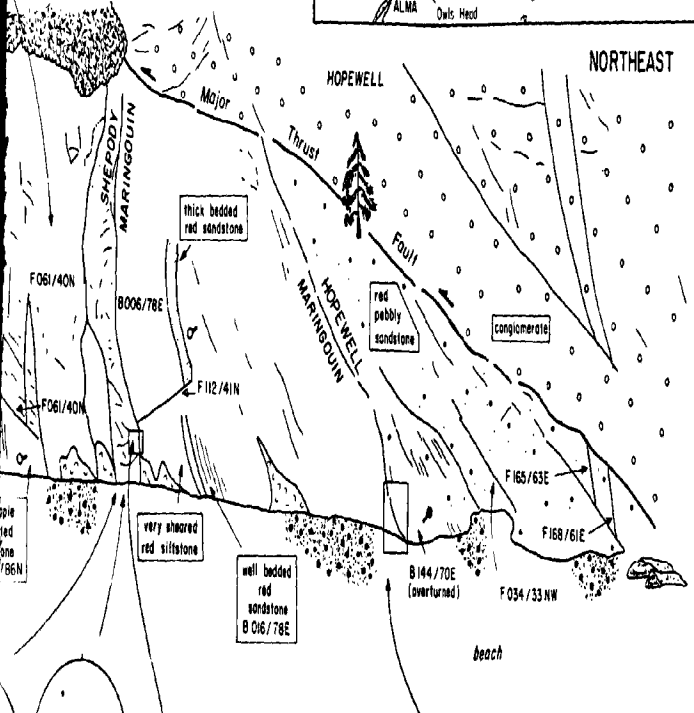


LOCALITY MAP



20 metres

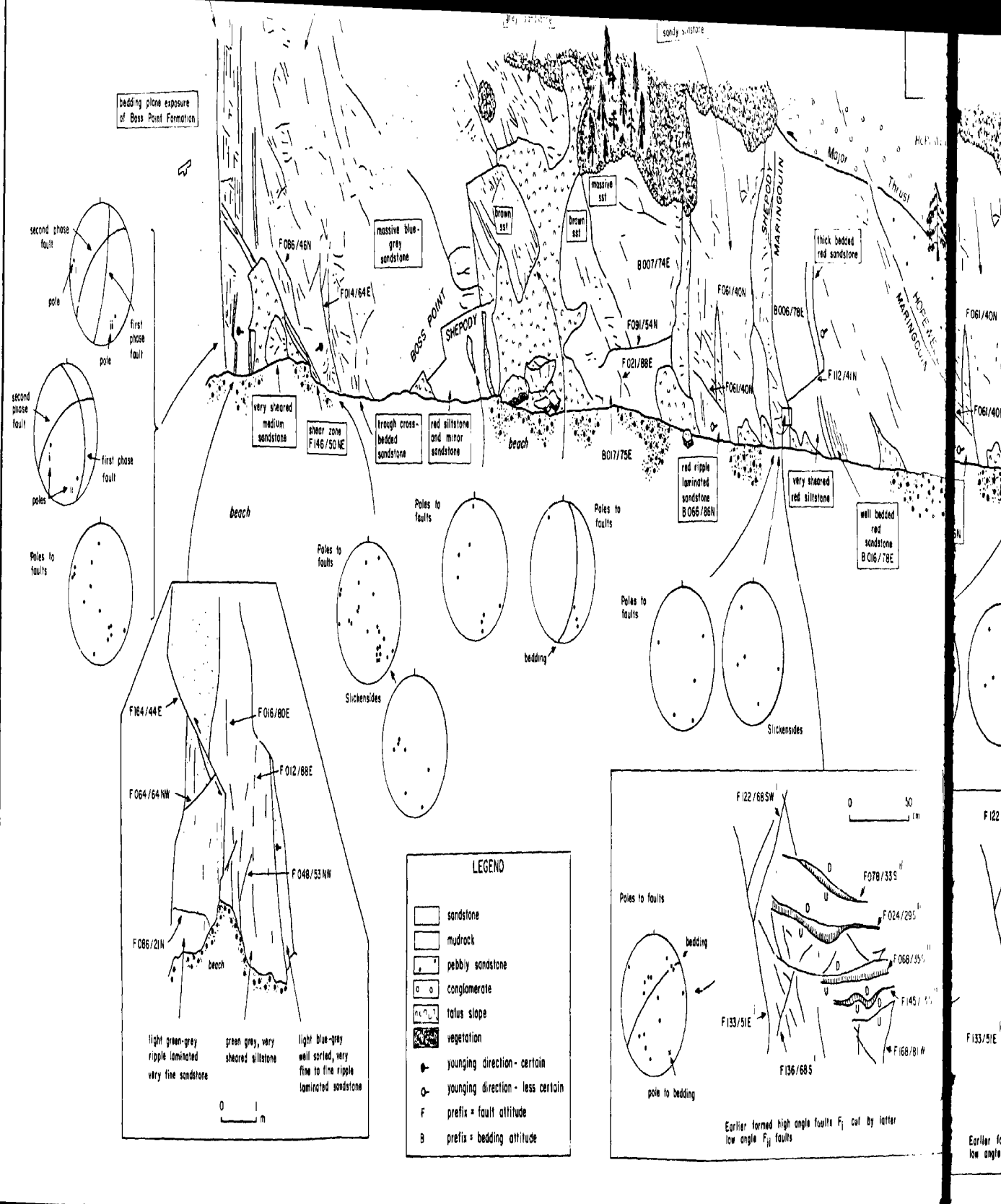
NORTHEAST

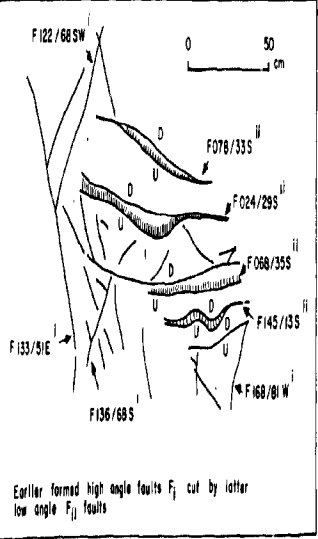
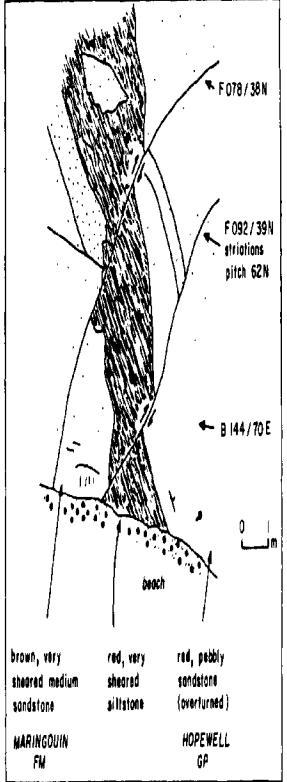
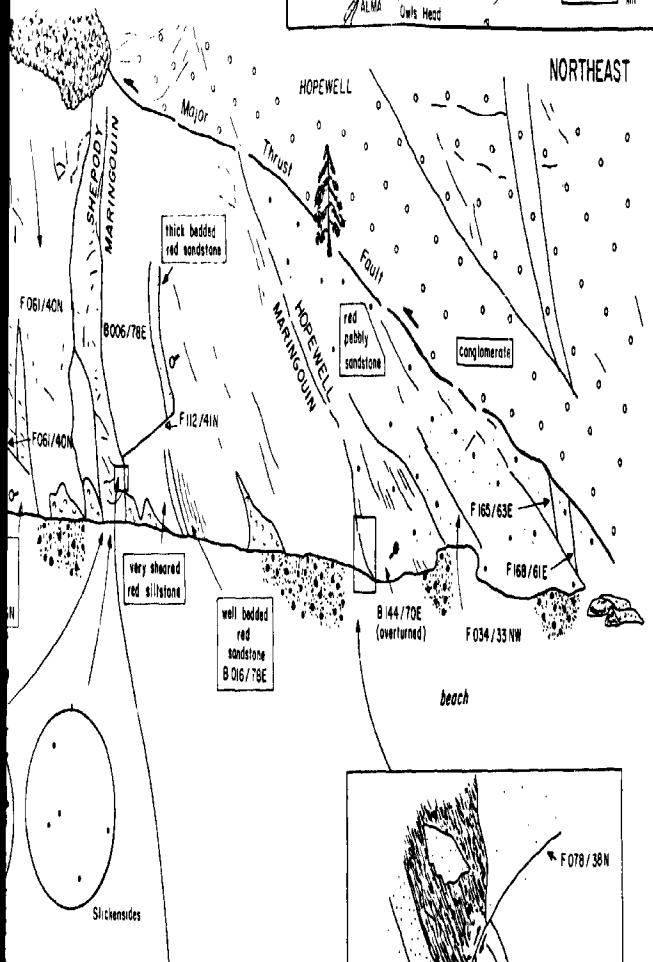


brown, very sheared medium sandstone red, very sheared siltstone red, pabbly sandstone (overturned)

Earlier formed high angle faults F₁ cut by latter low angle F₂ faults

HOPWELL





Earlier formed high angle faults F_i cut by letter low angle F_{ii} faults

brown, very sheared medium sandstone	red, very sheared siltstone	red, pebbly sandstone (overturned)
MERINGOUIN FM	HOPEWELL GP	

McLeod and Ruitenberg 1978, Nance 1987); all the other faults were dextral during the Carboniferous. Sinistral movement along the Harvey-Hopewell Fault was first suggested by Webb (1963) based on the correlation of coarse-grained Hopewell Group conglomerate lithologies east of the Hopewell Fault at Hopewell Cape, with once equivalent conglomerates (part of the same alluvial fan sequence), now displaced approximately 15 km to the south (Fig. 9.10).

9.1.5 The Harvey-Hopewell Fault Zone: Alma

The only well exposed fault zone in the study area occurs at Owls Head, 2.5 km NE of Alma (Fig. 9.11, inset A), where a 150 m wide fault zone is exposed (Plate 22a). No previous work has been undertaken at this locality, though it was mentioned by Webb (1963) who regarded it as a small splinter thrust west of the main Harvey-Hopewell Fault exposure at Dennis Beach.

At Owls Head, Hopewell Group conglomerate and breccia have been thrust west over Boss Point, Shepody and Maringouin formation lithologies (Figs. 9.11 & 9.12a, Plate 22a). Steeply dipping Boss Point Formation sandstones occur south of the thrust. Within the 150 m wide fault zone, fault-bounded blocks of highly sheared grey, reddish-grey and brown sandstone occur. The southwest portion of the shear zone consists of NE-dipping light green-grey

Plate 22

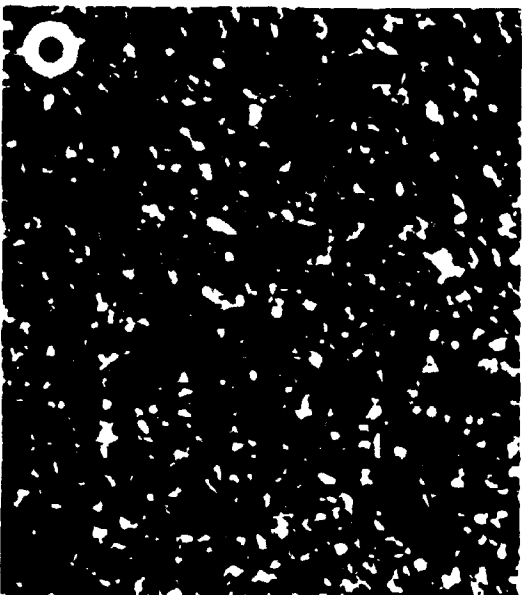
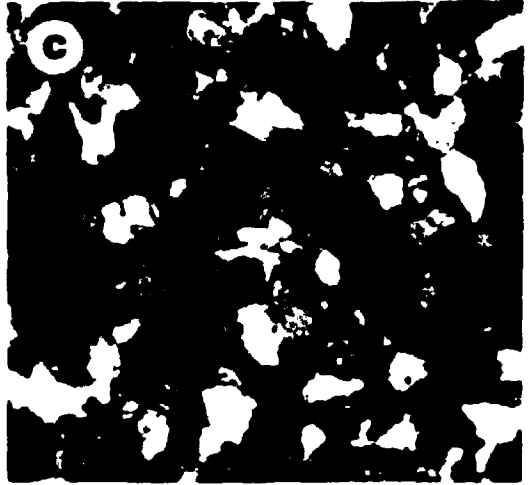
a) Photo of the 150 m wide shear zone at Owls Head (see Fig. 9.11). Overturned Boss Point Formation in extreme SW at left (A), is in fault contact with Boss Point Formation (B), Shepody Formation (C) and Maringouin Formation (D) within the fault zone. In the NE overturned Hopewell Group (E) occur beneath the thrust plane (arrowed). Prominent hill at extreme right (F) consists of Hopewell Group conglomerate and breccia.

b) Photomicrograph of Shepody Formation sandstone from the fault zone at Owls Head. View is in cross polarised light. Scale bar= 0.5 mm.

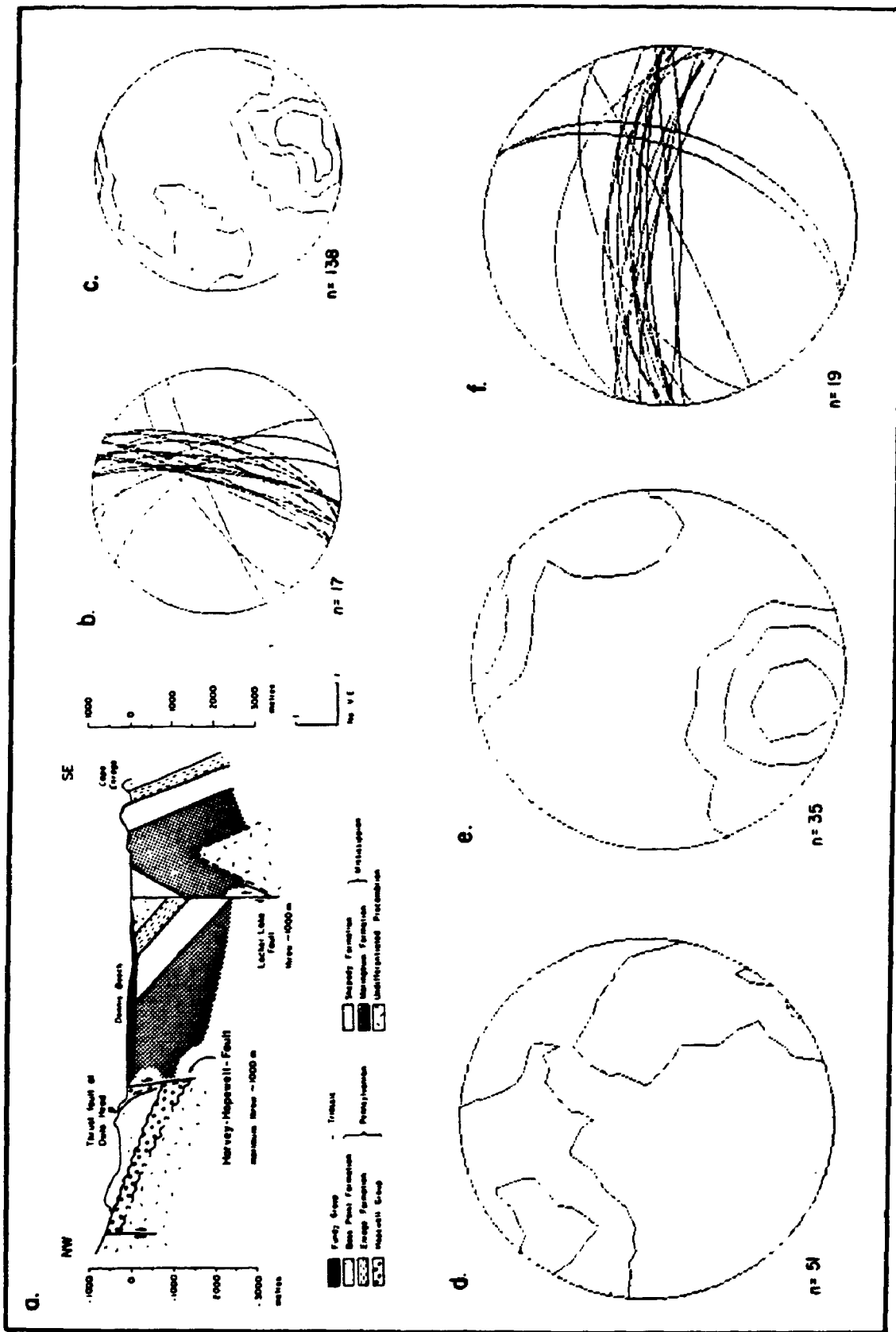
c) Photomicrograph of Shepody Formation sandstone from the inner cape, Cape Enrage. View is in cross polarised light. Scale bar= 0.5 mm.

d) Photomicrograph of Maringouin Formation silty fine-grained sandstone from the fault zone at Owls Head. View is in cross polarised light. Scale bar= 0.25 mm.

e) Photomicrograph of Maringouin Formation silty fine-grained sandstone from the inner cape, Cape Enrage. View is in cross polarised light. Scale bar= 0.25 mm.



- Fig. 9.12
- a) Cross section of the Harvey-Hopewell Fault zone at Owls Head (for location see Fig. 9.10).
 - b) Cyclographic traces of bedding within the fault zone at Owls Head.
 - c) Poles to faults within the fault zone at Owls Head.
 - d) Poles to faults within the Harvey-Hopewell Fault zone at Dennis Beach.
 - e) Poles to faults from the Boss Point Formation, southwest of the fault zone at Owls Head.
 - f) Cyclographic traces of calcite filled (tensional) calcite veins within the fault zone at Owls Head.



sandstone of the Boss Point Formation, in places overturned (Fig. 9.11). A series of faults separate these Boss Point Formation lithologies from reddish to brown sandstone and siltstone further to the east. These rocks are petrographically equivalent to the Shepody Formation (Namurian) exposed at Cape Enrage (Plate 22b & 22c). The northeastern section of the fault zone comprises deep red-brown siltstones and fine-grained sandstones (Fig. 9.11), which are petrographically similar to the Maringouin Formation (Viséan-Namurian) exposed at Cape Enrage (Plate 22d & 22e). Maringouin Formation rocks are faulted against a steeply dipping, overturned interval of Hopewell Group pebbly sandstone, which occur below the main thrust at the eastern margin of the fault zone (Fig. 9.11). The faulted contact between the Maringouin Formation and Hopewell Group is truncated by the latter formed thrust, and has in turn been cut by low angle W-E faults (see inset diagram, Fig. 9.11) that are probably related to Triassic-Jurassic transtensional stress.

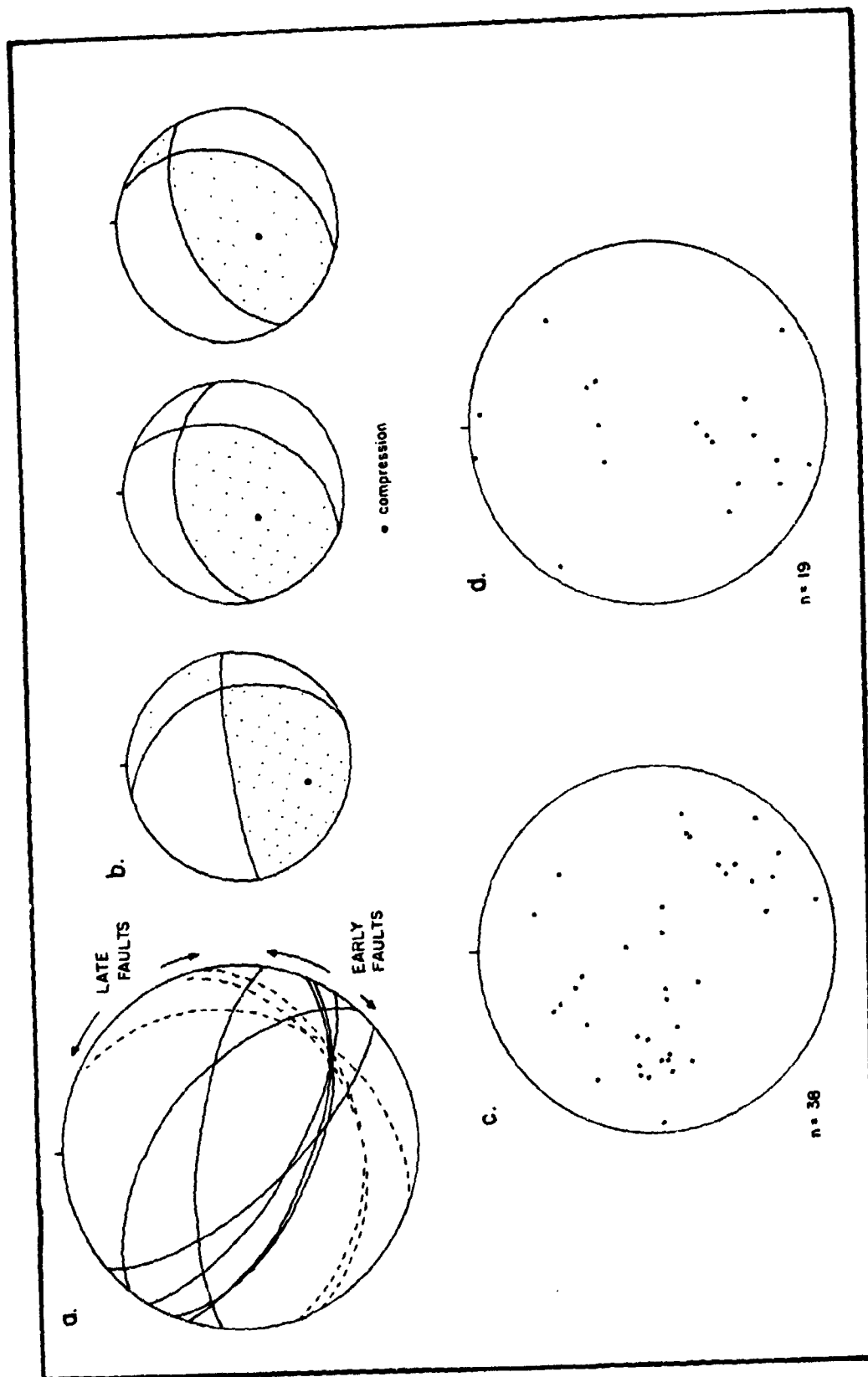
Bedding within the fault zone strikes N-S and is typically dipping at a steep angle to the east (Fig. 9.12b). Faults within the shear zone strike NE-SW and are near vertical (Fig. 9.12c), similar to the orientation of faults in the Hopewell Conglomerate, north of the fault zone exposure, but still within the Harvey-Hopewell Fault zone (Fig. 9.12d). In the Boss Point Formation south of the fault zone exposure, faults trend NW-SE (Fig. 9.12e).

Calcite filled tensional joints are common within the shear zone, and are oriented W-E (Fig. 9.12f), a trend which suggests that they are related to Triassic-Jurassic rifting.

Cross-cutting relationships in minor faults within the shear zone (Fig. 9.13a) commonly show that an earlier NW-SE oriented fault set (F_1), was cut by later formed, NE-trending faults (F_2), and W-E low-angle faults (F_3). Conjugate faults within the fault zone show consistent NE-SW directed compression (Fig. 9.13b), which is consistent with the dominant F_2 NE-SW trending faults being compressional or strike-slip. Striations are common throughout the fault zone exposure (Fig. 9.13c), and in general show moderate-angle, west-directed and SE-NW-directed movement planes, suggesting that a considerable dip-slip component was associated with the faulting. Striations adjacent to the Harvey-Hopewell Fault at Dennis Beach show south-directed movement directions (Fig. 9.13d), suggesting that this fault plane has had a different kinematic history to the thrust zone at Owls Head.

The dominant (F_2) NE-SW oriented fault pattern, and associated NE-SW compression indicates that many of the faults were strike-slip in nature, whereas the striations show a significant dip-slip component. It would not be unreasonable therefore for the faults to be transcurrent in nature.

- Fig. 9.13
- a) Fault solution for early F_1 and latter F_2 faults within the fault zone at Owls Head.
 - b) Conjugate fault couples from within the fault zone at Owls Head.
 - c) Striations from within the fault zone at Owls Head.
 - d) Striations from within the Harvey-Hopewell Fault zone at Dennis Beach.

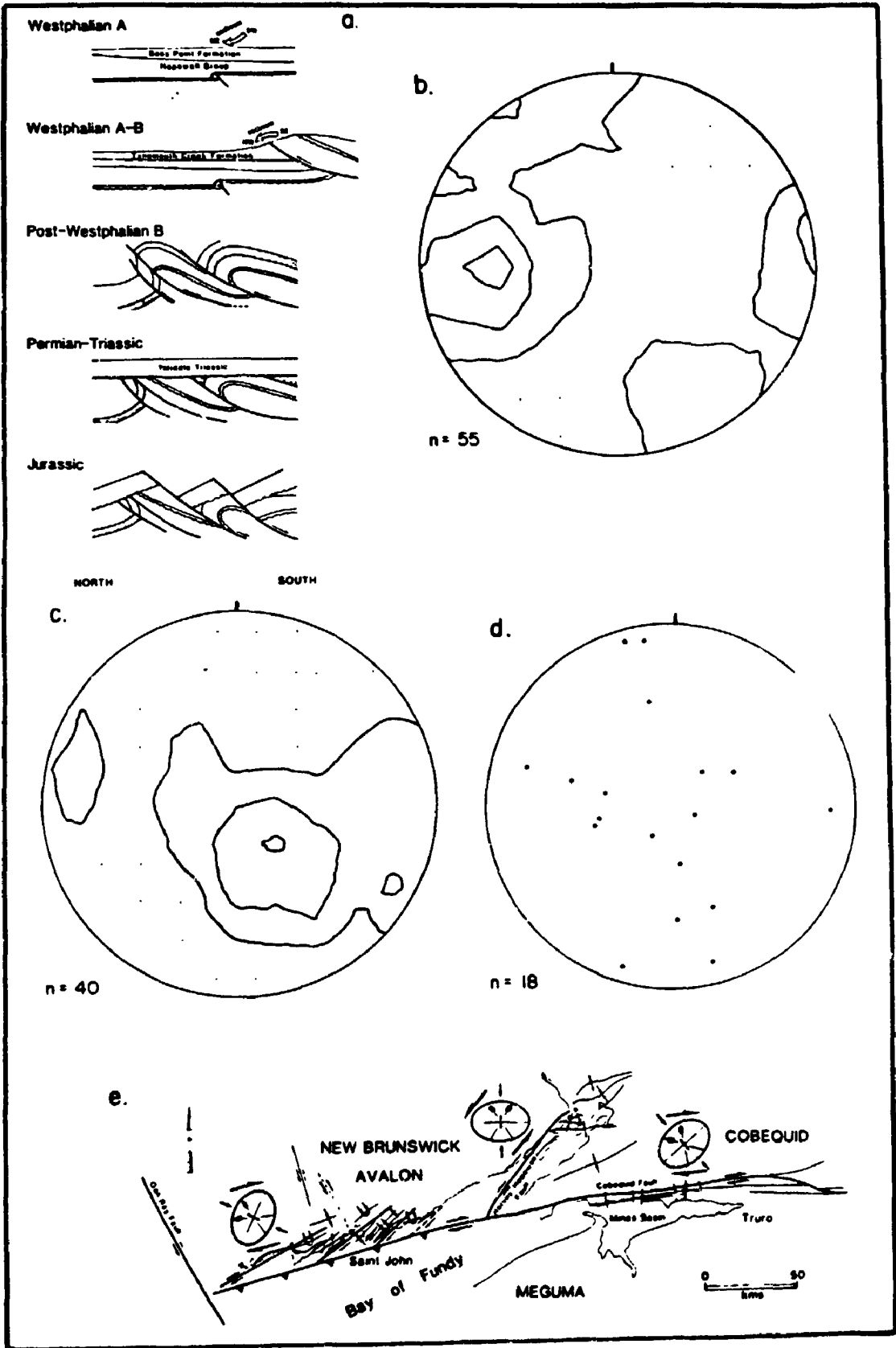


9.1.6 The Rogers Head Fault: Giffin Pond

A major shear zone exposure north of Giffin Pond, involves a moderately dipping thrust fault, which separates overturned Boss Point Formation sandstones from the Precambrian Coldbrook Volcanics. This locality, and the local structural evolution has previously been described by Plint and van de Poll (1984). It is not certain if this deformation is related to the Harvey-Hopewell Fault, but there is a strong possibility based on seismic work, that the Harvey-Hopewell Fault (or kinematically related structures) continues adjacent to the coast between Alma and St Martins (as suggested by Webb 1963, Nance 1987).

At Giffin Pond, deformation involved the northwest directed thrusting of the Coldbrook Volcanics and Boss Point Formation (Fig. 9.14a), deformation of which it has been suggested, commenced in the Westphalian B (Plint and van de Poll 1984). However the petrographic evidence reported in this study suggests that at least some of this movement began during Boss Point Formation (Westphalian A) time (see Chapter 4). Thrusting was related to a change in paleocurrent direction, from a SE-directed flow during Boss Point Formation time, to a NW-directed flow during deposition of the Tynemouth Creek Formation (Plint 1988). Paleocurrents recorded in this study from the very basal 20 m of the Tynemouth Creek Formation show a W-directed paleocurrent trend, suggesting that the change in

- Fig. 9.14 a) Model for the development of Westphalian thrusting and subsequent Jurassic extensional faulting in the Fundy coastal zone (from Plint & van de Poll 1984, Nance 1987).
- b) Poles to faults immediately below the Rogers Head Fault, north of Giffin Pond.
- c) Poles to faults >200m south of the Rogers Head Fault.
- d) Striations immediately below the Rogers Head Fault.
- e) Kinematic development of the Cobeguid and Harvey-Hopewell Faults as dextral and sinistral features, using the observed compression directions in Pennsylvanian strata. The strain ellipses (after Harding 1974) show that these two faults acted as conjugate pairs, and were associated with NE-SW fold axes (after Nance 1987).



paleocurrent related to thrusting, corresponds to the lithologic boundary between the Tynemouth Creek Formation and the Boss Point Formation. Thrusting and related sedimentation patterns are very similar to the south, where west-directed thrusting during the Westphalian B (and later), was related to the coarse-grained alluvial fan deposits of the Balls Lake Formation (Nance 1986, 1987).

Faults from the overturned Boss Point Formation sequence below the Rogers Head Fault (cf. Plint and van de Poll 1984, fig, 3), are dominantly high angle NE-trending structures (Fig. 9.14b), similar to the trend of faults from the less deformed Boss Point Formation further to the west (Fig. 9.14c). Striations are oriented west and SE-NW (Fig. 9.14d), very similar to the trend of striations from the Harvey-Hopewell Fault at Owls Head (Fig. 9.13c).

9.2 Tectonic Relationships in Older Carboniferous Units

No detailed examination was made of structures from other formations. However paleocurrents were routinely measured in many locations, and from these, certain conclusions may be drawn regarding the structural framework of the Cumberland sub-basin.

Paleocurrents from the Maringouin, Shepody and Claremont Formations (Figs. 9.15, 9.16 & 9.17) show similar trends to those of the Boss Point Formation (Fig. 8.1). Maringouin Formation paleocurrents are consistently to the

Fig. 9.15 Paleocurrent directions from ripple and climbing ripple lamination in the Maringouin Formation (Viséan-Namurian A).

MARINGOUIN FORMATION - Ripple & Climbing Ripple Lamination

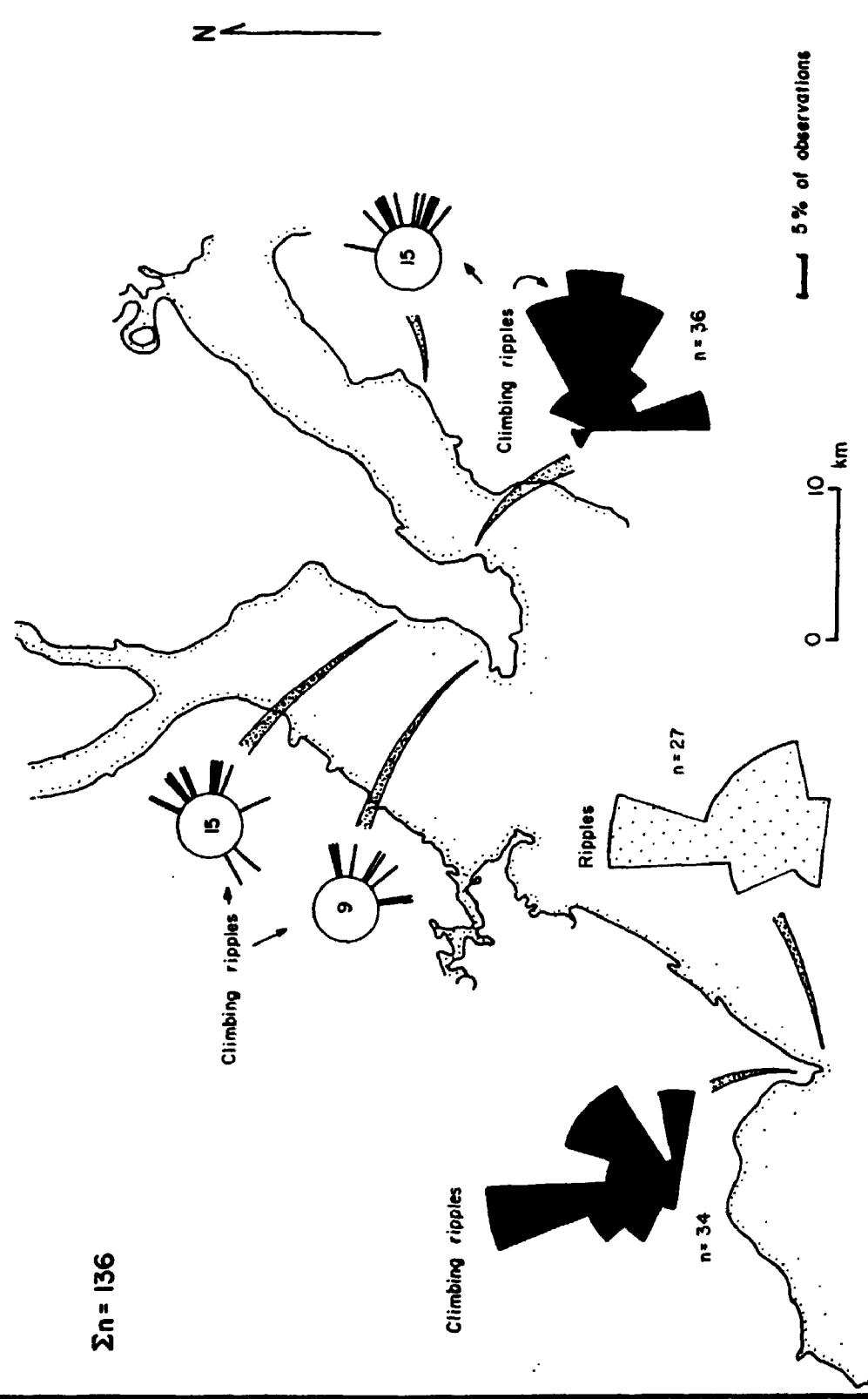


Fig. 9.16 Paleocurrent directions from trough cross-bedding
in the Shepody Formation (Namurian A).

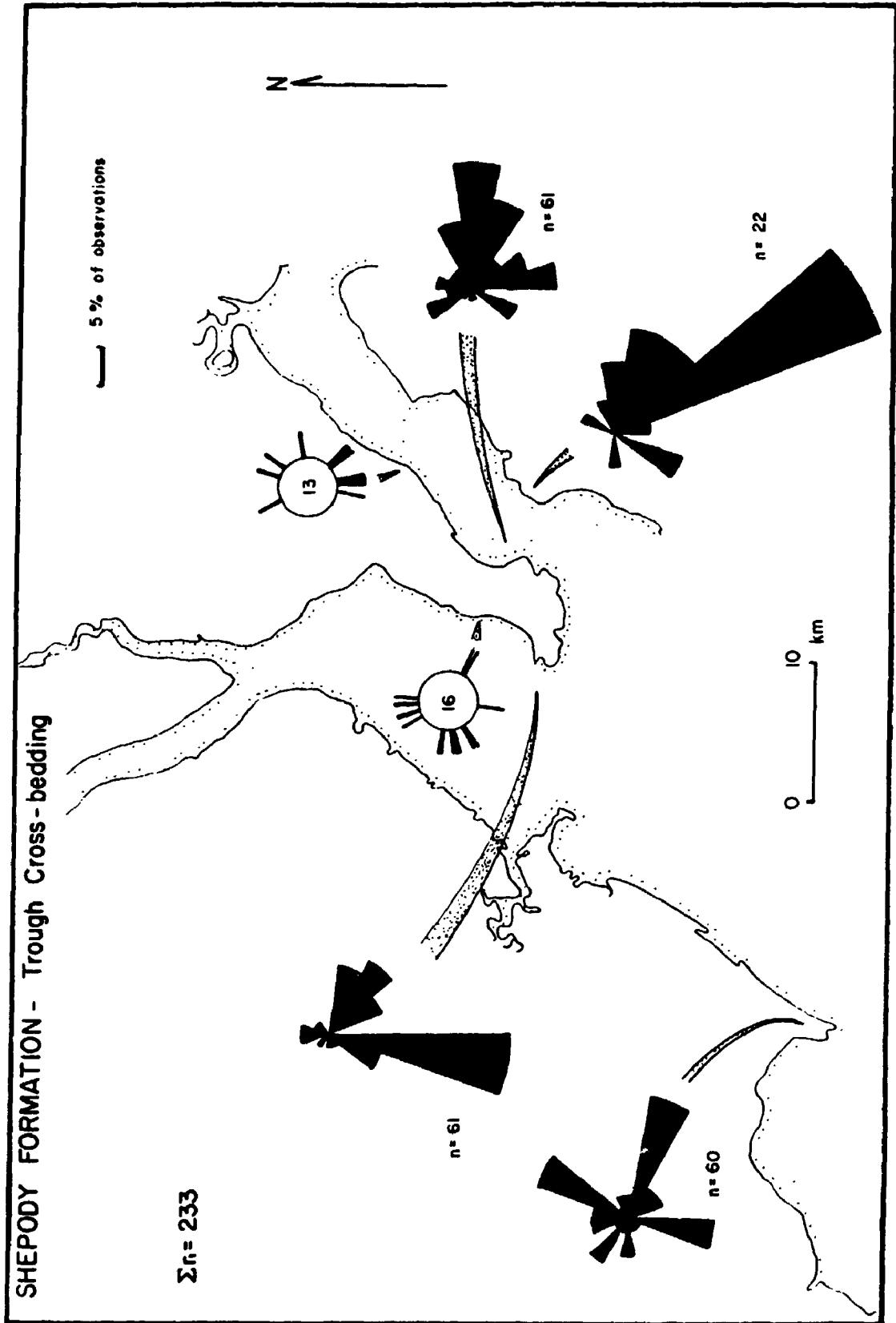
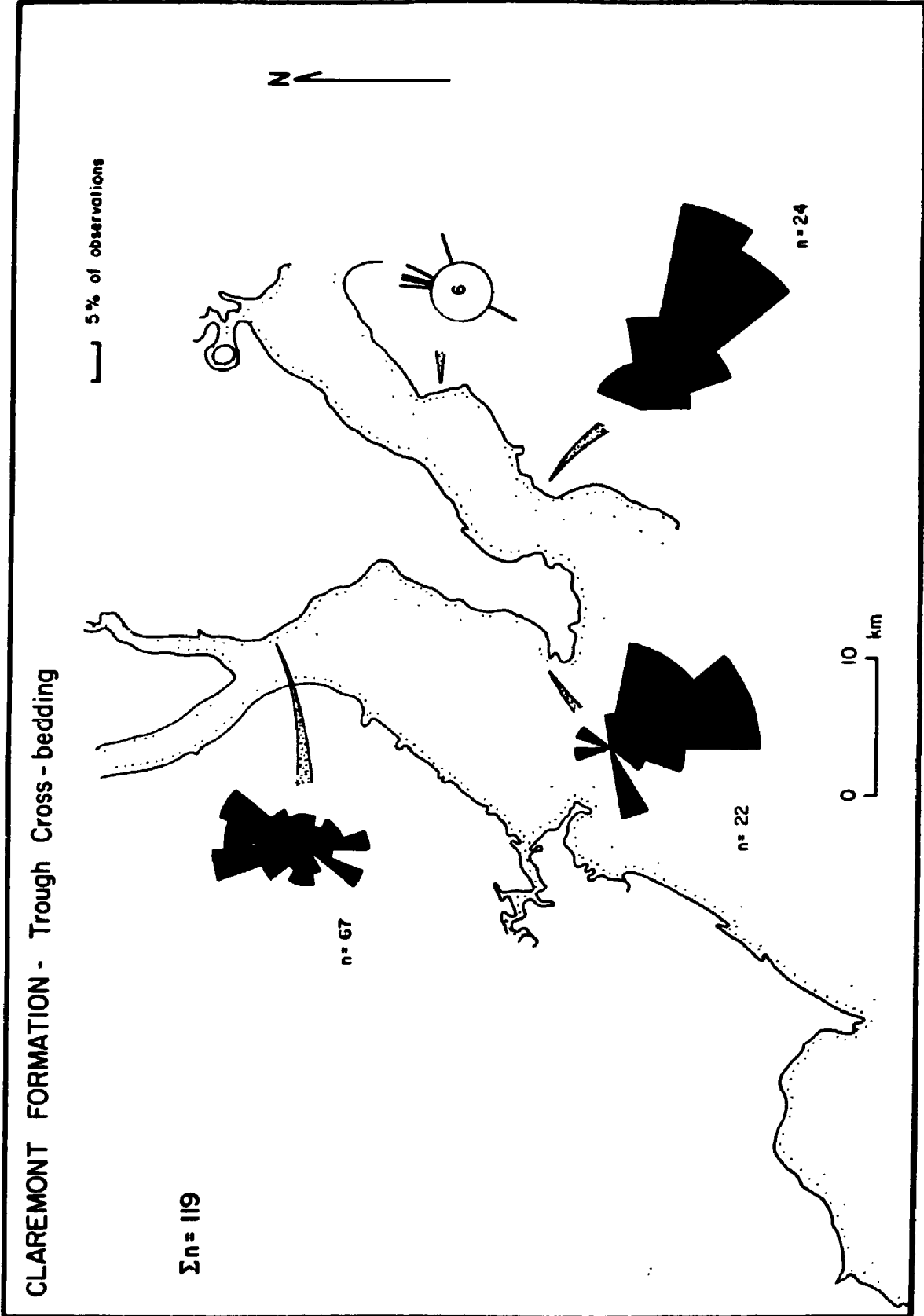


Fig. 9.17 Paleocurrent directions from trough cross-bedding in the Claremont Formation (Namurian B-Westphalian A).



north and east at Cape Enrage (a trend also indicated by the late B.R. Rust, pers comm. 1989), but swings to the east in the northern and eastern part of the Bay of Fundy region (Fig. 9.15). Paleocurrents from the Shepody Formation are similar (Fig. 9.16), but at Johnson Mills show a northerly and westerly trend which is comparable to the Boss Point Formation paleocurrents in this area (Fig. 8.1). Information for the Claremont Formation is limited (Fig. 9.17), but show dominantly easterly trends in the east, whereas at Dorchester paleocurrents are bipolar to the north and south. The similarity of paleocurrent data in these older Carboniferous units to that of the Boss Point Formation indicates that the paleogeography in the region did not change significantly between Viséan and Westphalian time, and further that the paleogeographic high recognised in the central portion of the Bay of Fundy (Chapters 6 & 8) during Boss Point Formation time, was probably also a physiographic feature throughout the Late Mississippian and Early Pennsylvanian.

9.3 Tectonic Models

Theories differ as to the exact origin of the sub-basins that make up the Maritimes Basin. A rift model was proposed by Belt (1968b) and later supported by McCutcheon and Robinson (1987), though most workers have suggested development associated with active tectonics, either as

pull-apart basins (Bradley 1982, D'Orsay 1986, Leger 1986, Nance 1987, Yeo & Ruixiang 1987), wrench basins (Fralick 1981, Fralick and Schenk 1981) or strike-slip basins (Gibling *et al.* 1987, Martel 1987). In respect to their tectonic development, the sub-basins of the Maritimes Basin appear similar to the pull-apart basins that developed in southern New England during the Carboniferous (Mosher 1983).

Pull-apart basins are defined as basins "formed by local crustal extension along strike-slip fault zones" (Zhang *et al.* 1989, p. 814). Carboniferous strike-slip activity along many of the faults in the Maritimes has been demonstrated (Bradley 1982, Donohoe and Wallace 1982, Leger 1986, Nance 1987, Yeo & Ruixiang 1987), and is supported from the data presented here.

The major faults that bound the sub-basins are well delineated, but work on their structural history has only recently been initiated (Eisbacher 1967, 1969, Donohoe and Wallace 1982, 1988, Yeo and Ruixiang 1986). A considerable amount of work still needs to be done mapping kinematic indicators in these fault zones and in equating fault movement with the sedimentary patterns adjacent to these faults. However a consensus is now emerging whereby regional variations in structural style, involving thrusting, strike-slip movement and extension, can be resolved within a wrench tectonic regime (Harding 1974, Harding and Lowell 1979).

Kinematically, the fault and fold geometry of the western Cumberland sub-basin can be explained in terms of the Cobequid-Chedabucto and Harvey-Hopewell Faults acting as a conjugate pair in a NW-SE or N-S compressional regime (Fig. 9.14e). This model is consistent with the compression directions determined from conjugate fault couples (this study) and with stress determinations made by Nance (1986, 1987). It also accounts for dextral movement on the Cobequid-Chedabucto Fault and sinistral movement on the Harvey-Hopewell Fault, and the NE-SW orientation of thrust faults, and the NE-SW orientation of regional folds (such as the Athol Syncline and Scotsburn Anticline; Fig. 1.2).

The sub-basins of the Maritimes developed adjacent to these strike-slip faults, as a result of dextral transpression (Martel 1987, Nance 1987), associated with movement on the Cobequid-Chedabucto Fault. Development of the dextral transpressive regime involved thrusting and the formation of positive flower structures at many localities along the Harvey-Hopewell Fault on the western side of the Cumberland sub-basin (Webb 1963, Plint and van de Poll 1984, Nance 1987); structures that are considered diagnostic of convergent wrench settings (Harding and Lowell 1979, Harding 1985). The location of these thrusts coincided with a major, right lateral compressive bend in the Cobequid-Chedabucto Fault during the Upper Carboniferous (Nance 1987). Namurian or possibly early

Westphalian structural deformation associated with the bend has recently been documented in western Nova Scotia along the Cobequid Fault (Waldron *et al.* 1989).

Modern analogues that incorporate plate boundaries and fluvial deposition in pull-apart basins include the Dead Sea Rift (Kashai and Crocker 1987, Ten Brink and Ben-Avraham 1989), the San Andreas Fault along major restraining bends (Sylvester 1988), and North Canterbury, New Zealand (Fruend 1971), though only the latter two involve pull-apart development at a restraining bend in the strike-slip faults.

CHAPTER 10

CONTROLS ON SEDIMENTATION

Traditionally fluvial successions are considered as spatially confined channel systems in which it is hard if not impossible to correlate isolated outcrops accurately or to make regional stratigraphic correlation of facies (Miall 1987, p.5). Recently however, several studies have demonstrated continuity between facies developed in ancient fluvial units (Blair 1987, Masson and Rust 1990), and that in so doing, considerable understanding can be made about the controls on depositional processes. The emphasis on architectural element analysis popularised by some workers (Miall 1985, 1988, Miall and Turner-Peterson 1989) is in part, a reflection of our increased understanding of fluvial stratal geometries.

The most striking feature of the Boss Point Formation is the sharply defined alternation between sandstone and siltstone packages. Stacked, erosionally based trough cross-bedded sandstone units, as much as 130 m thick, are overlain abruptly by siltstone, up to 40 m thick (Plate 5a). The tops of the stacked sandstone units are sharp; no transitional facies are present between these two lithologies (see section 7.3).

Although individual beds can not be correlated through the Bay of Fundy region, correlations can be confidently

made between thicker (>5 m thick) bedded mudrock and stacked sandstone successions (Figs. 7.7 & 7.8) based on similarity of facies, bounding surfaces, and correlation of paleosols. These regional correlations indicate that at least 8 large "megacycles" can be traced over a 20 km distance in the formation.

These key observations need to be accounted for in terms of the allocyclic (influences external to the catchment) and autocyclic (within catchment) mechanism or mechanisms which controlled sedimentation. Traditionally these include eustatic (Wanless and Shepard 1936), tectonic (Bott and Johnson 1967), climatic (Platt 1989a) and a variety of autocyclic controls (Moore 1957), and all of these have been invoked at different times for Carboniferous fluvial successions (see review in Leeder and Strudwick 1987).

Several mechanisms could explain the abrupt change between sandstone and siltstone observed in the Boss Point Formation, and the repetitive nature of these megacycles. Possible mechanisms include:

- Dam mechanisms
- Channel avulsion
- Changes in weather
- Changes in climate and/or vegetation
- Tectonic effects
- Eustatic effects

10.1 Dam Mechanisms

Dam mechanisms can easily change the pattern of fluvial

deposition, and are well known in fluvial settings. They include log and assorted riparian vegetation jams (Hickin 1984), damming by glaciers (Fahnestock and Bradley 1973) and coalescing of alluvial fans from adjacent margins of the flood plain. These phenomena are comparatively local features however, and can not readily explain the widespread patterns observed in the Boss Point Formation.

10.2 Channel Avulsion

Channel avulsion is an intrinsic feature of all braided channels (Smith 1973, Ashmore 1982, Bristow 1987, Smith et al. 1989), and is an important cause of changes in lithofacies recorded in vertical sections (see Chapter 7). Associated with the avulsions would be adjacent overbank fines, and their absence in the Boss Point Formation, suggests that other mechanisms operated.

10.3 Changes in Weather

Weather changes are those that occur in the order of a few days or months. It is possible for distinct lithofacies to be developed in response to weather patterns; sandstones and conglomerates being deposited during wet periods, whereas fine-grained sediments are deposited in dry intervals. In Chapter 6, it was suggested that a monsoonal weather pattern may have existed during

Boss Point Formation time, a notion that would be in accord with marked changes in sedimentation. However if such a mechanism did operate, clearly the thickness of each weather-related cycle would be correspondingly thin, and is certainly not a viable explanation for the cyclicity in the Boss Point Formation.

10.4 Changes in Climate and/or Vegetation

Climatic changes are those that occur in the order of 10 s of years, and it is common for example, for sands and coarse-grained material to be deposited during the rainy periods finer-grained material deposited during times of low rainfall. In principle, climatic changes are more likely to account for the thicknesses of the alternation between sandstone and siltstone observed in the Boss Point Formation, though it is not likely that some 130 m of sandstone could be deposited during a single climatic fluctuation, and it is extremely unlikely that the 8 megacycles observed in the Boss Point Formation would represent 8 climatic periods.

Changes in vegetation may be climatically controlled, deforestation leading to increased rates of erosion and hence coarser-grained deposition.

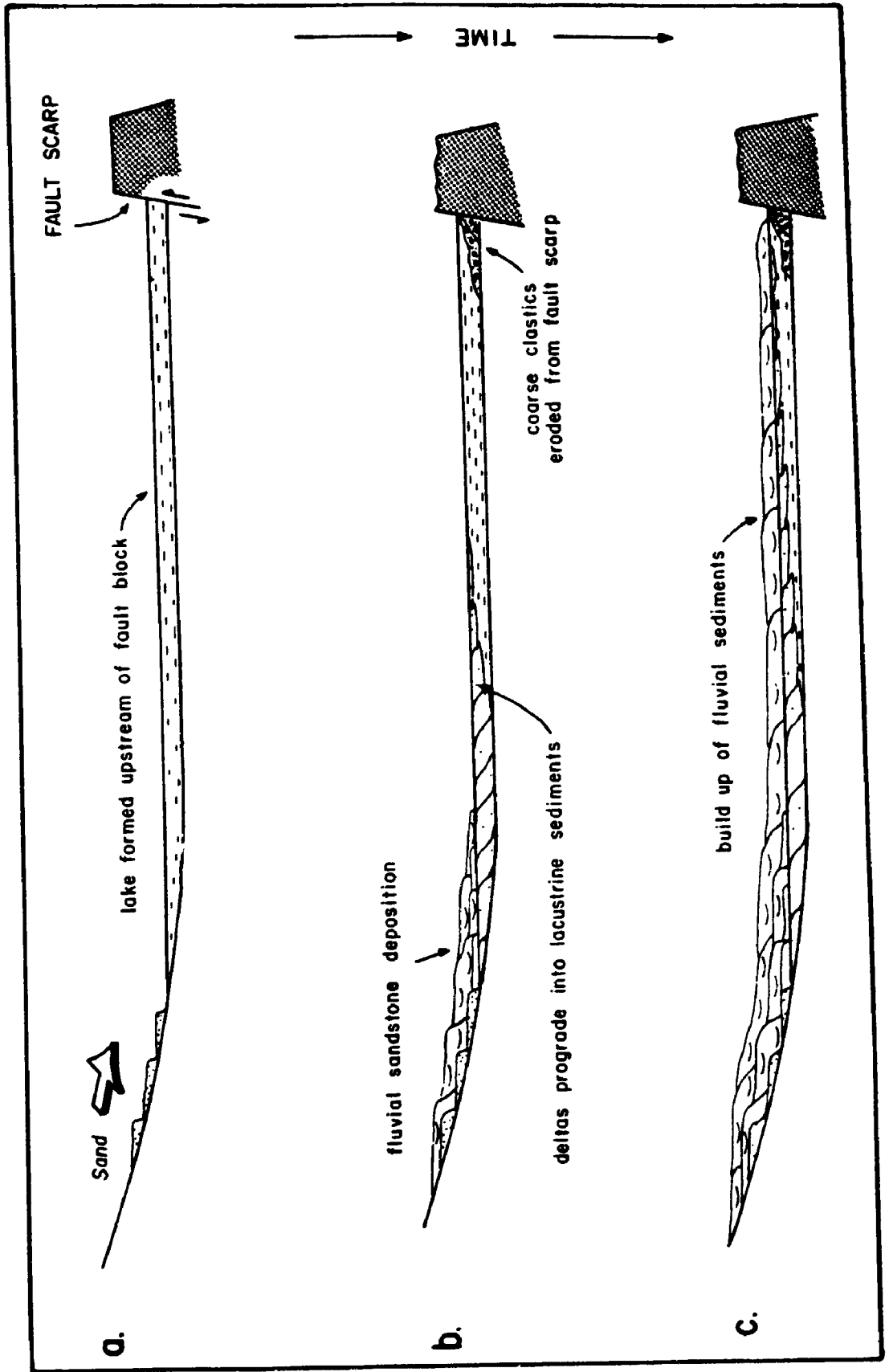
10.5 Tectonic Effects

Tectonic effects have been documented during sedimentation of the Boss Point Formation and can be clearly shown to effect both paleocurrents and sedimentary facies distributions (see Chapters 4, 6 & 9). As tectonism is inferred to have occurred during sedimentation, it is very likely that other faults were also active during the time of deposition of the formation. Little information can be gathered in this regard due to the limited outcrop, but penecontemporaneous faulting is known to have occurred immediately prior to the deposition of the Boss Point Formation in central Nova Scotia (the Millville formation; see Boehner et al. 1986).

Faulting in the lower part of the drainage profile may have changed local base level sufficiently to cause lakes to be developed in higher parts of the profile (Fig. 10.1), similar to those observed in the Boss Point Formation. Sandstones may have been deposited during times when faulting was relatively inactive, when the fault scarps were subdued by erosion (Fig. 10.1b & c). So little can ever be known about the Westphalian paleogeography that existed further downstream to the east, that the possibility of fault controlled sandstone and siltstone megacycles could never be entirely discounted.

Although faulting could account for the elevation of base level and the development of lakes, faulting *per se* would not promote the development of the subsequent

Fig. 10.1 Alluvial sedimentation patterns following initiation of a fault scarp in the lower reaches of the depositional profile. Initially (at time a), lacustrine sediments will be deposited upstream of the scarp. With time (b), sands will be deposited into the lake as a series of prograding deltas. At a later stage (time c), the entire lake will be infilled, and fluvial sandstones will rest either sharply on the underlying lacustrine siltstones, or will grade up from the siltstones. In either case, the contact at the base of the fluvial sandstones will not be erosive, unlike the relationship in the Boss Point Formation.



sandstone deposition phase. Once lakes developed, deltas would prograde into these lakes, and in time would infill them (Fig. 10.1b & c). This would be recorded in the geologic record as coarsening-upward cycles, capped by deltaic sands, roots and paleosols. Because the transition from lacustrine siltstone to fluvial sandstone will be *gradational*, a faulting mechanism by itself therefore cannot account for the large *erosional* surfaces preserved at the base of each sandstone unit of the Boss Point Formation.

10.6 Eustatic Effects

Eustasy too must be considered as a cause for the alternating sandstone and siltstone megacycles. Implicit from the early work on cyclothems (Wanless and Shepard 1936) and from subsequent work is that a relative sea level, and hence a base level fall will cause streams to erode, because of the increased gradient of the profile. The fluvial system will degrade by erosion proceeding upstream from the mouth.

Sandstones would be deposited during periods of falling sea level as gradients are increased, and there is a greater ability to erode and deposit sediment (cf. Atkinson 1986, Muto 1988), whereas siltstone will be deposited during rising relative sea levels as base levels are raised (see Dekker *et al.* 1987, Karistineos and Ioakim 1989).

Eustasy is therefore a plausible mechanism that could generate 8 sandstone and siltstone megacycles, each package representing a single eustatic cycle. As such, the term "sequence" may be used synonymously with megacycle to describe the alternation of these major sandstone and siltstone packages. Because their sharp erosional base, and extensive lateral continuity can be demonstrated, they conform to the definition of a *sequence* being "a relatively conformable succession of genetically related strata bounded by unconformities or their correlative conformities" (van Wagoner *et al.* 1988, p. 39).

Viewing the depositional system in this sequence stratigraphic context is a departure from previous work on sequence stratigraphy, which has dealt with marine depositional settings almost exclusively. Eustatic changes through time and the effects on stratal geometries are well recognised in marine depositional settings (van Wagoner *et al.* 1988), and, although it is appreciated, especially on theoretical grounds, that the same processes influence fluvial sedimentation, documented field studies of fluvial responses to eustasy are few. Important exceptions include work by McCave (1969), Plint (1983), Marzo *et al.* (1988), Muto (1988), Nelson *et al.* (1988), Nelson *et al.* (1989), and Miller *et al.* (1990).

Traditionally, studies of fluvial successions have emphasised lateral facies changes (Miall 1983, 1987). In recent years though, a number of studies have shown that

individual sedimentary packages can be traced over distances that range from several hundred metres to several kilometres (Atkinson 1986, Blair 1987, Miall and Turner-Peterson 1989, Masson and Rust 1990).

Despite early recognition that sea level fluctuations effect non-marine sedimentation (see for example Wanless and Shepard 1936), subsequent work has largely ignored the possible contribution of eustasy as a control on fluvial deposition (eg. Blair 1987, Kraus and Middleton 1987, Lawrence and Williams 1987, Miall 1987, Platt 1990a). No studies have taken as a basis the theoretical model proposed by Posamentier and Vail (1988) and assessed the fluvial response in this light, by applying it to a well documented geological analogue.

10.6.1 Sequence Stratigraphy in a Fluvial Setting - Theory

Eustatic controls on coastal plain sedimentation patterns have recently been addressed on a theoretical basis by Posamentier and Vail (1988). Their model assumes a passive margin setting under a constant and basinward-increasing rate of subsidence, and predicts changes in fluvial aggradation through changing eustasy.

Posamentier and Vail (1988) consider 3 arbitrary positions on the depositional profile, and predict the relative changes in the positions of these points with time, during eustatic fluctuations. These positions are:

The Equilibrium Point: The point along the depositional profile where the rate of eustatic change equals the rate of subsidence/uplift. It separates zones of rising and falling relative sea level.

Tectonic Hinge Point: The point along the depositional profile where subsidence is zero.

The Bayline: The demarcation line between fluvial and paralic/delta environments.

For their purpose, Posamentier and Vail (1988, their figure 8) take 8 positions on the eustatic curve (T_1 to T_8), and model the fluvial response at each time interval (Fig. 10.2).

During the time of the highest relative sea level (T_1), the equilibrium point and tectonic hinge will be coincident and well up the depositional profile in relation to the bayline. With a relative sea level fall (T_2 to T_3) the equilibrium point will migrate down the depositional profile, toward the bayline, until T_4 , when both the equilibrium point and the bayline correspond (Fig. 10.2). It is during the time period T_4 to T_6 that both the equilibrium point and the bayline migrate basinward (Figs. 10.2 & 10.3), and it is during this interval that fluvial deposition is predicted to occur by the model. After T_6 (the fall inflection point) the equilibrium point moves back up the depositional profile, faster than the bayline, such that alluvial deposition will be inhibited, and the depositional profile will be flooded (transgressed) as the bayline migrates up the profile. Posamentier and Vail (1988) don't entirely rule out the possibility of fluvial

Fig. 10.2 Response of sedimentation on a depositional profile to a eustatic cycle (after Posamentier and Vail 1988). E= the Equilibrium Point; T= Tectonic Hinge; B= Bayline as defined in the text.

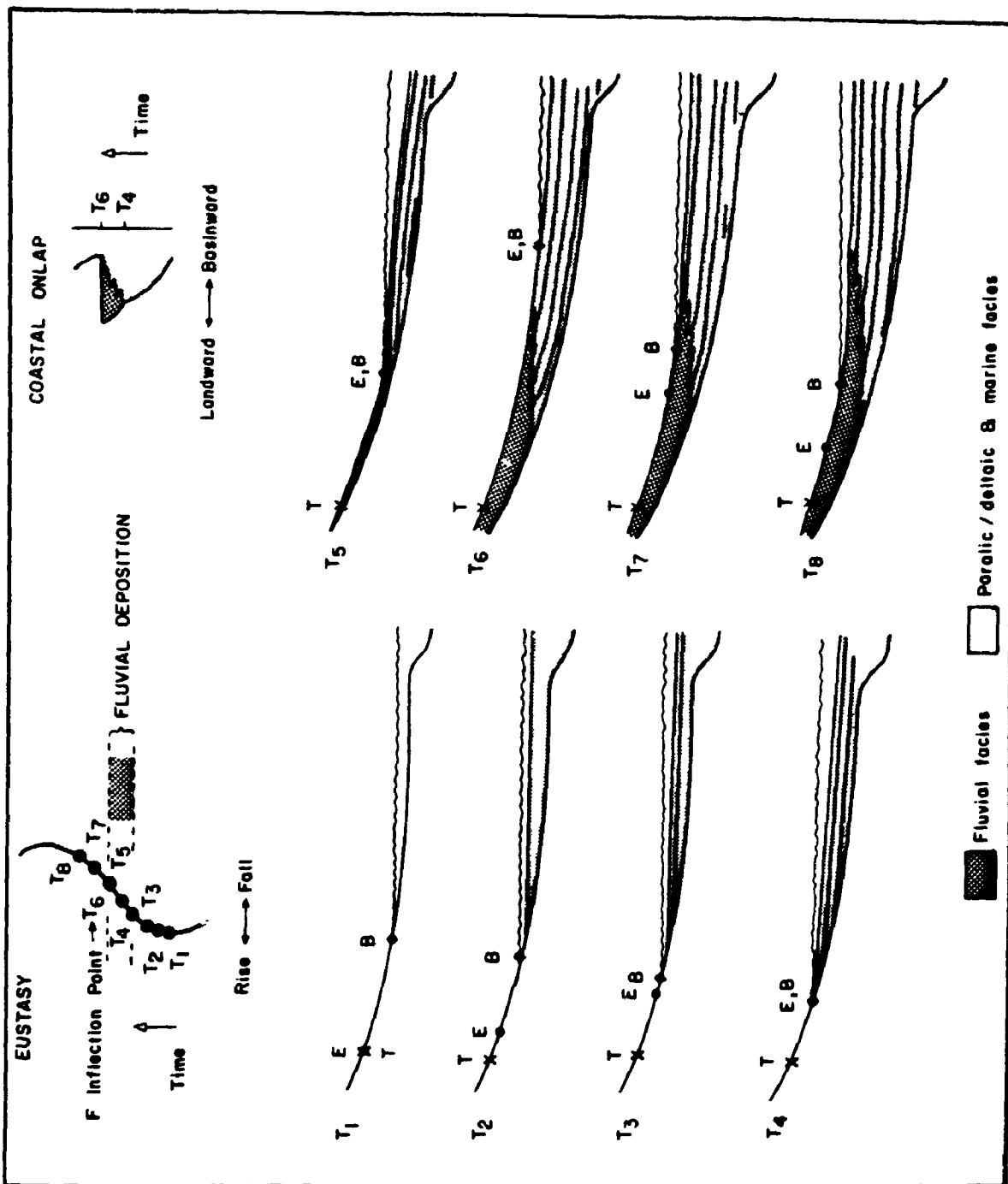
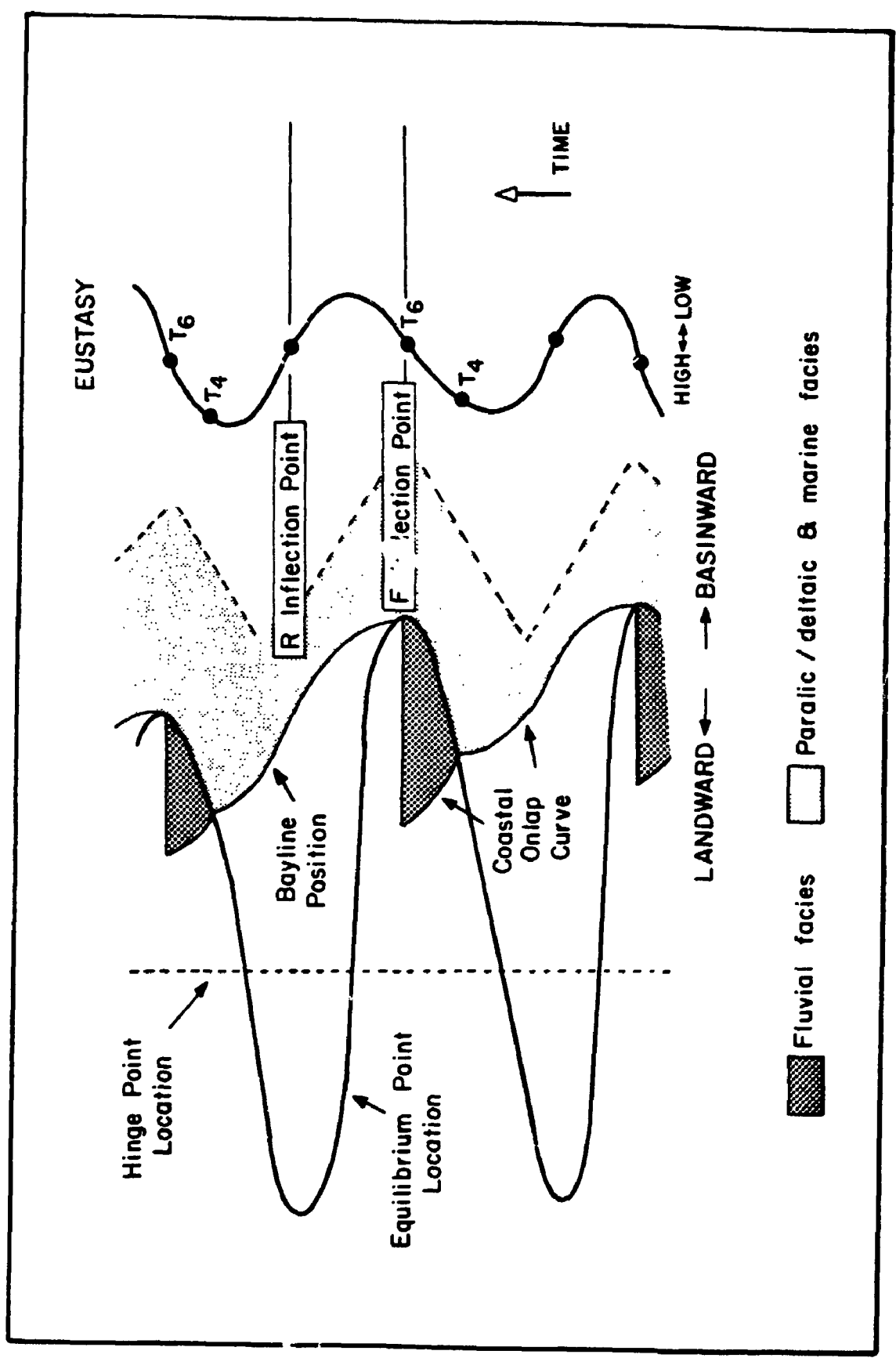


Fig. 10.3 Elements of the coastal onlap curve (after Posamentier et al. (1988)). The inflection points are positions on the eustatic curve where absolute slope or rate of change is greatest, the one on the falling limb being the F Inflection Point, the one on the rising limb being the R Inflection Point. Positions T_4 and T_6 are positions of the eustatic curve given in Fig. 10.2.



deposition before T_4 and after T_6 , but suggest that it is unlikely to be extensively developed (Figs. 10.2 & 10.3).

10.6.2 A Process-Response Model Based on the Boss Point Formation: Observed Versus Predicted Relationships

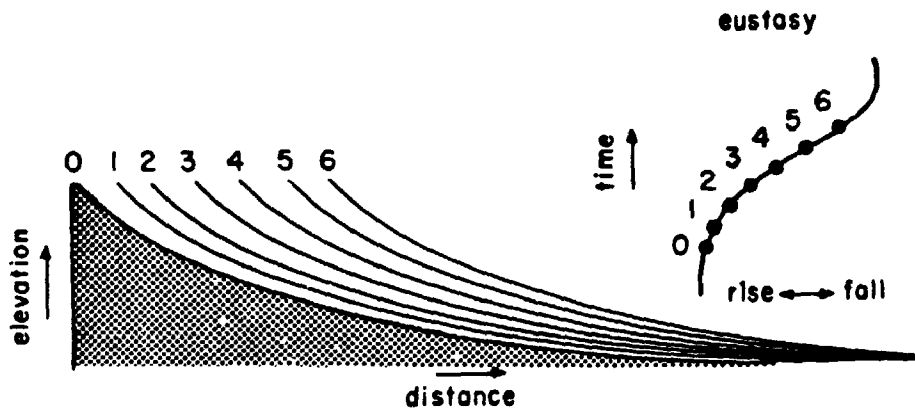
The Posamentier and Vail model serves as a useful reference from which to view fluvial deposition in ancient settings. However, using the Boss Point Formation as an ancient analogue it is apparent that some of the concepts proposed by the Posamentier and Vail model are not borne out by field observations. Several criticisms are presented below.

The change in depositional profile in response to relative sea level change modelled by Posamentier and Vail (Fig. 10.4), is clearly a gross exaggeration. Gradients of the order presented by their model are approximately 1 in 2, analogues to Himalayan proportions. Rather the great majority of the Boss Point Formation depositional profile would be of low gradient, in the order of 1 in 1000 to 1 in 10,000. It would be more realistic to consider a maximum gradient for the Boss Point Formation as 1 in 1000, which for example, would require a 10 km shift in the shoreline position to create space for 10 m of sediment.

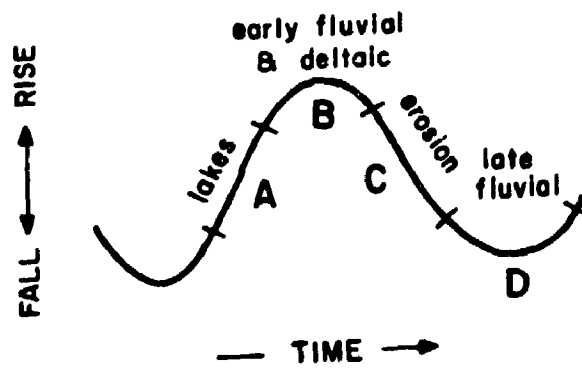
Accepting the tenet of the Posamentier and Vail model that sandstone deposition would occur during relative sea level fall, and siltstone deposition during relative sea

Fig. 10.4 Cartoon showing the relationship between falling sea level and accommodation on the depositional profile (after Posamentier and Vail 1988).

Fig. 10.5 Summary of depositional facies in relation to eustasy. For details see Fig. 10.6.



EUSTASY

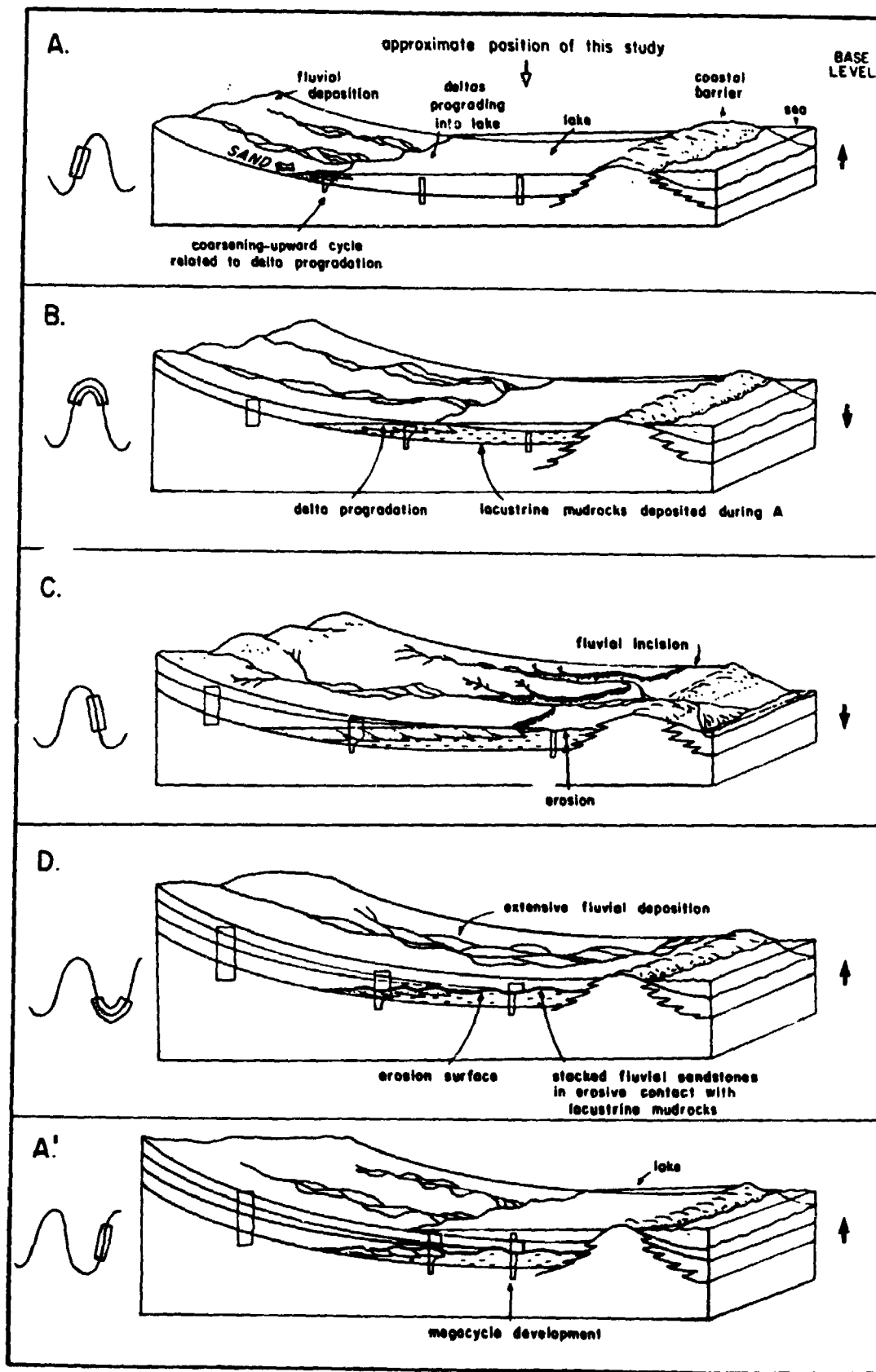


level rise, the response of the fluvial system to base level changes can be modelled sequentially (Fig. 10.5). For the present purpose, the eustatic curve can be divided into 4 compartments (A to D).

During a relative sea level rise (A; see Fig. 10.5), lacustrine facies will be deposited over the lower portions of the depositional profile (Fig. 10.6A). Coarser-grained fluvial clastics will be deposited only in the upper reaches. At some unspecified distance downstream, these coarser-grained clastics will interdigitate with the lacustrine facies (Fig. 10.6A), producing coarsening-upward deltaic units. The position of the deltas will vary spatially in time, and will be dependent on such factors as changes in sediment supply, discharge, subsidence or relative eustatic rise or fall.

However, at the maximum rate of relative sea level rise (the rise inflection point), the lacustrine facies would be expected to reach its maximum geographic development (ie. be the furthest distance up the depositional profile). Following the rise inflection point, the rate of addition of new space (accommodation) progressively diminishes to the eustatic highstand, after which accelerating eustatic fall reduces the accommodation. As a result, deltas which developed in the earlier rising eustatic phase will prograde basinward, down the depositional profile (Fig. 10.6B). Fluvial sedimentation will occur in the upper portions of the depositional profile, but the overall

Fig. 10.6 Summary of the deposition of the Boss Point Formation in relation to eustatic change. Lacustrine sediments were deposited at time A as relative sea level rose. Deltas prograding into the lake result in coarsening-upward cycles (time B), but as relative sea level falls, erosion initiated at the coast results in incision (time C), cutting a new depositional profile to the lowered base level. This erosion surface would be widespread, and erodes into the underlying transgressive and high stand deposits (lacustrine and deltaic facies). Stacked fluvial sandstone would be deposited on top of this erosion surface (time D).



stratigraphic response will be the development of deltaic coarsening-upward cycles, with lacustrine siltstone at the base, passing gradationally upward into coarser-grained sediments (perhaps rooted at the top). In time these deltas would prograde further into the lake (Fig. 10.6B).

Sandstone deposition will continue to occur throughout the depositional profile during eustatic fall. However, when the rate of eustatic fall exceeds the rate of subsidence (at C; Fig. 10.5), erosion will commence at the coast, and will cause the rivers to incise down to the new base level (Fig. 10.6C). This will be recorded in the geological record by a sharp, erosional contact of fluvial sandstones resting on previously deposited transgressive and highstand deposits, which in the Boss Point Formation are represented by lacustrine siltstones and coarsening-upward deltaic units (Fig. 10.6C).

Fluvial sedimentation will continue from the eustatic lowstand to the point of maximum sea level rise (at D; Fig. 10.6), when the elevation of the base level will start the next cycle of lacustrine deposition (at A'; Fig. 10.6).

The evolution of the depositional profile from A to D represents one megacycle in the Boss Point Formation, the sandstones interpreted as lowstand deposits, whereas the siltstones are interpreted as transgressive deposits (Figs. 10.5 & 10.6).

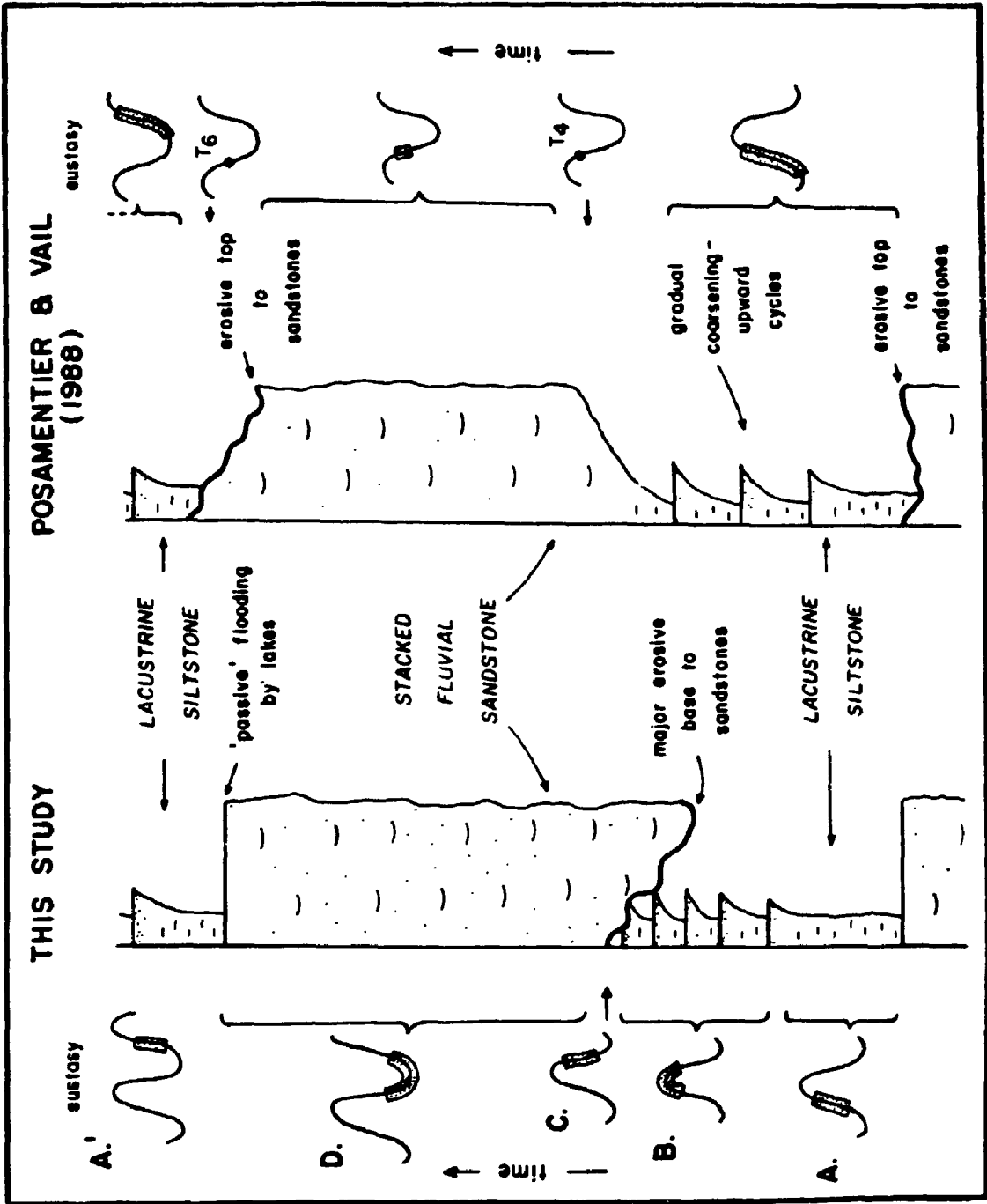
Clearly however, there are several major differences between the observations from the Boss Point Formation and

the model of Posamentier and Vail. The major feature of the Boss Point Formation megacycles is the erosive contact at the base of the sandstones (Fig. 10.7). In the Posamentier and Vail model however, the sands should gradually replace the siltstone, and the major truncation event corresponding to the fall inflection point, should occur at the top of the sandstone package (Fig. 10.7). In this respect the two scenarios are fundamentally different. The geologic record from the Boss Point Formation indicates that the major truncation occurs at the base of the sandstone; the base of the siltstone is in effect a "non event", representing passive flooding of the braidplain by the lake.

10.7 What were the Causes of Eustasy?

Accepting that eustasy can account for the megacyclic deposition in the Boss Point Formation, causes for the eustasy should also be considered. Eustasy can be explained in terms of volume changes of ocean basins brought about by earth deformation or volcanism (tectono-eustasy; see Summerhayes 1986), or to glaciations (glacio-eustasy). Tectono-eustasy during the Carboniferous can not be ruled out, especially as this was the period of the Alleghanian Orogeny, when changes in spreading rate could easily have influenced sea levels over the order of several million years (third-order cycles).

Fig. 10.7 The stratal relationships of the Boss Point megacycles, in response to eustatic changes, compared with the theoretic model of Posamentier and Vail (1988). The fundamental differences occur at the base of the stacked fluvial sandstone units. In the Boss Point Formation this contact is erosional and relates to falling relative sea level; in the Posamentier and Vail situation, this contact is gradational; in their model the most pronounced contact occurs at the top of the sandstone package.



The alternative explanation involving glacio-eustasy is well documented for the Carboniferous. The Pennsylvanian contains some of the best studied sedimentary cycles, and a great number of these have been attributed to glacio-eustatic effects, in both marine and non-marine environments (Wanless and Shepard 1936, Ross and Ross 1985, 1988, Saunders and Ramsbottom 1986, Leeder 1988, Collier et al. 1990) and many individual events can be correlated within and between continents (Ross and Ross 1985, 1988, Heckel 1986, Saunders and Ramsbottom 1986, Faulkner et al. 1990). Permo-Carboniferous glaciations have been recognised from all southern (Gondwana) continents (Crowell and Frakes 1975, Crowell 1978, Braakman et al. 1982, Caputo and Crowell 1985, Veevers and Powell 1987, Leeder 1988), and many of these have been previously used to explain Carboniferous cyclic sedimentation elsewhere in North America (Heckel 1986, Bird 1987, Gibling and Rust 1990).

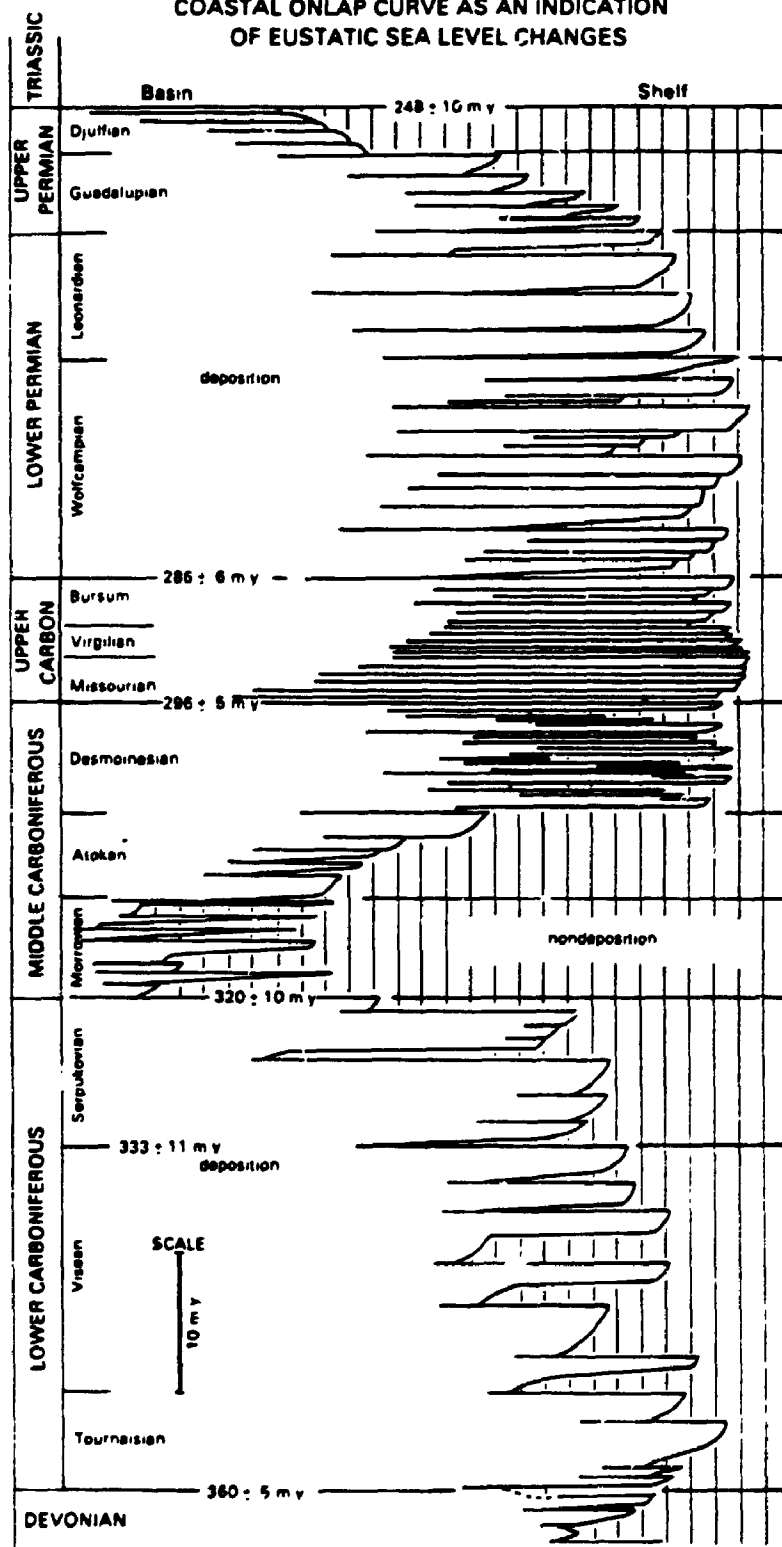
The largest Carboniferous glacial period was during the Early Pennsylvanian, that is, during Westphalian time (Fig. 10.8; Ross and Ross 1988, Brand 1989).

10.7.1 Causes of Glacial Cycles

It is tempting to speculate on the causes of the Carboniferous glacio-eustatic events. The most plausible explanation for the glacio-eustasy appears to be through variation in the orbital path of the Earth around the Sun,

Fig. 10.8 Coastal onlap curve for Carboniferous and Permian shelf sediments based on global data (from Ross and Ross 1988).

COASTAL ONLAP CURVE AS AN INDICATION OF EUSTATIC SEA LEVEL CHANGES



in that this distance has changed in a quasi-periodic fashion with time, in accordance with that predicted by Milankovitch theory (Imbrie et al. 1984).

Milankovitch theory predicts that the orbital path follows regular cycles with periods of approximately 19,000 to 23,000 years (precession), 41,000 years (obliquity) and 100,000 and 400,000 years (eccentricity). The longest cycles, those of eccentricity, are taken to have been constant through the last 400 Ma (after Lambeck 1980, p.388 and Walker and Zahnle 1986), whereas the shorter duration cycles attributed to precession and obliquity (influenced by variations in the Earth-Moon distance) have varied over geologic time (Collier et al. 1990). For the Carboniferous, the precession is calculated to have had a period of 21,400 years, and an obliquity of 31,100 years (Collier et al. 1990). Several workers have inferred sedimentary-cycles to be the result of climatic changes forced by orbital variations during the Carboniferous (Heckel 1986, Leeder 1988, Collier et al. 1990).

10.7.2 The Duration of Boss Point Formation Megacycles

Estimates for the duration of the Westphalian A vary considerably. Thus Harland et al. (1982) attribute 10 my (315-305 Ma; Fig. 2.1), whereas Hess and Lippolt (1986) attribute only 2 my (315-313 Ma) to the Westphalian A (Hess and Lippolt 1986, fig. 4, Leeder 1988, fig. 1). An

estimation of the duration of the Boss Point Formation megacycles is further compounded by the fact that Boss Point Formation deposition represents only a portion of the Westphalian A, as the upper part of the underlying Claremont Formation is also Westphalian A, as is the lower part of the overlying Cumberland Group and Tynemouth Creek Formation (Figs. 2.1 & 2.2). One may therefore speculate that the Boss Point Formation may have been deposited in anything between approximately 8 Ma (using the dates of Harland et al. (1982) and 1.5 Ma (using the dates of Hess and Lippolt (1986)). Thus, each of the 8 depositional megacycles in the Boss Point Formation may have lasted anywhere in the range 1,000,000 years to 190,000 years (using the age estimates of 8 and 1.5 Ma respectively).

A periodicity of approximately 190,000 years is similar to the cycle periods estimated for the Dinantian (Tournasian to Viséan) of northern England (240,000 to 190,000 years; Leeder 1988), and to the Silesian (Namurian to Stephanian) units of NW Europe (180,000 years; Leeder 1988). It is also very similar to the durations of around 200,000 years given for Westphalian A and B age marine cycles in Britain (Leeder 1988, Collier et al. 1990).

Clearly the chronological resolution for the Carboniferous (for discussion see Klein 1990) and the Westphalian A in general, and the dates for the Boss Point Formation in particular need considerable refinement, but it is tempting to speculate that the sandstone/siltstone

megacycles observed in the Boss Point Formation are

Milankovitch controlled fourth order cycles (0.1-1 m.y.).

CHAPTER 11

SUMMARY OF CONCLUSIONS

Chapter 1 - The Boss Point Formation has received little detailed scrutiny in recent times, despite a long history of largely stratigraphic description during the last 150 years. Recent work by Mitchell (1986) described siderite geochemistry and genesis, while van de Poll and Patel (1981, 1989, 1990) and Plint (1986, 1988) have discussed at some length the origin of ornamented mudrocks from the formation.

Chapter 2 - Revisions to the definition of the Boss Point Formation which is up to 860 m thick are suggested. At the type section at Boss Point, Nova Scotia, the base of the formation is not exposed. The top of the formation is placed at the base of a prominent local erosion surface which is associated with an inclined heterolithic stratification (lateral accretion) unit, which separates red, usually calcareous siltstones and minor sandstones above (Cumberland Group), from typically grey, noncalcareous sandstones and less abundant siltstones of the Boss Point Formation below. This revised formation boundary is 174 m stratigraphically below the previously accepted contact.

Chapter 3 - Coarse-grained units occur locally in the northern part of the study area. Trough cross-bedded gravel units are interpreted as coarse bedload braided channel deposits. Planar cross-bedded gravels are interpreted as bar facies, while massive gravels probably represent the internal parts of longitudinal bars. Breccia lithofacies occur in the eastern portion of the study area, and are interpreted as cohesive debris-flow deposits related to alluvial fan sedimentation around the fault controlled flanks of the basin.

Chapter 4 - Green-grey, noncalcareous well sorted fine-to lower medium-grained trough cross-bedded sandstones are by far the most abundant lithofacies in the formation. They were deposited as sinuous-crested dunes within fluvial channels. Pebbly sandstones occur throughout the formation and are common immediately overlying erosion surfaces (several metres relief), or at the base of trough cross-bedded cosets. Although bar forms represented by planar cross-bedded sandstones occur, they are seldom preserved. Horizontally laminated sandstones formed in both crevasse-splay and beach environments. Slightly finer-grained current ripple and climbing ripple laminated sandstones deposited by lower velocity flows are common. Rare occurrences of wavy bedforms are interpreted as 3-dimensional antidunes (deposited under upper flow regime conditions at the tops of fining-upward cycles) and

hummocky cross-stratification (storm related deposited developed within lacustrine settings). Inclined heterolithic stratification units occur at several localities within finer-grained siltstone lithofacies and are interpreted as meandering distributary channel deposits.

Chapter 5 - Finer-grained lithofacies are interpreted as lacustrine on the basis that individual bedded packages can be traced several kilometres (up to 20 km) across the basin. Massive and laminated siltstones are the most common lithologies, typically associated with nodular or cm-thick bedded siderite. Bioturbation is common as are *in situ* tree stumps. Siltstones rest sharply (sometimes marked by an erosion surface) ontop of sandstone units, and at one locality this contact displays runnels and adhesion ripples, suggesting that the lakes were infilled 'passively' so as to preserve these delicate features. Several localities show siltstone blocks (as much as 40 m diameter), and these can be shown at two localities to have been related to gravitational rotation of bank materials. Centimetre- and decimetre-thick ostracod-bearing limestones and coals occur through much of the central Bay of Fundy region.

Chapter 6 - Paleosols have not previously been recognised from the formation. Boss Point Formation paleosols consist

of both sandy and silty forms, and are associated with calcrete nodules and red and grey-green colour mottling. Their distribution is closely related to the Harvey-Hopewell Fault, which on the basis of paleocurrent trends in sandstone units, is thought to have been a paleogeographic high during sedimentation. The paleosols appear to have formed preferentially on this high. XRF analyses for representative paleosol profiles show consistently high Al_2O_3 (>20 weight percent), suggesting that these paleosols were extensively weathered, and were most probably weathered *in situ*. Calcrete morphologies include rhizoliths, ferroan calcite, crystic plasmic material, siltstone aggregates, fragmentary nodules and Mn-rich spherulitic siderites. The abundance of these calcrete nodules, together with the geochemistry and shrinkage-expansion related pseudoanticlines in silty paleosols, suggest a semi-arid paleoclimate during sedimentation. The paleosols are considered to represent ancient aridisols and vertisols. They were not related to podzolisation under tropical rainforest conditions as has been suggested for other Carboniferous paleosols in Maritime Canada.

Chapter 7 - The sandstone units of the Boss Point Formation are interpreted as braided river deposits formed from southeast and northerly flowing rivers that originated principally in highland areas adjacent to the basin, and

not from some distant Appalachian source as previous authors have suggested. Channel fill successions comprise fining-upward cycles between 2 and 25 m thickness. These cycles are typically sharp based, and are overlain for the majority of their thickness by trough cross-bedded sandstones. Planar cross-bedded, massive, horizontally laminated and pebbly sandstone lithofacies may occur in the lower portions of the cycles, but the upper portions are characterised by ripple cross-lamination, climbing ripples and finer-grained siltstones, paleosols and coals at the top of the fining-upward cycles. These sandstone-dominated intervals form stacked sandstone packages as much as 130 m thick. They are intercalated with thinner (up to 40 m thick) finer-grained sandstone and mudrock units comprising metre-thick coarsening-upward cycles, erosively based sandstone, sharp-based sandstone, thin-bedded sandstone, inclined heterolithic stratification and hummocky cross-stratification units of fluvio-lacustrine origin. Together the stacked sandstone packages together with the fluvio-lacustrine units form megacycle successions as much as 170 m thick, and these can be traced laterally for up to 20 km across the Bay of Fundy region.

Chapter 8 - Paleocurrent determinations have been made from cross-bedding, ripples, logs, parting lineations, flutes, rib and furrow and wave ripple crests. By far the most useful determinations come from over 4100 trough cross-

bedded sandstone measurements, which show southeast trends in the southern portion of the study area, and northern trends in the northern part of the region. This change in orientation appears to approximate the Harvey-Hopewell Fault, and suggests that this fault was a topographic high during sedimentation.

Chapter 9 - Much of the Boss Point Formation shows no evidence for faulting. More pervasive deformation occurs in the southwest adjacent to the Harvey-Hopewell Fault. An exposure at Owls Head shows thrust emplacement of Hopewell Group coarse clastics over locally overturned Boss Point, Shepody, Maringouin Formations and Hopewell Group lithologies, and is consistent with other localities described along a similar NE-trending thrust faults further to the southwest. Shearing within the 150 m wide fault zone at Owls Head shows an earlier NW-SE oriented fault set (F_1), which were cut by later formed, NE-trending faults (F_2), and W-E low-angle faults (F_3). Conjugate faults within the fault zone show NE-SW directed compression, which is consistent with the dominant F_2 NE-SW trending faults being compressional or strike-slip. Striations show moderate-angle movement directions suggesting a significant dip-slip, and probable transcurrent component on these faults.

Chapter 10 - Several mechanisms may have contributed to the sedimentation style of the Boss Point Formation, which in particular is characterised by the development of several megacycles. Most likely amongst these as controls on sedimentation are tectonism and eustasy. Tectonism, although acknowledged to have been active during sedimentation, is unlikely to have produced the observed stratal geometries, that is, sharp typically erosively based stacked sandstone packages. If tectonism were the primary sedimentary control, a transitional deltaic facies should separate lacustrine units below, from stacked sandstone units above. Eustatic effects are considered more likely to have controlled sedimentation, the lacustrine units being deposited during periods of relative sea level rise, the sandstones being deposited during periods of relative sea level fall or lowstand. The proposed model for deposition in the Boss Point Formation is fundamentally different to the recent theoretical model for fluvial deposition proposed by Posamentier and Vail (1988), especially in regard to the erosive base observed in the Boss Point Formation fluvial sandstones, and the sharp transition from sandstone into overlying lacustrine siltstone, and the essentially 'passive' flooding nature of this contact. A eustatic model for the Boss Point Formation would be in accord with glacioeustatic events recorded during the Permo-Carboniferous glaciation, which peaked during the deposition of the Boss Point Formation.

APPENDIX I

Summary of lithotype thicknesses and statistical parameters.

A. ENTIRE STUDY AREA

	# of Beds		Thickness (m)			
	En	%	En	%	Mean	Max ^a
Gt	82	2.6	111.5	1.78	1.36	7.5
Gms	121	3.8	105.4	1.68	0.87	7.3
Gp	12	0.4	27.3	0.43	2.28	14.3
§	1	-	0.6	-	0.60	0.6
Ss	354	11.2	376.2	5.99	0.62	3.0
St	1366	43.0	4069.2	64.72	2.98	8.4
Sp	6	0.2	2.5	0.04	0.41	1.3
Sm	137	4.3	252.4	4.01	1.84	11.8
Sh	89	2.7	132.1	2.10	1.48	8.4
Sr	424	13.4	424.0	6.74	1.00	6.2
Fm	471	14.8	678.9	10.81	1.44	12.0
Fl	29	0.9	49.5	0.79	1.71	5.5
B	10	0.3	15.5	0.25	1.55	1.5
P	29	0.9	32.3	0.51	1.11	2.2
¥	5	0.2	3.6	0.06	0.71	0.8
L	25	0.8	4.0	0.06	0.16	0.8
C	15	0.5	1.9	0.03	0.13	0.7
Totals	3176		6287.0 m			

Key:

Lithologic code after Miall (1978) or-

§ Breccia
 B Siltstone blocks
 ¥ Ball and Pillow

Gravel = 9.88 %
 Sand = 77.67 %
 Mudrocks
 (incl. paleosol, limestone & coal)
 = 12.45 %

B. RIVER JOHN SECTION, NOVA SCOTIA

	# of Beds		Σn	Thickness (m)			SD	
	Σn	%		%	Mean	Max ^m		Min ^m
Gt	4	14.3	1.8	5.2	0.4	0.8	0.2	0.28
Gms	1	3.6	0.2	0.6	0.2	0.2	0.2	-
S	1	3.6	0.6	1.8	0.6	0.6	0.6	-
Ss	1	3.6	0.8	2.4	0.8	0.8	0.8	-
St	15	53.6	23.2	68.9	1.6	4.5	0.2	1.04
Sh	1	3.6	1.2	3.6	1.2	1.2	1.2	-
Sr	4	14.3	5.1	15.2	1.3			1.82
P	1	3.6	0.8	2.4	0.8	0.8	0.8	-

Totals
28 33.7 m

Key:

Lithologic code after Miall (1978) or-

§ Breccia

Gravel = 10.0 % of total lithologic thickness
 Sand = 87.6 % " " " "
 Mudrocks
 (incl. paleosol)
 = 2.4 % " " " "

C. MALAGASH, NOVA SCOTIA

	# of Beds		Thickness (m)					
	En	%	En	%	Mean	Max ⁿ	Min ⁿ	SD
Gt	8	8.3	7.1	3.9	0.9	1.4	0.4	0.39
Gms	7	7.3	5.7	3.1	0.8	1.9	0.3	0.52
Ss	3	3.1	2.2	1.2	0.5	1.4	0.2	0.28
St	53	55.3	134.3	73.7	2.5	6.6	0.1	1.69
Sh	1	1.0	1.9	1.1	1.9	1.9	1.9	-
Sr	18	18.7	21.9	12.0	1.2	3.7	0.1	0.94
Fm	4	4.2	7.3	4.0	1.8	2.0	1.6	0.17
Fl	2	2.1	1.8	1.0	0.9	1.3	0.5	0.57

Totals 96 182.2 m

Key:

Lithologic code after Miall (1978)

Gravel = 8.2 % of total stratigraphic thickness
 Sand = 86.8 % " " " "
 Mudrocks = 5.0 % " " " "

D. HILLSBOROUGH, NEW BRUNSWICK

	# of Beds		Thickness (m)					
	Σn	%	Σn	%	Mean	Max ^a	Min ^a	SD
Gt	2	2.1	5.5	2.1	2.8	3.0	2.5	0.35
Gms	7	7.3	15.7	5.9	2.2	7.3	0.2	2.63
Gp	11	11.5	26.9	10.1	2.5	14.3	0.2	3.98
Ss	19	19.7	17.0	6.4	0.9	3.0	0.1	0.73
St	40	41.7	178.8	67.0	4.5	6.9	0.3	4.40
Sm	3	3.1	2.4	0.9	0.8	1.3	0.3	0.5
Sr	7	7.3	7.8	2.9	1.1	5.0	0.2	1.74
Fm	5	5.2	10.9	4.1	2.2	6.0	0.4	2.30
B	1	1.0	1.0	0.4	1.0	1.0	1.0	-
P	2	2.1	2.0	0.8	1.0	1.0	1.0	-

Totals 96

266.9 m

Key:

Lithologic code after Miall (1978) or-

B Siltstone blocks

Gravel = 24.5 % of total lithologic thickness
 Sand = 70.2 % " " " "
 Mudrocks
 (incl. paleosol)
 = 5.3 % " " " "

E. BEAUMONT, NEW BRUNSWICK

	# of Beds		Thickness (m)					SD
	Σn	%	Σn	%	Mean	Max ^m	Min ^m	
Gt	3	3.3	6.6	3.0	2.2	3.8	0.8	1.51
Gms	6	6.6	4.6	2.1	0.8	2.2	0.2	0.80
Ss	11	12.1	19.9	8.9	0.4	7.0	0.2	0.27
St	60	65.9	183.2	82.6	3.1	6.5	0.4	1.68
Sp	6	6.6	2.5	1.1	0.4	1.3	0.1	0.46
Sh	2	2.2	2.0	0.9	1.0	1.5	0.5	0.71
Sr	2	2.2	2.3	1.0	1.2	1.2	1.1	0.07
Fm	1	1.1	0.8	0.4	0.8	0.8	0.8	-

Totals 91 221.9 m

Key:

Lithologic code after Miall (1978)

Gravel = 14.0 % of total lithologic thickness
 Sand = 85.6 % " " " "
 Mudrocks = 0.4 % " " " "

F. DORCHESTER, NEW BRUNSWICK

	# of Beds		Thickness					
	Σn	%	Σn	%	Mean	Max ^a	Min ^a	SD
Gt	33	9.7	83.5	11.4	2.5	7.5	0.3	1.65
Gms	13	3.8	20.3	2.8	1.6	7.2	0.2	1.85
Ss	39	11.4	38.6	5.3	0.8	2.6	0.2	0.70
St	130	38.3	317.7	43.4	2.5	7.3	0.1	2.11
Sm	40	11.8	133.0	18.2	3.3	11.8	0.2	2.66
Sh	11	3.2	17.1	2.3	1.6	5.8	0.2	1.71
Sr	24	7.1	20.6	2.8	0.9	4.4	0.1	0.98
Fm	43	12.6	85.4	11.7	2.0	8.6	0.5	1.75
Fl	5	1.5	11.9	1.6	2.4	4.7	1.0	1.58

Totals 338

731.2 m

Key:

Lithologic code after Miall (1978)

Gravel = 19.5 % of total lithologic thickness
 Sand = 67.2 % " " " "
 Mudrocks = 13.3 % " " " "

G. JOHNSON MILLS, NEW BRUNSWICK

	# of Beds		Thickness (m)					
	En	%	En	%	Mean	Max ^a	Min ^a	SD
Gt	9	2.2	6.7	0.9	0.7	1.2	0.2	0.34
Gms	22	5.4	15.7	2.1	0.7	2.5	0.1	0.62
Ss	47	11.5	61.9	8.1	0.5	1.0	-	0.37
St	147	35.8	385.7	50.5	2.6	6.5	0.1	2.39
Sm	18	4.4	14.3	1.9	0.8	2.3	0.1	0.63
Sh	22	5.4	45.7	6.0	2.1	8.4	0.2	2.19
Sr	56	13.6	90.7	11.9	1.6	6.2	0.1	1.46
Fm	82	20.0	128.7	16.8	1.6	8.1	0.1	1.79
Fl	3	0.7	7.8	1.0	2.6	3.8	1.0	1.44
P	3	0.7	5.3	0.7	1.8	2.3	1.4	0.47
‡	1	0.2	1.0	0.1	1.0	1.0	1.0	-
L	1	0.2	0.2	-	0.2	0.2	0.2	-
Totals	411		763.5	m				

Key:

Lithologic code after Miall (1978) or-

‡ Ball and Pillow

Gravel = 11.1 % of total lithologic thickness
 Sand = 70.3 % " " " "
 Mudrocks
 (incl. paleosol & limestone)
 = 18.6 % " " " "

H. BOSS POINT, NOVA SCOTIA

	# of Beds		Thickness (m)					
	En	%	En	%	Mean	Max ^a	Min ^a	SD
Gt	5	1.2	6.0	0.9	1.2	1.7	0.3	0.55
Gms	4	1.0	1.3	0.2	0.3	0.6	0.2	0.19
Ss	61	14.6	70.9	11.1	0.5	3.9	0.1	0.35
St	153	36.6	388.5	60.6	2.5	7.6	0.1	2.60
Sm	14	3.4	10.6	1.7	0.8	3.0	0.1	0.79
Sh	10	2.4	5.2	0.8	0.5	1.8	0.1	0.50
Sr	85	20.4	67.0	10.5	0.8	5.3	0.1	0.97
Fm	72	17.3	82.9	12.9	1.2	7.3	-	1.98
Fl	2	0.5	1.6	0.2	0.8	1.5	0.1	0.99
B	3	0.7	3.6	0.6	1.2	1.3	1.1	0.10
L	4	1.0	0.4	0.1	0.1	0.2	0.1	0.07
C	2	0.5	1.0	0.2	0.5	0.7	0.2	0.32

Totals 417

640 m

Key:

Lithologic code after Miall (1978) or-

B Siltstone blocks

Gravel = 12.2 % of total stratigraphic thickness
 Sand = 73.8 % " " " "
 Mudrocks
 (incl. limestone & coal)
 = 14.0 % " " " "

I. ROCKPORT, NEW BRUNSWICK

	# of Beds		Thickness (m)					
	En	%	En	%	Mean	Max ^a	Min ^a	SD
Gt	3	1.0	2.3	0.4	0.8	1.1	0.6	0.29
Gms	6	2.1	4.9	1.0	0.8	1.5	0.2	0.47
Gp	1	0.3	0.4	0.1	0.4	0.4	0.4	-
Ss	28	9.7	26.8	5.4	0.5	4.9	0.1	0.58
St	125	42.9	357.9	71.5	2.9	6.8	0.1	1.89
Sm	9	3.1	4.7	0.9	0.5	1.5	0.1	0.47
Sh	4	1.4	2.8	0.6	0.7	1.1	0.2	0.42
Sr	35	12.0	23.9	4.8	0.7	3.0	0.1	0.68
Fm	66	22.6	70.1	14.0	1.1	10.4	0.1	1.64
Fl	2	0.7	4.0	0.8	2.0	3.0	1.0	1.41
P	2	0.7	1.7	0.3	0.9	1.1	0.6	0.35
L	4	1.4	0.7	0.1	0.2	0.4	-	0.17
C	6	2.1	0.7	0.1	0.1	0.2	-	0.06

Totals 291 500.7 m

Key:

Lithologic code after Miall (1978)

Gravel = 6.9 % of total lithologic thickness
 Sand = 77.8 % " " " "
 Mudrocks
 (incl. paleosol, limestone and coal)
 = 15.3 % " " " "

J. SLACKS COVE EAST, NEW BRUNSWICK

	# of Beds		Thickness (m)					SD
	En	%	En	%	Mean	Max ^m	Min ^m	
Gt	3	1.3	1.5	0.4	0.5	1.0	0.2	0.44
Gms	3	1.3	2.2	0.5	0.7	1.2	1.0	0.11
Ss	30	12.5	25.0	6.2	0.4	3.2	0.1	0.30
St	99	41.4	243.1	60.8	2.5	7.0	0.3	2.95
Sm	4	1.7	1.5	0.4	0.4	0.6	0.1	0.22
Sh	6	2.5	11.8	2.9	2.0	3.8	0.2	1.63
Sr	39	16.3	26.5	6.6	0.7	3.7	0.1	0.83
Fm	39	16.3	71.3	17.9	1.8	12.0	0.3	2.55
Fl	4	1.7	11.0	2.7	2.8	5.5	1.0	2.02
B	1	0.4	4.0	1.0	4.0	4.0	4.0	-
P	1	0.4	1.0	0.2	1.0	1.0	1.0	-
L	7	2.9	1.2	0.3	0.2	0.8	0.1	0.34
C	3	1.3	0.3	0.1	0.1	0.3	-	0.13
Totals	239		400.4 m					

Key:

Lithologic code after Miall (1978) or-

B Siltstone blocks

Gravel = 7.1 % of total lithologic thickness
 Sand = 70.7 % " " " "
 Mudrocks
 (incl. paleosol, limestone and coal)
 = 22.2 % " " " "

K. SLACKS COVE WEST, NEW BRUNSWICK

	# of Beds		Thickness (m)					SD
	Σn	%	Σn	%	Mean	Max ^a	Min ^a	
Ss	19	17.6	8.4	3.0	0.3	1.0	0.1	0.18
St	65	60.1	239.7	83.9	3.7	8.2	0.1	3.06
Sm	1	0.9	2.0	0.7	2.0	2.0	2.0	-
Sh	1	0.9	0.1	-	0.1	0.1	0.1	-
Sr	7	6.5	9.7	3.4	1.4	2.7	0.4	0.84
Fm	10	9.3	25.0	8.8	2.5	6.6	0.6	1.69
L	3	2.8	0.5	0.2	0.2	0.3	0.2	0.10
C	2	1.9	0.2	-	0.1	0.1	0.1	-
Totals	108		285.6 m					

Key:

Lithologic code after Miall (1978)

Gravel = 3.0 % of total lithologic thickness
 Sand = 88.0 % " " " "
 Mudrocks
 (incl. limestone and coal)
 = 9.0 % " " " "

L. CAPE MARINGOUIN, NEW BRUNSWICK

	# of Beds		Thickness (m)					SD
	En	%	En	%	Mean	Max ^a	Min ^a	
Gt	4	1.4	3.4	0.7	0.9	1.1	0.5	0.26
Ss	19	6.9	15.7	3.5	0.4	4.5	0.2	0.25
St	130	46.4	305.3	67.3	2.4	8.4	0.1	2.22
Sm	4	1.4	6.1	1.3	1.5	3.5	0.1	1.55
Sh	10	3.6	6.8	1.5	0.7	1.6	0.1	0.58
Sr	43	15.4	35.3	7.8	0.8	3.9	0.1	0.92
Fm	58	20.7	72.7	16.0	1.3	8.0	-	1.86
Fl	2	0.7	2.5	0.6	1.3	1.9	0.6	0.92
P	4	1.4	4.1	0.9	1.0	2.2	0.3	0.88
‡	2	0.7	1.1	0.2	0.6	0.8	0.3	0.35
L	2	0.7	0.7	0.2	0.4	0.7	-	0.48
C	2	0.7	0.1	-	-	0.1	-	0.02
Totals	280		453.7	m				

Key:

Lithologic code after Miall (1978) or-

‡ Ball and Pillow

Gravel = 4.2 % of total lithologic thickness
 Sand = 78.1 % " " " "
 Mudrocks
 (incl. paleosol, limestone & coal)
 = 17.7 % " " " "

M. GRINDSTONE ISLAND, NEW BRUNSWICK

	# of Beds		Thickness (m)					
	Σn	%	Σn	%	Mean	Max ^a	Min ^a	SD
Gt	2	1.2	2.7	0.7	1.4	1.9	0.8	0.78
Gms	11	6.8	8.1	2.2	0.7	1.6	0.2	0.40
Ss	5	3.1	5.5	1.5	1.3	2.1	0.2	0.85
St	63	38.9	247.0	67.0	3.9	6.8	0.2	5.29
Sm	8	4.9	17.2	4.7	2.1	9.0	0.4	2.90
Sh	19	11.7	22.9	6.2	1.2	5.6	0.2	1.25
Sr	23	14.2	24.6	6.7	1.1	2.9	0.1	0.96
Fm	20	12.3	31.2	8.5	1.6	11.5	0.2	2.68
Fl	5	3.1	3.1	0.8	0.6	1.0	0.2	0.37
B	3	1.9	2.7	0.7	0.9	1.5	0.4	0.56
P	3	1.9	3.8	1.0	1.3	2.0	0.3	0.84
Totals	162		368.6	m				

Key:

Lithologic code after Miall (1978)

B Siltstone blocks

Gravel = 4.4 % of total lithologic thickness
 Sand = 85.3 % " " " "
 Mudrocks
 (incl. paleosol)
 = 10.3 % " " " "

N. MARYS POINT, NEW BRUNSWICK

	# of Beds		Thickness (m)					SD
	Σn	%	Σn	%	Mean	Max ^a	Min ^a	
Gms	4	4.5	5.7	1.3	1.4	1.8	0.8	0.43
Ss	5	5.6	8.1	1.9	0.7	3.0	0.7	-
St	53	59.6	396.6	89.0	7.5	7.3	0.1	5.10
Sm	4	4.5	4.4	1.0	1.1	2.2	0.5	0.85
Sr	17	19.1	25.9	5.8	1.5	4.9	0.1	1.52
Fm	2	2.2	3.8	0.9	1.9	2.0	1.8	0.14
L	4	4.5	0.4	0.1	0.1	0.2	-	0.11
Totals	89		444.9 m					

Key:

Lithologic code after Miall (1978)

Gravel = 3.2 % of total lithologic thickness
 Sand = 95.8 % " " " "
 Mudrocks
 (incl. limestone)
 = 1.0 % " " " "

O. LONG ISLAND, NEW BRUNSWICK

	# of Beds		Thickness (m)					SD
	Σn	%	Σn	%	Mean	Max ⁿ	Min ⁿ	
Gt	1	2.1	1.8	1.6	1.8	1.8	1.8	-
Ss	8	16.6	8.5	7.8	0.6	3.8	0.2	0.46
St	30	62.5	79.4	72.5	2.7	4.7	0.3	1.53
Sm	4	8.3	10.0	9.1	2.5	4.2	1.0	1.40
Sh	2	4.2	3.5	3.2	1.8	1.9	1.6	0.21
Fl	2	4.2	4.5	4.1	2.3	3.1	1.4	1.20
B	1	2.1	1.8	1.6	1.8	1.8	1.8	-
Totals	48			109.5	m			

Key:

Lithologic code after Miall (1978) or-

B Siltstone blocks

Gravel = 6.8 % of total lithologic thickness
 Sand = 87.5 % " " " "
 Mudrocks = 5.7 % " " " "

P. TWO RIVERS, NEW BRUNSWICK

	# of Beds		Thickness (m)					
	Σn	%	Σn	%	Mean	Max ^a	Min ^a	SD
Gt	3	4.4	4.2	3.2	1.4	1.2	0.7	0.39
Gms	2	2.9	2.0	1.5	2.0	1.8	0.2	0.80
Ss	5	7.4	4.0	3.1	1.0	1.5	1.0	-
St	33	48.5	91.5	69.9	2.8	5.3	0.4	2.38
Sm	3	4.4	9.5	7.3	3.2	4.1	3.2	0.64
Sr	17	25.0	17.2	13.1	1.0	3.9	0.1	1.16
Fm	4	5.9	2.2	1.7	0.6	0.9	0.3	0.25
B	1	1.5	0.3	0.2	0.3	0.3	0.3	-
Totals	68		130.9 m					

Key:

Lithologic code after Miall (1978) or-

B Siltstone Blocks

Gravel	=	7.8 %	of total lithologic thickness
Sand	=	90.3 %	" " " "
Mudrocks	=	1.9 %	" " " "

Q. CAPE ENRAGE, NEW BRUNSWICK

	# of Beds		Thickness (m)					
	Σn	%	Σn	%	Mean	Max ⁿ	Min ⁿ	SD
Gt	1	0.6	0.6	0.2	0.6	0.6	0.6	-
Gms	28	16.1	16.8	5.3	0.6	3.5	0.2	0.64
Ss	12	6.8	23.6	7.4	0.3	4.0	0.2	0.07
St	70	40.3	200.2	63.1	2.9	5.0	0.2	2.42
Sm	10	5.7	9.0	2.8	0.9	2.2	0.2	0.72
Sh	7	4.0	8.9	2.8	1.3	3.2	0.4	1.12
Sr	18	10.4	26.9	8.5	1.5	6.1	0.2	1.67
Fm	24	13.8	29.1	9.2	1.3	5.5	0.2	1.38
P	4	2.3	2.4	0.7	0.6	1.1	0.3	0.37
Totals	174		317.3	m				

Key:

Lithologic code after Miall (1978)

Gravel = 12.9 % of total lithologic thickness
 Sand = 77.2 % " " " "
 Mudrocks
 (incl. paleosol)
 = 9.9 % " " " "

R. ALMA, NEW BRUNSWICK

	# of Beds		Thickness (m)					SD
	Σn	%	Σn	%	Mean	Max ^a	Min ^a	
Gt	1	0.8	1.2	0.5	1.2	1.2	1.2	-
Gms	5	3.9	2.3	0.9	0.5	1.1	0.1	0.31
Ss	26	19.6	26.8	10.9	0.7	5.0	0.1	0.39
St	55	43.3	155.9	63.0	2.8	5.5	0.5	2.38
Sm	3	2.4	6.6	2.7	2.2	2.5	1.8	0.36
Sh	1	0.8	2.2	0.9	2.2	2.2	2.2	-
Sr	19	15.0	14.1	5.7	0.7	3.6	0.3	1.01
Fm	11	8.7	28.3	11.4	2.6	5.5	0.8	1.73
Fl	1	0.8	0.9	0.3	0.9	0.9	0.9	-
B	1	0.8	3.1	1.3	3.1	3.1	3.1	-
P	3	2.4	4.5	1.8	1.5	2.1	1.1	0.53
¥	2	1.6	1.5	0.6	0.7	1.2	0.3	0.67

Totals 127 247.2 m

Key:

Lithologic code after Miall (1978) or-

B Siltstone blocks
 ¥ Ball and Pillow

Gravel = 12.3 % of total lithologic thickness
 Sand = 72.9 % " " " "
 Mudrocks
 (incl. paleosol
 = 14.8 % " " " "

T. GIFFIN POND, NEW BRUNSWICK

Overtuned sequence, immediately west of Rogers Head, beneath thrust (Lat. 45° 18' 40" N; Long. 65° 35' 05" W to Lat. 45° 18' 41" N; Long. 65° 34' 42" W).

	# of Beds		Thickness (m)					
	En	%	En	%	Mean	Max ^m	Min ^m	SD
Ss	3	7.5	6.1	6.4	2.0	3.3	1.2	1.12
St	22	55.0	67.2	70.3	3.1	7.2	0.2	2.16
Sm	5	12.5	12.9	13.5	2.6	5.8	1.3	1.84
Sr	4	10.0	1.7	1.8	0.4	0.7	0.1	0.25
Fm	6	15.0	7.8	8.0	1.3	2.2	0.1	1.12
Totals	40							95.65 m

Lithologic code after Miall (1978)

Gravel	=	6.4 %	of total lithologic thickness
Sand	=	85.6 %	" " " "
Mudrocks	=	8.0 %	" " " "

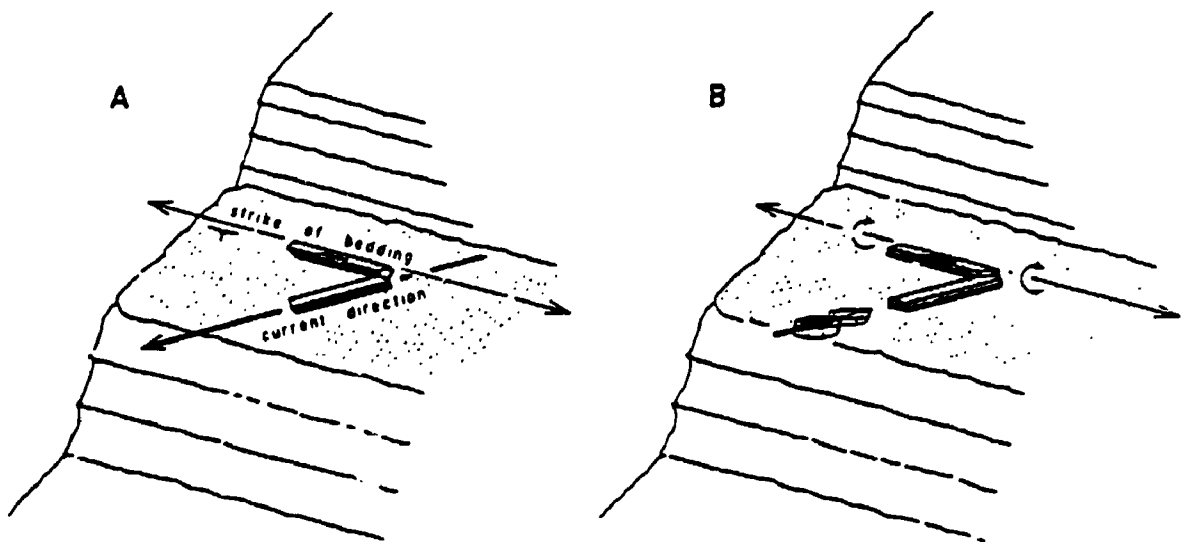
APPENDIX II

Direct Measurement of Paleocurrent Direction by the Carpenters Rule Method

A carpenters rule was used to determine paleocurrent directions for linear features such as logs, parting lineations, flutes etc.

One arm of the carpenters rule is aligned with the sedimentary feature, the other is oriented as a strike line (see A below). The best method to determine the strike line is to use a Brunton compass (or built-in spirit level) so that the horizontal is attained. By rotating the arm of the carpenters rule which had been aligned with the sedimentary feature, about the other arm (the strike line), the restored paleocurrent direction can be directly read by compass at the outcrop (see B below). The method can be applied to any dipping strata, including overturned beds. A little practice may be necessary in overturned sequences.

This method is useful where strata have not been adversely affected by plunging or regional folds, and has the great advantage that measurements can be made directly in the field and in very quick time, in comparison to stereographic restorations made back in the laboratory.



APPENDIX III

Petrography of Boss Point trough cross-bedded sandstones determined by point counting. Q= quartz; F= feldspar; L= lithics; Orth= orthoclase; Plag= plagioclase; SRF= sedimentary rock fragments; VRF= volcanic rock fragments and MRF= metamorphic rock fragments. All thin sections were treated with a solution of K-rhodizonate (after Houghton 1980), for the identification of orthoclase.

Sample	Q	F		SRF	L		Total
		Orth.	Plag.		VRF	MRF	
87.125	204	63	-	13	40	8	328
88.47	293	10	1	12	-	-	316
88.75	301	12	2	10	-	-	323
87.104	233	77	-	7	-	-	318
87.114	206	101	-	9	-	-	316
88.179	207	110	-	15	-	-	332
88.186	211	110	-	16	-	-	337
87.15	268	30	-	15	-	-	313
87.22	244	32	-	46	-	2	322
87.34	290	17	2	2	-	-	309
89.44	240	27	-	26	10	-	320

Key:

Sample	Locality	Stratigraphic Position
87.125	Giffin Pond, NB	26 m above basal exposure
88.47	Alma, NB	0.2 m above base
88.75	Alma, NB	154 m above base
87.104	Cape Enrage, NB	104 m above base
87.114	Cape Enrage, NB	226 m above base
88.179	Hillsborough, NB	120 m above base
88.186	Hillsborough, NB	457 m above base
87.15	Boss Point, NS	731 m above base
87.22	Boss Point, NS	610 m above base
87.34	Boss Point, NS	14 m above base
88.44	Malagash, NS	216 m above basal exposure

APPENDIX III

Petrography of Boss Point trough cross-bedded sandstones determined by point counting. Q= quartz; F= feldspar; L= lithics; Orth= orthoclase; Plag= plagioclase; SRF= sedimentary rock fragments; VRF= volcanic rock fragments and MRF= metamorphic rock fragments. All thin sections were treated with a solution of K-rhodizonate (after Houghton 1980), for the identification of orthoclase.

Sample	Q	F		SRF	L		Total
		Orth.	Plag.		VRF	MRF	
87.125	204	63	-	13	40	8	328
88.47	293	10	1	12	-	-	316
88.75	301	12	2	10	-	-	323
87.104	233	77	-	7	-	-	318
87.114	206	101	-	9	-	-	316
88.179	207	110	-	15	-	-	332
88.186	211	110	-	16	-	-	337
87.15	268	30	-	15	-	-	313
87.22	244	32	-	46	-	2	322
87.34	290	17	2	2	-	-	309
89.44	240	27	-	26	10	-	320

Key:

Sample	Locality	Stratigraphic Position
87.125	Giffin Pond, NB	26 m above basal exposure
88.47	Alma, NB	0.2 m above base
88.75	Alma, NB	154 m above base
87.104	Cape Enrage, NB	104 m above base
87.114	Cape Enrage, NB	226 m above base
88.179	Hillsborough, NB	120 m above base
88.186	Hillsborough, NB	457 m above base
87.15	Boss Point, NS	731 m above base
87.22	Boss Point, NS	610 m above base
87.34	Boss Point, NS	14 m above base
88.44	Malagash, NS	216 m above basal exposure

APPENDIX IV

SANDY PALEOSOLS

A. Dorchester paleosol description.

This paleosol occurs in a small bay, 1 km south of the wharf at Dorchester Cape (Long. 64° 32' 45"; Lat. 45° 51' 40") and at a stratigraphic position 337 m above the base of the Boss Point Formation (stratigraphic section 10). Colour designations follow the Rock Colour Chart of the Geological Society of America.

TOP

- 12 cm **Nodular calcrete:** pale green [10G 6/2], up to 10 cm diameter (generally 3-5 cm) nodular calcrete forming an indurated and erosion resistant band, interspersed with greyish green [10GY 5/2] calcareous, carbonaceous, very fine sandy siltstone. Gradational base.
- 7 - 9 cm **Sandstone:** greyish green [5G 5/2], noncalcareous, moderately indurated, apparently massive, well sorted fine sandstone. Contains brownish grey [5YR 4/1] blebs of noncalcareous, very fine sandy siltstone up to 5 cm diameter. Sharp, slightly irregular base- amplitude = 2 cm.
- 5 cm **Sandstone:** greyish green [10GY 5/2] and greenish grey [5G 6/1], noncalcareous, apparently massive, well sorted, very fine to fine sandstone with abundant greyish brown [5YR 3/2] colour mottling. Abundant pinkish grey [5YR 8/1] calcrete nodules up to 3 cm diameter (generally 0.5-1 cm) scattered throughout. Sharp irregular base- amplitude = 4 cm.
- 5 - 16 cm **Sandstone:** as above but with no calcrete. Red colour mottling at top. Sharp irregular base- amplitude = 11 cm.
- 35 cm **Sandstone:** as for 5 cm thick unit above. Gradational base. Cut by low angle shear.
- 35 cm **Sandstone:** Greyish green [5G 5/2] and pale green [10G 6/2], colour mottled, noncalcareous, well sorted, fine to lower medium sandstone with occasional <1 cm diameter calcrete nodules. Sharp

units) and slightly sandy siltstone (for green-grey units). Calcrete nodules up to 5 cm diameter throughout.

BASE

D. Alma paleosol description.

This paleosol occurs 500 m east of Alma beach (Long. 65° 55' 53"; Lat. 45° 35' 50") and at a stratigraphic position 68 m above the base of the Boss Point Formation (stratigraphic section 24). Colour designations follow the Rock Colour Chart of the Geological Society of America.

TOP

- 70 cm Siltstone: dark grey [N3](dominant) and greyish red purple [5RP 4/2](subordinate), colour mottled, noncalcareous, very fine sandy siltstone. Numerous <10 cm diameter calcrete nodules. Slickensided surfaces very common. Sharp irregular top- amplitude= 10 cm. Gradational base.
- 80 cm Siltstone: greyish green [10 GY 5/2] and greyish red [10R 4/2], colour mottled, noncalcareous, apparently massive, very fine sandy siltstone. Occasional <5 cm diameter nodular calcrete throughout. Faint vertical and sub-vertical and low-angle conjugate joints. Base poorly exposed.
- 20 cm Siltstone: greyish red [10R 4/2](dominant) and greyish green [10GY 5/2](subordinate), colour mottled, sheared, very fine sandy siltstone. Faint vertical, sub-vertical and low-angle conjugate joints. Gradational base.
- 40 cm Nodular Calcrete: Prominent, erosion resistant band comprising <15 cm diameter calcrete nodules.
- 15 cm Siltstone: as for 20 cm thick unit above.
- 50 cm Siltstone: greyish green [10GY 5/2](dominant) and greyish red [10R 4/2](subordinate), colour mottled, noncalcareous, apparently massive clayey siltstone with occasional <3 cm diameter calcrete nodules.

BASE

APPENDIX V

Major Oxide Data for Boss Point Paleosols determined by XRF analysis.

SANDY PALEOSOLS

A. Dorchester

	Sample					
	Top ← 89-15A	89-15C	89-15D	89-15E	89-15F	→ Base 89-15G
SiO ₂	50.80	67.15	68.35	65.50	58.91	64.12
TiO ₂	0.71	1.00	0.91	0.97	0.94	1.02
Al ₂ O ₃	12.85	15.95	14.68	16.52	20.16	15.13
Fe ₂ O ₃	3.06	5.59	5.21	3.99	6.49	8.81
MnO	0.59	0.04	0.06	0.09	0.06	0.10
MgO	0.93	1.49	1.25	1.37	1.76	0.80
CaO	13.78	0.12	0.84	2.03	0.80	1.03
K ₂ O	1.89	2.79	2.73	2.91	3.88	2.69
P ₂ O ₅	0.09	0.09	0.09	0.11	0.12	0.18
Na ₂ O	0.08	0.50	0.35	0.14	0.00	0.11
LOI	14.59	4.71	4.54	5.76	6.40	5.33
Total	99.37	99.43	99.02	99.39	99.52	99.31
CIA (%)	44.93	82.39	78.92	76.48	81.16	79.80

B. Cape Enrage

	Sample			
	Top ← 89-02D	89-02C	89-02B	→ Base 89-02A
SiO ₂	60.41	56.27	62.75	59.48
TiO ₂	1.06	1.01	1.01	1.05
Al ₂ O ₃	20.01	21.85	17.38	20.28
Fe ₂ O ₃	5.46	6.94	5.43	6.11
MnO	0.06	0.12	0.10	0.07
MgO	1.66	1.83	1.73	1.85
CaO	0.36	0.28	1.23	0.56
K ₂ O	4.02	4.56	3.44	4.14
P ₂ O ₅	0.19	0.17	0.19	0.19
Na ₂ O	0.30	0.09	0.54	0.46
LOI	6.04	6.71	5.38	5.73
Total	99.57	99.83	99.19	99.93
CIA (%)	81.04	81.59	76.94	79.72

APPENDIX V

Major Oxide Data for Boss Point Paleosols determined by XRF analysis.

SANDY PALEOSOLS

A. Dorchester

	Sample					
	Top ← 89-15A	89-15C	89-15D	89-15E	89-15F	→ Base 89-15G
SiO ₂	50.80	67.15	68.35	65.50	58.91	64.12
TiO ₂	0.71	1.00	0.91	0.97	0.94	1.02
Al ₂ O ₃	12.85	15.95	14.68	16.52	20.16	15.13
Fe ₂ O ₃	3.06	5.59	5.21	3.99	6.49	8.81
MnO	0.59	0.04	0.06	0.09	0.06	0.10
MgO	0.93	1.49	1.25	1.37	1.76	0.80
CaO	13.78	0.12	0.84	2.03	0.80	1.03
K ₂ O	1.89	2.79	2.73	2.91	3.88	2.69
P ₂ O ₅	0.09	0.09	0.09	0.11	0.12	0.18
Na ₂ O	0.08	0.50	0.35	0.14	0.00	0.11
LOI	14.59	4.71	4.54	5.76	6.40	5.33
Total	99.37	99.43	99.02	99.39	99.52	99.31
CIA (%)	44.93	82.39	78.92	76.48	81.16	79.80

B. Cape Enrage

	Sample			
	Top ← 89-02D	89-02C	89-02B	→ Base 89-02A
SiO ₂	60.41	56.27	62.75	59.48
TiO ₂	1.06	1.01	1.01	1.05
Al ₂ O ₃	20.01	21.85	17.38	20.28
Fe ₂ O ₃	5.46	6.94	5.43	6.11
MnO	0.06	0.12	0.10	0.07
MgO	1.66	1.83	1.73	1.85
CaO	0.36	0.28	1.23	0.56
K ₂ O	4.02	4.56	3.44	4.14
P ₂ O ₅	0.19	0.17	0.19	0.19
Na ₂ O	0.30	0.09	0.54	0.46
LOI	6.04	6.71	5.38	5.73
Total	99.57	99.83	99.19	99.93
CIA (%)	81.04	81.59	76.94	79.72

APPENDIX VI

Trace element data for Boss Point Formation paleosols
determined by XRF analysis (in ppm).

A. Cape Enrage - Silty Paleosol

	Sample			
	Top ←			→ Base
	89-03D	89-03C	89-03B	89-C3A
Nb	22	21	20	21
Zr	346	531	267	261
Y	27	39	27	27
Sr	177	88	281	274
Rb	222	186	259	262
Ba	621	347	529	663
Ga	43	29	48	48
Pb	17	22	21	20
Zn	116	96	130	131
Cu	12	9	8	31
Ni	45	48	49	50
Co	27	22	30	28
Cr	124	127	124	122
V	229	225	243	232

B. Dorchester - Sandy Paleosol

	Sample				
	Top ←				→ Base
	89-15A	89-15C	89-15E	89-15F	89-15G
Nb	17	22	20	19	21
Zr	361	473	472	331	262
Y	32	28	35	24	26
Sr	156	88	97	97	263
Rb	140	176	176	238	267
Ba	357	337	400	483	530
Ga	30	30	30	43	51
Pb	33	13	12	14	16
Zn	91	117	110	151	127
Cu	35	33	16	77	47
Ni	43	46	47	70	50
Co	14	24	21	29	33
Cr	145	140	146	157	121
V	209	249	256	260	239

APPENDIX VII

Electron microprobe analyses of rhizoliths (weight percent).

Siderite

Sample 89-02A, Cape Enrage (Nodule 1)

CaO	2.86
MgO	1.15
MnO	2.36
FeO	30.76
Total	37.13

Sample 89-02A, Cape Enrage (Nodule 2)

CaO	3.84
MgO	4.59
MnO	6.30
FeO	44.64
Total	59.37

Dolomite

Sample 89-02A, Cape Enrage (Nodule 3)

CaO	28.97
MgO	10.28
MnO	2.44
FeO	11.97
Total	53.66

Calcite

Sample 89-02A, Cape Enrage (Nodule 4)

CaO	43.28
MgO	0.92
MnO	2.73
FeO	8.55
Total	55.48

APPENDIX VII

Electron microprobe analyses of rhizoliths (weight percent).

Siderite

Sample 89-02A, Cape Enrage (Nodule 1)

CaO	2.86
MgO	1.15
MnO	2.36
FeO	30.76
Total	37.13

Sample 89-02A, Cape Enrage (Nodule 2)

CaO	3.84
MgO	4.59
MnO	6.30
FeO	44.64
Total	59.37

Dolomite

Sample 89-02A, Cape Enrage (Nodule 3)

CaO	28.97
MgO	10.28
MnO	2.44
FeO	11.97
Total	53.66

Calcite

Sample 89-02A, Cape Enrage (Nodule 4)

CaO	43.28
MgO	0.92
MnO	2.73
FeO	8.55
Total	55.48

Analyses from Outer Margins of Nodules

Analysis 1		Analysis 2	
CaO	4.97	CaO	2.72
MgO	2.03	MgO	2.14
MnO	6.60	MnO	8.86
FeO	44.93	FeO	44.63
Total	58.53	Total	59.35

Analysis 3		Analysis 4	
CaO	3.68	CaO	3.09
MgO	2.07	MgO	2.05
MnO	10.97	MnO	8.88
FeO	43.55	FeO	42.39
Total	60.27	Total	56.41

Analysis 5		Analysis 6	
CaO	4.66	CaO	2.93
MgO	2.08	MgO	2.32
MnO	9.12	MnO	11.74
FeO	44.64	FeO	43.65
Total	60.50	Total	60.64

MEAN FOR ALL ANALYSES (n= 15)

CaO	3.99
MgO	1.94
MnO	7.64
FeO	44.16
Total	57.74

Analyses from Radially Distributed Ferroan Calcite Within Nodules

Analysis 1		Analysis 2		Analysis 3	
CaO	43.73	CaO	46.40	CaO	48.11
MgO	0.75	MgO	0.39	MgO	0.36
MnO	3.07	MnO	3.48	MnO	3.19
FeO	7.05	FeO	4.15	FeO	5.90
Total	54.60	Total	54.42	Total	57.56

Analyses from Outer Margins of Nodules

Analysis 1

CaO	4.97
MgO	2.03
MnO	6.60
FeO	44.93
Total	58.53

Analysis 2

CaO	7.72
MgO	2.14
MnO	8.86
FeO	44.63
Total	59.35

Analysis 3

CaO	3.68
MgO	2.07
MnO	10.97
FeO	43.55
Total	60.27

Analysis 4

CaO	3.09
MgO	2.05
MnO	8.88
FeO	42.39
Total	56.41

Analysis 5

CaO	4.66
MgO	2.08
MnO	9.12
FeO	44.64
Total	60.50

Analysis 6

CaO	2.93
MgO	2.32
MnO	11.74
FeO	43.65
Total	60.64

MEAN FOR ALL ANALYSES (n= 15)

CaO	3.99
MgO	1.94
MnO	7.64
FeO	44.16
Total	57.74

Analyses from Radially Distributed Ferroan Calcite Within Nodules

Analysis 1

CaO	43.73
MgO	0.75
MnO	3.07
FeO	7.05
Total	54.60

Analysis 2

CaO	46.40
MgO	0.39
MnO	3.48
FeO	4.15
Total	54.42

Analysis 3

CaO	48.11
MgO	0.36
MnO	3.19
FeO	5.90
Total	57.56

APPENDIX IX

Mineralogy of clays within and surrounding spherulitic siderite nodules determined by electron microprobe analyses (weight percent).

Mineralogy for Clay Within Nodule (Smectite?)

Sample 88-65, Alma

SiO ₂	31.14
TiO ₂	0.41
Al ₂ O ₃	16.75
Cr ₂ O ₃	0.07
MnO	0.32
FeO	27.98
MgO	8.39
CaO	0.47
BaO	0.86
K ₂ O	0.13
Na ₂ O	0.02
F	0.76
Cl	0.05
Total	87.35

Dark Coloured Matrix Material Surrounding Nodules (Illite?)

Sample 88-65, Alma

SiO ₂	49.30
TiO ₂	0.33
Al ₂ O ₃	14.91
Cr ₂ O ₃	0.03
MnO	0.04
FeO	6.91
MgO	1.95
CaO	0.24
BaO	0.12
K ₂ O	5.33
Na ₂ O	0.09
F	0.00
Cl	0.00
Total	79.24

Light Coloured Matrix Material Surrounding Nodules
(Smectite?)

Sample 88-65, Alma

SiO ₂	28.07
TiO ₂	0.01
Al ₂ O ₃	16.74
Cr ₂ O ₃	0.02
MnO	0.16
FeO	32.86
MgO	4.55
CaO	0.23
BaO	0.05
K ₂ O	0.19
Na ₂ O	0.08
F	0.52
Cl	0.06
Total	83.54

APPENDIX X

Electron microprobe data for calcite infilling pore space (weight percent).

Outer Portion of Pore

CaO	55.64
MgO	1.42
MnO	0.15
FeO	0.00
Total	57.21

Middle Portion of Pore

CaO	40.22
MgO	2.37
MnO	16.53
FeO	0.62
Total	59.74

Central Portion of Pore

CaO	53.98
MgO	1.30
MnO	0.54
FeO	0.01
Total	55.83

APPENDIX XI

Major element results from Boss Point Formation calcrete nodules, determined by XRF analysis.

	Sample				
	C89-20B	C89-20E	C89-02A	C89-03A	C89-15A
SiO ₂	48.26	60.81	43.98	17.43	29.64
TiO ₂	0.67	0.89	0.73	0.25	0.44
Al ₂ O ₃	21.92	18.92	13.73	6.51	7.78
Fe ₂ O ₃	7.83	6.72	13.72	2.99	4.33
MnO	0.04	0.05	0.87	0.71	1.27
MgO	1.58	1.48	1.99	0.78	1.18
CaO	4.50	1.00	7.37	37.33	27.30
K ₂ O	4.32	3.76	2.77	1.34	1.24
P ₂ O ₅	3.08	0.17	0.27	0.26	0.38
Na ₂ O	0.00	0.10	0.23	0.00	0.00
LOI	7.52	5.57	13.52	31.32	25.45
Total	99.74	99.47	99.19	98.92	99.01

Samples are prefixed "C" to designate that they are calcrete nodules. Stratigraphic positions indicated in text figures. Samples are from the following localities:

- 89-20 Alma paleosol (silty)
- 89-02 Cape Enrage paleosol (sandy)
- 89-03 Cape Enrage paleosol (silty)
- 89-15 Dorchester paleosol (sandy)

Sample 89-20B is a ped* calcrete

Sample 89-20E is a ped, sparry calcite* and siltstone aggregate* calcrete

Sample 89-02A is a micritic* calcrete

Sample 89-03A is a micritic calcrete

Sample 89-15A is a ped calcrete

* For definition see text

APPENDIX XII

Trace elements for representative Boss Point Formation
calcrete nodule, determined by XRF analysis (in ppm).

	Sample
	C88-63
Nb	21
Zr	426
Y	30
Sr	120
Rb	227
Ba	546
Ga	37
Pb	23
Zn	118
Cu	39
Ni	56
Co	32
Cr	128
V	248

Sample comes from the paleosol at Alma (silty).

SUPPLEMENTARY APPENDIX

This appendix appears on microfiche in Volume II

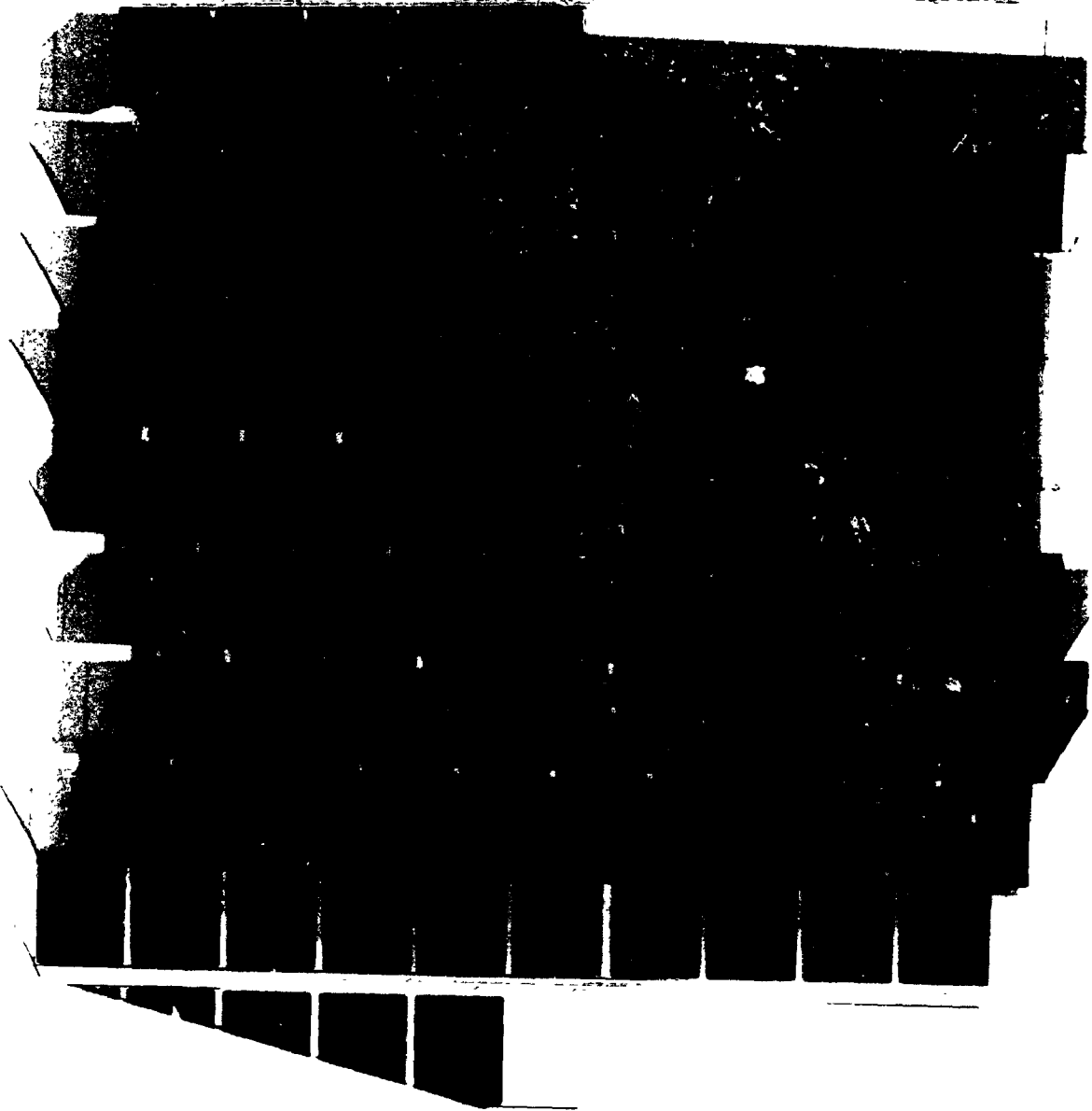
Location Details of Stratigraphic Sections Used in This Study

- Section 1- River John, Nova Scotia: Left bank of river, 1 km downstream of West and East Branch confluence (see Boehner *et al.* 1986, p. 49).
- Section 2- Malagash, Nova Scotia: Base of section begins at Malagash Point, opposite Saddle Island (below Chrysler of Canada house). Top of section is 2 km west on long coast near Treen Point.
- Section 3- Wallace Sandstone Quarry, Nova Scotia: Immediately behind township of Wallace. Permission required from owner Mr Stan Flynn who lives opposite to quarry entrance. Stone from this quarry used to build Parliament Buildings in Ottawa.
- Section 4- Wentworth, Nova Scotia: North portal of tunnel under railway line, Caldwell Brook. Contact of Boss Point Formation on Silurian Wilson Brook Formation exposed in tunnel (see Donohoe and Wallace 1982).
- Section 5- Halls Hill, New Brunswick: Road cutting along Highway 16.
- Section 6- Point de Bute Quarry, New Brunswick: Quarry 2 km west of Point de Bute township.
- Section 7- Mt Whatley Quarry, New Brunswick: Quarry just south of Mt Whatley, Highway 16.
- Section 8- Aulac, New Brunswick: Road cutting, north side of Trans-Canadian Highway.
- Section 9- British Settlement Quarry, New Brunswick: Quarry 3 km southwest of Sackville. Permission required from house opposite quarry entrance. See van de Poll & Patel (1990).
- Section 10- Dorchester, New Brunswick: Base in bay below Fillmore Hill, top at wharf near Cole Point.
- Section 11- Beaumont, New Brunswick: Base at Micmac Church, top at Fort Folly Point.

- Section 12- Hillsborough, New Brunswick: Base at Big Cape, top at old wharf near Hopewell Cape.
- Section 13- Johnson Mills, New Brunswick: Coastal exposures at Johnson Mills.
- Section 14- Boss Point, Nova Scotia: Coastal exposures north of Lower Cove.
- Section 15- Cape Maringouin, New Brunswick: Coastal exposures at Cape Maringouin.
- Section 16- Slacks Cove West, New Brunswick: Coastal exposures, base at west end of beach at Slacks Cove.
- Section 17- Slacks Cove East, New Brunswick: Coastal exposures, base at east end of beach at Slacks Cove.
- Section 18- Rockport, New Brunswick: Coastal exposures, base at south side of beach at Rockport.
- Section 19- Grindstone Island, New Brunswick: Coastal exposures along south shore, base at Jones Ledge, north side of island.
- Section 20- Marys Point, New Brunswick: Coastal exposures on north side of Marys Point.
- Section 21- Long Island, New Brunswick: Coastal exposures at Long Island, 4 km southwest of Marys Point.
- Section 22- Two Rivers, New Brunswick: Coastal exposures at river mouth, 9 km northeast of Cape Enrage.
- Section 23- Cape Enrage, New Brunswick: Coastal exposures, base at east end of beach. Danger from falling rocks (hardhat country). Tides are dangerous (be off section 2 hours either side of high tide).
- Section 24- Alma, New Brunswick: Coastal exposures north of beach. Danger from falling rocks (hardhat country). Tides are dangerous (be off section 1 hour either side of high tide).
- Section 25- Alma Baths, New Brunswick: Coastal exposures immediately south of Alma baths.
- Section 26- Giffin Pond, New Brunswick. Coastal exposures east of Giffin Pond, 6 km southwest of St Martins. Tides are dangerous around headland in middle of section (can not be passed 3 hours either side of high tide).
- Section 27- Elgin, New Brunswick: Road cutting above river, 6 km north of Goshen.

STRATIGRAPHIC COLUMNS # 1 of 9
- Boss Point formation
G.H. Brune PhD Thesis Supplementary Appendix

Information Graphics
Box 1873 Stn A
LONDON ON M6A 5H9



REFERENCES

- Ahmad, N. 1983. Vertisols. In: Pedogenesis and Soil Taxonomy II. The Soil Orders, L.P. Wilding, N.E. Smeck and G.F. Hall (eds.). Elsevier, p. 91-123.
- Allen, B.L. and Fanning, D.S. 1983. Composition and soil genesis. In: Pedogenesis and Soil Taxonomy I. Concepts and Interactions, L.P. Wilding, N.E. Smeck and G.F. Hall (eds.). Elsevier, p. 141-192.
- Allen, J.R.L. 1963. The classification of cross-stratified units. With notes on their origin. *Sedimentology*, v. 2, p. 93-114.
- Allen, J.R.L. 1965. Fining upward cycles in alluvial successions. *Liverpool and Manchester Geological Journal*, v. 4, p. 229-246.
- Allen, J.R.L. 1974. Studies in fluvial sedimentation: implications of pedogenic carbonate units, Lower Old Red Sandstone, Anglo-Welsh outcrop. *Geological Journal*, v. 9, p. 181-208.
- Allen, J.R.L. 1986. Pedogenic calcretes in the Old Red Sandstone facies (Late Silurian-Early Carboniferous) of the Anglo-Welsh area, southern Britain. In: *Paleosols Their Recognition and Interpretation*, V.P. Wright (ed.). Princeton University Press, Princeton, N.J., p. 58-86.
- Allen, J.R.L. and Williams, B.P.J. 1979. Interfluvial drainage on Silurian-Devonian alluvial plains in Wales and Welsh Borders. *Geological Society of London, Journal*, v. 136, p. 361-366.
- Altebaeumer, A.M. 1985. Organic geochemical investigation of selected oil shales of the Albert Formation, New Brunswick. *Bulletin of Canadian Petroleum Geology*, v. 33, p. 427-445.
- Ashmore, P.E. 1982. Laboratory modelling of gravel braided stream morphology. *Earth Surface Processes, Landforms*. v. 7, p. 201-225.
- Atkinson, C.D. 1986. Tectonic control on alluvial sedimentation as revealed by an ancient catena in the Capella Formation (Eocene) of Northern Spain. In: *Paleosols Their Recognition and Interpretation*, V.P. Wright (ed.). Princeton University Press, Princeton, N.J., p. 139-179.

- Ball, F.D., Sullivan, R.M. and Peach, A.R. 1981. Carboniferous Drilling Project. Report of Investigation 18. Mineral Resources Branch, New Brunswick Department of Natural Resources. 109p.
- Barr, S.M., Brisebois, D. and MacDonald, A.S. 1985. Carboniferous volcanic rocks of the Magdalen Islands, Gulf of St. Lawrence. *Canadian Journal of Earth Sciences*, v. 22, p. 1679-1688.
- Barr, S.M. and Raeside, R.P. 1989. Tectono-stratigraphic terranes in Cape Breton Island, Nova Scotia: Implications for the configuration of the northern Appalachian orogen. *Geology*, v. 17, p. 822-825.
- Barr, S.M. and White, C.E. 1988. Petrochemistry of contrasting late Precambrian volcanic and plutonic associations, Caledonian Highlands, Southern New Brunswick. *Maritime Sediments and Atlantic Geology*, v. 24, p. 353-372.
- Barrett, P.J. and Kohn, B.P. 1975. Changing sediment transport directions from Devonian to Triassic in the Beacon Super-Group of South Victoria Land, Antarctica. *In: Gondwana Geology. 3rd Gondwana Symposium, Canberra, Australia, 1973. Australian National University Press, Canberra. p. 15-35.*
- Barss, M.S., Hacquebard, P.A. and Howie, R.D. 1963. Palynology and stratigraphy of some Upper Pennsylvanian and Permian rocks of the Maritime Provinces. Geological Survey of Canada, Paper 63-3, 13p.
- Bell, W.A. 1914. Joggins Carboniferous section, Nova Scotia. Geological Survey of Canada Summary Report 1912, p. 360-371.
- Bell, W.A. 1944. Carboniferous rocks and fossil floras of northern Nova Scotia. Geological Survey of Canada Memoir 238, 276p.
- Belt, E.S. 1968a. Carboniferous continental sedimentation, Atlantic Provinces, Canada. Geological Society of America, Special Paper 106, p. 127-173.
- Belt, E.S. 1968b. Post-Acadian rifts and related facies, eastern Canada. *In: Studies of Appalachian Geology: Northern and Maritime, W.S. E-An Zen, W.S. White, J.B. Hadley and J.B. Thompson (eds.). Wiley Interscience, New York. p. 95-113.*
- Besly, B.M. and Fielding, C.R. 1989. Paleosols in Westphalian coal-bearing and red-bed sequences, Central and Northern England. *Palaeogeography,*

Palaeoclimatology, Palaeoecology, v. 70, p. 303-330.

- Besly, B.M. and Turner, P. 1983. Origin of red beds in a moist tropical climate (Etruria Formation, Upper Carboniferous, UK). *In: Residual Deposits: Surface Related Weathering Processes and Materials*, R.C.L. Wilson (ed.). Geological Society of London Special Publication 11, p. 131-147.
- Billi, P., Magi, M. and Sagri, M. 1987. Coarse-grained low-sinuosity river deposits: example from Plio-Pleistocene Valdarno Basin, Italy. *In: Recent Developments in Fluvial Sedimentology*, F.G. Ethridge, R.M. Flores and M.D. Harvey (eds.). Society of Economic Paleontologists and Mineralogists Special Publication 39, p. 197-203.
- Bird, D. 1987. The depositional environments of the Late Carboniferous, coal-bearing Sydney Mines Formation at Point Aconi, Cape Breton Island, Nova Scotia. Unpublished M.Sc. Thesis, Dalhousie University, Halifax. 343p.
- Blair, T. 1987. Tectonic and hydrologic controls on cyclic alluvial fan, fluvial, and lacustrine rift-basin sedimentation, Jurassic-Lowermost Cretaceous Todos Santos Formation, Chiapas, Mexico. *Journal of Sedimentary Petrology*, v. 57, p. 845-862.
- Bluck, B.J. 1979. Structure of coarse grained braided stream alluvium. *Transactions, Royal Society of Edinburgh*, v. 70, p. 181-221.
- Boehner, R.C., Calder, J.H., Carter, D.C., Donohoe, H.V., Ferguson, L., Pickerill, R.K. and Ryan, R.J. 1986. Basins of eastern Canada. *Symposium Field Trip. Atlantic Geoscience Society Special Publication 4*. 122p.
- Boehner, R.C., Ryan, R.J. and Carter, D.C. 1988. The Maritimes Basin: Basin, epieugeosyncline, taphrogeosyncline, horst-graben, wrench, successor, aulacogen, pull-apart, transpression? -basins, subbasins?- just a problem of semantics? *Atlantic Geoscience Conference Colloquium '88*. Antigonish, Nova Scotia. Abstract.
- Boothroyd, J.C. and Ashley, G.M. 1975. Process, bar morphology, and sedimentary structures on braided outwash fans, northeastern Gulf of Alaska. *In: Glaciofluvial and Glaciolacustrine Sedimentation*, A.V. Jopling and B.C. McDonald (Eds.). Society of Economic Paleontologists and Mineralogists Special Publication 23, p. 193-222.

- Bott, M.H.P. and Johnson, G.A.L. 1967. The controlling mechanism of Carboniferous cyclic sedimentation. *Quarterly Journal of the Geological Society, London*, v. 122, p. 421-441.
- Bown, T.M. and Kraus, M.J. 1987. Integration of channel and floodplain suites, I. Developmental sequence and lateral relations of alluvial paleosols. *Journal of Sedimentary Petrology*, v. 57, p. 587-601.
- Bowler, J.M. and Harford, L.B. 1966. Quaternary tectonics and the evolution of the Riverine Plain near Echuca, Victoria. *Journal of the Geological Society of Australia*, v. 13, p. 339-354.
- Braakman, J.H., Levell, B.K., Martin, J.H., Potter, T.L. and van Vliet, A. 1982. Late Paleozoic Gondwana glaciation in Oman. *Nature*, v. 299, p. 48-50.
- Bradley, D.C. 1982. Subsidence in Late Paleozoic basins in the northern Appalachians. *Tectonics*, v. 1, p. 107-123.
- Brand, U. 1989. Biogeochemistry of Late Paleozoic North American brachiopods and secular variation of seawater composition. *Biogeochemistry*, v. 7, p. 159-193.
- Brewer, R.C. 1964. *Fabric and Mineral Analysis of Soils*. Wiley, New York. 470p.
- Bridge, J.S. 1984. Largescale facies sequences in alluvial overbank environments. *Journal of Sedimentary Petrology*, v. 54, p. 583-588.
- Bridge, J.S. 1985. Paleochannel patterns inferred from alluvial deposits: a critical evaluation. *Journal of Sedimentary Petrology*, v. 55, p. 579-589.
- Bridge, J.S. and Leeder, M.R. 1979. A simulation model of alluvial stratigraphy. *Sedimentology*, v. 26, p. 617-644.
- Briggs, D.E.G., Plint, A.G. and Pickerill, R.K. 1984. *Arthropleura* trails from the Westphalian of eastern Canada. *Palaeontology*, v. 27, p. 843-855.
- Bristow, C.S. 1987. Brahmaputra River: channel migration and deposition. *In: Recent Developments in Fluvial Sedimentology*, F.G. Ethridge, R.M. Flores and M.D. Harvey (eds.). Society of Economic Paleontologists and Mineralogists Special Publication 39, p. 63-74.
- Cant, D.J. 1978. Development of a facies model for sandy braided river sedimentation: comparison of the South

- Saskatchewan River and the Battery Point Formation.
In: Fluvial Sedimentology, A.D. Miall (ed.). Canadian
Society of Petroleum Geologists Memoir 5, p. 627-639.
- Cant, D.J. and Walker, R.G. 1976. Development of a
braided-fluvial facies model for the Devonian Battery
Point Sandstone, Quebec. Canadian Journal of Earth
Sciences, v. 13, p. 102-119.
- Cant, D.J. and Walker, R.G. 1978. Fluvial processes and
facies sequences in the sandy braided South
Saskatchewan River, Canada. Sedimentology, v. 25, p.
625-648.
- Caputo, M.V. and Crowell, J.C. 1985. Migration of glacial
centres across Gondwana during the Paleozoic era.
Geological Society of America Bulletin, v. 96, p. 1020-
1036.
- Carling, P.A. 1990. Particle over-passing on depth-limited
gravel bars. Sedimentology, v. 37, p. 345-355.
- Clarke, D.B. and Muecke, G.K. 1985. Review of the petro-
chemistry and origin of the South mountain batholith
and associated plutons, Nova Scotia, Canada. In: High
Heat Production Granites, Hydrothermal Circulation and
Ore Genesis, Institute of Mining and Metallurgy,
London, England. p. 41-54.
- Coleman, J.M. 1969. Brahmaputra River: channel processes
and sedimentation. Sedimentary Geology, v. 3, p. 129-
239.
- Coleman, J.M. and Gagliano, S.M. 1965. Sedimentary
structures: Mississippi River deltaic plain. In:
Primary Sedimentary Structures and Their Hydrodynamic
Interpretation, G.V. Middleton (ed.). Society of
Economic Paleontologists and Mineralogists Special
Publication 12. p. 133-148.
- Collier, R.E.Ll., Leeder, M.R. and Maynard, J.R. 1990.
Transgressions and regressions: a model for the
influence of tectonic subsidence, deposition and
eustasy, with application to Quaternary and
Carboniferous examples. Geological Magazine, v. 127,
p. 117-128.
- Collinson, J.D. 1970. Bedforms of the Tana River, Norway.
Geographical Annalar, v. 52A, p. 31-56.
- Collinson, J.D. and Thompson, D.B. 1982. Sedimentary
Structures. George Allen and Unwin, London. 194p.
- Collinson, J.W., Stanley, K.O. and Vavra, C.L. 1980.

- Triassic fluvial depositional systems in the Fremouw Formation, Cumulus Hills, Antarctica. Proceedings of the Fifth International Gondwana Symposium. Gondwana Five. p. 141-148.
- Copeland, M.J. 1957. The arthropod fauna of the upper Carboniferous rocks of the Maritime Provinces. Geological Survey of Canada Memoir 286. 110p.
- Crowell, J.C. 1978. Gondwanan glaciation, cyclothems, continental positioning, and climatic change. American Journal of Science, v. 278, p. 1345-1372.
- Crowell, J.C. and Frakes, L.A. 1975. The late Paleozoic glaciation. In: Gondwana Geology, K.S.W. Campbell (ed.). Australian National University Press, Canberra. p. 313-331.
- Currie, K.L. 1984. A reconsideration of some geological relations near Saint John, New Brunswick. In: Current Research, Part A, Geological Survey of Canada, Paper 84-1A, p. 193-201.
- Dalrymple, R.W. 1984. Runoff microdeltas: a potential emergence indicator in cross-bedded sandstones. Journal of Sedimentary Petrology, v. 54, p. 825-830.
- Dam, G. and Andreasen, F. 1990. High-energy ephemeral stream deltas; an example from the Upper Silurian Holmstrand Formation of the Oslo Region, Norway. Sedimentary Geology, v. 66, p. 197-225.
- Dawson, J.W. 1868. Acadian Geology. MacMillan and Co., London. 2nd Edition. 694p.
- Dekker, F., Visser, C. and Dankers, P. 1987. The Primrose-Kirby area in the Southern Athabasca, Alberta, Canada: a detailed geological investigation. In: Exploration For Heavy Crude Oil and Natural Bitumen, R.F. Meyer (ed.). American Association of Petroleum Geologists Studies In Geology 25, p. 507-520.
- Dobkins, J.E. and Folk, R.L. 1970. Shape development on Tahiti-nui. Journal of Sedimentary Petrology, v. 40, p. 1167-1203.
- Donohoe, H.V. and Grantham, R.G. 1989. Geological Highway Map of Nova Scotia. 2nd Edition. Atlantic Geosciences Society, Halifax, Special Publication 1.
- Donohoe, H.V. and Wallace, P.I. 1982. Geological Map of the Cobequid Highlands, Nova Scotia. Nova Scotia Department of Mines and Energy.
- Donohoe, H.V. and Wallace, P.I. 1988. Movement history of

the Cobequid Fault Zone, Cobequid Highlands, northern Nova Scotia. Abstract. *Maritime Sediments and Atlantic Geology*, v. 24, p. 191-192.

- D'Orsay, M. 1986. Stratigraphy and sedimentology of Carboniferous rocks in the northwestern Minas Basin and Channel Region of Nova Scotia. Unpublished M.Sc. Thesis, University of New Brunswick. 301p.
- D'Orsay, M. and van de Poll, H.W. 1985. Quartz-grain surface textures: evidence for a tropical climate during the Middle Pennsylvanian in eastern Canada. *Canadian Journal of Earth Sciences*, v. 22, p. 786-790.
- Dott, R.H. and Bourgeois, J. 1982. Hummocky stratification: significance of its variable bedding sequences. *Geological Society of America Bulletin*, v. 93, p. 663-680.
- Duke, W.L. 1985. Hummocky cross-stratification, tropical hurricanes, and intense winter storms. *Sedimentology*, v. 32, p. 167-194.
- Duke, W.L. 1990. Geostrophic circulation or shallow marine turbidity currents? The dilemma of paleoflow patterns in storm-influenced prograding shoreline systems. *Journal of Sedimentary Petrology*, v. 60, p. 870-883.
- Eisbacher, G.H. 1967. Tectonic analysis in the Cobequid Mountains, Nova Scotia, Canada. Unpublished Ph.D. Thesis, Princeton University. 108p.
- Eisbacher, G.H. 1969. Displacement and stress field along part of the Cobequid Fault, Nova Scotia. *Canadian Journal of Earth Sciences*, v. 6, p. 1095-1104.
- Eisbacher, G.H. 1981. Late Mesozoic -Palaeogene Bowser Basin molasse and Cordilleran tectonics, western Canada. In: *Sedimentation and Tectonics in Alluvial Basins*. A.D. Miall (ed.). Geological Association of Canada Special Paper 23, p. 125-151.
- Elliott, T. 1974. Inter-distributary bay sequences and their genesis. *Sedimentology*, v. 21, p. 611-622.
- Elliott, T. 1976. The morphology, magnitude and regime of a Carboniferous fluvial-distributary channel. *Journal of Sedimentary Petrology*, v. 46, p. 70-76.
- Ells, R.W. 1885. Report on the geological formations of eastern Albert and Westmoreland counties. New Brunswick and of portions Cumberland and Colchester counties, Nova Scotia. Geological Survey of Canada

Annual Report for 1884-1885, v. 1E. 71p.

- Esteban, C.M. 1976. Vadose pisolite and caliche. American Association of Petroleum Geologists Bulletin, v. 60, p. 2048-2057.
- Ethridge, F.G. and Wescott, W.A. 1984. Tectonic setting, recognition and hydrocarbon reservoir potential of fan-delta deposits. In: Sedimentology of Gravels and Conglomerates, E.H. Koster and R.J. Steel (eds.). Canadian Society of Petroleum Geologists Memoir 10, p. 217-235.
- Evamy, B.D. 1963. The application of a chemical staining technique to a study of dedolomitisation. Sedimentology, v. 2, p. 164-170.
- Eyles, N. and Clark, B.M. 1986. Significance of hummocky and swaley cross-stratification in Late Pleistocene lacustrine sediments of the Ontario basin, Canada. Geology, v. 14, p. 679-682.
- Eynon, G. and Walker, R.G. 1974. Facies relationships in Pleistocene outwash gravels, southern Ontario: a model for bar growth in braided rivers. Sedimentology, v. 21, p. 43-70.
- Fahnestock, R.K. and Bradley, W.C. 1973. Knik and Matanuska Rivers, Alaska: a contrast in braiding. In: Fluvial Geomorphology, M. Morisawa (ed.). State University of New York, Binghamton. Publications in Geomorphology 4, p. 220-250.
- Falvey, D.A. and Deighton, I. 1982. Recent advances in burial and thermal geohistory analysis. Australian Petroleum Exploration Association Journal, v. 22, p. 65-81.
- Faulkner, T.J., Wright, V.P., Peeters, C. and Garvie, L. 1990. Cryptic exposure horizons in the Carboniferous Limestone of Portishead, Avon. Geological Journal, v. 25, p. 1-17.
- Felsche, J. 1978. Yttrium and lanthanides. Handbook of Geochemistry. Springer-Verlag, New York. v.11-5, p. A1-A42.
- Ferguson, R.I. and Werritty, A. 1983. Bar development and channel changes in the gravelly River Feschie, Scotland. In: Modern and Ancient Fluvial Systems, J.D. Collinson and J. Lewin (eds.). International Association of Sedimentologists Special Publication 6, p. 181-193.

- Fielding, C.R. 1984. Upper delta plain lacustrine and fluviolacustrine facies from the Westphalian of the Durham coalfield, NE England. *Sedimentology*, v. 31, p. 547-567.
- Fielding, C.R. 1989. Hummocky cross-stratification from the Boxvale Sandstone Member in the northern Surat Basin, Queensland. *Australian Journal of Earth Sciences*, v. 36, p. 469-471.
- Fitzpatrick, E.A. 1971. *Pedology: A Systematic Approach to Soil Science*. Oliver and Boyd, Edinburgh. 306p.
- Fletcher, H. 1892. Report on geological surveys and explorations in the Counties of Pictou and Colchester, Nova Scotia. *Geological Survey of Canada Annual Report*, v. 5, Part II, p. 5-193.
- Folk, R.L. 1974. *Petrology of Sedimentary Rocks*. Hemphill Publishing Co., Austin, Texas. 182p.
- Fralick, P.W. 1981. Tectonic and sedimentological development of a Late Paleozoic wrench basin: the eastern Cumberland Basin, Maritime Canada. Unpublished M.Sc. Thesis, Dalhousie University, Halifax. 175p.
- Fralick, P.W. 1989. Late Paleozoic basin development history of northern Nova Scotia. *Lithoprobe East, Report of Activities*, G. Quilan (ed.).
- Fralick, P.W and Schenk, P.E. 1981. Molasse deposition and basin evolution in a wrench tectonic setting: the Late Paleozoic, eastern Cumberland Basin, Maritime Canada. *In: Sedimentation and Tectonics in Alluvial Basins*, A.D. Miall (ed.). Geological Association of Canada Special Paper 23, p. 77-97.
- Francis, J.E. 1986. The calcareous paleosols of the basal Purbeck Formation (Upper Jurassic), Southern England. *In: Paleosols Their Recognition and Interpretation*, V.P. Wright (ed.). Princeton University Press, Princeton, N.J., p. 112-138.
- Freund, R. 1971. The Hope Fault, a strike slip fault in New Zealand. *New Zealand Geological Survey Bulletin* 86, 49p.
- Fritz, P., Binda, P.L., Folinsbee, F.E. and Krouse, H.R. 1971. Isotopic composition of diagenetic siderites from Cretaceous sediments in Western Canada. *Journal of Sedimentary Petrology*, v. 41, p. 282-288.
- Fyffe, L.R. and Barr, S.M. 1986. Petrochemistry and tectonic significance of Carboniferous volcanic rocks

- in New Brunswick. *Canadian Journal of Earth Sciences*, v. 23, p. 1243-1256.
- Gale, S.J. 1990. The shape of beach gravels. *Journal of Sedimentary Petrology*, v. 60, p. 787-789.
- Gardner, L.R. 1972. Origin of the Mormon Mesa caliche, Clark County, Nevada. *Geological Society of America Bulletin*, v. 83, p. 143-156.
- Gay, A.L. and Grandstaff, D.E. 1980. Chemistry and mineralogy of Precambrian paleosols at Elliot Lake, Ontario, Canada. *Precambrian Research*, v. 12, p. 349-375.
- Gersib, G.A. 1979. Meandering river deposits of the Upper Carboniferous, Port Hood Formation, Port Hood, Nova Scotia, Canada. Unpublished M.S. Thesis, University of Nebraska. 80p.
- Gersib, G.A. and McCabe, P.J. 1981. Continental coal-bearing sediments of the Port Hood Formation (Carboniferous), Cape Linzee, Nova Scotia, Canada. In: *Recent and Ancient Nonmarine Depositional Environments: Models for Exploration*, F.G. Ethridge and R.M. Flores (eds.). *Society of Economic Paleontologists and Mineralogists Special Publication 31*, p. 95-108.
- G-Farrow, C.E. and Mossman, D.J. 1988. Geology of Precambrian paleosols at the base of the Huronian Supergroup, Elliot Lake, Ontario, Canada. *Precambrian Research*, v. 42, p. 107-139.
- Gibling, M.R. 1989. Late Paleozoic drainage of the Appalachian Orogen: evidence from the coal basins of Atlantic Canada. 23rd Newcastle Symposium on Advances in the Study of the Sydney Basin, Newcastle, New South Wales. 31 March-2 April 1989. 8p.
- Gibling, M.R., Boehner, R.C. and Rust, B.R. 1987. The Sydney Basin of Atlantic Canada: a Late Paleozoic strike-slip basin in a collisional setting. In: *Sedimentary Basins and Basin-forming Mechanisms*, C. Beaumont and A.J. Tankard (Eds.). *Canadian Society of Petroleum Geologists Memoir 12*, p. 269-285.
- Gibling, M.R., Calder, J., Ryan, R., van de Poll, W. and Yeo, G. 1989. Pennsylvanian and Permian drainage in Atlantic Canada: lateral, intermontane flow from the Appalachian Orogen. *International Symposium on Intermountain Basins: Geology and Resources*. Chiang Mai, Thailand. 30 January-2 February 1989. p. 468.
- Gibling, M.R. and Rust, B.R. 1984. Channel margins in a

- Pennsylvanian braided, fluvial deposit: the Morien Group near Sydney, Nova Scotia, Canada. *Journal of Sedimentary Petrology*, v. 54, p. 773-782.
- Gibling, M.R. and Rust, B.R. 1987. Evolution of a mud-rich meander belt in the Carboniferous Morien Group, Nova Scotia, Canada. *Bulletin of Canadian Petroleum Geology*, v. 35, p. 24-33.
- Gibling, M.R. and Rust, B.R. 1990. Ribbon sandstones in the Pennsylvanian Waddens Cove Formation, Sydney Basin, Atlantic Canada: the influence of siliceous duricrusts on channel-body geometry. *Sedimentology*, v. 37, p. 45-65.
- Gibson, P.J. 1989. Petrology of two Tertiary oil shale deposits from Queensland, Australia. *Geological Society of London, Journal*, v. 146, p. 319-331.
- Gibson, P.J., Shaw, H.F. and Spiro, B. 1990. The formation of eogenetic siderites in Tertiary lacustrine oil shales of Queensland, Australia. *International Association of Sedimentologists Conference, Nottingham, August 1990. Abstract*. p. 494.
- Gilbert, R. and Shaw, J. 1981. Sedimentation in proglacial Sunwapta Lake, Alberta. *Canadian Journal of Earth Sciences*, v. 12, p. 1697-1711.
- Gile, L.H., Peterson, F.F. and Grossman, R.B. 1966. Morphological and genetic sequences of carbonate accumulation in desert soils. *Soil Science*, v. 101, p. 347-360.
- Goebel, K.A., Bettis, E.A. and Heckel, P.H. 1989. Upper Pennsylvanian paleosol in Stranger Shale and underlying Iatan Limestone, Southwestern Iowa. *Journal of Sedimentary Petrology*, v. 59, p. 224-232.
- Gore, P.J.W. 1989. Toward a model for open- and closed-basin deposition in ancient lacustrine sequences: the Newark Supergroup (Triassic-Jurassic), eastern North America. *Palaeogeography, Palaeoclimatology, Palaeoecology*, v. 70, p. 29-51.
- Goudie, A.S. 1973. *Duricrusts in Tropical and Subtropical Landscapes*. Clarendon Press, Oxford. 174p.
- Graves, M.C. 1982. Supplementary report No. 5 of the Carboniferous drilling project. Open File Report 82-30. Mineral Resources Division, New Brunswick Department of Natural Resources. 87p.
- Greenwood, B. and Sherman, D. 1986. Hummocky cross-

- stratification in the surf zone. Flow parameters and bedding genesis. *Sedimentology*, v. 33, p. 33-46.
- Gregory, D.I. and Schumm, S.A. 1987. The effects of active tectonics on alluvial river morphology. In: *River Channels Environment and Process*, K. Richards (Ed.). The Institute of British Geographers, Special Publications Series 17, Blackwell, p. 41-68.
- Groll, P.E. and Steidtmann, J.R. 1987. Fluvial responses to Eocene tectonism, the Bridger Formation, southern Wind River Range, Wyoming. In: *Recent Developments in Fluvial Sedimentology*, F.G. Ethridge, R.M. Flores and M.D. Harvey (eds.). Society of Economic Paleontologists and Mineralogists Special Publication 39, p. 253-262.
- Guion, P.D. 1987. Palaeochannels in mine workings in the High Hazles Coal (Westphalian B), Nottinghamshire Coalfield, England. *Journal of the Geological Society*, London, v. 144, p. 471-488.
- Gussow, W.C. 1953. Carboniferous stratigraphy and structural geology of New Brunswick, Canada. *American Association of Petroleum Geologists Bulletin*, v. 37, p. 1713-1816.
- Gustavson, T.C. 1978. Bed forms and stratification types of modern gravel meander lobes, Nueces River, Texas. (Abstract). In: *Fluvial Sedimentology*, A.D. Miall (ed.). Canadian Society of Petroleum Geologists Memoir 5, p. 851.
- Hacquebard, P.A. and Avery, M.P. 1984. Geological and geothermal effects on coal rank variations in the Carboniferous basin of New Brunswick. In: *Current Research, Part A. Geological Survey of Canada, Paper 84-1A*, p. 17-28.
- Hacquebard, P.A. and Cameron, A.R. 1989. Distribution and coalification patterns in Canadian bituminous and anthracite coals. *International Journal of Coal Geology*, v. 13, p. 207-260.
- Harding, T.P. 1974. Petroleum traps associated with wrench faults. *American Association of Petroleum Geologists Bulletin*, v. 58, p. 1290-1304.
- Harding, T.P. 1985. Seismic characteristics and identification of negative flower structures, positive flower structures, and positive structural inversion. *American Association of Petroleum Geologists Bulletin*, v. 69, p. 582-600.

- Harding, T.P. and Lowell, J.D. 1979. Structural styles, their plate tectonic habitats, and hydrocarbon traps in petroleum provinces. *American Association of Petroleum Geologists Bulletin*, v. 63, p. 1016-1058.
- Harland, W.B., Cox, A.V., Llewellyn, P.G., Pickton, C.A.G., Smith, A.G and Walters, R. 1982. Subdivisions of Phanerozoic Time. *A Geologic Time Scale*. Cambridge University Press.
- Harrison, R.S. 1977. Caliche profiles: indicators of near-surface subaerial diagenesis, Barbados, West Indies. *Bulletin of Canadian Petroleum Geology*, v. 25, p. 123-173.
- Hart, B.S. 1990. Sedimentology and Stratigraphy of the Upper Cretaceous Cardium Formation, in Northwestern Alberta and Adjacent British Columbia. Unpublished Ph.D. Thesis, University of Western Ontario. 505p.
- Hart, B.S. and Plint, A.G. 1989. Gravelly shoreface deposits: a comparison of modern and ancient facies sequences. *Sedimentology*, v. 36, p. 551-557.
- Haworth, R.T., Daniels, D.L., Williams, H. and Zietz, I. 1980. Bouguer Gravity Anomaly Map of the Appalachians. Scale 1:1 000 000. Project 27, International Geological Correlation Program and International Geodynamics Project. Memorial University of Newfoundland.
- Heckel, P.H. 1986. Sea-level curve for Pennsylvanian eustatic marine transgressive depositional cycles along midcontinent outcrop belt, North America. *Geology*, v. 14, p. 330-334.
- Hein, F.J. 1984. Deep-sea and fluvial braided channel conglomerates: a comparison of two case studies. In: *Sedimentology of Gravels and Conglomerates*, E.H. Koster and R.J. Steel (eds.). *Canadian Society of Petroleum Geologists Memoir 10*, p. 33-49.
- Hein, F.J. and Walker, R.G. 1977. Bar evolution and development of stratification in the gravelly, braided, Kicking Horse River, British Columbia. *Canadian Journal of Earth Sciences*, v. 14, p. 562-570.
- Hess, J.C. and Lippolt, H.J. 1986. $^{40}\text{Ar}/^{39}\text{Ar}$ ages on tonstein and tuff sanidines: new calibration points for the improvement of the Upper Carboniferous time scale. *Chemical Geology (Isotope Geoscience)*, v. 59, p. 143-154.
- Hesse, R. and Reading, H.G. 1978. Subaqueous clastic

- fissure eruptions and other examples of sedimentary transposition in the lacustrine Horton Bluff Formation (Mississippian), Nova Scotia, Canada. *In: Modern and Ancient Lake Sediments*, A. Matter and M.E. Tucker (eds.). Special Publication of the International Association of Sedimentologists 2, p. 241-257.
- Hickin, E.J. 1984. Vegetation and river channel dynamics. *Canadian Geographer*, v. 28, p. 111-126.
- Hobday, D.K. 1978. Geological evolution and geomorphology of the Zululand coastal plain. *In: Ecology and Biogeography of Lake Sibaya*. B.R. Allanson (ed.). Junk, The Hague. p. 1-20.
- Houghton, H.F. 1980. Refined techniques for staining plagioclase and alkali feldspars in thin section. *Journal of Sedimentary Petrology*, v. 50, p. 629-631.
- Hower, J., Eslinger, E.V., Hower, M.E. and Perry, E.A. 1976. Mechanisms of burial metamorphism of argillaceous sediment: 1) Mineralogical and chemical evidence. *Geological Society of America Bulletin*, v. 87, p. 725-737.
- Howie, R.D. 1988. Upper Paleozoic evaporites of eastern Canada. *Geological Survey of Canada Bulletin* 380. 120p.
- Howie, R.D. and Barss, M.S. 1975a. Paleogeography and sedimentation in the Upper Paleozoic, Eastern Canada. *In: Canada's Continental Margins and Offshore Petroleum Exploration*. Canadian Society of Petroleum Geologists Memoir 4, p. 45-57.
- Howie, R.D. and Barss, M.S. 1975b. Upper Paleozoic rocks of the Atlantic Provinces, Gulf of St Lawrence and adjacent continental shelf. *In: Offshore Geology of Eastern Canada*, W. van der Linden and J.A. Wade (eds.). Geological Survey of Canada, Paper 74-30, p. 35-50.
- Hubert, J.F. and Forlenza, M.F. 1988. Sedimentology of braided-river deposits in the Upper Triassic Wolfville redbeds, southern shore of Cobequid Bay, Nova Scotia, Canada. *In: Triassic-Jurassic Rifting: Continental Breakup and the Origin of the Atlantic Passive Margins*. Part A, W. Manspeizer (ed.). Developments in Geotectonics, Elsevier. p. 231-247.
- Hubert, J.F. and Mertz, K.A. 1984. Eolian sandstones in Upper Triassic-Lower Jurassic redbeds of the Fundy Basin, Nova Scotia. *Journal of Sedimentary Petrology*, v. 54, p. 798-810.

- Hutchinson, D.R., Klitgord, K.D., Lee, M.W. and Trehu, A.M. 1988. U.S. Geological Survey deep seismic reflection profile across the Gulf of Maine. Geological Society of America Bulletin, v. 100, p. 172-184.
- Hutchinson, D.R., Klitgord, K.D. and Trehu, A.M. 1987. Structure of the lower crust beneath the Gulf of Maine. Geophysical Journal of the Royal Astronomical Society, v. 89, p. 189-194.
- Imbrie, J., Hays, J.D., Martinson, D.G., McIntyre, A., Mix, A.C., Morley, J.J., Pisias, N.G., Prell, W. and Shackleton, N.J. 1984. The orbital theory of Pleistocene climate: support from a revised chronology of the marine $\delta^{18}O$ record. In: Milankovitch and Climate, A. Berger, J. Imbrie, J. Hays, G. Kukla and B. Saltzman (eds.). D. Riedel, Hingham, Massachusetts. p. 269-305.
- Irving, E. 1979. Paleopoles and paleolatitudes of North America and speculations about displaced terranes. Canadian Journal of Earth Sciences, v. 16, p. 669-694.
- Isbell, J.L. and Collinson, J.W. 1988. Fluvial architecture of the Fairchild and Buckley Formations (Permian), Beardmore Glacier area. Antarctic Journal of the United States, v. 23, p. 3-5.
- Jackson, R.G. 1978. Preliminary evaluation of lithofacies models for meandering alluvial streams. In: Fluvial Sedimentology, A.D. Miall (Ed.). Canadian Society of Petroleum Geologists Memoir 5, p. 543-576.
- James, N.P. 1972. Holocene and Pleistocene calcareous crust (caliche) profiles: criteria for subaerial exposure. Journal of Sedimentary Petrology, v. 42, p. 817-836.
- Joeckel, R.M. 1989. Geomorphology of a Pennsylvanian land surface: pedogenesis in the Rock Lake Shale Member, Southern Nebraska. Journal of Sedimentary Petrology, v. 59, p. 469-481.
- Jones, B. and Kwok-Choi Ng. 1988. The structure and diagenesis of rhizoliths from Cayman Brac, British West Indies. Journal of Sedimentary Petrology, v. 58, p. 457-467.
- Jones, C.M. 1977. The effects of varying discharge regimes on sedimentary structures in modern rivers. Geology, v. 5, p. 567-570.
- Kalkreuth, W. and Macauley, G. 1984. Organic petrology of selected oil shale samples from the Lower Carboniferous Albert Formation, New Brunswick, Canada. Bulletin of

- Canadian Petroleum Geology, v. 32, p. 38-51.
- Kalkreuth, W. and Macauley, G. 1987. Organic petrology and geochemical (rock-eval) studies on oil shales and coals from the Pictou and Antigonish areas, Nova Scotia, Canada. *Bulletin of Canadian Petroleum Geology*, v. 35, p. 263-295.
- Kaplan, S.S. 1980. The sedimentology, coal petrology, and trace element geochemistry of coal bearing sequences from Joggins, Nova Scotia, Canada, and Southeastern Nebraska, U.S.A. Unpublished Ph.D. Thesis, University of Pittsburgh, 304p.
- Karcz, I. 1969. Mud pebbles in a flash flood environment. *Journal of Sedimentary Petrology*, v. 39, p. 333-337.
- Karistineos, N. and Ioakim, C. 1989. Palaeoenvironmental and palaeoclimatic evolution of the Serres Basin (N. Greece) during the Miocene. *Palaeogeography, Palaeoclimatology, Palaeoecology*, v. 70, p. 275-285.
- Kashai, E.L. and Crocker, P.F. 1987. Structural geometry and evolution of the Dead Sea-Jordan rift system as deduced from new subsurface data. *Tectonophysics*, v. 141, p. 33-60.
- Kelley, D.G. 1967. Some aspects of Carboniferous stratigraphy and depositional history in the Atlantic Provinces. In: *Geology of the Atlantic Region*, E.R.W. Neale and H. Williams (eds.). Geological Association of Canada Special Paper 4, p. 213-227.
- Keppie, J.D. and Dallmeyer, R.D. 1987. Dating transcurrent terrane accretion: an example from the Meguma and Avalon composite terranes in the northern Appalachians. *Tectonics*, v. 6, p. 831-847.
- Kimberley, M.M. and Grandstaff, D.E. 1986. Profiles of elemental concentrations in Precambrian paleosols on basaltic and granitic parent materials. *Precambrian Research*, v. 32, p. 133-154.
- Kirk, M. 1989. Westphalian alluvial plain sedimentation, Isle of Arran, Scotland. *Geological Magazine*, v. 126, p. 407-421.
- Kirkham, R.V. 1985. Base metals in Upper Windsor (Codroy) Group oolitic and stromatolitic limestones in the Atlantic Provinces. In: *Current Research, Part A*. Geological Survey of Canada, Paper 85-1A, p. 573-585.
- Klappa, C.F. 1980. Rhizoliths in terrestrial carbonates: classification, recognition, genesis and significance.

Sedimentology, v. 27, p. 613-629.

- Klappa, C.F. 1983. A process-response model for the formation of pedogenic calcretes. *In: Residual Deposits: Surface Related Weathering Processes and Materials*, R.C.L. Wilson (ed.). Blackwell Scientific Publications, p. 211-220.
- Klein, G. deV. 1990. Pennsylvanian time scales and cycle periods. *Geology*, v. 18, p. 455-457.
- Kraus, M.J. 1984. Sedimentology and tectonic setting of Early Tertiary quartzite conglomerates, Northwest Wyoming. *In: Sedimentology of Gravels and Conglomerates*, E.H. Koster and R.J. Steel (eds.). Canadian Society of Petroleum Geologists Memoir 10, p. 203-216.
- Kraus, M.J. and Bown, T.M. 1986. Paleosols and time resolution in alluvial stratigraphy. *In: Paleosols Their Recognition and Interpretation*, V.P. Wright (ed.). Princeton University Press, Princeton, N.J. p. 180-207.
- Kraus, M.J. and Middleton, L.T. 1987. Constrasting architecture of two alluvial suites in different structural settings. *In: Recent Developments in Fluvial Sedimentology*, F.G. Ethridge, R.M. Flores and M.D. Harvey (eds.). Society of Economic Paleontologists and Mineralogists Special Publication 39, p. 253-262.
- Lambeck, K. 1980. *The Earth's Variable Rotation: Geophysical Causes and Consequences*. Cambridge University Press, Cambridge, UK. 449p.
- Langford-Smith, T. 1978. A select review of silcrete research in Australia. *In: Silcrete in Australia*, T. Langford-Smith (ed.). University of New England, Armidale, New South Wales. p. 1-11.
- Laury, R.L. 1971. Stream bank failure and rotational slumping: preservation and significance in the geologic record. *Geological Society of America Bulletin*, v. 82, p. 1251-1266.
- Lawrence, D.A. and Williams, B.P.J. 1987. Evolution of drainage systems in response to Acadian deformation: the Devonian Battery Point Formation, eastern Canada. *In: Recent Developments in Fluvial Sedimentology*, F.G. Ethridge, R.M. Flores and M.D. Harvey (eds.). Society of Economic Paleontologists and Mineralogists Special Publication 39, p. 287-300.

- Lawson, D.E. 1962. Sedimentology of the Boss Point Formation in southeastern New Brunswick. Unpublished M.Sc. Thesis, University of New Brunswick. 141p.
- Leckie, D.A. and Foscolos, A.E. 1986. Paleosols and Albian sea level fluctuations: preliminary observations from the northeastern British Columbia foothills. *In: Current Research, Part B, Geological Survey of Canada, Paper 86-1B, p. 429-441.*
- Leckie, D.A., Fox, C. and Tarnocai, C. 1989. Multiple paleosols of the Late Albian Boulder Creek Formation, British Columbia, Canada. *Sedimentology, v. 36, p. 307-323.*
- Leckie, D.A. and Walker, R.G. 1982. Storm- and tide-dominated shorelines in Cretaceous Moosebar-lower Gates interval; outcrop equivalents of Deep Basin gas trap in western Canada. *American Association of Petroleum Geologists Bulletin, v. 66, p. 138-157.*
- Leeder, M.R. 1973. Fluvial fining-upward cycles and the magnitude of paleochannels. *Geological Magazine, v. 110, p. 265-276.*
- Leeder, M.R. 1975. Pedogenic carbonates and flood plain sediment accretion rates: a quantitative model for alluvial arid-zone lithofacies. *Geological Magazine, v. 112, p. 257-270.*
- Leeder, M.R. 1976. Palaeogeographic significance of pedogenic carbonates in the topmost Old Red Sandstone of the Scottish Border Basin. *Geological Journal, v. 11, p. 21-28.*
- Leeder, M.R. 1988. Recent developments in Carboniferous geology: a critical review with implications for the British Isles and N.W. Europe. *Proceedings of the Geologists Association, v. 99, p. 73-100.*
- Leeder, M.R. and Strudwick, A.E. 1987. Delta-marine interactions: a discussion of sedimentary models for Yoredale-type cyclicity in the Dinantian of northern England. *In: European Dinantian Environments, J.M. Miller, A.E. Adams and V.P. Wright (eds.). Wiley, Chichester, p. 115-130.*
- Lefort, S.F. and van der Voo, B. 1981. A kinematic model for the collision and complete suturing between Gondwanaland and Laurasia in the Carboniferous. *Journal of Geology, v. 89, p. 537-550.*
- Leger, A. 1986. Transcurrent faulting history of southern New Brunswick. Unpublished M.Sc. Thesis, University of

New Brunswick. 170p.

- Legun, A.S. 1980. Sedimentology of the Clifton Formation (Upper Carboniferous) of northern New Brunswick: a semi-arid depositional setting for coal. Unpublished M.Sc. Thesis, University of Ottawa. 97p.
- Legun, A.S. and Rust, B.R. 1982. The Upper Carboniferous Clifton Formation of northern New Brunswick: coal-bearing deposits of a semi-arid alluvial plain. Canadian Journal of Earth Sciences, v. 19, p. 1775-1785.
- Leopold, L.B. and Wolman, M.G. 1957. River channel patterns: braided, meandering and straight. U.S. Geological Survey Professional Paper 282-B. 85p.
- Logan, W.E. 1845. Section of the Nova Scotia Coal Measures, as developed at the Joggins, on the Bay of Fundy, in descending order, from the neighbourhood of the West Ragged Reef to Minudie, reduced to vertical thickness. Geological Survey of Canada, Report of Progress for 1843. p. 92-159.
- Loncarevic, B.D., Barr, S.M., Raeside, R.P., Keen, C.E. and Marillier, F. 1989. Northeastern extension and crustal expression of terranes from Cape Breton Island, Nova Scotia, based on geophysical data. Canadian Journal of Earth Sciences, v. 26, p. 2255-2267.
- Longiaru, S., Rutherford, S. and Starkey, J. 1989. Microcomputer Workshop. Quantitative Petrofabric Analysis. 9th Annual Meeting, November 10-12, 1989. Structural Geology and Tectonic Division. Geological Association of Canada, London, Ontario. 68p.
- Love, D.W., Gutjahr, A. and Robinson-Cook, S. 1987. Location-dependent sediment sorting in bedforms under waning flow in the Rio Grande, Central New Mexico. In: Recent Developments in Fluvial Sedimentology, F.G. Ethridge, R.M. Flores and M.D. Harvey (eds.). Society of Economic Paleontologists and Mineralogists Special Publication 39, p. 37-47.
- Lyons, P.C. 1988. Alleghany orogeny - a misspelling(?) and web of confusion. Geology, v. 16, p. 91.
- McBride, E.F. and Yeakel, L.S. 1963. Relationship between parting lineation and rock fabric. Journal of Sedimentary Petrology, v. 33, p. 779-782.
- McCabe, P.J. 1978a. Bedforms from abandoned fluvial channels, Carboniferous, Maritime Provinces. (Abstract). In: Fluvial Sedimentology, A.D. Miall

- (ed.). Canadian Society of Petroleum Geologists Memoir 5, p. 854.
- McCabe, P.J. 1978b. Deposits of fine grained meandering rivers, with large discharge variations, in the Carboniferous of the Maritime Provinces, Canada. (Abstract). In: Fluvial Sedimentology, A.D. Miall (ed.). Canadian Society of Petroleum Geologists Memoir 5, p. 853-854.
- McCabe, P.J. 1979. Tectonic and climatic controls on the sedimentological evolution of a Carboniferous basin: the Namurian of the Cumberland Basin, Maritime Canada. (Abstract). 9th International Congress of Carboniferous Stratigraphy and Geology, Urbana, Illinois. p. 134.
- McCabe, P.J. 1984. Depositional environments of coal and coal-bearing strata. In: Sedimentology of Coal and Coal-Bearing Sequences, R.A. Rahmani and R.M. Flores (eds.). Special Publication of the International Association of Sedimentologists, v. 7, p. 13-42.
- McCave, I.N. 1969. Correlation of marine and non-marine strata, with example from Devonian of New York State. American Association of Petroleum Geologists Bulletin, v. 53, p. 155-162.
- Macauley, G., Ball, F.D. and Powell, T.G. 1984. A review of the Carboniferous Albert Formation oil shales, New Brunswick. Bulletin of Canadian Petroleum Geology, v. 32, p. 27-37.
- McCutcheon, S.R. and Calder, J.H. 1985. Boss Point Formation. In: Lexicon of Canadian Stratigraphy, Volume VI Atlantic Region, G.L. Williams, L.R. Fyffe, R.J. Wardle, S.P. Colman-Sadd and R.C. Boehner (eds.). Canadian Society of Petroleum Geologists, Calgary, p. 40-41.
- McCutcheon, S.R. and Robinson, P.T. 1987. Geological constraints on the genesis of the Maritimes Basin, Atlantic Canada. In: Sedimentary Basins and Basin-Forming Mechanisms, C. Beaumont and A.J. Tankard (eds.). Canadian Society of Petroleum Geologists Memoir 12, p. 287-297.
- McKerrow, W.S. and Ziegler, A.M. 1972. Paleozoic oceans. Nature (London), v. 240, p. 92-94.
- McLean, J.R. 1977. The Cadomin Formation: stratigraphy, sedimentology and tectonic implications. Bulletin of Canadian Petroleum Geology, v. 25, p. 792-827.
- McLeod, M.J. 1980. Geology and mineral deposits of the

Hillsborough area, map area V-22 and V-23 (Parts of 21H/15E and 21H/15W). Map report 79-6. Mineral Resources Branch, New Brunswick Department of Natural Resources.

- McLeod, M.J. and Ruitenbergh, A.A. 1978. Geology and mineral deposits of the Dorchester area, map area W-22, W-23 (21H/15E, 21H/16W). Map Report 78-4. Mineral Resources Branch, New Brunswick Department of Natural Resources.
- McMaster, R.L., de Boer, J. and Collins, B.P. 1980. Tectonic development of the southern Narragansett Bay and offshore Rhode Island. *Geology*, v. 8, p. 496-500.
- McPherson, J.G. 1979. Calcrete (caliche) palaeosols in fluvial redbeds of the Aztec Siltstone (Upper Devonian), Southern Victoria Land, Antarctica. *Sedimentary Geology*, v. 22, p. 267-285.
- Machette, M.N. 1985. Calcic soils of the southwestern United States. In: *Soils and Quaternary Geology of the Southwestern United States*, D.L. Weide (ed.). Geological Society of America Special Paper 203, p. 1-21.
- Marillier, F. and Verhoef, J. 1989. Crustal thickness under the Gulf of St Lawrence, northern Appalachians, from gravity and deep seismic data. *Canadian Journal of Earth Sciences*, v. 26, p. 1517-1532.
- Martel, A.T. 1987. Seismic stratigraphy and hydrocarbon potential of the strike-slip Sackville sub-basin, New Brunswick. In: *Sedimentary Basins and Basin-Forming Mechanisms*, C. Beaumont and A.J. Tankard (eds.). Canadian Society of Petroleum Geologists Memoir 12, p. 319-334.
- Martel, A.T. 1990. Stratigraphy, fluviolacustrine sedimentology and cyclicity of the Late Devonian-Early Carboniferous Horton Bluff Formation, Nova Scotia, Canada. Unpublished Ph.D. Thesis, Dalhousie University, Halifax, Nova Scotia. 297p.
- Marzo, M., Nijman, W. and Puigdefabregas, C. 1988. Architecture of the Castissent fluvial sheet sandstones, Eocene, South Pyrenees, Spain. *Sedimentology*, v. 35, p. 719-738.
- Mason, B. 1966. *Principles of Geochemistry*. John Wiley and Sons, New York. 329p.
- Masson, A.G. and Rust, B.R. 1990. Alluvial plain sedimentation in the Pennsylvanian Sydney Mines

- Formation, eastern Sydney Basin, Nova Scotia. *Bulletin of Canadian Petroleum Geology*, v. 38, p. 89-105.
- Meyer, R. and Pena dos Reis, R.B. 1985. Paleosols and alunite silcretes in continental Cenozoic of western Portugal. *Journal of Sedimentary Petrology*, v. 55, p. 76-85.
- Miall, A.D. 1973. Markov chain analysis applied to an ancient alluvial plain succession. *Sedimentology*, v. 20, p. 347-364.
- Miall, A.D. 1977. A review of the braided-river depositional environment. *Earth and Planetary Science Reviews*, v. 13, p. 1-62.
- Miall, A.D. 1978. Lithofacies types and vertical profile models in braided river deposits: a summary. *In: Fluvial Sedimentology*, A.D. Miall (ed.). Canadian Society of Petroleum Geologists Memoir 5, p. 597-604.
- Miall, A.D. 1983. Basin analysis of fluvial sediments. *In: Modern and Ancient Fluvial Sediments*, J.D. Collinson and J. Lewin (eds.). International Association of Sedimentologists Special Publication 6, p. 279-286.
- Miall, A.D. 1985. Architectural-element analysis; a new method of facies analysis applied to fluvial deposits. *Earth Science Review*, v. 22, p. 261-308.
- Miall, A.D. 1987. Recent developments in the study of fluvial facies models. *In: Recent Developments in Fluvial Sedimentology*, F.G. Ethridge, R.M. Flores and M.D. Harvey (eds.). Society of Economic Paleontologists and Mineralogists Special Publication 39, p. 1-9.
- Miall, A.D. 1988. Architectural elements and bounding surfaces in fluvial deposits: anatomy of the Kayenta Formation (Lower Jurassic), Southwest Colorado. *Sedimentary Geology*, v. 55, p. 233-262.
- Miall, A.D. and Turner-Peterson, C. 1989. Variations in fluvial style in the Westwater Canyon Member, Morrison Formation (Jurassic), San Juan Basin, Colorado Plateau. *Sedimentary Geology*, v. 63, p. 21-60.
- Middleton, L.T. and Trujillo, A.P. 1984. Sedimentology and depositional setting of the Upper Proterozoic Scanlan Conglomerate, Central Arizona. *In: Sedimentology of Gravels and Conglomerates*, E.H. Koster and R.J. Steel (eds.). Canadian Society of Petroleum Geologists Memoir 10, p. 189-201.

- Miller, K.G., Kent, D.V., Brower, A.N., Bybell, L.M., Feigenson, M.D., Olsson, R.K. and Poore, R.Z. 1990. Eocene-Oligocene sea-level changes on the New Jersey coastal plain linked to the deep-sea record. Geological Society of America Bulletin, v. 102, p. 331-339.
- Mitchell, B.E. 1986. Carbonate concretions in the Boss Point Formation, Cape Maringouin, New Brunswick. B.Sc. (Hons) Thesis, Mount Allison University, 74p.
- Moody-Stuart, M. 1966. High and low-sinuosity stream deposits with examples from the Devonian of Spitsbergen. Journal of Sedimentary Petrology, v. 36, p. 1102-1107.
- Moore, D.G. 1957. The Yoredale Series of Upper Wensleydale and adjacent parts of NW Yorkshire. Proceedings of the Yorkshire Geological Society, v. 31, p. 91-148.
- Morison, S.R. and Hein, F.J. 1987. Sedimentology of the White Channel gravels, Klondike area, Yukon Territory: fluvial deposits of a confined valley. In: Recent Developments in Fluvial Sedimentology, F.G. Etheridge, R.M. Flores and M.D. Harvey (eds.). Society of Economic Paleontologists and Mineralogists Special Publication 39, p. 205-216.
- Mosher, S. 1983. Kinematic history of the Narragansett Basin, Massachusetts and Rhode Island: constraints on late Paleozoic plate reconstructions. Tectonics, v. 2, p. 327-344.
- Mossman, D.J., Macey, J.F. and Lemmon, P.D. 1987. Diagenesis in the lacustrine facies of the Albert Formation, New Brunswick, Canada: a geochemical evaluation. Bulletin of Canadian Petroleum Geology, v. 35, p. 239-250.
- Mount, J.F. and Cohen, A.S. 1984. Petrology and geochemistry of rhizoliths from Plio-Pleistocene fluvial and marginal lacustrine deposits, East Lake Turkana, Kenya. Journal of Sedimentary Petrology, v. 54, p. 263-275.
- Mozley, P.S. 1989. Relation between depositional environment and the elemental composition of early diagenetic siderite. Geology, v. 17, p. 704-706.
- Muto, T. 1988. Stratigraphical patterns of coastal-fan sedimentation adjacent to high-gradient submarine slopes affected by sea-level changes. In: Fan Deltas: Sedimentology and Tectonic Settings, W.Nemec and R.J. Steel (eds.). Blackie and Son, p. 84-90.

- Nadeau, P.H., Wilson, M.J., McHardy, W.J. and Tait, J.M. 1985. The conversion of smectite to illite during diagenesis: evidence from some illitic clays from bentonites and sandstones. *Mineralogical Magazine*, v. 49, p. 393-400.
- Nadon, G.C. and Middleton, G.V. 1985. The stratigraphy and sedimentology of the Fundy Group (Triassic) of the St. Martins area, New Brunswick. *Canadian Journal of Earth Sciences*, v. 22, p. 1183-1203.
- Nance, R.D. 1986. Late Carboniferous tectonostratigraphy in the Avalon Terrane of southern New Brunswick. *Maritime Sediments and Atlantic Geology*, v. 22, p. 308-326.
- Nance, R.D. 1987. Dextral transpression and Late Carboniferous sedimentation in the Fundy coastal zone of southern New Brunswick. *In: Sedimentary Basins and Basin-Forming Mechanisms*, C. Beaumont and A.J. Tankard (eds.). *Canadian Society of Petroleum Geologists Memoir 12*, p. 363-377.
- Nanson, G.C., Young, R.W., Price, D.M. and Rust, B.R. 1988. Stratigraphy, sedimentology and Late-Quaternary chronology of the Channel Country of Western Queensland. *In: Fluvial Geomorphology of Australia*, R.F. Warner (ed.). *Academic Press*. p. 151-175.
- Naylor, H., Turner, P., Vaughan, D.J. and Fallick, A.E. 1989. The Cherty Rock, Elgin: a petrographic and isotopic study of a Permo-Triassic calccrete. *Geological Journal*, v. 24, p. 205-221.
- Nelson, C.S., Kamp, P.J.J. and Mildenhall, D.C. 1989. Late Pliocene distal silicic ignimbrites, Port Waikato, New Zealand: implications for volcanism, tectonics, and sea-level changes in South Auckland. *New Zealand Journal of Geology and Geophysics*, v. 32, p. 357-370.
- Nelson, C.S., Mildenhall, D.C., Todd, A.J. and Pocknall, D.T. 1988. Subsurface stratigraphy, paleoenvironments, palynology, and depositional history of the late Neogene Tauranga Group at Ohinewai, Lower Waikato Lowland, South Auckland, New Zealand. *New Zealand Journal of Geology and Geophysics*, v. 31, p. 21-40.
- Nemec, W. and Steel, R.J. 1984. Alluvial and coastal conglomerates: their significant features and some comments on gravelly mass-flow deposits. *In: Sedimentology of Gravels and Conglomerates*, E.H. Koster and R.J. Steel (Eds.). *Canadian Society of Petroleum Geologists Memoir 10*, p. 1-31.

- Nesbitt, H.W. 1979. Mobility and fractionation of rare earth elements during weathering of a granodiorite. *Nature*, v. 279, p. 206-210.
- Nesbitt, H.W., Markovics, G. and Price, R.C. 1980. Chemical processes affecting alkalis and alkaline earths during continental weathering. *Geochimica Cosmochimica Acta*, v. 44, p. 1659-1666.
- Nesbitt, H.W. and Young, G.M. 1982. Early Proterozoic climates and plate motions inferred from major element chemistry of lutites. *Nature*, v. 299, p. 715-717.
- Nesbitt, H.W. and Young, G.M. 1989. Formation and diagenesis of weathering profiles. *Journal of Geology*, v. 97, p. 129-147.
- Netterberg, F. and Caiger, J.H. 1983. A geotechnical classification of calcretes and other pedocretes. *In: Residual Deposits: Surface Related Weathering Processes and Materials*, R.C.L. Wilson (ed.). Blackwell Scientific Publications, p. 235-243.
- Nettleton, W.D. and Peterson, F.F. 1983. Aridisols. *In: Pedogenesis and Soil Taxonomy II. The Soil Orders*. L.P. Wilding, N.E. Smeck and G.F. Hall (eds.). Elsevier. p. 165-215.
- Norman, G.W.H. 1941. Hillsborough, Albert and Westmoreland counties, New Brunswick. Geological Survey of Canada, Map 646A.
- Norrish, K. and Hutton, J.T. 1969. An accurate X-ray spectrographic method for the analysis of a wide range of geological samples. *Geochimica et Cosmochimica Acta*, v. 33, p. 431-453.
- O'Brien, S.J., Wardle, R.J. and King, A.F. 1983. The Avalon Zone: a Pan-African terrane in the Appalachian Orogen of Canada. *Geological Journal*, v. 18, p. 195-222.
- Olsen, P.E. and Schische, R.W. 1990. Transtensional arm of the early Mesozoic Fundy rift basin: Penecontemporaneous faulting and sedimentation. *Geology*, v. 18, p. 695-698.
- Parkash, B., Awasthi, A.K. and Gohain, K. 1983. Lithofacies of the Markanda terminal fan, Kurukshetra district, Haryana, India. *In: Modern and Ancient Fluvial Systems*, J.D. Collinson and J. Lewin (eds.). International Association of Sedimentologists Special Publication 6, p. 337-344.

- Pe-Piper, G., Cormier, R.F. and Piper, D.J.W. 1989. The age significance of Carboniferous plutons of the western Cobequid Highlands, Nova Scotia. *Canadian Journal of Earth Sciences*, v. 26, p. 1297-1307.
- Picard, M.D. and High, L.R. 1981. Physical stratigraphy of ancient lacustrine deposits. *In: Recent and Ancient Nonmarine Depositional Environments*. F.G. Ethridge and R.M. Flores (eds.). Society of Economic Paleontologists and Mineralogists Special Publication 31, p. 233-259.
- Platt, N.H. 1989a. Climate and tectonic controls on sedimentation of a Mesozoic lacustrine sequence: the Purbeck of the W Cameros Basin, N. Spain. *Palaeogeography, Palaeoclimatology, Palaeoecology*, v. 70, p. 187-197.
- Platt, N.H. 1989b. Lacustrine carbonates and pedogenesis: sedimentology and origin of palustrine deposits from the Early Cretaceous Rupelo Formation, W. Cameros Basin, N. Spain. *Sedimentology*, v. 36, p. 665-684.
- Plint, A.G. 1983. Facies, environments and sedimentary cycles in the Middle Eocene, Bracklesham Formation of the Hampshire Basin: evidence for global sea-level changes? *Sedimentology*, v. 30, p. 625-653.
- Plint, A.G. 1985. Possible earthquake induced soft-sediment faulting and remobilization in Pennsylvanian alluvial strata, southern New Brunswick, Canada. *Canadian Journal of Earth Sciences*, v. 22, p. 907-912.
- Plint, A.G. 1986. Slump blocks, intraformational conglomerates and associated erosional structures in Pennsylvanian fluvial strata of eastern Canada. *Sedimentology*, v. 33, p. 387-399.
- Plint, A.G. 1988. Carboniferous to Triassic fault-styles and sedimentation, southern New Brunswick. Abstract. *Maritime Sediments and Atlantic Geology*, v. 24, p. 208.
- Plint, A.G. 1989. Slump blocks, intraformational conglomerates and associated erosional structures in Pennsylvanian fluvial strata of eastern Canada (reply). *Sedimentology*, v. 36, p. 145-150.
- Plint, A.G. and van de Poll, H.W. 1982. Alluvial fan and piedmont sedimentation in the Tynemouth Creek Formation (Lower Pennsylvanian) of southern New Brunswick. *Maritime Sediments and Atlantic Geology*, v. 18, p. 104-128.
- Plint, A.G. and van de Poll, H.W. 1984. Structural and

sedimentary history of the Quaco Head area, southern New Brunswick. *Canadian Journal of Earth Sciences*, v. 21, p. 753-761.

- Posamentier, H.W., Jervey, M.T. and Vail, P.R. 1988. Eustatic controls on clastic deposition I- conceptual framework. *In: Sea-Level Changes: an Integrated Approach*, C.K. Wilgus, B.S. Hastings, H. Posamentier, J. Van Wagoner, C.A. Ross and C.G.StC. Kendall (eds.). *Society of Economic Paleontologists and Mineralogists Special Publication 42*, p. 109-124.
- Posamentier, H.W. and Vail, P.R. 1988. Eustatic controls on clastic deposition II- sequence and system tract models. *In: Sea-Level Changes: an Integrated Approach*, C.K. Wilgus, B.S. Hastings, H. Posamentier, J. Van Wagoner, C.A. Ross and C.G.StC. Kendall (eds.). *Society of Economic Paleontologists and Mineralogists Special Publication 42*, p. 125-154.
- Prather, B.E. 1985. An Upper Pennsylvanian desert paleosol in the D-zone of the Lansing-Kansas City Groups, Hitchcock County, Nebraska. *Journal of Sedimentary Petrology*, v. 55, p. 213-221.
- Price, W.A. 1925. Caliche and pseudo-anticlines. *American Association of Petroleum Geologists Bulletin*, v. 9, p. 1009-1017.
- Price, W.A. 1933. Reynosa problem of south Texas, and the origin of caliche. *American Association of Petroleum Geologists Bulletin*, v. 17, p. 488-522.
- Ramos, A. and Sopeña, A. 1983. Gravel bars in low-sinuosity streams (Permian and Triassic, central Spain). *In: Modern and Ancient Fluvial Sediments*, J.D. Collinson and J. Lewin (eds.). *International Association of Sedimentologists Special Publication 6*, p. 301-312.
- Rast, N. 1988. Variscan-Alleghanian orogen. *In: Triassic-Jurassic Rifting. Continental Breakup and the Origin of the Atlantic Ocean and Passive Margin Part A*, W. Manspeizer (ed.). *Developments in Geotectonics*. Elsevier, p. 1-27.
- Reeves, C.C. 1970. Origin, classification and geologic history of caliche on the southern High Plains, Texas and eastern New Mexico. *Journal of Geology*, v. 78, p. 352-362.
- Reid, I. and Frostick, L.E. 1986. Flow dynamics and suspended sediment properties in arid zone flash floods. *Hydrological Processes*, v. 3, p. 239-253.

- Retallack, G.J. 1977. Triassic palaeosols in the Upper Narrabeen Group of New South Wales II: classification and reconstruction. *Journal of the Geological Society of Australia*, v. 24, p. 19-36.
- Retallack, G.J. 1981. Fossil soils: indicators of ancient terrestrial environments. In: *Palaeobotany, Palaeoecology and Evolution*, Volume 1, K.J. Niklas (ed.). Praeger Publishers, New York. p. 55-102.
- Retallack, G.J. 1983. A paleopedological approach to the interpretation of terrestrial sedimentary rocks: the mid-Tertiary fossil soils of Badlands National Park, South Dakota. *Geological Society of America Bulletin*, v. 94, p. 823-840.
- Retallack, G.J. 1984. Trace fossils of burrowing beetles and bees in an Oligocene paleosol, Badlands National Park, South Dakota. *Journal of Paleontology*, v. 58, p. 571-592.
- Retallack, G.J. 1985. Fossil soils as grounds for interpreting the advent of large plants and animals on land. *Philosophical Transactions of the Royal Society, London B*, v. 309, p. 105-142.
- Retallack, G.J. 1986. The fossil record of soils. In: *Paleosols Their Recognition and Interpretation*, V.P. Wright (ed.). Princeton University Press, Princeton, N.J., p. 1-57.
- Reyolds, P.H., Elias, P., Muecke, G.K. and Grist, A.M. 1987. Thermal history of the southwestern Meguma Zone, Nova Scotia, from an $^{40}\text{Ar}/^{39}\text{Ar}$ and fission track dating study of intrusive rocks. *Canadian Journal of Earth Sciences*, v. 24, p. 1952-1965.
- Robbin, D.M. and Stipp, J.J. 1979. Depositional rate of laminated soilstone crusts, Florida Keys. *Journal of Sedimentary Petrology*, v. 49, p. 175-180.
- Robinson, D. and Wright, V.P. 1987. Ordered illite/smectite and kaolinite/smectite as possible primary minerals in a Lower Carboniferous paleosol sequence, South Wales? *Clay Minerals*, v. 22, p. 109-118.
- Roliff, R.A. 1962. The Maritimes Carboniferous Basin of eastern Canada. *Geological Association of Canada, Proceedings* 14, p. 21-41.
- Ross, C.A. and Ross, J.P. 1985. Late Paleozoic depositional sequences are synchronous and worldwide. *Geology*, v. 13, p. 1984-197.

- Ross, C.A. and Ross, J.R.P. 1988. Late Paleozoic transgressive deposition. In: Sea Level Changes An Integrated Approach, C. K. Wilgus, B.S. Hastings, H. Posamentier, J. Van Wagoner and C.G. St. C. Kendall (eds.). Society of Economic Paleontologists and Mineralogists Special Publication 42, p. 227-247.
- Roy, R.L. 1977. La position stratigraphique déterminée paleomagnétiquement de sédiments carbonifères de Minudie Point, Nouvelle Ecosse: à propos de l'horizon repère magnétique de carbonifère. Canadian Journal of Earth Sciences, v. 14, p. 1116-1127.
- Roy, R.L. and Morris, W.A. 1983. A review of paleomagnetic results from the Carboniferous of North America: the concept of Carboniferous geomagnetic field horizon markers. Earth and Planetary Science Letters, v. 65, p. 167-181.
- Ruitenbergh, A.A., Giles, P.S., Venugopal, D.V., Buttner, S.M., McCutcheon, S.R. and Chandra, J. 1979. Geology and mineral deposits, Caledonia area. Mineral Resources Branch, New Brunswick Department of Natural Resources, Memoir 1. 213p.
- Rust, B.R. 1972. Structure and process in a braided river. Sedimentology, v. 18, p. 221-245.
- Rust, B.R. 1975. Fabric and structure in glaciofluvial gravels. In: Glaciofluvial and Glaciolacustrine Sedimentation, A.V. Jopling and B.C. McDonald (eds.). Society of Economic Paleontologists and Mineralogists Special Publication 23, p. 238-248.
- Rust, B.R. 1978. Depositional models for braided alluvium. In: Fluvial Sedimentology, A.D. Miall (ed.). Canadian Society of Petroleum Geologists Memoir 5, p. 605-625.
- Rust, B.R. 1981. Alluvial deposits and tectonic style: Devonian and Carboniferous successions in eastern Gaspé. In: Sedimentation and Tectonics in Alluvial Basins, A.D. Miall (ed.). Geological Association of Canada Special Paper 23, p. 49-76.
- Rust, B.R. 1984. Proximal braidplain deposits in the Middle Devonian Malbaie Formation of eastern Gaspé, Quebec, Canada. Sedimentology, v. 31, p. 675-695.
- Rust, B.R. and Gibling, M.R. 1990a. Braidplain evolution in the Pennsylvanian South Bar Formation, Sydney Basin, Nova Scotia, Canada. Journal of Sedimentary Petrology, v. 60, p. 59-72.
- Rust, B.R. and Gibling, M.R. 1990b. Three-dimensional

- antidunes as HCS mimics in a fluvial sandstone: the Pennsylvanian South Bar Formation near Sydney, Nova Scotia. *Journal of Sedimentary Petrology*, v. 60, p. 540-548.
- Rust, B.R., Gibling, M.R., Best, M.A., Dilles, S.J. and Masson, A.G. 1987. A sedimentological overview of the coal-bearing Morien Group (Pennsylvanian), Sydney Basin, Nova Scotia, Canada. *Canadian Journal of Earth Sciences*, v. 24, p. 1869-1885.
- Rust, B.R., Gibling, M.R. and Legun, A.S. 1984. Coal deposition in an anastomosing-fluvial system: the Pennsylvanian Cumberland Group south of Joggins, Nova Scotia, Canada. In: *Sedimentology of Coal and Coal-Bearing Sequences*, R.A. Rahmani and R.M. Flores (eds.). International Association of Sedimentologists Special Publication 7, p. 105-120.
- Rust, B.R. and Jones, B.G. 1987. The Hawkesbury Sandstone south of Sydney, Australia: Triassic analogue for the deposit of a large, braided river. *Journal of Sedimentary Petrology*, v. 57, p. 222-233.
- Rust, B.R. and Koster, E.H. 1984. Coarse alluvial deposits. In: *Facies Models*, R.G. Walker (ed.). Geoscience Canada, Reprint Series 1, p. 53-69.
- Rust, B.R. and Legun, A.S. 1983. Modern anastomosing-fluvial deposits in arid Central Australia, and a Carboniferous analogue in New Brunswick, Canada. In: *Modern and Ancient Fluvial Sediments*, J.D. Collinson and J. Lewin (eds.). International Association of Sedimentologists Special Publication 6, p. 385-392.
- Rust, B.R. and Nanson, G.C. 1989. Bedload transport of mud as pedogenic aggregates in modern and ancient rivers. *Sedimentology*, v. 36, p. 291-306.
- Ryan, R.J. 1984. Upper Carboniferous strata of the east half of the Tatamagouche Syncline, Cumberland Basin, Nova Scotia. In: *Current Research, Part A, Geological Survey of Canada, Paper 84-1A*, p. 473-476.
- Ryan, R.J. and Boehner, R.C. 1989. Cumberland and Pictou Group (Upper Carboniferous to Lower Permian) lithostratigraphic revisions in the Cumberland Basin and regional implications. Nova Scotia Department of Mines and Energy Report 89-3, p. 95-103.
- Ryan, R.J., Boehner, R.C., Calder, J. and Dolby, G. 1990. New palynological age dates, zonations, and stratigraphy in the Permo-Carboniferous strata of the Cumberland Basin, Nova Scotia. *Atlantic Geoscience*

- Society 1990 Symposium and Colloquium. Abstracts. p. 29.
- Ryan, R.J., Boehner, R.C., Deal, A. and Calder, J.H. in prep. Amherst, Springhill and Parrsboro Cumberland County. Cumberland Basin Geology Map. Nova Scotia Department of Mines and Energy, Halifax, Nova Scotia.
- Ryan, R.J., Calder, J., Donohoe, H.V. and Naylor, R. 1987. Late Paleozoic sedimentation and basin development adjacent to the Cobeguid Highlands massif, eastern Canada. In: Sedimentary Basins and Basin-Forming Mechanisms, C. Beaumont and A.J. Tankard (eds.). Canadian Society of Petroleum Geologists Memoir 12, p. 311-317.
- Salomons, W., Goudie, A.S. and Mook, W.G. 1978. Isotopic composition of calcrete deposits from Europe, Africa and India. Earth Surface Processes, v. 3, p. 43-57.
- Saunders, W.B. and Ramsbottom, W.H.C. 1986. The mid-Carboniferous eustatic event. Geology, v. 14, p. 208-212.
- Sawyer, E.W. 1986. The influence of source rock type, chemical weathering and sorting on the geochemistry of clastic sediments from the Quetico Metasedimentary Belt, Superior Province, Canada. Chemical Geology, v. 55, p. 77-95.
- Schäfer, A. and Sneh, A. 1983. Lower Rotliegend fluvio-lacustrine sequences in the Soar-Nahe Basin. Geologische Rundschau, v. 72, p. 1135-1146.
- Schenk, P.E. 1971. Southeastern Atlantic Canada, northwestern Africa, and continental drift. Canadian Journal of Earth Sciences, v. 8, p. 1218-1251.
- Schenk, P.E. 1978. Synthesis of the Canadian Appalachians. Caledonian-Appalachian Orogen of the North Atlantic Region. Geological Survey of Canada, Paper 78-13, p. 111-136.
- Schenk, P.E. 1981. The Meguma Zone of Nova Scotia—a remnant of western Europe, South America or Africa. In: Geology of the North Atlantic Borderlands, J. Wnkerr, A.J. Fergusson and L.C. Machan (eds.). Canadian Society of Petroleum Geologists Memoir 7, p. 119-148.
- Schmeisser, B.M. 1981. A narrative and structural history of Fort Cumberland 1755-1768. Parks Canada Monograph.
- Schumm, S.A. 1963. Sinuosity of alluvial rivers on the

- Great Plains. Geological Society of America Bulletin, v. 74, p. 1089-1100.
- Scotese, C.R., van der Voo, R., Johnson, R.E. and Giles, P.S. 1983. Paleomagnetic results from the Carboniferous of Nova Scotia. American Geophysical Union Geodynamic Series 12, p. 63-81.
- Searl, A. 1989. Pedogenic columnar calcite from the Oolite Group (Lower Carboniferous), South Wales. Sedimentary Geology, v. 62, p. 47-58.
- Semeniuk, V. and Meagher, T.D. 1981. Calcrete in Quaternary coastal dunes in southwestern Australia: a capillary-rise phenomenon associated with plants. Journal of Sedimentary Petrology, v. 51, p. 47-68.
- Semeniuk, V. and Searle, D.J. 1985. Distribution of calcrete in Holocene coastal sands in relationship to climate, Southwestern Australia. Journal of Sedimentary Petrology, v. 55, p. 86-95.
- Singer, A. 1988. Illite in arid soils, desert dust, and desert loess. Sedimentary Geology, v. 59, p. 251-259.
- Skehan, J.W., Murray, D.P., Hepburn, J.C., Billings, M.P., Lyons, P.C. and Doyle, R.G. 1979. The Mississippian and Pennsylvanian (Carboniferous) Systems in the United States - Massachusetts, Rhode Island and Maine. United States Geological Survey Professional Paper 1110-A.
- Smith, D.G. 1973. Aggradation of the Alexandra-North Saskatchewan River, Banff Park, Alberta. In: Fluvial Geomorphology, M. Morisawa (ed.). State University of New York, 4th Annual Symposium on Geomorphology, Binghamton, New York, p. 201-219.
- Smith, N.D. 1974. Sedimentology and bar formation in the upper Kicking Horse River, a braided outwash stream. Journal of Geology, v. 82, p. 205-223.
- Smith, N.D., Cross, T.A., Dufficy, J.P. and Clough, S.R. 1989. Anatomy of an avulsion. Sedimentology, v. 36, p. 1-23.
- Smith, W.D. and Gibling, M.R. 1987. Oil shale composition related to depositional setting: case study from the Albert Formation, New Brunswick, Canada. Bulletin of Canadian Petroleum Geology, v. 35, p. 469-487.
- Sneck, D.A. and Nance, R.D. 1988. Dextral transpression and Late Carboniferous deformation at Musquash Harbour, Southern New Brunswick. Abstract. Central Canada Geological Conference. University of Western Ontario,

- London, Ontario. p. 54.
- Sneed, E.D. and Folk, R.L. 1958. Pebbles in the lower Colorado River Texas: a study in particle morphogenesis. *Journal of Geology*, v. 66, p. 114-150.
- Sopher, C.D. and Baird, J.V. 1982. *Soils and Soil Management*. Reston Publishing Co., Reston, Virginia. 238p.
- Stalder, P.J. 1975. Cementation of Pliocene-Quaternary fluvial clastic deposits in and along the Oman Mountains. *Geologische en Mijnbouw*, v. 54, p. 148-156.
- Stanley, D.J., Krinitzsky, E.L. and Compton, J.R. 1966. Mississippi river bank failure, Fort Jackson, Louisiana. *Geological Society of America Bulletin*, v. 77, p. 859-866.
- Starkey, J. 1977. The contouring of orientation data represented in spherical projection. *Canadian Journal of Earth Sciences*, v. 14, p. 268-277.
- Staub, J.R. and Cohen, A.D. 1978. Kaolinite-enrichment beneath coals; a modern analog, Snuggedy Swamp, South Carolina. *Journal of Sedimentary Petrology*, v. 48, p. 203-210.
- Steel, R.J. 1974. Cornstone (fossil caliche)-its origin, stratigraphic and sedimentological importance in the New Red Sandstone, western Scotland. *Journal of Geology*, v. 82, p. 351-369.
- Steel, R.J. and Thompson, D.B. 1983. Structures and textures in Triassic braided stream conglomerates ('Bunter' Pebble Beds) in the Sherwood Sandstone Group, North Staffordshire, England. *Sedimentology*, v. 30, p. 341-367.
- Summerhayes, C.P. 1986. Sealevel curves based on seismic stratigraphy: their chronostratigraphic significance. *Palaeogeography, Palaeoclimatology, Palaeoecology*, v. 57, p. 27-42.
- Sylvester, A.G. 1988. Strike-slip faults. *Geological Society of America Bulletin*, v. 100, p. 1666-1703.
- Ten Brink, U.S. and Ben-Avraham, Z. 1989. The anatomy of a pull-apart basin: seismic reflection observations of the Dead Sea Basin. *Tectonics*, v. 8, p. 333-350.
- Thomas, R.G., Smith, D.G., Wood, J.M., Visser, J., Calverley-Range, E.A. and Koster, E.H. 1987. Inclined heterolithic stratification-terminology, description

- and significance. *Sedimentary Geology*, v. 53, p. 123-179.
- Tissot, B.P. and Welte, D.H. 1978. *Petroleum Formation and Occurrence*. Springer-Verlag. 538p.
- Tresse, K.L. and Wilkinson, B.H. 1982. Peat-marl deposition in a Holocene paludal-lacustrine basin-Sucker Lake, Michigan. *Sedimentology*, v. 29, p. 375-390.
- Tucker, M.E. 1981. *Sedimentary Petrology. An Introduction*. Blackwell Scientific Publications. 252p.
- Tye, R.S. and Coleman, J.M. 1989. Depositional processes and stratigraphy of fluviially dominated lacustrine deltas: Mississippi delta plain. *Journal of Sedimentary Petrology*, v. 59, p. 973-996.
- van de Poll, H.W. 1966. Sedimentation and paleocurrents during Pennsylvanian time in the Moncton Basin, New Brunswick. New Brunswick Department of Natural Resources Report, Investigation 1, 33p.
- van de Poll, H.W. 1970. Stratigraphical and sedimentological aspects of Pennsylvanian strata in southern New Brunswick. Unpublished Ph.D. Thesis, University College of Swansea, University of Wales, Swansea. 140p.
- van de Poll, H.W. 1972a. Stratigraphy and economic geology of Carboniferous basins in the Maritime Provinces, Field Excursion A60. 24th International Geological Congress, Montreal. 96p.
- van de Poll, H.W. 1972b. Geological map of New Brunswick (unpublished). Mineral Resources Branch, New Brunswick Department of Mines.
- van de Poll, H.W. 1983. The Upper Carboniferous Clifton Formation of northern New Brunswick: coal-bearing deposits of a semi-arid alluvial plain: Discussion. *Canadian Journal of Earth Sciences*, v. 20, p. 1212-1215.
- van de Poll, H.W. 1989. Lithostratigraphy of the Prince Edward Island redbeds. *Atlantic Geology*, v. 25, p. 23-35.
- van de Poll, H.W. and Patel, I.M. 1981. Flute casts and related structures on moulded silt injection surfaces in continental sandstone of the Boss Point Formation: southeastern New Brunswick, Canada. *Maritime Sediments and Atlantic Geology*, v. 17, p. 1-22.

- van de Poll, H.W. and Patel, I.M. 1989. Slump blocks, intraformational conglomerates and associated erosional structures in Pennsylvanian fluvial strata of eastern Canada (Discussion). *Sedimentology*, v. 36, p. 137-145.
- van de Poll, H.W. and Patel, I.M. 1990. An ornamented mudstone cavity, Boss Point Formation, Sackville, New Brunswick, Canada: evidence for mud intrusion and rheoplasis. *Sedimentology*, v. 37, p. 931-942.
- van der Voo, R., French, A.N. and French, R.B. 1979. A paleomagnetic pole position from the Upper Devonian Catskill red beds and its tectonic implications. *Geology*, v. 7, p. 345-348.
- Van Dijk, D.E., Hobday, D.K. and Tankard, A.J. 1978. Permo-Triassic lacustrine deposits in the eastern Karoo Basin, South Africa. In: *Modern and Ancient Lake Sediments*, A. Matter and M.E. Tucker (eds.). International Association of Sedimentologists Special Publication 2, p. 225-239.
- Van Houten, F.B. 1981. The odyssey of molasse. In: *Sedimentation and Tectonics in Alluvial Basins*, A.D. Miall (ed.). Geological Association of Canada Special Paper 23, p. 35-48.
- Van Wagoner, J.C., Posamentier, H., Mitchum, R.M., Vail, P.R., Sarg, J.F., Loutit, T.S. and Hardenbol, J. 1988. An overview of the fundamentals of sequence stratigraphy and key definitions. In: *Sea-Level Changes: An Integrated Approach*, C.K. Wilgus, B.S. Hastings, H. Posamentier, J. Van Wagoner, C.A. Ross and C.G. St. C. Kendall (eds.). Society of Economic Paleontologists and Mineralogists Special Publication 42, p. 39-45.
- Veevers, J.J. and Powell, C.McA. 1987. Late Paleozoic glacial episodes in Gondwanaland reflected in transgressive-regressive depositional sequences in Euramerica. *Geological Society of America Bulletin*, v. 98, p. 475-487.
- Waldron, J.W.F., Piper, D.J.W. and Pe-Piper, G. 1989. Deformation of the Cape Chignecto Pluton, Cobequid Highlands, Nova Scotia: thrusting at the Meguma-Avalon boundary. *Atlantic Geology*, v. 25, p. 51-62.
- Walker, J.C.G. and Zahnle, K.J. 1986. Lunar nodal tide and distance to the Moon during the Precambrian. *Nature*, v. 320, p. 600-602.
- Walker, R.G. and Cant, D.J. 1984. Sandy fluvial systems. In: R.G. Walker (ed.). *Facies Models*. 2nd Ed. Geoscience Canada, Reprint Series 1, p. 71-89.

- Walker, R.G., Duke, W.L. and Leckie, D.A. 1983. Discussion of "Hummocky stratification: significance and its variable bedding sequences". Geological Society of America Bulletin, v. 94, p. 1245-1249.
- Walls, R.A., Harris, W.B. and Nunan, W.E. 1975. Calcareous crust (caliche) profiles and early subaerial exposure of Carboniferous carbonates, northeastern Kentucky. Sedimentology, v. 22, p. 417-440.
- Wanless, H.R. and Shepard, F.P. 1936. Sea level and climatic changes related to late Paleozoic cycles. Geological Society of America Bulletin, v. 47, p. 1177-1206.
- Warren, J.K. 1983. Pedogenic calcrete as it occurs in Quaternary calcareous dunes in coastal South Australia. Journal of Sedimentary Petrology, v. 53, p. 787-796.
- Watts, N.L. 1980. Quaternary pedogenic calcretes from the Kalahari (southern Africa): mineralogy, genesis and diagenesis. Sedimentology, v. 27, p. 661-686.
- Webb, G.W. 1963. Occurrence and exploration significance of strike-slip faults in southern New Brunswick, Canada. American Association of Petroleum Geologists Bulletin, v. 47, p. 1904-1927.
- Weirich, F. 1986. The record of density-induced underflows in a glacial lake. Sedimentology, v. 33, p. 261-277.
- Williams, E.G., Guber, A.L. and Johnson, A. 1965. Rotational slumping and disconformities. Journal of Geology, v. 73, p. 534-547.
- Williams, E.P. 1974. Geology and petroleum possibilities in and around Gulf of St. Lawrence. American Association of Petroleum Geologists Bulletin, v. 58, p. 1137-1155.
- Williams, H. 1979. Appalachian Orogen in Canada. Canadian Journal of Earth Sciences, v. 16, p. 792-807.
- Williams, H. 1980. Tectonic Lithofacies Map of the Appalachian Orogen. International Geological Correlation Program, Project No. 27. The Appalachian-Caledonides Orogen. Scale 1:1 000 000. Memorial University of Newfoundland.
- Williams, H., Colman-Sadd, S.P. and Swinden, H.S. 1988. Tectonic-stratigraphic subdivisions of central Newfoundland. In: Current Research, Part B, Geological Survey of Canada, Paper 88-1B, p. 91-98.

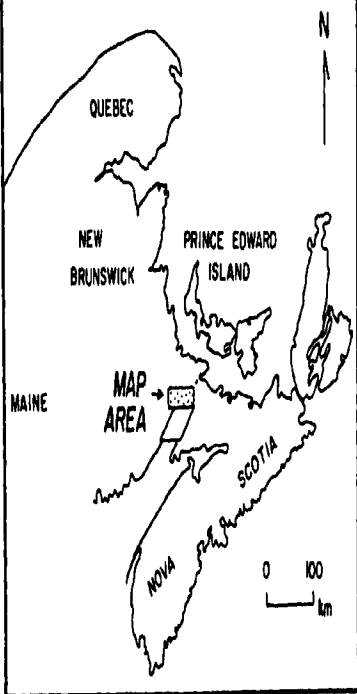
- Williams, H. and Hatcher, R.D. 1982. Suspect terranes and accretionary history of the Appalachian orogen. *Geology*, v. 10, p. 530-536.
- Wright, V.P. 1982. Calcrete paleosols from the Lower Carboniferous Llanelly Formation, South Wales. *Sedimentary Geology*, v. 33, p. 1-33.
- Wright, V.P. 1990a. Equatorial aridity and climatic oscillations during the early Carboniferous, southern Britain. *Journal of the Geological Society, London*, v. 147, p. 359-363.
- Wright, V.P. 1990b. Estimating rates of calcrete formation and sediment accretion in ancient alluvial deposits. *Geological Magazine*, v. 127, p. 273-276.
- Wright, W.J. 1922. Geology of the Moncton Map-Area. *Geological Survey of Canada Memoir* 129.
- Wright, W.J. 1950. Dorchester copper deposit. Assessment Files, Mineral Resources Branch, Department of Natural Resources, Sussex, New Brunswick.
- Wu, T-W. 1984. Geochemistry and Petrogenesis of some Granitoids in the Grenville Province of Ontario and their Tectonic Implications. Unpublished Ph.D. Thesis, University of Western Ontario. 2 Volumes. 622p.
- Yaalon, D.H. and Kalmar, D. 1978. Dynamics of cracking and swelling clay soils: displacement of skeletal grains, optimum depth of slickensides, and rate of intrapedonic turbation. *Earth Surface Processes*, v. 3, p. 31-42.
- Yeo, G.M. 1985. Upper Carboniferous sedimentation in northern Nova Scotia and the origin of Stellarton Basin. *In: Current Research, Part B, Geological Survey of Canada, Paper* 85-1B, p. 511-518.
- Yeo, G.M. and Ruixing, G. 1986. Late Carboniferous dextral movement on the Cobequid-Hollow Fault system, Nova Scotia: evidence and implications. *In: Current Research, Part A, Geological Survey of Canada, Paper* 86-1A, p. 399-410.
- Yeo, G.M. and Ruixiang, G. 1987. Stellarton Graben: an Upper Carboniferous pull-apart basin in northern Nova Scotia. *In: Sedimentary Basins and Basin-Forming Mechanisms*, C. Beaumont and A.J. Tankard (eds.). *Canadian Society of Petroleum Geologists Memoir* 12, p. 299-309.
- Zaitlin, B.A. and Rust, B.R. 1983. A spectrum of alluvial

deposits in the Lower Carboniferous Bonaventure Formation of western Chaleur Bay area, Gaspé and New Brunswick. Canadian Journal of Earth Sciences, v. 20, p. 1098-1110.

Zhang, P., Burchfiel, B.C., Chen, S. and Deng, Q. 1989. Extinction of pull-apart basins. Geology, v. 17, p. 814-817.

Zietz, I., Haworth, R.T., Williams, H. and Daniel, D.L. 1980. Magnetic Anomaly Map of the Appalachians. International Geological Correlation Program Project No. 27. The Appalchian-Caledonides Orogen. Scale 1:1 000 000. Memorial University of Newfoundland.

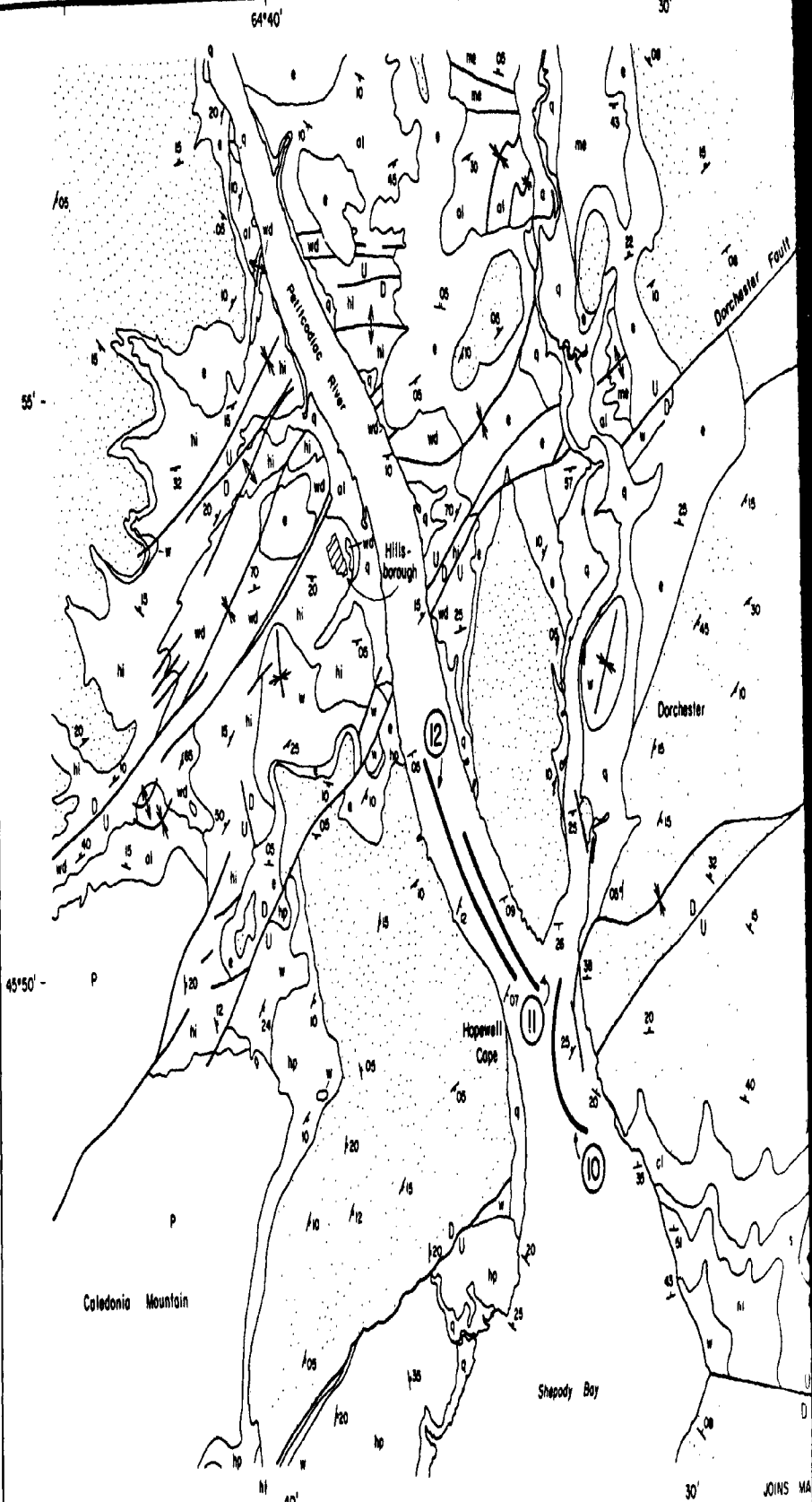
LOCALITY MAP



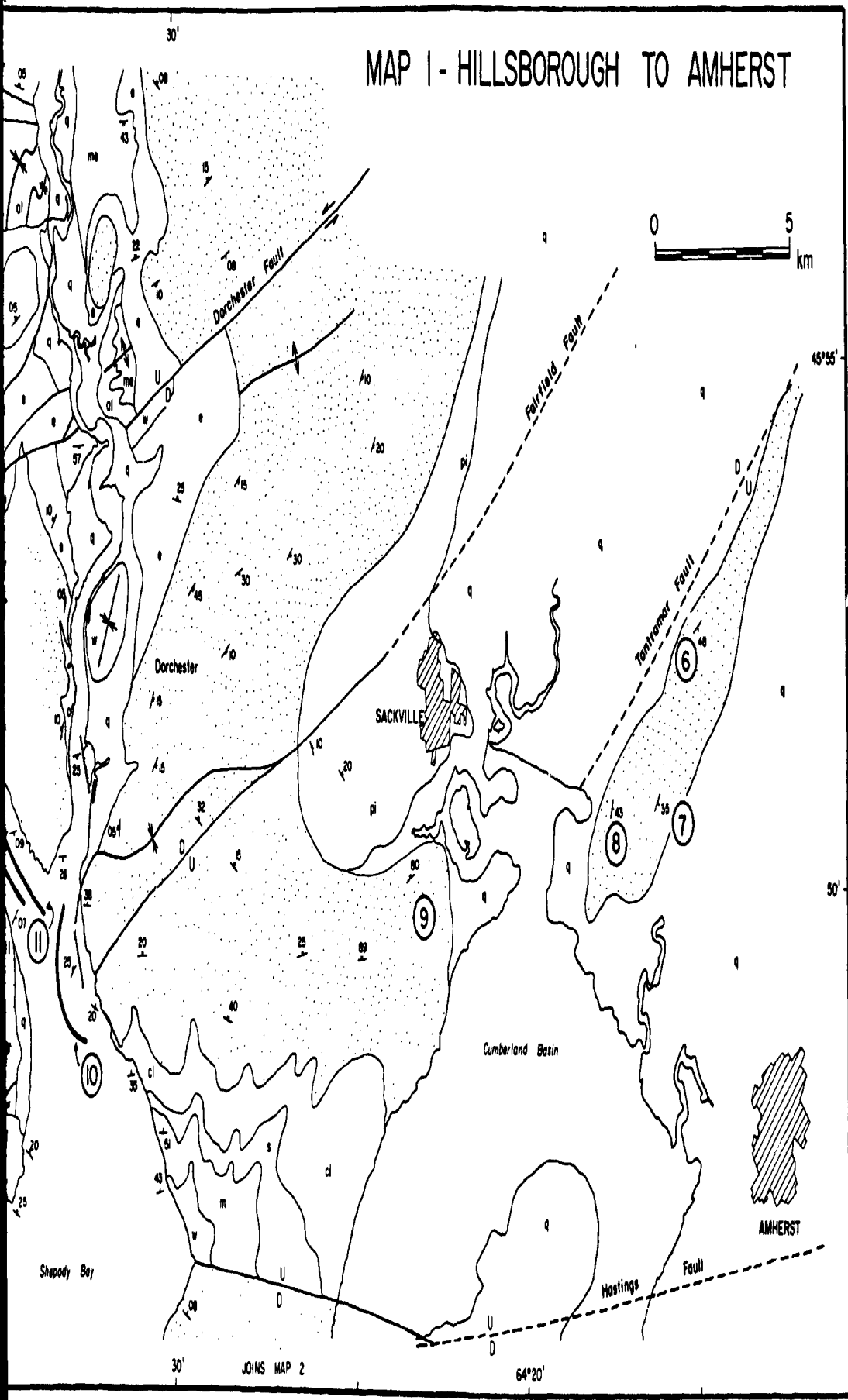
LEGEND

Quaternary	q	Undifferentiated sand, silt & peat
Permo-Carbonif.	pl	Pictou Group
	BOSS POINT FORMATION	
	e	Enrage Formation
Pennsylvanian	cl	Claremont Formation
	hp	Hopewell Group
	s	Shepody Formation
	m	Moringovin Formation
Mississippian	w	Windsor Group
	hi	Hillsborough Formation
	wd	Weldon Formation
	al	Albert Formation
	me	Memramcook Formation
	p	Undifferentiated Precambrian-Early Paleozoic basement (for details see Ruitenberg et al. 1975)

bedding altitude (this study)	bedding altitude (from previous workers)
anticline	syncline
fault (displacement shown)	fault (lateral movement shown)
contact	inferred continuity of structure
stratigraphic section	



MAP 1 - HILLSBOROUGH TO AMHERST

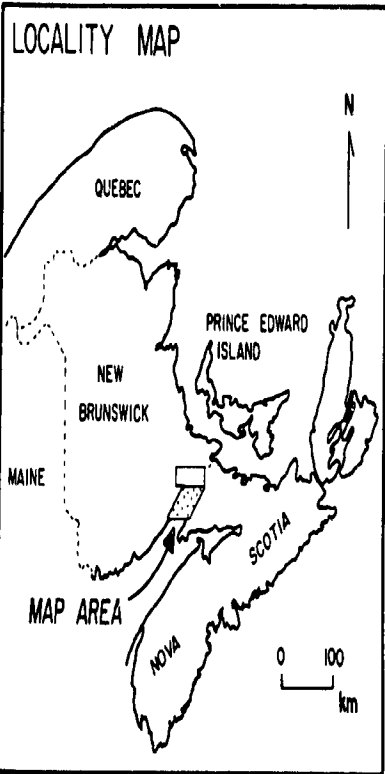


MAP 2 - ALMA TO BOSS POINT

50°

40°

JOINS MAP 1



Precambrian - Early Paleozoic
basement

RIVERSIDE-ALBERT

Cape Moringuin

CHIGNECTO BAY

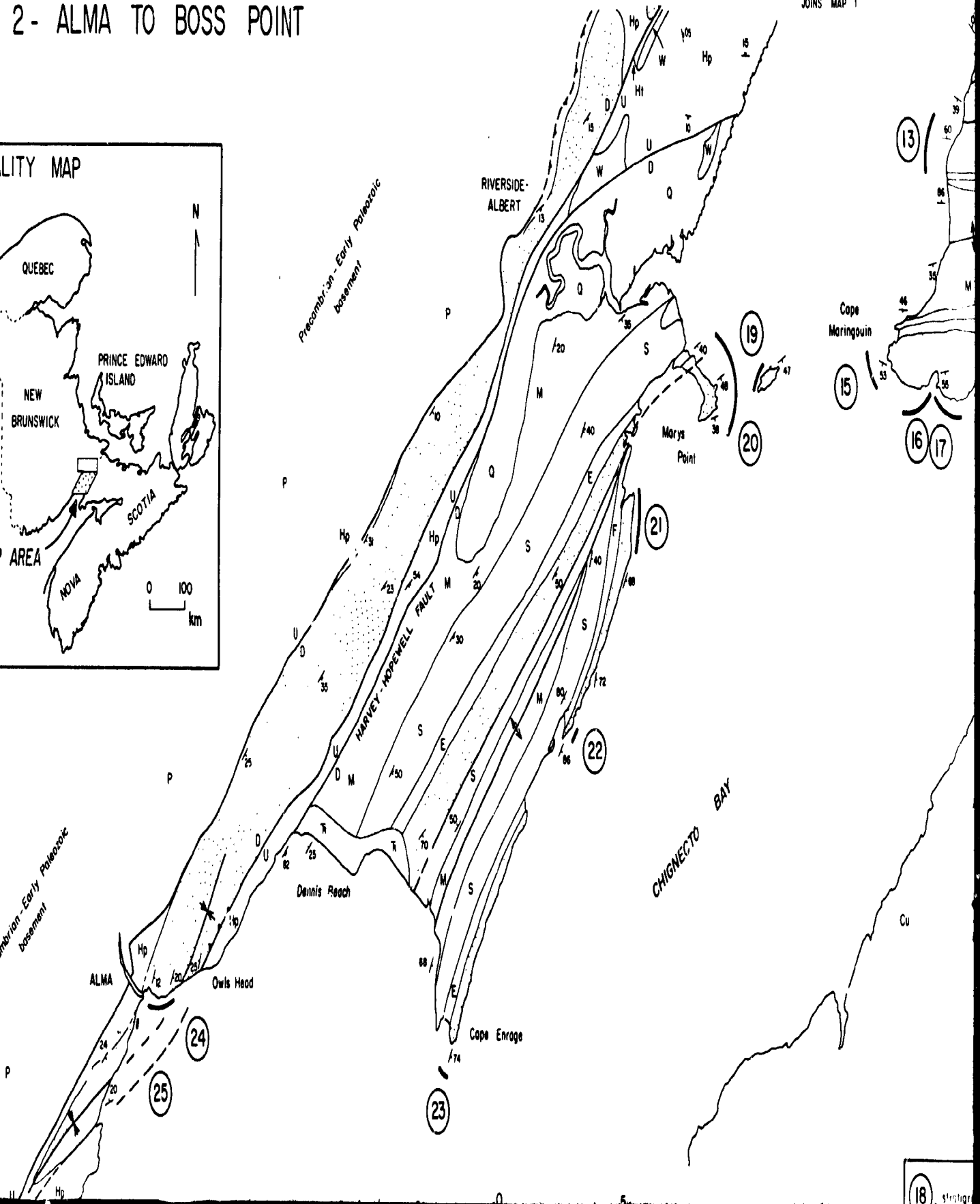
Dennis Beach

ALMA

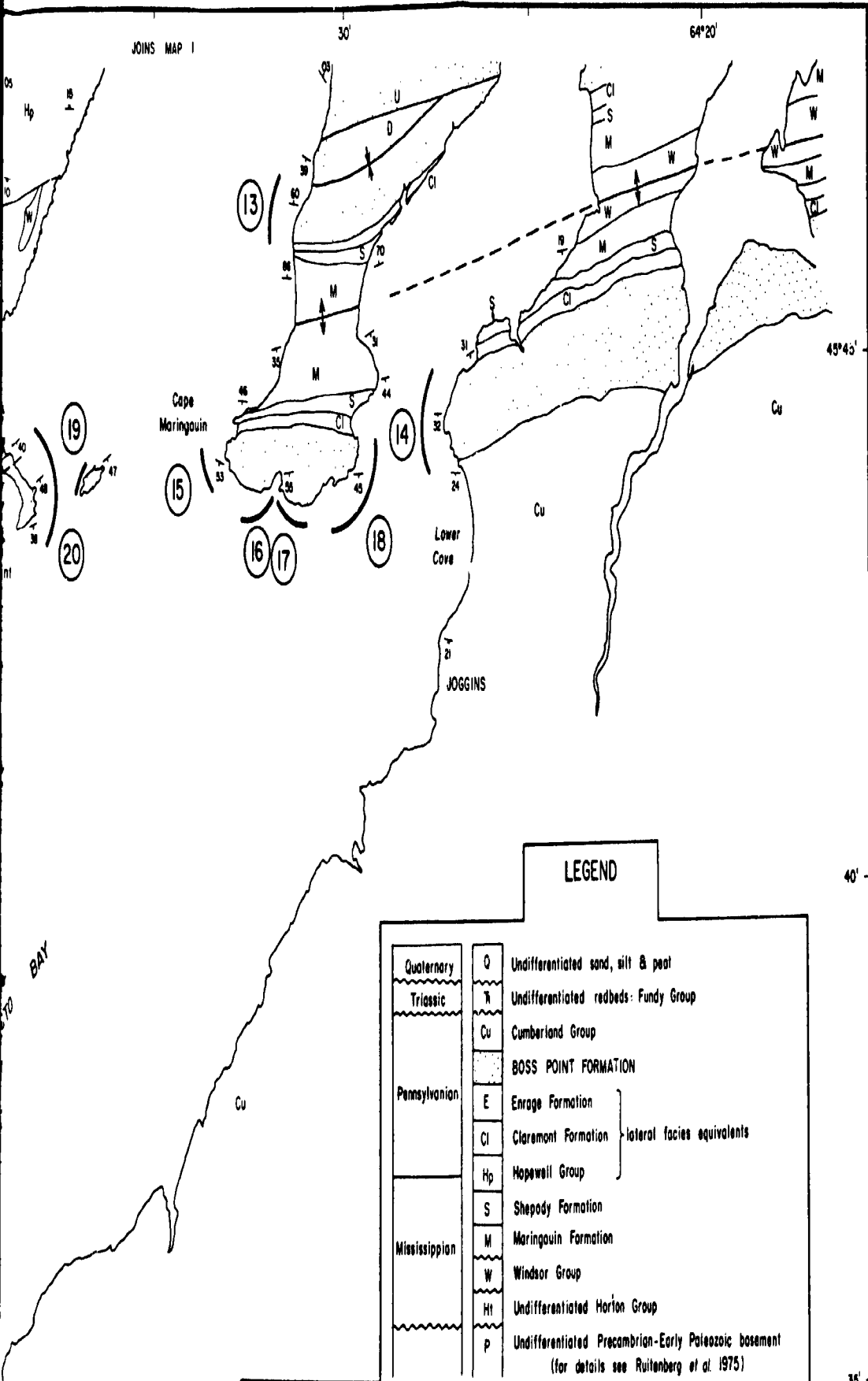
Owls Head

Cape Enrage

45° 35'



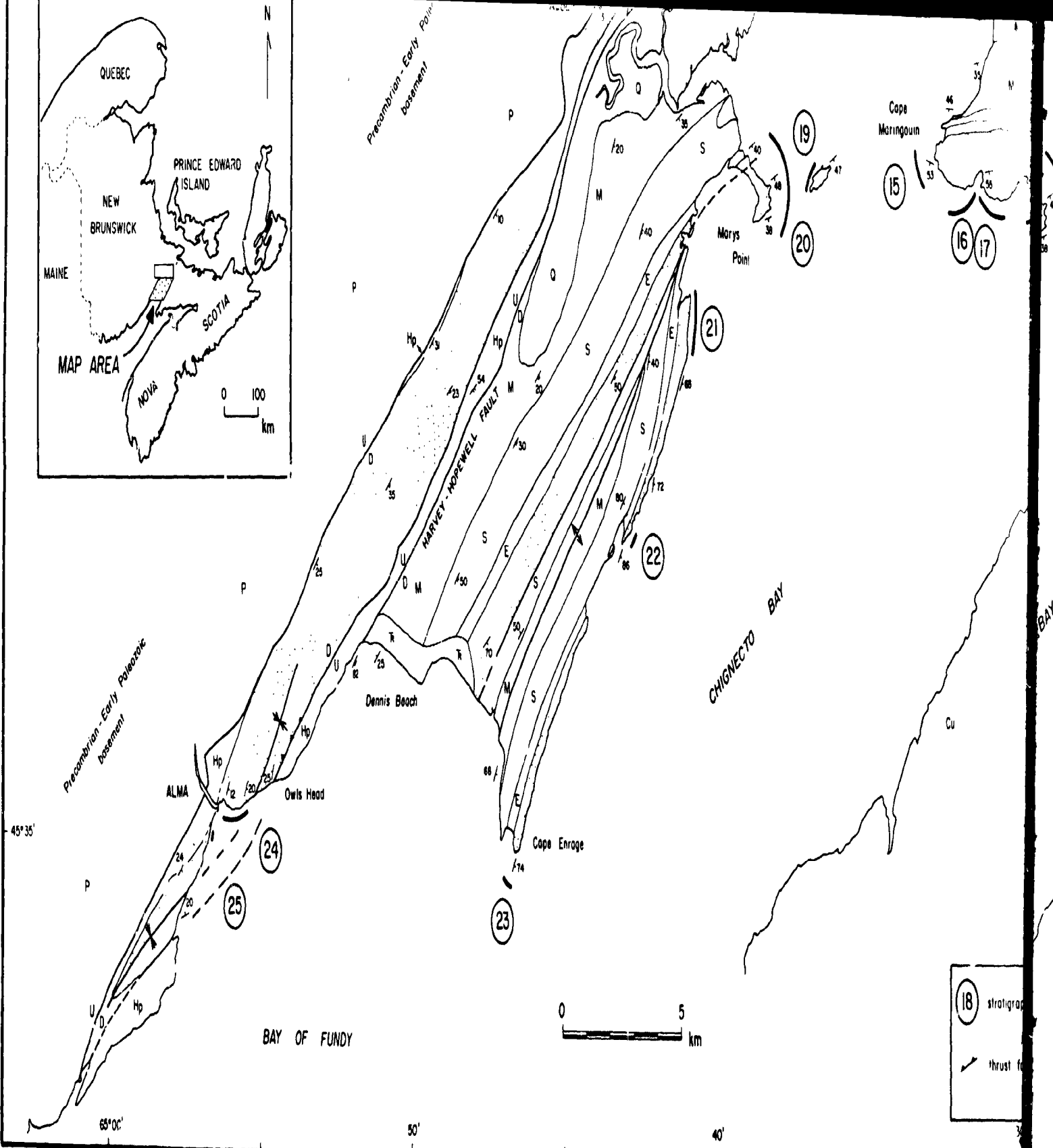
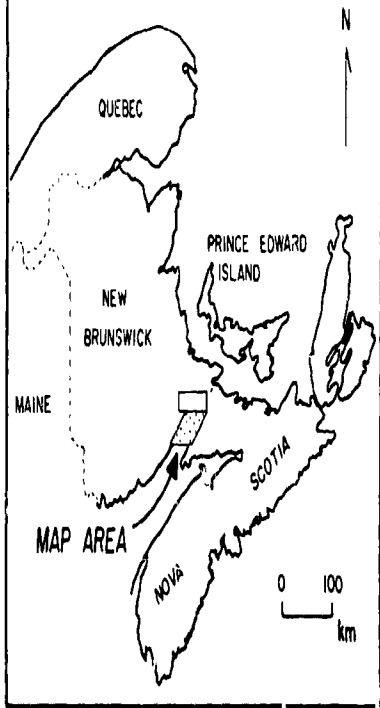
18



LEGEND

Quaternary	O	Undifferentiated sand, silt & peat
Triassic	N	Undifferentiated redbeds: Fundy Group
	Cu	Cumberland Group
		BOSS POINT FORMATION
Pennsylvanian	E	Enrage Formation
	Cl	Claremont Formation
	Hp	Hopewell Group
		} lateral facies equivalents
Mississippian	S	Shepody Formation
	M	Moringuin Formation
	W	Windsor Group
	H	Undifferentiated Horton Group
	P	Undifferentiated Precambrian-Early Paleozoic basement (for details see Ruitenberg <i>et al.</i> 1975)

(18) stratigraphic section ↗ bedding attitude (this study) ↘ bedding attitude (from previous workers)
 ▲ anticline ▼ syncline



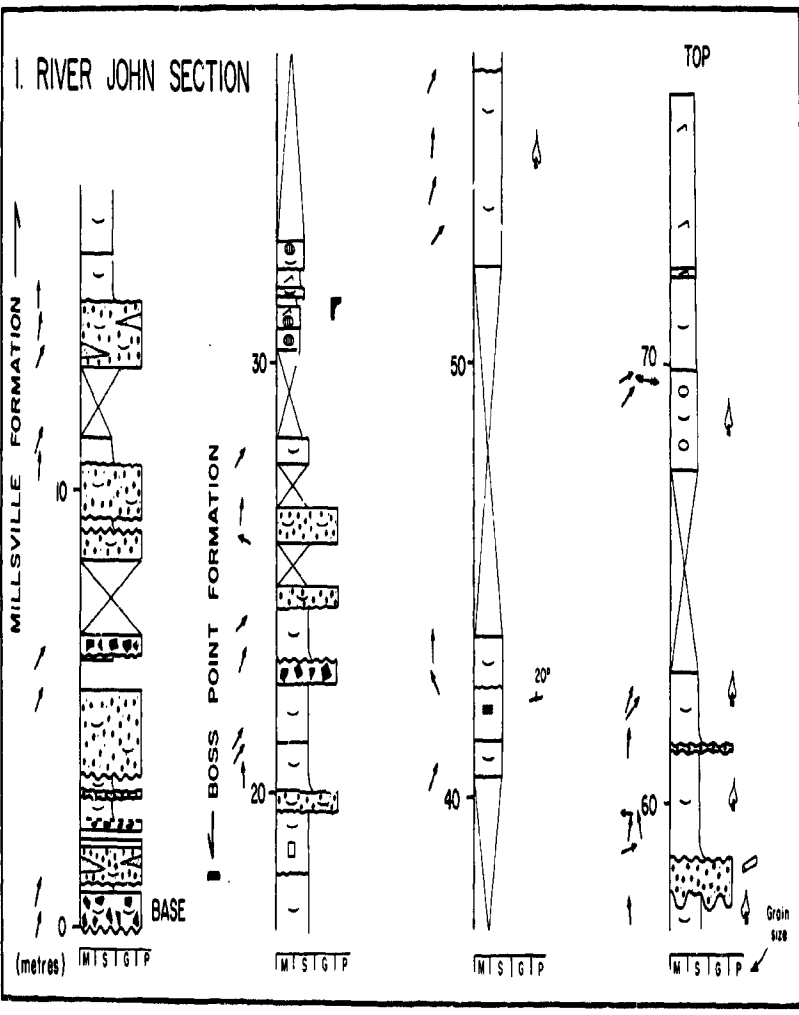
LEGEND

	trough cross-bedded sandstone		water expulsion structure		coarsening upward cycle
	planar cross-bedded sandstone		vertical calcareous tube (rhizolith)		finning upward cycle
	parallel laminated sandstone		adhesion ripple		shear zone
	current ripple laminated sandstone		antidune		slickensides
	wave ripple laminated sandstone		hummocky cross-stratification		tectonically deformed
	climbing ripple laminated sandstone		rill		interval not exposed
	massive sandstone		runzel mark		paleocurrent from cross-bedding
	pebbly sandstone		flute		paleocurrent from rib & furrow
	conglomerate		load cast		paleocurrent from current ripple
	breccia		gutter cast		paleocurrent from climbing ripple
	blue-grey mudrock		sole mark		paleocurrent from flute
	reddish mudrock		linear groove		paleocurrent from parting lineation
	siltstone blocks		obstacle/brush mark		paleocurrent from inclined heterolithic stratification
	inclined heterolithic stratification		convolute bedding		orientation of wave ripple crest
	coal		flame structure		orientation of rill
	coaly units		sandstone dyke		orientation of channel
	limestone		cone-in-cone		orientation of pebble long axis
	ball and pillow		polygon		massive bedding
	siltstone clast		calcareous concretion		fairly stratified
	siltstone clast with flute		calcrete nodule		well stratified
	outer margin		siderite nodule		bedding altitude
	irregular contact		pyrite		fault attitude
	conformable contact		ostracods		vein
	log debris		molluscs, bivalves & gastropods		sandstone dyke
	comminuted carbonaceous debris		fish scales		
	root horizon		bulbous structure		
	in situ tree		normal grading		
	paleosol		pseudoanticline		
	mudcrack		major erosion surface		
	orientation of logs		orientation of pebble long axes		

M mudrock
 S sandstone
 G granite
 P pebble

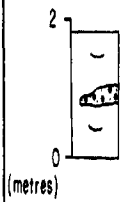
Grain size

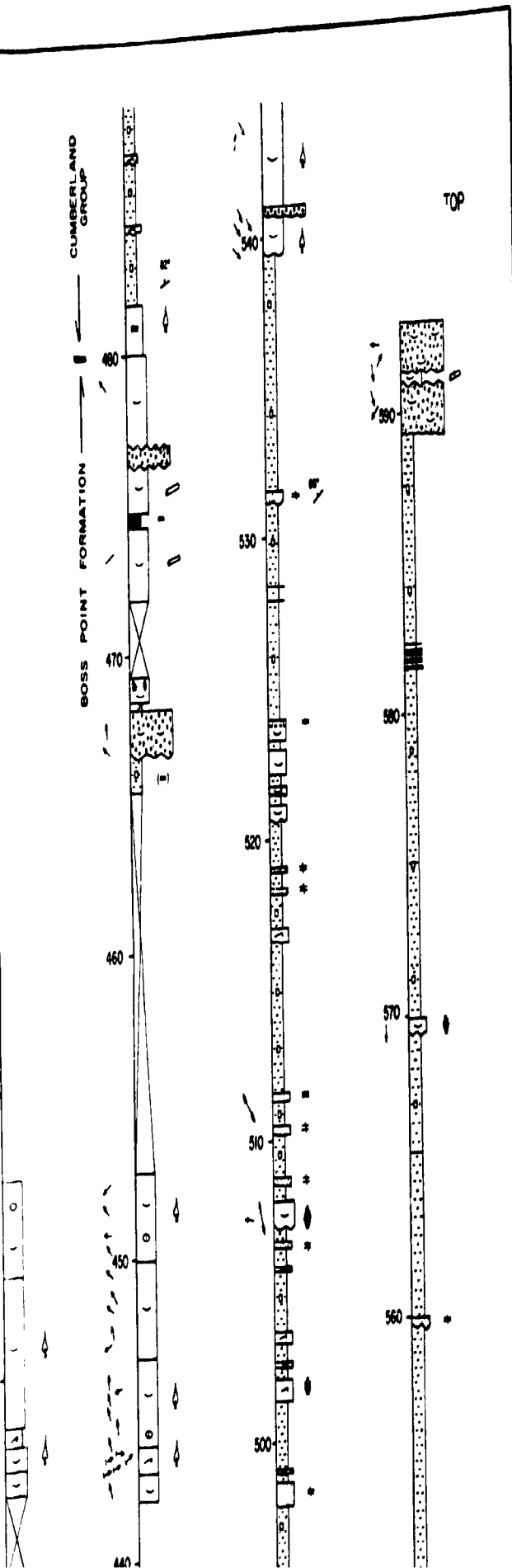
Stratigraphic Section 1
River John

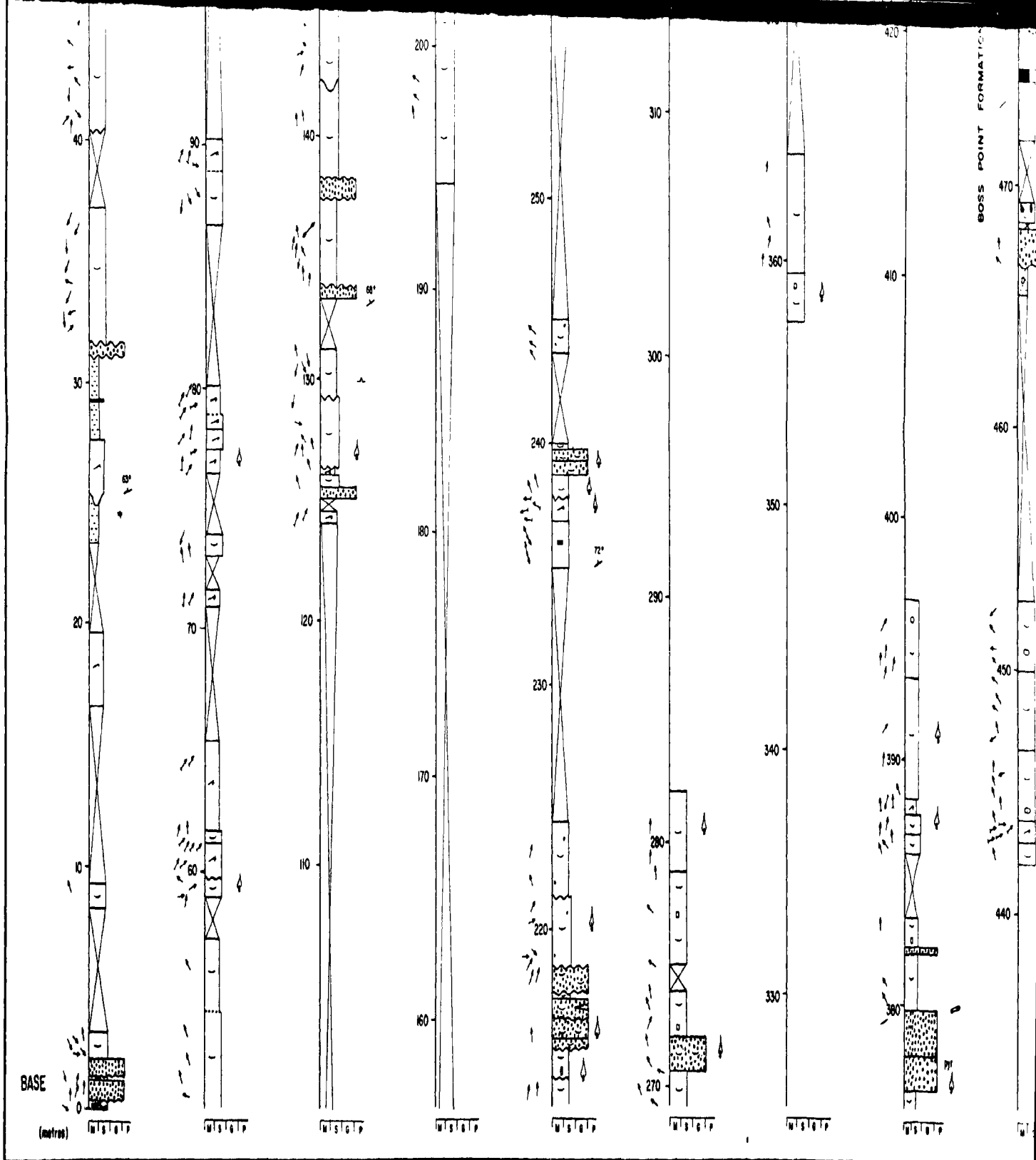


Stratigraphic Section 2
Malagash

RAILWAY TUNNEL, WENTWORTH





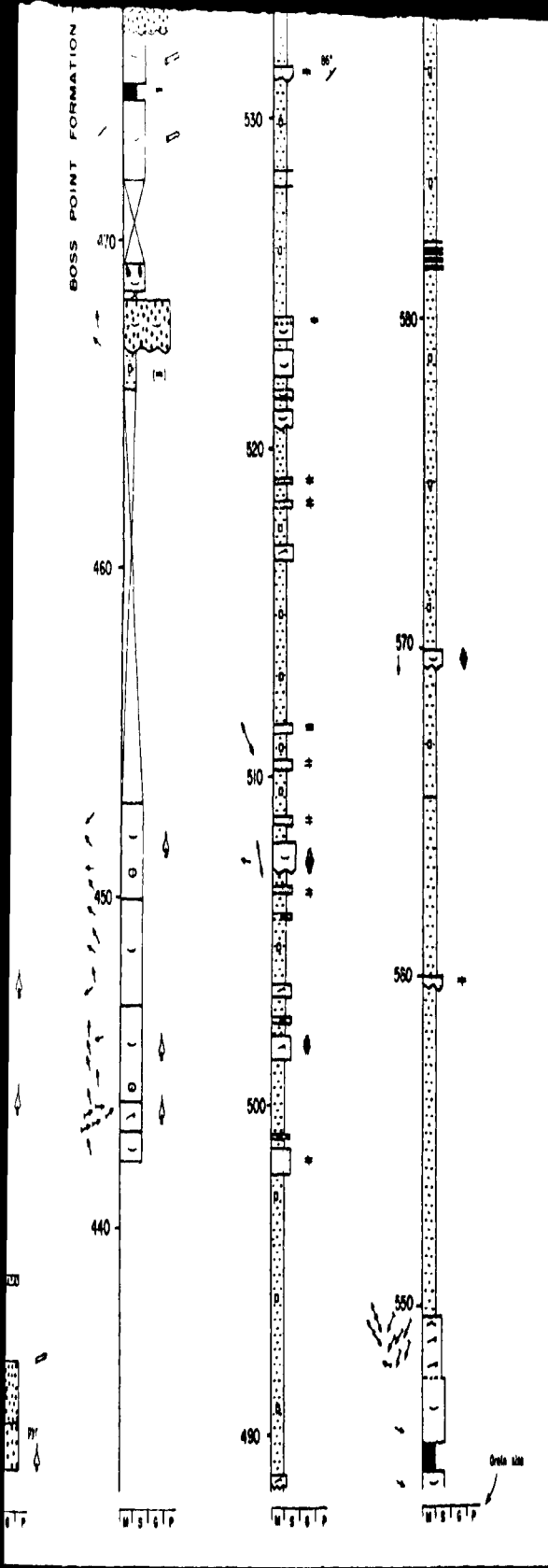


BASE

(metres)

BOSS POINT FORMATION

BOSS POINT FORMATION

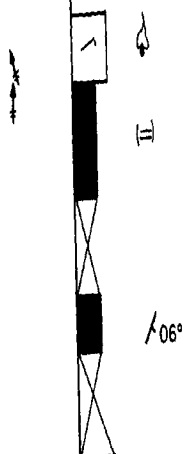


Stratigraphic Section 3
Wallace Quarry

3. WALLACE QUARRY

TOP

20



06°

10

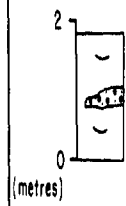
BASE

(metres) M S T G P

Grain size

Stratigraphic Section 4
Wentworth

RAILWAY TUNNEL, WENTWORTH



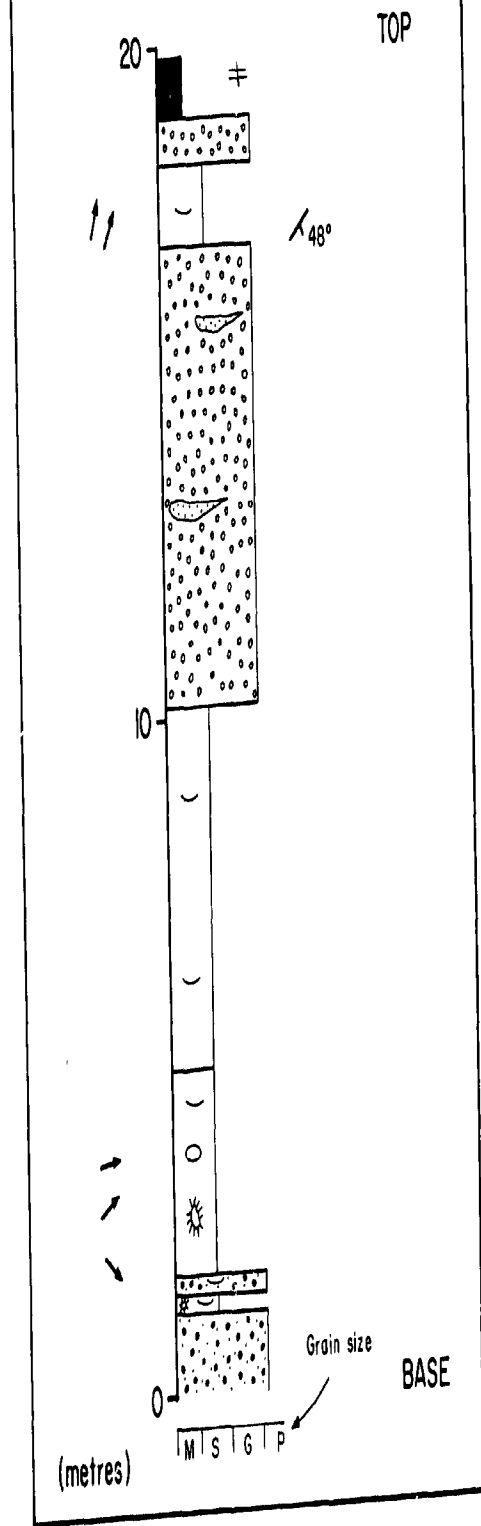
Stratigraphic Section 5
Halls Hill

HALLS HILL SECTION



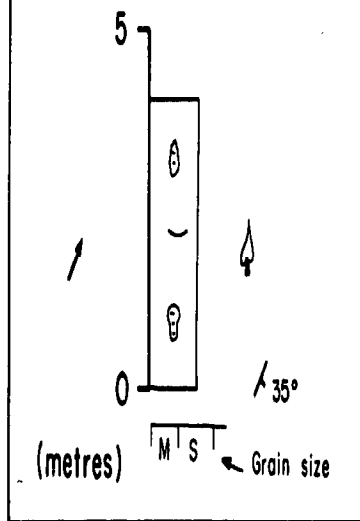
Stratigraphic Section 6
Pt de Bute Quarry

6. POINT DE BUTE QUARRY



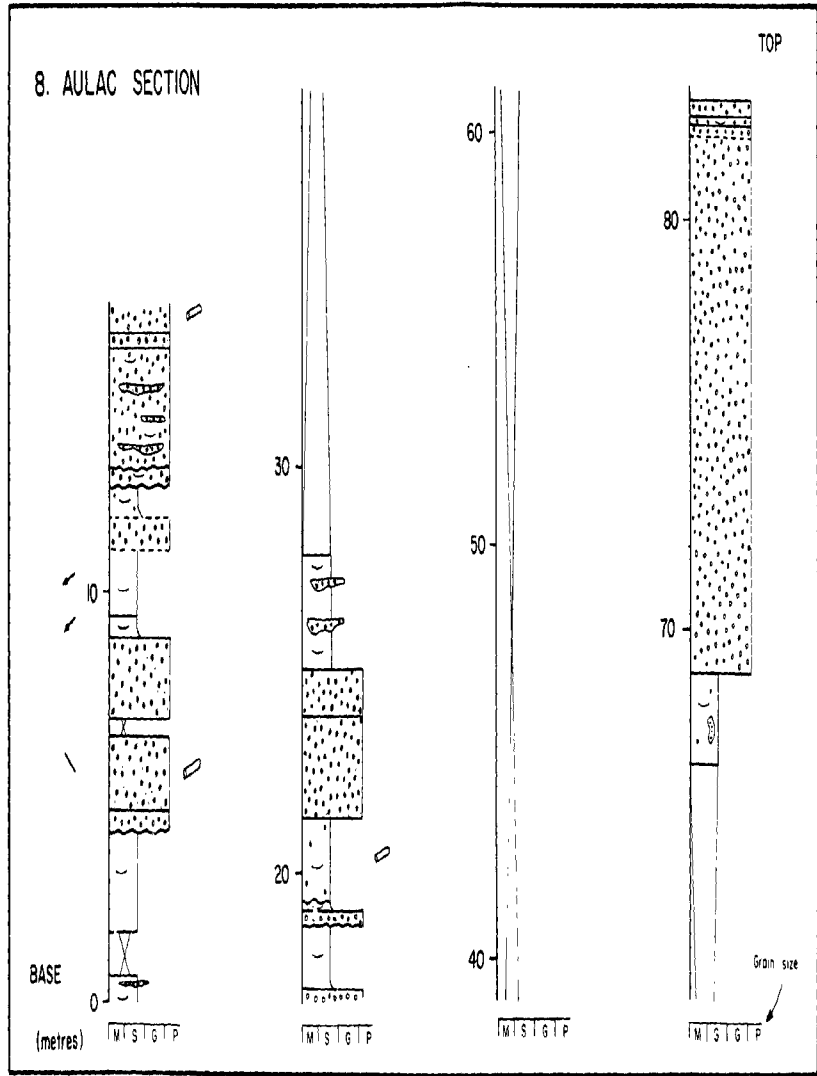
Stratigraphic Section ?
Mt. Whatley

7. MT WHATLEY QUARRY



Stratigraphic Section 8
Aulac

8. AULAC SECTION



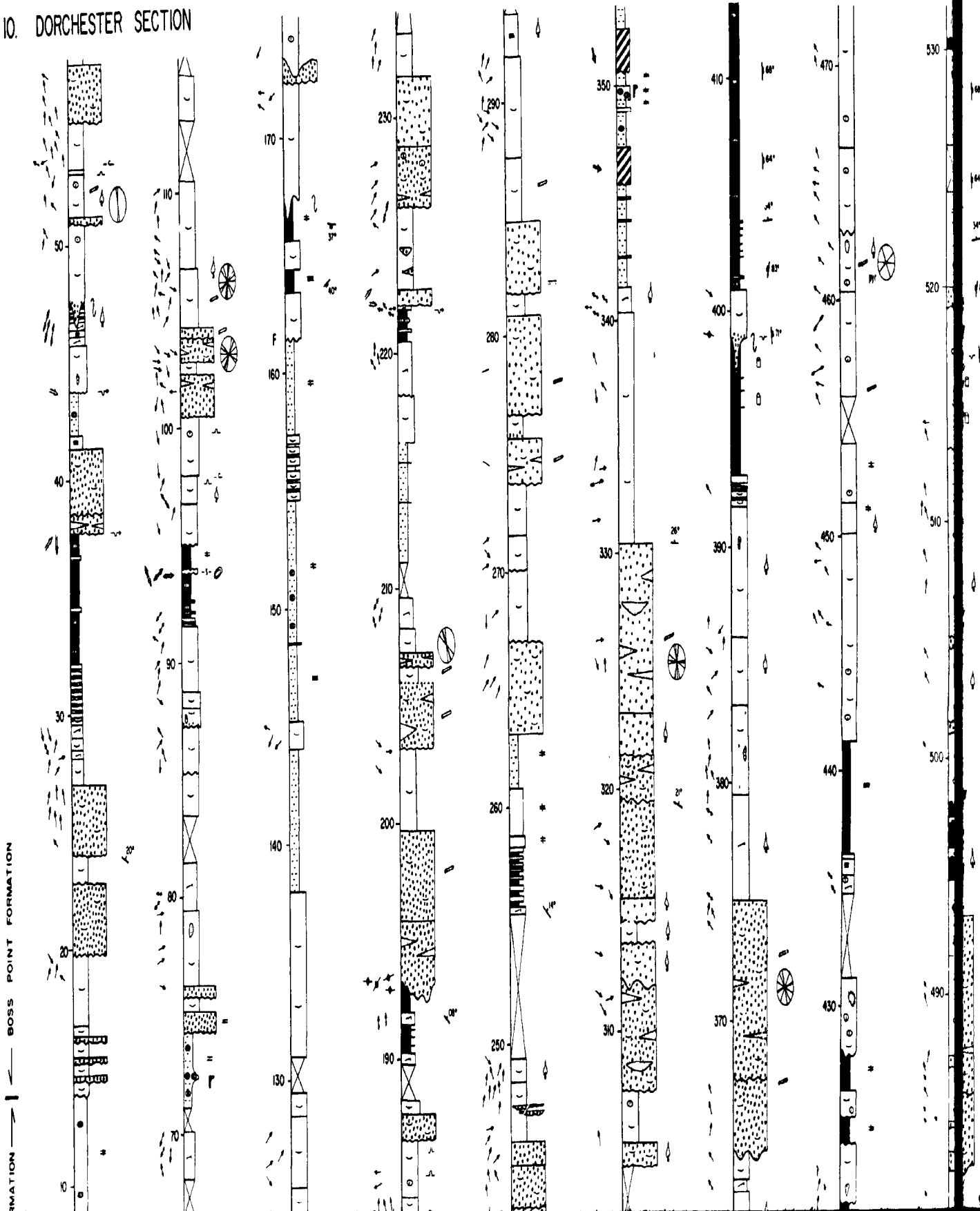
Stratigraphic Section 9
British Settlement

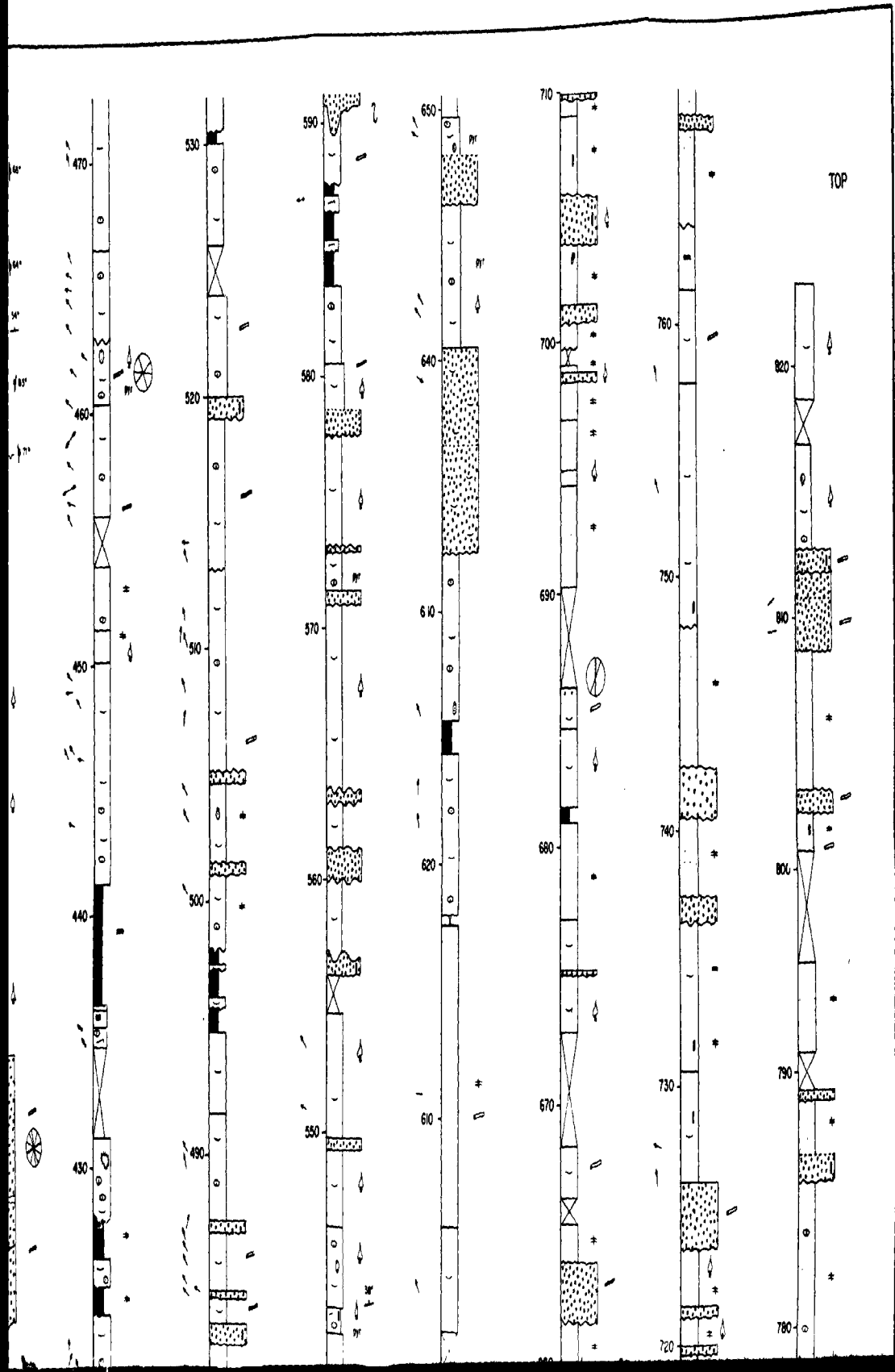
SANDSTONE QUARRY
BRITISH SETTLEMENT

Steeply dipping Boss Point Formation
sandstone - bedding attitude 094/67N

Stratigraphic Section 10
Dorchester

10. DORCHESTER SECTION

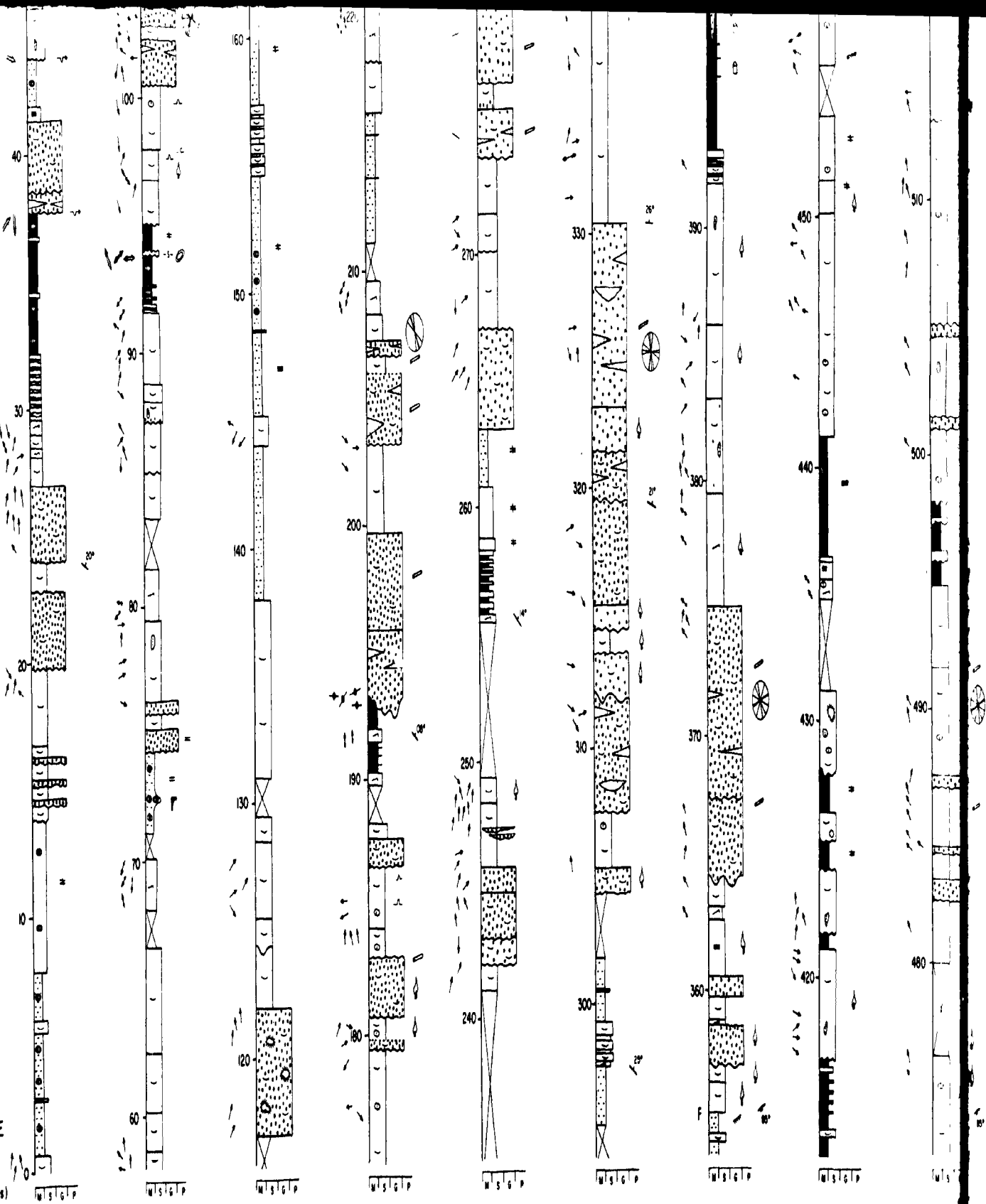


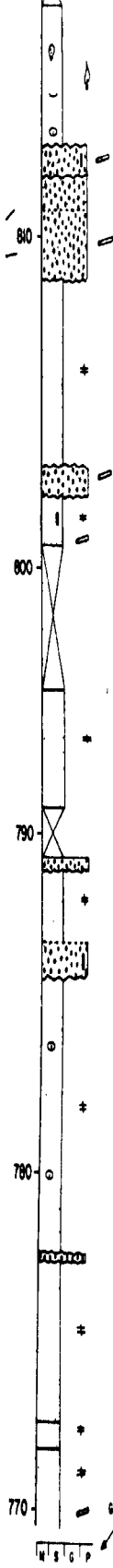
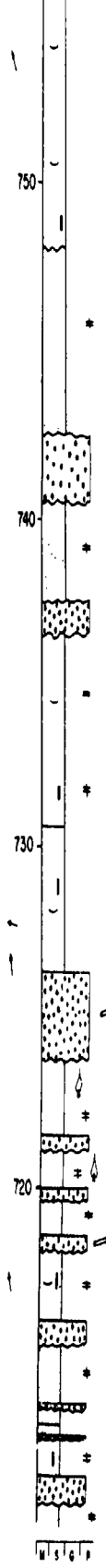
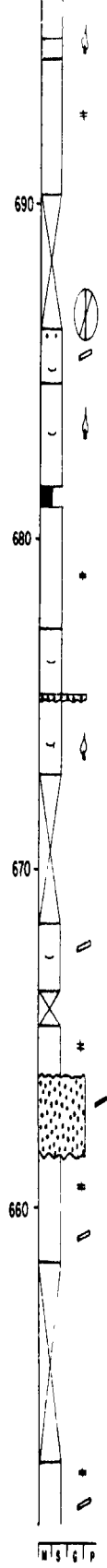
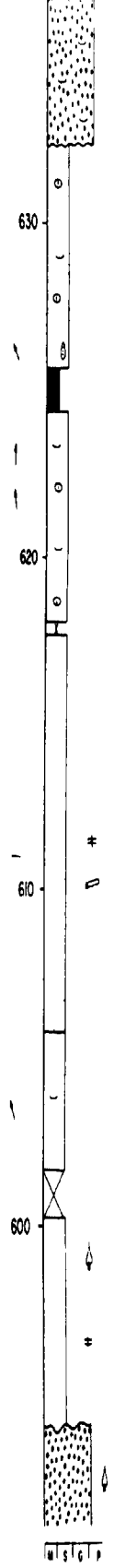
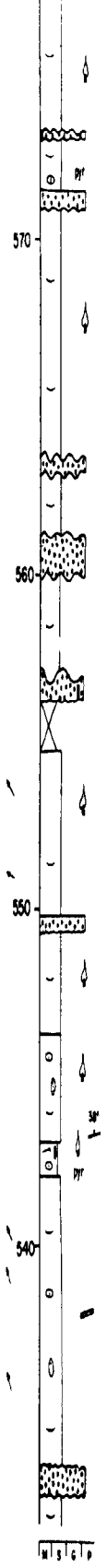
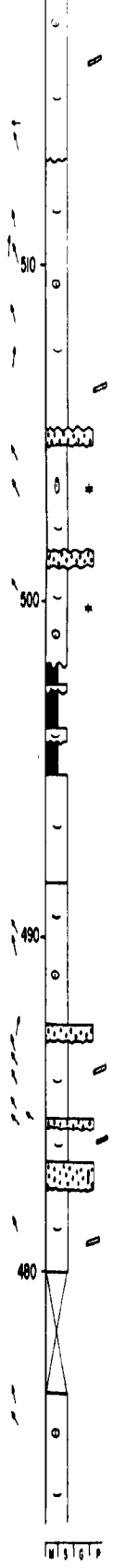


CLAREMONT FORMATION — BOSS POINT FORMATION

BASE

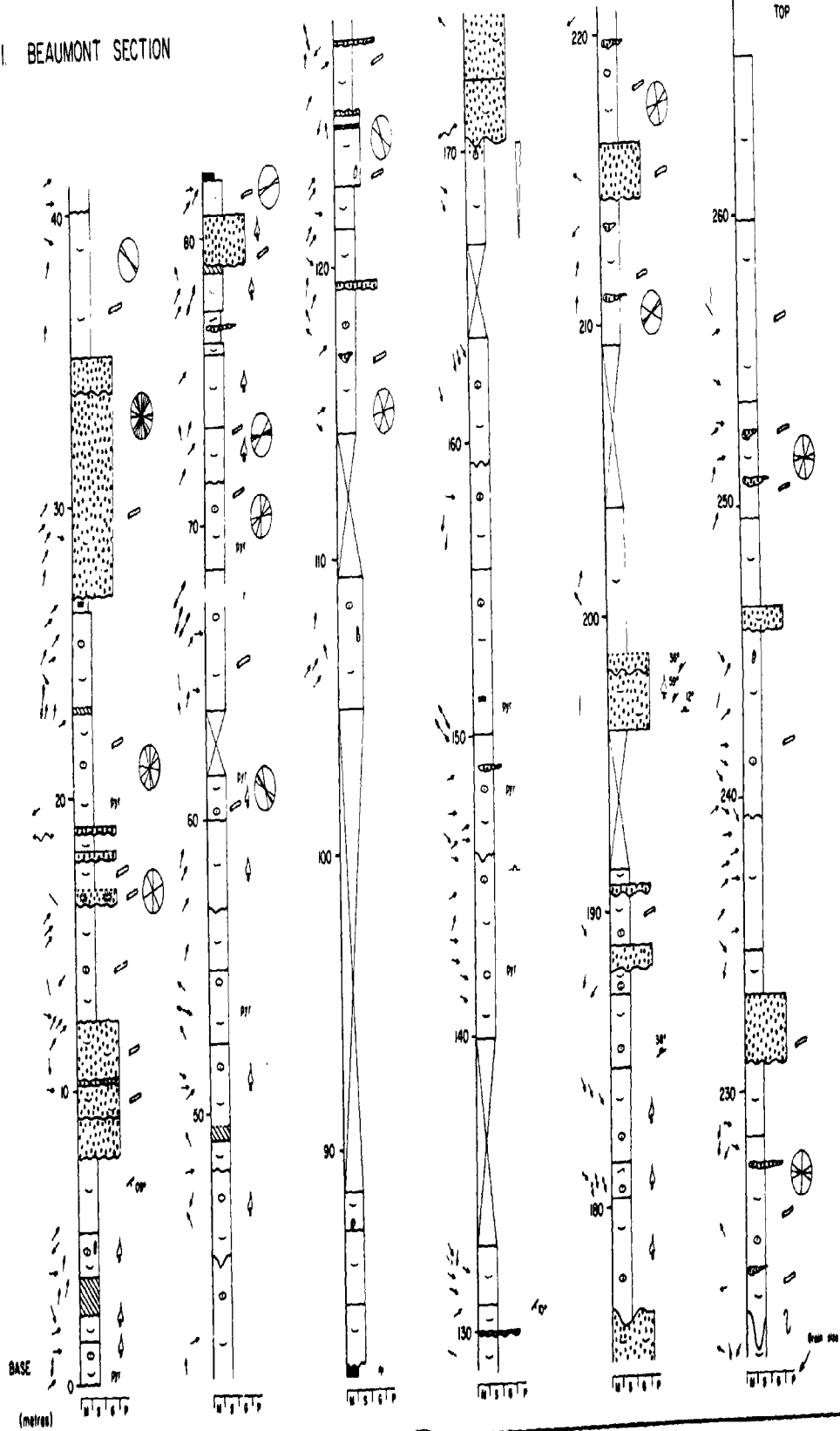
(metres)





Stratigraphic Section 11
Beaumont

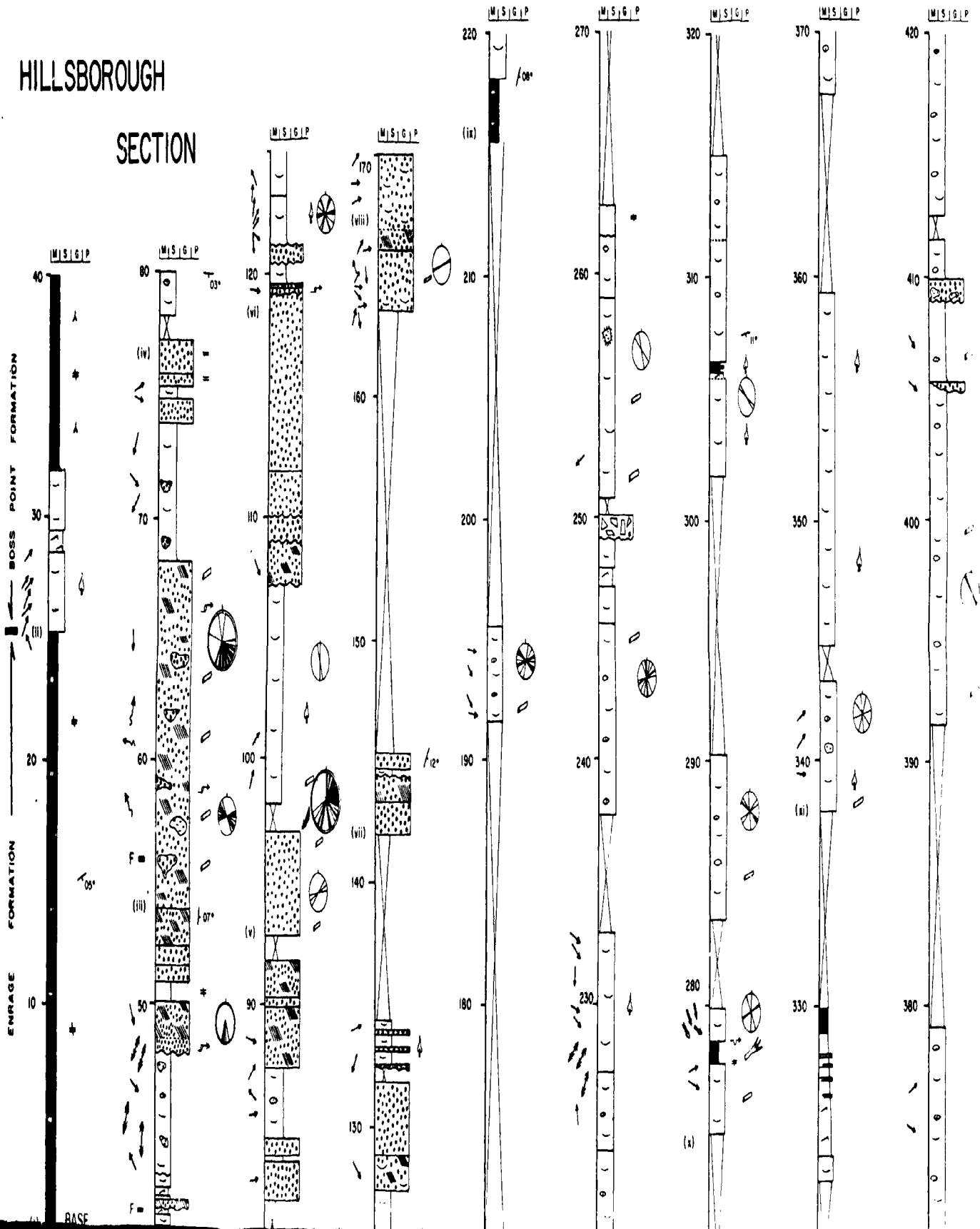
II. BEAUMONT SECTION

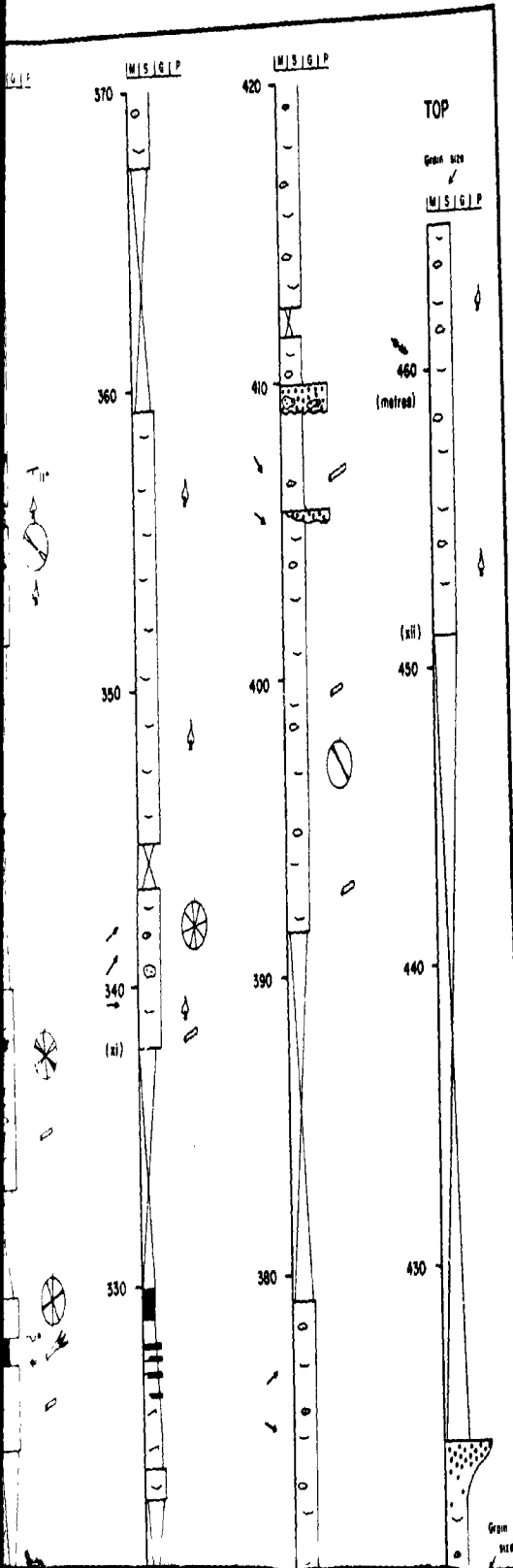


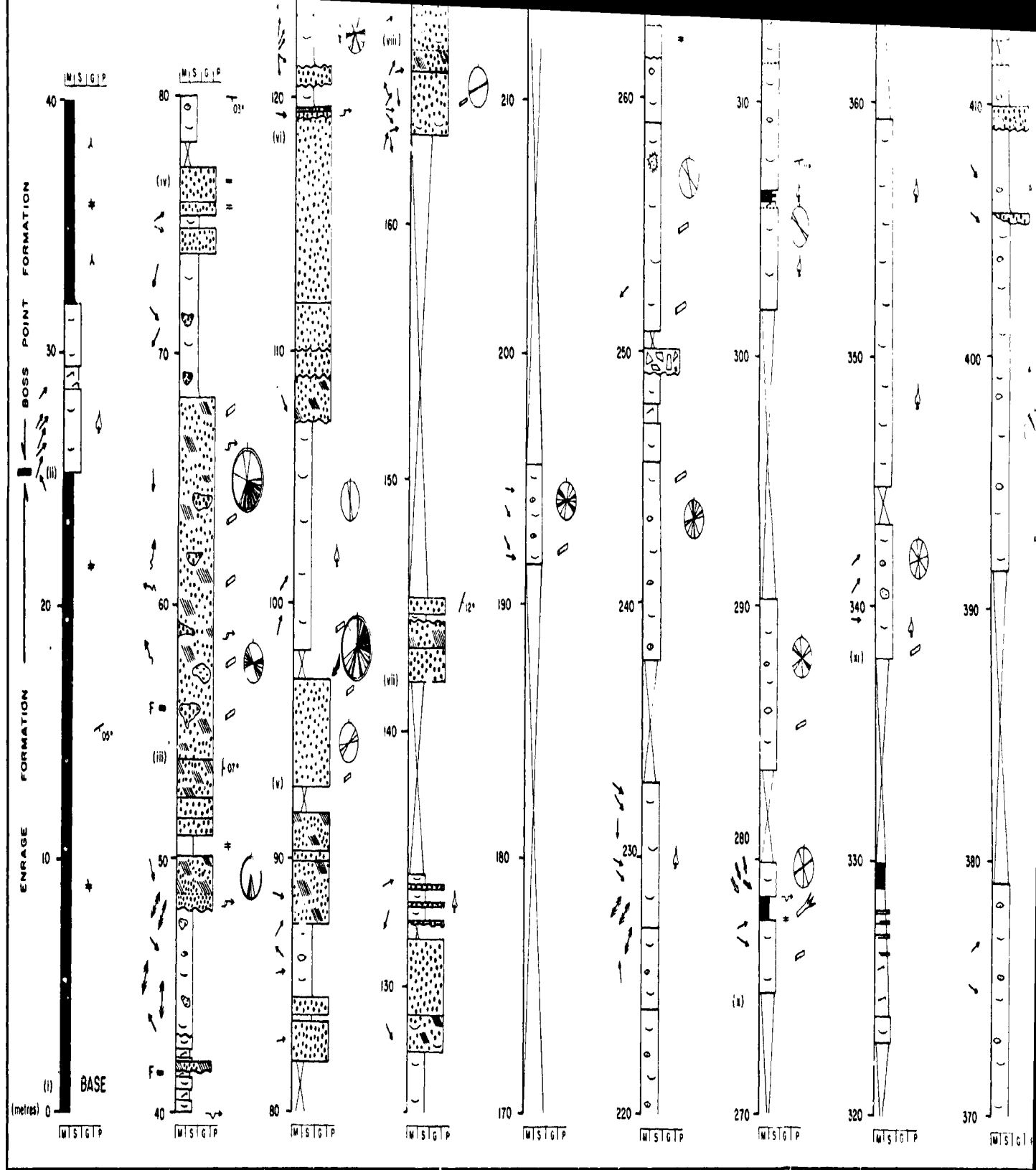
Stratigraphic Section 12
Hillsborough

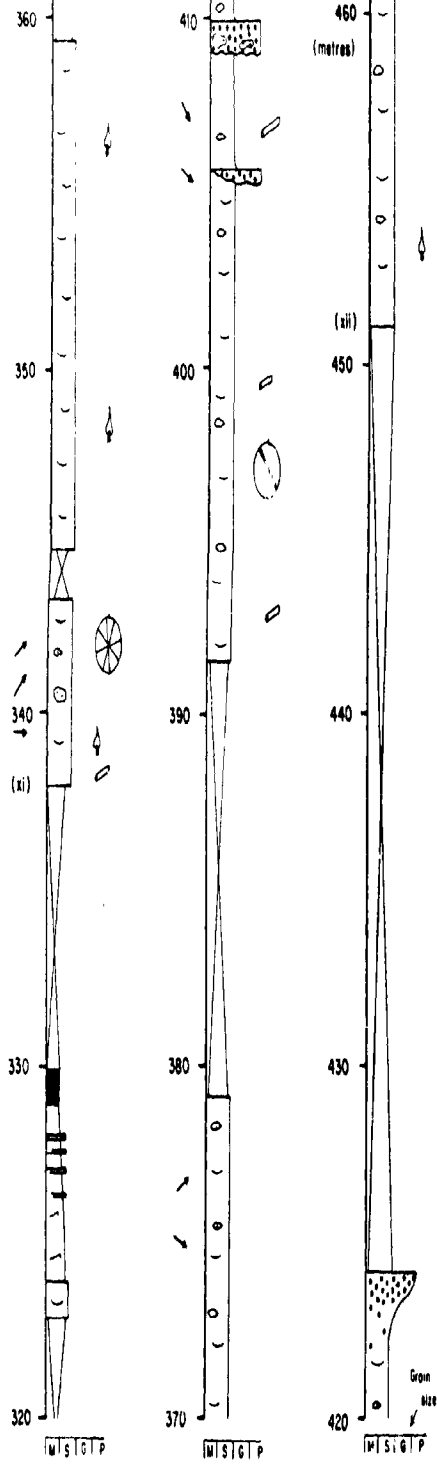
HILLSBOROUGH

SECTION



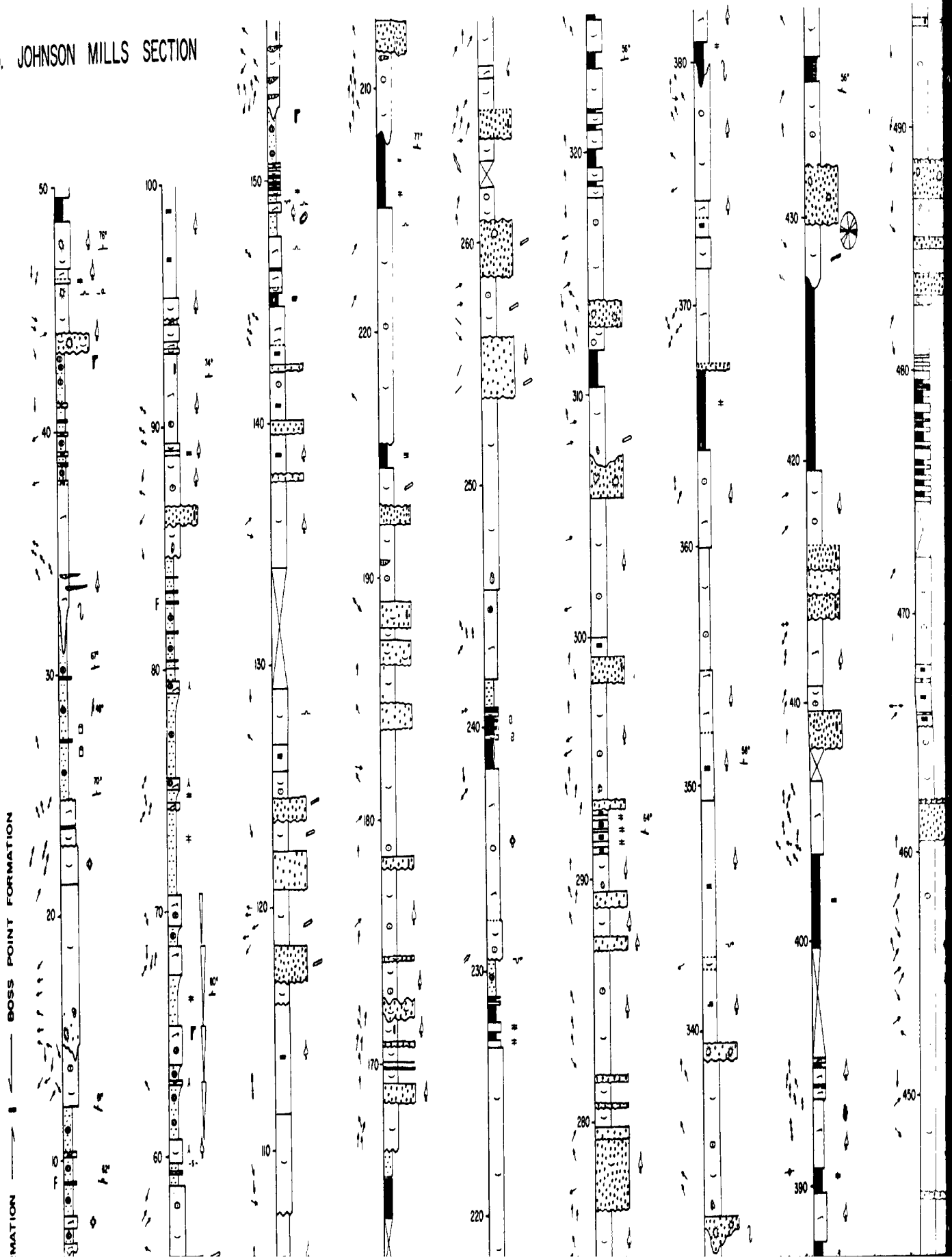


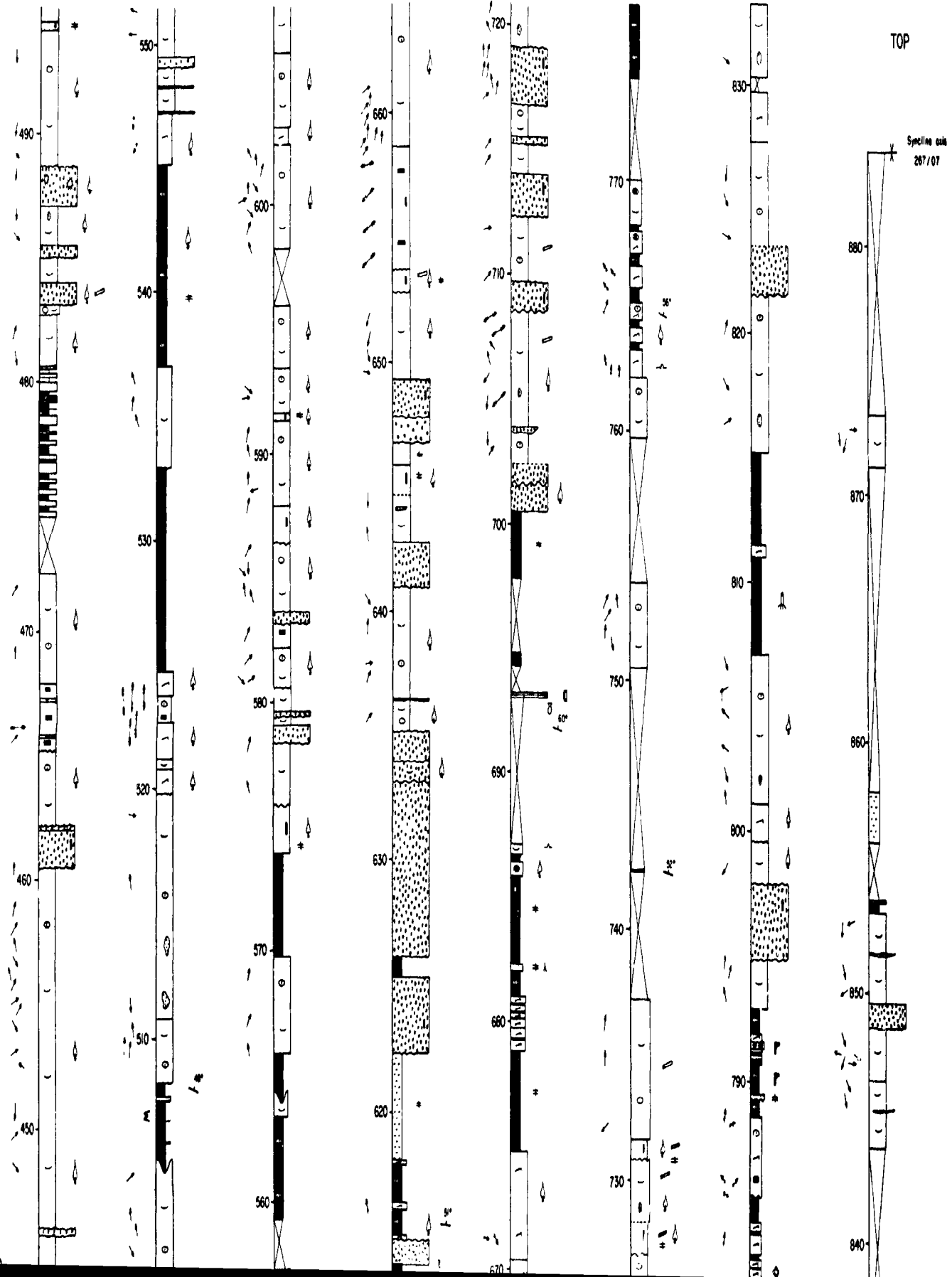




Stratigraphic Section 13
Johnson Mills

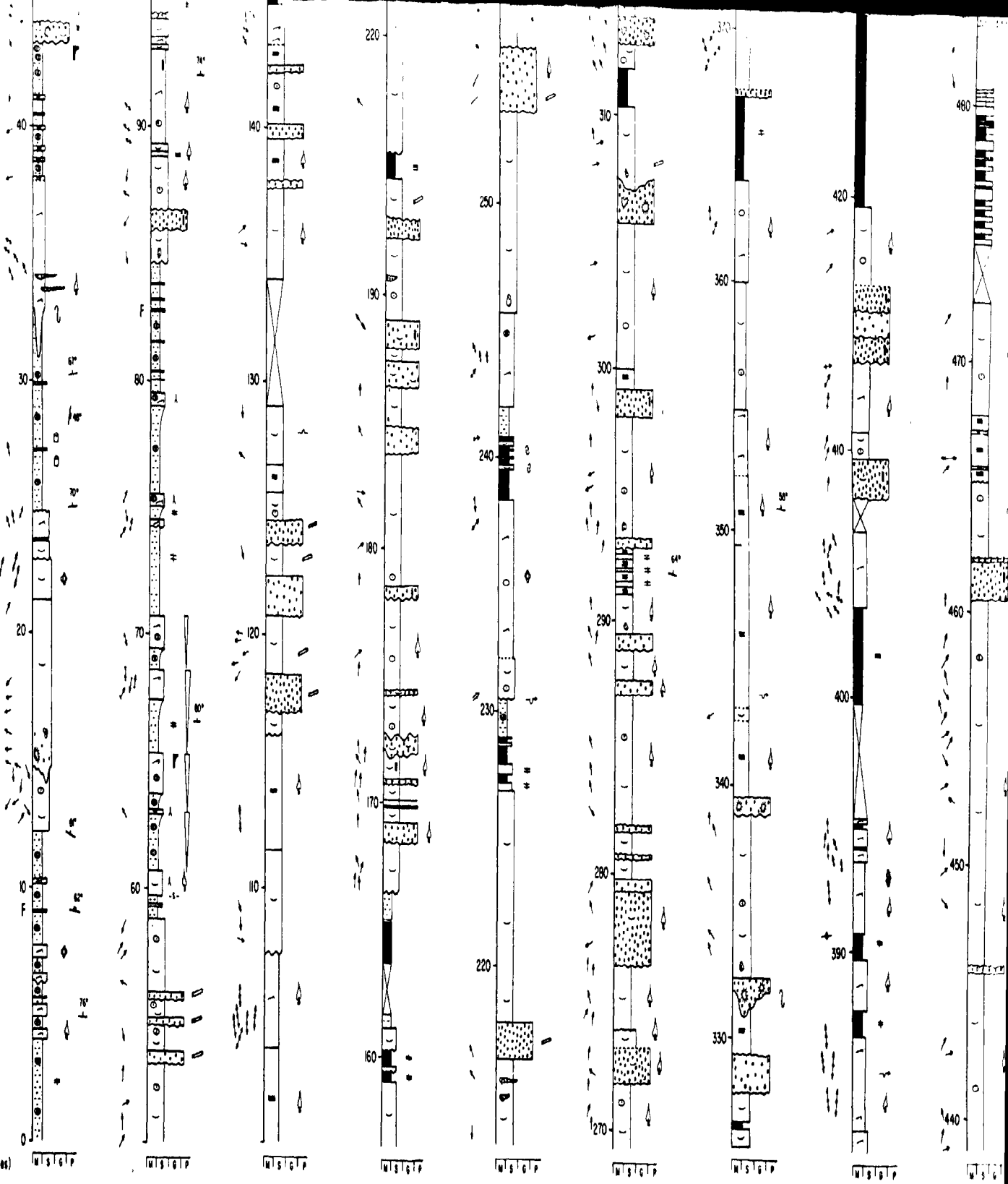
13. JOHNSON MILLS SECTION

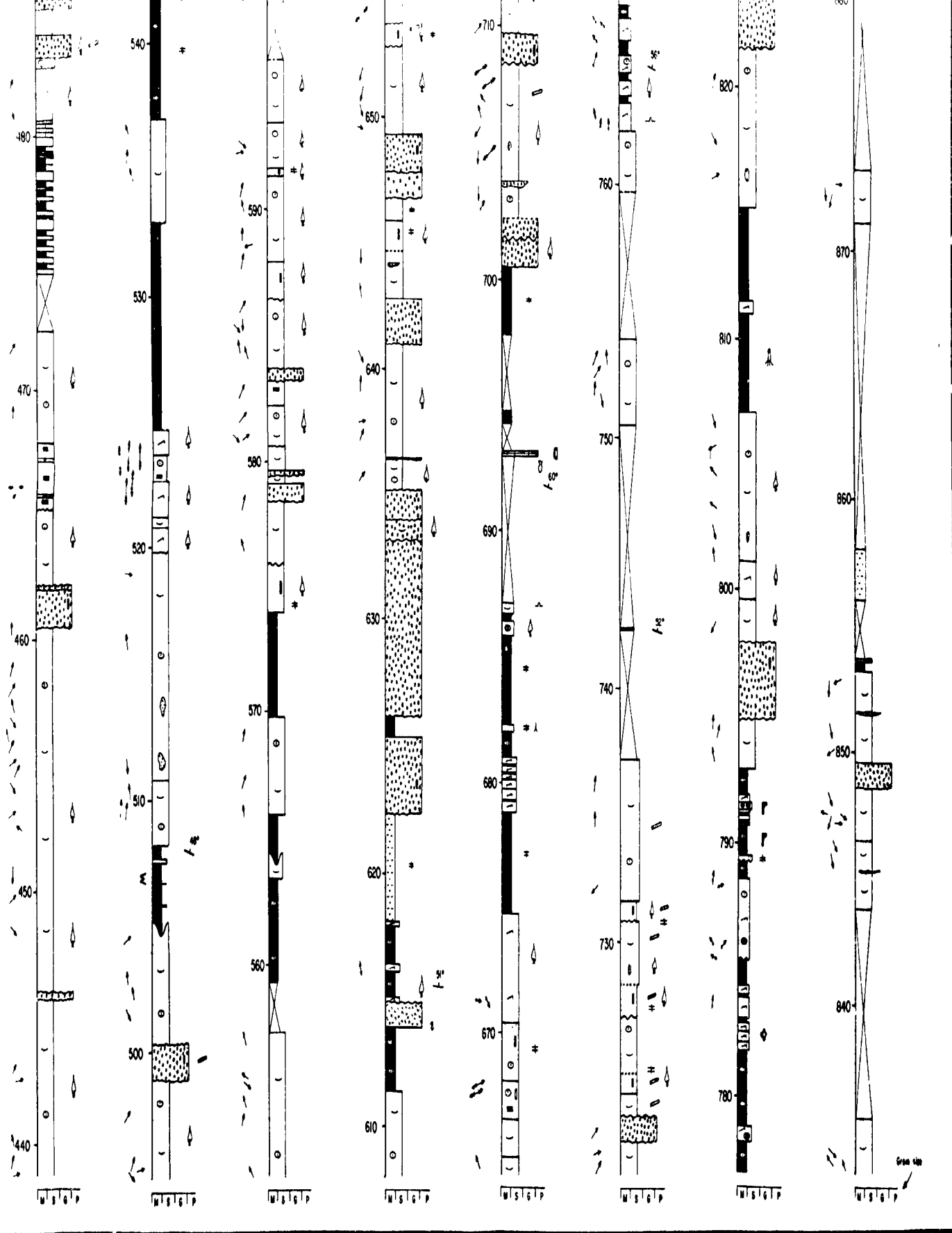




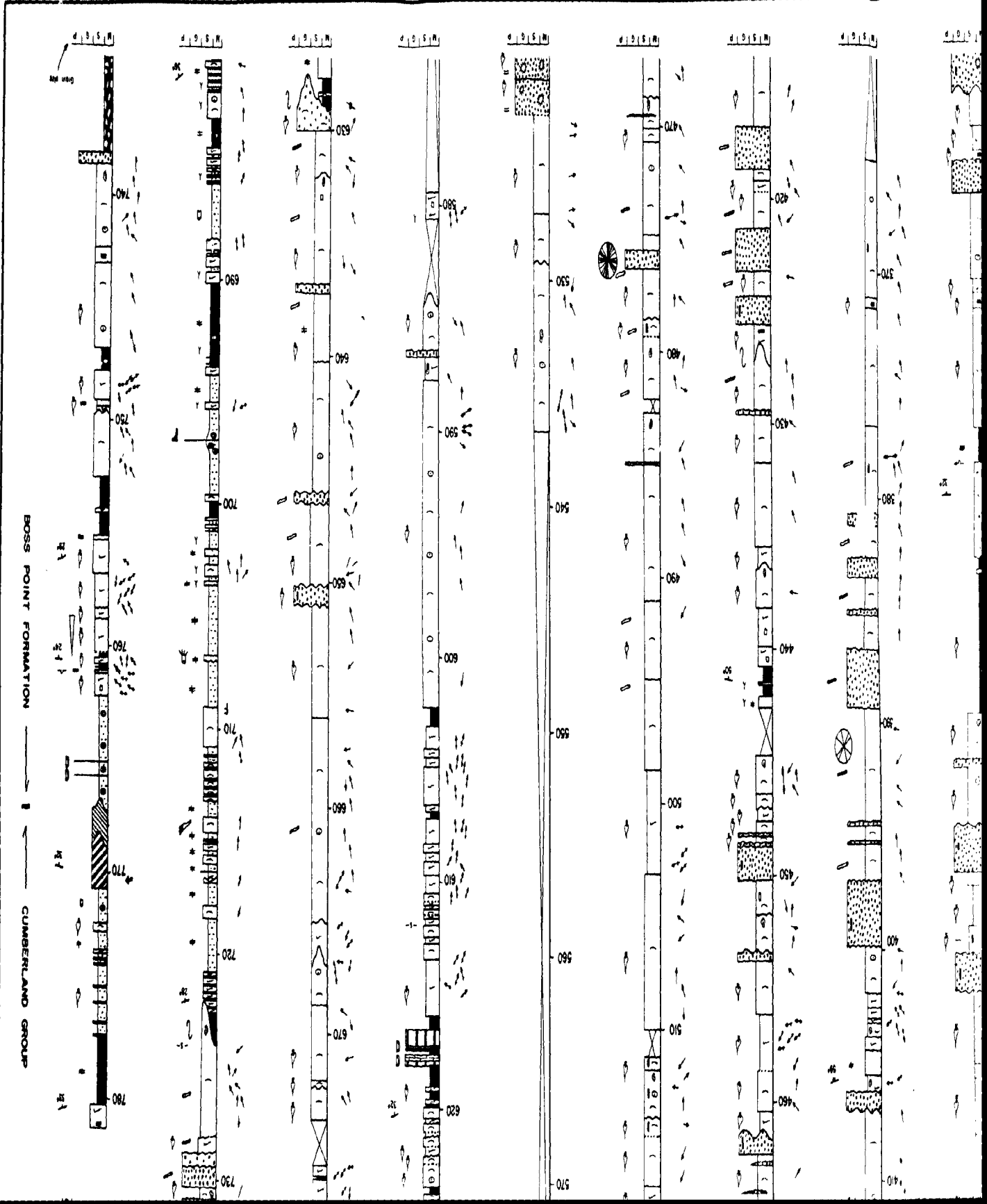
CLAREMONT FORMATION BOSS POINT FORMATION

(metres)





Stratigraphic Section 14
Boss Point

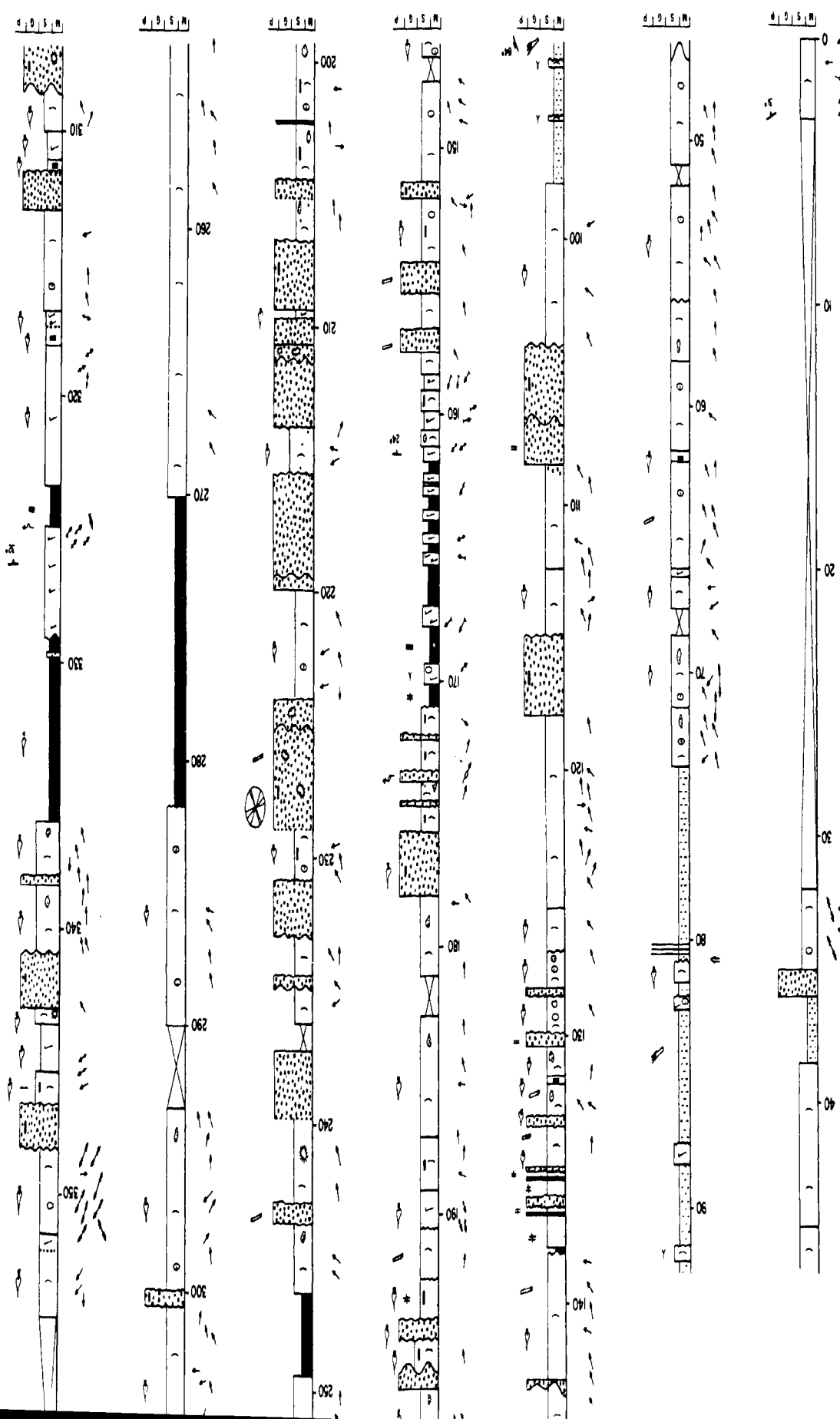


CLAREMONT FORMATION

BOSS POINT FORMATION

BASE

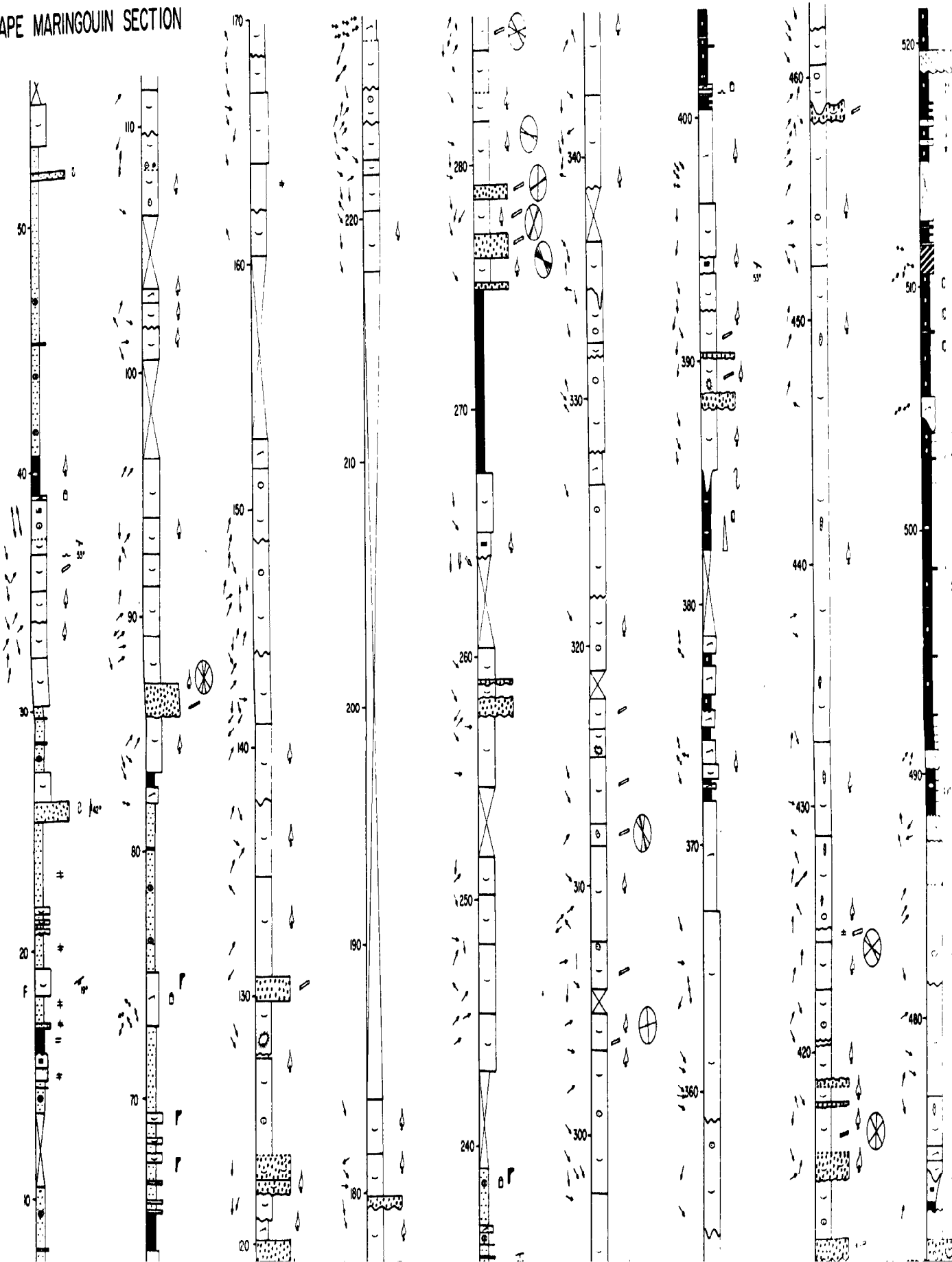
(metres)



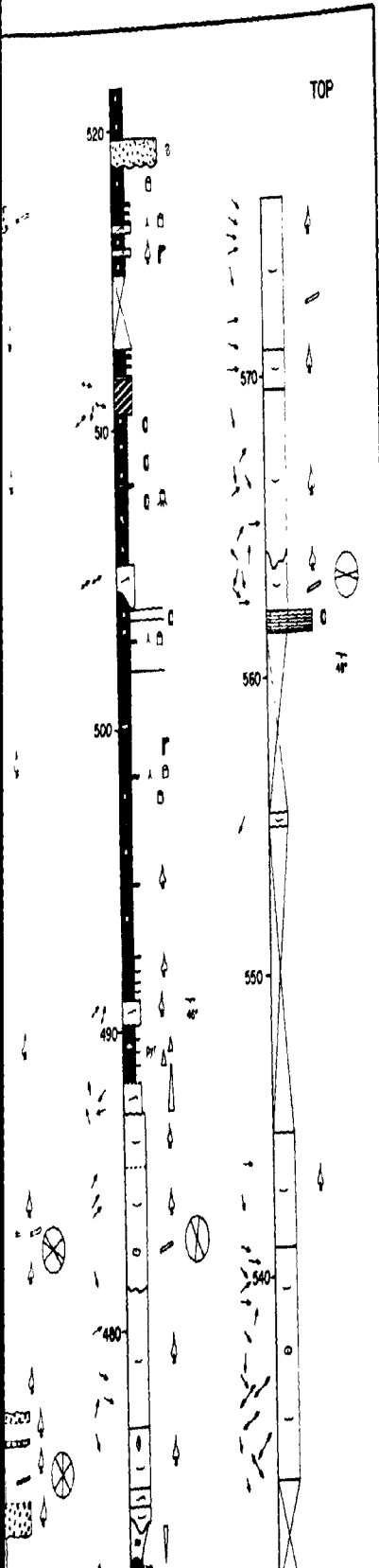
Stratigraphic Section 15
Cape Meringuin

15. CAPE MARINGOUIN SECTION

CLAREMONT FORMATION → BOSS POINT FORMATION



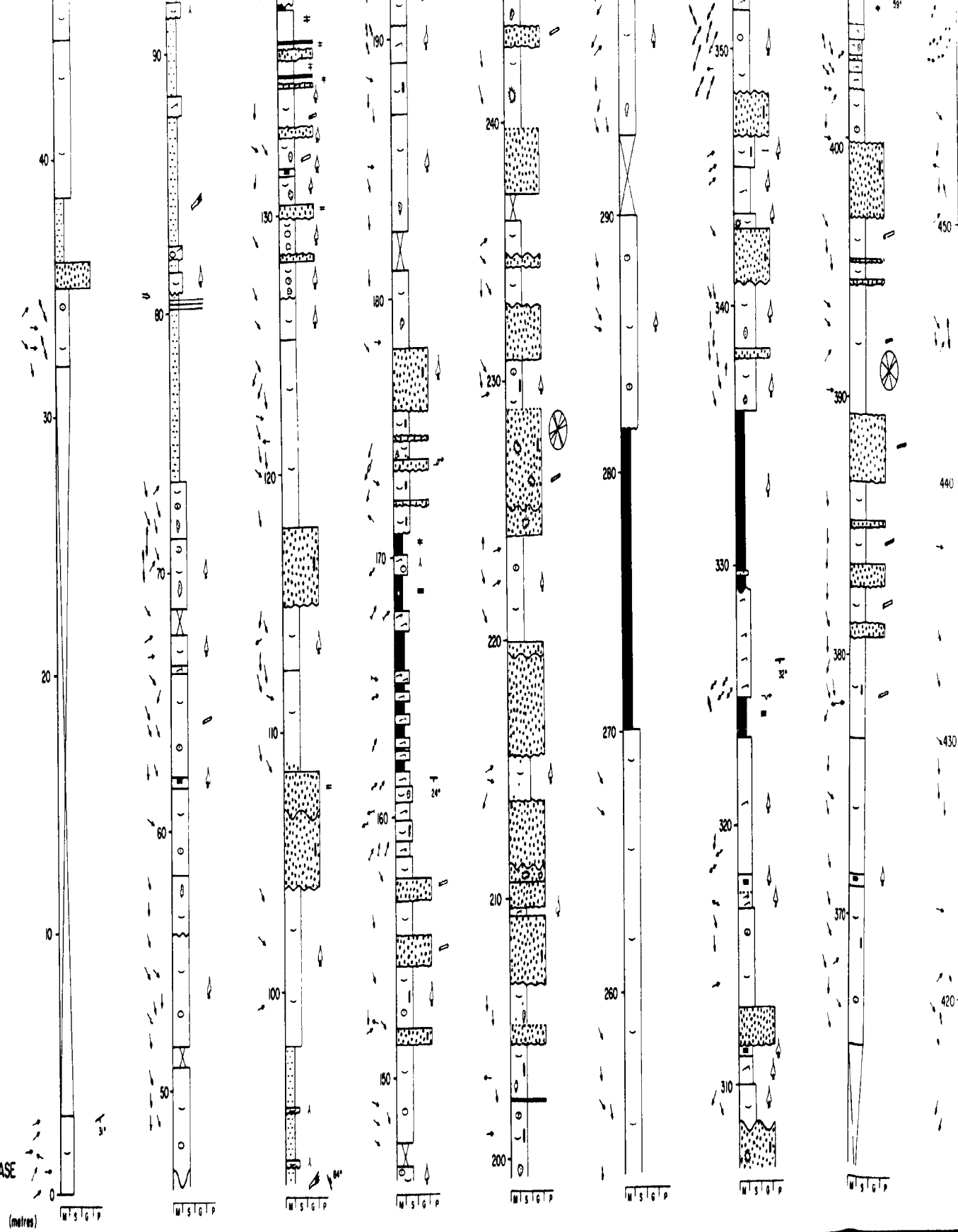
TOP



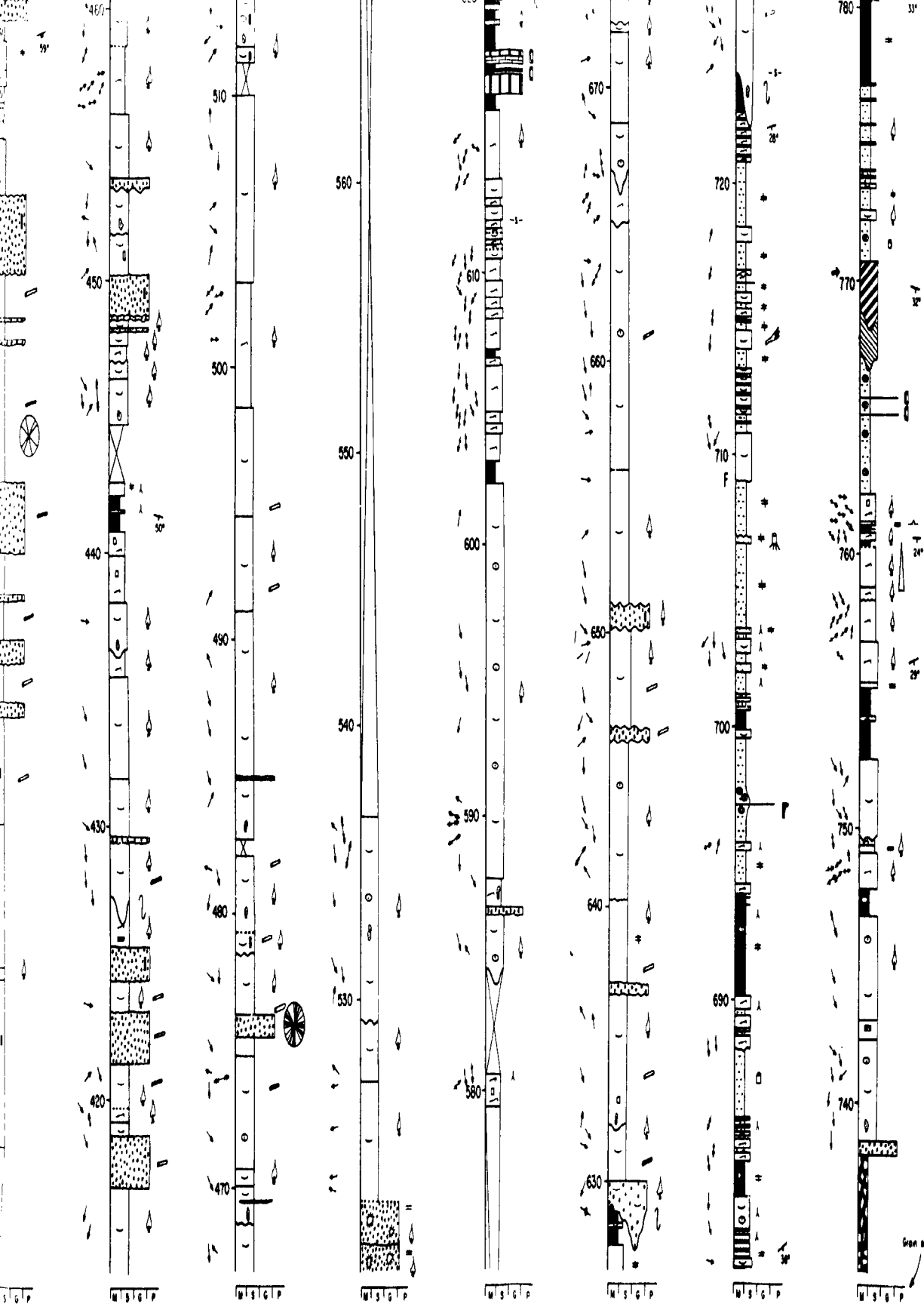
CLAREMONT FORMATION

BOSS POINT FORMATION

BASE



(metres)



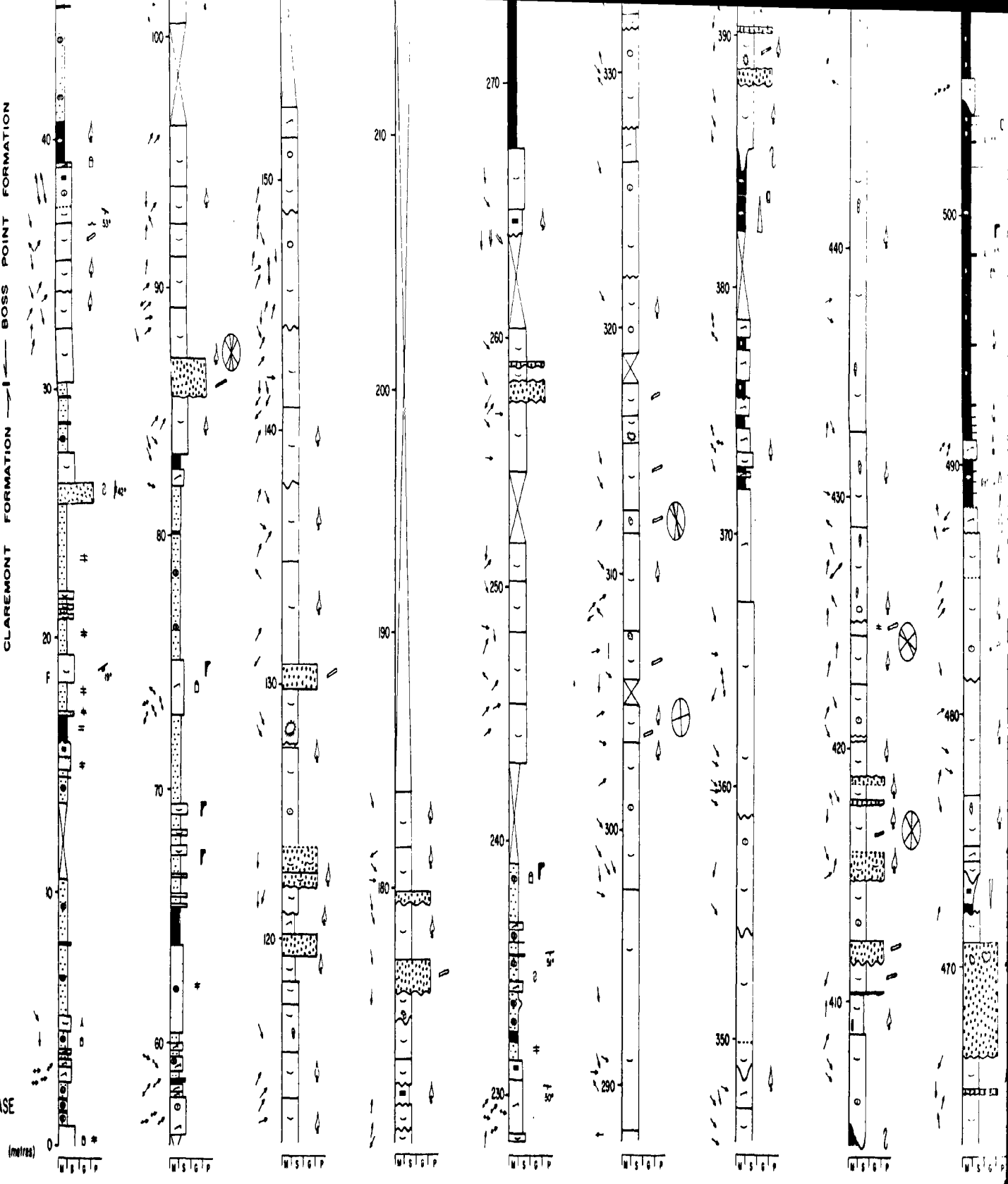
BOSS POINT FORMATION

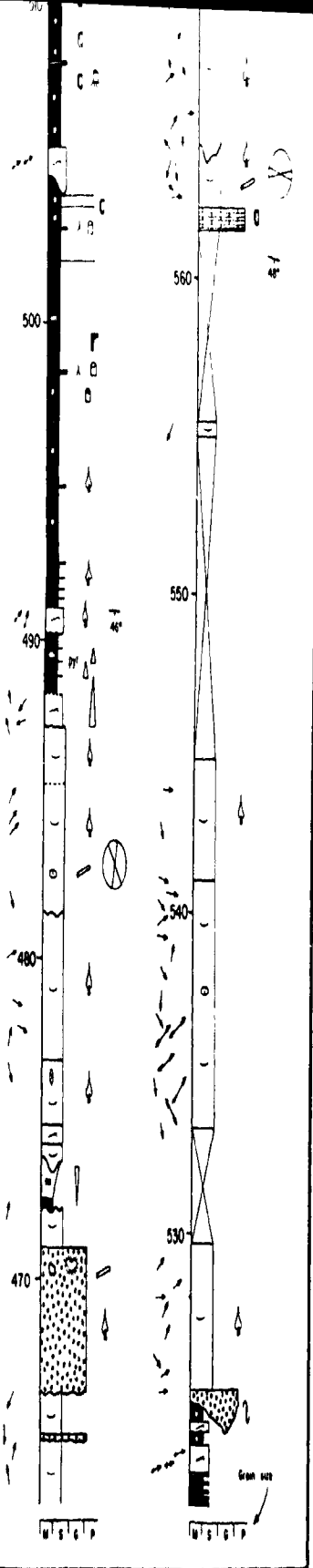
CUMBERLAND GROUP

Granite

CLAREMONT FORMATION — BOSS POINT FORMATION

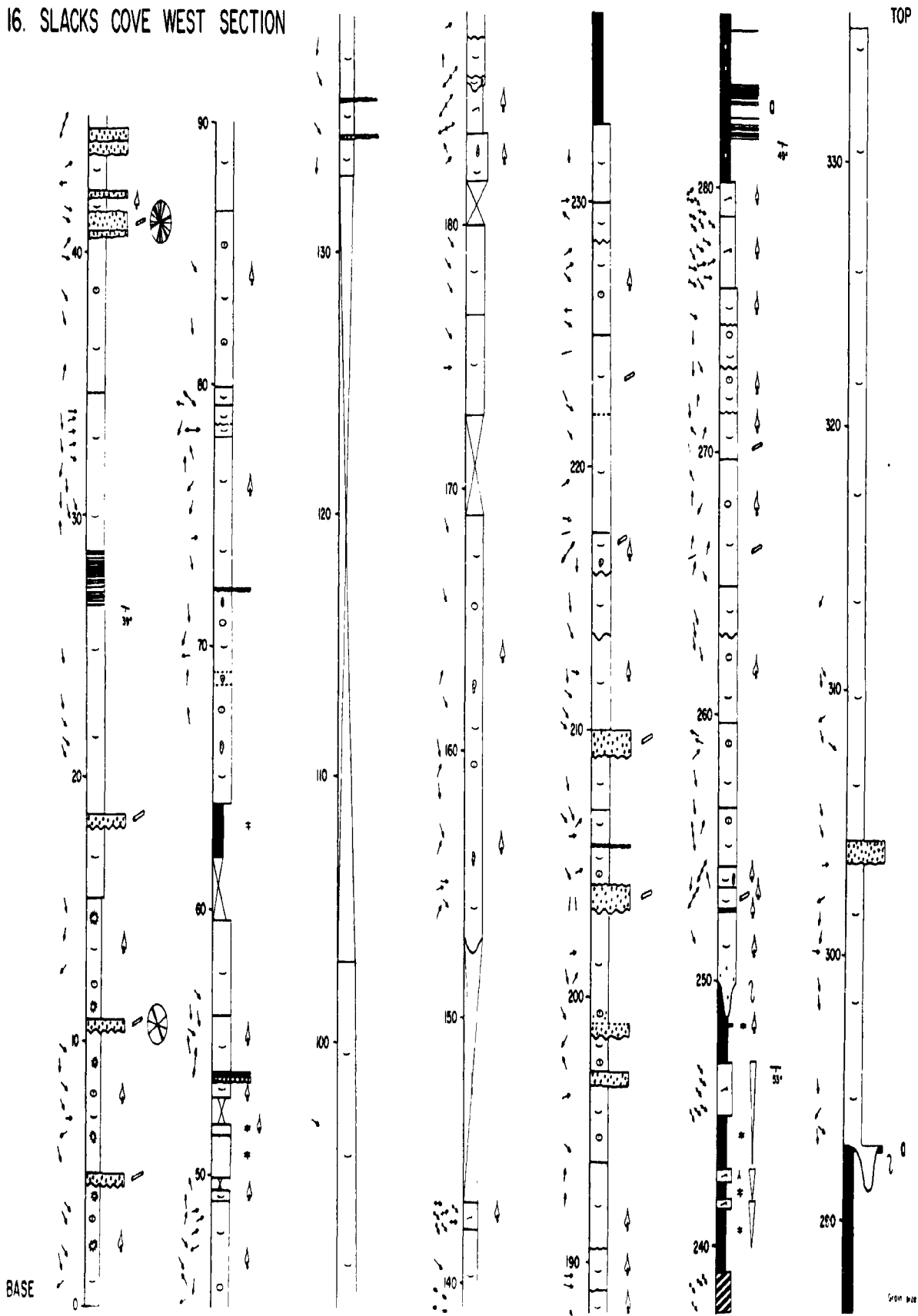
BASE





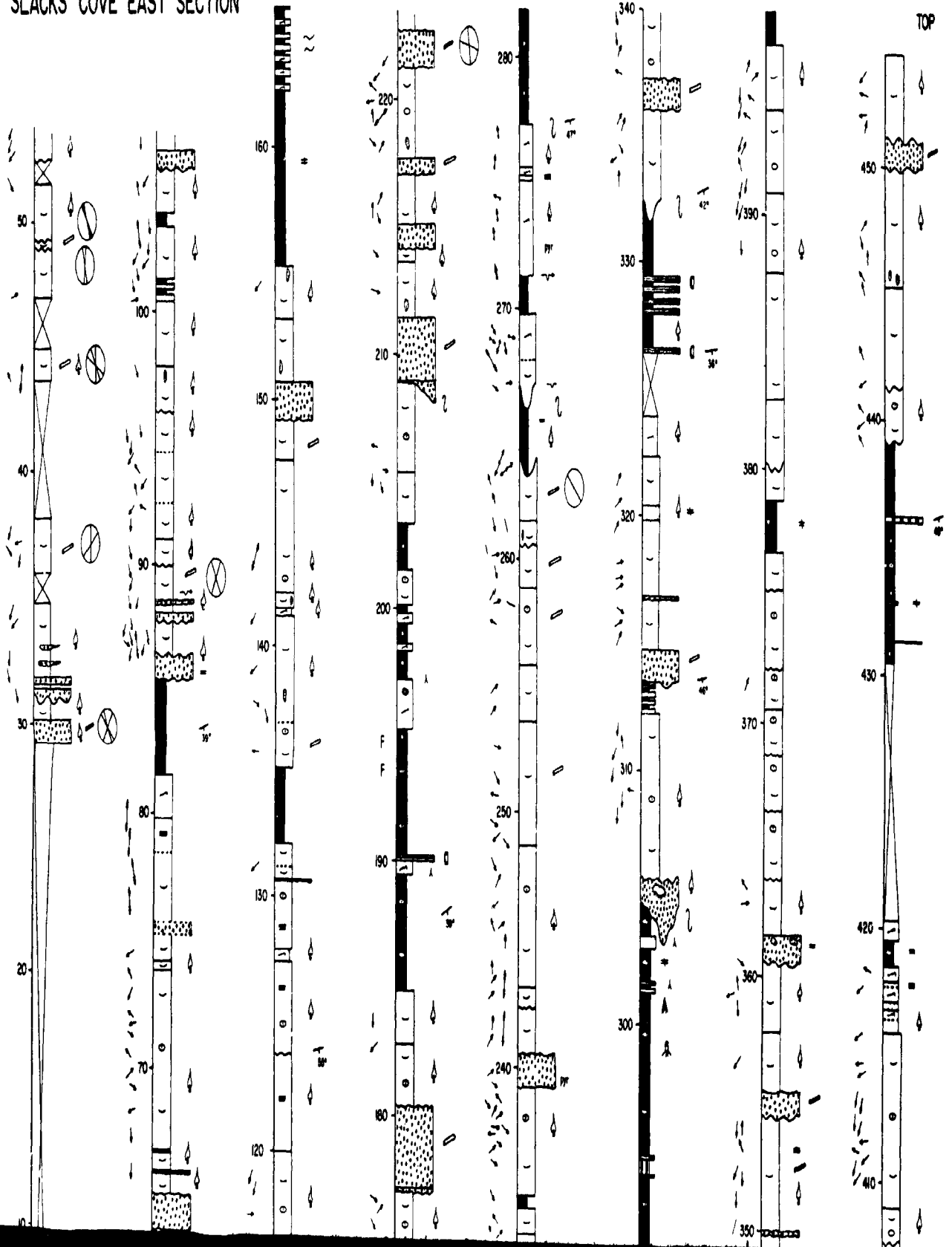
Stratigraphic Section 16
Slacks Cove West

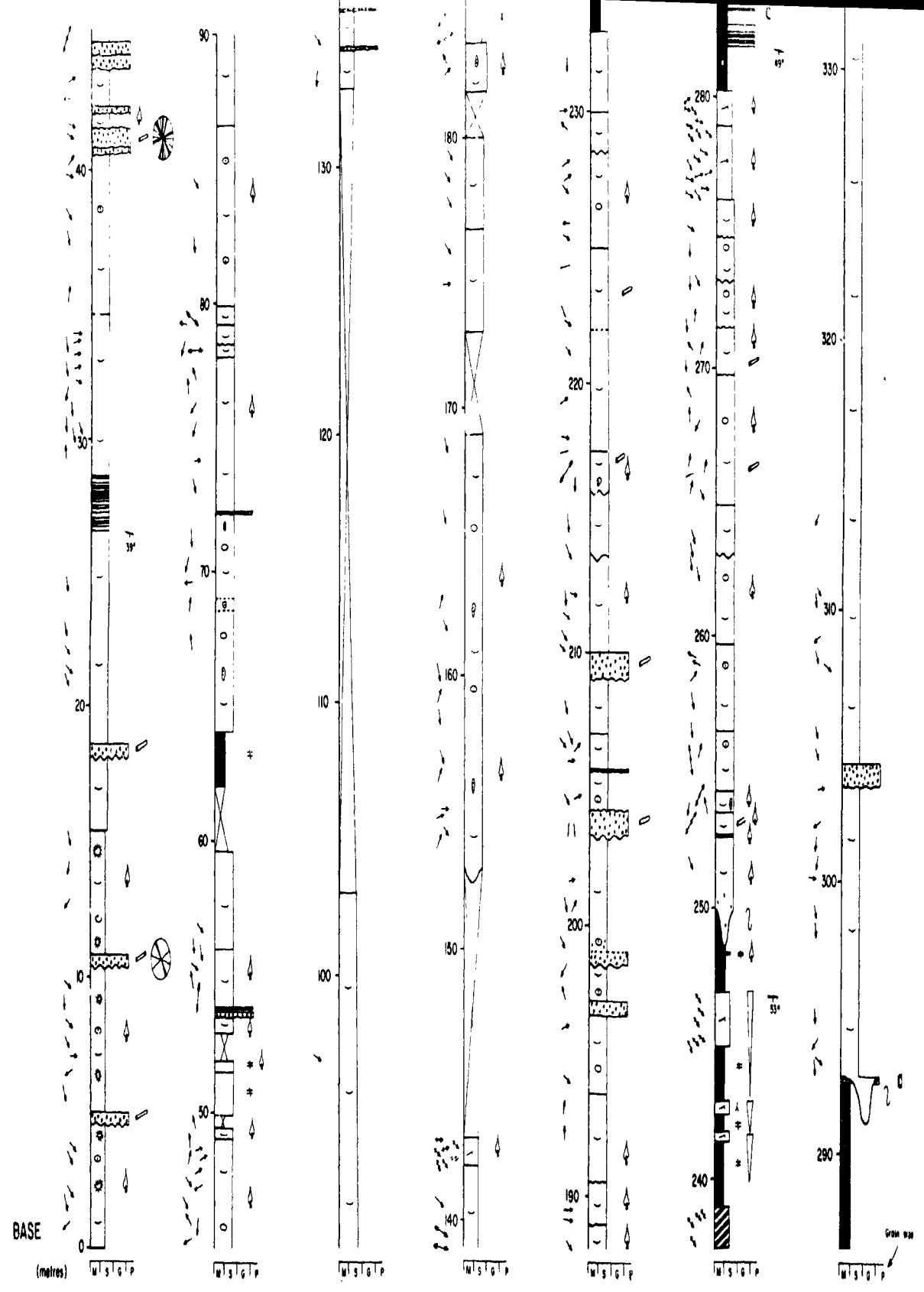
16. SLACKS COVE WEST SECTION



Stratigraphic Section 17
Slacks Cove East

17. SLACKS COVE EAST SECTION





BASE

(metres)

W S G P

W S G P

W S G P

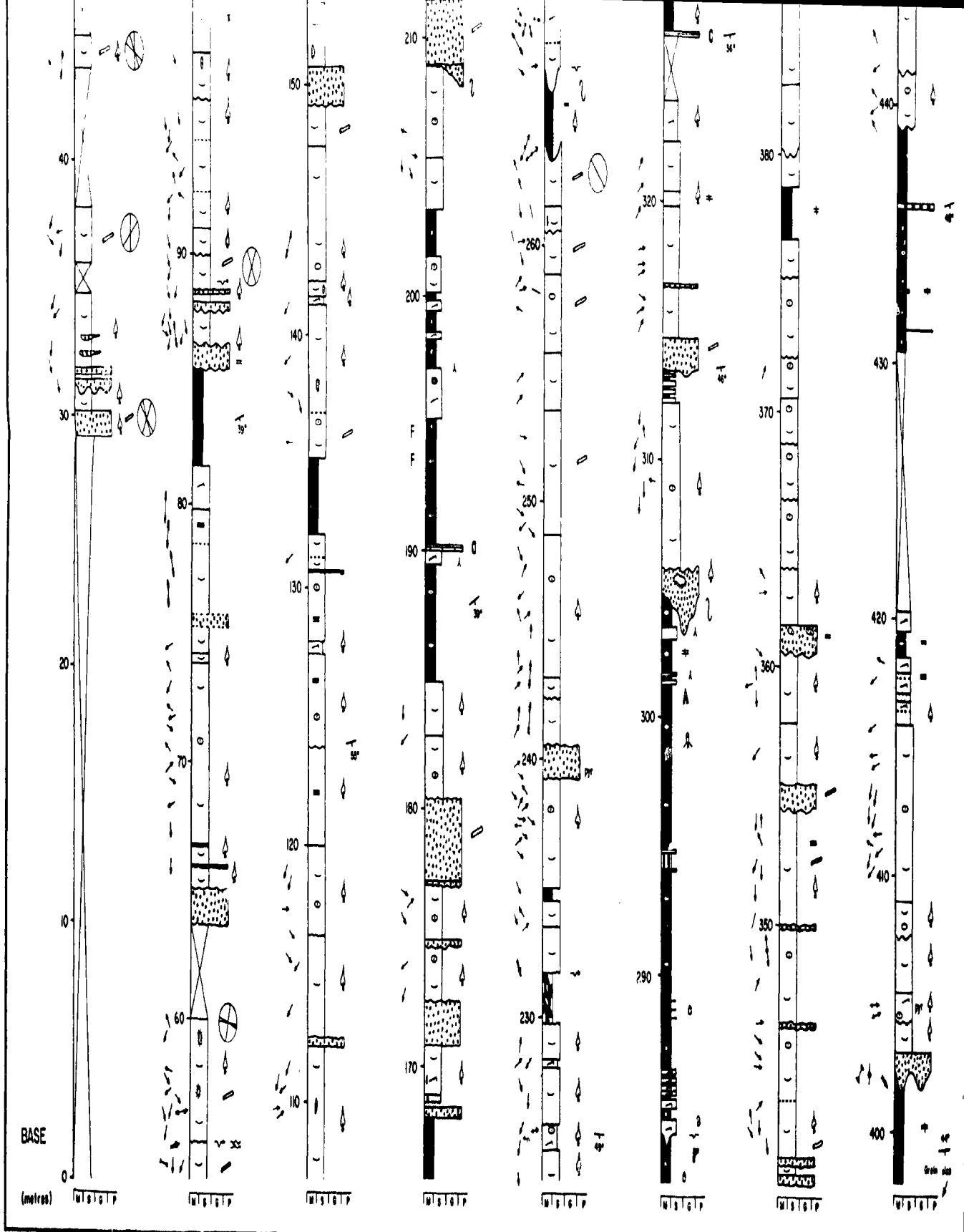
W S G P

W S G P

W S G P

W S G P

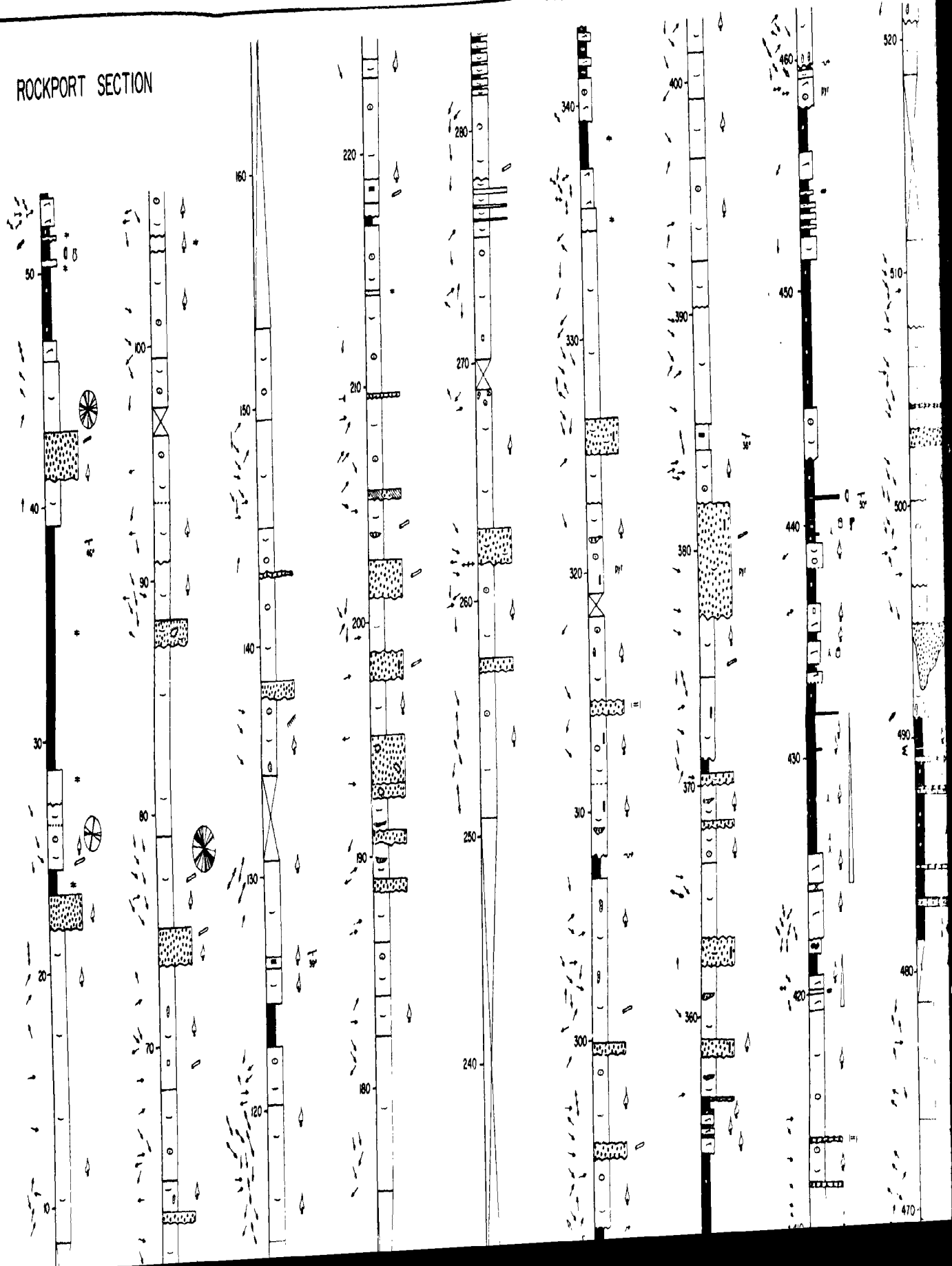
Gravel

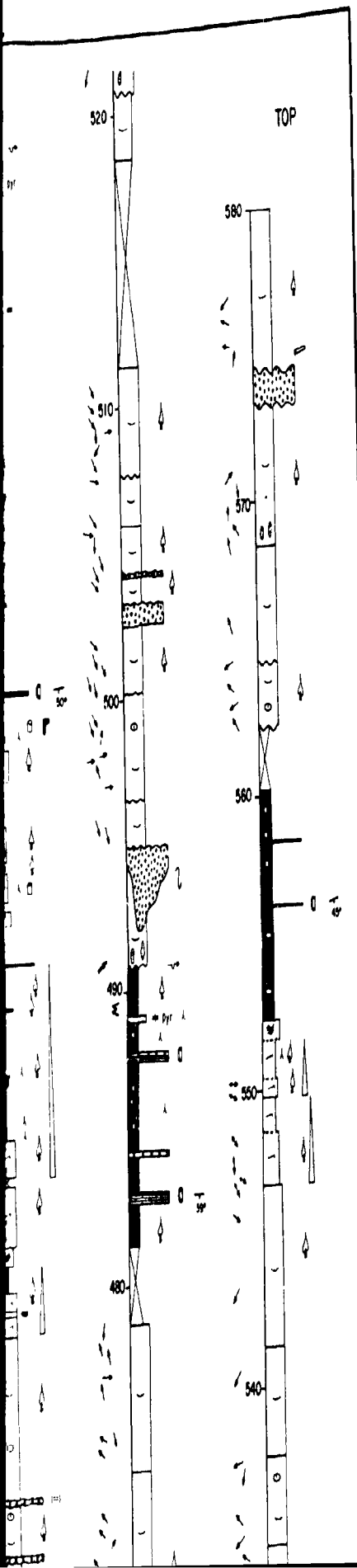


Stratigraphi
Rockport

Stratigraphic Section 18
Rockport

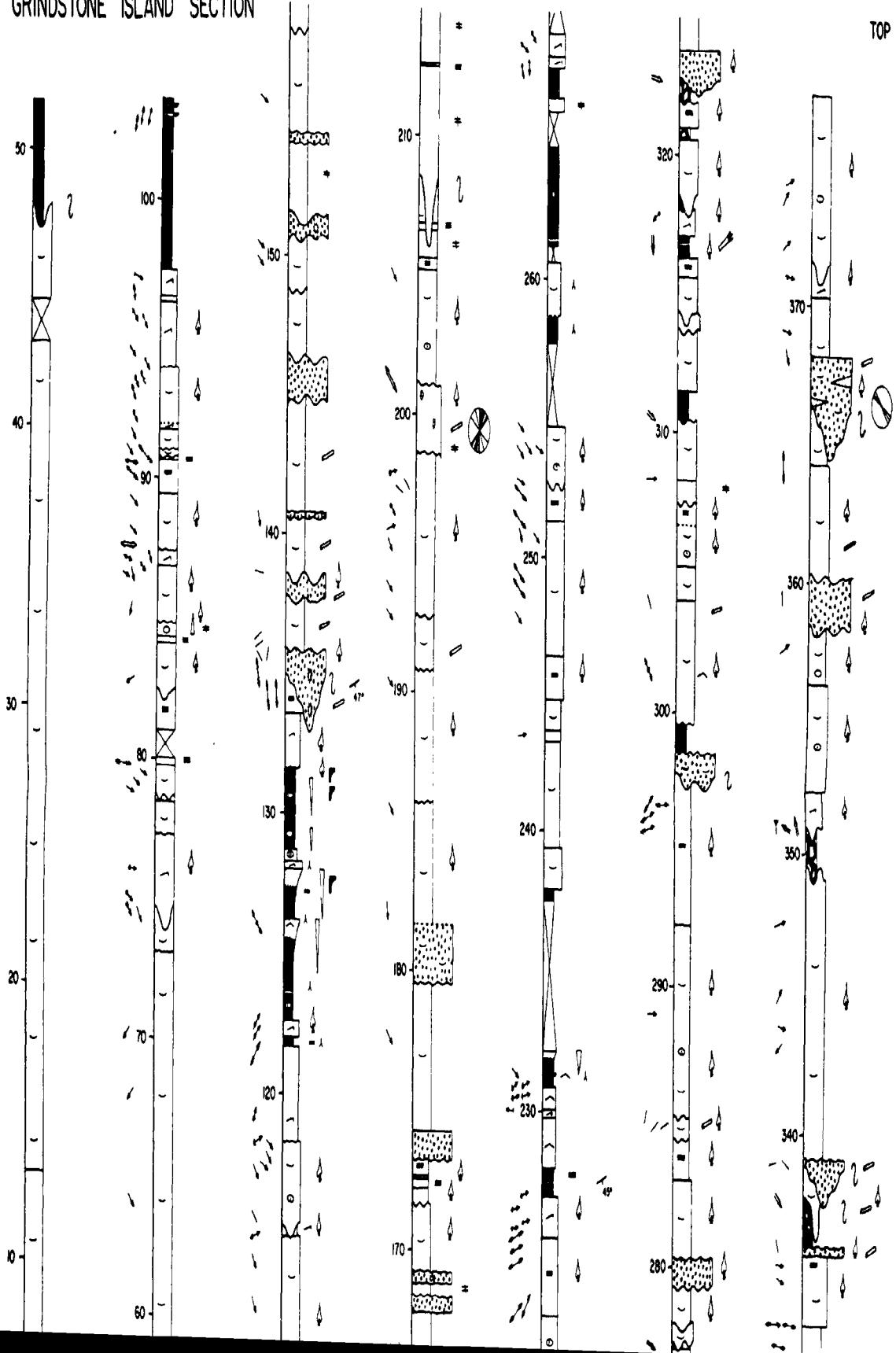
18. ROCKPORT SECTION

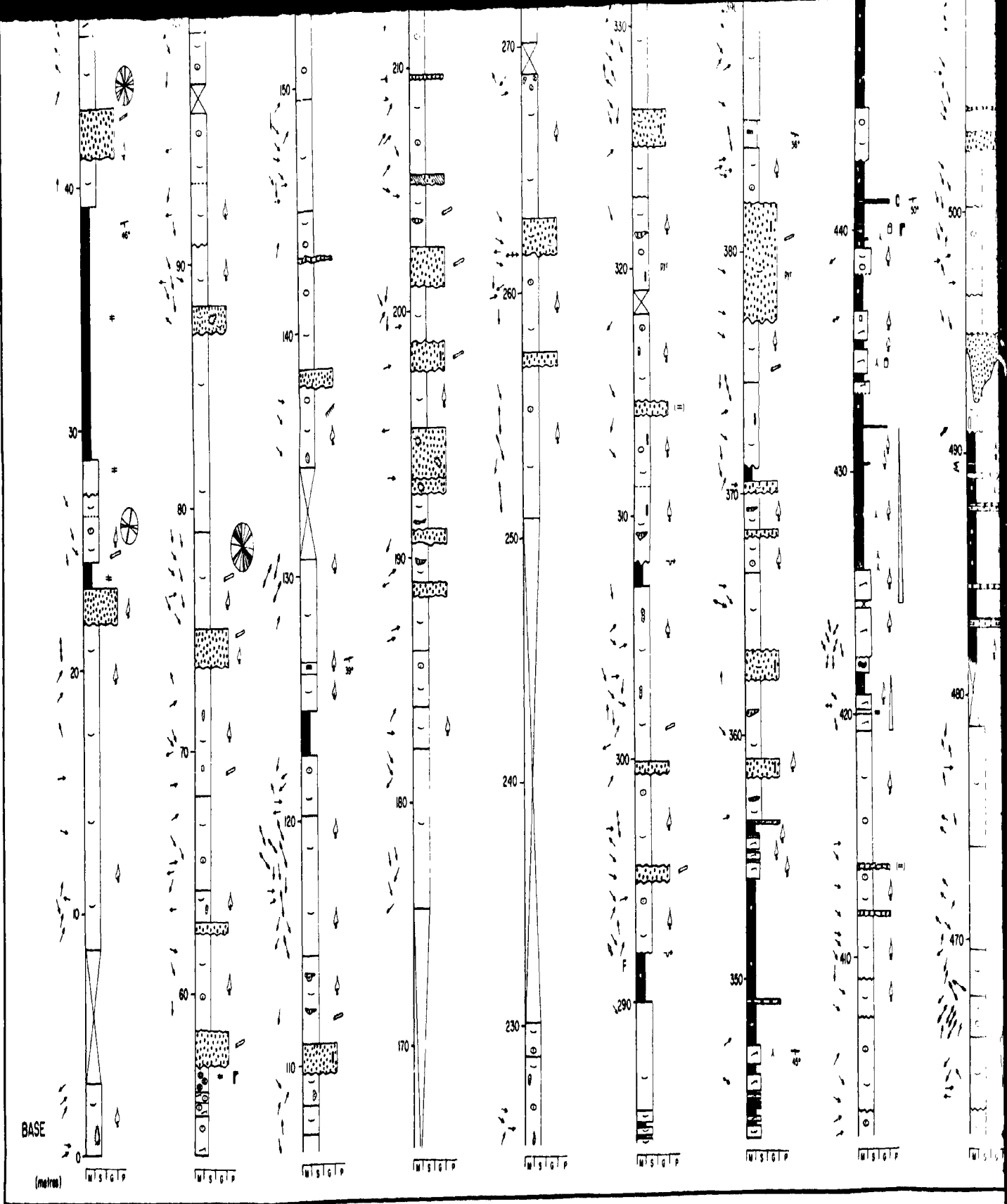




Stratigraphic Section 19
Grindstone Island

19. GRINDSTONE ISLAND SECTION





BASE

(metres)

WISGIP

WISGIP

WISGIP

WISGIP

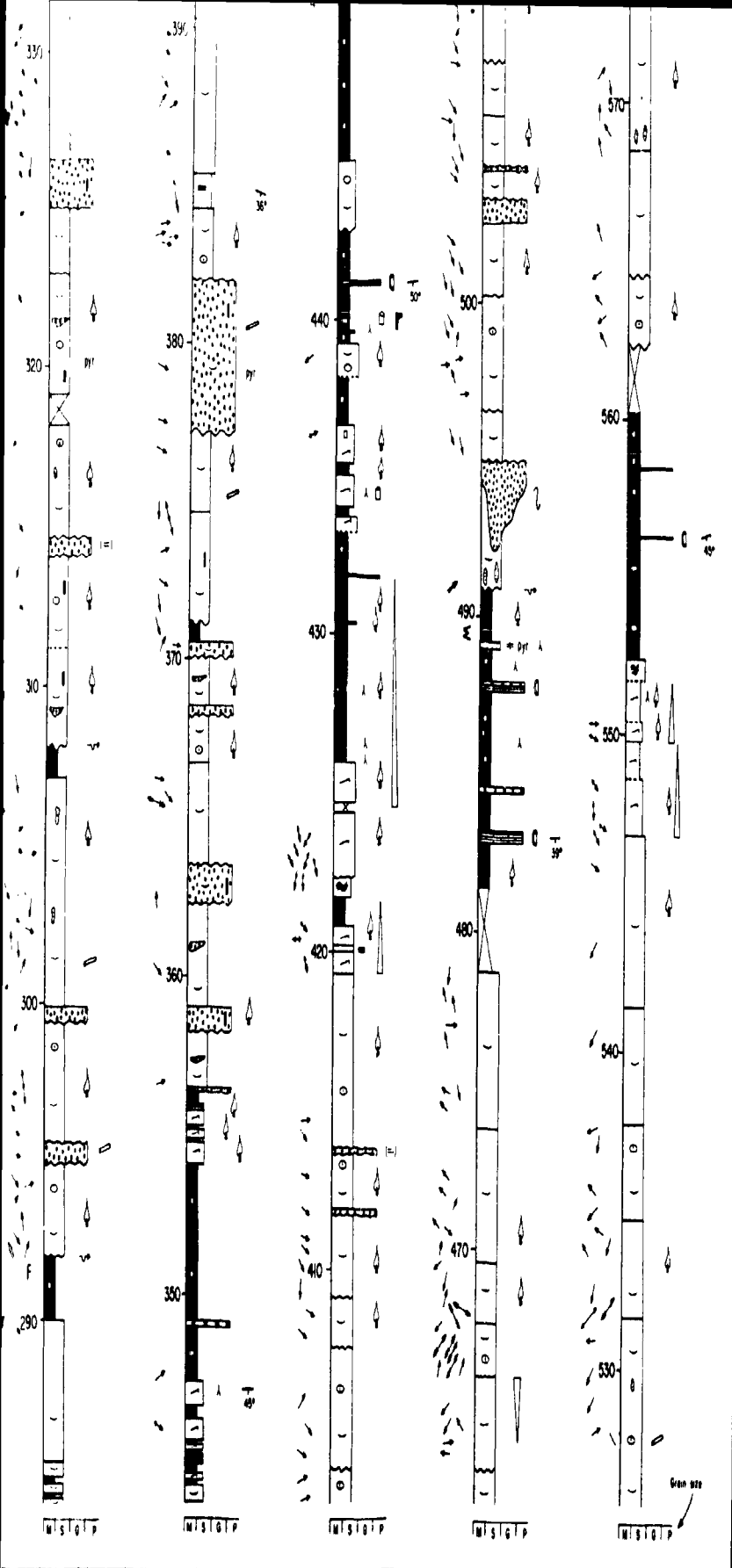
WISGIP

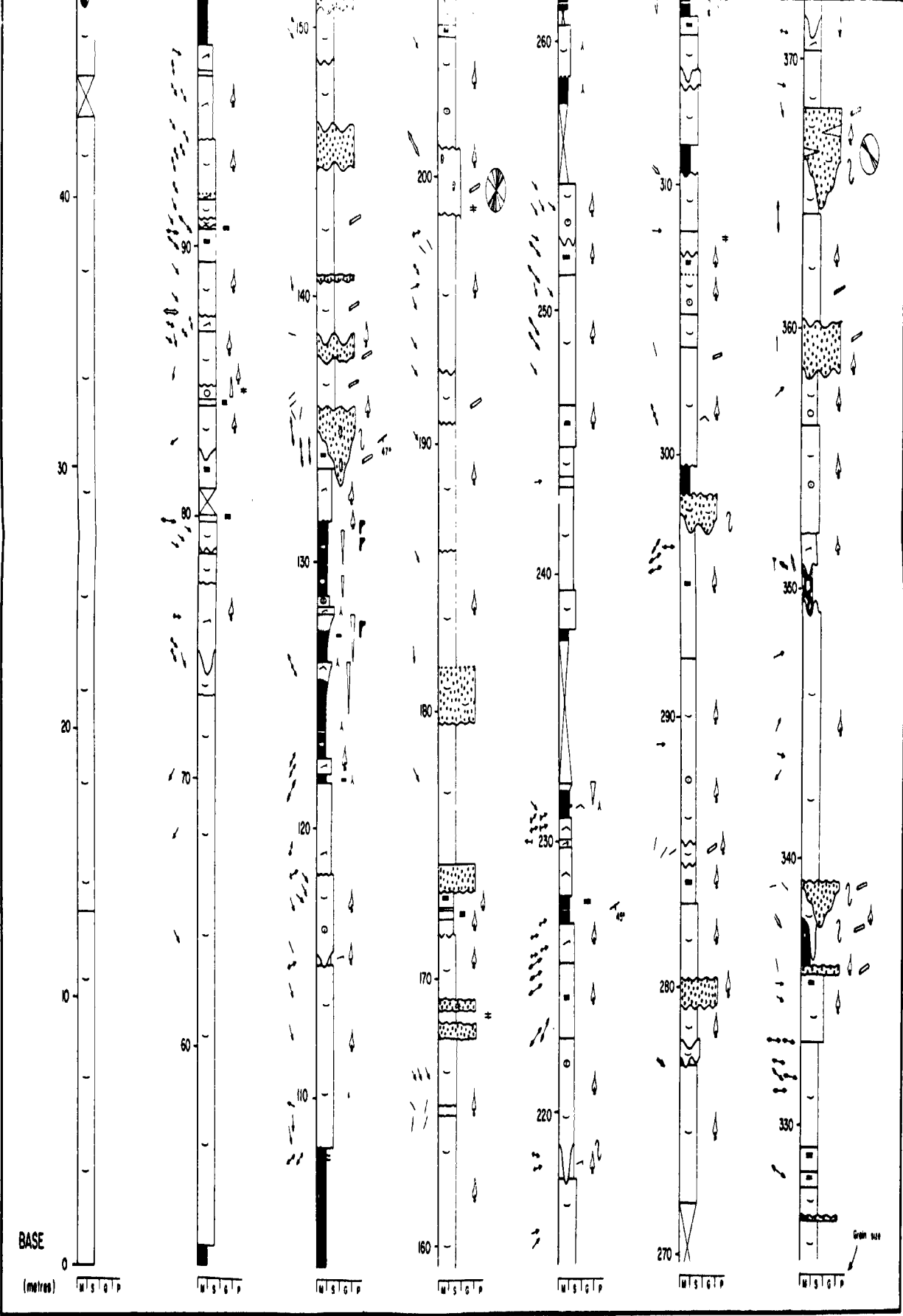
WISGIP

WISGIP

WISGIP

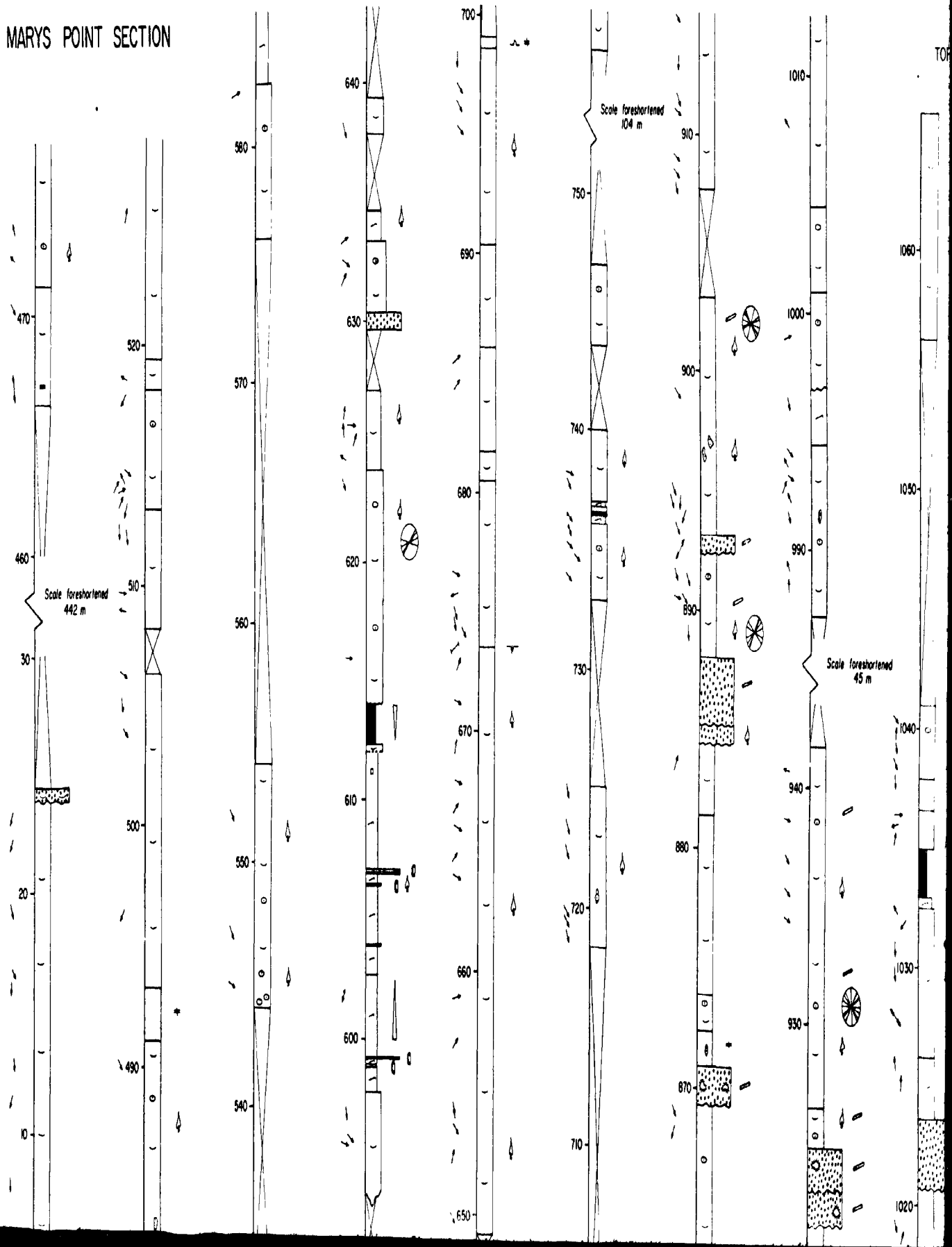
WISGIP

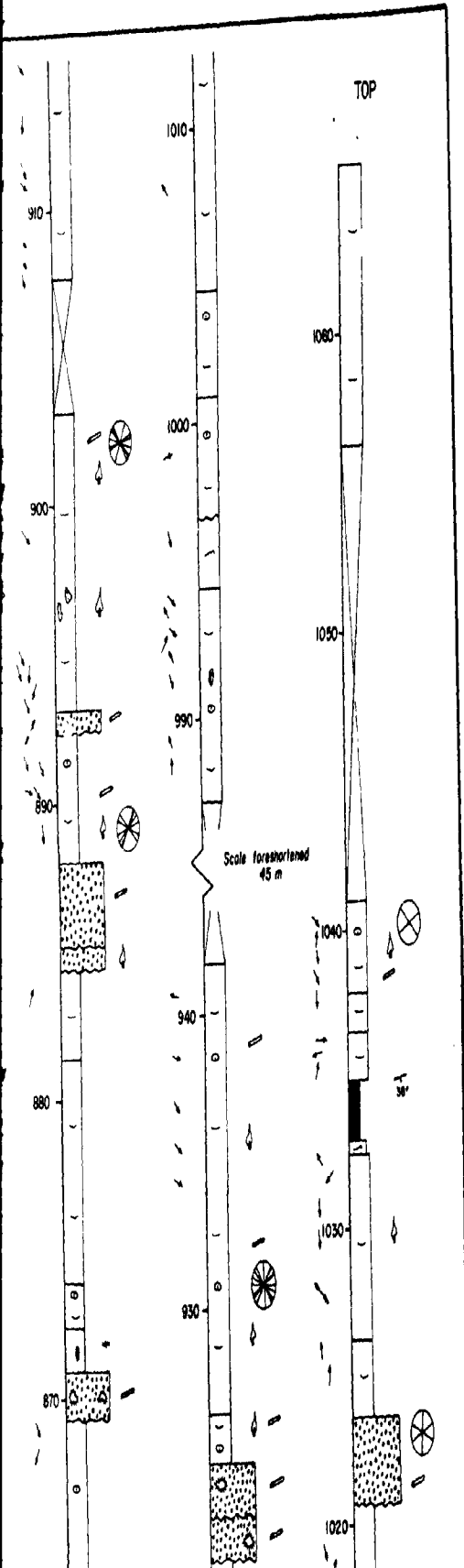




Stratigraphic Section 20
Marys Point

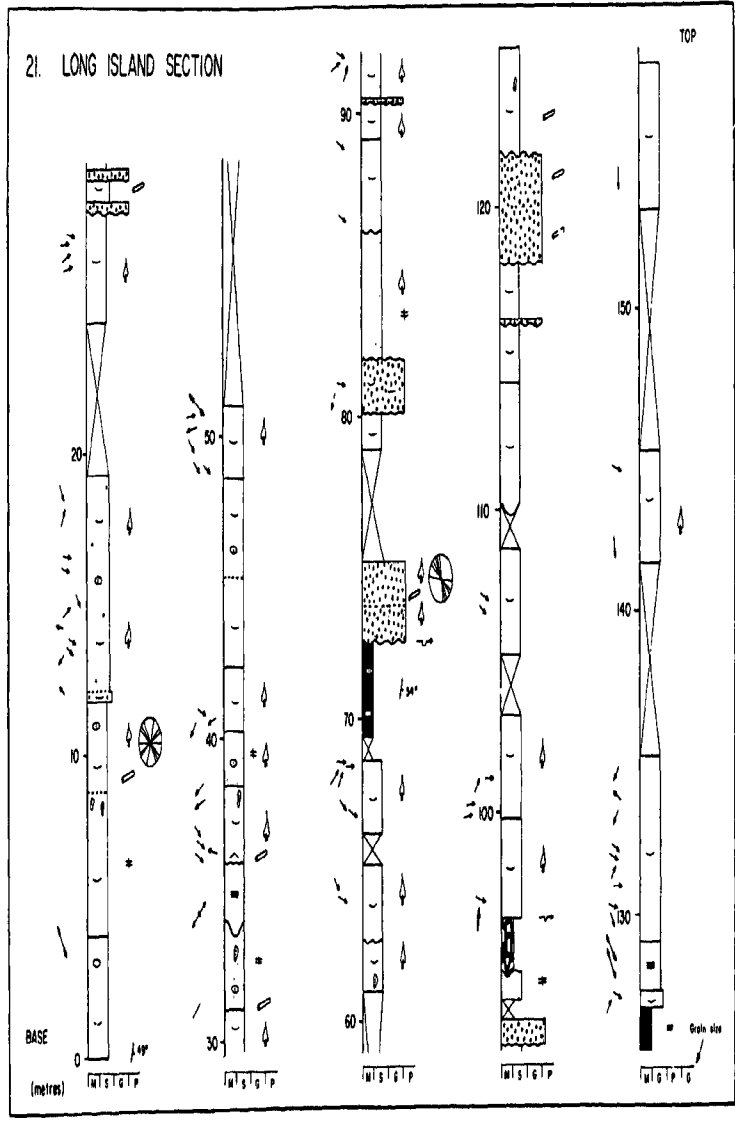
20. MARYS POINT SECTION

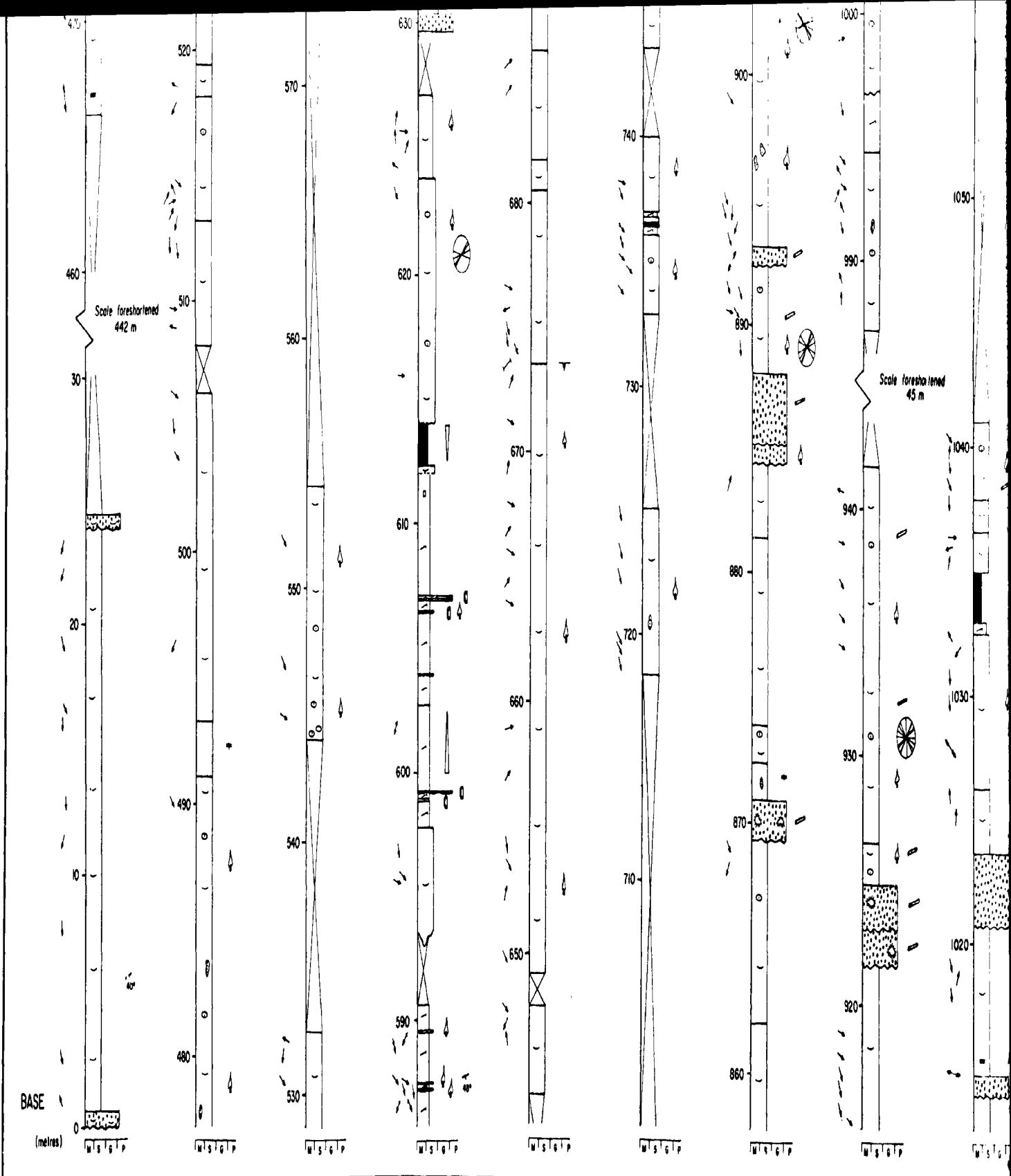


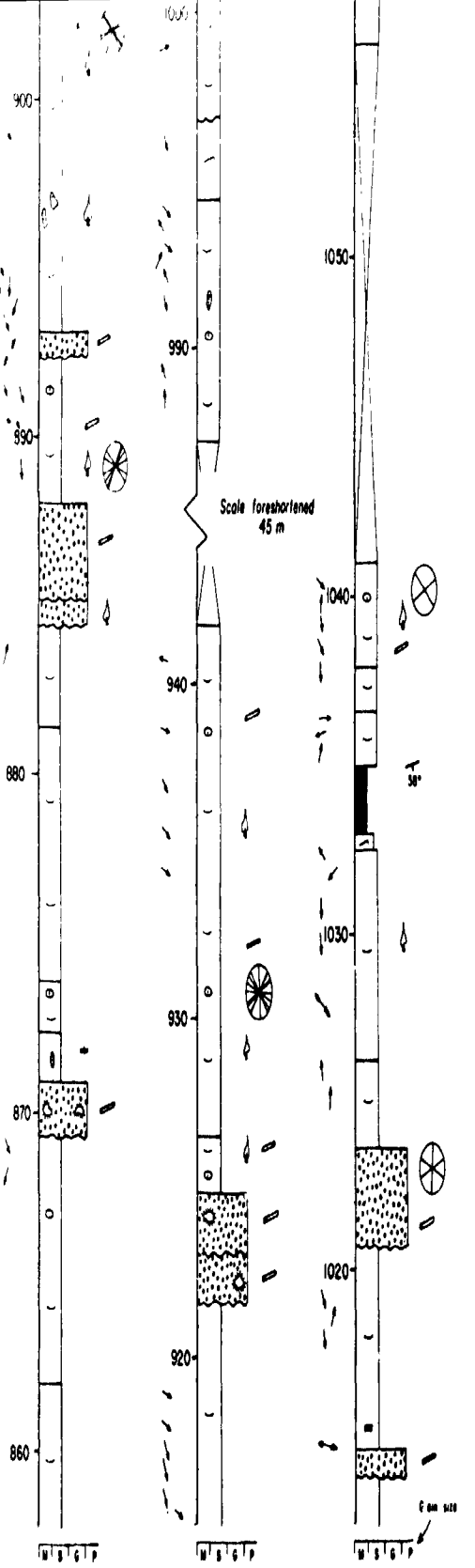


Stratigraphic Section 21
Long Island

21. LONG ISLAND SECTION





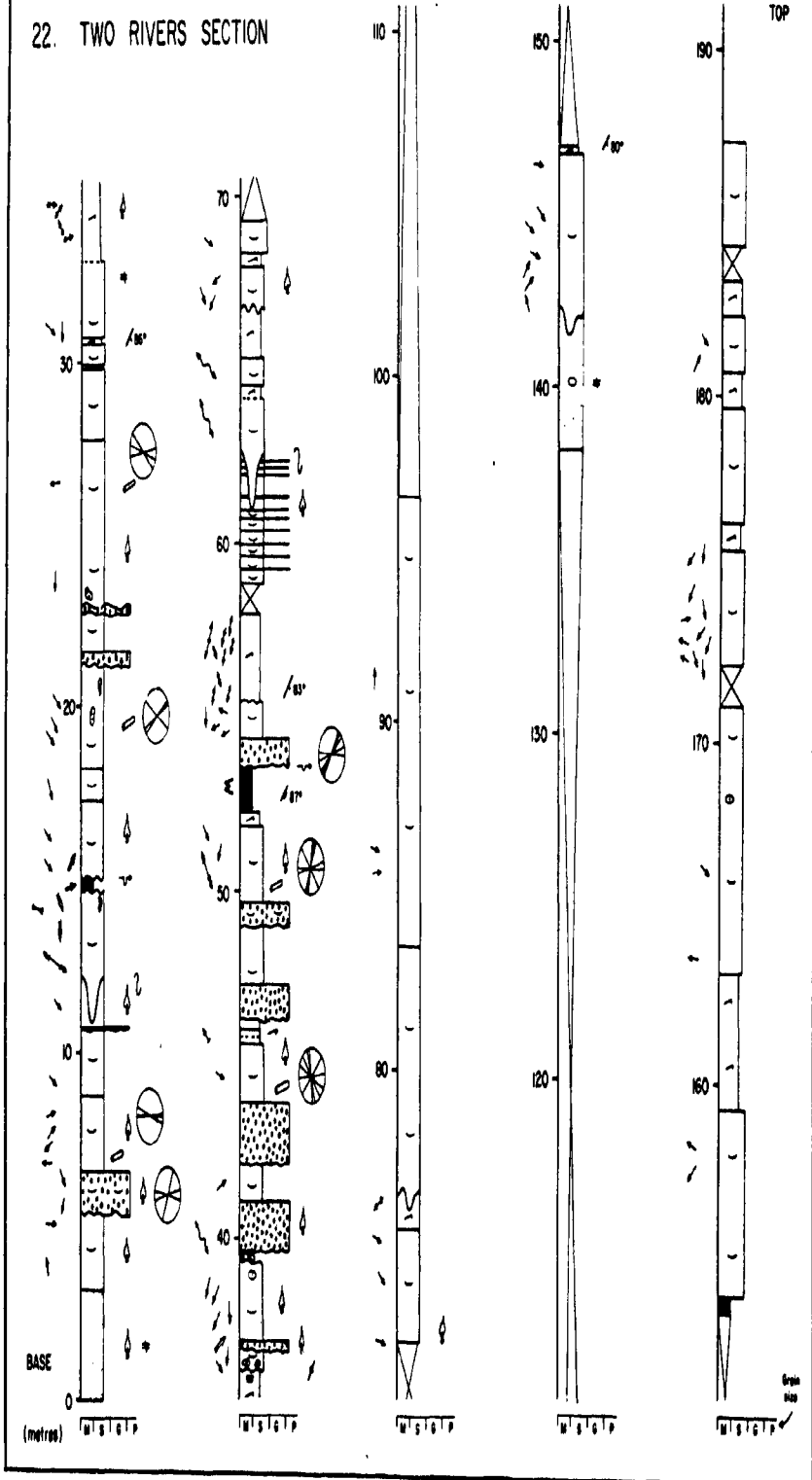


Scale foreshortened
45 m

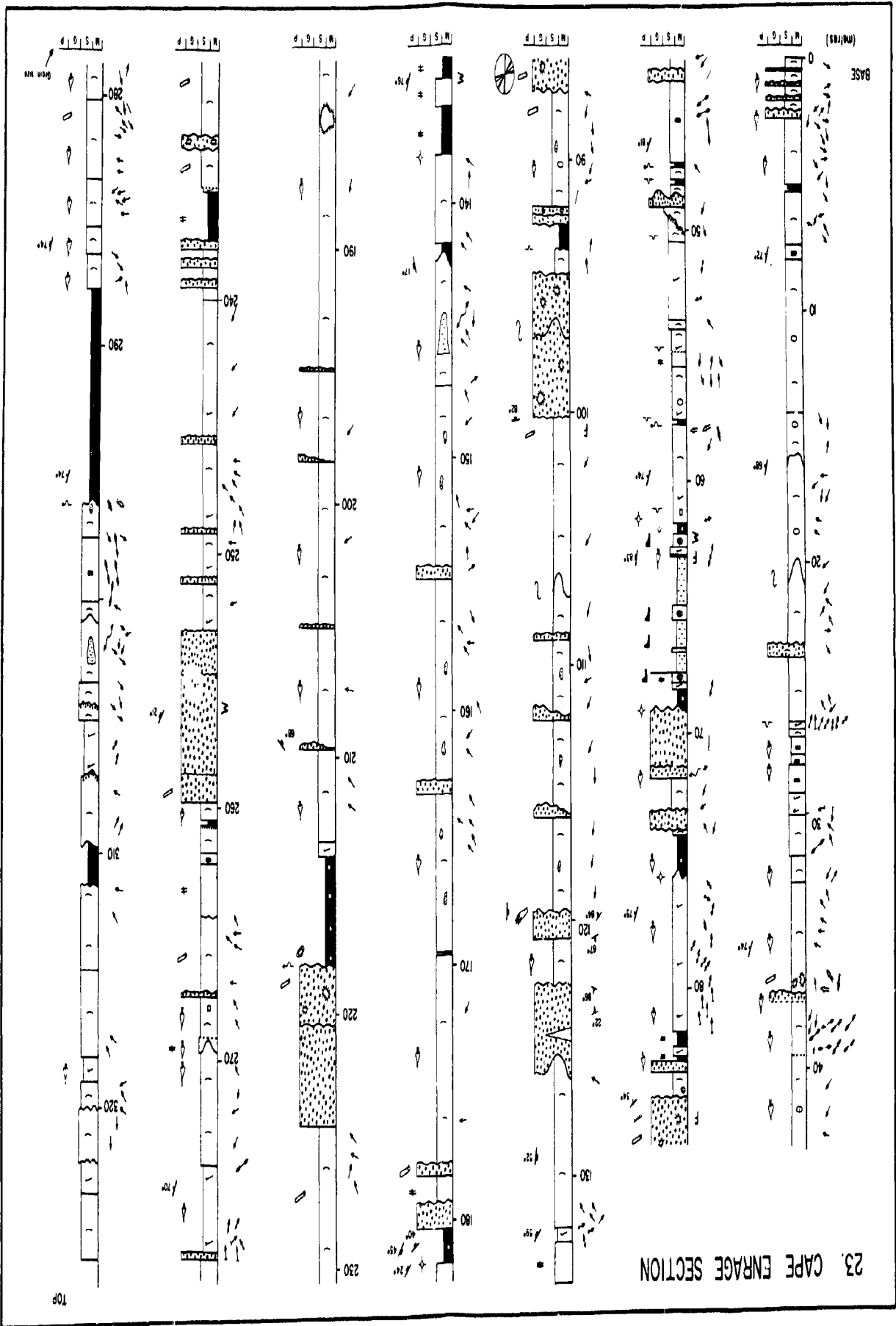
0 1 2 3 4 5

Stratigraphic Section 22
Two Rivers

22. TWO RIVERS SECTION

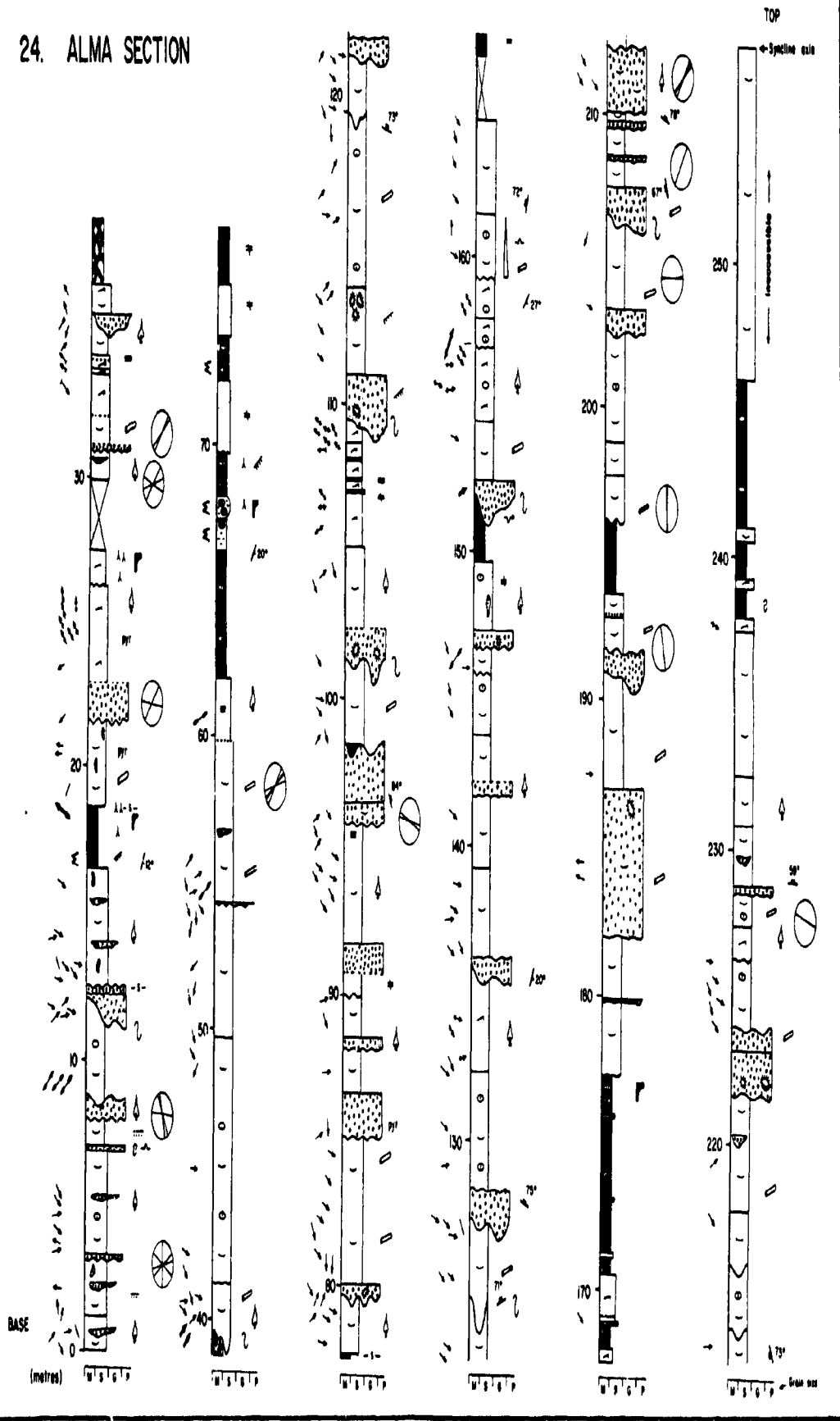


Stratigraphic Section 23
Cape Enrage



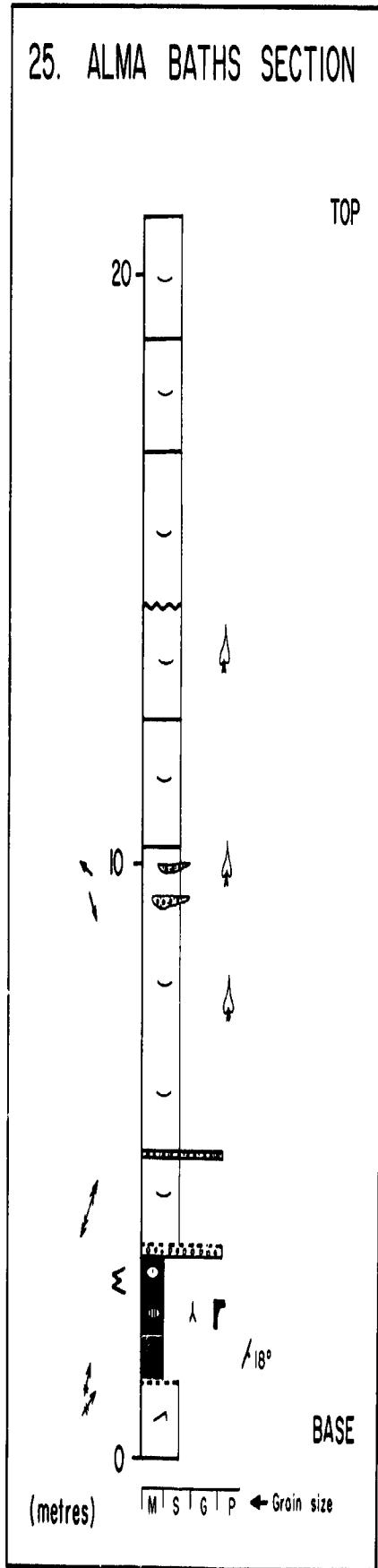
Stratigraphic Section 24
Alma

24. ALMA SECTION



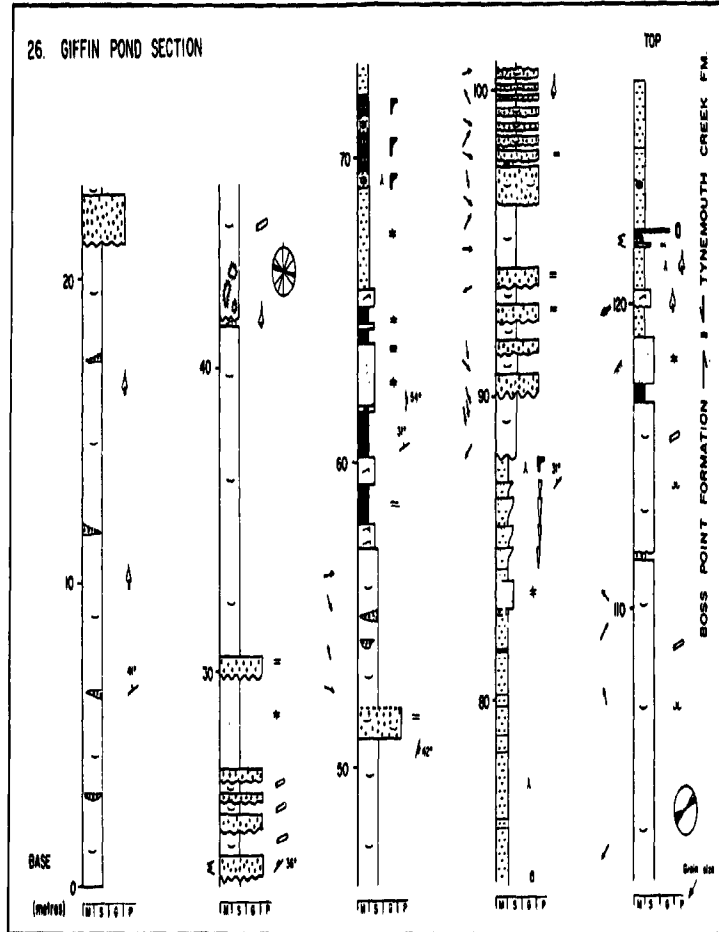
Stratigraphic Section 25
Alma Baths

25. ALMA BATHS SECTION

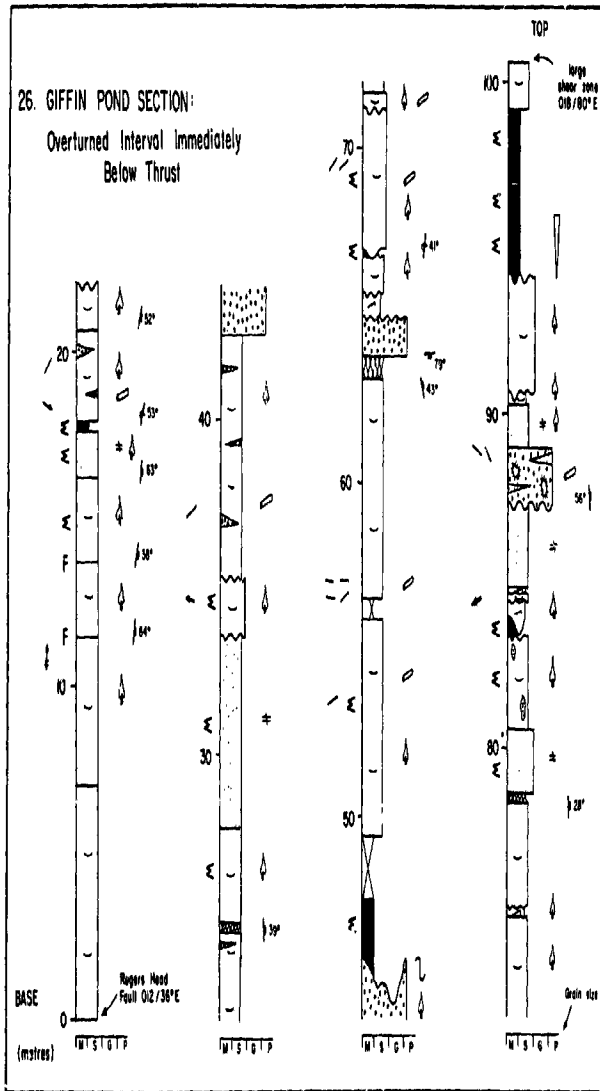


Stratigraphic Section 26
Giffin Pond

26. GIFFIN POND SECTION

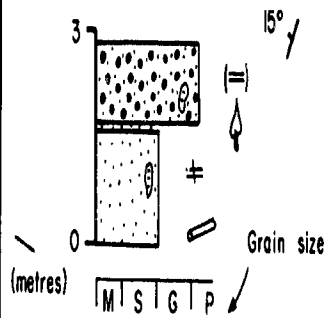


26. GIFFIN POND SECTION:
Overturned Interval Immediately
Below Thrust



Stratigraphic Section 27
Elgin

27. ELGIN SECTION



GRAIN SECTION

